Title
Number Theory in 3d Gravity and from 4d Gauge Theory

Author
Sun, Haoyu

Publication Date
2020

Peer reviewed|Thesis/dissertation

Number Theory in 3d Gravity and from 4d Gauge Theory

by

Haoyu Sun

A dissertation submitted in partial satisfaction of the

requirements for the degree of

Doctor of Philosophy

in

Physics

in the

Graduate Division

of the

University of California, Berkeley

Committee in charge:

Professor Ori J. Ganor, Chair
Professor Mina Aganagić
Professor Richard E. Borcherds

Summer 2020

Number Theory in 3d Gravity and from 4d Gauge Theory

Abstract

Number Theory in 3d Gravity and from 4d Gauge Theory

by

Haoyu Sun

Doctor of Philosophy in Physics

University of California, Berkeley

Professor Ori J. Ganor, Chair

String theory is very successful in connecting deep results between physics and mathematics. However, besides the appearance of modular forms in many supersymmetric partition functions, the relations between string theory and number theory are relatively weak, compared with geometry, algebraic/geometric topology and representation theory. In this thesis, we aim to strengthen the tie between high-energy physics and various aspects of number theory. We start by investigating Euclidean AdS_3 quantum gravity, with asymptotic boundary as either genus-one, namely torus, or higher-genus Riemann surfaces. We will see the appearance of the asymptotic analysis on coefficients in the Klein's j-function in Chapter 2, and two exotic finite-index subgroups of $SL(2,\mathbb{Z})$, with indices 24 and 384 respectively, in Chapter 3. In the end of that chapter, we also conjecture the existence of a series of finite-index subgroups for conformal boundary of any genus. Then we switch gear to the realm of p-adic numbers, and study the discrete semiclassical gravity on a Bruhat-Tits tree and its quotient, where we encounter a special representation of $PGL(2,\mathbb{Q}_p)$ and we explore its surprising relation to Chebyshev polynomials. At this point, we will have observed fascinating number-theoretic objects in studying 3d gravity and 2d conformal field theory. Finally, we present an example in which we are able to derive sophisticated number-theoretic identities, including the classic quadratic reciprocity by Gauss, from a careful use of first principles in string theory and 4d supersymmetric gauge theories.

To my family.

Contents

List of Figures

List of Tables

Acknowledgments

First and foremost, it is my great pleasure and honour to thank my advisor Professor Ori J. Ganor, without whom it is impossible for me to finish this thesis. His deep knowledge in string theory, and constant help along my journey through physics and mathematics as well as outside make my past six years at University of California, Berkeley the most intellectually inspiring period of time I have ever experienced.

I thank Professor Mina Aganagić and Professor Richard E. Borcherds for kindly serving on my thesis committee, and also Professor Holger Müller for attending my qualifying examination.

I owe a lot of gratitude towards my wonderful collaborators: Stephen Ebert, Yoon Pyo Hong, Andreas W. W. Ludwig, Zhu-Xi Luo, Chao-Ming Jian, Nathan Moore, Hai Song Tan, Nesty R. Torres-Chicon, Zhenghan Wang, and Meng-Yang Zhang. I am also appreciate to Yoon-Seok John Chae, Christian Ferko, and Zhengdi Sun for working together on several upcoming work.

Many advice and help on my research has been offered by faculty members outside of my thesis committee, such as Zheng-Cheng Gu, Thomas Hartman, Song He, Petr Hořava, Kristan Jensen, Andreas Karch, Alexander Maloney, Alessandro Tomasiello, Xi Yin, and I thank them all. I am especially indebted to Sergei Gukov, for his wonderful series of Idea Incubators at Caltech and guidance in understanding 3d-3d correspondence and his $\hat{Z}$ invariant.

My life at Berkeley was substantially enriched by friends, Erik Aldape, Yimu Bao, Chi-Ming Chang, Yixing Fu, Dmitry Galakhov, Qinghui Ge, Nathan Haouzi, Felip Kos, Shengzhi Alex Li, Zhengzhi Jack Ma, Mudassir Moussa, Ziwen Rui, Christian Schmid, Rahul Vijay, Sijia Viska Wei, Ziqi Yan, and Jiaobao Yang. I also thank Ning Bao, David Dunsky, Jacob Leedom, and Vijay Narayan for being on the team "Irrelevant Operators" with me for the intramural flag football.

I have the pleasure to spend quality time with colleagues and friends outside of Berkeley: Jordan Cotler, Alexander Frenkel, Dongmin Gang, Hao Geng, Wei Gu, Matthew Heydeman, Ziming Ji, Yuqi Li, Sarthak Parikh, Du Pei, Mauricio Romo, Kaiwen Sun, Yinan Wang, Hongyu Xiong, Fengjun Xu, Jingjin Yi, and Zhewei Yin.

I have had great time chatting with mathematicians and friends in math major at and outside of Berkeley: Ian Agol, Semeon Artamonov, Michael H. Freedman, Siqi He, Nicolai Yu. Reshetekhin, Alex A. Takeda, Su Tao, Peng Zhou, particularly on knot theory, hyperbolic 3-manifolds, representation theory and resurgence. I cannot imagine having a more excellent mathematician than Richard E. Borcherds on my committee; our conversations on quadratic reciprocity, monster module, p-adic L-function and representations among others largely facilitate my research.

My visit to the Kavli Institute for Theoretical Physics (KITP) at University of California, Santa Barbara during Spring 2019 is a memorable experience. I thank Xi Dong, Dongsheng Ge, Gary Horowitz, Ling-Yan Janet Hung, Donald Marolf, Sean McBride, Andrea Rocchetto, Eduardo Teste, Gustavo Joaquin Turiaci, Huajia Wang, Wayne Weng, Chih-Hung

Wu, Xiaochuan Wu, Shu Zhang, Yi Frank Zhang, Tianci Zhou for many useful conversations there. And a special gratitude goes to David J. Gross for being my mentor during my KITP graduate fellowship.

I would also like to take this opportunity to acknowledge my undergraduate mentors at UC Berkeley: Barbara Baker, Feng Li, and Jeffrey Tung, during my brief excursions into molecular biology and virology.

I thank staff members Joelle Miles and Donna K. Sakima for constant help on my administrative business.

Finally, I am grateful to my parents Meng and Jianpeng for their constant support and understanding during my study and research in college, in graduate school and beyond. I also thank my wife and collaborator, Zhuxi, for sharing joys and challenges in physics and life with me, and I thank my son Cliff for joining our exciting adventures.

Chapter 1

Introduction

String theory has remarkable connections to geometric topology, algebraic geometry and number theory. Here we further explore the deep ties between string theory and number theory, with an eye towards geometric topology in 3d.

1.1 First order formalism of 3d gravity

In 3d spacetime (either asymptotically anti-de Sitter, de Sitter, or Minkowski), Einstein gravity can be classically described by a non-chiral Chern-Simons gauge theory with a non-compact, possibly complex gauge group, depending on the signature of the metric being Lorentzian or Euclidean [1, 2] (for a review, see e.g., [3]). This is possible because 3d gravity has vanishing Weyl tensor and consequently no propagating degrees of freedom (no gravitational waves). Furthermore, after imposing the Einstein's equations, the Riemann tensor is completely defined in terms of the scalar curvature, so all possible solutions are locally equivalent to one with constant curvature everywhere. Consequently, the only possible differences between the solutions are global differences, for example, ones that change the topology.

The Chern-Simons theory is independent of the metric and can exist on any topological 3-manifold, so we will use a basis of the gravity theory that is coordinate-independent. Instead of the usual metric tensor field, we describe geometries using a vielbein field e^{μ}_{a}. It contains two types of indices: μ labels the general spacetime coordinate and a labels the local Lorentz laboratory coordinates. The vielbein or frame fields are roughly the matrix square root of the metric tensor $g_{\mu\nu}$ in a coordinate basis,

$$g_{\mu\nu} = e^{\mu}_{a} e^{\nu}_{b} \mu_{ab}, \tag{1.1}$$

where μ_{ab} is the flat Minkwoski metric $(-1, 1, 1, 1)$. They satisfy

$$e^{a}_{\mu} e^{\mu}_{b} = \delta^{a}_{b}, \quad e^{a}_{\mu} e^{\nu}_{a} = \delta^{\nu}_{\mu}. \tag{1.2}$$

The local Lorentz indices can be raised or lowered with the Lorentz metric, for example, $e_{\nu a} = \eta_{ab} e^{b}_{a}$, while the spacetime indices can be raised or lowered with the spacetime metric

$e^{\mu a} = g^{\mu\nu} e^a_\nu$. The vielbeins enable conversions between local Lorenz and spacetime indices, for example, $T_a = e^\mu_a T_\mu$.

The spin connection is defined as

$$\begin{aligned}\omega^{ab}_\mu &= e^a_\nu \Gamma^\nu_{\sigma\mu} e^{\sigma b} + e^a_\nu \partial_\mu e^{\nu b} \\ &= \frac{1}{2}\left[e^{\nu a}\left(\partial_\mu e^b_\nu - \partial_{nu} e^b_\mu\right) - e^{\nu b}\left(\partial_\mu e^a_\nu - \partial_{nu} e^a_\mu\right) - e^{\rho a} e^{\sigma b}\left(\partial_\rho e_{\sigma c} - \partial_\sigma e_{\rho c}\right) e^c_\mu\right],\end{aligned} \tag{1.3}$$

which is antisymmetric by construction.

The Riemann curvature tensor is then

$$R^{ab}_{\mu\nu} = \partial_\mu \omega^{ab}_\nu - \partial_\nu \omega^{ab}_\mu + [\omega_\mu, \omega_\nu]^{ab} = (d\omega + \omega \wedge \omega)_{\mu\nu}. \tag{1.4}$$

The 3d Einstein-Hilbert action is

$$\begin{aligned}S_{grav} &= \frac{1}{16\pi G}\int_{M_3} d^3x \sqrt{-g}(R - 2\Lambda) \\ &= \frac{1}{16\pi G}\int_{M_3} d^3x \left[e^a \wedge (2d\omega_a + \epsilon_{abc}\omega^b \wedge \omega^c) + \frac{\Lambda}{3}\epsilon_{abc} e^a \wedge e^b \wedge e^c\right].\end{aligned} \tag{1.5}$$

where the cosmological constant Λ is related to the AdS radius l by $\Lambda = -1/l^2$.

In Lorentzian signature[1], the isometry group of the global AdS_3 is $SO(2,2) \simeq SL(2,\mathbb{R}) \times SL(2,\mathbb{R})$, so we have two gauge fields $A = A^a T_a$ and $\bar{A} = \bar{A}^a T_a$ valued in the Lie algebra $sl(2,\mathbb{R})$, with generators

$$T^0 = \frac{1}{2}\begin{pmatrix} 0 & 1 \\ -1 & 0 \end{pmatrix}, \quad T^1 = \frac{1}{2}\begin{pmatrix} 1 & 0 \\ 0 & -1 \end{pmatrix}, \quad T^2 = \frac{1}{2}\begin{pmatrix} 0 & 1 \\ 1 & 0 \end{pmatrix}. \tag{1.6}$$

Then the Chern-Simons action is

$$S_{CS} = \frac{ik}{4\pi}\int \mathrm{Tr}\left(A \wedge dA + \frac{2}{3} A \wedge A \wedge A\right) - \frac{ik}{4\pi}\int \mathrm{Tr}\left(\bar{A} \wedge d\bar{A} + \frac{2}{3}\bar{A} \wedge \bar{A} \wedge \bar{A}\right) \tag{1.7}$$

By setting the gauge fields to be

$$A = \omega + e/l, \quad \bar{A} = \omega - e/l, \tag{1.8}$$

we see that

$$S_{grav} = S_{CS}, \tag{1.9}$$

with $k = l/4G$, which turns out to be quantized. This quantization is a consequence of Zamolodchikov's c-theorem [4], which states that in any continuously varying family of 2d CFTs, the central charge c is constant. More generally, the same is true for the left- and

[1]We defer the discussion using Euclidean signature to Chapters 2 and 3, where the isometry group is analytically continuated to $SL(2,\mathbb{C})$.

right-moving central charges c_L and c_R. And in AdS_3 gravity, k is related to the *Brown-Henneaux* central charge c of the boundary 2d Virasoro algebra, as introduced in Section 3.1, by $k = 6c$.

However, the identification (1.8) only works when the vielbein is invertible, which is true for classical solutions and small fluctuations around them. Nonperturbatively, the vielbein in Chern-Simons can be degenerate, i.e., there exists a classical solution with $A = \omega = e = 0$. It is unclear how to make sense of this degeneracy in gravity [5]. Furthermore, the equivalence between diffeomorphisms in gravity and gauge transformations in Chern-Simons is limited to the small ones which connect to identity continuously. Gravity also contains large diffeomorphisms, which lack a natural realization in the Chern-Simons theory [5].

In spite of these drawbacks, the Chern-Simons formulation does provide us with a toy model of gravity that is reasonably effective and exactly soluble, leading towards important insights.

1.2 (Topological) entanglement entropy

von Neumann entropy

In a quantum system spatially bipartited into regions A and B, the total Hilbert space is factorized[2]

$$\mathcal{H} = \mathcal{H}_A \otimes \mathcal{H}_B. \tag{1.10}$$

From the full density matrix of the system $\rho = \sum_i p_i |\psi_i\rangle \langle\psi_i|$, the reduced density matrix of subsystem A is the partial trace of ρ with respect to the degrees of freedom in subsystem B:

$$\rho_A = \mathrm{Tr}_B\, \rho, \tag{1.11}$$

satisfying $\mathrm{Tr}\, \rho_A = 1$. The von Neumann entropy is then defined as

$$S_A = -\,\mathrm{Tr}\, \rho_A \ln \rho_A. \tag{1.12}$$

In practice, it is often not easy to compute (1.12) directly. As an alternative approach, one can calculate the Rényi entropy of subsystem A defined as

$$S_A^{(n)} = \frac{1}{1-n} \ln \mathrm{Tr}\, \rho_A^n, \tag{1.13}$$

and take the limit

$$S_A = \lim_{n\to 1} S_A^n = -\lim_{n\to 1} \frac{\partial}{\partial n} \mathrm{Tr}\, \rho_A^n \tag{1.14}$$

using L'Hôspital's rule. Its connection with replica trick will be introduced in Section 2.2.

[2]Hilbert space in a continuous QFT is never factorizable [6], but it is OK for a QFT defined on a lattice.

For a system in a pure state $|\psi\rangle$, we apply the Schimdt decomposition to obtain orthonormal basis $\{|i\rangle_A\}$ of $\mathcal{H}_A$ and $\{|j\rangle_B\}$ of $\mathcal{H}_B$ such that

$$|\psi\rangle = \sum_i^{\min(\dim\mathcal{H}_A,\dim\mathcal{H}_B)} \lambda_i |i\rangle_A |j\rangle_B , \quad \sum_i \lambda_i^2 = 1, \quad \lambda_i \in [0,1]. \tag{1.15}$$

Then it is straightforward that for pure states, $S_A = S_B$. We also note that $S_A^n = S_B^n$ in this case.

For two density matrices ρ and σ, Umegaki's relative entropy [7]:

$$S(\rho||\sigma) = \mathrm{Tr}\left(\rho \ln \rho - \sigma \ln \sigma\right), \tag{1.16}$$

facilitates the proofs of some key properties of entanglement entropy. Measuring the distance between ρ and σ, the relative entropy is never negative and is zero if and only if $\rho = \sigma$, due to the positive spectral decompositions of ρ and σ required by unitarity. This non-negativity implies the triangle inequality of entanglement entropy

$$|S_A - S_B| \leq S_{AB}. \tag{1.17}$$

One can further define the mutual information between subsystems A and B:

$$I(A,B) \equiv S(\rho_{AB}||\rho_A \otimes \rho_B) = S_A + S_B - S_{AB} \geq 0 \tag{1.18}$$

This definition is favorable due to the cancellation of divergences in individual terms S_A, S_B and S_{AB}. Finally, for a tripartite system $\mathcal{H} = \mathcal{H}_A \otimes \mathcal{H}_B \otimes \mathcal{H}_C$, we obtain the strong subadditivity inequality:

$$S_{ABC} + S_B \leq S_{AB} + S_{BC}, \tag{1.19}$$

or equivalently, $I(A,B) \leq I(A,BC)$.

As an example of application, we turn our attention to low-dimensional systems. The entanglement entropy in a generic 2d CFT has been calculated by Calabrese and Cardy [8] (also less systematically by [9]). For the simplest case where region A is an interval of length L in an infinitely long 1d quantum system at zero temperature. The result is [10]

$$S_A = \frac{c}{3} \ln \frac{L}{a} + c_1', \quad S_A^{(n)} = \frac{c}{6}\left(1 + \frac{1}{n}\right) \ln \frac{L}{a} + c_n', \tag{1.20}$$

where non-universal constants are defined

$$c_n' \equiv \frac{\ln c_n}{1-n}, \quad c_1 = -\frac{\partial c_n}{\partial n}\Big|_{n=1}. \tag{1.21}$$

The lattice spacing a goes to zero in the continuum limit, rendering S_A with UV divergences. These results further enjoy generalizations for finite temperature, for finite system size, and also for region A consisted of multiple intervals, see for example [11, 12, 13, 14].

Other examples include the renowned Ryu-Takayanagi formula in holographic CFT [15], which will be an essential player in Chapter 2.

For topological phases

At the first glance, it is tempting to think that the entanglement entropy of a region A should be extensive, i.e., obey a volume law. This indeed happens for thermal states. For typical ground states, however, one finds the scaling of entropy is only linear in the circumference of the region (area law) [16]. Such systems have local short-ranged interactions, which require that quantum correlations between the region of interest and its exterior are established only through the neighborhood of its boundary. Additionally, if the system is in a topological phase, the quantum entanglement in the ground state will have global and topological properties that manifest themselves as a universal, subleading constant correction to the area law [17, 18]. In the case when subsystem A has a disk topology, the entanglement of region A has the form

$$S_A = \alpha L - \gamma, \tag{1.22}$$

where α is a non-universal coefficient that depends on the details of the system, L is the size of the boundary of A, and γ is a topological invariant called the *topological entanglement entropy* (TEE). The correction $-\gamma$ is always negative because it results from a global constraint consistent with the topological order. It can be computed by decomposing the system into four parts A, B, C, D. Then

$$\gamma = S_A + S_B + S_C - S_{AB} - S_{BC} - S_{AC} + S_{ABC} \tag{1.23}$$

is exactly the tripartite mutual information $I_3(A, B, C)$ of these regions. Equivalently, one can also write

$$I_3(A, B, C) = I(A, B) + I(A, C) - I(A, B \cup C). \tag{1.24}$$

In the case of a pure global state, by the strong subadditivity of entanglement entropy and the non-negativity of mutual information, the lower and upper bounds on $I_3(A, B, C)$ can be derived [19, 20]:

$$-2\min(S_A, S_B, S_C, S_D) \leq I_3(A, B, C) \leq \min(S_A, S_B, S_C, S_D). \tag{1.25}$$

In a chiral topological phase described by a modular tensor category (MTC), we have $\gamma = \ln \mathcal{D}$, where $\mathcal{D}$ is the total quantum dimension of the MTC

$$\mathcal{D} = \sqrt{\sum_i d_i^2}, \tag{1.26}$$

where d_i are quantum dimensions[3] of simple objects (or anyon types) of the MTC.

The TEE is sensitive to both the topological order/phase of the system, and the topology of the subsystems A, B. When the system is in an excited state, it also captures the feature of the quasiparticles inside each subsystem. One can thus extract the data of the topological

[3] d_i obtains its name because it tells how fast the size of the Hilbert space of multiple anyons of type i grows as we increase the number of anyons.

phase and even the mutual fractional statistics of quasiparticles from TEE [21]. TEE is also very accessible to numerical computations, such as applying density matrix renormalization groups (DMRG) [22] for a finite-size cylinder system bipartited by a flat cut to compute TEE [23].

1.3 The modular group $SL(2,\mathbb{Z})$ and its various congruence subgroups

Subgroups of $SL(2,\mathbb{Z})$ of finite or infinite indices are of great physical interests because it can describe discrete symmetries in various systems. Here we list a very incomplete list of places where $SL(2,\mathbb{Z})$ appears in high-energy and condensed matter theory:

- Mapping class group (MCG) of a two-dimensional torus T^2, and hence in modular transformation in 2d CFT, and rational/integral Dehn surgery in knot theory and 3-manifolds[4];
- Electromagnetic (Montonen-Olive) duality and S-duality in 4d $\mathcal{N}=4$ and $\mathcal{N}=2$ (Seiberg-Witten) gauge theories;
- $SL(2,\mathbb{Z})$ actions on (p,q) brane webs of D5- and NS5-branes;
- The axio-dilaton field in Type IIB string theory and F-theory transforms under $SL(2,\mathbb{Z})$. In particular, monodromy of τ around D7-branes, as well as on $[p,q]$ 7-branes, on which (p,q) 5-branes end;
- One-to-one correspondence between elliptic fibrations and $SL(2,\mathbb{Z})$ bundles in F-theory;
- Exchange of NS5 and D5 branes by the S action in the Type IIB dual description of 3d mirror symmetry [28];
- ...

We will study the first two aspects in Chapters 2-3 and Chapter 5, respectively.

Now the modular group $SL(2,\mathbb{Z})$ is a matrix Lie group defined as follows:

$$SL(2,\mathbb{Z}) = \left\{ \begin{pmatrix} a & b \\ c & d \end{pmatrix} \middle| a,b,c,d \in \mathbb{Z}, ad-bc=1 \right\}, \tag{1.27}$$

[4]In Dehn surgery [24], one cuts out a tubular neighborhood (isomorphic to a solid torus) of a knot inside a 3-manifold, and then glues back the solid torus with a diffeomorphism on its torus boundary, to get a new 3-manifold. The best known applications of Dehn surgery in physics are in Witten's series of work on Chern-Simons theory and Jones polynomial [25, 26, 27]. The surgery is usually performed on a closed 3-manifold, but it is also well-defined for 3-manifolds with boundary.

There is a variant called the *hyperbolic Dehn surgery*, in which one only fills in the cusps, which have torus boundaries, with certain solid tori to get a new hyperbolic 3-manifold, with or without cusps.

generated by two generators S and T with canonical representations:

$$S = \begin{pmatrix} 0 & -1 \\ 1 & 0 \end{pmatrix}, \quad T = \begin{pmatrix} 1 & 1 \\ 0 & 1 \end{pmatrix}. \tag{1.28}$$

The matrix S has order 4, while the matrix T has an infinite order and ST has order 6, serving as the defining relations.

It acts on elements τ on upper half-plane by the fractional linear fashion (3.8):

$$\tau \to \gamma \cdot \tau = \frac{a\tau + b}{c\tau + d}. \tag{1.29}$$

By using S and T generators, one can find the fundamental domain of $SL(2,\mathbb{Z})$ is the "key hole" region: $|\mathrm{Re}\,\tau| < 1/2$ and $|\tau| > 1$.

The method of decomposing a given element in $SL(2,\mathbb{Z})$ into a finite-length word

$$T^{p_1} S T^{p_2} S \dots T^{p_r} S T^{\#} \tag{1.30}$$

is to use continued fractions on the first column of the element [29]:

$$\frac{a}{c} = p_1 - \cfrac{1}{p_2 - \cfrac{1}{\ddots_{-\frac{1}{p_r}}}}, \tag{1.31}$$

or alternatively to use the standard all-plus convention for continued fraction:

$$\frac{a}{c} = q_1 + \cfrac{1}{q_2 + \cfrac{1}{\ddots_{+\frac{1}{q_r}}}} \equiv [q_1; q_2, \dots, q_r], \tag{1.32}$$

with $q_i = (-1)^{i+1} p_i$. Finally, the last power # in (1.30) is determined by solving

$$\begin{pmatrix} a & b \\ c & d \end{pmatrix} = \left(T^{p_1} S T^{p_2} S \dots T^{p_r} S\right) T^{\#}. \tag{1.33}$$

We also see that the decomposition is obviously non-unique. As a side note, this decomposition is also used when decomposing a rational Dehn surgery on an unknot into integral Dehn surgeries on a link of finitely many unknots.

Congruence subgroups

There are a variety of congruence subgroups of $SL(2,\mathbb{Z})$, with various fascinating properties, and we list the most basic three of them as follows.

Definition For an integer $N \geq 1$, the *principal congruence subgroup* $\Gamma(N)$ is defined as

$$\Gamma(N) = \left\{ \begin{pmatrix} a & b \\ c & d \end{pmatrix} \in SL(2,\mathbb{Z}) \,\middle|\, a, d \equiv 1 \,(\mathrm{mod}\, N),\ b, c \equiv 0 \,(\mathrm{mod}\, 0) \right\}, \tag{1.34}$$

i.e., the kernel of the homomorphism $\pi_N : SL(2,\mathbb{Z}) \to SL(2,\mathbb{Z}_N)$ induced by the reduction modulo N homomorphism $\mathbb{Z} \to \mathbb{Z}_N$. The formula for computing its finite index inside $SL(2,\mathbb{Z})$ will be presented in (A.39).

Definition With the above definition, a subgroup of $SL(2,\mathbb{Z})$ is called a *congruence subgroup* of level n if there exists $N \geq 1$ such that it contains the principal congruence subgroup $\Gamma(N)$, and n is the smallest such N. The level

Definition One example of a congruence subgroup is the so-called *Hecke congruence subgroup* of level N, defined as

$$\Gamma_0(N) = \left\{ \begin{pmatrix} a & b \\ c & d \end{pmatrix} \in SL(2,\mathbb{Z}) \middle| \, c \equiv 0 \,(\mathrm{mod}\, N) \right\}, \tag{1.35}$$

and its index inside $Sl(2,\mathbb{Z})$ is given by

$$|SL(2,\mathbb{Z}) : \Gamma_0(N)| = n \prod_{p|N} \left(1 + \frac{1}{p}\right). \tag{1.36}$$

Notice that S and T^2 generate a congruence subgroup of $SL(2,\mathbb{Z})$, called the *theta subgroup*

$$\Gamma_\theta = \left\{ \begin{pmatrix} a & b \\ c & d \end{pmatrix} \in SL(2,\mathbb{Z}) \middle| ac \equiv bd \equiv 0 \,(\mathrm{mod}\, 2) \right\}, \tag{1.37}$$

and is isomorphic to the Hecke congruence subgroup $\Gamma_0(2)$ [30, 31].[5]

One may ask "are all finite-index subgroups of $SL(2,\mathbb{Z})$ congruence subgroups?" It was already known by Felix Klein that the answer is no, and actually The number c_N of congruence subgroups in $SL(2,\mathbb{Z})$ of level N satisfies $\log c_N = O\left((\log N)^2/\log\log N\right)$. However, the number a_N of finite index subgroups of index N in $SL(2,\mathbb{Z})$ satisfies $N \log N = O(\log a_N)$, so most subgroups of finite index must be non-congruence.

1.4 $\mathcal{N} = 4$ super Yang-Mills and Type IIB string theory

$\mathcal{N} = 4$ Super Yang-Mills (SYM) plays a central role in high energy theory and also in this thesis. In order to derive its action, we first review the 4d $\mathcal{N} = 1$ superspace formalism.

[5]It is easy to check that

$$\langle S, T^2 \rangle = \left\{ A \in SL(2,\mathbb{Z}) \middle| A \equiv \begin{pmatrix} 1 & 0 \\ 0 & 1 \end{pmatrix} \text{ or } \begin{pmatrix} 0 & 1 \\ 1 & 0 \end{pmatrix} \mod 2 \right\},$$

and the conjugation class

$$\Gamma_0(2) = \begin{pmatrix} 1 & 0 \\ 1 & 1 \end{pmatrix} \Lambda \begin{pmatrix} 1 & 0 \\ 1 & 1 \end{pmatrix}^{-1}.$$

4d $\mathcal{N}=1$ superspace

In this case, we add anticommuting right- and left-handed Weyl spinor coordinates θ_α and $\theta_{\dot\alpha}$ to $\mathbb{R}^4$ to form the *superspace* $\mathbb{R}^{4|4}$, parametrized by new coordinates $z^A=(x^\mu,\theta_\alpha,\theta_{\dot\alpha})$. Then the expansion of a general superfield $F(x,\theta,\bar\theta)$ in terms of θ and $\bar\theta$ in terms of θ and $\bar\theta$ truncates at $\theta^2\bar\theta^2$. One of its important features is that components of F do not transform under an irrep of the supersymmetry algebra, and we impose conditions to get $\mathcal{N}=1$ chiral multiplet and $\mathcal{N}=1$ vector multiplet.

Chiral multiplets

$\Phi(x,\theta,\bar\theta)$ is determined by the constraint $\bar{\mathcal{D}}_{\dot\alpha}\Phi(x,\theta,\bar\theta)=0$, where

$$\bar{\mathcal{D}}_{\dot\alpha}=-\frac{\partial}{\partial\bar\theta^{\dot\alpha}}-i\theta^\alpha\sigma^\mu_{\alpha\dot\alpha}\frac{\partial}{\partial x_\mu}. \tag{1.38}$$

To find its components, we introduce new coordinates $y^\mu_\pm=x^\mu\pm i\theta\sigma^\mu\bar\theta$, satisfying $\bar{\mathcal{D}}y^\mu_+=0$.

Because of $\bar{\mathcal{D}}\theta=0$, we can Taylor expand the chiral superfield as:

$$\begin{aligned}\Phi(x,\theta,\bar\theta)=&\phi(y_+)+\sqrt{2}\theta\psi(y_+)+\theta^2F(y_+)\\ =&\phi(x)+i\theta\sigma^\mu\bar\theta\partial_\mu\phi(x)+\frac{1}{4}\theta^2\bar\theta^2\partial_\rho\partial^\rho\phi(x)+\sqrt{2}\theta\psi(x)-\frac{i}{\sqrt{2}}\theta^2\partial_\mu\psi(x)\sigma^\mu\bar\theta+\theta^2F(x),\end{aligned} \tag{1.39}$$

where $\phi(x)$ is a complex scalar, ψ is a left-handed Weyl spinor, and F is an auxiliary complex scalar, viewed as a Lagrange multiplier. Note that the lack of y_- coordinate justifies the name *chiral representation*, with superderivatives on different footings:

$$\mathcal{D}_\alpha=\frac{\partial}{\partial\theta^\alpha}+2i\sigma^\mu_{\alpha\dot\alpha}\bar\theta^{\dot\alpha}\frac{\partial}{\partial y^\mu_+},\quad \bar{\mathcal{D}}_{\dot\alpha}=-\frac{\partial}{\partial\bar\theta^{\dot\alpha}}. \tag{1.40}$$

Certainly, the anti-chiral multiplet satisfies the condition $\mathcal{D}_\alpha\Phi^\dagger(x,\theta,\bar\theta)=0$. Like before, in terms of y_+ and $\bar\theta$, $\Phi^\dagger$ also admits an expansion which is long-winded in chiral representation but simple in *antichiral representation*.

Vector multiplets

The vector superfield is defined by the covariant reality condition $V(x,\theta,\bar\theta)=V^\dagger(x,\theta,\bar\theta)$, constraining its expression to be

$$\begin{aligned}V(x,\theta,\bar\theta)=&C(x)+i\theta\chi(x)-i\bar\theta\bar\chi(x)+\frac{i}{2}\theta^2\left(M(x)+iN(x)\right)-\frac{i}{2}\bar\theta^2\left(M(x)-iN(x)\right)-\theta\sigma^\mu\bar\theta A_\mu(x)\\ &+i\theta\bar\theta^2\left(\bar\lambda(x)+\frac{i}{2}\bar\sigma^\mu\partial_\mu\chi(x)\right)-i\bar\theta^2\theta\left(\lambda(x)+\frac{i}{2}\sigma^\mu\partial_\mu\chi(x)\right)+\frac{1}{2}\theta^2\bar\theta^2\left(D(x)+\frac{1}{2}\partial_\rho\partial^\rho C(x)\right),\end{aligned} \tag{1.41}$$

where C, M, N are complex scalars, A is the gauge field, $\chi, \bar{\chi}, \lambda, \bar{\lambda}$ are fermions, and D is an auxiliary field.

To simplify the above expansion, we resort to the the gauge transformation $V \to V + \Phi + \Phi^*$, where Φ is the chiral multiplet, so that $C = M = N = \chi = \bar{\chi} = 0$, i.e., the *Wess-Zumino guage*. Now the multiplet is

$$V_{WZ}(x, \theta, \bar{\theta}) = -\theta\sigma^\mu A_\mu(x) + i\theta^2\bar{\theta}(x) - i\bar{\theta}^2\theta\lambda(x) + \frac{1}{2}\theta^2\bar{\theta}^2 D(x). \tag{1.42}$$

The superfield V may be viewed as the supersymmetric generalization of the Yang–Mills potential, so the supersymmetric field strengths are the following gauge-invariant chiral and antichiral superfields:

$$W_\alpha = -\frac{1}{4}\bar{\mathcal{D}}^2\left(e^{-V}\mathcal{D}_\alpha e^V\right), \quad \bar{W}_{\dot{\alpha}} = -\frac{1}{4}\mathcal{D}^2\left(\bar{\mathcal{D}}_{e^V\dot{\alpha}} e^{-V}\right). \tag{1.43}$$

Field content of 4d $\mathcal{N} = 4$ SYM

In 4d spacetime, the maximal amount of supersymmetry with a particle multiplet representation of spin ≤ 1 is $\mathcal{N} = 4$, corresponding to 16 preserved Poincaré supercharges. Each supercharge $Q_{a\alpha}$, $Q_{a\dot{\alpha}}$ changes the spin it acts on by 1/2, so all massless states with helicities between -1 and 1 are generated by acting with no more than $\mathcal{N}_{max} = 4$ different supercharges. Theories with more supersymmetry generators involve a spin-2 field, i.e., graviton,

Since any multiplet has to include spin-1 particles, all the $\mathcal{N} = 4$ theories must be constructed only from the massless vector multiplet, which contains:

- One vector field A_μ, forming a singlet representation **1** of $SU(4)_R$;
- Four Weyl fermions λ^a_α, $a = 1, \ldots, 4$, forming a fundamental representation **4** of $SU(4)_R$;
- Six real scalars ϕ^i, $i = 1, \ldots, 6$, forming an antisymmetric representation **6** of $SU(4)_R$.

There are two ways to obtain the Lagrangian of $\mathcal{N} = 4$ SYM. Since $\mathcal{N} = 4$ supersymmetric field theory is automatically $\mathcal{N} = 1$, we can use $\mathcal{N} = 1$ superspace to write down the theory. Alternatively, it can also be obtained by reducing from its parent, the unique 10d $\mathcal{N} = 1$ SYM, with spin-1 as the highest spin state, down to 4d.

$\mathcal{N} = 4$ SYM from $\mathcal{N} = 1$ superspace

The 4d $\mathcal{N} = 1$ superspace formulation of the 4d $\mathcal{N} = 4$ SYM needs three chiral superfields $\Phi_i, i = 1, 2, 3$ and the vector superfield V with strength W_α. With the normalization $\mathrm{Tr}(T_a T_b) = \delta_{ab}$ on the Lie algebra, the unique 4d $\mathcal{N} = 4$ Lagrangian density is

$$\mathcal{L} = \mathrm{Tr}\left[\int d^4\theta \Phi^{i\dagger} e^V \Phi^i e^{-V} + \frac{1}{8\pi}\,\mathrm{Im}\left(\tau \int d^2\theta W_\alpha W^\alpha\right) + \left(i g_{YM}\frac{\sqrt{2}}{6}\int d^2\theta \epsilon_{ijk}\Phi^i\left[\Phi^j, \Phi^k\right] + \text{h.c.}\right)\right], \tag{1.44}$$

where τ is the complex coupling constant defined as

$$\tau = \frac{\theta}{2\pi} + i\frac{4\pi}{g_{YM}^2} \in \mathbb{C}, \tag{1.45}$$

which will be of our main interest in Chapter 5, and W_α is the chiral spinor field in (1.43).

Use the field content in Section 1.4 to write out the components of superfields[6], the above action gives

$$\begin{aligned}\mathcal{L} = \mathrm{Tr}\Bigg(& -\frac{1}{2g_{YM}^2}F_{\mu\nu}F^{\mu\nu} + \frac{\theta}{16\pi^2}F_{\mu\nu}\tilde{F}^{\mu\nu} - i\bar{\lambda}^a\bar{\sigma}^\mu D_\mu\lambda_a - \sum_i D_\mu\phi^i D^\mu\phi^i \\ & + g_{YM}\sum_{a,b,i} C_i^{ab}\lambda_a\left[\phi^i,\lambda_b\right] + g_{YM}\sum_{a,b,i}\bar{C}_{iab}\bar{\lambda}^a\left[\phi^i,\bar{\lambda}^b\right] + \frac{g_{YM}^2}{2}\sum_{i,j}\left[\phi^i,\phi^j\right]^2\Bigg),\end{aligned} \tag{1.47}$$

where

$$F_{\mu\nu} = \partial_\mu A_\nu - \partial_\nu A_\mu + i\left[A_\mu, A_\nu\right] \tag{1.48}$$

is the usual non-abelian field strength, and D_μ is the covariant derivative acting on fields in adjoint representation by $D_\mu\cdot = \partial_\mu\cdot + i\left[A_\mu,\cdot\right]$. Moreover, $\tilde{F}_{\mu\nu} = \frac{1}{2}\epsilon_{\mu\nu\lambda}F^{\lambda\rho}$ is the Hodge dual, and $C^{ab}{}_i$ are Clebsh-Gordon coefficients combining two **4** representations into one **6** representation of $su(4)_R$.

Since the coupling constant is dimensionless and all fields are massless, the action of $\mathcal{N}=4$ SYM theory is scale invariant on the classical level. Remarkably, the scale invariance survives after quantization, due to its UV finiteness (finite instanton corrections) and its β-function vanishes to all orders in pertubation theory. In fact, it is a *superconformal* field theory (SCFT), but we will not go into its details.

$\mathcal{N}=4$ SYM from a dimensional reduction of 10d

We start from the 10d $\mathcal{N}=1$ Langrangian density

$$\mathcal{L} = \mathrm{Tr}\left(-\frac{1}{2}F_{mn}F^{mn} + \frac{i}{2}\bar{\Psi}\Gamma^m D_m\Psi\right), \tag{1.49}$$

where Γ^m are 10d Dirac matrices, F_{mn} is the field strength $F_{mn} = \partial_m A_n - \partial_n A_m + ig\left[A_m, A_n\right]$, and Ψ is a Majorana-Weyl spinor with 16 real components.[7] Both F_{mn} and Ψ both transform

[6] Expansion for W_α and $\bar{W}_{\dot\alpha}$ are given by

$$\begin{aligned} W_\alpha &= -i\lambda_\alpha(y_-) + \left[\delta_\alpha{}^\beta D(y_-) - \frac{i}{2}(\sigma^\mu\bar{\sigma}_\alpha^{\nu\beta})F_{\mu\nu}(y_-)\right]\theta_\beta + \theta^2\sigma^\mu_{\alpha\dot\alpha}\partial_\mu\bar{\lambda}^{\dot\alpha}(y_-), \\ \bar{W}_\alpha &= i\bar{\lambda}_{\dot\alpha}(y_+) + \left[\epsilon_{\dot\alpha\dot\beta}D(y_+) + \frac{i}{2}\epsilon_{\dot\alpha\dot\gamma}\left(\bar{\sigma}^\mu\sigma^\nu\right)_{\dot\beta}F_{\mu\nu}(y_+)\right]\bar{\theta}^{\dot\beta} - \epsilon_{\dot\alpha\dot\beta}\bar{\theta}^2\bar{\sigma}^{\mu\dot\beta\dot\alpha}\partial_\mu\lambda_\alpha(y_+).\end{aligned} \tag{1.46}$$

[7] The only other Majorana-Weyl spinor is in 2d spacetime, with a 1d real representation.

in the adjoint representation of the gauge group and thus the covariant derivative is

$$D_m\Psi = \partial_m\Psi + ig\,[A_m, \Psi]\,. \tag{1.50}$$

To perform a Kaluza-Klein reduction on a 6d torus T^6, we bipartite the index m into $\mu = 0, 1, 2, 3$ and $i = 1, \ldots, 6$. Firstly the 10d gauge field $A = A_m dx^m$ decomposes into a 4d gauge field with components A_μ and scalars ϕ_i which are the last six components of the 10d gauge field:

$$A_m = (A_\mu(x^\nu), \phi_i(x^\nu))\,. \tag{1.51}$$

We also assume that the fields A_μ and ϕ_i depend only on the first four coordinates x_μ, and are independent of the remaining coordinates. Note that ϕ_i transform trivially under a Lorentz transformation of the 4d coordinates x_μ and thus is a real scalar field in 4d while A_μ transforms as a vector. We find out gauge field strength:

$$F_{\mu i} = \partial_\mu\phi_i + ig[A_\mu, \phi_i] = D_\mu\phi_i, \quad F_{ij} = ig[\phi_i, \phi_j], \tag{1.52}$$

where D_μ is the 4d covariant derivative in (1.47).

The next step is to repeat the dimensional reduction above for the kinetic term $i\bar{\Psi}\Gamma^m D_m\Psi$ for the Majorana-Weyl spinor Ψ on T^6, where we decompose Γ^m into 4d Dirac matrices γ^μ and gamma matrices $\hat{\gamma}^i$ on T^6. It is not hard to show that we recover the 4d $\mathcal{N} = 4$ SYM action.

$\mathcal{N} = 4$ SYM as a worldvolume theory of D3-branes

In string theory, D-branes are higher-dimensional objects on which open strings can end. Perturbatively, this point of view is only reliable if the coupling constant for both open and closed strings is small, i.e., $g_s \ll 1$. Moreover, if we ignore massive string excitations of energy scale $\sim \sqrt{\alpha'}$, the dynamics of the open strings is described by a supersymmetric gauge theory living on the worldvolume of the D-branes. Massless closed string states give rise to 10d $\mathcal{N} = 1$ supergravity multiplet, while massless open string states form a 4d $\mathcal{N} = 4$ supermultiplet consisted of a gauge field A_μ, six real scalars ϕ_1 and their fermionic partners. Considering the rotation of worldvolume of D3-branes, A_μ correspond to open string excitations parallel to the D-branes while open string excitations transverse to the D-branes are scalar fields seen from the worldvolume.

The gauge group of the low-energy worldvolume theory is determined by Chan-Paton factors, *non-dynamical* degrees of freedom assigned to the endpoints of open strings connecting the various coincident D-branes. For example, the Chan-Paton factor λ_{ij} labels strings stretching between brane i and brane j, with $i, j = 1, \ldots, N$. The resultant matrix λ is an element of $u(N)$, the unique Lie algebra consistent with scattering amplitudes of *oriented* open strings, where N is the number of coincident D-branes. Therefore λ_{ij} can be chosen to be the entries of a Hermitian matrix. Although the Chan-Paton factors are global symmetries of the worldsheet action, the symmetry turns out to be local in the target

spacetime. Open strings ending on coincident D-branes can effectively be described by a non-Abelian gauge theory. More generally, *unoriented* strings are constructed by imposing the worldsheet parity transformation Ω:

$$\Omega : \sigma \to \sigma_0 - \sigma, \tag{1.53}$$

where $\sigma_0 = 2\pi$ for closed strings and $\sigma_0 = \pi$ for open strings. This transformation is a global symmetry, and can be viewed as an O-plane. With its presence, the low-energy gauge theory can have gauge group $SO(N)$ or $USp(N)$.

Now we study the low-energy *dynamics*, starting from the effective action for all massless string modes

$$S = S_{\text{closed}} + S_{\text{open}} + S_{\text{int}}, \tag{1.54}$$

where S_{int} is the interaction between open and closed strings, and S_{closed} is the action of 10d supergravity with higher derivative terms. S_{int} and S_{open} can be drived from Dirac-Born-Infeld (DBI) action and Wess-Zumino term. For simplicity, we first deal with one single D3-brane, whose worldvolume fields are bosonic coordinates $x^\mu, \mu = 0, \dots, 3$, while the six transverse directions have coordinates $x^i, i = 4, \dots, 9$ so that it is related to the six scalars by $x^{i+3} = 2\pi\alpha'\phi^i$. Now the pullback of the spacetime metric g_{MN} to the worldvolume under the embedding ϕ is

$$\phi^*(g_{MN}) = g_{\mu\nu} + 2\pi\alpha' \left(g_{i+3,\nu}\partial_\mu\phi^i + g_{\nu,j+3}\partial_\nu\phi^i\right) + (2\pi\alpha')^2 g_{i+3,j+3}\partial_\mu\phi^i\partial_\nu\phi^j, \tag{1.55}$$

which leads to the DBI action with a vanishing Kalb-Ramond field B_{MN}:

$$S_{DBI} = -\frac{1}{(2\pi)^3\alpha'^2 g_s}\int d^4x e^{-\phi}\sqrt{-\det\left[\phi^*(g_{MN}) + 2\pi\alpha' F\right]}. \tag{1.56}$$

Expanding $e^{-\phi}$ and $g_{MN} \approx \eta_{MN} + \kappa h_{MN}$, where h_{MN} is the metric fluctuation and[8] $\kappa = 8\pi^{7/2}\alpha'^2 g_s$, to leading order in α' we have

$$S_{\text{open}} = -\frac{1}{2\pi g_s}\int d^4x \left(\frac{1}{4}F^{\mu\nu} + \frac{1}{2}\eta^{\mu\nu}\partial^i_\mu\phi^i\partial_\nu\phi^i + \dots\right) \tag{1.58}$$

$$S_{\text{int}} = -\frac{1}{8\pi g_s}\int d^4x \left(\phi F^{\mu\nu}F_{\mu\nu} + \dots\right), \tag{1.59}$$

where dots represent terms of higher order in α'.

[8] κ is this value to make the kinetic term of h in the closed string action canonically normalized

$$\begin{aligned} S_{\text{closed}} =& \frac{1}{2\kappa^2}\int d^{10}\sqrt{-g}e^{-2\phi}\left(R + 4\partial_M\phi\partial^M\phi\right) + \dots \\ \sim& -\frac{1}{2}\int d^{10}x\partial_M h\partial^M h + \mathcal{O}(\kappa). \end{aligned} \tag{1.57}$$

In the case of N *coincident* D-branes, open strings between different branes are massless, and the effective coupling constant is gsN so the open string picture is valid for $gsN \ll 1$. To generalize the previous analysis, scalars and gauge fields are now valued in the adjoint representation of the gauge group $U(N)$: $\phi^i = \phi^{ia}T_a, A_\mu = A^a_\mu T_a$. After taking the trace to ensure gauge invariance, the gauge kinetic term is now $F^a_{\mu\nu}F^{a\mu\nu}$. We also need to replace the usual partial derivatives by covariant derivatives, and to leading order in α' we add to S_{open} a scalar potential

$$V = \frac{1}{2\pi g_s}\sum_{i,j}\text{Tr}\left[\phi^i,\phi^j\right]^2. \tag{1.60}$$

It is clear that in the limit $\alpha' \to 0$, the terms survived in S_{open} are the bosonic part of the action of $\mathcal{N}=4$ SYM with the identification

$$2\pi g_s = g^2_{YM}. \tag{1.61}$$

S_{int} is also zero in this limit, meaning that open and closed strings decouple. However, this limit is naïve as the following. If we pull out one D3-branes from the stack by a distance r in direction $i = 4,\ldots,9$, and consider only massless modes, this system is described by a $U(N-1)\times U(1)$ gauge theory rather than a $U(N)$ theory, i.e., the system is in a Higgs phase with vacuum expectation value (VEV) $\langle\phi^i\rangle = r/(2\pi\alpha')$. In the previous decoupling limit $\alpha' \to 0$, all field theory quantities need to be fixed, so in the correct limit called *Maldacena limit*, the ratio r/α' is fixed upon $\alpha' \to 0$.

Finally, by analyzing the closed string sector perspective of the same coincident D3-branes, we will get the celebrated Maldacena duality [32, 33], but we do not pursue it here because in this thesis we only study non-supersymmetric quantum gravity and the purely field-theoretc aspects of 4d $\mathcal{N}=4$ SYM, not any supergravity.

1.5 6d $(2,0)$ SCFT

This theory can facilitate understanding our double-Janus configuration in Chapter 5, and has a unique place in high energy theory: 6d is the highest dimension where a superconformal field theory (SCFT) can exist [34]. Those SCFTs are very exotic: for example, $(1,0)$ and $(2,0)$ theories have no Langrangian descriptions. In order to appreciate this point, we need to look at their field contents. First recall that a theory is said to have $\mathcal{N}=(n_l,n_r)$ supersymmetry when it has n_l chiral and n_r antichiral supersymmetries. The R-symmetry group of such a theory is $Sp(n_l)\times Sp(n_r)$. In 6d, a theory with a minimal amount of supersymmetry is then denoted as $\mathcal{N}=(1,0)$; it has 8 supercharges and a R-symmetry of $Sp(1)\simeq SU(2)$. The massless content of such a theory at low energy, and at a generic point on the moduli space, may include a combination of:

- A tensor multiplet, which contains a self-dual two-form $B_{[\mu\nu]}$, one left-handed Majorana spinor, and a single real scalar ϕ, whose VEV $\langle\phi\rangle$ parametrizes a tensor branch of the theory;

- Some number of vector multiplets contain a gauge field A_μ and a right-handed Weyl spinor field. Note that there is no scalar to parametrize the Coulomb branch of a $(1,0)$ theory as in more familiar gauge theories, so we refer to a nonzero VEV of a tensor multiplet as the "Coulomb branch" in 6d;
- A hypermultiplet contains a left-handed Weyl spinor and four real scalars ϕ_i, whose VEV's $\langle\phi_i\rangle$ parametrize the Higgs branch of the theory.

To consider 6d SCFTs with more supersymmetries and without gravity, the only two options are $\mathcal{N}=(1,1)$ and $\mathcal{N}=(2,0)$. First let us examine the field content of the former one. The only multiplet there is a $\mathcal{N}=(1,1)$ vector multiplet, which is made up of a $\mathcal{N}=(1,0)$ vector multiplet and hypermultiplet. Therefore, the $\mathcal{N}=(1,1)$ multiplet contains in the bosonic sector one vector field A_μ and four real scalars ϕ_i, for a total of $4+4=8$ degrees of freedom. The fermionic sector contains one Dirac spinor, that is to say one left-handed Weyl spinor and one right-handed Weyl spinor, for a total of $4+4=8$ degrees of freedom, agreeing with the bosonic amount. The R-symmetry is $Sp(1)\times Sp(1)\simeq Spin(4)$. Each spinor is a doublet under one of the two $Sp(1)$ groups, and the scalars transform under the $Spin(4)$ symmetry. The Lagrangian for this maximally supersymmetric theory is

$$S=\int d^6x\frac{1}{g_{6d}^2}F^a_{\mu\nu}F^{a\mu\nu}+\dots \tag{1.62}$$

where dots represents fermionic terms dictated by supersymmetry, and they have the same meaning in the rest of this section. It is IR-free, and since its coupling has mass dimension $[g_{6d}^2]=(\text{length})^2$, it is non-renormalizable.

The similar analysis for the $\mathcal{N}=(2,0)$ theory is much more interesting. The basic multiplet is no longer a vector multiplet, but an $\mathcal{N}=(2,0)$ tensor multiplet, made up of an $\mathcal{N}=(1,0)$ tensor multiplet and hypermultiplet. The bosonic sector now contains a self-dual two-form $B_{[\mu,\nu]}$ and five real scalars ϕ_i, for a total of $3+5=8$ degrees of freedom. The fermionic sector contains two left-handed Weyl spinors, again giving $4\times 2=8$ degrees of freedom. The R-symmetry is $Sp(2)\simeq Spin(5)$. The group $Sp(2)$ acts non-trivially on the fermions, while $Spin(5)$ rotates the scalars. The presence of the tensor $B_{[\mu,\nu]}$ is unusual in QFT, because it implies that some of the degrees of freedom of the $\mathcal{N}=(2,0)$ theory are described by nonlocal strings instead of the usual particles in QFT. The strings couple to the 2-form field via the coupling:

$$q\int_\Sigma B_{\mu\nu}d\sigma^{\mu\nu}+\dots, \tag{1.63}$$

where q is a charge, $d\sigma^{\mu\nu}$ is the area element of the string worldsheet. The strings in $(2,0)$ become tensionless because any scale has to vanish at the superconformal point. However, we can no longer mimic (1.62) to write down an action

$$S=\int d^6x\frac{1}{g_{6d}^2}F^a_{\mu\nu\rho}F^{a\mu\nu\rho}+\dots \tag{1.64}$$

where $F_{\mu\nu\rho} = \partial_{[\mu} B_{\nu\rho]}$, because the self-duality[9] of the tensor multiplet implies that the Hodge dual $F_{\mu\nu\rho} = \frac{1}{6}\epsilon^{\lambda\sigma\tau}_{\mu\nu\rho} F_{\lambda\sigma\tau}$, meaning that the tensor kinetic term in (1.64) vanishes. It turns out that the Lagrangian exists for a free (2,0) theory provided that $g_{6d}^2 = 1$, but it is impossible to study the interacting theory perturbatively.

6d $(2,0)$ from string theory and M-theory

The 6d $\mathcal{N} = (2,0)$ SCFT was discovered by Witten [35], when studying the Type IIB string compactified on K3 surfaces. To understand the type IIB side, we first study the Type IIA theory on the $\mathbb{R}^6 \times$K3 background, which is equivalent to the heterotic string on $\mathbb{R}^6 \times T^4$ by a string/string duality, from which enhanced gauge symmetry was found at certain singularities on the moduli space of K3 surfaces. The enhanced gauge symmetry means that extra string bound states emerge as gauge bosons at these singularities[10], which are locally $\mathbb{C}^2/\Gamma$ for some discrete subgroups Γ of $SU(2)$, allowing for an ADE classification.

However, because the Type IIB is chiral, it cannot admit the gauge multiplet introduced in Section 1.4, and there are no extra gauge bosons at those sigularities. Witten pointed out that the T-duality between Type IIA and Type IIB solves the apparant paradox. We can further compactify the Type IIA string on $\mathbb{R}^5 \times S^1 \times$ K3. Via T-duality, we could obtain an equivalent Type IIB theory on $\mathbb{R}^5 \times \tilde{S}^1 \times$ K3. Now we have particles in $\mathbb{R}^5$ for both configurations. In Type IIA, the enhanced gauge symmetry creates a new guage boson with mass $m \propto 1/\lambda_A$, where λ_A is the Type IIA string coupling. T-duality then implies that the Type IIB string obtains a massive gauge boson with $M \approx R_B/\lambda_B$ where R_B is the radius of $\tilde{S}^1$. If we then decompactify the Type IIB string from $\tilde{S}^1$, in $\mathbb{R}^6$ we will get a non-critical string, with a tension $T \propto 1/\lambda_B$. The dynamics of this non-critical string, which is anti-self-dual, couples to the 2-form field $B_{\mu\nu}$ with anti-self-dual field strength in the tensor multiplet, but does not couple to the 2-form field with self-dual field strength in the Type IIB supergravity multiplet, and it is hence described by the $(2,0)$ theory.

Later, Strominger [36] drew the connection between the 6d $(2,0)$ theory and the world-volume theory of multiple coincident M5-branes, on which M2-branes can end.[11] This configuration is the M-theoretic lift of the fundamental strings ending on the D4-brane in Type IIA string theory. M2-brane could be considered as a non-critical string in the M5-brane worldvolume, which is also described by the $(2,0)$ theory associated to the self-dual non-critical Type IIB string on K3. Strominger further showed that when two M5-branes are close to each other, this $(2,0)$ theory decouples from gravity and obtains the superconformal invariance, serving as a stepping stone for understanding the full M5-brane dynamics. On

[9] Self-dual QFTs really are exceptional objects in the moduli space of theories, just like sporadic groups, manifolds with exceptional holonomies, Platonic solids, and octonians in mathematics.

[10] A similar gauge symmetry enhancement appears at the T-duality critical radius $R = \sqrt{\alpha'}$, where α' is the string coupling constant.

[11] The low-energy effective theory of M-theory is the 11d supergravity theory, containing a 3-form gauge field C, under which two half-Bogomol'nyi–Prasad–Sommerfield (BPS) states, M5-branes and M2-branes, are magnetically and electically charged, respectively. They are electromagnetic duals of each other.

the other hand, the holographic dual of 6d $(2,0)$ has been proposed to be the M-theory on $AdS_7 \times S^4$ in Maldacena's original paper [32].

Starting from this connection with M5-brane worldvolume action, one can make great use of the $(2,0)$ theory to study difficult problems in lower-dimensional QFTs. Like in [35], when the 6d $(2,0)$ theory is toroidally compactified down to 4d, we get the $\mathcal{N}=4$ SYM theory. The modular transformation of the microscopic T^2 implies the S-duality of 4d theory [37]. Moreover, several correspondences have been constructed between lower-dimensional field theories from the compactifications of the 6d $(2,0)$ theory, e.g., the well-known AGT correspondence [38], the 3d-3d correspondence [39], and the more recent VOA$[M_4]$, a 2d $\mathcal{N}=(2,0)$ theory [40]. Finally, outside of high-energy theory, it also makes connections with condensed matter physics due to emergent fractional charges similar to the fractional quantum Hall effect (FQHE) [41].

1.6 Outline of the thesis

The rest of this thesis is organized as follows:

In Chapter 2, we study the Bekenstein-Hawking entropy of a two-sided BTZ black hole in Euclidean signature as a topological entanglement entropy. The entire spacetime has a torus asymptotic boundary. The definition of the monster double states depend on the asymptotic expansion of the Klein's J-function.

In Chapter 3, we study the Euclidean AdS/CFT dual with a boundary as a Riemann surface with an arbitrary genus, and mathematically rigorously proved that the only possible CFT dual to a with central charge smaller than 1, i.e., at strong coupling limit, is the Ising minimal model. We encounter a special index-3840 subgroup Γ_c in studying 3d pure gravity in AdS_3 with genus-two asymptotic boundary. Whether is it a congruence subgroup or not deserves a future study.

In Chapter 4, we study a discrete version of holography, in which the bulk spacetime is replaced by a Bruhat-Tits tree, representing the local number field $\mathbb{Q}_p$. We discovered some subtle relations between the representation theory of $\mathbb{Q}_p$ and Chebyshev polynomials, and a new class of eigenfunctions of Laplacian on the Burhat-Tits tree, among many other physical results.

In Chapter 5, we switch gears to investigate the concept of reciprocity. Reciprocity is a pivotal concept in number theory with a long history, dating back to Lagrange and Gauss in the 18th and 19th centuries. We present a purely physical derivation of these classic formulae from $\mathcal{N}=4$ SYM theory, abelian Chern-Simons theory and Type IIB string theory.

Chapter 2

Topological entanglement entropy in Euclidean AdS_3 via surgery

2.1 Introduction

Topological entanglement entropy (TEE), first introduced in condensed matter physics [17, 18], has been widely used to characterize topological phases. It is the constant subleading term (relative to the area-law term) in the entanglement entropy, only dependent on universal data of the corresponding topological phase.

At low energy, a large class of topological phases can be effectively described using Chern-Simons gauge theory with a compact, simple, simply-connected gauge group. When this is the case, TEE can be found using surgery [42] and replica trick [8] by computing the partition function on certain 3-manifolds. For compact gauge groups, TEE is expressed [42] in terms of modular S matrices of Wess-Zumino-Witten (WZW) rational conformal field theory (RCFT) on a compact Riemann surface, following the CS/WZW correspondence first described in geometric quantization by [25].

In three-dimensional spacetime, gravity can be classically described by Chern-Simons gauge theory with a non-compact, possibly complex gauge group [2, 43]. Specifically, in Euclidean picture with a negative cosmological constant $\Lambda = -1/l^2 < 0$, in the first-order formulation of general relativity, the spin connection ω combines with the "vierbein" e to make the holomorphic Chern-Simons gauge field $\omega + e/l$ and anti-holomorphic gauge field $\omega - e/l$ of gauge group $SL(2, \mathbb{C})$, where l is the AdS_3 curvature radius. The following questions thus arise naturally: is there a similar notion of TEE in 3d gravity? If so, can one compute the TEE for 3d gravity using surgery? Is the TEE related to modular S matrices of a CFT living on the conformal boundary? In [44], the authors proposed that the Bekenstein-Hawking entropy of a BTZ black hole [45, 46] in AdS_3 can be interpreted as TEE. The argument is supported by calculations using continuous and noncompact modular $\mathcal{S}$-matrices [47] in the possible dual Liouville CFT [48, 49, 50]. Unfortunately it is still not clear what is the meaning of this entanglement entropy, i.e., what are the two subregions or

components that are entangled together.

We are motivated by these questions to calculate TEE via 3d surgery in an Euclidean spacetime that is asymptotically AdS$_3$. In the case of thermal AdS$_3$, the constant time slice is a disk. We first bipartite this disk into two disks as shown in Figure 2.1, where a denotes the ratio between the interval length on the boundary circle that is contained in subregion A and the circumference of the full circle. After applying the replica trick, the glued manifold is a genus-n handlebody. Using one-loop partition function on this handlebody [51, 52, 53, 5, 54, 55], we derive an explicit expression for TEE, which vanishes in the low-temperature limit. Then we consider two disjoint thermal AdS$_3$'s and calculate the TEE between them,

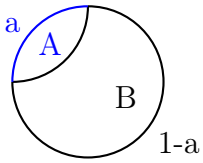

Figure 2.1: Bipartition of constant time slice of thermal AdS$_3$.

which turns out to be the thermal entropy of one thermal AdS$_3$. However, this does not mean any nontrivial entanglement between the two solid tori, and we support this argument by calculating the mutual information between them, which gives zero.

We also compute TEEs in an eternal BTZ background. In the Euclidean picture there is only one asymptotic region for the eternal BTZ black hole [56], which corresponds to the gluing of the two asymptotic regions of the two single-sided black holes in the Lorentzian picture. We show that TEE between the two single-sided black holes is equal to the Bekenstein-Hawking entropy of one single-sided black hole. The mutual information between them does not vanish and again equals to the Bekenstein-Hawking entropy, which guarantees the explanation of the result as supporting the ER=EPR conjecture in 3d bulk to be true [57, 58, 59].

Focusing on one single-sided black hole, we then derive an Entangling-Thermal relation, stating

$$\lim_{\text{Area}(\bar{A})\to 0}[S(A)-S(\bar{A})]=S_{BTZ}^{\text{thermal}}, \tag{2.1}$$

where A and $\bar{A}$ denotes the two complementary subregions. Quantities on both sides of this equation are intrinsically three-dimensional. The underlying physical reason of this relation is that, subregion A wraps the non-contractible loop of the constant time slice, while its complement $\bar{A}$ does not. The difference between S_A and $S_{\bar{A}}$ thus detects the effect of the non-contractible loop, which is exactly the outer horizon of the BTZ black hole. This relation is similar to but different from the thermal entropy relation [60] derived from the Ryu-Takayanagi formula [15], in that our result is topological and does not depend on geometrical details.

The full modular-invariant genus one partition function of three-dimensional pure gravity is a summation of classical geometries or gravitational instantons, which includes both

thermal AdS$_3$ and the BTZ black hole. At high temperatures, the full partition function is dominated by the $SL(2,\mathbb{Z})$ family of black hole solutions, whereas the low-temperature solution is dominated by the thermal AdS$_3$. We compute TEE for the full partition function with a bipartition between the two single-sided black holes in the high temperature regime and again observe ER=EPR explicitly. When Chern-Simons level $k_R = k_L = l/16G = 1$, after defining the quantum dimension data on the boundary Monster CFT with orbifolding, we see from the TEE calculation that the black hole geometries correspond to a topological phase in the bulk which contains a maximally-entangled superposition of 194 types of "anyons", labeled by the irreducible representations of the Monster group. This state, dubbed as *Moonshine double state*, has the similar property as the thermofield double state on the asymptotic boundary in that TEE between the anyon pairs is equal to the Bekenstein-Hawking entropy.

The rest of the chapter is organized as follows. In Section 2.2 we give a minimal introduction to the knowledge that facilitates the TEE calculation, including replica trick and Schottky uniformization. In Section 2.3 we show the calculation of TEE in thermal AdS$_3$, which amounts to the computation of the partition function on a genus n-handlebody. We also compute the TEE between two disjoint thermal AdS$_3$ and show their mutual information vanishes. Section 2.4 illustrates the TEE calculation for BTZ black holes for several different bipartitions. We discuss the relations with ER=EPR and show that mutual information between the two single-sided black holes is equal to the Bekenstein-Hawking entropy. We further propose an Entangling-Thermal relation for single-sided black holes. Then in Section 2.5 we demonstrate the TEE of the full modular-invariant partition function after summing over geometries and present the quantum dimension interpretation. The system is mapped to a superposition of 194 types of "anyons". Comments on the implication of TEE on the Hawking-Page transition and the outlook can be found in Section 2.6.

2.2 Review of relevant components

In this section we will introduce basic concepts that are essential to understanding the rest of the chapter.

"Surgery" and Replica Trick

Surgery was originally invented by Milnor [61] to study and classify manifolds of dimension greater than three.[1]. In this work we use this concept in a broader sense, i.e., as a collection of techniques used to produce a new finite-dimensional manifold from an existing one in a controlled way. Specifically, it refers to cutting out parts of a manifold and replacing it by a part of another manifold, matching up along the cut.

As a warm-up, we review the usage of surgery in the entanglement calculation of 2d CFT for a single interval at finite temperature $T = 1/\beta$ [8]. The interval A lies on an infinitely long line whose thermal density matrix is denoted as ρ. The reduced density matrix of

[1]For 3-manifolds, there are famous variants such as (hyperbolic) Dehn surgery [24].

subregion A is then defined as $\rho_A = \mathrm{tr}_{\bar{A}}\rho$, where the trace $\mathrm{tr}_{\bar{A}}$ over the complement of A only glues together points that are not in A, while an open cut is left along A. Entanglement entropy between A and its complement $\bar{A}$ is then $S_A = -\mathrm{tr}\rho_A \ln \rho_A$. The matrix logarithm is generally hard to compute, so alternatively one applies the replica trick to obtain an equivalent expression, with proper normalization (so that the resultant quantity is 1 when being analytically continued to $n = 1$):

$$S(A) = -\frac{d}{dn}\left(\frac{\mathrm{tr}(\rho_A^n)}{(\mathrm{tr}\rho_A)^n}\right)\Bigg|_{n=1}. \tag{2.2}$$

Now the problem reduces to the computation of $\mathrm{tr}(\rho_A^n)$. Using surgery, one can interpret it as the path integral on the glued 2-manifold [62]. An example for $n = 3$ is shown in Figure 2.2, where the left panel sketches ρ_A^3, and the right panel is $\mathrm{tr}(\rho_A^3)$. In this case with a finite temperature, S_A is not necessarily equal to $S_{\bar{A}}$.

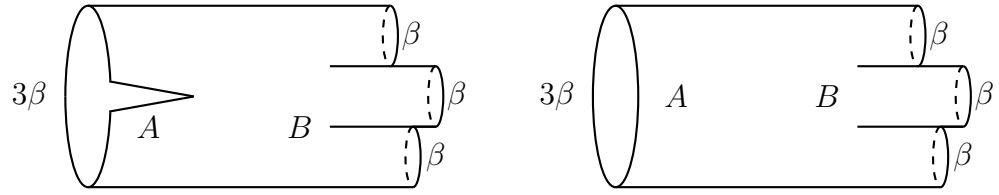

Figure 2.2: Left: Sketch of ρ_A^3. Right: Sketch of $\mathrm{tr}\rho_A^3$

This operation can be extended to 3-manifolds in a straightforward way, as shown in [42]. The authors calculated examples where the constant time slices are closed surfaces and restricted to ground states, so that the β cycle is infinitely long.

The constant time slices that we are interested in for Euclidean AdS$_3$ are all open surfaces with asymptotic conformal boundaries, and the quantum states do not necessarily belong to the ground state Hilbert subspace. Details will be presented in Sections 2.3 and 2.4.

Conformal Boundary and $\mathbb{H}^3/\Gamma$

We now introduces the hyperbolic three-space $\mathbb{H}^3$ that describes the Euclidean AdS$_3$. It is the 3d analogue of hyperbolic plane, with the standard Poincare-like metric

$$ds^2 = \frac{dy^2 + dzd\bar{z}}{y^2}, \tag{2.3}$$

where $y > 0$ and z is a complex coordinate.

Any 3-manifold M having a genus n Riemann surface Σ_n as its conformal boundary that permits a complete metric of constant negative curvature can be constructed using Schottky uniformization. The idea is to represent the 3-manifold M as the quotient of $\mathbb{H}^3$ by a Kleinian

group Γ [63], which is a discrete subgroup of $SL(2,\mathbb{C})$ as well as a discrete group of conformal automorphisms of Σ_n.

The conformal boundary of $\mathbb{H}^3$ is a sphere at infinity, S^2_∞, on which Γ acts discretely, except for a *limit set* of accumulation points of Γ denoted by $\Lambda(\Gamma)$. The complement $\Omega(\Gamma) = S^2_\infty - \Lambda(\Gamma)$ is called the domain of discontinuity. Then the 3-manifold M has boundary $\Omega(\Gamma)/\Gamma$, a well-defined quotient.

In particular, when M is a handlebody, Γ reduces to a Schottky group, which is freely finitely generated by the *loxodromic* elements[2] $\gamma_1, \ldots, \gamma_n \in SL(2,\mathbb{C})$, that acts on S^2_∞ as a fractional linear transformation. Among these generators, there are $3n-3$ independent complex parameters, which are coordinates on the Schottky space, a covering space of the complex moduli of the Riemann surface.

Each $\gamma \in \Gamma$ is completely characterized by its fixed points and its multiplier q_γ. An eigenvalue q_γ is defined through the unique conjugation of γ under $SL(2,\mathbb{C})$: $z \mapsto q_\gamma z$ with $|q_\gamma| < 1$. More explicitly, denoting η, ξ as the fixed points of γ, one has

$$\frac{\gamma(z)-\eta}{\gamma(z)-\xi} = q_\gamma \frac{z-\eta}{z-\xi}. \tag{2.4}$$

Within the Schottky group Γ, there are primitive conjugacy classes $\langle \gamma_1, \ldots, \gamma_n \rangle$ of Γ, with "primitive" meaning that γ is not a positive power of any other element in Γ.

Solid Tori Classified as $M_{c,d}$

The physical spacetimes we are concerned about in this chapter are all solid tori, i.e., the $n = 1$ case in the previous subsection. They have toroidal conformal boundaries, so the Schottky group actions is relatively simple.

After these topological constructions, we can further classify them into the $M_{c,d}$ family according to their geometries. This family first appeared in the discussion of classical gravitational instantons which dominate the path integral in [64], and is further explained in [5] and [65].

In this case, $\Lambda(\Omega)$ composes of the north and south poles of S^2_∞. Since solid tori have boundaries $T^2 \cong \Omega(\Gamma)/\Gamma$, $\pi_1(\Omega(\Gamma))$ must be a subgroup of $\pi_1(T^2)$, so $\pi_1(\Omega(\Gamma))$ can only be isomorphic to $\mathbb{Z}\oplus\mathbb{Z}$, $\mathbb{Z}$, or the trivial group. When $\pi_1(\Omega(\Gamma)) = \mathbb{Z}\oplus\mathbb{Z}$, $\Omega(\Gamma)$ has to be a Riemann surface of genus 1, which cannot be isomorphic to an open subset of S^2_∞. When $\pi_1(\Omega(\Gamma))$ is trivial, $\Omega(\Gamma)$ is a simply-connected universal cover of T^2, so that Γ has to be $\mathbb{Z}\oplus\mathbb{Z}$. It is easily seen from (2.3) that if $\Gamma \cong \mathbb{Z}\oplus\mathbb{Z}$, then although $\mathbb{H}^3/(\mathbb{Z}\oplus\mathbb{Z})$ has a toroidal boundary at $y = 0$, there is a cusp at $y \to \infty$, whose sub-Plackian length scale invalidates semi-classical treatments.

The only possibility is thus $\pi_1(\Omega(\Gamma)) = \mathbb{Z}$, where Γ can be either $\mathbb{Z}$ or $\mathbb{Z}\oplus\mathbb{Z}_n$. The latter yields M to be a $\mathbb{Z}_n$-orbifold, indicating the existence of massive particles, which are not allowed in pure gravity. To avoid undesirable geometries such as cusps and orbifolds in the

[2]They are of the form (2.5).

contributions to path integral [54, 5], we restrict our Schottky group to be $\Gamma \cong \mathbb{Z}$, generated by the matrix

$$W = \begin{pmatrix} q & 0 \\ 0 & q^{-1} \end{pmatrix} \tag{2.5}$$

where $|q| < 1$.

The boundary torus is thus obtained by quotiening the complex z-plane without the origin by $\mathbb{Z}$. Redefine $z = e^{2\pi i\omega}$, so ω is defined up to $\omega \to \omega + 1$, and W acts by $\omega \to \omega + \ln q/2\pi i$. Hence, the complex modulus of the torus is $\tau \equiv \ln q/2\pi i$, defined up to a $PSL(2,\mathbb{Z})$ Möbius transformation $\tau \sim (a\tau + b)/(c\tau + d)$, where integers a, b, c, d satisfy $ad - bc = 1$.

When constructing a solid torus from its boundary torus, τ is defined only up to $\tau \sim \tau + \mathbb{Z}$ by a choice of solid filling, completely determined by the pair (c, d) of relatively prime integers. This is because the flip of signs $(a, b, c, d) \to (-a, -b, -c, -d)$ does not affect q, and once (c, d) are given, (a, b) can be uniquely determined by $ad - bc = 1$ up to a shift $(a, b) \to (a, b) + t(c, d)$, $t \in \mathbb{Z}$ which leaves q unaffected. We call these solid tori $M_{c,d}$'s, and any $M_{c,d}$ can be obtained from $M_{0,1}$ via a modular transformation on τ. Physically, $M_{0,1}$ is the Euclidean thermal AdS$_3$ and $M_{1,0}$ is the traditional Euclidean BTZ black hole obtained from Wick rotating the original metric in [45]. Excluding $M_{0,1}$, $M_{c,d}$'s are collectively called the $SL(2,\mathbb{Z})$ family of Euclidean black holes, to be discussed in Section 2.5.

2.3 Thermal AdS$_3$

The Euclidean thermal AdS$_3$ has the topology of a solid torus $M_{0,1}$, whose non-contractible loop is parametrized by the Euclidean time. The constant time slice is thus a disk D^2 with a boundary S^1, perpendicular to the non-contractible loop.

Bipartition into Two Disks

We bipartite the disk into upper and lower subregions A and B, both having the topology of a disk. The solid torus is then turned into a sliced bagel as in Figure 2.3. Boundary of each subregion contains an interval lying on the S^1. In the following we will denote the ratio between the length of one interval and the circumference of the boundary S^1 to be a, satisfying $0 \leq a \leq 1$. Except for the symmetric case where $a = 1/2$ and the two subregions are equivalent, generally $S_A \neq S_B$.

As introduced in Section 2.2, one then glues each of n copies of subregion B separately while gluing the n copies of subregion A together. The resultant 3-manifold is an n-handlebody, which is a filled genus-n Riemann surface, shown in Figure 2.3. (In the special case of $n = 1$, the handlebody reduces to a solid torus.)

With a proper normalization, the entanglement entropy corresponding to subregion A is then

$$S_{TAdS} = -\frac{d}{dn}\left(\frac{Z(n\text{-handlebody})}{Z(1\text{-handlebody})^n}\right)\Bigg|_{n=1}. \tag{2.6}$$

Figure 2.3: Left: bipartition of the thermal AdS_3. Right: the glued 3-manifold is a flat bouquet-like n-handlebody.

Contribution to the path integral around a classical saddle point for an n-handlebody takes the form

$$Z(n) = \exp\left[kS_0(n) + \sum_i k^{-i+1} S_i(n)\right], \tag{2.7}$$

where $k^{-i+1}S_i(n)$ is the i-loop free energy of boundary graviton excitations. At tree level ($i = 0$), $Z_{tree}(n\text{-handlebody})$ can be derived assuming the dual CFT is an extremal CFT [52][3],

$$Z_{tree}(n) = \prod_{\gamma \text{ prim.}} \prod_{m=1}^{\infty} |1 - q_\gamma^m|^{24k}, \tag{2.8}$$

with the product running over primitive conjugacy classes of γ, q_γ being the multiplier of γ introduced in Section 2.2, and $k = l/16G$.

In general the two products are hard to evaluate. However, in the low-temperature regime when thermal AdS_3 dominates, the leading contribution to the infinite product over m comes from $m = 1$. Furthermore, the product over γ is dominated by a single-letter contribution [55, 66], $\prod_{\gamma \text{ prim.}} |1 - q_\gamma| \approx |1 - q_1|^{2n}$. Combining these, we obtain

$$Z_{tree}(n) \approx \prod_{\gamma \text{ prim.}} |1 - q_1|^{24k} = |1 - q_1|^{48nk}, \tag{2.9}$$

with q_1 a function of n and a, having the form

$$q_1 = \frac{\sin^2(\pi a)}{n^2 \sin^2(\pi a/n)} e^{-2\pi\beta}. \tag{2.10}$$

At one-loop ($i = 1$) level, the general expression for $Z_{loop}(n\text{-handlebody})$ can be derived from either the boundary extremal CFT [52, 53] or the bulk heat kernel method [54]. They

[3]This partition function is motivated by the Liouville action of a single free boson on a handlebody, and is conjectured in [52] as a modular form of weight $12k$ to avoid singularities of special functions.

both depend on the Schottky parametrization of the boundary genus n-Riemann surface. The result is

$$Z_{loop}(n) = \prod_{\gamma \text{ prim.}} \prod_{m=2}^{\infty} \frac{1}{|1-q_\gamma^m|} \approx \frac{1}{|1-q_1^2|^{2n}}, \tag{2.11}$$

in the low-temperature regime $q_1 \ll 1$. Plugging $Z(n\text{-handlebody}) = Z_{tree}(n)Z_{loop}(n)$ into (2.6), we obtain

$$S_{TAdS}(a) \approx \left[96ke^{-2\pi\beta} + (96k-8)e^{-4\pi\beta} + O(e^{-6\pi\beta})\right](\pi a \cot(\pi a) - 1)\,. \tag{2.12}$$

The terms containing k come from tree-level, while others are one-loop contributions. The entire expression approaches to zero very fast in the low-temperature regime $\beta \to \infty$ for any k. The dependence of the above result on a distinguishes itself from the original definition [17, 18] of TEE, which is a universal constant. We note that a enters as the boundary condition on the constant time slice, and has nothing to do with the leading area-law term in usual expressions of entanglement entropies.

When subregion A is "nothing", i.e., $a \to 0$, $\pi a \cot(\pi a) \to 1$, thus the TEE between subregions A and B vanishes. When A is instead "everything", i.e., $a \to 1$, $\pi a \cot(\pi a) \to -\infty$, balanced by the smaller $e^{-2\pi\beta} \ll 1$ at low temperatures. We observe that apart from the $a \to 0$ case, the TEE for thermal AdS_3 is always negative. Another important case is when $a = 1/2$ so that the two subregions are symmetric. In this case we have

$$S_{TAdS}\left(a = \frac{1}{2}\right) \approx -\left[96ke^{-2\pi\beta} + (96k-8)e^{-4\pi\beta} + O(e^{-6\pi\beta})\right]. \tag{2.13}$$

Two Disjoint Thermal AdS$_3$

Now we take two non-interacting thermal AdS_3's as the whole system, represented by two disjoint solid tori $M_{0,1}$. There are two non-interacting, non-entangled, identical CFTs living on their asymptotic boundaries. One would naïvely expect the TEE between these two solid tori to be zero, which is not really the case. To calculate the entanglement entropy between these two solid tori, one can simply use

$$S_{TAdS} = -\frac{d}{dn}\left(\frac{Z_{0,1}(n\tau)Z_{0,1}(\tau)^n}{Z_{0,1}(\tau)^{2n}}\right)\Bigg|_{n=1}. \tag{2.14}$$

We have used the shorthand notation $Z_{0,1}(\tau) = Z_{0,1}(\tau, \bar{\tau})$ to take into account both holomorphic and anti-holomorphic sectors. The partition function $Z_{0,1}(n\tau)$ comes from gluing n copies of solid torus A, which is a new solid torus with modular parameter $n\tau$.

Meanwhile, $Z_{0,1}(\tau)^n$ comes from gluing individually the n copies of solid torus B. We can simply multiply the contributions from A and B together because they are disjoint. Then we can plug these into the expression for the solid torus partition function, i.e., the

1-handlebody result from (2.8) and (2.10),

$$Z_{0,1}(\tau) = |q|^{2k} \prod_{m=2}^{\infty} |1-q^m|^{-2}. \tag{2.15}$$

In the low temperatures, we can approximate $q = e^{2\pi i\tau} = e^{-2\pi\beta}$ as a small number and thus at leading order $Z_{0,1}(\tau) \approx q^{-2k}(1-q^2)^{-2}$.

After straightforward calculations we obtain

$$S_{TAdS} \approx 2(1+4\pi\beta)e^{-4\pi\beta}. \tag{2.16}$$

This contains only the loop contribution, i.e., the semi-classical result is zero. For comparison, we also calculate the canonical ensemble thermal entropy of a single thermal AdS_3 at temperature β^{-1}: $S^{\text{thermal}}_{TAdS} = \ln Z(\text{1-handlebody}) - \beta Z(\text{1-handlebody})^{-1}\frac{\partial Z(\text{1-handlebody})}{\partial\beta}$. It has the low-temperature form

$$S^{\text{thermal}}_{TAdS} \approx 2(1+4\pi\beta)e^{-4\pi\beta}, \tag{2.17}$$

which again solely comes from loop contributions. We immediately observe that the thermal entropy of a single thermal AdS_3 is the same as the TEE between two independent thermal AdS_3's.

This does *not* imply that there are nontrivial topological entanglement between the two copies of thermal AdS_3, but simply reveals the insufficiency of using entanglement entropy as an entanglement measure at finite temperatures. For example, consider two general subsystems A and B with thermal density matrices ρ_A and ρ_B and combine them into a separable system,

$$\rho = \rho_A \otimes \rho_B. \tag{2.18}$$

These two subregions are thus obviously non-entangled. But if one attempts to calculate the entanglement entropy between A and B by tracing over B, one can still get an arbitrary result depending on the details of ρ_A. If we choose $\rho_A = |\psi\rangle\langle\psi|$ where $|\psi\rangle$ is some pure state, then the entanglement entropy will be zero. If instead we choose $\rho_A = \frac{1}{\dim(\mathcal{H}_A)}\mathbb{1}$ as the proper normalized identity matrix, then the entanglement entropy will be $\ln(\dim(\mathcal{H}_A))$. So depending on the choice of ρ_A, one can obtain any value of the entanglement entropy between these minimum and maximum values. This shortcoming is due to the fact that now the entanglement entropy calculation involves undesired classical correlations in mixed states.

To address this issue, we look at the topological mutual information between the two solid tori,

$$I(A,B) = S(A) + S(B) - S(A\cup B), \tag{2.19}$$

so that the thermal correlations can be canceled. Following similar replica trick calculations, one easily obtain $S(A\cup B) = 2S(A) = 2S(B)$, thus the mutual information vanishes and there exists no nontrivial topological entanglement between the two disjoint thermal AdS_3's. We will observe in the next section that this statement no longer holds true for an eternal BTZ black hole.

2.4 BTZ black holes

We will explore in this section the topological entanglement in the bulk of Euclidean BTZ black hole.

BTZ Geometry

It has been speculated for a long time that the 3d gravity is rather trivial because besides local fluctuations, there is no gravitational wave due to the vanishing Weyl tensor. However in the year of 1992, authors of [45] proposed a new type of AdS-Schwarzschild black hole with Lorentzian metric

$$ds_L^2 = -N_L^2 dt_L^2 + N_L^{-2} dr^2 + r^2(d\phi + N_L^\phi dt)^2, \tag{2.20}$$

where the *lapse* and *shift* functions have the form $N_L^2 = -8GM_L + \frac{r^2}{l^2} + \frac{16G^2J_L^2}{r^2}, N_L^\phi = -\frac{4GJ_L}{r^2}$. G is the 3d Newton constant, l the curvature radius of AdS$_3$, and M_L, J_L are the mass and angular momentum of the black hole, respectively. The outer and inner horizons are defined by

$$\tilde{r}_\pm^2 = 4GM_L l^2 \left(1 \pm \sqrt{1 - \frac{J_L^2}{M_L^2 l^2}}\right). \tag{2.21}$$

Let $t_L \equiv it$ and $J_L \equiv iJ$, and we perform the Wick rotation to get

$$ds^2 = N^2 dt^2 + N^{-2} dr^2 + r^2(d\phi + N^\phi dt)^2, \tag{2.22}$$

with $N^2 = -8GM + \frac{r^2}{l^2} - \frac{16G^2J^2}{r^2}, N^\phi(r) = -\frac{4GJ}{r^2}$. The horizons are now given by

$$r_\pm^2 = 4GMl^2 \left(1 \pm \sqrt{1 + \frac{J^2}{M^2 l^2}}\right). \tag{2.23}$$

The Euclidean BTZ black hole is locally isometric to the hyperbolic 3-space $\mathbb{H}^3$ and is globally described by $\mathbb{H}^3/\Gamma$ with $\Gamma \cong \mathbb{Z}$. The topology is a solid torus, and one can make it explicit by performing the following coordinate transformations [67]

$$\begin{aligned}
x &= \sqrt{\frac{r^2 - r_+^2}{r^2 - r_-^2}} \cos\left(\frac{r_+}{l^2}t + \frac{|r_-|}{l}\phi\right) \exp\left(\frac{r_+}{l}\phi - \frac{|r_-|}{l^2}t\right), \\
y &= \sqrt{\frac{r^2 - r_+^2}{r^2 - r_-^2}} \sin\left(\frac{r_+}{l^2}t + \frac{|r_-|}{l}\phi\right) \exp\left(\frac{r_+}{l}\phi - \frac{|r_-|}{l^2}t\right), \\
z &= \sqrt{\frac{r_+^2 - r_-^2}{r^2 - r_-^2}} \exp\left(\frac{r_+}{l}\phi - \frac{|r_-|}{l^2}t\right) > 0.
\end{aligned} \tag{2.24}$$

They bring the metric (2.22) to the 3d upper half-space with $z > 0$, representing $\mathbb{H}^3$. Further changing to the spherical coordinates $(x, y, z) = (R\cos\theta\cos\chi, R\sin\theta\cos\chi, R\sin\chi)$, we finally arrive at

$$ds^2 = \frac{l^2}{\sin^2\chi}\left(\frac{dR^2}{R^2} + \cos^2\chi d\theta^2 + d\chi^2\right). \tag{2.25}$$

In order to incorporate the periodicity of the Schwarzschild angular coordinate ϕ in (2.22), we require terms in (2.25) to obey the global identifications

$$(R, \theta, \chi) \sim \left(Re^{2\pi r_+/l}, \theta + \frac{2\pi|r_-|}{l}, \chi\right). \tag{2.26}$$

Now it is clear that the fundamental region for (2.25) is the solid slice between inner and outer hemispheres centered at the origin in Figure 2.4 with radii $R = 1$ and $R = e^{2\pi r_+/l}$, respectively, with an opening of $2\pi|r_-|/l$ or 2π (if $r_- = 0$) in azimuthal angle (in the θ direction).[4] For each fixed $\chi \in [0, \pi/2]$, the two hemispheres are identified along the radial direction, and two segments bounding the azimuthal opening angle are also identified, forming a torus. Hence, the segment on the z-axis between two hemispheres corresponds to the outer horizon, and it is mapped to the central cord of solid torus, i.e., the fundamental region, at $\chi = \pi/2$ (the boundary torus is at $\chi = 0$).

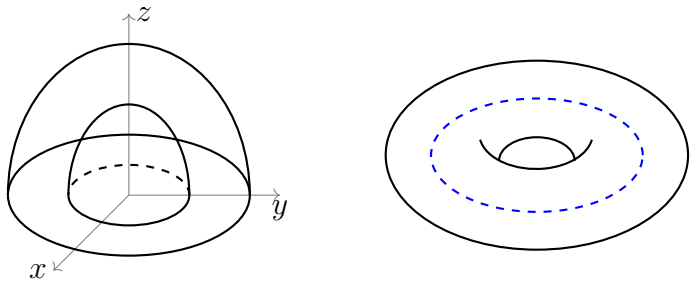

Figure 2.4: Left: The spherical coordinates on $\mathbb{H}^3$, which convert the original AdS-Schwarzschild metric (2.20) of BTZ black hole into the right picture. Right: Topology of the Euclidean BTZ black hole is a solid torus. Horizon is the blue dashed line threading the central cord of the solid torus. The Euclidean time runs in the meridian direction.

Finally, to ensure that the coordinate transformations in (2.24) are non-singular (contain no conical singularities) at the z axis ($r \to r_+$), we must require periodicity in the arguments of the trigonometric functions there. That is, we must identify

$$\frac{1}{2\pi l}(\phi, t) \sim \frac{1}{2\pi l}(\phi + \Phi, t + \beta), \tag{2.27}$$

[4]The fundamental region looks just like a slice of cheese, which is not drawn here. See Figure 12.2 in [68] for an illustration.

where $\Phi = \frac{|r_-|}{r_+^2 - r_-^2}$, $\beta = \frac{r_+ l}{r_+^2 - r_-^2}$. We combine the real pair (Φ, β) into one single complex variable

$$\tau \equiv \Phi + i\beta, \tag{2.28}$$

which is the complex modular parameter of the boundary torus.

For convenience, in the rest of this chapter, unless stated otherwise, we only focus on non-rotating Euclidean BTZ black hole, so that τ is pure imaginary and $r_- = 0$.

TEE between Two One-Sided Black Holes and Mutual Information

Following [57, 58, 59, 69], an eternal Lorentzian AdS black hole has two asymptotic regions and can be viewed as two black holes connected through a non-traversable wormhole. It is also suggested from the dual CFT perspective that the entanglement entropy between the CFTs living on the two asymptotic boundaries is equal to the thermal entropy of one CFT. Motivated by this, we are interested in calculating the TEE between the two single-sided black holes in the bulk.

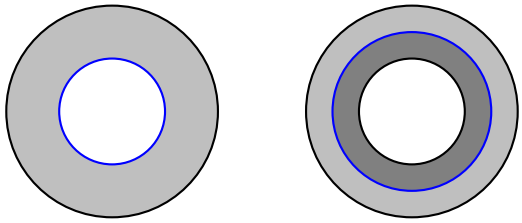

Figure 2.5: Left: Constant time slice of each single-sided BTZ black hole is an annulus. The inner boundary in blue denotes the horizon. Time evolution of this slice corresponds to rotating angle π around the inner blue boundary. Right: Gluing the constant time slices of single-sided black holes R (light grey) and L (dark grey) along the horizon (blue line) in the middle.

However, for the Euclidean BTZ black hole (2.22) and (2.25), the metrics only cover the spacetime outside the horizon of one single-sided black hole. Everything inside the horizon is hidden, so is another single-sided black hole. In order to make the computation of TEE between two single-sided black holes possible, we take an alternative view of the solid torus $M_{1,0}$, as in Figure 2.5. In the left panel, we sketch the constant time slice of the right single-sided black hole, called R. It is the constant θ slice in metric (2.25) with an annulus topology, whose inner boundary is identified with the horizon. In the right panel, we glue the two constant time slices for black holes L and R along the horizon. Then there comes the most important step: we fold the annulus of black hole L along the horizon, so that it coincides with the annulus of black hole R. To obtain the full spacetime geometry, one rotates the constant time slice of L about the horizon *counterclockwise* by π, while rotating the constant time slice of R about the horizon *clockwise* by π. Namely, the two annuli meet

twice: one at angle 0, the other at π. The resultant manifold is a solid torus, same as the $M_{1,0}$ introduced before. Hence one can view this solid torus either as one single-sided black hole R with modular parameter $\tau = i\beta$, or as two single-sided black holes L and R, each contributing $\tau' = i\beta/2$.

It might concern some readers that the CFTs living on the asymptotic boundaries of L and R in the Lorentzian picture are now glued together. We note that this is a feature of the Euclidean picture: due to the different direction of evolutions, we have $\mathrm{CFT}_L(t) = \mathrm{CFT}_R(-t)$. At $t = 0$, these obviously coincide. Then at $t = \beta/2$, this gives $\mathrm{CFT}_L(t = \beta/2) = \mathrm{CFT}_R(t = -\beta/2)$. Using the fact that in the Euclidean picture we have $-\beta/2 = -\beta = 2 + \beta = \beta/2$, we arrive at $\mathrm{CFT}_L(t = \beta/2) = \mathrm{CFT}_R(t = \beta/2)$, thus they coincide again and the two CFTs are glued together. This is consistent with the fact that in the Euclidean signature, there should only be one asymptotic region, as shown in [56].

Now we can calculate the TEE between the constant time slices of L and R, which we denote as A and B. Importantly, since in general the result can be time dependent, we specify the cut to be done at $t = 0$. Shown in the left panel of Figure 2.6, each subregion contributes τ' to the modular parameter of the solid torus. We sketch one copy of ρ_A in the right panel.

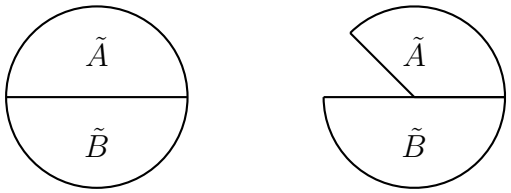

Figure 2.6: The disk perpendicular to the horizon, which pierces the center of the disk. Left: Here, parts $\tilde{A}$ and $\tilde{B}$ in spacetime are respectively formed by rotating both spatial subregions A and B by $\pm\pi$. Right: The graphical representation of ρ_A, with a wedge missing in spacetime subregion $\tilde{A}$.

To find $S(A)$, we need to calculate the partition function of the 3-manifold that correspond to $\mathrm{tr}\rho_A^n$. We first enlarge the missing wedge in the right panel of Figure 2.6 and shrink the size of A, B. To add the second copy of ρ_A, one should glue A_1 to B_2, with B_2 glued with A_2, as shown in Figure 2.7. Note that this differs from the usual way of doing replica tricks, where A_1 is always glued to A_2. This is again a result of the opposite directions of time evolutions for L and R: the B spatial slice at $t = \beta/2$ should always be identified with the A spatial slice at $t = \beta/2$. One can then follow this procedure and glue n-copies of ρ_A.

The resultant 3-manifold is a solid torus with modular parameter $2n\tau'$, since each copy of $\tilde{A}$ contributes τ' and the same goes for $\tilde{B}$. Replica trick then gives

$$S_{BTZ}(A) = -\frac{d}{dn}\left(\frac{Z_{1,0}(2n\tau')}{Z_{1,0}(2\tau')^n}\right)\Bigg|_{n=1}. \tag{2.29}$$

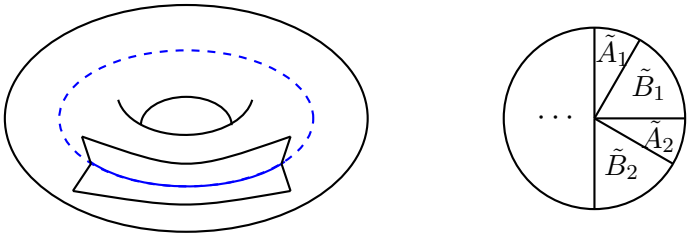

Figure 2.7: Left: front view of the pictorial representation of ρ_A. Notice that the cutaway wedge runs along the longitude (non-contractible loop) of the solid torus, with its vertex on the horizon. Right: Graphical representation of $\mathrm{tr}\rho_A^n$. The disk is perpendicular to the horizon.

Partition function $Z_{1,0}(\tau)$ can be obtained from that of the thermal AdS_3 by a modular transformation $\tau \to -1/\tau$,

$$Z_{1,0}(\tau) = |q_-|^{-2k} \prod_{m=2}^{\infty} \frac{1}{|1-q_-^m|^2}, \tag{2.30}$$

where we have defined $q_- \equiv e^{-2\pi i/\tau} = e^{-2\pi/\beta}$. In the high-temperature regime $\beta \ll 1$, the above reduces to $Z_{1,0}(\tau) \approx e^{4\pi k/\beta}\left(1-e^{-4\pi/\beta}\right)^{-2}$. Substituting it into (2.29), one obtains at leading order

$$S_{BTZ}(A) = \frac{8\pi k}{\beta} - 2e^{-4\pi/\beta}\left(\frac{4\pi}{\beta}-1\right) + O(e^{-6\pi/\beta}). \tag{2.31}$$

where the first term comes from tree level and is identified with the Bekenstein-Hawking entropy. The above expression matches with the thermal entropy of one single-sided black hole at one-loop,

$$S_{BTZ}^{\text{thermal}}(A) = \ln Z_{1,0}(\tau) - \beta Z_{1,0}(\tau)^{-1}\frac{\partial Z_{1,0}(\tau)}{\partial \beta} = S_{BTZ}(A). \tag{2.32}$$

Remarkably, this equation holds true regardless of $Z_{1,0}(\tau)$'s specific form.

It might be confusing at first that the Bekenstein-Hawking entropy, usually viewed as an area-law term, appears in the calculation of topological entanglement entropy. To make it explicit that the results above are TEEs instead of the full entanglement entropy, alternatively we can use $Z_{1,0}(\tau)$ derived from supersymmetric localization method in Chern-Simons theory on 3-manifolds with boundaries [70]. Following the replica trick, we find exactly the same expression[5]. Since Chern-Simons theory is a topological quantum field theory, the resulting entanglement entropy is a TEE. The horizon area r_+ should be understood as a topological quantum number of the theory.

[5]The supersymmetric localization method involves boundary fermions. We need to remove the contribution from the boundary fermions to match with the partition function (2.30)

In the calculation of TEE between two disjoint thermal AdS$_3$'s, as stated in Section 2.3, we have seen that a nonzero TEE is not enough to guarantee true nontrivial entanglement between two subregions because of the possible contribution from classical correlations. So we resort to the mutual information $I(A, B)$ between two single-sided black holes. We then need to find $S(A \cup B)$. Since in the Euclidean picture we are no longer at a pure state, it is not necessary that $S(A \cup B)$ vanishes, although $A \cup B$ consists the entire system.

We start with bipartiting the system into $A \cup B$ and C at $t = 0$, as shown in Figure 2.8. C is a very small region whose area will finally be taken to zero.

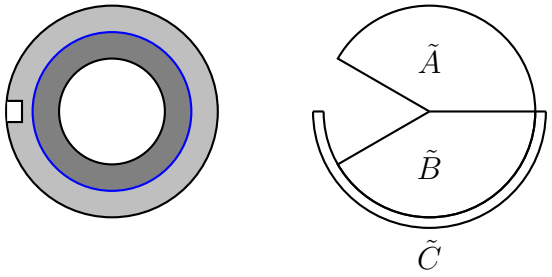

Figure 2.8: Left: Subregion C is the small white square in the constant time slice. Right: One copy of ρ_A. The picture shows the disk perpendicular to the horizon. The thin layer surrounding the lower half circle corresponds to $\tilde{C}$, the spacetime region resulting from C.

The glued manifold is a solid torus with modular parameter $2n\tau'$, exactly the same form as that in Figure 2.6. The contributions from C vanish because C is still contractible in the glued manifold and we can safely take their area to be zero. Plugging (2.30) into the replica trick formula (2.29), we again obtain

$$S_{BTZ}(A \cup B) = S_{BTZ}^{\text{thermal}}(A). \tag{2.33}$$

So indeed the TEE of $A \cup B$ does not vanish. Combining these, we find that the mutual information is the same as the Bekenstein-Hawking entropy for a single-sided black hole:

$$I(A, B) = S_{BTZ}(A) + S_{BTZ}(B) - S_{BTZ}(A \cup B) = S_{BTZ}^{\text{thermal}}(A). \tag{2.34}$$

Note that, had we naïvely taken the full partition function of the eternal BTZ black hole to be $Z_{1,0}(\tau)^2$, namely, the two single-sided black holes are independent and non-entangled so that their partition functions can be multiplied together, then $S_{BTZ}(A \cup B)$ would have been twice $S_{BTZ}^{\text{thermal}}(A)$ and the mutual information would have vanished. So the nonzeroness of mutual information indicates nontrivial entanglement between L and R.

There is still another surgery that can yield $S_{BTZ}^{\text{thermal}}(A)$: (1) restrict to the right single-sided black hole R as the full spacetime, which is a solid torus with modular parameter τ, obtained from rotating the constant time slice of it by 2π (if $r_- = 0$); (2) thicken the horizon S^1 to a narrow annulus inside the spatial slice of the solid torus R; (3) calculate the TEE

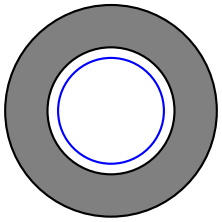

Figure 2.9: With the absence of black hole L, bipartitions of the constant time slice of black hole R lead to $Z_{1,0}(n\tau)$ after gluing. The gray area corresponds to subregion A, and the width of the annulus B will be taken to zero.

between the thin solid torus generated by thickened horizon, denoted by $\hat{B}$, and the rest, denoted by $\hat{A}$; (4) and finally take the limit that thickness of solid torus $\hat{B}$ goes to zero.

The bipartition of the constant slice in this case is sketched in Figure 2.9. In this bipartition, the obtained TEE is between the exterior and the interior of horizon, rather than that between two single-sided black holes. The glued manifold is again represented by $Z_{1,0}(n\tau)$ and the replica trick yields the Bekenstein-Hawking entropy.

We have thus come to a conclusion that the followings are equal:

(a) TEE between the two single-sided black holes,

(b) TEE between the exterior and the interior of the horizon for a single-sided black hole,

(c) thermal entropy of one single-sided black hole,

(d) mutual information between the two single-sided black holes.

The equivalence of (a) and (c) supports the ER=EPR conjecture [57, 58, 59] in the Euclidean AdS$_3$ case. The equivalence between (b) and (c) shows explicitly from the bulk perspective that one should view the thermal entropy of a black hole as entanglement entropy (see for example [71]).

In general for a rotating BTZ black hole, although there is an inner horizon at $r = r_-$, the z-axis still represents the outer horizon at $r = r_+$ in the spherical coordinates (2.24) for the upper $\mathbb{H}^3$. Hence, the replica trick described earlier still applies to a rotating BTZ black hole with modular parameter $\tau = \Phi + i\beta$, where Φ is the angular potential, the conjugate variable to angular momentum. Geometrically, we just need to put $r = |r_-|$ "inside" the inner edge of the constant time slice, so that it is not observable.[6]

The Entangling-Thermal Relation

In [60], the authors showed a relation (2.35) for a single-sided BTZ black hole between the entanglement entropy of CFT on the conformal boundary and the Bekenstein-Hawking

[6] A similar situation will be described in Appendix A.1.

entropy:

$$\lim_{l\to 0}(S_A(L-l)-S_A(l))=S^{\text{thermal}}, \tag{2.35}$$

where $S_A(L-l)$ is the entanglement entropy of a subregion A on the boundary 1+1d CFT with an interval length $(L-l)$, and S^{thermal} is the thermal entropy in the bulk. In this section, we propose another similar but different Entangling-Thermal relation.

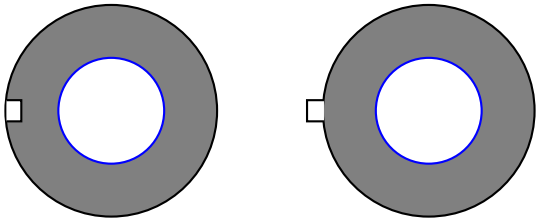

Figure 2.10: Bipartition of the constant time slice. Left and right panels are equivalent.

We first consider the bipartition of the constant time slice as in Figure 2.10 for a single-sided black hole. We put the separation between two subregions away from the horizon, so that region B generates the white contractible region in the left panel. The right panel is equivalent to the left one, and will be convenient for visualization of the gluing. We will call the glued manifold as the "ring", because after time evolution, region $B=\overline{A}$ (the complement) will glue to itself and form a ring around the solid torus, as shown in the middle panel of Figure 2.11, where the small white part corresponds to the unglued part in the left panel. Hence, a single copy is the middle panel: away from the ring, the open wedge running around the longitude is the same as that in the left panel of Figure 2.7.

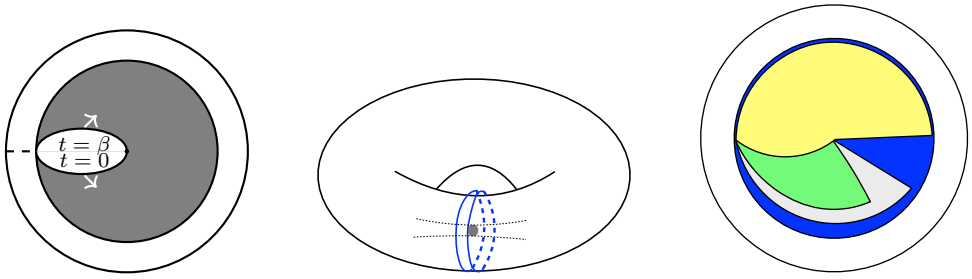

Figure 2.11: Left: The side view of $\text{tr}\rho_A$ for the "ring"; the dashed line is only used to separate $t=0$ and $t=\beta$ ends of the grey region. Middle: the front view of $\text{tr}\rho_A$ for the "ring" configuration. Right: the side view of $\text{tr}\rho_A^4$ inside the "ring" of the first $\text{tr}\rho_A$.

Naïvely it seems that one is unable to glue n copies of the above geometry, since the ring blocks a portion of the wedge's opening. However, there do exist a unique embedding from n copies to $\mathbb{R}^3$ up to homotopy equivalence, as shown in the right panel of Figure 2.11: one

first stretches the grey region in the left panel to the blue area in right panel, and glue a second light grey copy so that its $t = 0$ edge are glued to the $t = \beta$ edge of the blue copy; now one repeats this process for green and yellow regions and so on, still preserving the replica symmetry. Notice that rings from gray, green and yellow copies are not in this piece of paper, but on parallel planes above or below. Then one puts rings from each copy side by side on the boundary torus, which requires each ring to be infinitesimally thin since n is arbitrarily large. The resultant manifold is again a solid torus of modular parameter $n\tau$. So the replica trick calculation follows the previous equation (2.29) and gives

$$\lim_{\text{Area}(\tilde{A})\to 0} S(A) = S_{BTZ}^{\text{thermal}}. \tag{2.36}$$

For completeness, we note that Figure 2.11 has another limiting case, where the width of the ring covers almost the entire longitudinal direction of the solid torus, and its depth occupies a considerable portion of the radial direction, as shown in Figure 2.12. Now in order to put rings side by side upon gluing n copies, we need to stretch the non-contractible direction for n times to accommodate them, so that the resultant manifold is approximately a solid torus with modular parameter τ/n. Now plug $Z_{1,0}(\tau/n)$ into (2.29):

$$\lim_{\text{Area}(A)\to 0} S(A) = -\frac{d}{dn}\left(\frac{Z_{1,0}(\tau/n)Z_{1,0}(\tau)^n}{Z_{1,0}(\tau)^{2n}}\right)\Bigg|_{n=1} = \ln Z_{1,0}(\tau) + \tau\frac{d}{d\tau}Z_{1,0}(\tau). \tag{2.37}$$

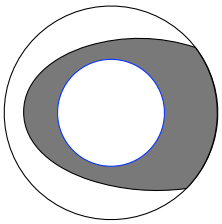

Figure 2.12: Another limit of the ring configuration.

Using $Z_{1,0}(\tau) \approx e^{4k\pi/\beta}(1 + 2e^{-4\pi/\beta})$ again, we obtain

$$\lim_{\text{Area}(A)\to 0} S(A) = 2\left(\frac{4\pi}{\beta} + 1\right)e^{-4\pi/\beta}, \tag{2.38}$$

which vanishes at high temperature. Note that here is no k-dependence, meaning we can observe the one-loop effect directly.

Now we consider the complementary bipartition of Figure 2.11, as shown in Figure 2.13, where the grey region is generated by B in Figure 2.10. The gluing here is simple: since the unglued cut in the grey region $\tilde{A}$ is parallel to the longitude, n copies should be arranged around a virtual axis tangent to the annulus. The resultant manifold is a vertical n-handlebody.

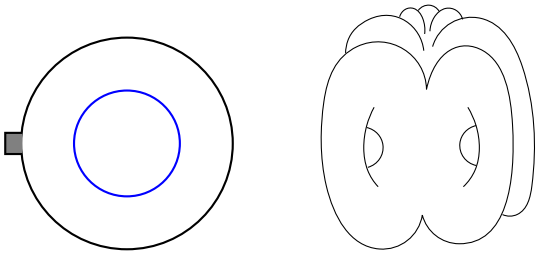

Figure 2.13: Left: The complementary bipartition which leads to $S_{\bar{A}}$. Right: The glued manifold is a vertical bouquet-like handlebody.

One can calculate the corresponding TEE following a parallel procedure in the calculation of thermal AdS$_3$ in Section 2.3. The partition function of the glued manifold is

$$Z(n) = \prod_{\gamma \text{ prim.}} \prod_{m=1}^{\infty} |1 - q_\gamma^m|^{24k} \times \prod_{\gamma \text{ prim.}} \prod_{m=2}^{\infty} \frac{1}{|1 - q_\gamma^m|}, \tag{2.39}$$

where the first and second factors come from tree level and one-loop, respectively. The products are over primitive conjugacy classes of $\gamma \in \Gamma$. In the high-temperature regime, this expression can be simplified by the single-letter word approximation $\prod_{\gamma \text{ prim.}} |1-q_\gamma| \approx |1-q_1'|^{2n}$, so that

$$Z(n, q_1') \approx \frac{|1 - q_1'|^{48nk}}{|1 - q_1'^2|^{2n}}. \tag{2.40}$$

Here q_1' can be obtained from q_1 in (2.10) using a modular transformation,

$$q_1'(n, a) = \frac{\sinh^2(\pi a/\beta)}{n^2 \sinh^2(\pi a/n\beta)} e^{-2\pi/\beta}. \tag{2.41}$$

The replica trick then gives

$$S(\bar{A}) = -\frac{d}{dn} \left[\frac{Z(n, q_1'(n))}{Z(1, q_1'(1))^n} \right] \Bigg|_{n=1}. \tag{2.42}$$

This is explicitly written as

$$S(\bar{A}) = 96k \left(\frac{\pi a}{\beta} - 2 \right) e^{-2\pi/\beta} + 8(12k - 1) \left(\frac{\pi a}{\beta} - 2 \right) e^{-4\pi/\beta} + O(e^{-6\pi/\beta}). \tag{2.43}$$

We now take the limit $a \to 0$ because this corresponds to the limit where the grey region in Figure 2.13 goes to zero, so that:

$$\lim_{\text{Area}(\bar{A}) \to 0} S(\bar{A}) \equiv \lim_{a \to 0} S(\bar{A}) = -192k e^{-2\pi/\beta} - 16(12k - 1) e^{-4\pi/\beta} + O(e^{-6\pi/\beta}), \tag{2.44}$$

which vanishes at high temperature. The infinitesimally negative value is a quirk due to approximation on q_γ's.

Combining equations (2.36) and (2.44), one obtains the *Entangling-Thermal relation:*

$$\lim_{\text{Area}(\bar{A})\to 0}[S(A)-S(\bar{A})]=S_{BTZ}^{\text{thermal}}, \tag{2.45}$$

We give this relation a different name from the two-dimensional thermal entropy relation in the dual CFT calculation (2.35) because this is not merely a generalization of it in one higher dimension. The thermal entropy relation (2.35) relates the entanglement entropy on the dual CFT with the thermal entropy of black hole in the bulk, while the entangling-thermal relation connects the topological entanglement entropy and thermal entropy both in the bulk gravitational theory. Additionally, the explanation for thermal entropy relation relies on the geometrical detail (minimal surfaces) in the bulk [60], while the entangling-thermal relation is of topological origin. In the first bipartition in Figure 2.11, subregion A sees the non-contractible loop and the nontrivial flux threading through the hole inside the annulus. In the second bipartition in Figure 2.13, subregion A does not completely surround the non-contractible circle, i.e., the horizon. The difference between them thus characterizes the non-contractible loop.

Finally we remark that there are several cases in which gluing procedures are not available. The no-gluing criterion is that, as long as the boundary of a subregion is contractible and not anchored on the boundary S^1, the spatial slice is not n-glueable. Also, a single copy in which glued region B completely surrounds region except for the inner edge is not n-glueable.

2.5 Summation over geometries

The partition functions of thermal AdS$_3$, $Z_{0,1}(\tau)$, and BTZ black hole, $Z_{1,0}(\tau)$, are not modular-invariant by themselves. To obtain the full modular-invariant partition function, one needs to sum over the pair of parameters (c,d) for $Z_{c,d}$. This can alternatively be written as the summation over modular transformations of $Z_{0,1}$ as follows:

$$Z(\tau)=\sum_{\Gamma_\infty\backslash SL(2,\mathbb{Z})}Z_{c,d}(\tau)=\sum_{\Gamma_\infty\backslash SL(2,\mathbb{Z})}Z_{0,1}\left(\frac{a\tau+b}{c\tau+d}\right), \tag{2.46}$$

where $\Gamma_\infty\backslash SL(2,\mathbb{Z})$ denotes the right coset space of Γ_∞ in $SL(2,\mathbb{Z})$ [72], and Γ_∞ is the translational subgroup generated by the 2×2 matrix $T\equiv\begin{pmatrix}1&1\\0&1\end{pmatrix}$ with action $\tau\to\tau+1$. Solid torus filling and Schottky parametrization are invariant under Γ_∞, and the summation over the coset space is to make the full partition function invariant under both $T:\tau\to\tau+1$ and $S:\tau\to-1/\tau$.

Note that in the previous sections we have used $Z_{c,d}(\tau)=Z_{c,d}(\tau,\bar{\tau})$ as the shorthand for the product of holomorphic and anti-holomorphic pieces, whereas in this section we return

to the notation that $Z_{c,d}(\tau)$ describes the holomorphic part of the partition function only. The anti-holomorphic part can easily be found as $\bar{Z}(\bar{\tau})$ and $Z(\tau,\bar{\tau}) = Z(\tau)\bar{Z}(\bar{\tau})$.

Modular-invariant partition function of the form (2.46) is unique for the most negative cosmological constant ($k = 1$) [51, 73] and was investigated in more general situations ($k > 1$) in [5]. An important theorem due to [73] is that the moduli space of Riemann surfaces of genus one is itself a Riemann surface of genus zero, parametrized by the j-function. Consequently, any modular-invariant function can be written as a function of it. The J-function is defined as

$$\begin{aligned} J(\tau) &\equiv \frac{1728 g_2(\tau)^3}{g_2(\tau)^3 - 27 g_3(\tau)^2} - 744 \\ &= q^{-1} + 196884q + 21493760q^2 + 864299970q^3 + 20245856256q^4 + \dots \end{aligned} \tag{2.47}$$

where $q = e^{2\pi i\tau}$ as usual, and $g_2(\tau) \equiv 60G_4(\tau)$ and $g_3(\tau) \equiv 140G_6(\tau)$, where G_{2k} are holomorphic Eisenstein series of weight $2k$, $k \geq 2$, defined as $G_{2k} \equiv \sum_{(m,n)\neq(0,0)} (m+n\tau)^{-2k}$.

Since the pole in the full partition function $Z(q)$ at $q = 0$ is of order k (due to the holomorphic tree-level contribution of thermal AdS_3, q^{-k}), it must be a polynomial in J of degree k,

$$Z(q) = \sum_{j=0}^{k} a_i J^i = \sum_n c(k,n) q^n. \tag{2.48}$$

For $k = 1$ we simply have $Z(q) = J(q)$. It has been obtained from modular or Rademacher sum on multiple occasions, see e.g., [65, 74, 72]. The coefficients of $J(q)$ in front of q^n was known to be intimately related to the dimensions of irreducible representations of the monster group $\mathbb{M}$, the largest sporadic group. It has $2^{46} \cdot 3^{20} \cdot 5^9 \cdot 7^6 \cdot 11^2 \cdot 13^3 \cdot 17 \cdot 19 \cdot 23 \cdot 29 \cdot 31 \cdot 41 \cdot 47 \cdot 59 \cdot 71 \approx 8 \times 10^{53}$ group elements and 194 conjugacy classes. Dimensions of the irreducible representations of the monster group can be found in the first column of its character table [75]: 1, 196883, 21296876, 842609326, 18538750076, 19360062527 ....

After John McKay's observation $196884 = 1 + 196883$, Thompson further noticed [76]:

$$\begin{aligned} 21493760 &= 1 + 196883 + 21296876, \\ 864299970 &= 2 \times 1 + 2 \times 196883 + 21296876 + 842609326, \\ 20245856256 &= 2 \times 1 + 3 \times 196883 + 2 \times 21296876 + 842609326 + 19360062527. \end{aligned} \tag{2.49}$$

This phenomenon is dubbed "monstrous moonshine" by Conway and Norton [77], later proved by Borcherds [78].

The author of [51] conjectures that for cosmological constant $k \equiv l/16G \in \mathbb{Z}$, quantum 3d Euclidean pure gravity including BTZ black holes can be completely described by a rational CFT (RCFT) called extremal self-dual CFT (ECFT) with Brown-Henneaux central charge [79] $(c_L, c_R) = (24k, 24k)$, which is factorized into a holomorphic and an anti-holomorphic pieces. An ECFT is a CFT whose lowest dimension of primary field is $k + 1$, and it has a sparsest possible spectrum consistent with modular invariance, presenting a finite mass gap.

The only known example is the $k = 1$ one with a monster symmetry, constructed by Frenkel-Lepowsky-Meurman (FLM) [80] to have partition function as $J(q)$, but its uniqueness has not been proved. The existence of ECFTs with $k > 1$ is conjectured to be true [51] and is still an active open question [81, 82].

In this section we will mainly focus on the $k = 1$ case.

TEE for the Full Partition Function

The modular-invariant partition function is still defined on a solid torus. We will again consider the bipartition that separate the two single-sided black holes, similar to the story in Section 2.4. It is justified in Appendix A.1 that one can still cut $SL(2,\mathbb{Z})$ family of BTZ black holes along their outer horizons, which lie in the core of the solid torus. So one just needs to plug the partition function $J(q)$ into the replica trick formula. At low temperatures, $q = e^{-2\pi\beta}$ is small, so that the full partition function will be dominated by the q^{-1} term with almost trivial thermal entropy and TEE, trivial in the sense that there are no tree-level contributions. At high temperatures, richer physics is allowed. Below we calculate the TEE of the full partition function in this regime.

Generally, the coefficient in front of q^n in the partition function $Z(q)$ for any k can be written as

$$c(k,n) = \sum_{i=0}^{193} \mathbf{m}_i(-k,n) d_i, \tag{2.50}$$

where each d_i is the dimension of the corresponding irreducible representations M_i of $\mathbb{M}$, and $\mathbf{m}_i(-k,n)$ is the multiplicity of the irreducible representation M_i in the decomposition similar to (2.49). It is guaranteed to be a non-negative integer. At large n, $\mathbf{m}_i(-k,n)$ has the following asymptotic form [83],

$$\mathbf{m}_i(-k,n) \sim \frac{d_i |k|^{1/4}}{\sqrt{2}|\mathbb{M}||n|^{3/4}} e^{4\pi\sqrt{|kn|}}. \tag{2.51}$$

Now we restrict to the $k = 1$ case and let n to be a variable. After taking care of the anti-holomorphic part, the replica trick (2.29) gives the following TEE

$$S_{\text{full}}(A) = S_{\text{full}}^{\text{thermal}} = 2\ln J(q) - 2\beta J(q)^{-1} \frac{\partial J(q)}{\partial \beta}. \tag{2.52}$$

Note that this is again the same as the expression for calculation of thermal entropy in the canonical ensemble. (Using $\beta = l/r_+ = 1/\sqrt{M} = 1/\sqrt{n}$, n is viewed as a function of β so the second term in (2.52) is nonzero.) The computation of $S_{A\cup B}$ for the entire $SL(2,\mathbb{Z})$ family of black holes is also similar to that of $M_{1,0}$ calculated in Section 2.4. The result is again equal to the thermal entropy, based on the fact that the $SL(2,\mathbb{Z})$ family of black holes are all solid tori with horizons living in the core. This implies that the system is again in a mixed state due to Euclideanization, as expected in [84, 85]. The mutual information $I(A,B)$ is also the thermal entropy, parallel to the discussion in Section 2.4.

In the high-temperature expansion, we only take the q^n term $J_n(q)$ from the summation in $J(q)$ to calculate TEE because this desired term has a coefficient exponentially larger than those at lower temperatures[7]:

$$J_n(q) = \sum_{i=0}^{193} \frac{d_i^2}{|\mathbb{M}|} \frac{e^{4\pi\sqrt{n}}}{\sqrt{2}n^{3/4}} q^n. \tag{2.53}$$

Mathematically the two copies of d_i in d_i^2 are both the dimension of irreducible module M_i of the monster group, which will be explained in detail later in Section 2.5. But physically they have different origins: one is the contribution from a single M_i as shown in equation (2.50), while the other is probability amplitude for M_i to appear in the summation as in equation (2.51). Namely, there is a correspondence between the partition function $J(q)$ and a pure state in the bulk, which is a superposition of all different M_i's:

$$|\Psi\rangle = \sum_{i=0}^{193} \frac{d_i}{\sqrt{|\mathbb{M}|}} |i, i^*\rangle. \tag{2.54}$$

In analogy to topological phases, the state is a *maximally-entangled state of* 194 *types of "anyons"* labelled by the irreducible representations of the Monster group $\mathbb{M}$. The d_i that appears explicitly in (2.54) corresponds to that in (2.51), whereas $|i, i^*\rangle$ means a quasiparticle-antiquasiparticle pair labeled by M_i and contributes another d_i, which correspond to the one in (2.50). In [86], the authors proposed from abstract category theory, that the ER=EPR realization in the context of TQFT should be exactly of the form (2.54). We will show later that this specific maximally-entangled superposition is the bulk TQFT version of the thermofield double state on the dual CFTs.

Applying to equation (2.53) the identity for finite groups: $\sum_i d_i^2 = |\mathbb{M}|$, we arrive at

$$J_n(q) = \frac{e^{4\pi\sqrt{n}}}{\sqrt{2}n^{3/4}} q^n = \frac{1}{\sqrt{2}} \beta^{3/2} e^{2\pi/\beta}. \tag{2.55}$$

Plugging it into (2.52) and taking into account the anti-holomorphic part, we again recover the Bekenstein-Hawking entropy:

$$S_{\text{full}}(A) = \frac{8\pi}{\beta} + 3\ln\beta - \ln 2 - 3. \tag{2.56}$$

The first three terms agree with Witten's asymptotic formula for Bekenstein-Hawking entropy [51], and provides an additional term -3. Remarkably, the "anyons" become invisible in TEE after the summation over i. This is exactly due to the appearance of the maximally-entangled superposition in equation (2.54). Had we taken another state where only one single M_j appears with probability amplitude 1 and all the others appear with amplitude 0, the corresponding contribution would have been proportional to $\ln\left(d_j/\sqrt{|\mathbb{M}|}\right)$ instead of 0.

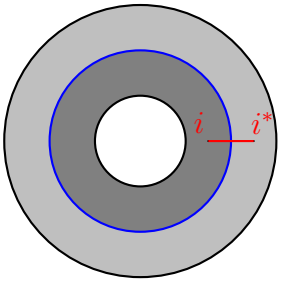

Figure 2.14: Constant time slice of the eternal BTZ black hole as in Figure2.5. The Wilson line corresponding to the quasiparticle-antiquasiparticle pair i, i^* intersects with horizon both on the constant time slice and in the 3d bulk.

The latter matches with the entanglement entropy calculations in [87, 88, 89] for an excited state labeled by j in a rational CFT.[8]

In our case, the creation of the quasiparticle-antiquasiparticle pair i and i^* can be represented by a Wilson line, as shown in Figure 2.14. The Wilson line intersects the non-contractible loop of the solid torus, i.e., the horizon, which is the reason why it can be detected by a cut along the horizon.

To make full understanding of the "anyon" picture, we rewrite state (2.54) as

$$|\Psi\rangle = \frac{1}{\sqrt{J(q)}} \sum_{i=0}^{193} e^{-\frac{\beta}{2}E_i} |i, i^*\rangle, \tag{2.57}$$

where the energy level corresponding to the "anyon" pair i, i^* is described by the quantum dimension of M_i:

$$E_i = -\frac{1}{\beta} \ln \left[\frac{d_i^2}{|\mathbb{M}|} J_n(q) \right]. \tag{2.58}$$

Denoting $|i, i^*\rangle \equiv |i\rangle|i^*\rangle$, one can trace over all the $|i^*\rangle$'s and obtain the reduced density matrix

$$\rho_A = \sum_i e^{-\beta E_i} |i\rangle\langle i|, \tag{2.59}$$

which is just the thermal density matrix for "anyons", and different types of anyons i form an ensemble. Using the expression for energy levels (2.58), the entanglement entropy between the "anyon" pair can be easily calculated as

$$S_\Psi(A) = S^{\text{thermal}}(A) = S_{\text{full}}(A), \tag{2.60}$$

where we have added the anti-holomorphic contribution. Thus the state (2.57) has the similar property as the thermofield double state does, in that the entanglement entropy between the

[7] We will take into account all terms of $J(q)$ in Appendix A.2.

[8] This disappearance of "anyons" in the TEE for a maximally-entangled superposition is also expected in the context of topological phases, see equation (40) of [42], where one takes $|\psi_j|$ there to be d_j/D.

quasiparticle-antiquasiparticle pair is equal to the thermal entropy of one quasiparticle. We call this state in the 3d bulk as the *Moonshine double state*, in which the pair of "anyons" are separated by the horizon, just like the two single-sided black holes L and R are separated by it.

Unfortunately it has a shortcoming: as a pure state, the Moonshine double state above cannot reproduce the result of nonzero $S(A \cup B)$ (2.33). To account for this, one could modify the final total quantum state as

$$\rho = |\tilde{\Psi}\rangle\langle\tilde{\Psi}| \otimes \rho_{\text{th}}, \tag{2.61}$$

where the modified moonshine double state now reads $|\tilde{\Psi}\rangle = \frac{1}{\sqrt[4]{J(q)}} \sum_{i=0}^{193} e^{-\frac{\beta}{2}\tilde{E}_i} |i, i^*\rangle$ with $\tilde{E}_i = -\frac{1}{\beta} \ln \left[\frac{d_i^2}{|\mathbb{M}|} J_n(q)^{1/2} \right]$. These energy levels lead to the partition function $Z(q) = J(q)^{1/2}$. When one bipartites the system into two two single-sided black holes A and B, one can see from straightforward computation that $|\tilde{\Psi}\rangle$ will contribute half of Bekenstein-Hawking entropy. The newly introduced ρ_{th} is purely thermal and exhibits no non-local correlations between A and B, so that its von Neumann entropy is extensive and scales with volume. When one bipartites the system into the two single-sided black holes A and B, it will give half of the Bekenstein-Hawking entropy. Combining the contribution from $|\tilde{\Psi}\rangle$, we recover $S_{\tilde{\Psi}}(A) = S^{\text{thermal}}(A)$, the Bekenstein-Hawking entropy. When considering $S(A \cup B)$, the modified moonshine double state contributes nothing as a pure state, while the result for ρ_{th} is simply $S^{\text{thermal}}(A)$, matching with the calculations in (2.33).

Another caveat is that since $\ln J$ is approximately the Bekenstein-Hawking entropy, the leading term in E_i scales with $-\beta^{-2} \sim -n$. So in order to have a genuine quantum theory, our theory has to have a UV cutoff scale at a certain n. Furthermore, apart from the asymptotic expression (2.51) which gives rise to the tree-level Bekenstein-Hawking entropy, there is the remainder formula [90] for coefficients of q^n in the whole partition function $J(q)$ which is possibly related to the one-loop contribution to TEE. For general $k \in \mathbb{Z}_+$, the remainder formula reads

$$\begin{aligned} c(k,n) = \frac{k e^{4\pi\sqrt{kn}}}{\sqrt{2}(kn)^{3/4}} \Bigg[1 + \sum_{m=1}^{p-1} \frac{(-1)^m (1,m)}{(8\pi\sqrt{kn})^m} + \frac{r_p(kn)}{(kn)^{p/2}} + \frac{\sqrt{2}n^{3/4}}{e^{4\pi\sqrt{n}}} S(k,n) \\ + \frac{1}{k^{1/4}} \sum_{1 \le r < k} \frac{r^{1/4} a_{-r}(k)}{e^{4\pi\sqrt{n}(\sqrt{k}-\sqrt{r})}} \left(1 + \sum_{m=1}^{p-1} \frac{(-1)^m (1,m)}{(8\pi\sqrt{kn})^m} + \frac{r_p(kn)}{(kn)^{p/2}} + \frac{\sqrt{2}n^{3/4}}{e^{4\pi\sqrt{n}}} S(k,n) \right) \Bigg], \end{aligned} \tag{2.62}$$

where $p(x)$ is the integer partition of $x \in \mathbb{Z}_+$, and

$$\begin{aligned} &(1,k) \equiv \prod_{j=0}^{k-1} \frac{4 - (2j+1)^2}{4^k k!}, \quad a_r(k) \equiv p(r+k) - p(r+k-1), \\ &|r_p(n)| \le \frac{|(1,p)|}{\sqrt{2}(4\pi)^p} + 62\sqrt{2} e^{-2\pi\sqrt{n}} n^{p/2}, \quad 0 < \frac{\sqrt{2}n^{3/4}}{e^{4\pi\sqrt{n}}} S(k,n) \le \frac{1}{4}\zeta^2\left(\frac{3}{2}\right) \frac{(rn)^{3/2}}{e^{4\pi\sqrt{rn}}}. \end{aligned} \tag{2.63}$$

To check this claim, one could restrict to the $k = 1$ monstrous case and plug this expression into (2.52). Alternatively one may fix n and view the $c(k, n)$ as the number of possible microstates at fixed energy, i.e., in the micro-canonical ensemble. One then performs a unilateral forward Laplace transform to return to canonical ensemble and then plug it into (2.52). Computations in both methods are in general complicated, and we do not pursue it here.

We provide another perspective towards the loop contribution in Appendix A.2 by plugging in the whole J function instead of only one large n term. We observe that the loop correction is negative, consistent with both the thermal AdS_3 case in Section 2.3 and the BTZ case in Section 2.4.

d_i's as Quantum Dimensions

In this section we provide more mathematical details and show that d_i equals the quantum dimension of the irreducible module M_i of $|\mathbb{M}|$. An ECFT at $k = 1$ is a special vertex operator algebra (VOA) $V^\natural$ whose automorphism group is the Monster group $\mathbb{M}$. This VOA, also known as the moonshine module [80], is an infinite-dimensional graded representation of $\mathbb{M}$ with an explicit grading:

$$V^\natural = \bigoplus_{n=-1}^{\infty} V_n^\natural, \tag{2.64}$$

where every $V_n^\natural$ is an $\mathbb{M}$-module, called a homogeneous subspace. It can be further decomposed into

$$V_n^\natural \simeq \bigoplus_{i=0}^{193} {M_i}^{\oplus \mathbf{m}_i(-1,n)}, \tag{2.65}$$

with M_i labeling the irreducible $\mathbb{M}$-modules, and $\mathbf{m}_i(-1, n)$ is the multiplicity of M_i. This is the same multiplicity that appears in (2.50). (For ECFTs with general k, we have a tower of moonshine modules [83] $V^{(-k)} = \bigoplus_{n=-k}^{\infty} V_n^{(-k)}$, where $V_n^{(-k)}$'s are all irreducible $\mathbb{M}$-modules. For each summand, one can similarly define $\mathbf{m}_i(-k, n)$ as the multiplicity of the $\mathbb{M}$-modules M_i in $V_n^{(-k)}$, so that $V_n^{(-k)} \simeq \bigoplus_{i=0}^{193} M_i^{\oplus \mathbf{m}_i(-k,n)}$.)

Since we restrict to the holomorphic part of $Z(\tau, \overline{\tau})$ in this section, the entire dual CFT contains the ECFT above as a holomorphic piece. Furthermore, it is diagonal, i.e., its Hilbert space is a graded sum of tensor products of holomorphic and anti-holomorphic sectors:

$$\mathcal{H} \cong \bigoplus_{\alpha \in \mathbb{C}} \mathcal{M}_\alpha \otimes \overline{\mathcal{M}}_\alpha, \tag{2.66}$$

where $\mathcal{M}_\alpha$ and $\overline{\mathcal{M}}_\alpha$ are indecomposable representations of right and left Virasoro algebras. Since Virasoro action is built into the VOA axioms [91], these are also modules of the right and left monstrous VOAs, so $V^\natural$ admits induced representations from representations of the Virasoro algebra [92]. Obviously there are infinite number of Virasoro primaries, and $V^\natural$ is

not an RCFT in this sense. However, $V^\natural$ is a typical example of a holomorphic/self-dual VOA, i.e., there is only one single irreducible $V^\natural$-module which is itself. Knowing that there is only one VOA-primary, one can reorganize Virasoro fields in $\mathcal{M}_\alpha$ and $\overline{\mathcal{M}}_\alpha$ into irreducible representations of $V^\natural$, by introducing the graded dimension of the $V^\natural$-module N, defined as

$$\mathrm{ch}_q N \equiv \mathrm{tr}_N q^{L_0} = \sum_{n=0}^{\infty} \dim N_n q^n, \tag{2.67}$$

where L_0 is the usual Virasoro generator and N_n's are homogeneous subspaces of N labelled by eigenvalues of L_0. (Note that we have omitted the overall prefactor $q^{-c/24}$ often appeared in literature.) The above procedure is similar to regrouping an infinite number of Virasoro primaries in WZW models into finite Kac-Moody primaries.

To explain the d_i appearing in (2.53), it is natural to consider quantum dimensions associated to $V^{\mathbb{M}}$ consisted of fixed points of the action by $\mathbb{M}$ on $V^\natural$. By theorem 6.1 in [93], we have the following decomposition of $V^\natural$

$$V^\natural \simeq \bigoplus_{i=1}^{194} V_i^{\mathbb{M}} \otimes M_i \tag{2.68}$$

as $V^{\mathbb{M}} \times \mathbb{M}$-modules, for the 194 $V^{\mathbb{M}}$-submodules $V_i^{\mathbb{M}}$ in $V^\natural$ with $V^{\mathbb{M}} = V_1^{\mathbb{M}}$, where M_i denotes an irreducible module for $\mathbb{M}$ with character d_i. This $V^{\mathbb{M}}$ is a sub-VOA of $V^\natural$ of CFT type [94], and is called the *monster orbifold*, because it is obtained from orbifolding $V^\natural$ by its automorphism group $\mathbb{M}$ [95], in the same sense as orbifolding the Leech lattice VOA by $\mathbb{Z}/2\mathbb{Z}$ in the FLM construction.

The standard definition of the quantum dimension of a VOA-module N with respect to a general VOA V is [93]

$$\mathrm{qdim}_V N = \lim_{q\to 1^-} \frac{\mathrm{ch}_q N}{\mathrm{ch}_q V}. \tag{2.69}$$

The quantum dimensions of submodules of orbifold VOA V^G obtained from orbifolding V by a subgroup $G \subseteq \mathrm{Aut}(V)$ only recently found their applications in quantum Galois theory [93]. In our case, the quantum dimensions of all $V_i^{\mathbb{M}}$'s with respect to $V^{\mathbb{M}}$ were first calculated to be $\mathrm{qdim}_{V^{\mathbb{M}}} V_i^{\mathbb{M}} = d_i$ in [83], using the asymptotic formula for multiplicities of $\mathbb{M}$-modules M_i in Fourier coefficients of j-invariant, bypassing the knowledge of $V^{\mathbb{M}}$'s rationality, which is still only conjectured to be true.

The remaining question is to define in parallel a quantum dimension for the the $\mathbb{M}$-modules in the above pair $\left(V_i^{\mathbb{M}}, M_i\right)$. The definition (2.69) does not directly apply to an $\mathbb{M}$-module, but one can extend the definition using the n-graded dimension of $\mathbb{M}$-modules M_i's. We define $\mathrm{ch}_q M_i$ as [9]

$$\mathrm{ch}_q M_i \equiv \sum_\sigma j_\sigma \cdot \overline{\chi_i(\sigma)}. \tag{2.70}$$

[9] We are deeply grateful to Richard E. Borcherds for suggesting this alternative formula. It is similar to the generating function of multiplicity $\mathbf{m}_i(-1, n)$ in Section 8.6 of [83], but without normalization by $1/|\mathbb{M}|$.

Here $j_\sigma \equiv \sum_{n=-1}^{\infty} \chi_{V_n^\natural}(\sigma) q^n$ is the monstrous McKay-Thompson series for each σ as well as the unique Hauptmodul for a genus-0 subgroup Γ_σ of $SL(2,\mathbb{R})$ for each σ [77, 78]. σ belongs to an index set with order 171, deduced from the 194 conjugacy classes of $\mathbb{M}$. The difference $194 - 171 = 23$ can be understood from the one-to-one correspondence between conjugacy classes and irreducible representations of $\mathbb{M}$: most of the 194 irreducible representations have distinct dimensions, except for 23 coincidences. σ's are only sensitive to the dimensions of the corresponding irreducible representations. $\overline{\chi_i(\sigma)}$ is complex conjugation of the character of the irreducible representation M_i of the 171 "conjugacy classes" σ.[10] At large n, summation in $\mathrm{ch}_q M_i$ is dominated by the first Hauptmodul for the identity element of $\mathbb{M}$, which is exactly the Klein's invariant $j(q)$, so that

$$\lim_{q\to 1^-} \mathrm{ch}_q M_i \approx j(q) \times d_i. \tag{2.71}$$

In other words, one can view $\mathrm{ch}_q M_i$ as a function $\mathrm{ch}_q M_i(g)$ on group $\mathbb{M}$, and when defining the quantum dimension in (2.70), we take the value when its argument is the identity element.

With this, we can define the quantum dimension of $\mathbb{M}$-modules M_i in (2.65) relative to $V^\natural$ as

$$\mathrm{qdim}_{V^\natural} M_i \equiv \lim_{q\to 1^-} \frac{\mathrm{ch}_q M_i}{\mathrm{ch}_q V^\natural} = \lim_{n\to\infty} \frac{\dim (M_i)_n}{\dim V_n^\natural}. \tag{2.72}$$

Here $\mathrm{ch}_q V^\natural = J(q)$ by applying (2.69) to $V^\natural$, which is a $V^\natural$-module of itself. Combining the discussions above, the quantum dimension is just

$$\mathrm{qdim}_{V^\natural} M_i = d_i. \tag{2.73}$$

The d_i's that appeared explicitly in (2.53) of the TEE calculation are quantum dimensions of M_i, while those in (2.51) are quantum dimensions of $V_i^{\mathbb{M}}$. They coincide numerically. As we mentioned before, the rationality of $V^{\mathbb{M}}$ is widely conjectured to be true[11], and by a theorem of Huang [98], the module category of any rational, C_2-cofinite VOA is modular, i.e., it is a modular tensor category with a non-degenerate $\mathcal{S}$-matrix [99, 100]. If one believes in the *rationality conjecture*, then $\mathrm{qdim}_{V^{\mathbb{M}}} V_i^{\mathbb{M}}$'s have a well-defined interpretation in terms of modular $\mathcal{S}$-matrices of the orbifold CFT $V^{\mathbb{M}}$:

$$d_i = S_{i0}/S_{00}. \tag{2.74}$$

Note that these 194 "anyons" are the pure charge exitations in the corresponding topological ordered system described by the modular tensor category associated with the orbifold VOA $V^{\mathbb{M}}$.

[10] In literature this is often denoted by $\overline{\mathrm{tr}(\sigma|M_i)}$ or $\overline{\mathrm{tr}(M_i(\sigma))}$ or $\overline{\mathrm{ch}_{M_i}(\sigma)}$ as well.

[11] Unfortunately, the conjecture has only been proved only when the subgroup of the automorphism group is solvable [96, 97], which is not our case.

2.6 Discussion and outlook

In the high-temperature regime, the full modular-invariant partition function (2.46) is dominated by the black hole solution $Z_{1,0}(\tau)$, while in the low-temperature regime, it is dominated by $Z_{0,1}(\tau)$, the thermal AdS_3 solution [65, 5]. It is widely believed that there exists a Hawking-Page [101, 102] transition at the critical temperature $\beta \sim 1$, or $r_+ \sim l$. However, there is no consensus on whether this transition really exists [5, 103, 104], or if it exists, whether it is a first-order or a continuous phase transition [105, 106, 107, 108, 109, 110], or something else that is more subtle. In this section we offer a clue from the TEE perspective.

We compare the $a = 1$ (defined in Figure 2.1) case in (2.12) of thermal AdS_3 and the Figure 2.9 case of a single-sided black hole, for their subregion A's both cover the whole space. One then observes that even at the tree level, TEE of BTZ and thermal AdS_3 have different signs. A natural guess would thus be that, if the transition exists, it should be topological and happen at where the TEE changes sign.

Our definition of topological entanglement entropy is the constant subleading term in the expression for entanglement entropy, which is in general different from the tripartite information as used in [17]. For topological phases in condensed matter physics, these two formulations differ by a factor of two and are both negative. For gravitational theories in the bulk, our topological entanglement entropies can be either positive (as in BTZ black hole case) or negative (as in the thermal AdS_3 case). To calculate the tripartite information, one can use the surgery method presented in this chapter and find its time dependence, which at late times is negative of the Bekenstein-Hawking entropy [111]. This matches with the results in CFTs with gravitational duals, it is expected that the tripartite information should be negative [112] and that for thermofield double state, it equals the negative of the Bekenstein-Hawking entropy [19].

Quantum dimensions also appears in the calculation of left-right entanglement in RCFT [113]. One might perform similar computations in the orbifold VOA $V^{\mathbb{M}}$ appeared in Section 2.5, by using the Ishibashi boundary CFT states that were constructed in [114] for open bosonic strings ending on D-branes.

Given the "anyonic" interpretation in Section 2.5, one natural question to ask is that, to what extent 3d pure quantum gravity can be described as a theory of topological order. Naïvely one would expect the corresponding topological order to be the 3d Dijkgraaf-Witten theory of the monster group $\mathbb{M}$, which gives rise to the same modular tensor category as the one given by orbifold CFT $V^{\mathbb{M}}$ as explained in Section 2.5. On the other hand, it is also natural to expect the corresponding topological order to be the one which is effectively described by the double $SL(2,\mathbb{C})$ Chern-Simons theory. It would be highly non-trivial to find a mechanism that reconciles these two theories.

Another remark is that we have specified the bipartitions to be done at $t = 0$ in Section 2.4, while in general the result can be time-dependent. In the latter case one can still use the surgery method proposed in this chapter to find the TEE or Rényi entropies, which can serve as an indicator of scrambling [115, 116].

A final mathematically motivated direction is the following. Vaughn Jones considered

how one von Neumann algebra can be embedded in another and developed the subfactor theory [117]. In general, the Jones program is about how to embed one *infinite* object into another, reminiscent of field extensions in abstract algebra, and quantum dimension is defined exactly in this spirit. It would be interesting to see how subfactor theory in general can help connect topological phases and pure quantum gravity [118].

Chapter 3

Establishing strongly-coupled 3d AdS quantum gravity with Ising dual using all-genus partition functions

3.1 Introduction and summary of results

A way of looking at 3d pure gravity with negative cosmological constant using partition functions and modular properties was initiated in work by Dijkgraaf et al. [65], Witten [51], and Maloney and Witten [5]. In a pioneering paper [119], Castro et al. argued that two well-known Conformal Field Theories (CFT) in two-dimensional space time, i.e., Ising and tricritical Ising minimal models [120, 121], are dual to pure Einstein quantum gravity in three-dimensional spacetime with negative cosmological constant, i.e., in Anti-de Sitter spacetime (AdS_3).[1] These are theories of strongly-coupled gravity where the AdS radius l is of the order of the Planck scale. The arguments provided by Castro et al. in support of these dualities at the corresponding values of the Brown-Henneaux [79] central charges $c = 3l/2G$ (G is the 3d Newton constant) consisted in demonstrating a match between the gravity partition function of Euclidean AdS_3 spacetime when its asymptotic boundary is a 2d torus T^2, with the torus partition function of the corresponding 2d minimal model CFT.

To be specific, one can think of the finite-temperature partition function of pure Einstein gravity in Euclidean AdS_3 as being written as a path integral. The latter is formally a sum over every smooth 3-manifold X whose asymptotic boundary is a torus T^2,

$$Z_{\rm grav}(\tau,\bar\tau) = \int_{\partial X = T^2} \mathcal{D}g_{\mu\nu}\; e^{-c\; S_E[g_{\mu\nu}]}, \tag{3.1}$$

with τ the conformal structure parameter of the boundary torus, the Brown-Henneaux central charge $c = 3l/2G$ playing the role of the inverse gravity coupling constant (large in

[1] In the same paper similar arguments are also presented for certain versions of theories of higher spin quantum gravity. See also Footnote 3.

the semi-classical regime). $S_E[g_{\mu\nu}]$ is the Einstein-Hilbert action with $g_{\mu\nu}$ the complete Riemannian metric tensor on X. One will need to both sum over all different geometries of the bulk 3-manifold X with the same equivalence class of conformal structures (i.e., the same conformal class) on the boundary torus, as well as integrate over all different boundary metrics connected by small diffeomorphisms, i.e., those isotopic to the identity. The *full* gravitational path integral can then be written as

$$Z_{\text{grav}} = \sum_{X \ (\text{where } \partial X = T^2)} Z(X, \tau), \tag{3.2}$$

where $Z(X, \tau)$ denotes the contribution from the sum over all metrics related by small diffeomorphisms on a particular 3-manifold X with a fixed conformal structure parameter τ on the asymptotic torus boundary, while the summation over X means summing over different τ's in the same conformal class.

In the semi-classical (large c) limit, the smooth 3-manifolds X contributing to the path integral turn out to be only those which admit classical solutions, i.e., which are saddle points[2] of the Einstein-Hilbert action $S_E[g]$, and only solid tori are commonly considered, see [5, 64, 65]. Following the logic pursued in previous work [51, 65, 119] on this problem, the gravitational path integral can then be thought of as being organized as a sum over classical solutions, along with a *full* treatment of *all* quantum fluctuations around each saddle point. For the case of solid tori X, different saddles correspond to inequivalent ways of filling in the bulk X of the boundary torus T^2, and are related to each other by $SL(2, \mathbb{Z})$ modular transformations. The gravity partition function (3.2) can then be obtained as the sum of inequivalent images of a certain "vacuum seed" partition function in Euclidean AdS_3 under the action of $SL(2, \mathbb{Z})$. Physically, this "vacuum seed" describes the gravitational partition function of thermal AdS_3 where the spatial cycle of the boundary torus T^2 is contractible in the bulk, whereas the cycle of Euclidean time is not. This corresponds to a particular solid torus X, for example see Figure 3.1. As argued in [119], the gravitational "vacuum seed" partition function can be obtained exactly by using the remarkable and fundamental results of Brown and Henneaux [79]; this is reviewed in Section 3.2 below, and the result summarized in the next paragraph. After action on the "vacuum seed" gravitational partition function with a non-trivial modular transformation, the spatial cycle may no longer be contractible in the bulk while the temporal cycle may now be; in that case the corresponding gravitational partition function describes physically that of a BTZ black hole [45]. The sum over modular transformations in $SL(2, \mathbb{Z})$ appearing in (3.2) can also be seen to originate from general coordinate invariance, independent of invoking semi-classical notions such as saddle points, because non-trivial modular transformations correspond to large diffeomorphisms, not continuously connected to the identity; in the gravitational path integral for

[2]One main conclusion of [5] is that in the weak-coupling/semiclassical regime, one has to include geometries corresponding to *complex* saddle points of $S_E[g]$ in order to have a Hilbert space interpretation of the gravity theory. However, since here we are only concerned with the strongly coupled regime, we are not bound by these considerations.

the "vacuum seed" partition function, on the other hand, these large diffeomorphisms are thought to be excluded. (This complementary point of view was also stressed in [119].)

As was argued in [119], with certain assumptions the gravitational "vacuum seed" partition function turns out to be precisely equal to the vacuum character of the dual CFT. Furthermore, owing to the fact that the vacuum character of rational CFTs is invariant under a certain finite index subgroup of the modular group $SL(2,\mathbb{Z})$ [122, 123], the modular sum in (3.2) over the infinite group $SL(2,\mathbb{Z})$ of modular transformations reduces in fact to the sum over a finite number of right cosets of that finite index subgroup in $SL(2,\mathbb{Z})$ when the Brown-Henneaux central charge c is equal to that of a unitary conformal minimal model CFT [120, 121]. For Brown-Henneaux central charge $c = 1/2$, the resulting finite sum was shown in [119] to be proportional to the partition function of the 2d Ising CFT on the torus T^2.

Based on the above analysis of solid tori X, Castro et al. argued in [119] that amongst all [120, 121] the unitary Virasoro minimal models with central charge $c < 1$, only the Ising and tricritical Ising CFTs are dual to pure Einstein gravity at the corresponding values of the Brown-Henneaux central charge.[3] A possible gravitational explanation of this observation could be as follows: It turns out that amongst all unitary Virasoro minimal CFTs with central charge $c < 1$, only the Ising and tricritical Ising CFTs satisfy the condition that the conformal weights h of all non-trivial primary states are larger than $c/24$. In CFTs with large central charge c, this inequality describes a necessary condition that a primary state of conformal weight h can be interpreted as being dual to a black hole [126]. Assuming that this condition is still valid in the strong-coupling regime where c is not large, Ising and tricritical Ising would be the only unitary minimal model CFTs with $c < 1$ in which all primary states can be interpreted as being dual to black holes. All other $c < 1$ unitary minimal model CFTs would then contain, in addition to black holes, other primary *matter* fields, and these CFTs could thus not be dual to pure Einstein gravity. (We will come back in Appendix A.3 to the interpretation of primary states in the Ising CFT as states dual to black holes in strongly-coupled Einstein gravity, by suggesting a possible expression for their Bekenstein-Hawking entropy.)

The focus of the present chapter is pure Einstein quantum gravity on Euclidean 3-manifolds X whose asymptotic boundaries ∂X are *higher-genus* Riemann surfaces. This arises physically because 3-manifolds X whose boundaries are Riemann surfaces of higher

[3]Some of the $\mathcal{W}_N$ minimal models, were also conjectured in [119] to be possibly dual to higher-spin gravity theories instead of being dual to pure Einstein gravity. This is due to the existence of an extended chiral conformal algebra, generated by conserved currents possessing (conformal) spins with values ranging from 3 up to N. These currents generalize the spin-2 stress-energy tensor $T_{\mu\nu}$ which generates "pure graviton" excitations in the pure Einstein gravity discussed in Section 3.2, and lead to a "truncated version" of higher spin Vasiliev gravity, the latter containing generalized graviton excitations of arbitrary integer spin (see, e.g., [124, 125]). As it is well known, the presence of extended chiral conformal algebras can lead to multiple modular invariants in 2d CFTs, but by extending the "vacuum seed" to the vacuum representation of the extended chiral algebra, a single modular invariant can be built, and generalizations to higher spin gravity of the Virasoro arguments leading to Ising and Tricritical Ising are possible as described in [119] based on genus-one considerations.

genus $g \geq 2$, are known [52, 54, 56, 127, 128, 129, 130] to be the Euclidean spacetimes corresponding to multi-boundary wormholes in Lorentzian signature. X is commonly restricted to handlebodies, and we will follow this assumption here; more complicated saddles such as non-handlebodies were studied in [131] in the semi-classical regime. We plan to come back to this issue in future work. There is a variety of interesting and important physical questions related to such multi-boundary wormholes (see, e.g., [69] for a relatively recent discussion), and a complete description of the duality between 3d quantum gravity and the associated 2d CFT at the asymptotic boundary must include all those spacetimes. In other words, any proposed duality must also be valid in any such multi-boundary wormhole spacetime. For that reason, it is important to investigate the duality between quantum gravity in AdS_3 and the CFT on the asymptotic boundary at higher genus $g \geq 2$.

For the gravitational partition function at general genus g, there is again formally a sum over geometries of the smooth handlebody X and over its boundary geometries

$$Z_{\text{grav}}(\Omega, \bar{\Omega}) = \int_{\partial X = \Sigma_g} \mathcal{D} g_{\mu\nu} \; e^{-c \; S_E[g_{\mu\nu}]}, \tag{3.3}$$

where the "period matrix" Ω, a $g \times g$-dimensional symmetric complex matrix, completely parametrizes the conformal structure of the genus g Riemann surface Σ_g constituting the boundary of X. The gravitational path integral can then again be written in the form

$$Z_{\text{grav}} = \sum_{X \;\; (\text{where } \partial X = \Sigma_g)} Z(X, \Omega), \tag{3.4}$$

where $Z(X, \Omega)$ stands for the contribution from the sum over all metrics connected by small diffeomorphisms on a particular smooth handlebody X with a fixed period matrix Ω on its asymptotic boundary Σ_g, while the summation over X means summing over different period matrices Ω in the same conformal class.

Different Euclidean saddles can be constructed by specifying which cycles of the Riemann surface Σ_g are contractible in the interior of the 3-manifold X, and such cycles are mapped into each other under the action of the mapping class group (MCG) Γ_g of the Riemann surface Σ_g. To compute the gravitational path integral in (3.4), our strategy is analogous to the torus case: We again start with the contribution from a certain gravitational "vacuum seed" partition function $Z_{\text{vac}}(\Omega, \bar{\Omega})$ corresponding to the trivial saddle and perform a modular sum to write the complete partition function in (3.4) in the following more explicit form

$$Z_{\text{grav}}(\Omega, \bar{\Omega}) = \sum_{\gamma \in \Gamma_c \backslash \Gamma_g} Z_{\text{vac}}(\gamma\Omega, \bar{\gamma}\bar{\Omega}). \tag{3.5}$$

Here, Γ_c denotes the subgroup of the MCG Γ_g of the Riemann surface Σ_g (the latter being an infinite group) which leaves the "vacuum seed partition function" $Z_{\text{vac}}(\Omega, \bar{\Omega})$ invariant, and $\Gamma_c \backslash \Gamma_g$ is the right coset space; it is over this coset space that the sum in (3.5) is performed. Whether this sum has an infinite or a finite number of terms depends in general (a): on the

value of the Brown-Henneaux central charge, and (b): on the genus g. When the sum is infinite, there is no natural procedure to associate a value to it.[4] In this chapter, we show that for all theories of pure Einstein gravity in AdS_3 with Brown-Henneaux central charge $c < 1$, this sum is finite and unique *only* when $c = 1/2$, corresponding to the dual CFT at the asymptotic boundary to be the Ising CFT. Therefore we argue that in the strong-coupling regime of Brown-Henneaux central charge $c = 3l/2G < 1$, pure Einstein gravity is only dual to a 2d CFT if $c = 1/2$.

We arrive at this conclusion by extending the results obtained for genus one by Castro et al. [119]. Recall that, as mentioned above, Castro et al. argued solely based on genus-one considerations that the only 2d CFTs with central charge $c < 1$ that can be dual to pure Einstein gravity in AdS_3 at the corresponding Brown-Henneaux central charges are the Ising and the Tricritical Ising CFTs of central charges $c = 1/2$ and $c = 7/10$, respectively. The results we obtain in the present chapter, based on consideration of *arbitrary* genus g, are two-fold:

(i) *For Brown-Henneaux central charge* $c = 1/2$. After first identifying the gravitational genus-g "vacuum seed" partition function, we observe that the orbit of the vacuum seed under the MCG action is dictated by a projective representation ρ_g of the MCG Γ_g that is identical to the projective representation induced by the holomorphic conformal blocks of the 2d Ising CFT. We then show, using the properties of ρ_g, that the action of the MCG Γ_g on the vacuum seed generates an orbit that is always a finite set for any genus g and, hence, leads only to a *finite* sum in (3.5). We further prove that this projective representation ρ_g is *irreducible*, which, by Schur's Lemma, leads to the conclusion that the finite sum in (3.5) for the gravitational partition function is unique, and is precisely proportional to the partition function of the 2d Ising CFT.[5] The key mathematical results that we prove in this chapter and that underlie our physics conclusions on the quantum gravity partition function at $c = 1/2$ are: (1) The representation ρ_g, when viewed as a mapping from the MCG Γ_g to a unitary group, has a *finite* image set for any genus g, and (2) the projective representation ρ_g of the MCG Γ_g is always *irreducible* for any genus g. These results are obtained by exploiting the connection between the 2d Ising CFT and the 3d Ising topological quantum field theory (TQFT). We first provide a simplified discussion on these results in Section 3.3 for the genus-two case, and continue with the discussion of the general genus g case in Section 3.4.

(ii) *For Brown-Henneaux central charge* $c = 7/10$. While the genus-one considerations

[4] A natural regularization scheme would require a probability measure on the (infinite) MCG that is also invariant under "translations" (i.e., under group multiplications). A group with such a translation-invariant measure that is further finitely additive (the measure of a finite disjoint union of sets is the sum of the measures of these sets) is called amenable. All MCGs are non-amenable as they contain non-abelian free groups as subgroups. Subgroups of amenable groups are amenable and non-abelian free groups are known to be non-amenable. It follows that there are no natural regularization schemes to sum over MCGs in this sense. However, this theorem does not apply to summations over cosets such as the regularized sum considered for genus one in [5]. It is not clear how to generalize their treatment to higher genus at the current stage.

[5] The physical significance of the factor of proportionality is not entirely clear at this point.

by Castro et al. [119] would permit the conclusion that pure Einstein gravity in AdS_3 at $c = 7/10$ is dual to the 2d Tricritical Ising CFT at the asymptotic boundary, their arguments do not carry over to higher genus $g \geq 2$. (As discussed above, consideration of arbitrary genus is necessary for a complete description of a duality.) We arrive at this conclusion by considering the 3d TQFT related to the 2d Tricritical Ising CFT at $c = 7/10$. We show that, at Brown-Henneaux central charge $c = 7/10$, the sum occurring in the $g \geq 2$ gravitational partition function (3.5) has an infinite number of terms and cannot be naturally regularized, as explained in Footnote 4. A detailed discussion will be provided in Section 3.4.

The remainder of this chapter is organized as follows. In Section 3.2, we review the torus case. Section 3.3 presents a discussion of the genus-two case, while Section 3.4 presents a complete discussion and proof for general genus g, which is independent of the previous section and is more mathematically involved. The difficulty in extending to the Tricritical Ising case is discussed in more detail at the end of Section 3.4. Several Appendices spell out various details. In the last appendix A.3, the duality is used to compute the gravitational entropy and we find a resemblance to the topological correction to the entanglement entropy occurring in the context of topological phases of matter.

3.2 Gravitational partition function with torus asymptotic boundary

The simplest Euclidean smooth 3-manifold X that contributes to the sum in (3.2) is that of thermal AdS_3, topologically a solid torus. It is described in the semi-classical limit ($c \gg 1$) by the following metric

$$ds^2 = l^2 \left(d\rho^2 + \cosh^2 \rho \; dt_E^2 + \sinh^2 \rho \; d\phi^2 \right), \tag{3.6}$$

where $\phi \sim \phi + 2\pi$ denotes a spatial cycle which is contractible in the bulk of X, and the Euclidean time t_E parametrizes a non-contractible cycle. Defining $z = -t_E + i\phi$, the complex coordinate z parametrizes points on the asymptotic boundary ($\rho \to \infty$) of X, and it is periodically identified according to

$$z \sim z + 2\pi i n \sim z + 2\pi i m\tau, \;\; m, n \in \mathbb{Z}, \tag{3.7}$$

where the first identification is automatic (due to the periodicity of ϕ), while the second is to construct the thermal AdS_3 space-time, and τ is the complex parameter specifying the conformal structure of the boundary torus. Large diffeomorphisms, i.e., elements of the MCG, act on this conformal structure parameter as

$$\tau \to \gamma \cdot \tau = \frac{a\tau + b}{c\tau + d}, \quad \gamma = \begin{pmatrix} a & b \\ c & d \end{pmatrix} \in SL(2, \mathbb{Z}). \tag{3.8}$$

Note that the large diffeomorphisms do not change the conformal structure on the boundary torus. Therefore, all conformal structure parameters $\gamma \cdot \tau$ with $\gamma \in SL(2, \mathbb{Z})$ (in other words,

all τ's related to each other by the MCG) specify the same conformal structure. Each of $\gamma\tau$ gives a classical Euclidean solution to the Einstein's equation [64], i.e., a valid saddle point of (3.1). These may or may not be different saddle points depending on the choice of γ. For example, the combination $a = 0$, $b = 1$, $c = -1$, $d = 0$ realizes a modular S transformation, which maps $\tau \mapsto -1/\tau$ and the resultant saddle is the Euclidean BTZ black hole [45]. It is related to thermal AdS_3 by exchanging the spatial and temporal cycles, consistent with the defining feature of a Euclidean BTZ black hole - the existence of a a temporal cycle contractible in the bulk. It was shown in [5] that the only smooth solutions to the equation of motion with torus boundary conditions are the ones above, but not all these solutions labeled by γ are inequivalent. Specifically, an overall sign flip of a, b, c, d does not change the saddle, neither does a constant integer shift $(a, b) \to (a, b) + n(c, d)$ generated by the modular T transformation. Physically, the latter observation corresponds to the fact that adding a contractible cycle to a non-contractible cycle leaves the non-contractible cycle still non-contractible. We denote the subgroup of $SL(2, \mathbb{Z})$ generated by T by Γ_∞. So in the semi-classical regime, different saddles are labeled by different right cosets of Γ_∞ in $SL(2, \mathbb{Z})$, or equivalently by integers (c, d) corresponding to solid tori $M_{c,d}$. Notice that all solid tori $M_{c,d}$ share the same hyperbolic metric (3.6), because by a famous theorem of Sullivan [132, 133, 134], for a fixed conformal class of the asymptotic boundary, the bulk is a *unique* smooth and infinite-volume hyperbolic 3-manifold, with a rigid complete metric.

These saddle-point Euclidean spacetimes $M_{c,d}$ can be obtained from the corresponding Lorentzian ones via analytical continuation, which amounts to taking the Schottky double of its Lorentzian $t = 0$ constant time slice [56, 129]. The Schottky double of a surface is essentially two copies of the surface glued along their boundaries, i.e., a closed surface. (For a surface without a boundary, the Schottky double is two disconnected copies of the surface, with all moduli replaced by their complex conjugates in the second copy.) In Figure 3.1, we depict the examples of Euclidean thermal AdS_3 with $(c, d) = (0, 1)$ and the Euclidean BTZ black hole $(c, d) = (1, 0)$, as well as their constant time slices. Both are non-rotating[6] and possess an equal time $t = 0$ surface with a $\mathbb{Z}_2$ time-reversal symmetry.

It turns out that in the strongly coupled regime, Γ_∞ is enhanced to a larger group Γ_c (a "new gauge symmetry") [119], which is a finite index subgroup of $SL(2, \mathbb{Z})$. Hence the inequivalent manifolds X are then labeled by right cosets $\gamma \in \Gamma_c \backslash SL(2, \mathbb{Z}) \equiv \Gamma$ and one can write

$$Z_{\text{grav}}(\tau, \bar{\tau}) = \sum_{\gamma \in \Gamma} Z_{\text{vac}}(\gamma\tau, \gamma\bar{\tau}), \tag{3.9}$$

where Z_{vac} is the partition function of the "vacuum seed", by which we here mean here that of thermal AdS_3 spacetime.

[6]For a definition see Appendix A.4.

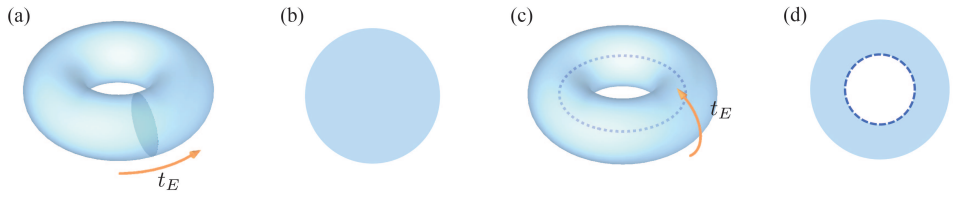

Figure 3.1: From left to right: (a) Geometry for Euclidean thermal AdS_3, with time going along the longitudinal direction; (b) The constant time slice of (a) is a disk; (c) Geometry for Euclidean BTZ black hole, with the event horizon being the dashed line in the core of the solid torus; (d) Constant time slice of (c) is an annulus,where the inner boundary is the event horizon.

Vacuum seed

To compute $Z_{\text{vac}}(\tau, \bar{\tau})$, one needs to evaluate in the path integral (3.1) the contribution from metrics that are continuously connected to thermal AdS_3. In this subsection (and only here), we temporarily resort to Lorentzian signature for convenience. These metrics differ from that of empty AdS_3, the Lorentzian counterpart of the Euclidean thermal AdS_3, by small diffeomorphisms that preserve the Brown-Henneaux boundary conditions

$$ds^2 \sim l^2 \left[d\rho^2 + \frac{1}{4} e^{2\rho}(-dt^2 + d\phi^2) + O(\rho^0) \right] \tag{3.10}$$

at large ρ.

The classical phase space of the theory is the same as the configuration space of all classical excitations that are continuously connected to the global AdS_3 ground state metric (3.6). Brown and Henneaux [79] observed[7] that the phase space charges $H(\zeta_n)$ corresponding to such small diffeomorphisms ζ_n satisfy the Virasoro algebra

$$i\{H[\zeta_n], H[\zeta_m]\} = (n-m)H[\zeta_{m+n}] + \frac{c}{12} n(n^2-1)\delta_{n,-m}, \tag{3.11}$$

with central charge $c = 3l/2G$ and $\{\cdot,\cdot\}$ is the Dirac braket. Acting on the ground state with these charge operators, one obtains the boundary graviton states, whose norms $||\zeta||^2 = \{H[\zeta^*], H[\zeta]\}$ must be positive. Upon performing canonical quantization as proposed in [79, 119], Dirac brackets are promoted to commutators, while charge operators are promoted to operators representing the generators of the Virasoro algebra,

$$L_n \equiv H[\zeta_n], \quad \bar{L}_n \equiv H[\bar{\zeta}_n]. \tag{3.12}$$

Then the vacuum state is annihilated by L_0 and $\bar{L}_0$, as well as other Virasoro lowering operators. This state corresponds semi-classically to empty Lorentzian AdS_3. The conformal

[7] See also, e.g., the compact review in [126].

symmetry constrains the theory strongly, and the boundary gravitons are described by the states obtained by acting with chains of Virasoro raising operators on the vacuum, i.e., these are the descendant states $L_{-n_1}\cdots L_{-n_k}|0\rangle$, with $n_i > 1$. Our desired partition function Z_{vac} is then the generating function that counts these states.

In the strongly coupled regime of Brown-Henneaux central charge $c < 1$, the requirement of unitarity constrains the central charge to the values $c = 1 - 6/m(m+1)$ corresponding to the 'Virasoro minimal model' CFTs, where m is an integer larger than two. Furthermore, eliminating the null states gives the vacuum (identity) character of an irreducible highest-weight representation of the Virasoro algebra (see for example [135]),

$$Z_{\text{vac},\, g=1} = \text{Tr}_{\text{vac}}\; q^{L_0}\bar{q}^{\bar{L}_0} = |\chi_{1,1}(\tau)|^2, \quad \text{where } q = e^{2\pi i\tau}. \tag{3.13}$$

Here the subscript r, s of a general character $\chi_{r,s}$ denotes indices of the Kac table that label all possible irreducible representations of the Virasoro algebra at this central charge (where $r = 1, 2, ..., m-1$ and $s = 1, 2, ..., m$), and[8]

$$\chi_{r,s} = \frac{q^{(1-c)/24}}{\eta(\tau)}\left[q^{h_{r,s}} + \sum_{l=1}^{\infty}(-1)^l\left(q^{h_{r+lm,s(-1)^l+(m+1)[1-(-1)^l]/2}} + q^{h_{r,s(-1)^l+l(m+1)+(m+1)[1-(-1)^l]/2}}\right)\right], \tag{3.14}$$

with $\eta(\tau) = q^{1/24}\prod_{n=1}^{\infty}(1-q^n)$ the Dedekind eta function and the highest weight $h_{r,s}$ given by

$$h_{r,s} = \frac{[(m+1)r - ms]^2 - 1}{4m(m+1)}. \tag{3.15}$$

Modular sum and duality to the Ising CFT

The simplest minimal model is the Ising CFT with $c = 1/2$. There are three irreducible representations of the Virasoro algebra satisfying $h_{1,1} = 0$, $h_{2,1} = 1/2$ and $h_{1,2} = 1/16$. The partition function of the theory is simply the diagonal modular invariant

$$Z_{\text{Ising}}(\tau, \bar{\tau}) = |\chi_{1,1}(\tau)|^2 + |\chi_{1,2}(\tau)|^2 + |\chi_{2,1}(\tau)|^2, \tag{3.16}$$

where the three summands are conformal characters of the identity, energy and spin operators, respectively [135]. These characters can also (for Ising) be expressed in terms of the Riemann or Jacobi theta function, as reviewed in Appendix A.5, equation (A.33).

[8] The character is known [136, 137] to take the form $\eta(\tau)q^{-(1-c)/24}\chi_{r,s} = \sum_{k\in\mathbb{Z}}\left(q^{h_{r+2km,s}} - q^{h_{r+2km,-s}}\right) \equiv S$. Using the identity $h_{r+lm,s+l(m+1)} = h_{r,s}$ for all $l \in \mathbb{Z}$, which follows from (3.15) by inspection, one can bring the expression above into the form $S = q^{h_{r,s}} + \sum_{k=1}^{\infty}\left[q^{h_{r+2km,s}} + q^{h_{r,s+2k(m=1)}}\right] - \left[\left(\sum_{k=0}^{\infty} q^{h_{r+(2k+1)m,-s+(m+1)}}\right) + \left(\sum_{k=1}^{\infty} q^{h_{r,-s+2k(m+1)}}\right)\right]$. After expressing this as a single sum over l from $l = 1$ to ∞, where $l = 2k$ for even l, and $l = (2k+1)$ for odd l, the sum S is easily seen to yield the result presented in the following equation.

On the other hand, the gravitational partition function is obtained by summing all images of the vacuum character under $\Gamma \equiv \Gamma_c \backslash SL(2,\mathbb{Z})$, the right coset space of Γ_c in $SL(2,\mathbb{Z})$, as

$$Z_{\text{grav}}(\tau,\bar{\tau}) = \sum_{\gamma\in\Gamma} |\chi_{1,1}(\gamma\tau)|^2, \tag{3.17}$$

where Γ_c is the set of all "pure gauge transformations" of the vacuum, which are defined to be those elements of $SL(2,\mathbb{Z})$ that act trivially on the modulus of the vacuum character, $|\chi_{1,1}|$:

$$\Gamma_c = \{\gamma \in SL(2,\mathbb{Z}) |\ |\chi_{1,1}(\gamma\tau)| = |\chi_{1,1}(\tau)|\}. \tag{3.18}$$

This is a finite index subgroup as proven in [122], so the summation in (3.17) has a finite number of terms, unlike the $c > 1$ Farey-tail cases that were discussed in [65, 5]. We will see in later sections that the finiteness property, seen here at genus one, extends (for Ising) to the case of higher genus. Starting from the "vacuum seed" $|\chi_{1,1}|^2$, (3.13), and repeatedly acting on it with the generators

$$S = \begin{pmatrix} 0 & -1 \\ 1 & 0 \end{pmatrix}, \quad T = \begin{pmatrix} 1 & 1 \\ 0 & 1 \end{pmatrix} \tag{3.19}$$

of $SL(2,\mathbb{Z})$, one finds 24 inequivalent contributions, which sum up to

$$Z_{\text{grav}} = 8 Z_{\text{Ising}}. \tag{3.20}$$

The physical meaning of this constant factor of 8 is at present unclear, while its mathematical meaning, along with extra new results on Γ_c that go beyond those presented in [119], are collected in Appendix A.6. Therefore we see the equality of the partition functions of pure Einstein gravity in AdS_3 at Brown-Henneaux central charge $c = 3l/2G = 1/2$ and that of the Ising CFT, at genus one.

3.3 Gravitational partition functions with genus-2 asymptotic boundaries

Now we generalize the discussion of the duality between Euclidean AdS_3 and Virasoro minimal model CFTs to genus two. The current section is more "physical" or intuitive, compared to Section 3.4 which discusses the case for arbitrary genus and will be more mathematically involved. We will focus on the $c = 3l/2G = 1/2$ theory and present its gravitational partition function as well as its relation to the Ising CFT in Section 3.3, followed by a review of the relevant mathematical concepts in Section 3.3.

Gravitational partition function

Similar to the genus-one case, the key assumption in the computation of the gravitational partition function is that the path integral is equal to the contribution from classical saddle

points and the full set of quantum fluctuations around them, irrespective of the fact that the Brown-Henneaux central charge is now of order one.

As briefly reviewed in the last section, the analytical continuation from Lorentzian to Euclidean signature basically amounts to taking a Schottky double. When the Lorentzian geometry contains three asymptotic regions, its constant time slice is a pair of pants. The boundary of the corresponding Euclidean spacetime is thus obtained (following the notion of the Schottky double, mentioned above) by gluing two pairs of pants together, thereby obtaining a genus-two Riemann surface. Different ways of gluing give distinct saddles and correspond to different choices of contractible cycles in the bulk. In Figure 3.2, we sketch three bulk geometries that possess a $\mathbb{Z}_2$ time-reflection symmetry [69]. The left one depicts the case which corresponds to three disconnected thermal AdS_3 spacetimes in Lorentzian signature. The green circles label the interfaces between the two pairs of pants. The middle panel describes the Euclidean version of the three-sided wormhole. The right figure is the case with one copy of thermal AdS_3 and a BTZ black hole. Different bulk saddles can be transformed into each other by the action of the MCG (whose definition will be reviewed in Section 3.3).

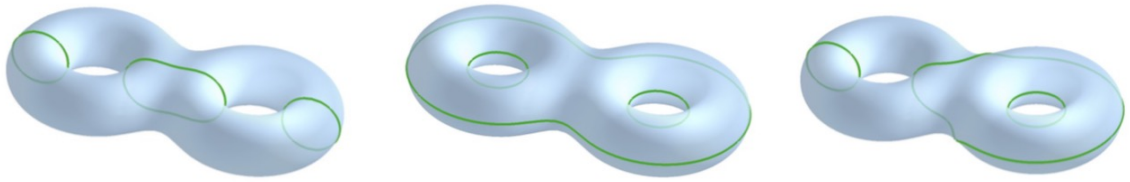

Figure 3.2: Different Euclidean saddles with $\mathbb{Z}_2$ time-reflection symmetry. They analytically continue to three copies of thermal AdS_3 (left), three-sided wormhole (middle), and one thermal AdS_3 plus a BTZ black hole (right). The areas encircled by the green lines are the sets of fixed points of the action of the $\mathbb{Z}_2$ symmetry.

The full partition function can thus be written as the modular sum of one of the saddles, namely as that of the vacuum saddle without black holes,

$$Z_{\text{grav}}(\Omega,\bar{\Omega}) = \sum_{\gamma\in\Gamma} Z_{\text{vac}}(\gamma\Omega,\bar{\gamma}\bar{\Omega}), \tag{3.21}$$

where $\Gamma = \Gamma_c\backslash\Gamma_g$ is the right coset space in the MCG Γ_g of the Riemann surface Σ_g with respect to Γ_c, the symmetry group that leaves Z_{vac} invariant. - Here $g = 2$. The 2×2-dimensional complex, symmetric period matrix Ω is a higher-genus generalization of the modular parameter τ in genus one, whose definition is presented in Section 3.3 below. The conformal structure on the asymptotic boundary is specified by the period matrix Ω. All period matrices Ω related to each other by the MCG correspond to the *same* conformal structure.

Vacuum seed

We are interested in the case where the bulk gravity is a genus-two handlebody, which can be viewed as three solid cylinders that meet at a cup and a cap (each being a "3-ball" - the interior of a 2-dimensional sphere), compare e.g., Figure 3.4. We will choose the notation for the elementary cycles depicted in Figure 3.3 below. The vacuum sector Z_{vac} dominates the

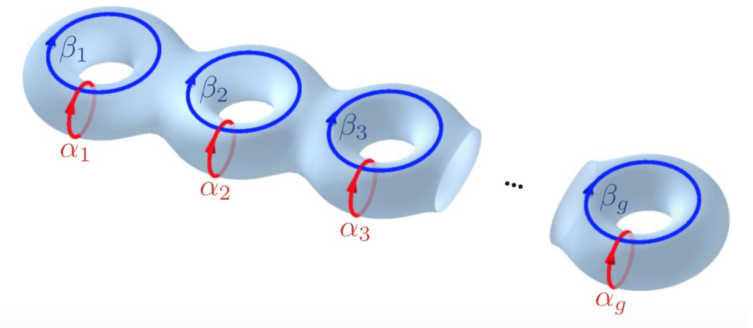

Figure 3.3: The canonical homology basis for Σ_g.

full partition function in the low-temperature limit, which we define to be the limit where the three solid cylinders are long and thin, like in Figure 3.4. (This is analogous to the genus-one case, where in the low-temperature limit, the dominant geometry is the one whose boundary torus has a longitude much larger than its meridian.) In this limit, a natural local coordinate system can be chosen, such that a constant time slice is a disjoint union of three disks, i.e., the cross sections of the three solid cylinders (see Figure 3.4), while the time direction is along the longitudinal direction of the cylinders.[9] Such a topology analytically continues to three copies of thermal AdS_3. Namely, all the α-cycles in Figure 3.3 need to be contractible in the bulk.

For a bulk geometry with a higher-genus asymptotic boundary, we believe that the as-

[9]From a TQFT point of view, this corresponds to the case where only the trivial anyons propagate in the long cylinders. The relationship with TQFT is discussed briefly in Appendix A.5 and will be generally described in Section 3.4.

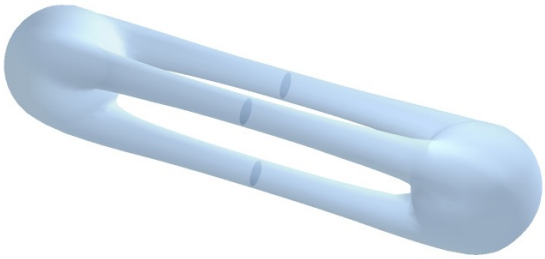

Figure 3.4: The low-temperature or long-cylinder limit of the genus-two geometry.

sociation with the Brown-Henneaux central charge $c = 3l/2G$ is still valid.[10] Recall in the genus-one case, the boundary torus describes the time evolution of graviton states living on the boundary of a disk. When the Brown-Henneaux central charge is $c = 1/2$, these states correspond to the quantum states of the 2d Ising CFT in the vacuum sector $\chi_{1,1}$ (and $\bar{\chi}_{1,1}$). For genus two and in the local coordinate system where a constant time slice consists of three disjoint disks (see Figure 3.4), the boundary graviton states live on the boundary of each disk. Hence locally, the boundary graviton states correspond to three copies of $\chi_{1,1}$ states (and $\bar{\chi}_{1,1}$ states). Globally, the former should correspond to states in the vacuum conformal block of the Ising CFT at genus two (the analogue of the $\chi_{1,1}$ sector for genus one), which we denote by χ_{vac}. Therefore, we assume Z_{vac} to be of the same form as the partition function of the Ising vacuum conformal block. This assumption is a natural extension of results in [52, 140]. In the large-c and the pinching limit of the genus-2 asymptotic boundary, the author of [52] calculated the vacuum seed of AdS_3 to order$1/c^2$. This was then shown to match exactly with the partition function of the vacuum conformal block of a 2d large-c CFT [140]. Naturally, we expect this match to hold to all orders of $1/c$, thereby justifying the assumption.

The full partition function of the 2d Ising CFT theory on a Riemann surface of arbitrary

[10] In their original paper [79], given the global AdS_3 metric with ρ being the radial direction,

$$ds^2 = -\left(\frac{\rho^2}{l^2}\right) dt^2 + \left(\frac{l^2}{\rho^2}\right) d\rho^2 + \rho^2 d\phi^2,$$

after quotienting it by some discrete subgroup of the isometry group of global AdS_3, off-diagonal entries of the new metric need to satisfy the asymptotic conditions

$$g_{t\rho} \sim \mathcal{O}(1/\rho^3), \quad g_{t\phi} \sim \mathcal{O}(1), \quad g_{\rho\phi} \sim \mathcal{O}(1/\rho^3),$$

in order to produce two copies of Virasoro algebras with central charge c on the boundary. In principle, these conditions can be checked here using the Fefferman-Graham metric for asymptotic AdS_{d+1}, constructed basically by shooting geodesics inwards from the boundary [138, 139]: $ds^2 = g_{\rho\rho}d\rho^2 + g_{ij}dx^i dx^j = \frac{l^2 d\rho^2}{4\rho^2} + \frac{1}{\rho}\tilde{g}_{ij}(\rho, x)dx^i dx^j$, where the d-dimensional metric $\tilde{g}_{ij}(\rho, x)$ is the ρ-dependent Euclidean boundary metric.

genus was worked out in [141] using a $\mathbb{Z}_2$ orbifold of the free compactified boson theory, and in [142] using a single, non-interacting Majorana fermion. In the formulation using the Majorana fermion, a choice of boundary conditions (spin structure) has to be imposed. The contribution from each choice of boundary conditions or spin structure can be written as the norm of the regularized determinant of the corresponding chiral Dirac operator. The determinant can further be separated into two factors, one being the Riemann theta function of the corresponding spin structure (whose definition will be reviewed in Section 3.3), while the other is independent of spin structures and only a function of the metric. In what follows, the former will be denoted as the classical contribution to the partition function, and the latter will be called the quantum contribution. (Note this has a different meaning from the "quantum" used to describe gravitational theories which are beyond semiclassical regime. The word "quantum" here stems from the fact that this universal factor accounts for the quantum fluctuations of the boson fields in the $\mathbb{Z}_2$ orbifold.) For more details about the quantum contribution, we refer to Appendix A.5. In fact, not only the full partition of the 2d Ising CFT, but each of the conformal blocks also factorizes into a classical and a quantum piece. Given the identification of the gravitational vacuum seed and the vacuum conformal block of the 2d Ising CFT, discussed above, we can write $Z_{\text{vac}} = Z^{\text{cl}}_{\text{vac}} Z^{\text{qu}}_{\text{vac}}$ (where "cl" stands for classical and "qu" stands for quantum). In the following discussion, we will be interested in how the different sectors or conformal blocks in the theory transform into each other under the MCG. For this purpose, it is enough to temporarily ignore the overall quantum factor that is the same for all conformal blocks and focus on the classical contribution of the gravitational vacuum seed

$$Z^{\text{cl}}_{\text{vac}}(\Omega,\bar{\Omega}) = |\chi^{\text{cl}}_{\text{vac}}(\Omega)|^2 = \frac{1}{16}\left|\sum_{b_1,b_2\in\{0,1/2\}} \vartheta^{1/2}\begin{bmatrix} a_1=0 & a_2=0 \\ b_1 & b_2\end{bmatrix}(0|\Omega)\right|^2, \tag{3.22}$$

where $|\chi^{\text{cl}}_{\text{vac}}(\Omega)|^2$ is the classical contribution to the vacuum conformal block of the 2d Ising CFT, and where ϑ denotes the conventional Riemann theta function (see (3.32) of Section 3.3 for a review of relevant notations). Here, $a_{1,2}$ should be viewed as the two components of the characteristic vector $\mathbf{a} = (a_1, a_2)$ appearing in the theta function for the genus-2 case. Similarly, $b_{1,2}$ are the two components of the characteristic vector $\mathbf{b} = (b_1, b_2)$. The number of components of these characteristic vectors is given by the genus g in general. We explain in the following the specific choice of theta functions ϑ appearing in the above expression.

We know that along a contractible cycle, the boundary condition for a fermion has to be anti-periodic.[11] Since, as discussed above, in the gravitational vacuum seed all the α-cycles in Figure 3.3 need to be contractible, all the corresponding boundary conditions on the (Majorana) fermion along those cycles need to be anti-periodic. Consequently, the top characteristic vector of the theta functions that are relevant for the vacuum sector is zero,

[11] This is the natural boundary condition for fermions since they anti-commute. See also for example [142, 135, 69]. Periodic boundary conditions for fermions would imply a singularity inside the cycle, often called a $\mathbb{Z}_2$-vortex, or Majorana fermion zero mode.

i.e., $a_1 = a_2 = 0$. Furthermore, the vacuum sector must be an equal-weight summation over both even and odd fermion number parities along every β-cycle. This means $Z^{\rm cl}_{\rm vac}$ has to be the modulus square of an equal-weight linear combination of the square root of Riemann theta functions that appear in equation (3.22), as displayed in that same equation.

The above form (3.22) for $Z^{\rm cl}_{\rm vac}$ is also analogous to the classical contribution to the vacuum seed on the *torus*. The latter, as reviewed in (A.33) of Appendix A.5, is the equal-weight sum of the square roots of all theta functions whose characteristic 'vector' $\mathbf{a} = (a_1)$ is zero. On the torus, this has a natural Hamiltonian interpretation that exists due to a global notion of time (leading to a clean separation of 1D space and 1D time), which is absent at higher genus.[12]

In the pinching limit where the bulk 'cylinder' connecting the two tori pinches off [141], i.e., where $\Omega_{12}, \Omega_{21} \to 0$, the (classical) vacuum seed partition function (3.22) reduces to $|\chi^{\rm cl}_{1,1}(\tau_1)\ \chi^{\rm cl}_{1,1}(\tau_2)|^2$, which is the product of the classical parts of the two torus vacuum seeds $|\chi_{1,1}(\tau_1)|^2$ and $|\chi_{1,1}(\tau_2)|^2$ of two tori with modular parameters τ_1 and τ_2.

One can check that (3.22) is invariant under a genus-two generalization of Γ_∞, see Appendix A.7. This is a subgroup of the genus-two MCG Γ_g,[13] generated [52] by integer shifts of matrix elements of the period matrix Ω, as well as the $SL(2,\mathbb{Z})$ transformation that acts on Ω by conjugation $\Omega \mapsto A\Omega A^T$. The genus-2 generalization of the group Γ_∞ is the classical symmetry of the vacuum seed at large c, and it is enhanced in the case of strong coupling ($c < 1$) to the previously mentioned group Γ_c, a subgroup of $\Gamma_{g=2}$ which is larger than Γ_∞. This new "gauge symmetry" will be relevant in the modular sum as it turns out to be a finite-index subgroup.

As a consistency check of (3.22), in the low-temperature or long-cylinder limit depicted in Figure 3.4, the leading contribution to $Z^{\rm cl}_{\rm vac}$ needs to be equal to that of the total classical contribution to the full Ising partition function at genus two in the same limit, as explained in Appendix A.8. The long-cylinder limit can be taken in the following way: The genus-two Riemann surface can be described as a hyperelliptic curve, which is the set of solutions to the following equation (see for example [143] for a recent discussion of this)

$$y(z)^2 = \prod_{k=1}^{3} \frac{z - u_k}{z - v_k}. \tag{3.23}$$

[12]Namely, at genus one there are four (one of them vanishing) holomorphic partition functions, $\chi_{\sigma_x,\sigma_{t_E}} \equiv Tr_{\mathcal{H}_{\sigma_x}}(\sigma_{t_E})^F q^{L_0}$, where F denotes the fermion parity operator, $\sigma_x, \sigma_{t_E} = \pm 1$. Here $\mp\sigma_x$ denotes spatial (anti-)periodicity whereas $\mp\sigma_{t_E}$ denotes Euclidean temporal (anti-)periodicity. These holomorphic partition functions are proportional to $\vartheta^{1/2}\begin{bmatrix} a \\ b \end{bmatrix}$ with $a = (1-\sigma_x)/2$ and $b = (1-\sigma_{t_E})/2$. One then sees from (A.33) of Appendix A.5 that the torus vacuum character $\chi_{1,1}$ is proportional to the sum of the square-roots of theta functions with $a = 0$, summed over $b = 0$ and $b = 1/2$. The sum appearing in (3.22) is the natural generalization of this genus-one expression to genus two.

[13]Basic facts about this genus-two generalization of Γ_∞ will be discussed in Appendix A.7 where this group is referred to as $\Gamma^{[2]}_\infty$.

Such a surface is a two-sheeted branched cover of the Riemann sphere, the points on which are parametrized by z, and the two sheets are labeled by the choice of the root y which solves (3.23). There is a $\mathbb{Z}_2$ "replica symmetry" generated by $y \to -y$, which physically corresponds to the time reversal symmetry discussed above in Figure 3.2, and the corresponding text. The covering map has $2 \times 3 = 6$ branch points (u_k, v_k). Monodromy of z around one of the six branch points shifts $y \to -y$ and moves from one sheet to the other. The locations of the branch points span the moduli space[14] of the Riemann surface. Consequently, the period matrix can be expressed in terms of the branch points [144], and the long-cylinder limit corresponds to taking $u_k - v_k$ to be small for $k = 1, 2, 3,$. To obtain the vacuum seed partition function, the resulting period matrix Ω is inserted into (3.22). For the case of the long-cylinder limit at general genus g, one simply replaces the number 3 appearing in (3.23) by $g + 1$, and proceeds in an analogous fashion.

A final remark is that, for our gravitational vacuum seed partition function Z_{vac} to be identical with that of the vacuum conformal block of the boundary CFT (up to some constant factor), we further need to discuss the cup and cap regions, where three cylinders join. We argue that the three-point correlation functions that describe the graviton scattering processes in the gravity theory match those in the boundary conformal theory[15].

Genus two modular sum

With the above expression for the vacuum seed, we now perform the sum over the images of the action with the MCG ("modular sum") as in (3.21) at $g = 2$.[16]. We will first provide the numerical results, and then give a mathematical argument for the finiteness of the modular sum. Independently, we will present later in Section 3.4 another simple proof from a TQFT perspective for arbitrary genus.

As reviewed in Section 3.3, the subgroup of the MCG which acts non-trivially on the period matrix is $Sp(4, \mathbb{Z})$. The generators of $Sp(2g, \mathbb{Z})$ are reviewed in Appendix A.7. By acting repeatedly with the two generators of $Sp(4, \mathbb{Z})$ on the vacuum seed partition function, we find 3840 inequivalent contributions with the aid of *Mathematica*.[17] These modular

[14]This is a $g = 2$ coincidence, for general genus g the moduli space $\mathcal{M}_g$ of a Riemann surface Σ_g has real dimension $6g - 6$, while the number of real branches is $2g + 2$.

[15]At genus one, a related but somewhat different two-to-one scattering process in AdS_3 between the bulk duals of the light primaries O and χ, whose conformal weights less than $c/12$, is described in [145]. Their CFT three-point function is found to have the *same form* as the gravitational scattering amplitude between their gravitational duals in the BTZ background, with a proportionality factor only dependent on the saddle geometry. Although this process is not necessarily in pure gravity, this result is in support of our argument about the form of Z_{vac}.

[16]Instead of $Z^{\text{cl}}_{\text{vac}}$, we use the full quantum conformal block $Z_{\text{vac}} = |\chi_{\text{vac}}|^2$ in the modular sum. The quantum contribution and issues related to it, are discussed in Appendices A.7 and A.5.

[17]This set is invariant under the action of Torelli group introduced in Section 3.3 below. The Torelli group acts by multiplying $\{\vartheta[1/2, 1/2; 1/2, 1/2](\Omega) \cdot \vartheta^*[1/2, 1/2; 1/2, 1/2](\Omega)\}^{1/2}$ by a minus sign, which can be explicitly verified in the pinching limit using the formalism in [141] and straightforwardly carries over to the general case away from that limit. Only this specific theta function product is affected by the Torelli group action, because it is related to the sector (conformal block) $\chi_{\sigma\psi\sigma}$ (in the language of Appendix A.5),

images sum up to 384 times the partition function Z_{Ising} of the 2d Ising CFT at genus two of Appendix A.5):

$$Z_{\text{grav}} = 384 Z_{\text{Ising}}. \tag{3.24}$$

The factor $10 = 3840/384$ is simply the dimension of the conformal block basis, or simply the number of linearly independent Riemann theta functions. The physical meaning of the constant factor 384 in (3.24) is unclear at this point.

We emphasize that all the above arguments are gravitational ones that solely come from the three-dimensional bulk. In the remainder of this section, we support the above computation by a mathematical explanation for the finiteness of the summation in the partition function [as in (3.21)].

In the Ising case, there exists[18] a short exact sequence for any genus g,

$$1 \to \rho_g(D_g) \to \rho_g(\Gamma_g) \to Sp(2g, \mathbb{Z}_2) \to 1, \tag{3.25}$$

where $\rho_g(\Gamma_g)$ is the image group of the MCG Γ_g represented as matrices in the basis of Riemann theta functions, D_g is the subgroup of the MCG that acts trivially on $H_1(\Sigma_g, \mathbb{Z}_2)$, and $\rho_g(D_g)$ is the corresponding image group. The latter turns out to always be a subgroup of $\mathbb{Z}_8^N$, where N is a finite positive integer.

Since $\rho_g(D_g)$ is abelian (see Appendix A.9), (3.25) gives a central extension of $Sp(2g, \mathbb{Z}_2)$. Such central extensions are classified by the second cohomology group

$$H^2(Sp(2g, \mathbb{Z}_2),\ \rho_g(D_g)). \tag{3.26}$$

For every group element $h \in Sp(2g, \mathbb{Z}_2)$ and $n \in \rho_g(D_g)$, there is an element (n, h) in $\rho_g(\Gamma_g)$, satisfying the group multiplication $(n_1, h_1) \cdot (n_2, h_2) = (\omega(h_1, h_2) n_1 n_2, h_1 h_2)$, where $\omega(h_1, h_2)$ is a 2-cocycle with $\rho_g(D_g)$ coefficients. Alternatively, one can interpret the above short exact sequence in terms of projective representations. Irreducible representations of the MCG Γ_g correspond to the irreducible projective representations of $Sp(2g, \mathbb{Z}_2)$, where the projective phases are given by $\rho_g(D_g)$.

Since Z_{vac} involves taking the modulus square of the vacuum character, the overall phases of $\rho_g(D_g)$ will not matter. We can simply focus on the summation over elements of $Sp(2g, \mathbb{Z}_2)$ that act non-trivially on the absolute values of the theta functions. At genus $g = 2$, $Sp(4, \mathbb{Z}_2)$ turns out to be equal to the permutation group S_6 and contains $6! = 720$ elements. Due to the short exact sequence (3.25), the image group of Γ_g is clearly finite.

In Section 3.4, we will present an alternative simple proof for the finiteness of $\rho_g(\Gamma_g)$ that works for arbitrary genus, from a topological field theory perspective.

Review of the relevant concepts

We first describe the homology of orientable, finite-type two-dimensional surfaces Σ_g of genus g. When Σ_g is compact, its homology groups are free, with $\dim H_0(\Sigma_g) = 1$, $\dim H_1(\Sigma_g) = 2g$,

where there is a fermion ψ in the middle of the genus-two handlebody (denoted by b in Figure A.1, i.e., $b \to \psi$), which acquires a negative sign upon the Dehn twist along the separating curve.

[18] This is a generalization of the mathematical result in [146] which is explained in Appendix F.

$\dim H_2(\Sigma_g) = 1$. One can choose a canonical homology basis α_i, β_i with $1 \leq i \leq g$ for $H_1(\Sigma_g)$ as in Figure 3.3. Any closed curve on Σ_g generates a homology class, which can be uniquely decomposed into the classes generated by α_i, β_i. They are normalized with respect to the algebraic intersection number $J(C_1, C_2)$ between two simple closed curves C_1 and C_2, by

$$J(\alpha_i, \alpha_j) = J(\beta_i, \beta_j) = 0, \quad J(\alpha_i, \beta_j) = -J(\beta_i, \alpha_j) = \delta_{ij}. \tag{3.27}$$

There are g pairs of holomorphic and anti-holomorphic one-forms on Σ_g, denoted by $\{\omega_i, \bar{\omega}_i\}$ $(i = 1, \cdots, g)$, which satisfy the normalization condition

$$\oint_{\alpha_i} \omega_j = \delta_{ij}. \tag{3.28}$$

The period matrix defined by

$$\oint_{\beta_i} \omega_j = \Omega_{ij} \tag{3.29}$$

is then a $g \times g$ complex symmetric matrix, with a positive-definite imaginary part.[19] Analogous equations as above hold for the anti-holomorphic counterparts $\bar{\omega}_i$ and $\bar{\Omega}_{ij}$. The period matrix Ω generalizes the modular parameter τ for the torus, completely parametrizing the conformal structure of Σ_g. Note that a conformal structure of Σ_g can be specified by different period matrices that are related to each other by the MCG.[20]

The MCG Γ_g of a genus-g Riemann surface Σ_g is the group of all isotopy classes of orientation preserving diffeomorphisms of Σ_g. It is generated by Dehn twists around the cycles C of Σ_g. A Dehn twist acts by excising a tubular neighborhood of C inside Σ_g, twisting the latter by 2π, and then gluing it back to the rest of the surface. There are two generators for each handle, and one for each closed curve linking the holes of two neighboring handles.

Γ_g leaves the intersections (3.27) invariant, thus acting on the canonical homology basis by $Sp(2g, \mathbb{Z})$ transformations. The $Sp(2g, \mathbb{Z})$ transformations act on the period matrix by

$$\gamma = \begin{pmatrix} A & B \\ C & D \end{pmatrix} \in Sp(2g, \mathbb{Z}), \quad \gamma : \Omega \to (A\Omega + B)(C\Omega + D)^{-1}, \tag{3.30}$$

where A, B, C, D are g by g matrices. At genus $g = 2$, the minimal number of generators of $Sp(4, \mathbb{Z})$ is two [147]; these are reviewed in Appendix A.7. For $Sp(2g, \mathbb{Z})$ with $g \geq 3$ the minimal number of generators is three [148].

Some elements of Γ_g act trivially on the canonical homology basis, leaving it invariant. These elements are diffeomorphisms homotopic to the identity and they form a normal subgroup of Γ_g, known as the Torelli group $\mathcal{I}_g$ [149, 150]. For genus two, $\mathcal{I}_g$ is infinitely

[19] An alternative normalization for Ω more suitable for computation is considered in Appendix A.8.

[20] The moduli space $\mathcal{M}_g$, the space of conformal structures of Σ_g, has real dimension $6g - 6$. The *Torelli map* from $\mathcal{M}_g$ to the space of Ω's quotiented by the MCG Γ_g is injective, intuitively because the latter has real dimension $g(g+1)$, so the parametrization is complete.

generated by Dehn twists around the separating curve, i.e., the curve that separates the genus two surface into two tori. For $g \geq 3$, besides the ones that twist around the separating curves, there exists another type of generator, called the "bounding pair map". A bounding pair map is the composition of a twist along a non-separating curve C_1 and an inverse twist along another non-separating curve C_2 which is disjoint from C_1 but represents the same homology class as C_1. So $C_1 \cup C_2$ separates Σ_g into two subsurfaces having $C_1 \cup C_2$ as their common boundary. These two kinds of generators are shown in Figure 3.5.

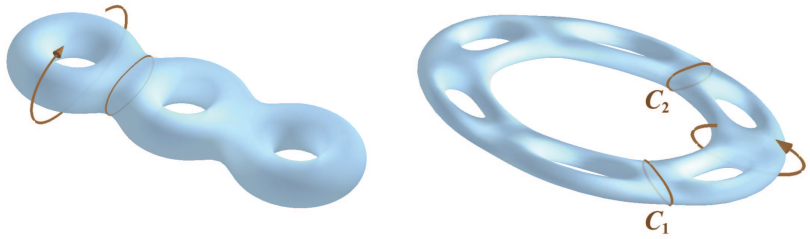

Figure 3.5: Generators of the Torelli group $\mathcal{I}_g$. Left: Dehn twist along a separating curve. Right: the bounding pair map.

In summary, we have the following non-splitting short exact sequence,

$$1 \to \mathcal{I}_g \to \Gamma_g \to Sp(2g, \mathbb{Z}) \to 1. \tag{3.31}$$

Riemann or Siegel theta functions, which depend on two g-dimensional row vectors $\mathbf{a}, \mathbf{b} \in \mathbb{R}^g$ called characteristics, are defined by the following infinite sum [151, 152, 153, 154],

$$\vartheta \begin{bmatrix} \mathbf{a} \\ \mathbf{b} \end{bmatrix} (\mathbf{z}|\Omega) \equiv \sum_{\mathbf{n} \in \mathbb{Z}^g} \exp\left(i\pi(\mathbf{n}+\mathbf{a}) \cdot \Omega \cdot (\mathbf{n}+\mathbf{a}) + 2\pi i(\mathbf{n}+\mathbf{a}) \cdot (\mathbf{z}+\mathbf{b})\right), \tag{3.32}$$

where $\mathbf{z} \in \mathbb{R}^g$ is a g-dimensional vector.

In this chapter, we will be interested in and limit our discussion to the Ising case described by a single Majorana fermion species, where the characteristic vectors are $\mathbf{a}, \mathbf{b} \in (\frac{1}{2}\mathbb{Z})^g$. In this case there is, associated with each theta function, the notion of a *spin-structure* of characteristics $\begin{bmatrix} \mathbf{a} \\ \mathbf{b} \end{bmatrix}$, denoting a $2 \times g$-matrix. The spin structure is called to be even or odd depending on whether $4\mathbf{a} \cdot \mathbf{b}$ is even or odd, respectively. This can be seen from the following identity

$$\vartheta \begin{bmatrix} \mathbf{a} \\ \mathbf{b} \end{bmatrix} (-\mathbf{z}|\Omega) = (-1)^{4\mathbf{a}\cdot\mathbf{b}} \vartheta \begin{bmatrix} \mathbf{a} \\ \mathbf{b} \end{bmatrix} (\mathbf{z}|\Omega). \tag{3.33}$$

Additionally, due to the identity

$$\vartheta \begin{bmatrix} \mathbf{a}+\mathbf{n} \\ \mathbf{b}+\mathbf{m} \end{bmatrix} (\mathbf{z}|\Omega) = e^{2\pi i \mathbf{a}\cdot\mathbf{m}} \vartheta \begin{bmatrix} \mathbf{a} \\ \mathbf{b} \end{bmatrix} (\mathbf{z}|\Omega), \tag{3.34}$$

where $\mathbf{m}$, $\mathbf{n} \in \mathbb{Z}^g$, it is enough to only consider $\mathbf{a}, \mathbf{b} \in (\frac{1}{2}\mathbb{Z}_2)^g$. At genus g, there are $2^{g-1}(2^g-1)$ odd spin structures and $2^{g-1}(2^g+1)$ even ones. The theta functions $\vartheta(\Omega)$ *always* vanish for odd spin structures, which is obvious from (3.33).

Riemann theta functions are also weight-1/2 modular forms. From now on we will denote $\vartheta(0|\Omega)$ by $\vartheta(\Omega)$ for convenience. When their argument Ω is acted on by $\gamma = \begin{pmatrix} A & B \\ C & D \end{pmatrix} \in Sp(2g, \mathbb{Z})$, they transform as [142, 154]:

$$\vartheta \begin{bmatrix} \mathbf{a}' \\ \mathbf{b}' \end{bmatrix} (\gamma\Omega) = \epsilon(\gamma) e^{-i\pi\phi(\mathbf{a},\mathbf{b})} \det(C\Omega + D)^{1/2} \vartheta \begin{bmatrix} \mathbf{a} \\ \mathbf{b} \end{bmatrix} (\Omega), \tag{3.35}$$

where

$$\begin{Bmatrix} \mathbf{a}' \\ \mathbf{b}' \end{Bmatrix} = \begin{pmatrix} D & -C \\ -B & A \end{pmatrix} \begin{Bmatrix} \mathbf{a} \\ \mathbf{b} \end{Bmatrix} + \frac{1}{2} \begin{Bmatrix} (CD^T)_d \\ (AB^T)_d \end{Bmatrix}, \tag{3.36}$$

and

$$\phi(\mathbf{a}, \mathbf{b}) = \left(\mathbf{a}D^T B\mathbf{a} + \mathbf{b}C^T A\mathbf{b}\right) - \left[2\mathbf{a}B^T C\mathbf{b} + \left(\mathbf{a}D^T - \mathbf{b}C^T\right)\left(AB^T\right)_d\right], \tag{3.37}$$

which is Ω-independent.

In (3.36), $\begin{Bmatrix} \cdot \\ \cdot \end{Bmatrix}$ means concatenating two g-dimensional row vectors into a single $2g$-dimensional column vector, i.e., $\begin{Bmatrix} \mathbf{a} \\ \mathbf{b} \end{Bmatrix} \equiv \begin{bmatrix} \mathbf{a}^T \\ \mathbf{b}^T \end{bmatrix}$ where $\cdot^T$ denotes the matrix transpose, whereas $(\cdot)_d$ denotes the g-dimensional row vector whose entries are the diagonal elements of the $g \times g$ matrix appearing inside the parentheses ( ). The subtle phase $\epsilon(\gamma)$ is always an eighth root of unity independent of $\mathbf{a}$ and $\mathbf{b}$, and incidentally, if $\gamma = I_{2g} \bmod 2$, then $\epsilon^2(\gamma) = e^{\pi i \mathrm{Tr}(D-1)/2}$.

We note that the action of the group $Sp(4, \mathbb{Z})$ on the Riemann theta functions at genus $g = 2$ defines a 10-dimensional projective, not a linear representation. The explicit forms of the matrix representations of the (two) generators of the group are displayed in Appendix A.7.

A conjecture on index of $SL(2, \mathbb{Z})$ subgroups for higher genus

Here we digress a little bit and present a conjecture without much numerical evidence, following comments from Shu-Heng Shao and Edward Witten [155].

From genus 1 and 2 cases, we see that the partition functions of $c = 1/2$ gravity and Ising model do not exactly agree, but are proportional to each other. If we were to try interpreting the numerical factor between Z_{grav} and Z_{Ising} as a contribution from the topological term on the boundary Riemann surface, then we should have the following form

$$Z_{\text{grav}} = Ae^{-a\chi} Z_{\text{Ising}}, \tag{3.38}$$

where $\chi = 2 - 2g$ is the Euler characteristic for genus g, and a, A are universal constants. Then we can extrapolate the index of the enhanced symmetry group $\Gamma_c \subset SL(2, \mathbb{Z})$ from the

data on genus 1 and 2. Because $\chi = 0$ for torus, we see from (3.20) that $A = 8$, and (3.24) tells us that $e^{2a} = 48$. Then a genus-3 surface has $\chi = -4$, so the numerical factor in front of Z_{Ising} should be $8\,(e^{2a})^2 = 18,432$ according to (3.38).

Finally, according to the discussion following (3.24), the index of Γ_c should be the factor times the number of non-vanishing (i.e., even) Riemann theta functions on the genus-3 surface, which is $2^{g-1}(2^g + 1) = 36$, so the index should be $663,552$. Unfortunately, the computational power required to obtain this number is much greater than that used for genus 2, and we have not finished running the code at this point. Nevertheless, we would still like to propose the following conjecture:

Conjecture The index of the enhanced symmetry group Γ_c in $SL(2,\mathbb{Z})$ is

$$\boxed{8\,(2^g + 1)\,96^{g-1}}. \tag{3.39}$$

If this result were true, it would be extremely dramatic because of the following reason. According to our ansatz (3.22) for the vacuum seed, the number of Riemann theta functions with all zero entries on the first row on a genus-g Riemann surface is 2^g. Then the algorithm of computing the index of Γ_c by counting how many new Riemann theta function show up in total (as shown in Appendix A.7) tells us that, by fully forgetting about $Sp(2g,\mathbb{Z})$ modular transformations, we obtain the most naïve upper bound on the index

$$[2^{g-1}(2^g + 1)]^{2^g}, \tag{3.40}$$

but (3.39) shows that starting from Z_{vac}, all $Sp(2g,\mathbb{Z})$ transformations only connect a *doubly exponentially* small portion of all Riemann theta functions as g grows.

It would also be a very interesting problem to study its potential congruence and other number-theoretic properties.

3.4 Gravitational partition functions with boundaries of arbitrary genus

In this section, we discuss the full gravitational partition function at Brown-Henneaux central charge $c = 1/2$ with an asymptotic boundary being a Riemann surface of arbitrary genus following the same strategy as in the genus-2 case. The full gravitational partition function Z_{grav} at Brown-Henneaux central charge $c = 1/2$ with a genus-g asymptotic boundary Σ_g is again formulated as a sum over the contributions from different saddle points which are all related to the "vacuum seed" contribution Z_{vac} by the action of the MCG Γ_g of the asymptotic boundary Σ_g. Given the period matrix Ω that specifies the conformal structure on the asymptotic boundary Σ_g, we should write the full gravitational partition function as

$$Z_{\text{grav}}(\Omega,\bar{\Omega}) = \sum_{\gamma\in\Gamma} Z_{\text{vac}}(\gamma\Omega,\bar{\gamma}\bar{\Omega}), \tag{3.41}$$

where $\Gamma = \Gamma_c \backslash \Gamma_g$ is the right coset space, the MCG Γ_g, of its subgroup Γ_c that leaves the vacuum seed invariant. In this sum, the term with trivial γ represents the contribution from the vacuum sector (as known as the "vacuum seed") while other terms present the contributions from other saddle points.

In the following, we will first argue in Section 3.4 that the vacuum seed $Z_{\text{vac}}(\Omega, \bar{\Omega})$ at Brown-Henneaux central charge $c = 1/2$ can be identified with the vacuum conformal block of the 2d Ising CFT on the asymptotic boundary Σ_g with the same period matrix Ω. Then, we will show that the Γ_g-orbit $\{Z_{\text{vac}}(\gamma\Omega, \bar{\gamma}\bar{\Omega}) | \gamma \in \Gamma_g\}$ of the vacuum seed, which appears in (3.41), is dictated by the projective representation ρ_g of the MCG Γ_g induced by the holomorphic conformal blocks of the 2d Ising CFT on Σ_g. Subsequently, we will prove in Section 3.4 a mathematical result stating that ρ_g, viewed as a mapping from Γ_g to a unitary group, has a *finite* image set $\text{im}(\rho_g)$, which has the immediate consequence that the sum $\sum_{\gamma \in \Gamma_g}$ in (3.41) is *finite*. Furthermore, in Section 3.4, we will prove another mathematical result stating that the MCG representation ρ_g is *irreducible*. Using the irreducibility of ρ_g, we can show that the finite sum in (3.41) for the full gravitational partition function is precisely proportional to the partition function of the 2d Ising CFT on the asymptotic boundary Σ_g. In Section 3.4, we establish duality between 3d AdS quantum gravity at Brown-Henneaux central charge $c = 1/2$ and 2d Ising CFT. There, we will also further comment on our arguments for the gravitational vacuum seed $Z_{\text{vac}}(\Omega, \bar{\Omega})$. In Section 3.4, we will discuss, from the perspective of the higher-genus partition function, the fundamental difficulty in extending the duality to the case with Brown-Henneaux central charge $c = 7/10$.

Vacuum seed

Similar to the discussion of the genus-2 asymptotic boundary, to identify the vacuum seed, namely the gravitational partition function contributed by the vacuum sector, we start with a handlebody X with a genus-g asymptotic boundary $\partial X = \Sigma_g$. The classical saddle point geometry on such a handlebody X is asymptotically AdS_3 [52, 54, 56, 127, 128, 129, 130]. As stated in Section 3.3, we believe that the asymptotic behavior of the geometry ensures that the Brown-Henneaux central charge $c = 3l/2G$ is still applicable even if the boundary genus g is larger than 1. In the following, we will always focus on the case with Brown-Henneaux central charge $c = 1/2$.

As far as topology goes, the genus-g handlebody X can be viewed as two 3-balls (the interiors of two 2-dimensional spheres) connected by $g+1$ solid cylinders. A genus-3 example is shown in Figure 3.6.[21] Similar to the genus-2 discussion, we believe that the vacuum seed Z_{vac} should dominate the (full) gravitational partition function on the 3-manifold X in the limit where the boundary period matrix Ω is chosen such that, for each of the solid cylinder regions, the boundary circumference is much shorter than the length of the cylinder. In such a limit, it is natural to consider a (local) coordinate system such that the Euclidean

[21] In this chapter, we only study handlebodies in 3 dimensions. A genus-g (3-dimensional) handlebody means a handlebody with a genus-g 2-dimensional boundary.

time direction is along the longitudinal direction of each solid cylinder region. The Hilbert space of quantum gravity states should then be associated to a constant-time slice, which is a disjoint union of the cross sections of each of the solid cylinders, namely the disjoint union of $g+1$ disks. For example, for $g=3$, the Hilbert space of quantum gravity states should be associated with a disjoint union of 4 disks as shown in Figure 3.6.

Recall that in the discussion of the case with a genus-1 asymptotic boundary, the quantum gravity states defined on a single disk are the boundary graviton states that form the irreducible (identity) representation of the Virasoro algebra with the corresponding Brown-Henneaux central charge c. For $c=1/2$ in particular, the boundary graviton states on a single disk are in one-to-one correspondence with quantum states of the 2d Ising CFT within the $|\chi_{1,1}|^2$ sector.

Coming back to the genus-g handlebody, we now need to assign a Hilbert space to the disjoint union of $g+1$ disks. We naturally expect the Hilbert space to be identified as the tensor product of $g+1$ copies of boundary graviton states obtained in the genus-1 discussion. In this picture, each solid cylinder region physically describes the time evolution of the boundary graviton states.

So far, we have have been discussing the solid cylinder regions of the handlebody. Each of the 3-ball regions in the handlebody glues together all of the solid cylinders. Physically, each of them should describe the scattering process of $g+1$ boundary graviton states. Since the boundary graviton states are in one-to-one correspondence with the quantum states of the 2d Ising CFT, we further make the proposal that the vacuum seed, $Z_{\text{vac}}(\Omega,\bar{\Omega})$, is identical to the vacuum conformal block of the 2d Ising CFT on the asymptotic boundary Σ_g with period matrix Ω[22], which we naturally expect to factorize into holomorphic and the anti-holomorphic pieces, i.e.,

$$Z_{\text{vac}}(\Omega,\bar{\Omega}) = \chi_{\text{vac}}(\Omega)\bar{\chi}_{\text{vac}}(\bar{\Omega}), \tag{3.42}$$

where $\chi_{\text{vac}}(\Omega)$ and $\bar{\chi}_{\text{vac}}(\bar{\Omega})$ are the respective holomorphic and anti-homolorphic vacuum conformal blocks of the 2d Ising CFT on the genus-g surface Σ_g with period matrix Ω. In fact, our proposed form of the vacuum seed is simply a natural extension of results in [52] and [140]. To be more specific, [52] calculates the vacuum seed of the pure 3d AdS gravity with a genus-2 asymptotic boundary in the large-c limit and also in the degeneration limit of the boundary. The result is obtained to the order $1/c^2$. [140] shows that the vacuum conformal block of a 2d large-c CFT matches exactly with the result of [52] to all the orders calculated. Naturally, such a matching is expected to hold to all orders of $1/c$. Hence, (3.42) is a reasonable assumption when we take $c=1/2$. In addition, we will also see in the following subsections that a vacuum seed of the form of ((3.42)) does yield a sensible expression for the full gravitational partition function through the modular sum (3.41).

[22]In the vacuum conformal block of the 2d Ising CFT, the states propagating along the boundary of the solid cylinder regions all belong to the irreducible representation of the Virasoro algebra (and its anti-holomorphic copy) associated with $|\chi_{1,1}|^2$.

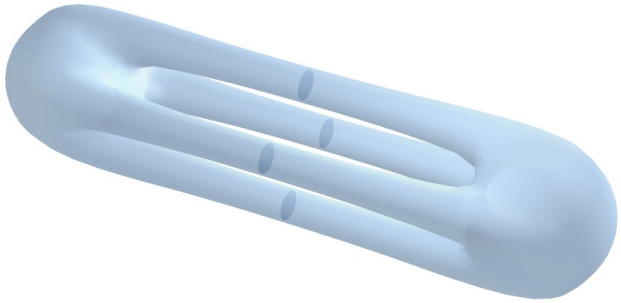

Figure 3.6: A handlebody with a genus-3 asymptotic boundary. Each shaded disk shown should be associated with a Hilbert space of the boundary graviton states which form the representation of the Virasoro algebra with $c = 1/2$.

Finiteness of the Modular Sum

To perform the modular sum (3.41), we need to ensure that the summation over the set of right cosets, $\Gamma = \Gamma_c \backslash \Gamma_g$, is finite. Γ_g is the MCG of the asymptotic boundary Σ_g and Γ_c is the subgroup of Γ_g that leaves the vacuum seed $Z_{\text{vac}}(\Omega, \bar{\Omega})$ invariant. The finiteness of the set Γ is mathematically equivalent to the finiteness of the orbit of the vacuum seed Z_{vac} under the MCG action, namely the finiteness of the set $\{Z_{\text{vac}}\left(\gamma\Omega, \bar{\gamma}\bar{\Omega}\right) | \gamma \in \Gamma_g\}$. In Section 3.4, we have argued that the vacuum seed Z_{vac} is given by the product of the holomorphic and anti-holomorphic vacuum conformal blocks of the 2d Ising CFT. Therefore, the MCG orbit of the vacuum seed Z_{vac} is dictated by the Γ_g action on the conformal blocks of the 2d Ising CFT on Σ_g.

Σ_g is a genus-g Riemann surface. Considering only the holomorphic vacuum conformal block χ_{vac}, the 2d Ising CFT has a total of $N_g = 2^{g-1}(2^g + 1)$ holomorphic conformal blocks on Σ_g. They form an N_g-dimensional vector space which admits a Γ_g action:

$$\chi_i(\gamma\Omega) = \sum_{i'=1}^{N_g} \Big(\rho_g(\gamma)\Big)_{ii'} \chi_{i'}(\Omega). \tag{3.43}$$

Here $\gamma \in \Gamma_g$, where $\chi_i(\Omega)$ with $i = 1, 2, .., N_g$ denote the N_g different holomorphic conformal blocks of the 2d Ising CFT on the surface Σ_g, and $\rho_g(\gamma) \in U(N_g)$ is an $N_g \times N_g$ unitary matrix that depends on γ (but not on the period matrix Ω). In fact, ρ_g is a projective representation of the MCG Γ_g: For any $\gamma, \gamma' \in \Gamma_g$, $\rho_g(\gamma)\rho_g(\gamma')$ is equal to $\rho_g(\gamma\gamma')$ up to a $U(1)$ phase. The Γ_g action on the anti-holomorphic conformal blocks of the 2d Ising CFT is naturally given by the complex-conjugated version of (3.43). Therefore, we will only discuss the representation ρ_g that dictates the Γ_g action on the holomorphic conformal blocks in the following discussion.

When viewed as a map from Γ_g to $U(N_g)$, ρ_g has an image set $\rho_g(\Gamma_g) \equiv \{\rho_g(\gamma) | \gamma \in \Gamma_g\}$ which is a subset of $U(N_g)$. In the following, we will prove that $\rho_g(\Gamma_g)$ is a finite set.

Combining (3.42) and (3.43), it is straightforward to see that the finiteness of the set $\rho_g(\Gamma_g)$ directly implies the finiteness of the MCG orbit $\{Z_{\text{vac}}\left(\gamma\Omega, \bar{\gamma}\bar{\Omega}\right) | \gamma \in \Gamma_g\}$ and, consequently, leads to the conclusion that the modular sum (3.41) is finite.

We will prove the finiteness of $\rho_g(\Gamma_g)$ by contradiction. Let's assume that $\rho_g(\Gamma_g)$ is an infinite set. First, we show that this assumption leads to the consequence that $\{\text{Tr}\,\rho_g(\gamma)|\gamma \in \Gamma_g\}$ also has to be an infinite set. Since $\rho_g(\gamma) \in U(N_g)$, $|\,\text{Tr}\,\rho_g(\gamma)| \leq N_g$. To show that $\{\text{Tr}\,\rho_g(\gamma)|\gamma \in \Gamma_g\}$ is an infinite set, it is sufficient to show that, for any small number $\epsilon > 0$, we can either find (i) a pair of elements $\gamma, \gamma' \in \Gamma_g$ such that $0 < |\,\text{Tr}\,\rho_g(\gamma) - \text{Tr}\,\rho_g(\gamma')| < \epsilon$ or (ii) an element $\gamma'' \in \Gamma_g$ such that $N_g - \epsilon < |\,\text{Tr}\,\rho_g(\gamma'')| < N_g$.[23] First, we start with a sufficiently small $\epsilon' > 0$. Since $U(N_g)$ is a compact space, the assumption that $\rho_g(\Gamma_g)$ is an infinite set guarantees the existence of a pair of elements $\gamma, \gamma' \in \Gamma_g$ such that $0 < \|\rho_g(\gamma) - \rho_g(\gamma')\| < \epsilon'$ where $\|\cdot\|$ represents the Frobenius norm.[24] $\rho_g(\gamma)$ is not identical to $\rho_g(\gamma')$. But we still need to distinguish two situations depending on whether $\rho_g(\gamma)$ and $\rho_g(\gamma')$ differ by only a $U(1)$ phase or not. In first situation where $\rho_g(\gamma)$ differs from $\rho_g(\gamma')$ by a $U(1)$ phase, the sufficiently small ϵ' can guarantee that $0 < |\,\text{Tr}\,\rho_g(\gamma) - \text{Tr}\,\rho_g(\gamma')| < \epsilon$. Hence, we find the pair of elements γ, γ' described in (i). In second situation where $\rho_g(\gamma)$ is not proportional to $\rho_g(\gamma')$, we notice $\rho_g(\gamma^{-1}\gamma')$, which is equal to $\rho_g(\gamma)^{-1}\rho_g(\gamma')$ up to a $U(1)$ phase, is then not proportional to the identity operator. Then, with $\gamma'' = \gamma^{-1}\gamma'$, $|\,\text{Tr}\,\rho_g(\gamma'')| < N_g$. However, with a sufficiently small ϵ', $\rho_g(\gamma'')$ can be arbitrarily close to the identity operator up a $U(1)$ phase. Therefore, we have $N_g - \epsilon < |\,\text{Tr}\,\rho_g(\gamma'')| < N_g$. Hence, we find the element γ'' described in (ii). Now, we can conclude that the assumption that $\rho_g(\Gamma_g)$ is an infinite set has a consequence that $\{\text{Tr}\,\rho_g(\gamma)|\gamma \in \Gamma_g\}$ also has to be an infinite set.

In the remainder of this subsection, we will show that $\{\text{Tr}\,\rho_g(\gamma)|\gamma \in \Gamma_g\}$ in fact cannot be an infinite set and, hence, that the assumption that $\rho_g(\Gamma_g)$ is an infinite set is incorrect.

For any $\gamma \in \Gamma_g$, $\text{Tr}\,\rho_g(\gamma)$ can be interpreted as a partition function of the 3d Ising topological quantum field theory (TQFT). The 3d Ising TQFT is closely related to the 2d Ising CFT. In particular, the 3d Ising TQFT assigns a N_g-dimensional Hilbert space to the genus-g surface Σ_g whose basis vectors are in one-to-one correspondence with the holomorphic conformal blocks of the 2d Ising CFT on Σ_g [99]. The details of this correspondence will be reviewed in the next subsection. A Γ_g action γ on the genus-g surface Σ_g induces a unitary transformation within the 3d Ising TQFT Hilbert space which is exactly given by $\rho_g(\gamma)$. $\text{Tr}\,\rho_g(\gamma)$ can be interpreted as the 3d Ising TQFT partition function $Z_{\text{iTQFT}}(M_\gamma)$ evaluated on the mapping torus $M_\gamma \equiv \frac{[0,1]\times\Sigma_g}{(0,x)\sim(1,\gamma(x))}$. The mapping torus M_γ is a 3-manifold obtained from gluing the two Σ_g boundary components of the Cartesian product $[0,1] \times \Sigma_g$ with an MCG action γ performed on one of the Σ_g components. For a general 3-manifold M^3, the 3d Ising TQFT partition can be expressed as [156, 157]

$$Z_{\text{iTQFT}}(M^3) = \sum_{\text{spin structure } \zeta} e^{\frac{2\pi i}{16}\mu(M^3,\zeta)}, \tag{3.44}$$

[23] The full details of mathematical rigor for the rest of this paragraph will be presented in Appendix A.10.

[24] The Frobenius norm $\|A\|$ of a matrix A is defined as the square root of the sum of the absolute squares of its elements, namely $\|A\| = \sqrt{\text{Tr}(A^\dagger A)}$.

where $\sum_\zeta$ represents the summation over all spin structures ζ on M^3 and $\mu(M^3,\zeta)$ is Rokhlin's μ-invariant[25] of the 3-manifold M^3 with the spin structure ζ. The invariant $\mu(M^3,\zeta)$ is defined modulo 16 and is always an even integer. For a general 3-manifold M^3, the number of spin structures on M^3 is equal to $|H^1(M^3,\mathbb{Z}_2)| = |H_1(M^3,\mathbb{Z}_2)|$. Here, we are viewing H^1 and H_1 as groups. $|\cdot|$ means the order of the group in this context. For the mapping torus M_γ of Σ_g, we can consider the following long exact sequence (see, e.g., Example 2.48 of [158]),

$$... \to H_n(\Sigma_g,\mathbb{Z}_2) \to H_n(\Sigma_g,\mathbb{Z}_2) \to H_n(M_\gamma,\mathbb{Z}_2) \to H_{n-1}(\Sigma_g,\mathbb{Z}_2) \to ..., \tag{3.45}$$

which implies an upper bound on the number of spin structures on M_γ that only depends on g but not γ:

$$|H^1(M_\gamma,\mathbb{Z}_2)| = |H_1(M_\gamma,\mathbb{Z}_2)| \leq |H_1(\Sigma_g,\mathbb{Z}_2)| \times |H_0(\Sigma_g,\mathbb{Z}_2)|. \tag{3.46}$$

The inequality above is a direct consequence of the $H_1(\Sigma_g,\mathbb{Z}_2) \to H_1(M_\gamma,\mathbb{Z}_2) \to H_0(\Sigma_g,\mathbb{Z}_2)$ part of the long exact sequence (3.45).[26] Therefore, according to (3.44), for any $\gamma \in \Gamma_g$,

$$\begin{aligned} &\operatorname{Tr}\rho_g(\gamma) = Z_{\text{iTQFT}}(M_\gamma) \\ &\in \left\{ \sum_{n=0,2,4,...,14} a_n e^{\frac{2\pi i}{16}n} \;\middle|\; a_n \in \mathbb{Z},\ 0 \leq a_n \leq |H_1(\Sigma_g,\mathbb{Z}_2)| \times |H_0(\Sigma_g,\mathbb{Z}_2)| \right\}. \end{aligned} \tag{3.47}$$

Notice that the set given in the second line a finite set. Therefore, $\{\operatorname{Tr}\rho_g(\gamma)|\gamma \in \Gamma_g\}$ cannot be an infinite set, which is in contradiction to the consequence of the assumption that $\rho_g(\Gamma_g)$ is an infinite set. Now, we can conclude that $\rho_g(\Gamma_g)$ has to be a finite subset of $U(N_g)$. It follows that the modular sum (3.41) is finite.

This proof of the finiteness of the modular sum (3.41) relies on the expression of the vacuum seed Z_{vac} (3.42) that we argued for in Section 3.4. In fact, as long as the vacuum seed Z_{vac} can be written as a product of a holomorphic and an anti-holomorphic conformal block of the 2d Ising CFT (or even as a sum of products of this type), the proof given in this subsection is still applicable and the modular sum (3.41) is still finite.

[25] For (M^3,ζ), it is defined as the signature of the intersection form of any smooth compact spin 4-manifold with the spin boundary (M^3,ζ).

[26] With the map $H_1(M_\gamma,\mathbb{Z}_2) \to H_0(\Sigma_g,\mathbb{Z}_2)$ in (3.45) viewed as a linear map between vector spaces (over $\mathbb{Z}_2$), the sum of the dimensions of its kernel and its image is equal to the dimension of $H_1(M_\gamma,\mathbb{Z}_2)$. The image of the linear map $H_1(M_\gamma,\mathbb{Z}_2) \to H_0(\Sigma_g,\mathbb{Z}_2)$, as a vector space over $\mathbb{Z}_2$, has a dimension less than or equal to the dimension of $H_0(\Sigma_g,\mathbb{Z}_2)$. From the fact that (3.45) is exact, the kernel of the map $H_1(M_\gamma,\mathbb{Z}_2) \to H_0(\Sigma_g,\mathbb{Z}_2)$ has the same dimension as the image of the map $H_1(\Sigma_g,\mathbb{Z}_2) \to H_1(M_\gamma,\mathbb{Z}_2)$ whose dimension is smaller than or equal to the dimension of the vector space $H_1(\Sigma_g,\mathbb{Z}_2)$. Therefore, the dimension of the vector space $H_1(M_\gamma,\mathbb{Z}_2)$ is not greater than the sum of the dimensions of $H_0(\Sigma_g,\mathbb{Z}_2)$ and of $H_1(\Sigma_g,\mathbb{Z}_2)$, which implies (3.46).

Irreducibility of the MCG representation and the modular sum

With the modular sum (3.41) proven to be finite, the full gravitational partition function $Z_{\text{grav}}(\Omega, \bar{\Omega})$ is then, by construction, invariant under any Γ_g action on the asymptotic boundary Σ_g. Since a MCG action generally transforms the holomorphic (anti-holomorphic) vacuum conformal blocks of the 2d Ising CFT into a linear superposition of all holomorphic (anti-holomorphic) conformal blocks, we expect the modular sum (3.41), together with the vacuum seed (3.42), to yield

$$Z_{\text{grav}}(\Omega, \bar{\Omega}) = \sum_{i,i'=1}^{N_g} B_{ii'} \bar{\chi}_{i'}(\bar{\Omega}) \chi_i(\Omega), \tag{3.48}$$

where B is a $N_g \times N_g$ matrix. The invariance of $Z_{\text{grav}}(\Omega, \bar{\Omega})$ under the action of the MCG implies that

$$\rho_g(\gamma)^\dagger B \rho_g(\gamma) = B, \tag{3.49}$$

for any $\gamma \in \Gamma_g$. Importantly, as we will prove later in this subsection, the projective representation ρ_g of the MCG Γ_g is *irreducible*. As a consequence, by Schur's lemma, B has to be proportional to the identity matrix to satisfy (3.49). Therefore, the full gravitational partition function satisfies

$$Z_{\text{grav}}(\Omega, \bar{\Omega}) \propto \sum_{i=1}^{N_g} \bar{\chi}_i(\bar{\Omega}) \chi_i(\Omega). \tag{3.50}$$

In the following, we will present the proof of the irreducibility of the MCG representation ρ_g.

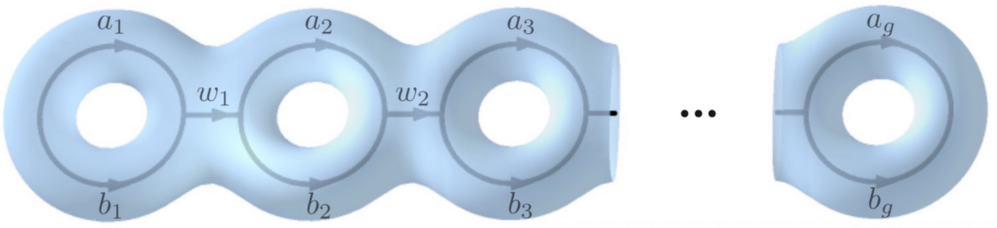

Figure 3.7: $a_{1,2,\ldots,g}$, $b_{1,2,\ldots,g}$, $w_{1,2,\ldots,g-1} \in \{1, \sigma, \psi\}$. Fusion rules need to be applied at each trivalent vertex for the fusion diagram to be admissible.

First, we review the connections between the 2d Ising CFT and 3d Ising TQFT that will be useful for the proof of the irreducibility of the representation ρ_g. On the genus-g surface Σ_g, there are N_g holomorphic conformal blocks in the 2d Ising CFT and there are N_g orthogonal quantum states in the 3d Ising TQFT. Each of the holomorphic conformal blocks

has a corresponding TQFT quantum state and vice versa. Each of holomorphic conformal blocks and its corresponding TQFT quantum state can be represented by an admissible fusion diagram as shown in Figure 3.7. Each line in the fusion diagram is labeled by 1, σ or ψ. That is to say, in Figure 3.7, all the labels $a_{1,2,...,g}$, $b_{1,2,...,g}$ and $w_{1,2,..,g-1}$ take values in the set $\{1, \sigma, \psi\}$. The labels $\{1, \sigma, \psi\}$ should be viewed as the labels for the primary fields in the 2d (chiral) Ising CFT and, equivalently, also as the labels for the anyons (or objects or particles) in the 3d Ising TQFT. Note that the lines in the fusion diagrams are also directed. In general, a directed line carrying an anyon label a is equivalent to the line with the opposite direction and with the label $\bar{a}$, namely the label for the anti-particle of a. The directions of all the lines in Figure 3.7 are chosen merely as a convention. In fact, in 3d Ising TQFT, each of 1, σ and ψ is its own antiparticle. Therefore, it should not cause confusion even if we don't specify the directions of the lines in a fusion diagram in in the discussion below. Also, 1 represents the trivial anyon in the 3d Ising TQFT and the trivial (identity) primary operator in the 2d Ising CFT. In the fusion diagram, a line labeled by 1 can also be erased. Only a so-called admissible fusion diagram corresponds to a holomorphic conformal block or a TQFT quantum state on Σ_g. For the fusion diagram in Figure 3.7 to be admissible in the 2d Ising CFT or the 3d Ising TQFT, we first need to require $a_1 = b_1$ and $a_g = b_g$. Moreover, an admissible fusion diagram also requires each trivalent vertex to be admissible. Each trivalent vertex has two incoming (outgoing) lines and one outgoing (incoming) line. If the anyons a and b labeling the two incoming (outgoing) lines have a fusion product $a \times b$ that contains the anyon c labeling the one outgoing (incoming) line, the trivalent vertex is admissible. The full set of fusion rules of the 3d Ising TQFT (or the 2d Ising CFT) is given by

$$\begin{aligned} &1 \times 1 = 1, \quad 1 \times \sigma = \sigma, \quad 1 \times \psi = \psi, \\ &\psi \times 1 = \psi, \quad \psi \times \sigma = \sigma, \quad \psi \times \psi = 1, \\ &\sigma \times 1 = \sigma, \quad \sigma \times \psi = \sigma, \quad \sigma \times \sigma = 1 + \psi. \end{aligned} \tag{3.51}$$

One can directly show (see below) that there are N_g admissible fusion diagrams (with different anyon labels $a_{1,2,..,g}$, $b_{1,2,..,g}$ and $w_{1,2,..,g-1}$) of the form shown in Figure 3.7, where $N_g = 2^{g-1}(2^{g-1} + 1)$ is the dimension of the representation ρ_g of the MCG discussed above.

We will denote the Ising TQFT quantum state (and its correspond Ising-CFT conformal block) by the corresponding fusion diagram labels. For example, the Ising TQFT quantum state associated to the fusion diagram shown in Figure 3.7 will be denoted as $|\{a_i\}, \{b_i\}, \{w_i\}\rangle$. Physically, in the language of 3d TQFT, one can think of an admissible fusion diagram as describing the world lines of anyon. Therefore, in the discussion below, we will also refer to a fusion diagram as an anyon diagram. The correspondence between the state $|\{a_i\}, \{b_i\}, \{w_i\}\rangle$ and its fusion diagram can be understood as follows. The state $|\{a_i\}, \{b_i\}, \{w_i\}\rangle$ on Σ_g can be viewed as generated by the 3d Ising TQFT path integral on a genus-g handlebody H_g such that $\partial H_g = \Sigma_g$, and such that the corresponding fusion diagram (or anyon diagram) is embedded in the core of H_g (in the same configuration as shown in Figure 3.7). In particular, there is a "special" state $|\text{vac}\rangle \equiv |\{a_i = 1\}, \{b_i = 1\}, \{w_i = 1\}\rangle$

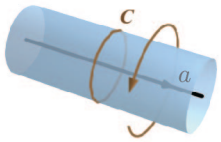

Figure 3.8: The Dehn twist along the non-contractible loop C only yields a $U(1)$ phases $e^{i2\pi h_a}$ that depends on the label a.

with all of the labels on the fusion diagram set to be 1. The state $|\text{vac}\rangle$ can be viewed as the result of the Ising TQFT path integral on the handlebody H_g without an anyon diagram inside (remember that anyon lines labeled by 1 can be erased). The so-defined TQFT state $|\text{vac}\rangle$ corresponds to the holomorphic vacuum conformal block $\chi_{\text{vac}}(\Omega)$ of the 2d Ising CFT.

Because of the correspondence between the holomorphic conformal blocks of the 2d Ising CFT and the states on Σ_g of the 3d Ising TQFT, the MCG Γ_g acts on the states $|\{a_i\},\{b_i\},\{w_i\}\rangle$ via the same representation ρ_g. The Γ_g action on the Ising-TQFT states can also be understood as follows. In the picture where the Ising-TQFT states are generated by the Ising TQFT path integral on a handlebody H_g with an anyon diagram, the MCG action on $\Sigma_g = \partial H_g$ should be extended to the whole handlebody H_g. Such an extended action of Γ_g deforms the anyon diagram inside H_g. The deformed anyon diagram can be rewritten in terms of a linear superposition of anyon diagrams of the original shape shown in Figure 3.7 with different anyon labels. That is to say that when a state $|\{a_i\},\{b_i\},\{w_i\}\rangle$ is acted on by an element $\gamma \in \Gamma_g$ of the MCG, the resulting state is in general a superposition of many states with different anyon labels in their fusion diagrams:

$$\begin{aligned}&\rho_g(\gamma)|\{a_i\},\{b_i\},\{w_i\}\rangle\\ &= \sum_{a_i',b_i',w_i'=\{1,\sigma,\psi\}} \langle\{a_i'\},\{b_i'\},\{w_i'\}|\rho_g(\gamma)|\{a_i\},\{b_i\},\{w_i\}\rangle \quad |\{a_i'\},\{b_i'\},\{w_i'\}\rangle. \end{aligned} \tag{3.52}$$

A particularly simple case is when the MCG action is a Dehn twist ν_C along a loop C that is threaded by a single anyon line labeled by a (as is shown in Figure 3.8). Such a Dehn twist does not change the shape of the anyon diagram, the action $\rho_g(\nu_C)$ only yields extra $U(1)$ phase $e^{i2\pi h_a}$ on the state represented by the anyon diagram, where h_a depends on the anyon label a:

$$h_1 = 0, \quad h_\sigma = 1/16, \quad h_\psi = 1/2. \tag{3.53}$$

Here h_a can be viewed as the conformal weight of the primary field labeled by a in the 2d (chiral) Ising CFT. Also, in the 3d Ising TQFT language, we can view $e^{i2\pi h_a}$ as the topological spin of the anyon labeled by a.

In the following, we will show that ρ_g is an irreducible projective representation of the MCG Γ_g. In fact, the irreducibility of ρ_g is equivalent to the statement that the

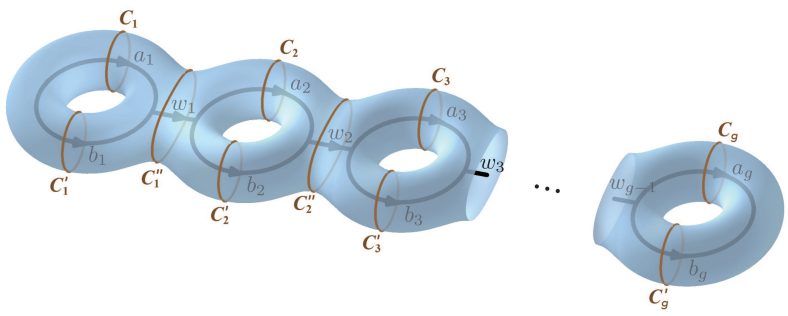

Figure 3.9: The Dehn twists along the loops $C_{1,2,..,g}$, $C'_{1,2,..,g}$ and $C''_{1,2,..,g-1}$ can distinguish all of the states $|\{a_i\},\{b_i\},\{w_i\}\rangle$

$\mathbb{C}$-linear matrix algebra $\mathbb{C}[\rho_g]$ generated by $\rho_g(\Gamma_g)$ (through addition and matrix multiplication) is identical to the *full* matrix algebra $\mathbb{M}_{N_g}$ of all $N_g \times N_g$ complex matrices, namely $\mathbb{C}[\rho_g] \cong \mathbb{M}_{N_g}$. Obviously, $\mathbb{C}[\rho_g] \subseteq \mathbb{M}_{N_g}$. Therefore, what we need to prove is that $\mathbb{M}_{N_g} \subseteq \mathbb{C}[\rho_g]$. The strategy of the proof is to explicitly construct all the operators of the form $|\{a_i\},\{b_i\},\{w_i\}\rangle\langle\{a'_i\},\{b'_i\},\{w'_i\}|$ within $\mathbb{C}[\rho_g]$.

We will first construct the projection operators $|\{a_i\},\{b_i\},\{w_i\}\rangle\langle\{a_i\},\{b_i\},\{w_i\}|$, which will be denoted as $P_{\{a_i\},\{b_i\},\{w_i\}}$ in the following discussion, for any state $|\{a_i\},\{b_i\},\{w_i\}\rangle$. For this purpose, we can focus on the set of non-intersecting loops $C_{1,2,..,g}$, $C'_{1,2,..,g}$ and $C''_{1,2,..,g-1}$ shown in Figure 3.9. The Dehn twists ν_{C_i}, $\nu_{C'_i}$ and $\nu_{C''_i}$ along each of these loops commute with each other. A state $|\{a_i\},\{b_i\},\{w_i\}\rangle$ with a fixed set of labels $a_{1,2,..,g}$, $b_{1,2,..,g}$ and $w_{1,2,..,g-1}$ is a simultaneous eigenstate of all such Dehn twists:

$$\begin{aligned}
&\rho_g(\nu_{C_j})|\{a_i\},\{b_i\},\{w_i\}\rangle = e^{i2\pi h_{a_j}}|\{a_i\},\{b_i\},\{w_i\}\rangle, \qquad \text{for } j=1,2,...,g\\
&\rho_g(\nu_{C'_j})|\{a_i\},\{b_i\},\{w_i\}\rangle = e^{i2\pi h_{b_j}}|\{a_i\},\{b_i\},\{w_i\}\rangle, \qquad \text{for } j=1,2,...,g\\
&\rho_g(\nu_{C''_j})|\{a_i\},\{b_i\},\{w_i\}\rangle = e^{i2\pi h_{w_j}}|\{a_i\},\{b_i\},\{w_i\}\rangle, \qquad \text{for } j=1,2,...,g-1.
\end{aligned} \tag{3.54}$$

Since $e^{i2\pi h_1}$, $e^{i2\pi h_\sigma}$, $e^{i2\pi h_\psi}$ are all different, one can use the set of Dehn twists ν_{C_i}, $\nu_{C'_i}$ and $\nu_{C''_i}$ to fully distinguish all the states $|\{a_i\},\{b_i\},\{w_i\}\rangle$. Building on this, we can construct the following projection operators associated with any loop C and an anyon label 1, σ, or ψ within $\mathbb{C}[\rho_g]$:

$$\begin{aligned}
P_1(C) &\equiv \frac{1}{16}\sum_{n=1}^{16}\rho_g\left(\nu_C^n\right),\\
P_\sigma(C) &\equiv \left(1-e^{2\pi i/8}\right)^{-1}\left(\mathbb{1}-\rho_g\left(\nu_C^2\right)\right),\\
P_\psi(C) &= \mathbb{1}-P_1(C)-P_\sigma(C),
\end{aligned} \tag{3.55}$$

where $\nu_C \in \Gamma_g$ represents the Dehn twist along the loop C and $\mathbb{1}$ represents the $N_g \times N_g$

identity matrix. Choosing C to be C_j, C'_j or C''_j, we see that

$$\begin{aligned} P_a(C_j)|\{a_i\},\{b_i\},\{w_i\}\rangle &= \delta_{a,a_j}|\{a_i\},\{b_i\},\{w_i\}\rangle, \qquad \text{for } j=1,2,...,g \\ P_b(C'_j)|\{a_i\},\{b_i\},\{w_i\}\rangle &= \delta_{b,b_j}|\{a_i\},\{b_i\},\{w_i\}\rangle, \qquad \text{for } j=1,2,...,g \\ P_w(C''_j)|\{a_i\},\{b_i\},\{w_i\}\rangle &= \delta_{w,w_j}|\{a_i\},\{b_i\},\{w_i\}\rangle, \qquad \text{for } j=1,2,...,g-1, \end{aligned} \tag{3.56}$$

where $a_i, b_i, w_i \in \{1, \sigma, \psi\}$. Any projector $P_{\{a_i\},\{b_i\},\{w_i\}}$ onto a given state $|\{a_i\},\{b_i\},\{w_i\}\rangle$ can then be written as a product of $P_a(C_j)$, $P_b(C'_j)$ and $P_w(C''_j)$. Therefore, all projection operators $P_{\{a_i\},\{b_i\},\{w_i\}}$ belong to $\mathbb{C}[\rho_g]$.

Next, we will show that all the operators of the form $|\text{vac}\rangle\langle\{a_i\},\{b_i\},\{w_i\}|$ can be constructed within $\mathbb{C}[\rho_g]$. Upon inspection we observe that in any admissible fusion diagram of the form shown in Figure 3.7, the labels w_i for $i=1,2,...,g-1$ can only take values 1 or ψ. We will first focus on the case with $w_i=1$ for all $i=1,2,...,g-1$. In this case, an admissible diagram further requires $a_i=b_i$ for all $i=1,2,...,g$. Therefore, the relevant states in this case are of the form $|\{a_i\},\{b_i=a_i\},\{w_i=1\}\rangle$, which will be denoted by $|\{a_i\}\rangle$ in short hand in the following discussion. The anyon diagram of $|\{a_i\}\rangle$, after we have erased all the lines carrying label 1, is simply a disjoint union of anyon loops labeled by $a_{1,2,...,g}$. To construct an operator of the form $|\text{vac}\rangle\langle\{a_i\}|$ in $\mathbb{C}[\rho_g]$, it is sufficient to find an MCG element γ such that $\langle\text{vac}|\rho_g(\gamma)|\{a_i\}\rangle \neq 0$ which allows us to write $|\text{vac}\rangle\langle\{a_i\}|$ as $|\text{vac}\rangle\langle\text{vac}|\rho_g(\gamma)|\{a_i\}\rangle\langle\{a_i\}|$ up to a non-zero multiplicative constant. Remember that we have already constructed the operators $|\text{vac}\rangle\langle\text{vac}|$ and $|\{a_i\}\rangle\langle\{a_i\}|$ within $\mathbb{C}[\rho_g]$. Therefore, we only need to find the suitable MCG element γ.

In principle, the choice of γ can depend on the state $|\{a_i\}\rangle$. Interestingly, we can show that there is a specific MCG element $\gamma_0 \in \Gamma_g$ that works for all $|\{a_i\}\rangle$. The MCG element γ_0 can be identified as follows. Consider the disjoint union of two copies of a genus-g handlebody H_g and H'_g whose boundaries are given by two identical copies Σ_g and Σ'_g of the *same* Riemann surface, i.e., $\Sigma_g = \partial H_g$ and $\Sigma'_g = \partial H'_g$. In general, we can perform a MCG action $\gamma \in \Gamma_g$ on Σ'_g and then glue it to Σ_g. This procedure glues the two genus-g handlebodies H_g and H'_g into a single closed 3-manifold that depends on the choice of γ. There exists an element γ_0 such that the resulting closed 3-manifold is the 3-sphere S^3. We will show that $\langle\text{vac}|\rho_g(\gamma_0)|\{a_i\}\rangle \neq 0$ for any states $|\{a_i\}\rangle$. Again, consider the setup with two copies H_g and H'_g of the genus-g handlebody. Performing the 3d Ising-TQFT path integral on H_g (without any anyon diagram) yields the state $|\text{vac}\rangle$ on its boundary $\partial H_g = \Sigma_g$. Now, we embeded the anyon diagram of $|\{a_i\}\rangle$, which is a collection of disjoint anyon loops labeled by $a_{1,2,..,g}$ respectively, in H'_g. The TQFT path integral on H'_g then yields the state $|\{a_i\}\rangle$ on its boundary $\partial H'_g = \Sigma'_g$. When Σ'_g is acted on by γ_0 and then glued to Σ_g, we obtain a 3d Ising TQFT path integral on S^3 together with the anyon diagram that was originally embedded in H'_g. The result of such a path integral is exactly $\langle\text{vac}|\rho_g(\gamma_0)|\{a_i\}\rangle$. Since the anyon diagram involved here is a disjoint union of anyon loops labeled by $a_{1,2,..,g}$ respectively, the Ising TQFT path integral on S^3 with such anyon diagrams is definitely non-vanishing. Therefore,

$$\langle\text{vac}|\rho_g(\gamma_0)|\{a_i\}\rangle \neq 0, \tag{3.57}$$

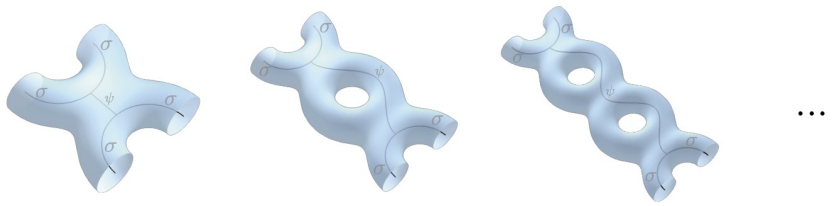

Figure 3.10: Local configurations of fusion diagrams with some of the w_i labels taking the value ψ

for any choice of $a_{1,2,\ldots,g}$. Consequently, we can conclude that the operators of the form $|\text{vac}\rangle\langle\{a_i\}|$ all belong to $\mathbb{C}[\rho_g]$. By Hermitian conjugation, the any operator of the form $|\{a_i\}\rangle\langle\text{vac}|$ also belongs to $\mathbb{C}[\rho_g]$.

Now, we are ready to construct the operators $|\text{vac}\rangle\langle\{a_i\},\{b_i\},\{w_i\}|$ with some of the w_i labels equal to ψ. When some of the w_i labels equal to ψ, the anyon diagram associated to $|\{a_i\},\{b_i\},\{w_i\}\rangle$ must be in one of the configurations shown in Figure 3.10 in the vicinity of the diagram where the w_i labels take the value ψ. In the Ising TQFT, we have the following linear relations between the diagrams

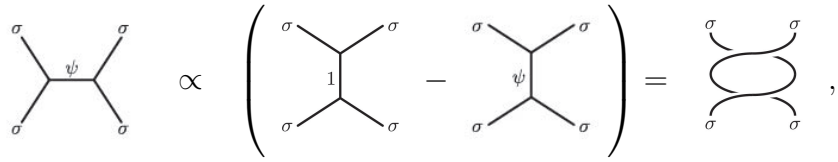

(3.58)

which can help us relate an anyon diagram with some of the w_i labels equal to ψ to another diagram with less of the w_i labels equal to ψ. For example, the leftmost configuration shown in Figure 3.10 obeys

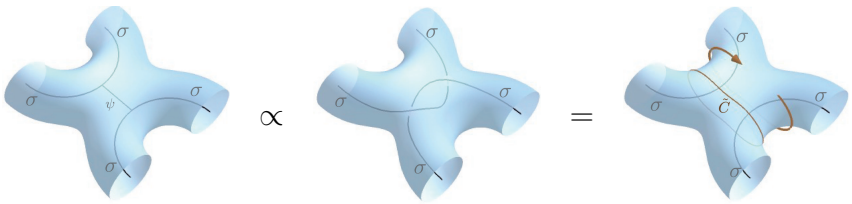

(3.59)

where the relation between the first two diagrams is a graphical representation of the relation (3.58). The last equality in (3.59) means that a Dehn twist along the loop $\tilde{C}$ can transform the rightmost diagram shown in (3.59), before it was acted on by the Dehn twist, to the diagram shown in the middle of the same equation. Remember that the Dehn twist along $\tilde{C}$ on the surface should be extended into the interior of the handlebody leading to the transformation from the third diagram to the second in (3.59). Thus, Equation (3.59) shows an example to use Dehn twists to relate a diagram with a w_i label equal to ψ to another diagram without such a w_i label. A similar relation can also be obtained for the second

configuration shown in Figure 3.10:

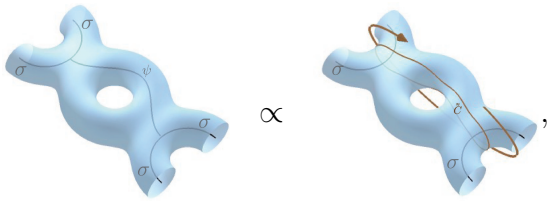

(3.60)

where a Dehn twist along $\tilde{\tilde{C}}$ is performed. In fact, similar procedures can be carried out on all of the configurations shown in Figure 3.10 (and their generalizations that are not depicted). Therefore, all of the states $|\{a_i\},\{b_i\},\{w_i\}\rangle$ with some w_i labels equal to ψ can be obtained from the states the states without such w_i labels, i.e., the states $|\{a_i\}\rangle$, by applying one or a sequence of Dehn twists of the type shown above. Consequently, all the operators $|\text{vac}\rangle\langle\{a_i\},\{b_i\},\{w_i\}|$ and $|\{a_i\},\{b_i\},\{w_i\}\rangle\langle\text{vac}|$ can be obtained from multiplying the operators of the form $|\text{vac}\rangle\langle\{a_i\}|$ or $|\{a_i\}\rangle\langle\text{vac}|$ with the unitary operators associated to the proper set of Dehn twists.

Having constructed all of the operators $|\text{vac}\rangle\langle\{a_i\},\{b_i\},\{w_i\}|$ and $|\{a_i\},\{b_i\},\{w_i\}\rangle\langle\text{vac}|$ (regardless of the value of the w_i labels) within $\mathbb{C}[\rho_g]$, we can simply obtain via matrix multiplication operators of the more general form $|\{a'_i\},\{b'_i\},\{w'_i\}\rangle\langle\{a_i\},\{b_i\},\{w_i\}|$, which form a complete basis for the full matrix algebra $\mathbb{M}_{N_g}$, within $\mathbb{C}[\rho_g]$. At this point, we have completed the proof for $\mathbb{C}[\rho_g] \cong \mathbb{M}_{N_g}$ and, hence, for the irreducibility of the (projective) representation ρ_g of the MCG for a general g.

Duality to 2d Ising CFT

In Section 3.4, we proposed the expression (3.42) for the vacuum seed in terms of the product of the holomorphic and anti-holomorphic vacuum conformal blocks of the 2d Ising CFT. Based on this proposed vacuum seed, we proved the finiteness of the "gravitational" modular sum (3.41) in Section 3.4 and obtained the final expression (3.50) of the gravitational partition function Z_{grav} up to a multiplicative constant in Section 3.4. We need to emphasize that, in our discussion, the result (3.50) is purely a consequence of our arguments for the vacuum seed Z_{vac} which were made from the gravity bulk perspective, as well as of the mathematical results that we proved including the finiteness of $\rho_g(\Gamma_g)$ and the irreducibility of the MCG representation ρ_g. In fact, even if Z_{vac} is not of the form (3.42), as long as it be written as a product of a holomorphic and an anti-holomorphic conformal block of the 2d Ising CFT (or even as a sum of products of this type), we can still conclude the finiteness of the modular sum (3.41) and further obtain the *same* expression (3.50) for Z_{grav}, based on our mathematical results, i.e., the finiteness of $\rho_g(\Gamma_g)$ and the irreducibility of ρ_g.

The right hand side of (3.50) can also be naturally identified with the (full) partition function of the 2d Ising CFT on the Riemann surface Σ_g with period matrix Ω. We therefore conclude that, at Brown-Henneaux central charge $c = 1/2$, and for genus g, the full gravitational partition function $Z_{\text{grav}}(\Omega,\bar{\Omega})$ with a genus-g asymptotic boundary Σ_g is always

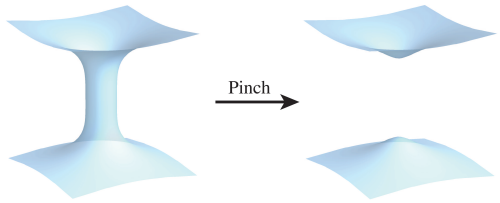

Figure 3.11: A schematic picture for pinching off a long cylinder.

proportional to the partition function of the 2d Ising CFT $Z_{\text{Ising}}(\Omega, \bar{\Omega})$ on Σ_g:

$$Z_{\text{grav}}(\Omega, \bar{\Omega}) \propto \sum_{i=1}^{N_g} \chi_i(\Omega)\bar{\chi}_i(\bar{\Omega}) = Z_{\text{Ising}}(\Omega, \bar{\Omega}). \tag{3.61}$$

At this point, we would like to come back to our proposed expression (3.42) for the vacuum seed. In Section 3.4, we have already provided physical arguments that suggest that (3.42) is a natural expression for the vacuum seed. Now, we would like to further substantiate this proposal (3.42) by commenting on the resulting gravitational partition function Z_{grav} (3.61). (3.61) is a sensible result from the following perspectives. Firstly, the gravitational partition function (3.61) for arbitrary genus g is compatible with and is the natural extension of the genus-one result obtained in [119]. Secondly, the gravitational partition function (3.61), in the "pinching limits", is self-consistent and is consistent with the genus-one result obtained in [119]. The pinching limit we focus on here is the limit of the period matrix Ω of the asymptotic boundary Σ_g in which some part of the asymptotic boundary Σ_g is stretched into a very long cylinder and eventually can be effectively viewed as pinched off. Figure 3.11 is a schematic picture for pinching off a long cylinder. In the gravity context, such a pinching limit has previously only been investigated, to the best of our knowledge, in semi-classical gravity [52, 159]. With the gravitational partition function given by (3.61), we can now study the pinching limit of strongly coupled gravity with Brown-Henneaux central charge $c = 1/2$. In the pinching limit, intuitively, we expect the genus of the asymptotic boundary to be effectively reduced by 1. Hence, we expect a reduction of a gravitational partition function with a genus-g boundary to one with a genus-$(g-1)$ boundary. This physical intuition is indeed consistent with (3.61), since the partition function of 2d Ising CFT on a genus-g surface indeed reduces to that on a genus-$(g-1)$ surface in the pinching limit [141].

Starting with a genus-g asymptotic boundary, we can take successive pinching limits such that the genus of the resulting asymptotic boundaries eventually reduces to $g = 1$. In this case, (3.61) implies that the gravitational partition function eventually reduces, up an overall multiplicative constant, to the product of genus-one partition functions of the 2d Ising CFT. This result is again consistent with [119]. Here, we have provided general arguments for the behavior of the gravitational partition function in the pinching limits using (3.61) and using the behavior of the 2d Ising CFT partition in the same limit. In Appendix A.5, we provide

an example of analytic studies of the pinching limit of the gravitational partition function with genus-two asymptotic boundaries. Having provided arguments that substantiate the result (3.61) [and thereby its starting point (3.42)], we would like to conclude that based on a natural choice for the vacuum seed, we establish duality between 3d AdS quantum gravity at Brown-Henneaux central charge $c = 1/2$ and the 2d Ising CFT using the all-genus partition functions.

Besides the gravitational partition function, the mathematical result that ρ_g is an irreducible projective representation of the MCG Γ_g of the Riemann surface Σ_g for any g also has an interesting implication purely for the 2d Ising CFT. It was proven in [137] that, up to a multiplicative constant, there is only one unique modular invariant partition function that can be constructed using 2d Ising CFT conformal blocks on a genus-one surface. To the best of our knowledge, there is no generalization of such a proof to higher-genus surfaces in previous works. Our result that ρ_g is an irreducible representation of Γ_g implies that, up to a multiplicative constant, for any fixed genus g, there is always a unique partition function constructed from Ising-CFT conformal blocks that is invariant under the MCG Γ_g action on a genus-g surface.

Difficulty in extending beyond the 2d Ising CFT

Solely based on the consideration of gravitational partition functions with genus-1 asymptotic boundary, Castro et al. [119] argued that, for Brown-Henneaux central charge $c < 1$, the only 2d CFTs that can be dual to pure Einstein gravity in AdS_3 at the corresponding Brown-Henneaux central charge c are the Ising and the Tricritical Ising CFTs of central charges $c = 1/2$ and $c = 7/10$. Our results obtained in the previous subsections on the all-genus partition functions has established duality between 3d AdS quantum gravity at Brown-Henneaux central charge $c = 1/2$ and the 2d Ising CFT.

However, as we will show later in this subsection, the consideration of higher-genus partition functions at $c = 7/10$ reveals a fundamental difficulty in establishing duality between 3d gravity at Brown-Henneaux central charge $c = 7/10$ and the Tricritical Ising CFT.

At Brown-Henneaux central charge $c = 7/10$, we can follow the same reasoning as in Section 3.4 to argue that the corresponding gravitational vacuum seed at $c = 7/10$ with a genus-g asymptotic boundary Σ_g should be identified as the vacuum conformal block of the 2d Tricritical Ising CFT on Σ_g. Hence, the modular sum (3.41) at $c = 7/10$ is dictated by the MCG Γ_g representation ρ'_g that governs how the holomorphic conformal blocks of the 2d Tricritical Ising CFT transform under the action of Γ_g. In complete analogy with the connection between the 2d Ising CFT and the 3d Ising TQFT, the information about the MCG representation ρ'_g (which is associated with the holomorphic conformal blocks of the 2d Tricritical Ising CFT) is fully contained in the 3d Tricritical Ising TQFT, which can be mathematically described, equivalently, by the chiral Tricritical Ising Modular Tensor Category (MTC) [99, 160].

By inspection, this MTC contains a sub-Modular Tensor Category called Fib, with the

so-called Fibonacci Fusion Rules[27] (see, e.g., [161]). It follows from a very general Theorem by Müger [162] that the Tricritical Ising MTC at $c = 7/10$ must then be the tensor product of the sub MTC Fib and the MTC associated to the chiral Ising CFT. This factorization implies that the MCG representation ρ'_g given by the Tricritical Ising MTC must be a tensor product of an MCG representation given by the MTC Fib and an MCG representation given by the MTC of the 2d chiral Ising CFT. Each of these MCG representations mentioned here can be viewed as a map from the MCG to a unitary group.

Finally, a fundamental Theorem by Freedman, Larsen and Wang [163] states that the MCG representations given by the MTC Fib has an infinite image set.[28] It then immediately follows that the image set of ρ'_g must also be infinite, i.e., the set $\rho'_g(\Gamma_g)$, where Γ_g is the MCG of the genus-g Riemann surface, is an infinite set. This result implies that at Brown-Henneaux central charge $c = 7/10$, the modular sum of the gravitational partition function in (3.41) cannot be defined for genus $g \geq 2$ because the sum occurring in this equation has an infinite number of terms and cannot be naturally regularized, as discussed in Footnote Footnote 4.

[27]The MTC Fib has only two labels (="simple objects" or "particles" or "anyons" types) which, when denoted by 1 and x, possess the Fusion Rules $x \times x = 1 + x$, $1 \times x = x \times 1 = x$, $1 \times 1 = 1$. Strictly speaking, the MTC Fib that is needed here is the conjugate of the MTC Fib typically used in the literature [161].

[28]In fact, this image set is dense in a unitary group, a result that, as is well known, is related to the fundamental importance of the Fib MTC for the subject of fault-tolerant quantum computation.

Chapter 4

Probing holography in p-adic CFT

4.1 Introduction

Explorations in the past three decades between the interplay of algebraic number theory and string theory have been emerging. Once one defines the p-adic norm, a well-known phenomenon appears in string scattering amplitudes from adelic products. We can construct the real Veneziano amplitude $A^{(\infty)}(s,t,u)$ for the open bosonic string theory at tree-level from the product over all prime numbers of the p-adic Veneziano amplitudes $A^{(p)}(s,t,u)$ [164, 165]

$$A^{(\infty)}(s,t,u) = \left[\prod_p A^{(p)}(s,t,u)\right]^{-1} = B_\infty(1-k_1\cdot k_2, 1-k_1\cdot k_3) \equiv \int_{\mathbb{R}} dx |x|_\infty^{-k_1\cdot k_2} |1-x|_\infty^{-k_1\cdot k_3}, \tag{4.1}$$

where $|x|_\infty$ is the usual norm in $\mathbb{R}$ and s,t,u are the Mandelstam variables which are expressed in terms of the tachyon momenta k_1, k_2, k_3, so that $k_i^2 = 2$. An interpretation of the p-adic string is given by [166], where the open string worldsheet is replaced by a Bruhat-Tits tree (defined in Section 4.2 therein) and its boundary as the p-adic numbers.

Recently inspired by this perspective, Gubser et al. [167] and Heydeman et al. [168] proposed a toy model of a non-Archimedean version for the Euclidean AdS/CFT correspondence [32]. In the simplest topology, the usual continuous bulk is replaced by an infinite, symmetric, and homogeneous (i.e., no preferred central vertex) tree of uniform valency $p+1$. This tree, known as the *Bruhat-Tits tree* (or *Bethe lattice*), is expressed as the left coset space

$$T_p \equiv PGL\,(2,\mathbb{Q}_p)\,/PGL\,(2,\mathbb{Z}_p)\,, \tag{4.2}$$

where $PGL\,(2,\mathbb{Q}_p)$ is the p-adic global conformal group[1], whose maximal compact open subgroup is $PGL\,(2,\mathbb{Z}_p)$. The definition (4.2) is reminiscent of the hyperbolic 3-space $\mathbb{H}^3 \simeq SL(2,\mathbb{C})/SU(2)$ with boundary $\mathbb{P}^1(\mathbb{C})$, describing Euclidean asymptotic AdS_3. Additionally,

[1]It is a *totally disconnected locally compact (TDLC)* group, with respect to the $\mathbb{Q}_p$ topology as explained in Section 10.5 in [169], but not compact. Its subgroup $PSL\,(2,\mathbb{Q}_p)$ is neither compact nor open.

for the *unramified* finite Galois extension $\mathbb{Q}_{p^n}$ of $\mathbb{Q}_p$, the tree T_{p^n} has valency $p^n + 1$ and boundary $\partial T_{p^n} = P^1(\mathbb{Q}_{p^n})$. Using unramified extensions, we are not limited to just one-dimensional boundaries but we can think of Euclidean AdS_{n+1} analogous to T_{p^n}.

With this specific discretization of the bulk, one can put physical degrees of freedom on its vertices. The simplest case is to introduce scalars. Furthermore, the tree as well as its dual graph can be identified with tensor networks in order to study bulk reconstruction, quantum error-correction codes [168, 170] and holographic RG flow [171].

One can study more general fields, such as spins, on the trees. The first realization of spins in p-adic AdS/CFT was introduced by Gubser et al. [172, 173] with results on the bulk dual to non-scalar operators and dynamical gauge fields. In particular, they computed the holographic two-point correlator of an operator $\mathcal{O}_\psi$ dual to a spin state $|\psi\rangle$. One of the main conclusions was that the fermionic two-point correlator is of similar form to the scalar two-point correlator up to normalization and a non-trivial sign character resembling the operators' statistics.

There are other exotic and interesting applications in the context of the p-adics. An example is to understand higher-order versions of the Klebanov-Tarnopolsky model for both the real and p-adic cases. Recently in [174], the authors analyzed the situation for q propagators at each interaction vertex as well as found an adelic product relation between the p-adic and real eigenvalues of the ladder operator integral to calculate four-point correlators. In addition, [174] provided nice comparisons with matrix field theory regarding the propagators' symmetry group.

Another use of p-adic is to use the Berkovich space to iencode the renormalization group flow of the energy spectrum of the theory of a particle-in-a-box [175].

Given these progresses, the status quo of p-adic AdS/CFT seems rather one-sided in the sense that the p-adic CFT is not well-formulated, because a Hilbert space is absent. Melzer [176], and later Harlow et al. [177] and Gubser-Parikh [178], have shed some light on its OPE structure, but its partition function and local conformal algebra were not duly explored. As mentioned earlier, it is very natural to describe global AdS_n as a Bruhat-Tits tree. One well-known phenomenon studied in 3d gravity is the BTZ black hole. Heydeman et al. [168] formulated a p-adic BTZ black hole, and it serves as one motivation for this chapter in the hope of extracting meaningful information for p-adic CFTs. We calculated the bulk partition function and showed it has many key features as in [5], such as Bekenstein-Hawking area law in 3d gravity. We hope this partition function could initiate future works to match the boundary CFT data.

A meaningful direction to gain more insight on the holographic p-adic CFT's structure is to study the constraints on the averaged three-point coefficients for p-adic BTZ black holes as done in regular BTZ black holes [145]. We found the averaged three-point coefficient for a p-adic BTZ black hole in the limit of large horizon l to obey a similar exponentially-decaying behavior $e^{-\Delta l}$ as for regular BTZ black holes [145], where Δ is a boundary CFT data. One would hope to recover this result purely from the Lie algebra representation of the holographic p-adic CFT. However, we make a strong argument against the existence of a local algebra, and therefore we turn to the group representations, where a classification theorem

comes in handy. We analyze each case, and propose a way of checking which representation of p-adic CFT fits the genus-1 bulk calculation.

The rest of this chapter is organized as follow. In Section 4.2, we review mathematical and physical concepts relevant to p-adic AdS/CFT. In Section 4.3, we solve Laplace problems on Bruhat-Tits trees and p-adic BTZ black hole geometries via linear recurrence, and therefore obtain the partition functions, whose various implications are discussed. In Section 4.4, we calculate the one-loop Witten diagram describing the 1-to-2 scattering between two types of bulk scalars dual to light primary fields on the boundary in the background of a p-adic BTZ black hole, and the result imposes a constraint on potentially precise formulations on p-adic CFTs. In Section 4.5, we review the representation theory on $PGL(2, \mathbb{Q}_p)$. Furthermore, we present an analysis on possible group representations as Hilbert spaces for p-adic CFTs. Finally, we conclude with a discussion of the results and future directions in Section 4.6.

4.2 Summary of p-adic concepts

p-adic numbers

As mentioned in the introduction, in constructing the p-adic AdS/CFT correspondence, the non-Archimedean field $\mathbb{Q}_p$ plays an important role. We briefly review Archimedean and non-Archimedean fields before discussing $\mathbb{Q}_p$. Let $\mathbb{F}$ be any field with a norm $|\cdot|_{\mathbb{F}}$ which obeys the standard axioms[2] for any $x, y \in \mathbb{F}$ [179]:

1. $|x|_{\mathbb{F}} \geq 0$ and is saturated when $x \equiv 0$;
2. $|x \cdot y|_{\mathbb{F}} = |x|_{\mathbb{F}} \cdot |y|_{\mathbb{F}}$;
3. $|x + y|_{\mathbb{F}} \leq |x|_{\mathbb{F}} + |y|_{\mathbb{F}}$ (triangle inequality).

When $\mathbb{F}$ is *Archimedean*, its norm obeys $\sup\{|n|_{\mathbb{F}} : n \in \mathbb{Z}\} = \infty$; whereas when $\mathbb{F}$ is *non-Archimedean*, its norm obeys $\sup\{|n|_{\mathbb{F}} : n \in \mathbb{Z}\} = 1$. The major difference between Archimedean and non-Archimedean fields is that only the latter has ultrametricity [169]:

$$|x + y|_{\mathbb{F}} \leq \sup\left(|x|_{\mathbb{F}}, |y|_{\mathbb{F}}\right), \tag{4.3}$$

implying that all triangles over an non-Archimedean field are isosceles.

Characteristic of $\mathbb{F}$ is defined as the least n such that when one adds up n copies of $1 \in \mathbb{F}$, one obtains zero. Naturally, $\mathbb{Q}$, $\mathbb{R}$, and $\mathbb{C}$ are fields of characteristic zero, while the set of residue classes modulo a prime p is a field of characteristic p [180]. We are concerned with $\mathbb{Q}_p$, a *characteristic zero non-Archimedean field*. To obtain degree n unramified extensions $\mathbb{Q}_{p^n}$, we adjoin $\mathbb{Q}_p$ by a primitive $(p^n - 1)^{\text{th}}$ root of unity [180].

[2]Rigorously speaking, in algebraic geometry and algebraic number theory, these axioms define the term "*valuation*" or "*absolute value*", differing from the "norm" in functional analysis, whose *absolute homogeneity* replaces the second axiom here. However, we still abuse the term "norm" throughout this chapter.

For any prime number p, $\mathbb{Q}_p$ is a completion of $\mathbb{Q}$ with respect to the p-adic norm $|\cdot|_p$ [169]. To define $|\cdot|_p$, we note that any $x \in \mathbb{Q}_p \backslash \{0\}$ has a unique p-adic expansion

$$x = \underbrace{...a_3a_2a_1a_0}_{\text{in } \mathbb{Z}_p} . \underbrace{a_{-1}a_{-2}...a_{v_p}}_{\text{fractional part of } x} \equiv \sum_{n=v_p}^{\infty} a_n p^n, \tag{4.4}$$

where $a_n \in \{0, 1, \cdots, p-1\}$, and v_p is the smallest integer index such that $a_{v_p} \neq 0$ [165]. The p-adic norm of x is then defined as

$$|x|_p = p^{-v_p}. \tag{4.5}$$

Notice that although $0 \in \mathbb{Q}_p$ has no p-adic expansion, we naturally define $|0|_p = 0$.

One can ask do other completions of $\mathbb{Q}$ exist? The answer is given by Ostrowski's theorem [169]: *the only non-trivial norms on $\mathbb{Q}$ are those equivalent to the $|\cdot|_p$ or the ordinary norm $|\cdot|_\infty$*. In other words, $\mathbb{Q}_p$ and $\mathbb{R}$ are the only completions of $\mathbb{Q}$. For unramified extensions of Ostrowski's theorem for $\mathbb{Q}_{p^n}$, see [179, 181].

We here list notations for subsets of $\mathbb{Q}_p$ used in later sections. We denote the multiplicative group of the p-adic field as $\mathbb{Q}_p^\times \equiv \mathbb{Q}_p \backslash \{0\}$, the ring of integers of $\mathbb{Q}_p$ as $\mathbb{Z}_p \equiv \{x \in \mathbb{Q}_p : |x|_p \leq 1\}$, and the set of units in $\mathbb{Q}_p$ as $\mathbb{U}_p \in \mathbb{Z}_p$ such that $\forall x \in \mathbb{U}_p, |x|_p = 1$.

Bruhat-Tits tree

The Bruhat-Tits tree is an infinite tree structure built on equivalence classes of the $\mathbb{Q}_p^2$-lattice $\mathcal{L}$ which are spanned by two linearly independent vectors $u, v \in \mathbb{Q}_p^2$:

$$\mathcal{L} \equiv \left\{ au + bv \in \mathbb{Q}_p^2 | a, b \in \mathbb{Z}_p \right\}. \tag{4.6}$$

The equivalence relation between the two $\mathbb{Q}_p^2$-lattices $\mathcal{L}$ and $\mathcal{L}'$ is defined as: $\mathcal{L} \sim \mathcal{L}'$ if $\mathcal{L} = c\mathcal{L}'$ for some $c \in \mathbb{Q}_p^\times$.

Based on these definitions, a Bruhat-Tits tree is then constructed by assigning each equivalence class of the $\mathbb{Q}_p^2$-lattice to one vertex on the tree. It is straightforward to see that by applying the $PGL(2, \mathbb{Q}_p)$ group actions on a lattice equivalence class in the following fashion

$$M : l = (u, v) \to (Mu, Mv), \quad M \in GL(2, \mathbb{Q}_p), \tag{4.7}$$

we obtain another new equivalence class. Any subgroup which is conjugate to $PGL(2, \mathbb{Z}_p)$ will leave a lattice equivalence class invariant, so the Bruhat-Tits tree T_p is identified with the coset $PGL(2, \mathbb{Q}_p)/PGL(2, \mathbb{Z}_p)$.

On the tree we also need to clarify the meaning of an edge between two vertices. Therefore, a relation between two lattice equivalence classes $\mathcal{L}$ and $\mathcal{L}'$ is introduced as described in [166] and reviewed in the Appendix of [182]: they are called *incident* if $p\mathcal{L} \subset \mathcal{L}' \subset \mathcal{L}$, and we connect them by an edge.

Using this incident relation to define edges on the Bruhat-Tits tree has two advantages. Firstly, this relation is reflexive, so the Bruhat-Tits tree becomes unoriented, with exactly one edge between two adjacent vertices. Secondly, $PGL(2,\mathbb{Q}_p)$ action on the tree preserves the incident relation between any two lattice classes, leaving the number of edges between any two vertices invariant. If we use the edge number as a natural metric on the tree, then we see that $PGL(2,\mathbb{Q}_p)$ is its *isometry group*. This fact is significant, because in usual AdS/CFT, the bulk isometry group is to be identified with the boundary conformal group. Indeed, the suitable conformal group for the tree boundary $\mathbb{P}^1(\mathbb{Q}_p)$ is the same $PGL(2,\mathbb{Q}_p)$, acting in a fractional linear fashion. Therefore, we consider the Bruhat-Tits tree as the only candidate for p-adic AdS bulk.[3]

Apart from the formal definition, a Bruhat-Tits tree is also visualized as Figure 4.1 in

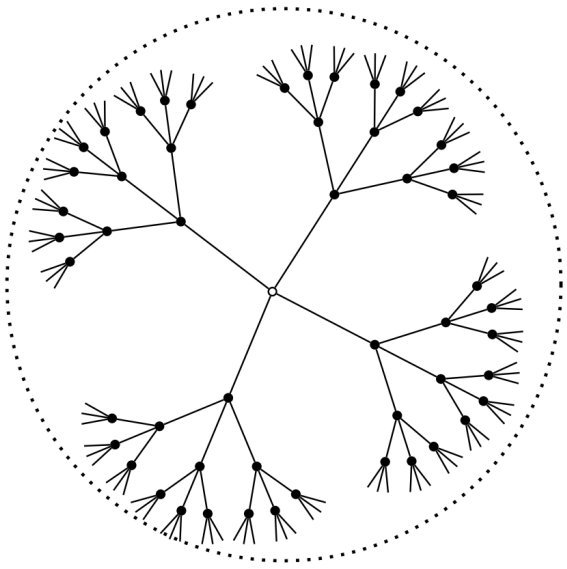

Figure 4.1: The Bruhat-Tits tree for the 3-adic numbers. The boundary $\partial T_3 = P^1(\mathbb{Q}_3)$ represents the infinity.

the representation as follows. From [182], we know that incident to any lattice class (u,v), there are always $p+1$ other lattice classes: (pu,v) and $(u+nv,pv)$ where $n \in \mathbb{F}_p$ taking p possible values, indicating that the Bruhat-Tits tree is homogeneous with valency $p+1$.

Given the valency, there is a good way to translate the tree into p-adic numbers. Because any p-adic number has a unique expansion (4.4), it is determined by a unique sequence of (a_n), $a_n \in \mathbb{F}_p$. We assign coordinates (z,z_0) on the Bruhat-Tits tree, where z_0 is the prime number p's exponent, regarded as a level in the tree, and z is a p-adic number up to $\mathcal{O}(z_0)$ precision. Therefore, each path on the Bruhat-Tits tree from $(z_0 \to \infty)$ to the boundary

[3]Iterative refinements on vertices of a Bruhat-Tits tree in the context of holography is proposed in Section 5.3 of [167], and is later extended in [183].

$\mathbb{P}^1(\mathbb{Q}_p)$ uniquely represents a p-adic number. This is graphically presented in terms of a "trunck" and "branches" in [167].

An invitation to p-adic CFTs

The majority of CFTs of our interests are "one-dimensional" ones, however, we will see that all higher-dimensional p-adic CFTs are very similar to ordinary 2d CFTs. We review Melzer's axioms [176] on p-adic CFTs. They must have operator product expansion algebras (OPA), just like ordinary CFTs. The main difference between ordinary and p-adic CFTs is that local derivatives do not exist in the latter due to $\mathbb{Q}_p$ being totally disconnected.[4] More explicitly, this is seen by applying Leibniz's rule to $\mathbb{C}$-valued characteristic (or indicator) functions over $\mathbb{Q}_p$, all of which are locally constant [176]. Finally, to make the OPA complete, all fields are primary (4.12):

$$\phi'_a(x')(dx')^{\Delta} = \phi_a(x)(dx)^{\Delta}, \tag{4.8}$$

and the following OPE must exist

$$\phi_m(x)\phi_n(y) = \sum_a C^a_{mn}(x,y)\phi_a(y) \tag{4.9}$$

with $C^a_{mn}(x,y) \in \mathbb{R}$.

Here Δ is the conformal dimension, dx is the Haar measure defined on $\mathbb{Q}_p$, and the transformation $x \to x' \in P^1(\mathbb{Q}_p)$ is a fractional linear one:

$$x \to x' = \frac{ax+b}{cx+d}, \quad \begin{pmatrix} a & b \\ c & d \end{pmatrix} \in GL(2,\mathbb{Q}_p), \tag{4.10}$$

so the Haar measure and scalar field transform respectively as:

$$dx \to dx' = \left|\frac{ad-bc}{(cx+d)^2}\right|_p dx, \tag{4.11}$$

$$\phi_a(x) \to \phi'_a\left(\frac{ax+b}{cx+d}\right) = \left|\frac{ad-bc}{(cx+d)^2}\right|_p^{-\Delta} \phi_a(x). \tag{4.12}$$

Since the bulk is a Bruhat-Tits tree and the boundary consists of p-adic numbers, evaluating correlators are more convenient than that in the ordinary case. For instance, the general two- and three-point functions for local operators $\mathcal{O}_1, \mathcal{O}_2, \mathcal{O}_3, \ldots$ with different conformal dimensions $\Delta_1, \Delta_2, \Delta_3, \ldots$ respectively are of similar form to real CFTs' [167]:

$$\langle \mathcal{O}_1(z_1)\mathcal{O}_2(z_2)\rangle = \frac{C_{\mathcal{O}_1\mathcal{O}_2}}{|z_{12}|_p^{2\Delta_1}}, \qquad \langle \mathcal{O}_1(z_1)\mathcal{O}_2(z_2)\mathcal{O}_3(z_3)\rangle = \frac{C_{\mathcal{O}_1\mathcal{O}_2\mathcal{O}_3}}{|z_{12}|_p^{\Delta_{12}}|z_{23}|_p^{\Delta_{23}}|z_{31}|_p^{\Delta_{31}}}, \tag{4.13}$$

[4] By totally disconnected for the p-adic numbers, we mean that two open sets are totally disjoint. Whereas the Archimedean field $\mathbb{R}$ is a connected metric space.

up to contact terms. Here $z_{ij} \equiv z_i - z_j$, $\Delta_{12} \equiv \Delta_1 + \Delta_2 - \Delta_3$, and the z_i-dependence is completely fixed by the invariance under fractional linear transformations. Ultrametricity constrains three- and four-point functions to be exact in cross-ratios in the p-adic norm, unlike the usual ones [167, 176]. The OPE coefficients form an associative algebra and primary operators can have *arbitrary* dimensions, but the unit operator must have dimension 0.

Another property worth mentioning about p-adic CFTs is that they are automatically *unitary* unlike their Archimedean counterparts. However, as opposed to finite-dimensional representations of the local $sl(2,\mathbb{C})$ in usual 2d CFTs, the p-adic global conformal group $PGL(2,\mathbb{Q}_p)$ lacks a Lie algebra, leading to the absence of a central charge or a good notion of state-operator correspondence.[5] Despite lacking both local conformal algebra and descendants, we will discuss in Section 4.5 on allowed group representations of a p-adic CFT.

p-adic AdS/CFT and BTZ black hole

In order to construct a p-adic version of the BTZ black hole, we first review the ordinary BTZ black hole, a classic black hole solution to the 3d Einstein equation [45]. A *non-rotating* Euclidean BTZ black hole is described by the following complete Riemannian metric [186]:

$$ds^2 = \left(r^2 - r_+^2\right) dt^2 + \frac{1}{r^2 - r_+^2} dr^2 + r^2 d\phi^2, \tag{4.14}$$

where r_+ is the outer horizon radius[6], related to the ADM energy and central charge of the boundary 2d CFT by [145]

$$r_+ = \sqrt{\frac{12E}{c} - 1}. \tag{4.15}$$

Similarly, a p-adic BTZ black hole can also be formulated by solving classical equations of motion. In [187], Gubser et al. proposed to use edge length dynamics to formulate "gravity" (beyond linearized regime) on Bruhat-Tits trees, and even though large diffeomorphisms were seemingly not included there, this "gravity" does result in BTZ black holes with non-uniform lengths, incorporating topological changes by the 1-cycle. Their idea has been generalized to weighted graphs [188, 189].

However, to avoid technicalities above, we choose to review the p-adic BTZ black hole constructed instead by *Schottky uniformization* as proposed in [168], in which the black hole is a quotient of the Bruhat-Tits tree (analogue of the zero-temperature AdS_3), similar to the construction of a regular Euclidean BTZ black hole [46].

In Euclidean AdS_3/CFT_2 at zero temperature, the bulk is identified with the hyperbolic space $\mathbb{H}^3$ and the boundary is the *sphere at infinity* S^2_∞, on which its conformal group is

[5] Examples of ordinary 2d CFTs with $c = 0$ include special classes of logarithmic CFTs, see, e.g., [184, 185].

[6] This metric is in a compact form, nevertheless agreeing with (2.22) upon setting $J = 0$ (non-rotating) and $l = 1$.

$PSL(2,\mathbb{C})$, same as the isometry group of $\mathbb{H}^3$. *Schottky uniformization* provides us a way to construct higher genus elliptic curves on the conformal boundary. In this complex case, a genus-1 closed curve corresponds to T^2 torus and the solid torus bulk is topologically equivalent to the BTZ black hole. Generally for a genus-n curve, *Schottky uniformization* starts from picking a $PSL(2,\mathbb{C})$ discrete subgroup called *Schottky group* Γ with n generators $\{\gamma_1, \cdots, \gamma_n\}$. Each γ_i has fixed points in S^2_∞, and the genus-n curve is constructed as S^2_∞/Γ after removing those fixed points. The authors in [168, 170] extended this procedure to construct the p-adic BTZ black hole, which we will review and follow.

For a genus-1 boundary, $\Gamma = q^{\mathbb{Z}}$ is generated by $q \in \mathbb{C}^\times$. Fixed points $0, \infty$ of the action by q need to be removed from $\mathbb{P}^1(\mathbb{C})$ before taking the quotient. We define the *domain of discontinuity* $A = \mathbb{P}^1(\mathbb{C}) \setminus \{0, \infty\}$ and hence the quotient $C \equiv A/q^{\mathbb{Z}}$. Meanwhile, we also take the quotient of the bulk $\mathbb{H}^3$, and the total quotient space is $\mathbb{H}^3/q^{\mathbb{Z}} \cup C$, which is visualized as a solid torus. We should mention that the generator γ can be written in terms of parameter $q = e^{2\pi i\tau}$, where $\tau \in \mathbb{C}$ is the torus' moduli.

In the BTZ black hole (4.14), r_+ is a solution-classifying parameter to be realized in *Schottky uniformization*. Note that the *Schottky group* $q^{\mathbb{Z}}$'s generator γ can be written as [5, 168]:

$$\begin{pmatrix} q^{\frac{1}{2}} & 0 \\ 0 & q^{-\frac{1}{2}} \end{pmatrix} \in PSL(2,\mathbb{C}). \tag{4.16}$$

The *Schottky parameter* q is written in terms of horizon radius $q = e^{2\pi r_+}$ [168, 170], so $r_+ = \frac{1}{2\pi}\log q$, proportional to the Bekenstein-Hawking entropy.

A torus T^2 is the same as a complex lattice $\mathbb{Z} + \tau\mathbb{Z}$, $\tau \in \mathbb{C}$, while in the p-adic case, this viewpoint is not true due to $p^\infty \to 0$ forcing many lattice equivalence classes to be 0. However, we could still select one *Schottky group* Γ, a discrete subgroup of $PGL(2,\mathbb{Q}_p)$ to form genus-n curves from $\mathbb{P}^1(\mathbb{Q}_p)$. The genus-one curve is the Tate uniformized elliptic curve $E_q = \mathbb{Q}_p^\times/q^{\mathbb{Z}}$ and genus-n curve is the Mumford curve. We demonstrate the genus-one example by picking Γ generated by $q \in \mathbb{Q}_p^\times$, so that

$$\Gamma = \left\langle \begin{pmatrix} q & 0 \\ 0 & 1 \end{pmatrix} \right\rangle. \tag{4.17}$$

Again we remove its fixed points, which are still $\{0, \infty\}$, from $\mathbb{P}^1(\mathbb{Q}_p)$, then the total space including bulk and boundary is $B = T_p \cup (\mathbb{P}^1(\mathbb{Q}_p) \setminus \{0, \infty\})$, where T_p is the Bruhat-Tits tree from Section 4.2. The quotient $B/q^{\mathbb{Z}}$ is visualized as a graph with one regular polygon at the center. On each vertex of the polygon, a "Bruhat-Tits" inhomogeneous subtree is attached as seen in Figure 4.2.

This graph could also be considered as a p-adic BTZ black hole, whose horizon area is the number of edges l of the central polygon, with l related to the Schottky parameter q via $l = \log_p |q|_p$.[7] This also adds a restriction: $|q|_p > 1$. In Sections 4.3 and 4.4, we will use the above graph as the p-adic BTZ black hole and perform calculations on it.

[7]The $\log_p$ denotes the ordinary logarithm with base p, not the p-adic logarithm.

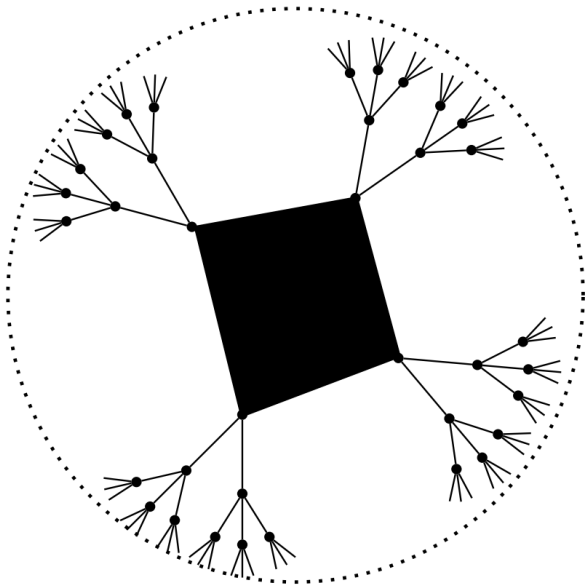

Figure 4.2: ($l = 3$, $p = 3$) BTZ black hole is at the center. The dotted lines represent the Bruhat-Tits tree structure repeating itself in a fractal fashion.

4.3 Path integrals

In this section, we try to calculate the partition function of the boundary p-adic CFT directly from the bulk by resorting to the Gubser-Klebanov-Polyakov-Witten (GKPW) dictionary. Recall for a boundary CFT local operator $\mathcal{O}$ [190, 191]

$$Z_{\text{grav}}[\phi^i_\partial(x); \partial M] = \left\langle \exp\left(-\sum_i \int_{\partial M} d^d x \phi^i_\partial(x) \mathcal{O}^i(x) \right) \right\rangle_{\text{CFT on } \partial M}, \tag{4.18}$$

with the boundary condition on bulk scalar field $\phi^i(z, x) = z^{d-\Delta}\phi^i_\partial(x) +$ (subleading) as $z \to 0$, where z is the radial coordinate.

When we set field values ϕ^i_∂ on the conformal boundary to be zero, it is expected to calculate the CFT partition function, see e.g., Eq.(72) in [167].

In our case, the bulk path integral on a Bruhat-Tits tree, is

$$Z_{\text{tree}} = \int \mathcal{D}\phi_a e^{-S_{\text{tree}}[\phi_a]}, \tag{4.19}$$

where the action $S_{\text{tree}}[\phi_a]$ is for massive scalar fields with sources on the tree, and the subscript "a" labels vertices. Naturally, this action is [167]

$$S_{\text{tree}}[\phi_a] = \sum_{\langle ab \rangle} \frac{1}{2} (\phi_a - \phi_b)^2 + \sum_a \left(\frac{1}{2} m_p^2 \phi_a^2 - J_a \phi_a \right) \tag{4.20}$$

with a and b labelling the tree's vertices and $\sum_{\langle ab\rangle}$ refers to summing over adjacent vertices on the tree, and J_a is a source.

As expected, the linearized equations of motion for a scalar field ϕ_a are

$$\left(\Box + m_p^2\right)\phi_a = J_a, \tag{4.21}$$

but with a modification to the regular Laplacian. The modification is that the Laplacian here is the lattice/graph Laplacian[8] and is defined as a a positive definite operator

$$\Box\phi_a \equiv \sum_{\langle ab\rangle}(\phi_a - \phi_b). \tag{4.22}$$

With this Laplacian to our disposal, the desired partition function is easily calculable via

$$Z_\phi = \frac{1}{\sqrt{\left(\Box + m_p^2\right)'}}, \tag{4.23}$$

where the superscript $'$ means omitting zero modes, which is absent as we will see later.

Another way to obtain the partition function is through the use of a tensor network formulation for p-adic AdS/CFT by [171]. These authors put a tensor network on the Bruhat-Tits tree, similar to [168] but different from the dual graph in [170]. Then by making analogies with ordinary *diagonal* CFTs[9], their proposed "torus" partition function is[10]:

$$\sum_a |q|^{\Delta_a}. \tag{4.24}$$

Here a labels all primary fields, and Δ_a's correspond to arbitrary scaling dimensions according to Melzer's axioms, and are compatible with the associative operator product algebra. Conspicuously, multiplicities here are all one, which is not the case for ordinary non-diagonal 2d CFTs.

A caveat is that our calculations are only for bulk scalar fields and not for the real gravitational contributions to the presumably full bulk path integral.[11] In the following three subsections, we first turn off the mass m_p^2, and then turn it back on near the end of this section.

[8] Connection Laplacian [167] and Hodge Laplacian [168, 187] are proved to be equivalent on Bruhat-Tits tree.

[9] *"Diagonal"* means that torus partition functions are diagonal invariants, such as Liouville theory and (A, A)-series minimal models, e.g., Ising model. Non-diagonal CFTs are the majority, and include logarithmic CFTs, $\widehat{su}(2)$ WZW models in D and E series, and (A, D)-, (A, D)-, (A, E)- and (E, A)-seires Virasoro minimal models, where (A_4, D_4), i.e., the 3-state Potts model being the simplest one.

[10] To be precise, it is a genus-1 Tate curve on the boundary of Bruhat-Tits tree.

[11] Attempts at formulating gravity on Bruhat-Tits trees include [187], but our techniques do not apply to calculating gravitational partition functions there.

Laplace problem on Bruhat-Tits trees

As promised, in this subsection and the next, we study massless scalars, which are dual to boundary marginal operators in the usual AdS/CFT context [168, 191].

We first define a few concepts on the Bruhat-Tits tree to be used in later sections. On this homogeneous tree, one can arbitrarily pick the central point and assign any vertex with "depth n," the number of edges going outwards from the center to that vertex, and the center has depth 0.

When we talk about scalar fields on the Bruhat-Tits tree, we refer to a real-valued scalar function globally defined on each vertex of the tree. The spectrum has been considered in to some extent, for example in [192], and here we solve the problem in more settings.

We show the isotropy of the spectrum, i.e., the lack of angular modes, as follows: one starts from the conformal boundary placed at a fictitious finite radial cut-off, which will later be taken to infinity, with boundary condition $\phi|_{\partial T_p} \equiv \phi_N = 0$, then p of them connect to one inner point with value ϕ_{N-1}. This point connects to a point further inwards with field value ϕ_{N-2}. Following the definition of Laplacian (4.22) and denoting the eigenvalue of the function $\phi_i, i = 1, \ldots, N$ as λ, there is a local recursion relation around the valency-$(p+1)$ vertex:

$$p(\phi_{N-1} - 0) + (\phi_{N-1} - \phi_{N-2}) = \lambda\phi_{N-1}, \tag{4.25}$$

implying $\phi_{N-2} = (p+1-\lambda)\phi_{N-1}$. Now at the depth $n = N-1$, for another point connecting to the point with value ϕ_{N-1}, we suppose it has another value $\tilde{\phi}_{N-1} \neq \phi_{N-1}$. This value must satisfy the same relation (4.25) with a fixed ϕ_{N-2}. Thus, we have $\tilde{\phi}_{N-1} = \phi_{N-1}$. By induction on depth n, one can show that all field values of the same depth n on the Bruhat-Tits tree are equal and we denote them as ϕ_n; this is due to the fact that the single central vertex is reached in the same number of steps starting from any boundary points.

We consider the sourceless case where $J = 0$ in (4.21). The recursion relation starting from $n = 2$ for ϕ_n now reads

$$p(\phi_{n-1} - \phi_n) + (\phi_{n-1} - \phi_{n-2}) = \lambda\phi_{n-1}, \tag{4.26}$$

whose characteristic equation has two roots:

$$\alpha_\pm = \frac{1 + p - \lambda \pm \sqrt{(\lambda - p - 1)^2 - 4p}}{2p}. \tag{4.27}$$

Field value at depth n equals the general solution to the linear recurrence (4.26)

$$\phi_n = c_+\alpha_+^n + c_-\alpha_-^n, \tag{4.28}$$

and we solve for coefficients $c_\pm$ with two initial conditions at depths 1 and 2:

$$\phi_1 = \left(1 - \frac{\lambda}{p+1}\right)\phi_0, \quad \phi_2 = \frac{p+1-\lambda}{p}\phi_1 - \frac{\phi_0}{p} = \left(1 - \frac{2\lambda}{p} + \frac{\lambda^2}{p+p^2}\right)\phi_0, \tag{4.29}$$

where ϕ_0 at the center is not fixed. The coefficients are

$$c_\pm = \left[\frac{1}{2} \pm \frac{p^2 - 1 - \lambda p + \lambda}{2(p+1)\sqrt{(p+1-\lambda)^2 - 4p}}\right] \phi_0. \tag{4.30}$$

Now we treat (4.28) as an degree-n polynomial equation in λ. Numerically we see that somewhat surprisingly, all roots of the equations for any n and p (primes and non-primes alike) are real. And in particular, when n is odd, there is one universal root $\lambda = p+1$. Also, the constant term in the polynomial $\phi_n(p, \lambda, \phi_0)$ is always ϕ_0, while the coefficient of the highest-degree term is always $(-1)^N \phi_0 / \left(p^N + p^{N-1}\right)$. Then by Vieta's formula, the product of all roots of the polynomial in λ is

$$p^N + p^{N-1} \tag{4.31}$$

which is in fact insensitive to the exact boundary value of ϕ_N.

Since $-\log\det(\Box)$ is radius-like divergent $\sim N$, in principle we are supposed to regularize it by local counterterms. We notice that the number of boundary points is also $p^N + p^{N-1}$, which dominates the number of points in the bulk for large N:

$$\frac{(p+1)p^N - 2}{p-1} \xrightarrow{N\to\infty} \frac{p}{p-1}\left(p^N + p^{N-1}\right). \tag{4.32}$$

Giving this observation, let us first recall that in the usual $\mathrm{AdS}_3/\mathrm{CFT}_2$, there are several places where various divergences appear. First, in the one-loop determinant of $\Box + m^2$ for a massive scalar on $\mathbb{H}^3$ [54],

$$\frac{1}{2}\mathrm{Vol}\left(\mathbb{H}^3\right) \int \frac{dt}{t} \frac{e^{-(m^2+1)t}}{(4\pi t)^{3/2}}, \tag{4.33}$$

there are $1/t$ UV divergence and $\mathrm{Vol}(\mathbb{H}^3)$ IR divergence, both removable by local counterterms. In another context, for the on-shell Einstein-Hilbert action with constant metric:

$$\frac{1}{16\pi G} \int d^3x \sqrt{g}\,(R - 2\Lambda) = \frac{V}{4\pi G l^2}, \tag{4.34}$$

where the cosmological constant $\Lambda = -1/l^2$ with l being the AdS_3 radius, and V is the spacetime volume, one can introduce a height cutoff ϵ in the upper-half space model. Then the regularized volume becomes [56]:

$$V_\epsilon(r) = \pi l^3 \left(\frac{r^2}{2\epsilon^2} - \frac{1}{2} - \ln\frac{r}{\epsilon}\right), \tag{4.35}$$

where the first boundary-area divergence can be removed by adding a boundary term local in boundary metric, and the second logarithmic divergence can be removed by a local counterterm as well.

In our case, the situation is different from these usual cases, since our boundary area appears in e^S instead of the action S. The naïve speculation is that the volume (i.e., number of vertices) on a Bruhat-Tits tree grow exponentially instead of power-law. By mimicking the removal of boundary-area divergence in ordinary AdS_3 above, we propose the partition function:

$$\boxed{Z_{\text{tree}} = \left(\frac{p}{p-1}\right)^{1/2}}. \tag{4.36}$$

We then investigate the behavior of the smallest and the largest eigenvalues of the Laplacian $\Box$ as $N \to \infty$ at a fixed p. We used Newton's method to find the upper bound on λ_1 and the lower bound on λ_N, and they seem to converge numerically; although intermediate eigenvalues do not converge, which is natural since the amount of them increases as N increases. For example, see Figure 4.3 when $p = 5$ and $N = 3, \ldots, 51$ blue for their convergence. Via Newton's method, we obtain the lower bound $\sim$1.52786 after 8036 iterations, and the upper bound $\sim$10.4721 after 474 iterations.

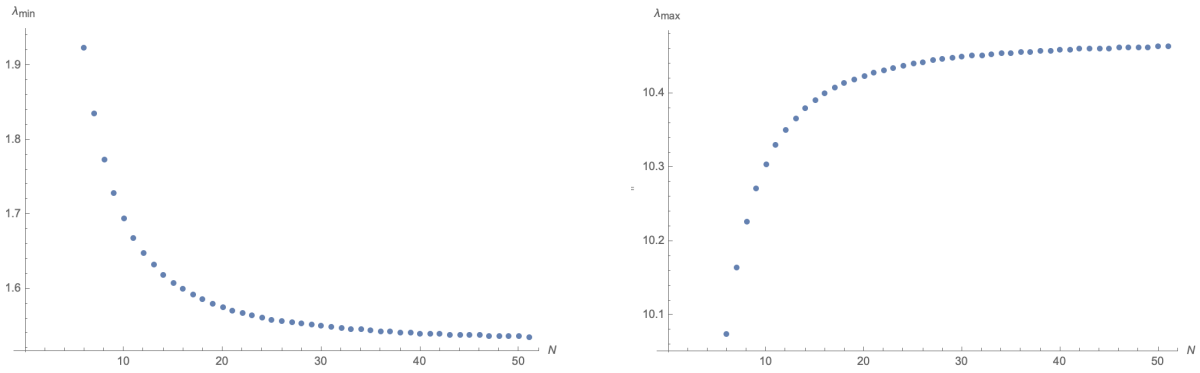

(a) Convergence of the smallest eigenvalues.

(b) Convergence of the largest eigenvalues.

Figure 4.3: Numerical bounds on the smallest and the largest eigenvalues via *Mathematica*'s `NSolve`, as the fictitious boundary cutoff N increases up to 51. They agree with results from Newton's method.

Now we pursue in finding the eigenfunctions on Bruhat-Tits trees. Unlike discrete Laplacians on a multidimensional regular rectangular grid with Dirichlet boundary conditions, the universal solutions to the second-order linear recurrence cannot be expressed in terms of a linear combination of Chebyshev polynomials of the first and the second kinds due to the nontrivial topology of Bruhat-Tits trees. The first expression in (4.29) contains a constant term ϕ_0, so there is no inner product over a finite real interval $[-a, a]$ which makes ϕ_1 and ϕ_2 orthogonal to each other. Another way to see this impossibility is that there is a linear term in λ for the second expression in (4.29).

Numerically, we observe that the decay is almost exponential, but faster than the asymptotically decay $\sim z^{-1/2}$ of Bessel functions of first and second kinds $J_\alpha(z)$ and $Y_\alpha(z)$. In

Figure 4.4, we plot the real part[12] of $\log(\phi_n/\phi_0), n = 1, \ldots, 51, N = 51$. The large but finite negative value is an artifact that we can only compute for finite N; ideally we should get $\log 0$. Notice that although their semi-log plots look almost the same, at least to the naked eye. However, if one plots their face values, they look quite different and consistent with the approximate orthogonality.

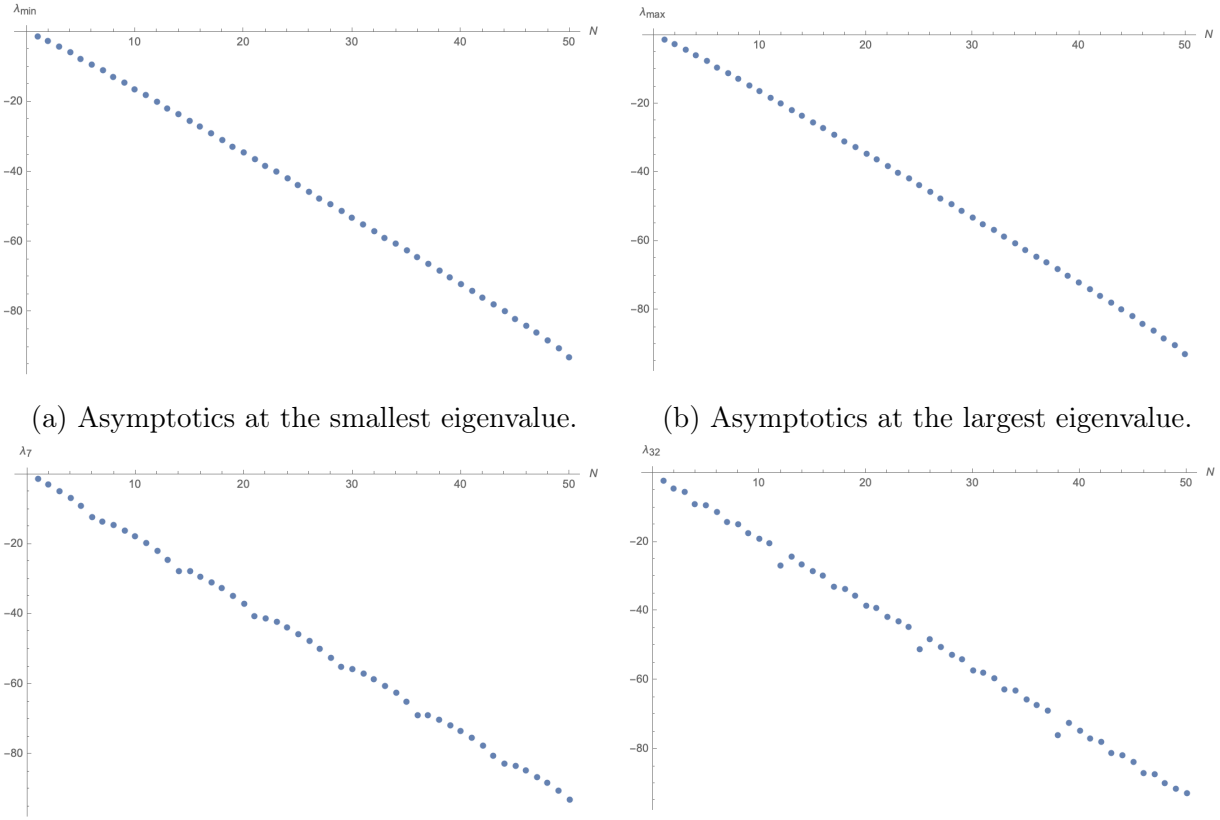

(a) Asymptotics at the smallest eigenvalue.

(b) Asymptotics at the largest eigenvalue.

(c) Asymptotics at the 7^{th} largest eigenvalue.

(d) Asymptotics at the 32^{th} largest eigenvalue.

Figure 4.4: Asymptotics of $\mathrm{Re}\left[\log(\phi_n/\phi_0)\right]$ evaluated at different eigenvalues as the cutoff N increases, with $p = 41$.

On the other hand, within the exponentially decaying envelope, ϕ_n is discretely oscillating around zero as n increases. This oscillatory behavior is shown in Figure 4.5 after stripping off the exponential envelope.

Based on numerics, for a radial cutoff at depth N, we propose the following ansatz:

$$\boxed{\phi_{n,i} = p^{-n/2}\cos\left(kn\frac{i-1}{N-1}\pi + \psi\right)\phi_{0,i}}, \tag{4.37}$$

[12]The field value ϕ_n can be negative at many different depths n.

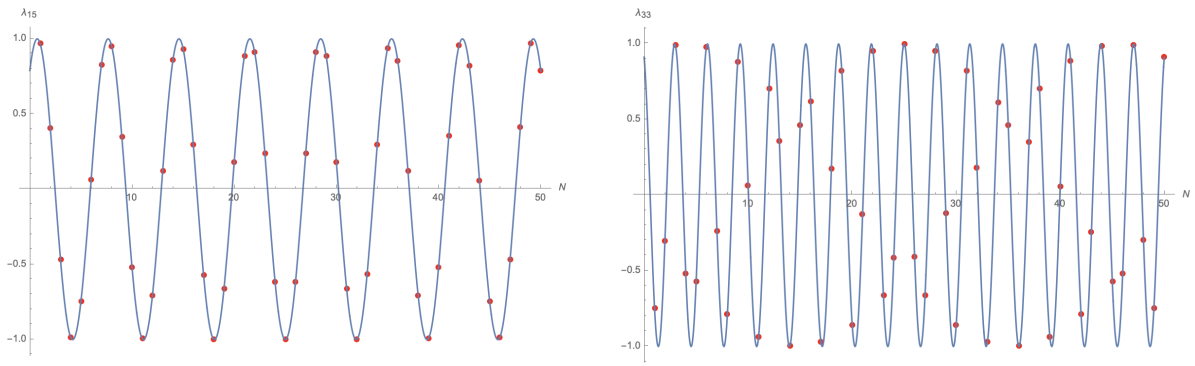

(a) Oscillation of ϕ_n/ϕ_0 at the 15^{th} largest eigenvalue for $p = 239$.

(b) Oscillation of ϕ_n/ϕ_0 at the 33^{th} largest eigenvalue for $p = 239$.

Figure 4.5: Oscillations of eigenvalues over the cutoff N, where red dots are data points from *Mathematica*'s `NSolve`, and blue sinusoidal curves with phase shifts are fittings with frequencies $n\frac{i-1}{N-1}\pi$ for the ϕ_n/ϕ_0 at the i^{th} largest eigenvalue, $n = 1, \ldots, N-1$, $i = 1, \ldots, N$.

where $1 \leq i \leq N$ labels N eigenvalues, n is the depth, and k and ψ are to be determined. After plugging this ansatz for $\phi_{n,i}$ into the recurrence relation (4.26), we obtain:

$$\begin{aligned} 0 =& p^{1/2} \sin\left(kn\frac{i-1}{N-1}\pi + \psi\right) + (\lambda_i - p - 1)\sin\left(k\frac{(i-1)(n-1)}{N-1}\pi + \psi\right) \\ &+ p^{1/2}\sin\left(k\frac{(i-1)(n-2)}{N-1}\pi + \psi\right) \\ =& \sin\left(k\frac{(i-1)(n-1)}{N}\pi + \psi\right)\left[2p^{1/2}\cos\left(k\frac{i-1}{N-1}\pi\right) + (\lambda_i - p - 1)\right]. \end{aligned} \tag{4.38}$$

The eigenvalues are asymptotically

$$\boxed{\lambda_i = p + 1 - 2p^{1/2}\cos\left(k\frac{i-1}{N-1}\pi\right)}. \tag{4.39}$$

Integer k in the frequency in (4.37) can freely vary *ab initio*, but by simply plotting the spectrum $\{\lambda_i\}$ agaisnt i at a fixed N, we can see that the profile is monotonically decreasing as in Figure 4.6. Hence k is fixed to be 1. The validity of this frequency is numerically tested up to $p = 2477$ (larger p's do not increase computational complexity significantly). However, the phase shift ψ in (4.37) has to be determined numerically and is conveniently unimportant for us.

The eigenvalues (4.39) are exact only if they correspond to $\phi_{n,i}$ in (4.37) at large depth n [i.e., far away from the initial condition (4.29] at the center) and $N \to \infty$. For $p = 5$, we see that the largest and the smallest eigenvalues are asymptotically $6 \pm 2\sqrt{5}$. These are

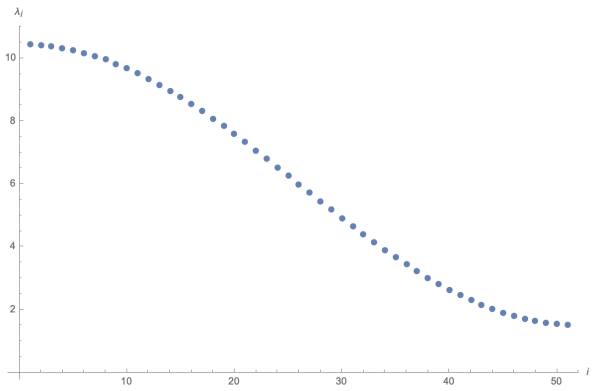

Figure 4.6: The spectrum $\{\lambda_i\}$ of Laplacian $\Box$ when the cutoff is $N = 51$, ordered from the largest to the smallest, agreeing with (4.39) with $k = 1$. The horizontal axis is $1 \leq i \leq N$, not cutoff N or depth n.

consistent with results from Newton's method as well as Vieta's formula in the sense that the summation of the eigenvalues (4.39) is exactly $(p+1)N$. Additionally, all the eigenvalues are confined within an interval $\left[-2\sqrt{p}, 2\sqrt{p}\right]$.[13]

Overall, this is a different spectral decomposition of Laplacian on Bruhat-Tits tree than the plane-wave basis [166, 168, 192], in that eigenfunctions here may oscillate around zero. Also a key feature of discrete Laplacian here on trees is that solutions to the Laplace's equation averaged over the circular boundary $P^1(\mathbb{Q}_p)$ is not equal to the value at the center, as opposed to the continuous Laplacian.

Finally, it is a trivial exercise to change the valency to $p^n + 1$ in the recurrence (4.26) and repeat everything above if one wants to study the scalar on T_{p^n} which models AdS_{n+1}.

Laplace problem on BTZ graphs

We now turn to study the Laplace problem for BTZ black holes. Conceptually, to calculate the determinant of Laplacian $\Box$, we are not able to use its heat kernel as did in [54] for continuous AdS_3, because the BTZ graph is essentially a constant-time slice [168], and there is no good notion of "time".

In terms of recursion relations here, the only modification on the linear recurrence for a BTZ graph are the initial conditions on ϕ_1 in terms of ϕ_0 as explained below.

The major difference between a p-adic BTZ black hole and Bruhat-Tits tree is that the field values on the event horizon (depth 0) could be different. Given the horizon's area l, the field values are labeled as $\phi_{0,0}, \phi_{0,1}, \ldots, \phi_{0,s}, \ldots, \phi_{0,l-1}$, where a specific s labels a horizon vertex as well as the entire subtree rooted at that vertex mentioned in Figure 4.2.

[13] Similarly-looking bounds on eigenvalues in the context of principal series representation of $GL(2, \mathbb{Q}_p)$ without boundary conditions on a Bruhat-Tits tree were obtained in [192] (Theorem 5.4.2).

Now, as shown in Figure 4.7, we go inwards from the boundary (at depth N) where all the fields vanish and label the field value on the layer next to the boundary as ϕ_{N-1}. All following discussions are on the subtree rooted at vertex s on the horizon.

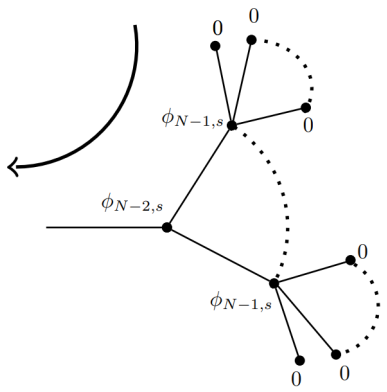

Figure 4.7: Going from the boundary towards the center, with the initial condition (4.40).

The initial condition on the boundary of subtree s is

$$\phi_{N-2,s} = (p+1-\lambda_t)\phi_{N-1,s}, \quad t = 0, \ldots, l-1, \tag{4.40}$$

where $\phi_{N,s}$ is a free parameter, and the subscript t in eigenvalue λ_t will be explained later below (4.50).[14] The linear recursion relation towards the central horizon is exactly the same as (4.26):

$$\phi_{n-2,s} + (\lambda_t - p - 1)\phi_{n-1,s} + p\phi_{n,s} = 0, \quad 2 \leq n \leq N-1, \tag{4.41}$$

in the "reversed" order, and the field values are

$$\phi_{n,s} = c_{+,t}\left(\phi_{N-1,s}\right) \cdot \alpha_{+,t}^{N-1-n} + c_{-,t}\left(\phi_{N-1,s}\right) \cdot \alpha_{-,t}^{N-1-n}, \tag{4.42}$$

where coefficients $\left[c_{+,t}\left(\phi_{N-1,s}\right), c_{-,t}\left(\phi_{N-1,s}\right)\right]$ and solutions $(\alpha_{+,t}, \alpha_{-,t})$ to the characteristic equation of (4.41) are both pairs of Galois conjugates as before[15].

We denote the ratio between field values on the first layer (depth 1) and those on the horizon as $k \equiv \phi_{1,s}/\phi_{0,s}$. This ratio k is isotropic around the loop, i.e., without a subscript

[14] Although t shares the same range as s, it has a *different* physical meaning, and by definition it is independent of s, which is obvious because λ_t is a global quantity.

[15] Although they will not enter the rest of our analysis, we have

$$\alpha_{\pm,t} = \frac{(1+p-\lambda_t) \pm \sqrt{(1+p-\lambda_t)^2 - 4p}}{2}. \tag{4.43}$$

s, because it is solely determined by the recursion relation (4.41) for $n = 2$. At a fixed depth n, although $\phi_{n,s}$ may vary among subtrees rooted at different horizon vertices s, they remain homogeneous within the same subtree as explained right below (4.25).

However, k still depends on $\alpha_{\pm,t}$ and thus λ_t, so we denote it by $k_t(\lambda_t)$. We examine the recursion relation around the event horizon:

$$\phi_{0,s+2} - [(p-1)(1-k_t(\lambda_t)) - \lambda_t + 2]\,\phi_{0,s+1} + \phi_{0,s} = 0, \quad s = 0, \ldots, l-1, \tag{4.44}$$

with the periodic boundary condition[16] $\phi_{0,0} = \phi_{0,l}$, as shown in Figure 4.8.

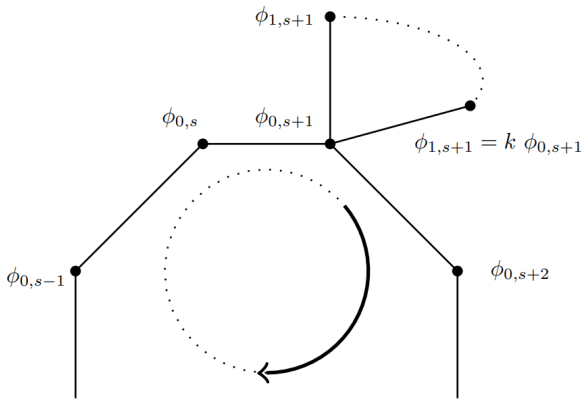

Figure 4.8: Going around the horizon with recursive relation (4.44).

On the other hand, the necessary and sufficient condition for the existence of periodicity in a second-order linear recurrence like (4.44) is that the two solutions r_+, r_- to its quadratic characteristic equation are roots of unity (not necessarily primitive). Suppose $r_+ = e^{2\pi i \frac{w}{q}}$ is the q^{th} root of unity and $r_- = e^{2\pi i \frac{w'}{q'}}$ is the q'^{th} root of unity, then their period is $\text{lcm}(q, q')$. In our casem the period is l, the horizon length.

The solutions to the characteristic equation of (4.44) are:

$$r_{\pm,t} = \frac{1}{2}\left\{[(p-1)\,(1-k_t(\lambda_t)) - \lambda_t + 2] \pm \sqrt{[(p-1)(1-k_t(\lambda_t)) - \lambda_t + 2]^2 - 4}\right\}, \tag{4.45}$$

then it is clear from Vieta's formula that

$$(p-1)(1-k_t(\lambda_t)) - \lambda_t + 2 = +2\cos\left(\frac{2\pi t}{l}\right) \tag{4.46}$$

[16] We might consider anti-periodic boundary conditions for fermions as in [172], and intuitively all l later on will be replaced by $2l$.

and

$$\sqrt{4-\left[(p-1)(1-k_t(\lambda_t))-\lambda_t+2\right]^2}=+2\sin\left(\frac{2\pi t}{l}\right). \tag{4.47}$$

If we denote the discriminant in (4.45) as δ, then we note that it is impossible to have

$$+\frac{\sqrt{\delta}}{2i}=\sin\frac{2\pi}{q}\ \text{ and }\ -\frac{\sqrt{\delta}}{2i}=\sin\frac{2\pi}{q'},\quad 0<q\neq q'\leq l,\quad l=\text{lcm}(q,q')>2, \tag{4.48}$$

i.e., different denominators in the exponents of roots of unity r_+ and r_-, because

$$\sin\frac{2\pi}{q}+\sin\frac{2\pi}{q'}=2\sin\left(\frac{q+q'}{qq'}\pi\right)\cos\left(\frac{q'-q}{qq'}\pi\right)=0 \tag{4.49}$$

indicates that $(q+q')/qq'=0,1$ or $(q'-q)/qq'=1/2,3/2$. The first equation implies that $q=q'=2$ and the second equation implies that $q=1,q'=2$. Hence, r_+ and r_- are both l^{th} roots of unity, and are complex conjugates to each other.

Then we have

$$k_t(\lambda_t)=1-\frac{1}{p-1}\left(2\cos\left(\frac{2\pi t}{l}\right)+\lambda_t-2\right),\quad t=0,\ldots,l-1, \tag{4.50}$$

with double degeneracies $k_t\left(\lambda_t\right)=k_{l-t}(\lambda_{l-t})$, and t now labels oscillation modes, answering Footnote 14. To avoid overcounting, we observe that pairs – $[k_t(\lambda_t),\lambda_t]$ and $[k_{l-t}(\lambda_{l-t}),\lambda_{l-t}]$ – correspond to the same mode along the horizon, because $t\Longleftrightarrow l-t$ is equivalent to swapping solutions $r_{+,t}$ and $r_{-,t}$ to (4.45), so that upon solving the initial conditions $\phi_{0,0}=A+B$ and $\phi_{0,1}=Ar_{+,t}+Br_{-,t}$, all $\phi_{0,s}$'s are invariant under this swapping. Then the maximum value of t should be $\lfloor l/2\rfloor$.

Let us take a deeper look into this $k_t(\lambda_t)$, by stepping outwards away from the horizon. Starting from depth 1, we adopt the same recursion as used in the Bruhat-Tits tree case. Therefore, the recursion relation here stays the same as (4.26) for any depth $n>2$, implying that solutions $\alpha_\pm$ to the characteristic equation are unchanged as in (4.27). When $n=2$, the field value ϕ_{n-2} in (4.26) is replaced by $\phi_{0,s},s=0,\ldots,l-1$, and ϕ_{n-1} in (4.26) becomes $\phi_{1,s}=k_t(\lambda_t)\phi_{0,s}$. Then, the initial condition here gives:

$$\tilde{c}_{\pm,t}\left(\phi_{0,s}\right)=\left(\frac{1}{2}\pm\frac{(p+1)(p+1-\lambda_t)-4p\cos\left(\frac{2\pi t}{L}\right)}{2(p-1)\sqrt{(1+p-\lambda_t)^2-4p}}\right)\phi_{0,s}. \tag{4.51}$$

Numerically, we observe that the coefficient of the highest degree in λ_t for the polynomial $\phi_{N,s}=\left(\tilde{c}_{+,t}\left(\phi_{0,s}\right)\cdot\alpha_{+,t}^N+\tilde{c}_{-,t}\left(\phi_{0,s}\right)\cdot\alpha_{-,t}^N\right)\phi_{0,s}$ is $(-1)^N\phi_{0,s}/\left(p^N-p^{N-1}\right)$, where $\alpha_{+,t}$ and $\alpha_{-,t}$ are the same as in (4.42). Thus, the constant term is

$$\frac{1}{p^N-p^{N-1}}\left(p^N+p^{N-1}+2\sum_{i=0}^{N-2}p^i-2\cos\left(\frac{2\pi t}{l}\right)\sum_{i=0}^{N-1}p^i\right)\phi_{0,s}. \tag{4.52}$$

The product of all roots is *independent* of index s:

$$p^N + p^{N-1} + 2\frac{p^{N-1}-1}{p-1} - 2\frac{p^N-1}{p-1}\cos\left(\frac{2\pi t}{l}\right). \tag{4.53}$$

Note that (4.53) is the product of eigenvalues for one specific t. In order to account for all modes when computing $\det\Box$, we must multiply contributions from all $t = 0, \ldots, \lfloor l/2 \rfloor$, and for convenience we shift t by 1 in the product.

To multiply $\lceil l/2 \rceil$ terms of (4.53) together, we recall that roots of $T_n(x)$, the Chebyshev polynomial of the first kind of degree n, are

$$x_k = \cos\left(\frac{2k-1}{2n}\pi\right), \quad k = 1, \ldots, n, \tag{4.54}$$

called *Chebyshev nodes* in interval $[-1, 1]$, and hence (see, e.g., [193])

$$T_n(x) = 2^{n-1}\prod_{k=1}^{n}\left[x - \cos\left(\frac{(2k-1)\pi}{2n}\right)\right]. \tag{4.55}$$

Then it is not hard to see, using the reflection symmetry $T_n(-x) = (-1)^n T_n(x)$, for coprime α and β, we have

$$\boxed{\prod_{k=1}^{\beta}\left[2x \pm 2\cos\left(\frac{2\pi k\alpha}{\beta} + \theta\right)\right] = 2\left[T_\beta(x) + (\pm 1)^\beta(-1)^{\alpha\beta+\alpha}\cos(\beta\theta)\right]}, \tag{4.56}$$

which leads us to the desired product:

$$\begin{aligned}
&\prod_{t=1}^{\lceil l/2 \rceil}\left\{\frac{p^N-1}{p-1}\left[\left(2\frac{p^{N-1}-1}{p-1} + p^{N-1} + p^N\right)\Big/\frac{p^N-1}{p-1} - 2\cos\left(\frac{2\pi t}{l}\right)\right]\right\} \\
&= \begin{cases}
\left(\frac{p^N-1}{p-1}\right)^{\frac{l}{2}}\left[2T_l\left(\frac{p^{N-1}(p^2+1)-2}{2(p^N-1)}\right) - 2\right]^{\frac{1}{2}} & l \text{ even}, \\
\left(\frac{p^N-1}{p-1}\right)^{\frac{l}{2}}\left[2T_l\left(\frac{p^{N-1}(p^2+1)-2}{2(p^N-1)}\right) - 2\right]^{\frac{1}{2}}\left[\frac{p^{N+1}+p^{N-1}-2+2(p^N-1)\cos\left(\frac{\pi}{l}\right)}{p-1}\right]^{\frac{1}{2}} & l \text{ odd}.
\end{cases}
\end{aligned} \tag{4.57}$$

For large N, we have:

$$\begin{cases}
\sqrt{2}\left(\frac{p^N}{p-1}\right)^{\frac{l}{2}}\left[T_l\left(\frac{p^2+1}{2p}\right) - 1\right]^{\frac{1}{2}} & l \text{ even}, \\
\sqrt{2}\left(\frac{p^N}{p-1}\right)^{\frac{l}{2}}\left[T_l\left(\frac{p^2+1}{2p}\right) - 1\right]^{\frac{1}{2}}\left[\frac{p^{N-1}(p^2+1+2p\cos(\pi/l))}{p-1}\right]^{\frac{1}{2}} & l \text{ odd}.
\end{cases} \tag{4.58}$$

Since N is really an infinite quantity, we need to fully forget all subleading terms in (4.58). Because of this, there are no descendants and agrees with Melzer's non-Archimedean CFT axioms [176], and Chebyshev polynomials do not serve as counterparts of the usual degeneracy-counting function $1/\eta(-1/\tau)$ in 2d CFTs.

Furthermore, if l and p are not small, we use the explicit expression

$$T_l(x) = \cosh\left(l\text{arccosh}x\right), x \geq 1, \tag{4.59}$$

then we obtain

$$\boxed{\begin{cases} \left(\frac{p^{N+1}}{p-1}\right)^{\frac{l}{2}} & l \text{ even}, \\ \left(\frac{p^{N+1}}{p-1}\right)^{\frac{l+1}{2}} \left(\frac{p+1}{p}\right) & l \text{ odd}. \end{cases}} \tag{4.60}$$

Now we can already see that $\det(\Box)$ is divergent exponentially as p^{lN} when $N \to \infty$, which is very different from the number of boundary points $l(p-2)(p-1)^{N-1}$, or the total number of points in the BTZ graph lp^N. So we cannot directly obtain a finite answer using the similar argument which leads to (4.36), and the unregularized partition function is:[17]

$$\boxed{Z_{\text{BTZ}} = \begin{cases} \left(\frac{p-1}{p^{N+1}}\right)^{\frac{l}{4}} & l \text{ even}, \\ \left(\frac{p-1}{p^{N+1}}\right)^{\frac{l+1}{4}} \left(\frac{p}{p+1}\right) & l \text{ odd}. \end{cases}} \tag{4.61}$$

Apart from the divergence, (4.61) is very similar to the partition function of a BTZ black hole in the usual Euclidean AdS_3 at leading order, as reviewed in Appendix B.3.

In summary, we have to undergo three recurrences to solve the Laplace problem on a p-adic BTZ black hole:

1. *From the asymptotic boundary to the horizon*[18]*, using recurrence (4.41);*[19]
2. *Go around the horizon once, using recurrence (4.44);*
3. *From the horizon to the asymptotic boundary, using recurrence (4.26).*

Since the recurrence relation (4.41) for depth $n > 2$ is the same as the one in Bruhat-Tits tree (4.26), the asymptotic behavior of eigenfunction and eigenvalues stay the same as in (4.37) and (4.39), respectively. We are still in the "evanescent wave" basis as in Section 4.3.

Now we perform the non-Wick-rotated inverse Laplace transform on the partition function (4.61) to obtain the density of states. To this end, we need to do two radical things:

- Firstly, we strip off the divergent factor in (4.61) by hand, since otherwise the density of states to be obtained would be very negative numbers;
- Secondly, we regard l as "$1/\beta \sim i/\tau > 0$" for a non-rotating BTZ. Although in our p-adic setup, there is no mathematically rigorous $\tau \in \mathbb{C}$, in order to do the integral transform, we need to turn on an auxiliary imaginary part of the inverse temperature momentarily, so that $\tilde{\beta} = \beta + i\beta', \beta' \in \mathbb{R}$.

[17] Since our divergence originates from a divergent number of eigenvalues as $N \to \infty$, one might try zeta function regularization. However, since eigenvalues here are complicated factors of Chebyshev polynomials, we do not see an easy way out; we hope to revisit this issue in the future.

[18] Skipping *Step 1* results in a messy situation, as explained in Appendix B.2.

[19] The sole purpose of recurrence (4.41) is to show the isotropy of k around the horizon, and the isotropy of $\phi_{n,s}$ within the subtree s.

Then going from the canonical ensemble to the microcanonical ensemble, we have

$$\rho(E)=\mathcal{L}^{-1}\left\{Z_{\mathrm{BTZ}}\left(\tilde{\beta}\right)\right\}(E)=\begin{cases}\frac{1}{2\pi i}\int_{\beta-i\infty}^{\beta+i\infty}d\tilde{\beta}e^{\tilde{\beta}E}\,(p-1)^{1/4\tilde{\beta}} & l \text{ even},\\ \frac{1}{2\pi i}\int_{\beta-i\infty}^{\beta+i\infty}d\tilde{\beta}e^{\tilde{\beta}E}\,(p-1)^{1/4\tilde{\beta}+1/4}\left(\frac{p}{p+1}\right) & l \text{ odd}.\end{cases} \tag{4.62}$$

However, the second expression cannot be evaluated explicitly, so we focus on the high-temperature limit as $\beta\to 0$ so that $1/4\tilde{\beta}+1/4\approx 1/4\tilde{\beta}$, and from now on we do not treat even and odd l separately, because they only differ by a factor $\frac{p}{p+1}$. Then we get

$$\rho(E)=\frac{\ln(p-1)}{8}{}_0F_1\left(;2;\frac{E\ln(p-1)}{4}\right)+\delta(E), \tag{4.63}$$

for all primes p, where ${}_0F_1$ is the *confluent hypergeometric limit function*, and is related to the modified Bessel function of the first kind as

$$I_\alpha(x)=\frac{(x/2)^\alpha}{\Gamma(\alpha+1)}{}_0F_1\left(;\alpha+1;\frac{x^2}{4}\right). \tag{4.64}$$

In (4.63), we have $\propto I_1\left(\sqrt{E\ln(p-1)}\right)$, and it goes to zero as $E\to 0$. Its asymptotic behavior of ${}_0F_1$ as $x\to\infty$ is

$${}_0F_1\left(;\alpha;x\right)\approx x^{-(\alpha-1)/2}\Gamma(\alpha)\frac{e^{2\sqrt{x}}}{\sqrt{2\pi\sqrt{x}}}\left(1-\frac{4(\alpha-1)^2-1}{16\sqrt{x}}+\dots\right) \tag{4.65}$$

so in semi-classical limit, for positive energy, we discard Dirac delta and its derivative in (4.62). When $p>3$, we have

$$\boxed{\rho(E)\approx\frac{\ln^{1/4}(p-1)}{\sqrt{2\pi}}e^{\sqrt{E\ln(p-1)}}E^{-3/4}\left(1-\frac{3}{8\sqrt{E\ln(p-1)}}+\mathcal{O}(E^{-1})+\dots\right)}. \tag{4.66}$$

Finally and straightforwardly, the Bekenstein-Hawking-like entropy is

$$S\approx\sqrt{E\ln(p-1)}-\frac{3}{4}\ln E+\frac{1}{4}\ln\left(\ln(p-1)\right)-\frac{1}{2}\ln(2\pi)-\dots, \tag{4.67}$$

where the second term is the famous logarithmic correction terms previously discovered in [194, 195]. This result is also consistent with the "species problem" [196] because we are calculating scalar fields all the time. One can also derive the Cardy-like formula [197, 198, 199] via saddle point approximation on (4.62).

The usual Benkenstein-Hawking entropy of black holes from Cardy-like formula has $4\pi\sqrt{Ek}$ as the leading term [5], where k is proportional to the Brown-Henneaux central

charge $3l/2G_N$ [79]. By comparing this with (4.67), we see that our $\ln(p-1)$ is like k. However this raises a puzzle, because increasing valency of the tree should increase the curvature, corresponding to decreasing k in the continuous AdS_3.[20] We will discuss this near the end.

Another standalone case of (4.63) is $p = 3$, since $\ln 2 < 0$, and the asymptotic expansion (4.65) is only true when $|\arg x| < \pi/2$. Now ${}_0F_1$ is related to the Bessel function of the first kind as

$$J_\alpha(x) = \frac{(x/2)^\alpha}{\Gamma(\alpha+1)} {}_0F_1\left(;\alpha+1;-\frac{x^2}{4}\right), \tag{4.68}$$

and $J_\alpha(x)$ has the following asymptotics for real $x \to \infty$:

$$J_\alpha(x) \approx \sqrt{\frac{2}{\pi x}} \cos\left(x - \frac{\alpha\pi}{2} - \frac{\pi}{4}\right), \tag{4.69}$$

so the semiclassical limit of density of states is

$$\rho(E)|_{p=2} \approx 2\sqrt{2}\frac{(-\ln 2)^{3/4}}{\sqrt{\pi}} E^{-3/4} \cos\left(\sqrt{-E\ln 2} - \frac{3\pi}{4}\right), \tag{4.70}$$

which is a pathological result due to the oscillatory nature. It seem that a 3-adic BTZ black hole is unstable.

The continuous integral transform (4.62) is justified because in high-temperature regime $l \to \infty$, the separation between two adjacent discrete inverse temperatures is $\sim 1/l^2$. On the other hand, if we do not perform coarse-graining, we need to do the discrete inverse Laplace transform. Superficially, the discrete inverse Laplace transform has the same expression as the one used in going from canonical partition function $Z_N(\beta)$ for N particles to grand partition function $\mathcal{Z}(\beta,\mu)$:

$$\mathcal{Z}(\beta,\mu) = \sum_{N=0}^{\infty} \left(e^{\mu\beta}\right)^N Z_N(\beta), \tag{4.71}$$

but here the temperature is held fixed, and particle number is the analogue of p-adic discrete temperature.[21] Unfortunately in our case, the Z-transform does not yield a closed form so we stick to the continuous approximation (4.62).

Let us examine more details on the density of states. At low energy E_0, we integrate the density of states (4.63) over the interval $[E_0, E_0+\epsilon]$ with a small but finite ϵ

$$\int_{E_0}^{E_0+\epsilon} dE\rho(E) = \frac{\ln(p-1)}{8} {}_0F_1\left(;2;\frac{E\ln(p-1)}{4}\right)\Bigg|_{E_0}^{E_0+\epsilon}, \tag{4.72}$$

[20] Since the Bruhat-Tits tree has no holonomy, defining a Riemann tensor is arduous. Yau et al. [200] were able to define a Ricci curvature κ_{xy} on graphs without a Riemann tensor, but in terms of the edge lengths a_{xy}, from which Gubser et al. [187] found that on-shell the tree has a constant negative Ricci curvature $\kappa_{xy} = -2\frac{p-1}{p+1}$ and the edge length fluctuations are massless modes.

[21] This transform is also called a unilateral Z-transformation, with the less common but equivalent definition where powers are positive, same as probability generating functions.

although there is no particle interpretation in ordinary 2d CFTs (roughly because their correlators have no simple poles), and we expect so in p-adic CFT, in the bulk we can view the tree as a lattice, and number of vertices equals the number of degrees of freedom (or "particles"), which is lp^N. The low-energy limit of (4.72) is

$$\frac{1}{8}{}_0F_1\left(;2;\frac{\ln(p-1)E_0}{4}\right)\ln(p-1)\epsilon+\frac{1}{128}{}_0F_1\left(;3;\frac{\ln(p-1)E_0}{4}\right)\ln^2(p-1)\epsilon^2+\mathcal{O}(\epsilon^3). \quad (4.73)$$

Small-argument behavior of ${}_0F_1$ is just 1, so we have:

$$\frac{1}{8}\ln(p-1)\epsilon+\frac{1}{128}\ln^2(p-1)\epsilon^2+\mathcal{O}(\epsilon^3)<\frac{1}{16}\ln(p-1)\sum_{i=1}^{\infty}(i+1)\epsilon^i=\frac{\epsilon(2-\epsilon)}{16(\epsilon-1)^2}\ln(p-1), \quad (4.74)$$

which is a constant polynomial in total number of "particles", hence satisfying the sparsity condition on in [201, 202] on the number of low-energy eigenstates in a gapless 1D system with a local Hamiltonian[22], hence in principle one is able to approximate the Hilbert subspace near the ground state in the supposedly dual p-adic CFT. This may be worth investigating in the future.

Turning on the scalar mass

Here we again turn off the source J in (4.21), and now we have a Helmholtz-like wave equation

$$\left(\Box+m_p^2\right)\phi_a=0. \quad (4.75)$$

The on-shell masses squared of a bulk scalar in (4.20) are real [167, 168]:

$$m_p^2=-\frac{1}{\zeta_p(\Delta-1)\zeta_p(-\Delta)}=-(p+1)+2\sqrt{p}\,\cosh\left[\left(\Delta-\frac{1}{2}\right)\ln p\right], \quad (4.76)$$

where the p-adic or "finite" local zeta function $\zeta_p(s)$ is defined as:

$$\zeta_p(s)\equiv\frac{1}{1-p^{-s}}, \quad (4.77)$$

which obtains its name because the real Riemann zeta function $\zeta_\infty(s)$ can be constructed from Euler's adelic product:

$$\zeta_\infty(s)\equiv\sum_{n=1}^{\infty}\frac{1}{n^s}=\prod_{\text{primes}p}\zeta_p(s)=\prod_p\frac{1}{1-p^{-s}}. \quad (4.78)$$

Then we have the Breitenlohner-Freedman (BF) bound $m_{BF,p}^2=-1/\zeta_p(-n/2)^2$, and

$$p^{\Delta_\pm}=\frac{1}{2}\left[(1+p^n+1/m^2)\pm\sqrt{(1+p^n+1/m^2)^2-4p^n}\right]. \quad (4.79)$$

[22]We thank Ning Bao for pointing out these references.

Due to the inversion symmetry of $\zeta_p(s)$, m^2 in (4.76) is invariant under $\Delta \to 1-\Delta$.

We adopt the same convention on the solutions to (4.76) as in [167], i.e., $\Delta = \Delta_+ > n/2$. Then for massless scalars, $\Delta = n$, so we are restricted to $\Delta = 0, 1$ when $n = 1$.

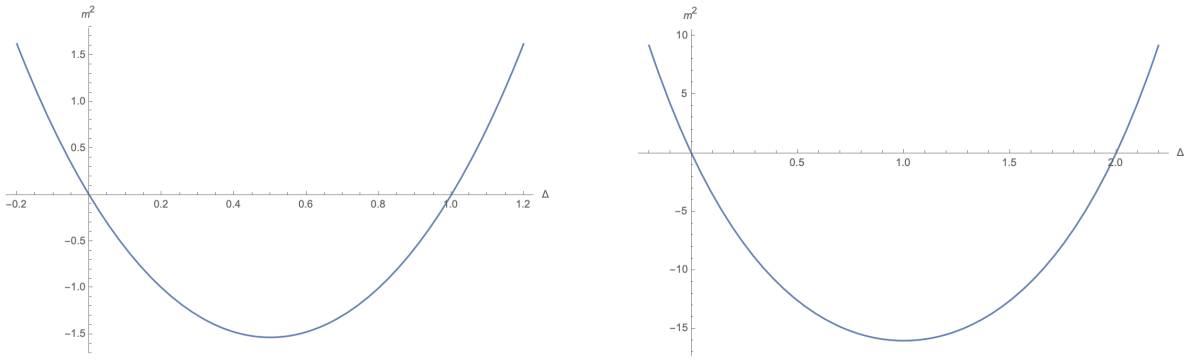

(a) $p = 5$, $n = 1$. (b) $p = 5$, $n = 2$.

Figure 4.9: Scalar mass m^2 as a function of conformal dimension Δ. $m^2 > 0$ when $\Delta > n$.

Now we hope to calculate partiton function when ϕ is massive, which amounts to calculating the determinant of $\Box + m^2\mathbb{1}$. We relate the field polynomial $\phi_N^{\text{tree}}(\lambda)$ ($\phi_{n,s}^{\text{BTZ}}(\lambda_t)$ for BTZ black holes) resulting from the boundary condition $\phi|_{\partial T} \equiv \phi_N = 0$ with the "monic" (up to $(-1)^N$) characteristic polynomial $P_N(\lambda) = \prod_{i=1}^N (\lambda_i - \lambda) = \det(\Box - \lambda\mathbb{1})$ of the Laplacian $\Box$. What we have calculated in the previous two subsections are essentially $P_N(0)$, the constant term of $P_N(\lambda)$, and now we perturbatively investigate $P_N(-m^2)$, i.e., the determinant $\det(\Box + m^2\mathbb{1}) = \prod_{i=1}^N (\lambda_i + m^2)$.

It is important that λ_i's are always greater than the BF bound $m_{BF,p^n} = -1/\zeta_p(-n/2)^2$, which is $m_{BF,p} = -\left(\sqrt{p}-1\right)^2$ for $n = 1$, whose absolute value is strictly smaller than all eigenvalues for both Bruhat-Tits trees and BTZ black holes in (4.39). Hence, we will not encounter issues of alternating signs upon calculating determinants of $\Box + m^2\mathbb{1}$.

In principle, one could possibly use minimal polynomials for Gaussian integers to study powers of Galois conjugates. However, we will proceed in a more combinatorial approach.

On Bruhat-Tits trees

Since the polynomial $\phi_N(\lambda)$ in λ always has the constant term 1, we need to rescale it to be monic up to $(-1)^N$:

$$\boxed{P_N^{\text{tree}}(\lambda) \equiv \phi_N^{\text{tree}}(\lambda)/\phi_0^{\text{tree}} \prod_{i=1}^N \lambda_i = \left(p^N + p^{N-1}\right) \phi_N^{\text{tree}}(\lambda)/\phi_0^{\text{tree}}}, \tag{4.80}$$

where $P_N^{\text{tree}}(\lambda)$ is defined in (4.28), so that $P_N^{\text{tree}}(0) = p^N + p^{N-1}$.

By denoting $x \equiv p - \lambda + 1$, we can rewrite $P_N^{\text{tree}}(\lambda)$ as

$$\frac{1}{2(2p)^N}\sum_{k=0}^{n}\binom{N}{k}x^k(x^2-4p)^{\frac{N-k-1}{2}}\left\{(x^2-4p)^{\frac{1}{2}}\left(1+(-1)^{N-k}\right)+\frac{p-1}{p+1}x\left[\left(1+(-1)^{N-k-1}\right)\right]\right\}. \tag{4.81}$$

Repeatedly applying the binomial theorem in a nested fashion gives us the following results:

- The linear term of $P_N^{\text{tree}}(\lambda)$ is, since $p \neq 1$:

$$\left(-Np^{N-1}-2\sum_{i=1}^{N-1}ip^{i-1}\right)\lambda = \frac{(N+2p-Np^2)p^N-2p}{p(p-1)^2}\lambda, \tag{4.82}$$

  which goes to $-N\frac{p+1}{p-1}p^{N-1}\lambda$ when N is large;

- The quadratic term is

$$\begin{aligned}&\sum_{i=0}^{N-2}p^i\left[\frac{(i+1)(i+2)}{2}+(i+1)(i+2)(N-i-2)\right]\lambda^2\\ =&\frac{1}{2p(p-1)^4}\left[(N^2-N)p^{N+3}-(N^2+5N-6)p^{N+2}-(N^2-5N-6)p^{N+1}\right.\\ &\left.+(N^2+N)p^N-(4N+6)p^2+(4N-6)p\right]\lambda^2,\end{aligned} \tag{4.83}$$

  which goes to $N^2\frac{p+1}{2(p-1)^2}p^{N-1}\lambda^2$ when N is large.

So for small $|m^2| < 1$, we have the unregularized partition function $Z_{\text{tree}}(m \to 0)$:

$$\begin{aligned}\det\left(m^2\mathbb{1}+\Box\right) = P_N^{\text{tree}}\left(-m^2\right) &= \left(p^N+p^{N-1}\right)\left(1+\frac{N}{p-1}m^2+\frac{1}{2}\left(\frac{N}{p-1}m^2\right)^2+\dots\right)\\ &= \boxed{\left(p^N+p^{N-1}\right)e^{\frac{Nm^2}{p-1}}},\end{aligned} \tag{4.84}$$

where the regularization factor $p^N + p^{N-1} \propto (4.32)$ is now manifest.

For completeness, we look into the large-mass limit, where only high-degree terms in $P_N^{\text{tree}}(\lambda)$ matter.

- The λ^{N-1} term is $-(-1)^N N(p+1)\lambda^{N-1}$. So in order to ignore the λ^{N-2} term, we need m^2 to be larger than N;

- The λ^{N-2} term is

$$\frac{1}{2}(-1)^N\left[N(N-1)p^2+2(N-1)^2p+N(N-1)-2\right]\lambda^{N-2}, \tag{4.85}$$

  which goes to $\frac{1}{2}(-1)^N N^2(p+1)^2\lambda^{N-2}$ when N is large;

- The coefficient of λ^{N-3}, a degree 3 polynomial in p involves first-order linear recurrence with variable coefficient for p^i coefficients f_N, such as

$$f_N = f_{N-1} + N(N-1)/2, \tag{4.86}$$

but in the end we have

$$\begin{aligned} -(-1)^N \Bigg\{ & \frac{N(N+1)(N-4)}{6} + 2 + \frac{N(N-2)(N-3)}{2} p \\ & + \left[\frac{N(N^2-5N+8)}{2} - 2 \right] p^2 + \frac{N(N-1)(N-2)}{6} p^3 \Bigg\}, \end{aligned} \tag{4.87}$$

which goes to $-\frac{1}{6}(-1)^N N^3 (p+1)^3 \lambda^{N-3}$ when N is large.

Then collectively we have the unregularized partition function:

$$\begin{aligned} & Z_{\text{tree}}(m \to \infty) \\ &= \left(p^N + p^{N-1}\right) m^{2N} \left(1 + \frac{N(p+1)}{m^2} + \frac{1}{2} \left(\frac{N(p+1)}{m^2} \right)^2 + \frac{1}{6} \left(\frac{N(p+1)}{m^2} \right)^3 + \cdots \right) \\ &= \boxed{\left(p^N + p^{N-1}\right) m^{2N} e^{\frac{N(p+1)}{m^2}}}, \end{aligned} \tag{4.88}$$

Now we discuss the conditions on Δ when $|m^2|$ is small. In order to have $0 < -m^2 \ll 1$, we write $\Delta = 1 + \epsilon$ where $\epsilon \ll 1$. So we have

$$\left(1 - p^{n-\Delta}\right)\left(p^{\Delta} - 1\right) \ll 1, \tag{4.89}$$

where n denotes the unramified extension $\mathbb{Q}_{p^n}$, then we get

$$\epsilon \ll \frac{\ln\left[\frac{p^{1-n}}{2}\left(2 + p^n - \sqrt{p^{2n}+4}\right)\right]}{\ln p}. \tag{4.90}$$

and similarly, for $\Delta = 1 - \epsilon$, we need $-1 \ll -m^2 < 0$, and we get

$$\epsilon \ll \frac{\ln\left[\frac{p}{2}\left(1 - p^{-n}\sqrt{p^n(p^n-4)}\right)\right]}{\ln p} \tag{4.91}$$

From this expression we also see that when $n = 1$, the smallest prime p is 5, consistent with the result from density of states in Section 4.2.

On BTZ black holes

The characteristic polynomial for Laplacian on BTZ black hole is different from $P_N^{\text{tree}}(\lambda)$. It is rescaled from the field polynomial[23] $\phi_{N,s}^{\text{BTZ}}(\lambda_t)$ at the cutoff depth N to

$$\boxed{P_N^{\text{BTZ}}(\lambda_t) \equiv \prod_{t=1}^{\lceil l \rceil} \tilde{P}_{N,t}^{\text{BTZ}}(\lambda_t) = \left(p^N - p^{N-1}\right)^l \prod_{t=1}^{\lceil l \rceil} \phi_{N,s}^{\text{BTZ}}\left(\lambda_t\right) / \phi_{0,s}^{\text{BTZ}}}, \tag{4.92}$$

so that $P_N^{\text{BTZ}}(\lambda_t)$ and $\tilde{P}_{N,t}^{\text{BTZ}}(\lambda_t)$ are monic up to $(-1)^{Nl}$ and $(-1)^N$, respectively, and $P_N^{\text{BTZ}}(0)$ agrees with (4.57).

Let us first consider when the mass $|m^2|$ is small. The linear term in λ_t in $\tilde{P}_{N,t}^{\text{BTZ}}(\lambda_t)$ for one specific t is

$$\begin{aligned} &\left[-Np^{N-1} + \left(\cos\left(\frac{2\pi t}{l}\right) - 1\right) \sum_{i=1}^{N-1} 2i(N-i)p^{N-i-1}\right] \lambda_t \\ =& -\left(Np^{N-1} + 4\sin^2\left(\frac{\pi t}{l}\right) \frac{N(p^N+1)(p-1) - (p^N-1)(p+1)}{(p-1)^3}\right) \lambda_t, \end{aligned} \tag{4.93}$$

which goes to

$$-\left(\frac{Np^N}{(p-1)^2} + 4Np^{N-1}\sin^2\left(\frac{\pi t}{l}\right)\right) \lambda_t \tag{4.94}$$

when N is large.

For small m^2, we only calculate $\tilde{P}_{N,t}^{\text{BTZ}}\left(-m^2\right)$ up to the linear term in λ_t, written in shorthand:

$$A\cos\left(\frac{2\pi t}{l}\right) + B \tag{4.95}$$

where

$$A \equiv -\frac{2m^2\left(-(p+1)p^N + N(p-1)\left(p^N+1\right) + p + 1\right)}{(p-1)^3} - \frac{2\left(p^N-1\right)}{p-1} \tag{4.96}$$

$$B \equiv m^2 Np^{N-1} + \frac{2m^2\left(-(p+1)p^N + N(p-1)\left(p^N+1\right) + p + 1\right)}{(p-1)^3} + p^{N-1} + \frac{2\left(p^{N-1}-1\right)}{p-1} + p^N, \tag{4.97}$$

then $\lceil l \rceil$ terms multiply together to be

$$P_N^{\text{BTZ}}\left(-m^2\right) = \begin{cases} \sqrt{2}(-A/2)^{\frac{l}{2}}\left[T_l\left(-B/A\right) - 1\right]^{\frac{1}{2}} & l \text{ even}, \\ \sqrt{2}(-A/2)^{\frac{l}{2}}\left[T_l\left(-B/A\right) - 1\right]^{\frac{1}{2}}\left(A\cos\left(\pi/l\right) + B\right)^{\frac{1}{2}} & l \text{ odd}, \end{cases} \tag{4.98}$$

[23]Here the subscript is "s" not "t", because this polynomial depends on the initial field value $\phi_{0,s}$ on horizon, as written above (4.52).

where $-B/A$ expanded up to the first order in m^2 is

$$\begin{aligned}\frac{p^{N+2}+p^N-2p}{2p\left(p^N-1\right)}+\frac{p^{N-1}\left(p^{N+1}+p^N-2Np+2N-p-1\right)}{2\left(p^N-1\right)^2}m^2+\mathcal{O}\left(m^4\right)\\ \xrightarrow{N\to\infty}\frac{p^2+1}{2p}+\frac{p+1}{2p}m^2\end{aligned}. \tag{4.99}$$

Because $dT_l(x)/dx = lU_{l-1}(x)$, where $U_l(x)$ is the Chebyshev polynomial of the second kind, when both l and p are not small, we get the unregularized BTZ partition function:

$$\begin{aligned}Z_{\mathrm{BTZ}}(m\to 0) &= P_N^{\mathrm{BTZ}}\left(-m^2\right)\\ &\approx\begin{cases}\left(1+\frac{lm^2}{2p}\right)^{\frac{1}{2}}\left(\frac{p^{N+1}}{p-1}\right)^{\frac{l}{2}}\left(1+\frac{Nm^2}{(p-1)^2}\right)^{\frac{l}{2}} & l \text{ even},\\ \left(1+\frac{lm^2}{2p}\right)^{\frac{1}{2}}\left(\frac{p^{N+1}}{p-1}\right)^{\frac{l}{2}}\left(1+\frac{Nm^2}{(p-1)^2}\right)^{\frac{l}{2}}\left(A\cos\left(\frac{\pi}{l}\right)+B\right) & l \text{ odd},\end{cases}\end{aligned} \tag{4.100}$$

which recovers (4.60) when $m^2 = 0$.

For large mass $|m^2|$, we calculate the λ_t^{N-1} term in $\tilde{P}_{N,t}^{\mathrm{BTZ}}(\lambda_t)$ to be

$$(-1)^N\left(2\cos\left(\frac{2\pi t}{l}\right)-N(p+1)\right)\lambda_t^{N-1}, \tag{4.101}$$

and the λ_t^{N-2} term is

$$(-1)^N\left(\frac{N(N-1)}{2}(p^2+1)+(N-1)^2p+1-2(N-1)\cos\left(\frac{2\pi t}{l}\right)\right)\lambda_t^{N-2}, \tag{4.102}$$

so we have terms with the three highest degrees added up to

$$\begin{aligned}\tilde{P}_{N,t}^{\mathrm{BTZ}}\left(-m^2\right) =& m^{2N}+m^{2N-2}\left(N(p+1)-2\cos\left(\frac{2\pi t}{l}\right)\right)\\ &+m^{2N-4}\left(\frac{N(N-1)}{2}(p^2+1)+(N-1)^2p+1-2(N-1)\cos\left(\frac{2\pi t}{l}\right)\right)\\ &+\ldots,\end{aligned} \tag{4.103}$$

and when N is large it is

$$C\cos\left(\frac{2\pi t}{l}\right)+D, \tag{4.104}$$

where

$$C\equiv -2m^{2N}\left(\frac{1}{m^2}+\frac{N}{m^4}\right),\ D\equiv m^{2N}\left(1+\frac{N(p+1)(2m^2+N+Np)}{2m^4}\right), \tag{4.105}$$

then $\lceil l \rceil$ terms multiply together to

$$P_N^{\mathrm{BTZ}}\left(-m^2\right) = \begin{cases} \sqrt{2}(-C/2)^{\frac{l}{2}} \left[T_l\left(-D/C\right)-1\right]^{\frac{1}{2}} & l \text{ even}, \\ \sqrt{2}(-C/2)^{\frac{l}{2}} \left[T_l\left(-D/C\right)-1\right]^{\frac{1}{2}} \left(C\cos\left(\pi/l\right)+D\right)^{\frac{1}{2}} & l \text{ odd}, \end{cases} \tag{4.106}$$

where $-D/C$ up to the first oreder in m^2 is

$$\frac{N}{4}(p+1)^2 + \frac{1}{4}\left(1-p^2\right)m^2 + \mathcal{O}\left(m^4\right) + \ldots \tag{4.107}$$

so explicitly the unregularized BTZ partition function for very large m^2 is

$$\boxed{Z_{\mathrm{BTZ}}(m\to\infty) \approx \begin{cases} m^{lN-l}\left(1+\frac{N}{m^2}\right)^{\frac{l}{2}} \left(\frac{N(p+1)^2}{2}+\frac{(1-p^2)m^2}{2}\right)^{\frac{1}{2}} & l \text{ even}, \\ m^{lN-l}\left(1+\frac{N}{m^2}\right)^{\frac{l}{2}} \left(\frac{N(p+1)^2}{2}+\frac{(1-p^2)m^2}{2}\right)^{\frac{1}{2}} \left(C\cos\left(\frac{\pi}{l}\right)+D\right) & l \text{ odd}, \end{cases}} \tag{4.108}$$

4.4 One-loop Witten diagrams

In the work by Kraus and Maloney [145], they proposed a duality between higher-energy states on the conformal boundary and semi-classical gravity in AdS_3 for the BTZ black hole. They showed that a bulk Witten diagram with two types of perturbative (i.e., not massive conical defects) scalar fields in the bulk is equivalent to the average value of the three-point coefficient $\overline{\langle E|\mathcal{O}|E\rangle}$, where $|E\rangle$ is the high-energy state dual to the BTZ black hole, and $\mathcal{O}$ is the operator dual to one type of the light scalars. Here, the average of the three-point coefficient is taken over all states with energy E

$$\overline{\langle E|\mathcal{O}|E\rangle} \equiv \frac{\langle E|\mathcal{O}|E\rangle}{\rho(E)}, \tag{4.109}$$

where $\rho(E)$ is the density of states given explicitly by the asymptotic Cardy formula [197, 198, 199]. In Section 4.2, we reviewed a way to construct a p-adic version of the BTZ black hole as the quotient space of the Bruhat-Tits tree by the p-adic Schottky group $q^{\mathbb{Z}}$. In this section, we propose to use Kraus-Maloney's technique in p-adic BTZ configuration and calculate the analogous Witten diagram.[24] This calculation provides a dual interpretation for the boundary p-adic CFT averaged three-point coefficient, which in principle could be independently derived from a pure CFT calculation.

Review on BTZ black hole calculation by Kraus-Maloney

In this section, we provide a brief overview of Kraus and Maloney's results [145] on the bulk and boundary sides, as well as list their assumptions.

[24] Another name for Witten diagrams in p-adic AdS are called "subway diagrams" [167].

Cardy formula for three-point coefficients in 2d CFTs

High and low energy spectra of a CFT are related by modular invariance, i.e., $\mathcal{Z}(\beta) = \mathcal{Z}\left((2\pi)^2/\beta\right)$. Analogously, modular invariance can be used to refer high and low dimensional operators as "heavy" and "light" respectively. This can be used to obtain results on the asymptotic spectral density weighted by OPE coefficients. Kraus and Maloney used modular invariance in the torus one-point function to estimate light-heavy-heavy three-point coefficients $\langle E|\mathcal{O}|E\rangle$ for a BTZ black hole. They proved that the averaged three-point coefficient from the bulk in the large horizon limit and from the boundary in the high-temperature limit agree.

The three-point coefficients are easily found by taking the inverse Laplace transform and using the saddle point approximation in the high-temperature limit for a primary operator $\mathcal{O}$

$$\langle\mathcal{O}\rangle = \mathrm{Tr}_{\mathcal{H}_{S^1}}\,\mathcal{O}\; e^{-\beta H} = \sum_i \langle i|\mathcal{O}|i\rangle\; e^{-\beta E_i}, \tag{4.110}$$

where we trace over CFT states on the thermal circle and these coefficients are constrained by modular invariance.

The asymptotic behavior of the light-heavy-heavy coefficient is exponentially suppressed. The suppression depends on the central charge c and conformal dimensions of operators $\mathcal{O}$ and χ, which are light primary operators dual to AdS_3 bulk scalars $\phi_\mathcal{O}$ and ϕ_χ, with energy $E_\mathcal{O}, E_\chi \ll \frac{c}{12}$. To compute the averaged three-point function coefficient, the last ingredient we need is the density of states which is given by the Cardy formula in the large E limit [197, 198, 199]. In this limit, the final result of the averaged three-point function coefficient is

$$\overline{\langle E|O|E\rangle} \approx C_{\mathcal{O}\chi\chi} r_+^{\Delta_\mathcal{O}} e^{-2\pi\Delta_\chi r_+}, \tag{4.111}$$

which matches precisely in the bulk calculation done in Section 4.4.

Witten diagram calculation in AdS_3

The bulk theory has an interaction term $\phi_\mathcal{O}\phi_\chi^2$ with coupling $C_{\mathcal{O}\chi\chi}$. The cubic vertex integrated over the entire BTZ AdS spacetime in Figure 4.10 is

$$\overline{\langle E|O|E\rangle} = C_{\mathcal{O}\chi\chi}\int dr dt_E d\phi\; r\; G_{bb}\left(r;\Delta_\chi\right) G_{b\partial}\left(r,t_E,\phi;\Delta_\mathcal{O}\right). \tag{4.112}$$

We want to match the integral (4.112) in the large r_+ limit to the CFT result (4.111) for the asymptotic three-point coefficient. The BTZ black hole is obtained from global AdS_3 via periodic identifications (i.e., $\mathrm{AdS}_3/\mathbb{Z}$ under $\phi \sim \phi + 2\pi$), which allows us to preform the method of images to obtain the BTZ black hole propagator from global AdS_3. The BTZ black hole propagator is

$$G_{bb}\left(r,r'\right) = -\frac{1}{2\pi}\sum_{n=-\infty}^{\infty}\frac{e^{-\Delta\sigma_n(r,r')}}{1-e^{-2\sigma_n(r,r')}}, \tag{4.113}$$

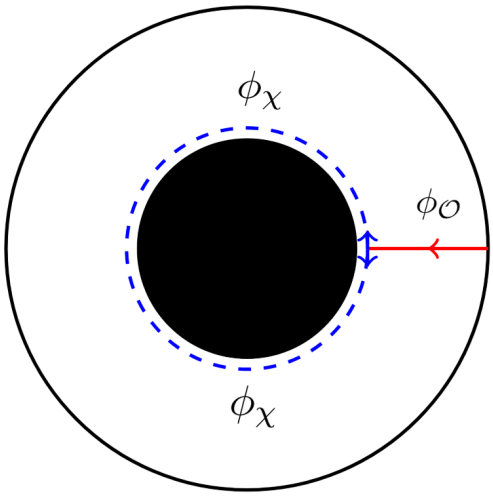

Figure 4.10: As illustrated in the Witten diagram for the regular BTZ black hole, a light scalar field $\phi_\mathcal{O}$ is emanated from the boundary to the horizon and splits into a pair of light fields ϕ_χ that wrap around the horizon.

where $\sigma_n(r, r')$ is the geodesic distance between r and the n^{th} image of r'. There is an apparent UV-divergent tadpole for the $n = 0$ term; however, this can be easily cancelled by a local counterterm and other terms $n \neq 0$ are finite. As we will see in Section 4.4, this type of UV divergence is absent in the case for p-adic BTZ black holes due to the form of the Green function, but a tadpole term remains present. Additionally, Kraus and Maloney considered the scalar fields to be massive: $E_\mathcal{O} \approx m_\mathcal{O} \gg 1, E_\chi \approx m_\chi \gg 1$ such that $m_\mathcal{O}, m_\chi \ll c$.

In the large r_+ limit, the averaged three-point coefficient is

$$\overline{\langle E|O|E\rangle} \approx C_{\mathcal{O}\chi\chi} r_+^{\Delta_\mathcal{O}} e^{-2\pi\Delta_\chi r_+}. \tag{4.114}$$

p-adic version Witten diagram calculation

Previously, we reviewed that the p-adic BTZ black hole is constructed as a quotient space of the Bruhat-Tits tree and is visualized as a central polygon with a sub-Bruhat-Tits rooted tree attached to each vertex of the polygon. The central polygon is the horizon of the p-adic BTZ black hole with area $l = -ord_p(q) = \log_p |q|_p$ and q is the generator of Schottky group $q^\mathbb{Z}$. Considering the construction of the p-adic BTZ black hole, we choose a new set of coordinates (n, h) to parametrize bulk points. The label of vertices on the horizon, to which bulk points attach (directly or indirectly), are represented by $n = 0, 1, \cdots, l-1$. Whereas $h = 0, 1, \cdots, \infty$ represents the number of edges between the attached central vertex and that bulk point.

Under this parametrization, in order to calculate the similar Witten diagram mentioned in [145], we replace the original integration over AdS space with a summation over all bulk

points (n, h) on the quotient space of the Bruhat-Tits tree

$$\overline{\langle E|\mathcal{O}|E\rangle} \approx C_{\mathcal{O}\chi\chi} \sum_{(n,h)} d(n,h) G_{bb}(n,h;\Delta_\chi) G_{b\partial}(n,h;x,\Delta_\mathcal{O}), \tag{4.115}$$

where $x \in \mathbb{Q}_p$ is the boundary coordinate of the operators $\mathcal{O}$, Δ_χ and $\Delta_\mathcal{O}$ are scaling dimensions of operators χ and $\mathcal{O}$. $d(n,h)$ counts the number of vertices sharing the same coordinate (n,h).

There are two different cases that we need to calculate separately. The first case is both the bulk and boundary points are attached to the same central vertex. The second case is both the bulk and boundary points are attached to different vertices. We denote the central vertex attached by the boundary point as vertex 0, such that these two cases are $n = 0$ and $n \neq 0$.

Propagators revisited in BTZ background

In Section 4.2, we introduced the p-adic BTZ black hole as the quotient space $T_p/q^\mathbb{Z}$, which is different from the original Bruhat-Tits tree T_p. One obvious distinction is that the quotient space loses some global symmetries.[25] Remember that the normal Bruhat Tits tree has a perfect homogeneity, and in principle, we could choose any local vertex to be a central point. However, the p-adic BTZ background certainly has some predetermined central vertices, which has been shown in Figure 4.2 as vertices of the central polygon.

Given the global symmetry breaking, we should question whether the theory defined on the p-adic BTZ black hole would deviate from the normal Bruhat-Tits tree theory defined by the action (4.20), and more importantly, whether the propagators (i.e., Green functions as the main characters of Witten diagram calculation shown above) would also change. Fortunately, by observations, we find that even though the global symmetry is broken by a topological change, the local features of the graph are still preserved. In other words, the valency of each vertex is still $p + 1$, same as on the Bruhat-Tits tree. Meanwhile, since the p-adic BTZ black hole is also an undirected graph with an infinite number of vertices, we should expect the action (4.20) to still be valid in the BTZ black hole background. However, when we compute the propagators, the equations of motion has sources inserted on some vertices. The symmetry loss of the BTZ black hole will also cause the symmetry loss to the solutions of these equations of motions. For instance, on the Bruhat-Tits tree, no matter where we insert the source, due to homogeneity of the tree, the solution will be homogeneous. However, in the BTZ black hole case, the depth of vertices, where we insert the source, from the horizon will indeed affect the solutions and subsequently the solutions will be different from those on a normal Bruhat-Tits tree.

One approach to compute the propagators in the background of an ordinary Euclidean BTZ black hole is the method of images [54, 145], which will be demonstrated in the next

[25] Global symmetries under action by the isometry group, e.g., $PGL(2, \mathbb{Q}_p)$ in the context of Bruhat-Tits trees. When we quotient $P^1(\mathbb{Q}_p)$ by the Schottky group $q^\mathbb{Z}$, the isometry group is then broken to a subgroup of $PGL(2, \mathbb{Q}_p)$.

subsection. Instead, we can also straightforwardly start from the solution to the equation of motion with a source insertion. This provides us a sanity check for the use of method of images. In general, due to the loss of symmetries, solving the equation of motion with sources inserted in arbitrary vertices on the p-adic BTZ is arduous, but we can still use the residual symmetries to evaluate a simple case.

Suppose we use the same action (4.20) for the p-adic BTZ background. Meanwhile, we restrict our calculations to the case where only one current source J is coupled to the vertex 0 on the horizon, without other source couplings. The equation of motion is then:

$$\left(\Box + m_p^2\right)\phi_i = \begin{cases} J & i = C_0 \\ 0 & \text{otherwise} \end{cases}, \tag{4.116}$$

yielding the propagator:

$$G_{bb}\left(C_0, a\right) = \frac{\phi_a}{J}, \tag{4.117}$$

where ϕ_a is the field value to an arbitrary vertex a and C_0 represents the vertex 0 on the horizon.

We should mention that the solution does depend on the specified boundary condition. In order to find the same class of solutions as those on the Bruhat-Tits tree, we specify the boundary condition:

$$\lim_{i \to \partial T_p} \phi_i = 0. \tag{4.118}$$

For simplicity, we set the mass m_p of the scalar field ϕ_i to be 0.

In Section 4.3, we demonstrated a way to solve Laplace's equation by using linear recursion in the scalar fields. Here, we follow a similar technique. We denote the vertices on the horizon as C_n where $n = 0, \cdots, l-1$. Consider one specific vertex C_i, the subtree rooted at C_n is solved by using a recursion relation:

$$(p+1)\phi_{h,n} = p\phi_{h+1,n} + \phi_{h-1,n}, \tag{4.119}$$

where the vertices on the subtree are parametrized by h, the depth of a vertex with respect to C_i. From Section 4.3, we know the solution to this recursion relation is:

$$\phi_{h,n} = a + bp^{-h}, \tag{4.120}$$

where a, b are two free variables that are fixed by the boundary conditions. We first enforce the boundary condition (4.118) to set $a = 0$, so $\phi_{h,n} = \phi_{C_n} p^{-h}$.

We also need to determine all field values ϕ_{C_n} on the horizon. This requires us to use the recursive equations on the horizon for $n \neq 0$:

$$(p+1)\phi_{C_n} = \phi_{C_{n-1}} + \phi_{C_{n+1}} + \frac{p-1}{p}\phi_{C_n} \tag{4.121}$$

The equation on vertex 0 is modified by the source:

$$(p+1)\phi_{C_0} = \phi_{C_{l-1}} + \phi_{C_1} + \frac{p-1}{p}\phi_{C_0} + J. \tag{4.122}$$

These linear equations can solved either numerically or analytically. We demonstrate a simple example where $l = 3$ and obtain the following solutions to (4.121):

$$\begin{aligned} \phi_{C_0} &= \frac{1}{p-\frac{1}{p}}\left(1+\frac{2}{p^3-1}\right)J \\ \phi_{C_1} &= \phi_{C_2} = \frac{1}{p-\frac{1}{p}}\frac{p^2+p}{p^3-1}J. \end{aligned} \tag{4.123}$$

In (4.76), we gave a correspondence between the mass of a bulk scalar field and the scaling dimension of a boundary operator. For a massless scalar, the corresponding scaling dimension is $\Delta = 1$. Then we rewrite the propagators (4.123) in a convenient way

$$\begin{aligned} G_{bb}(C_0, C_0) &= \frac{\zeta_p(2\Delta)}{p^\Delta}\left(1+\frac{2}{p^{\Delta l}-1}\right) \\ G_{bb}(C_0, C_n) &= \frac{\zeta_p(2\Delta)}{p^\Delta}\frac{p^n+p^{l-n}}{p^{\Delta l}-1}. \end{aligned} \tag{4.124}$$

In the subsequent subsections, we will see directly that these results are consistent with the results given by method of images in [168] for both bulk-to-bulk and bulk-to-boundary propagators.

$n = 0$ case

For the $n = 0$, the boundary point x and the bulk point b are in the same subtree rooted at, without loss of generality, the central vertex 0. The Witten diagram in Figure 4.11 is what is needed to calculate the averaged three-point coefficient.

To calculate this Witten diagram, we must determine two main factors: the bulk-to-bulk and bulk-to-boundary propagators. Since both fields χ and $\mathcal{O}$ are normal perturbative scalar fields, we directly derive the bulk-to-bulk propagator on the Bruhat-Tits tree by finding the tree Laplacian's Green function, which has a simple form[26] [167, 168]

$$G_{bb}(z, z_0; w, w_0) = p^{-\Delta_\chi d(z,z_0;w,w_0)}, \tag{4.125}$$

where the function $d(\cdot,\cdot)$ gives the geodesic distance. In the previous subsection, we provide a way to compute the Green function in p-adic BTZ background by solving the sourced equation of motion (4.122). In general, that approach is doable but complicated. Fortunately, the p-adic BTZ background is realized as the quotient space of the normal Bruhat-Tits tree,

[26] Here we omit the normalization factor $\frac{\zeta_p(2\Delta)}{p^\Delta}$ in [167].

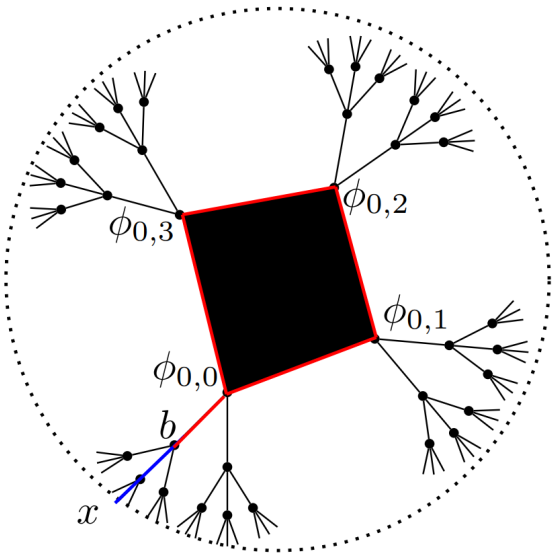

Figure 4.11: Witten diagram in the p-adic BTZ black hole ($p = 3, l = 3, n = 0$). Red line: the bulk-to-bulk propagator. Blue line: the bulk-to-boundary propagator.

so we use the method of images to solve the equations given the solutions in the parent space. Following [145], we use the method of images to derive the bulk-to-bulk propagator from vertex b to itself. Using the (n, h) parametrization as mentioned before, we obtain

$$G_{bb}(n,h) = p^{-\Delta_\chi d(b,b)} + 2\sum_{i=1}^{\infty} p^{-2\Delta_\chi h} p^{-i\Delta_\chi l} = 1 + \frac{2p^{-2\Delta_\chi h}}{p^{\Delta_\chi l} - 1}, \tag{4.126}$$

where the summation is over all images of b under the action of the Schottky group, and the index i is regarded as the winding number around the horizon. Comparing this result with solution (4.124) by setting $h = 0$, we see the two results agree up to a normalization factor $\zeta_p(2\Delta)/p^\Delta$ we omitted in (4.125). Notice that there is a constant 1 appearing in the bulk-to-bulk propagator. This is the tadpole term which usually causes divergence in the normal AdS spacetime. Although it does not cause a divergence in our case, it is still unphysical. Fortunately, we are able to cancel this tadpole term by adding a local counterterm $\sum_i c_i \phi_i$ into the action, where i is the label of bulk vertices. The renormalized bulk-to-bulk propagator is:

$$G_{bb}^{\text{renorm}}(n,h) = \frac{2p^{-2\Delta_\chi h}}{p^{\Delta_\chi l} - 1} \tag{4.127}$$

The bulk-to-boundary propagator is derived from the bulk-to-bulk propagator by moving one point to the boundary.[27] Notice that if we were to directly take this limit in (4.125),

[27]This limiting process is safe here, but it would be naïvely wrong when one were to calculate two-point correlators, as explained in Section 4 of [167].

it would vanish due to $d(z, z_0; w, w_0) \to \infty$. Therefore, we need to perform a regularization prescription provided in Section 3 of [167]. The bulk-to-boundary propagator on the Bruhat-Tits tree is derived via [167]:

$$G_{b\partial}(z, z_0; x) = \lim_{\delta_x \to 0} |\delta_x|_p^{-\Delta} G_{bb}(z, z_0; w, w_0). \tag{4.128}$$

Given a bulk point (w, w_0), we denote any boundary point which is reached by an oriented path $(z, z_0) \to (w, w_0)$ as y. The supremum of $|y - x|_p$ is denoted by δ_x. When we move (w, w_0) to the boundary point x, the limit is taken as $\delta_x \to 0$. Clearly, some prescription factor $|\delta_x|_p^{-\Delta} \to \infty$ is required so the bulk-to-boundary propagator does not vanish.

In [168, 166], another regularization procedure is provided. Instead of taking the asymptotic limit of the bulk-to-bulk propagator, they regularized the geodesic distance. The main feature there is that A. V. Zabrodin defined $d_{reg}(C, x) = 0$ [166], where C is a vertex on the horizon and x is the boundary point in the subtree rooted at C. By inspection, we realize that these two regularization methods are equivalent and both are consistent with the recursive derivation in Section 4.4. We then say these regularizations are anomaly-free under $PGL(\mathbb{Q}_p)$. Setting the geodesic distance of $d_{reg}(C, x) = 0$ is the same as factoring $p^{d(C,x)\Delta}$ out from the non-regularized propagator. $p^{d(C,x)\Delta} \to \infty$ plays the same role as $|\delta_x|^{-\Delta}$. Therefore, we freely choose one regularization approach and use the method of images to find the bulk-to-boundary propagator. The bulk-to-boundary propagator is given as [168]:

$$G_{b\partial}(b, x) = p^{-\Delta d_{reg}(b,x)} + \frac{2p^{-\Delta h}}{p^{\Delta l} - 1}. \tag{4.129}$$

For the $n = 0$ case, we combine the two propagators to obtain the averaged three-point coefficient

$$\overline{\langle E|\mathcal{O}|E\rangle}_{n=0} \approx C_{\mathcal{O}\chi\chi} \sum_{(0,h)} d(0, h) \left(p^{-\Delta_{\mathcal{O}} d_{reg}(b,x)} + \frac{2p^{-\Delta_{\mathcal{O}} h}}{p^{\Delta_{\mathcal{O}} l} - 1} \right) \frac{2p^{-2\Delta_\chi h}}{p^{\Delta_\chi l} - 1}, \tag{4.130}$$

where $d(0, h)$ denotes the degeneracy of vertices with the coordinate $(0, h)$. Notice that there is a unique path from the horizon vertex 0 to the boundary point x as well as a unique intersection point between the path from the bulk point b to the boundary point x and the path from vertex 0 to x. In order to compute the summation, we introduce one more parameter i to represent the intersection point between the two paths. Additionally, the parameter i will parametrize the bulk point b. By using the parameters (n, h, i), we rewrite

the summation in terms of a nested geometrical series:

$$\begin{aligned}\overline{\langle E|\mathcal{O}|E\rangle}_{n=0} \approx & C_{\mathcal{O}\chi\chi}\sum_{i=0}^{\infty}\left(p^{\Delta_{\mathcal{O}}i}\frac{2p^{-2\Delta_\chi i}}{p^{\Delta_\chi l}-1}+\sum_{h=i+1}^{\infty}(p-2)p^{h-i-1}p^{\Delta_{\mathcal{O}}(2i-h)}\frac{2p^{-2\Delta_\chi h}}{p^{\Delta_\chi l}-1}\right)\\ &+C_{\mathcal{O}\chi\chi}\frac{2}{p^{\Delta_{\mathcal{O}}l}-1}\frac{2\left(1+\frac{p-1}{p(p^{\Delta_{\mathcal{O}}+2\Delta_\chi-1}-1)}\right)}{p^{\Delta_\chi l}-1}\\ =&C_{\mathcal{O}\chi\chi}\left[\frac{2\left(1+\frac{p-2}{p(p^{\Delta_{\mathcal{O}}+2\Delta_\chi-1}-1)}\right)}{(p^{\Delta_\chi l}-1)(1-p^{\Delta_{\mathcal{O}}-2\Delta_\chi})}+\frac{4\left(1+\frac{p-1}{p(p^{\Delta_{\mathcal{O}}+2\Delta_\chi-1}-1)}\right)}{(p^{\Delta_{\mathcal{O}}l}-1)\,(p^{\Delta_\chi l}-1)}\right].\end{aligned} \tag{4.131}$$

In order to make the geometrical series converge for the above summations, we find inequalities between the scaling dimensions of operator $\mathcal{O}$ and χ:

$$\Delta_{\mathcal{O}}+2\Delta_\chi>1, \Delta_{\mathcal{O}}<2\Delta_\chi. \tag{4.132}$$

The first inequality is automatically satisfied, as mentioned in Section 4.3, we use the convention in [167] that $\Delta=\Delta_+>1/2$. The second inequality adds an extra constraint on the dimension of the operator $\mathcal{O}$. When $\Delta_{\mathcal{O}}$ is small enough, our calculation is well-defined until $\Delta_{\mathcal{O}}$ saturates the inequality (4.132). Further regularization is required for this. However, the second inequality is only related to coefficients independent of the horizon length l. Therefore, it will not affect the asymptotic behaviors for large l.

$n\neq 0$ case

This case is simpler than $n=0$. The Witten diagram is now visualized as Figure 4.12. The bulk-to-bulk propagator is the same as (4.126), while the bulk-to-boundary propagator is slightly different [168]. We evaluate the summations (4.115) as follows:

$$\begin{aligned}\overline{\langle E|\mathcal{O}|E\rangle}_{n\neq 0} \approx & C_{\mathcal{O}\chi\chi}\sum_{n=1}^{l-1}\sum_{(n,h)}d(n,h)\frac{p^{\Delta_{\mathcal{O}}(l-n)}+p^{\Delta_{\mathcal{O}}n}}{p^{\Delta_{\mathcal{O}}l}-1}p^{-\Delta_{\mathcal{O}}h}\frac{2p^{-2\Delta_\chi h}}{p^{\Delta_\chi l}-1}\\ =&C_{\mathcal{O}\chi\chi}\sum_{n=1}^{l-1}\frac{p^{\Delta_{\mathcal{O}}(l-n)}+p^{\Delta_{\mathcal{O}}n}}{p^{\Delta_{\mathcal{O}}l}-1}\frac{2\left(1+\frac{p-1}{p\left(p^{\Delta_{\mathcal{O}}+2\Delta_\chi-1}-1\right)}\right)}{p^{\Delta_\chi l}-1}\\ =&4C_{\mathcal{O}\chi\chi}\frac{p^{\Delta_{\mathcal{O}}l}-p^{\Delta_{\mathcal{O}}}}{(p^{\Delta_{\mathcal{O}}}-1)(p^{\Delta_{\mathcal{O}}l}-1)}\frac{1+\frac{p-1}{p(p^{\Delta_{\mathcal{O}}+2\Delta_\chi-1}-1)}}{p^{\Delta_\chi l}-1}\end{aligned} \tag{4.133}$$

In this case, we have no issues for divergences in the geometrical series. The only requirement $\Delta_{\mathcal{O}}+2\Delta_\chi>1$ has already been shown to be satisfied in previous subsection.

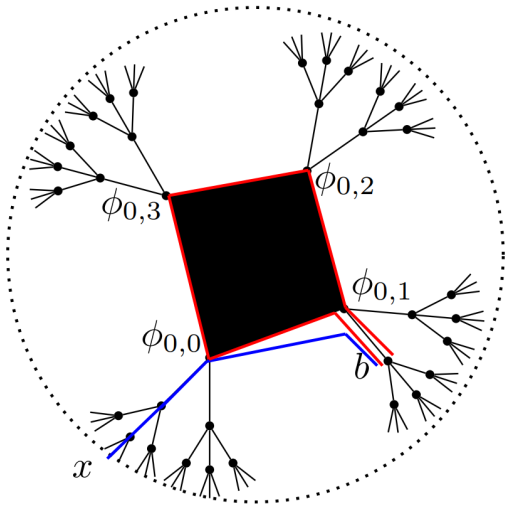

Figure 4.12: Witten diagram in the p-adic BTZ blac khole ($p = 3, l = 3, n \neq 0$). Red line: the bulk-to-bulk propagator. Blue line: the bulk-to-boundary propagator.

After having the contributions from both $n = 0$ and $n \neq 0$ cases, we then get the full expression for the averaged three-point coefficient:

$$\begin{aligned}\overline{\langle E|\mathcal{O}|E\rangle} &= \overline{\langle E|\mathcal{O}|E\rangle}_{n=0} + \overline{\langle E|\mathcal{O}|E\rangle}_{n\neq 0} \\ &= 2C_{\mathcal{O}\chi\chi}\left[\frac{1+\frac{p-2}{p\left(p^{\Delta_{\mathcal{O}}+2\Delta_\chi-1}-1\right)}}{(p^{\Delta_\chi l}-1)(1-p^{\Delta_{\mathcal{O}}-2\Delta_\chi})} + 2\frac{1+\frac{p-1}{p\left(p^{\Delta_{\mathcal{O}}+2\Delta_\chi-1}-1\right)}}{(p^{\Delta_\chi l}-1)\,(p^{\Delta_{\mathcal{O}}}-1)}\right] \\ &= C'_{\mathcal{O}\chi\chi}\frac{1}{p^{\Delta_\chi l}-1} \xrightarrow{l\to\infty} \boxed{C'_{\mathcal{O}\chi\chi}p^{-\Delta_\chi l}}\end{aligned} \tag{4.134}$$

The coefficient $C'_{\mathcal{O}\chi\chi}$ is viewed as the three-point coefficient $\langle\chi|\mathcal{O}|\chi\rangle$ and absorbs all factors independent of the horizon length l. In the last line, we show that as $l \to \infty$, the averaged three point coefficient $\overline{\langle E|\mathcal{O}|E\rangle}$ has an asymptotic behavior with an exponential dependence on horizon length l.

Physical implications

By comparing (4.114) with our average three-point coefficient (4.134), we find that l is a p-adic counterpart of $2\pi r_+$ which is the outer horizon area of a normal BTZ black hole. If we rewrite $p^{-\Delta_\chi l}$ as $e^{-\ln p\Delta_\chi l}$, it will become reminiscent to $e^{-2\pi\Delta_\chi r_+}$ in (4.114). However, in the p-adic case, we miss a counterpart to $r_+^{\Delta_{\mathcal{O}}}$. This term can be realized as the dominant normalization factor r_+^{Δ} in the bulk-to-boundary propagator of a normal Euclidean BTZ black hole [145]. Physically, it can be thought as the horizon radius being probed by the particle

$\mathcal{O}$ entering the bulk from the boundary. In a continuum spacetime, the horizon radius is well defined by a Riemannian metric. Whereas in the p-adic BTZ graph, the black hole is represented by a polygon which has no radius measured by the graph's metric. Therefore, when the particle ϕ is emanated into the p-adic BTZ background, it cannot measure the radius of horizon as well as unable to create a term including the horizon radius and its scaling dimension $\Delta_{\mathcal{O}}$.

In Section 4.3, we provided calculations on the p-adic CFT partition function and density of states. However, our knowledge is primitive on the modular transformations for p-adic genus-1 Tate curves. If we understand the modular transformation, we can obtain the averaged three point coefficient entirely from the CFT side. Our averaged three-point coefficient displays an unconventional feature compared to the Euclidean BTZ case to then indicate that the p-adic modular transformation is nontrivial. We will explore this aspect further in future works.

Last but not the least, our geometries only capture AdS length scale effects, and miss contributions coming from "small loops" which can be trivial, as stressed in [183]. It would be nice to see if the bulk calculation can be reproduced from the p-adic CFT side.

4.5 p-Adic representations

The proposed p-adic AdS/CFT correspondence provides tools to understand some features of the boundary p-adic CFT. However, for a general (not necessarily holographic) CFT, the bulk/boundary duality cannot allow us to study the theory comprehensively. In order to fully solve a general p-adic CFT, a Hilbert space interpretation is necessary. For example, independent of the bulk calculations in Section 4.4, if one wants to compute the one-point function of a primary operator $\mathcal{O}$ of p-adic CFT, analogous to $\langle\mathcal{O}\rangle_\tau = \mathrm{Tr}_{\mathcal{H}}\,\mathcal{O}q^{L_0-\frac{c}{24}}\overline{q}^{\overline{L}_0-\frac{c}{24}}$ with $q \equiv e^{2\pi i\tau}$ in an ordinary 2d CFT, one would hope to have p-adic exponentials, and analogues of Virasoro generators L_0 and $L_{\pm1}$ as well as Verma modules.

In a normal quantum field theory, its Hilbert space could be constructed based on representations of Lie algebra $\mathfrak{g}$ associated to the global or internal symmetry group G. In a p-adic CFT, the global symmetry group is $PGL\,(2,\mathbb{Q}_p)$, so analogous to ordinary CFTs, we should study Lie algebra representations of this group. Typically, a p-adic CFT is a quantum field theory with complex-valued (or real-valued) fields over $\mathbb{Q}_p$, which restricts our interests to a vector space V over $\mathbb{C}$ as the representation space. In [176], Melzer showed the nonexistence of local derivatives over $\mathbb{Q}_p$. Meanwhile, in the usual context of Lie algebra, we can always define the exponential map $\exp : \mathfrak{g} \to G$, while in p-adic case, the exponential function of p-adic numbers does not converge nicely [180]. Moreover, it is a totally disconnected group, its corresponding would-be Lie algebra "$\mathfrak{pgl}\,(2,\mathbb{Q}_p)$" does not exist. The Virasoro-like local conformal algebra never shows up.

Although we cannot find any suitable complex representation of Lie algebra, we still hope to directly study representations of the global conformal group $PGL\,(2,\mathbb{Q}_p)$. Actually, several recent papers indeed explore the power of group representations in quantizing a theory, such

as Jackiw-Teitelboim gravity [203] and spinors on AdS_2 [204], in that their Hilbert spaces can be partially[28] defined by group representations of $SL(2,\mathbb{R})\times U(1)/\mathbb{Z}$ or $\widetilde{SL(2,\mathbb{R})}$. There are numerous types of $PGL\left(2,\mathbb{Q}_p\right)$ representations, so we add some reasonable assumptions to narrow down our search list. Since all p-adic CFTs are unitary [176], we expect a suitable representation to also be *unitary*. Notice that any unitary irreducible representations (irreps) of $PGL\left(2,\mathbb{Q}_p\right)$ naturally induces a $GL\left(2,\mathbb{Q}_p\right)$ unitary irreps, so that we could study unitary irreps of $GL\left(2,\mathbb{Q}_p\right)$ and canonically restrict them onto the subgroup $PGL\left(2,\mathbb{Q}_p\right)$. Another advantage to study $GL\left(2,\mathbb{Q}_p\right)$ comes from the classification theorem on all of its unitary irreps. In the rest of this section, we will analyze this theorem and evaluate the suitability of all unitary irreps as physical Hilbert spaces over $\mathbb{C}$ of p-adic CFTs. Rather than being mathematically rigorous, we provide sufficient amount of evidence.

Troubles with Lie algebras

The usual Iwasawa decomposition[29] still holds for TDLC groups of our interests, such as $SL\left(2,\mathbb{Q}_p\right)$ or $PGL\left(2,\mathbb{Q}_p\right)$. Any element of $SL\left(2,\mathbb{Q}_p\right)$, the commutator subgroup of $GL\left(2,\mathbb{Q}_p\right)$, as presented in [168], can be decomposed into a product of special conformal transformation, rotation, dilatation, and translation as shown respectively:

$$\begin{pmatrix} p^m a & b \\ c & p^{-m}a^{-1}(1+bc) \end{pmatrix} = \begin{pmatrix} 1 & 0 \\ cp^{-m}a^{-1} & 1 \end{pmatrix} \begin{pmatrix} a & 0 \\ 0 & a^{-1} \end{pmatrix} \begin{pmatrix} p^m & 0 \\ 0 & p^{-m} \end{pmatrix} \begin{pmatrix} 1 & bp^{-m}a^{-1} \\ 0 & 1 \end{pmatrix}, \quad (4.135)$$

where $a,b,c\in\mathbb{Q}_p$ and $|a|_p=1$. The decomposition of $PGL\left(2,\mathbb{Q}_p\right)$ is similar, but up to a $\pm$ sign on the total determinant.[30]

One might believe that the exponential map from Lie algebras to the usual matrix group $GL(n,\mathbb{C})$ works for p-adic groups as well, but this is unfortunately incorrect. Indeed, one could define a tangent space and Lie algebra functor near the identity of $SL\left(2,\mathbb{Q}_p\right)$ [205], but the total disconnectedness of the group poses a serious problem. For $z\in\mathbb{Q}_p$, the p-adic exponential is defined as

$$\exp(z)\equiv\sum_{n=0}^{\infty}\frac{z^n}{n!}, \quad (4.136)$$

which diverges at the identity since the radius of convergence is $|z|_p<p^{-1/(p-1)}$.

Another fundamental reason is as follows. Having a tangent space T_e at the identity e of the group analytical manifold $PGL\left(2,\mathbb{Q}_p\right)$, it is natural to introduce a one-parameter subgroup $\phi:\mathbb{F}\to PGL\left(2,\mathbb{Q}_p\right)$, where $\mathbb{F}$ is a number field, which is $\mathbb{R}$ for usual connected Lie groups. ϕ also defines vector fields on the group manifold. Moreover, one can build an exponential map to recover local features of the group via Lie algebra. Thus,

$$\exp:\mathbb{F}\to PGL\left(2,\mathbb{Q}_p\right),\ t\mapsto e^{tL}, \quad (4.137)$$

[28] Some Lie algbera data such as quadratic Casimir are still required.

[29] For real semisimple Lie groups, it is defined via their Lie algebras.

[30] Each sign sector is similar to a connected component of the usual Lorentz group $SL(2,\mathbb{C})$. For the Iwasawa decomposition of $GL\left(2,\mathbb{Q}_p\right)$, see Proposition 4.2.1 in [169].

with the Lie algebra element $L \in T_e$. Consequently, we must select the correct number field $\mathbb{F}$ for the parameter t. $\mathbb{R}$ is ruled out due to the disconnectedness of p-adic groups. The only remaining candidate is $\mathbb{Q}_p$. However, another issue arises when we consider the representation of $PGL(2, \mathbb{Q}_p)$. With the representation space V over $\mathbb{C}$, we expect for any $g \in PGL(2, \mathbb{Q}_p)$, its image $\pi(g) \in GL(V)$ whose entries are all $\mathbb{C}$-valued. From the exponential map, we see that the image can always be written as

$$\pi(g) = e^{tM}, \tag{4.138}$$

where $M = \pi(L)$ is the image of the Lie algebra element L.[31] However, t and entries of M are in different number fields with different norms, so the multiplication tM is forbidden, and the Lie algebra representation over $\mathbb{C}$ cannot exist. Since there is no well-defined Lie algebra or "infinitesimal generators" for the dilatation operator L_0, it is a little bit dubious to discuss a "state-operator correspondence" used in [171] and hence radial quantization.

However, we should also mention the possibility to construct a Lie algebra representation over $\mathbb{Q}_p$ [206, 207]. In these cases, we need to consider Hilbert spaces over $\mathbb{Q}_p$ though, inconsistent with Melzer's axioms for p-adic CFTs.

Admissible representations of $GL(2, \mathbb{Q}_p)$ in general

Due to the troubles on the existence of p-adic Lie algebra, we turn our attention to group representations. The unitarity of p-adic CFTs directs us to unitary representations, which are subspaces of the physical Hilbert spaces as usual.

We start from the representation vector space V over $\mathbb{C}$. Let $GL(V)$ be the space of all automorphisms of V, and π be the following homomorphism

$$\pi : GL(2, \mathbb{Q}_p) \to GL(V). \tag{4.139}$$

Given an inner product[32] $(\cdot, \cdot)$ on V, a *unitary* representation (π, V) of G satisfies

$$(\pi(g) \cdot v, \pi(g) \cdot w) = (v, w), \quad \forall g \in G,\ v, w \in V. \tag{4.140}$$

Clearly, this definition is *relative* to the prescribed inner product on V. If V is not equipped with an inner product which makes (π, V) unitary, one can ask if (π, V) can be made unitary by choosing an appropriate inner product [169]. To this end, a representation (π, V) is defined as *unitarizable* if there exists[33] an inner product $(\cdot, \cdot)$ such that (4.140) holds. Moreover, it is straightforward to turn a unitary representation V into a complete metric space [208,

[31] The Lie algebra elements are complex-valued matrices.

[32] Formally speaking, this is a positive-definite Hermitian form, and is equivalent to the usual pairing between bras and kets.

[33] Existence of inner products is the first thing to look for in group representations. For example, for $SL(2, \mathbb{R})$ in JT gravity, among four types of its unitary irreps, trivial and complementary series representations are not considered [203] due to the lack of inner product. All of its finite-dimensional representations are non-unitary as well [204].

209], and therefore a Hilbert space; in fact the space of unitary admissible representations of $GL(2,\mathbb{Q}_p)$ is a proper subspace of the space of $\mathbb{C}$-Hilbert representations of $GL(2,\mathbb{Q}_p)$. Notice that inner products here do not rely on the dual (or *contragredient*) representation of V.

We further assume that we are dealing with irreps. According to the admissibility theorem[34], all unitary irreps of a p-adic reductive group such as $GL(2,\mathbb{Q}_p)$ [213] are admissible, so we only consider admissible ones. This is also empirically reasonable, because at least for real and complex Lie groups, their irreps naturally appearing in PDEs, geometry, number theory and physics are all admissible [214]. The admissibility theorem was originally proved in [215] and later illustrated in [216][35] (Section II.2.2). These were recently improved upon to work for more general TDLC groups, see [217] and [218] (Corollary 6.30).

Now to be complete, we present the definition of an admissible representation. An *admissible* representation (π, V) of G requires that the subspace of V fixed by any compact open subgroup of G is finite-dimensional [169, 218, 216]. It also has to be *smooth*, meaning that for $v \in V$, the function

$$\begin{pmatrix} a & b \\ c & d \end{pmatrix} \mapsto \pi\left(\begin{pmatrix} a & b \\ c & d \end{pmatrix}\right)\cdot v, \quad \forall \begin{pmatrix} a & b \\ c & d \end{pmatrix} \in GL(2,\mathbb{Q}_p) \tag{4.141}$$

is smooth, i.e., locally constant[36] [169, 219, 220]. Furthermore, a smooth irrep is admissible [169] (Theorem 6.1.11 therein). Dual representations of admissible representations are all admissible [169].

Finally we summarize the relations between various $GL(2,\mathbb{Q}_p)$ representations in Figure 4.13. Automorphic representations are not considered at all, because they are adelic over all prime numbers.

Finite-dimensional admissible representations

We start our discussion on finite-dimensional admissible irreps. These representations appear reasonable at first sight because they are consistent with the absence of descendants in p-adic CFTs. This is also reasonable especially when there are only a finite number of primaries. However, all finite-dimensional smooth irreps of $GL(2,\mathbb{Q}_p)$ are trivial in the sense that they are one-dimensional complex vector spaces such that the images of $GL(2,\mathbb{Q}_p)$ act as scalar multiplications as stated below [169].

Theorem *Let (π, V) be a finite-dimensional* ***smooth irrep*** *of $GL(2,\mathbb{Q}_p)$, then $V \cong \mathbb{C}$ and $\exists$ a multiplicative character ω: $\mathbb{Q}_p^\times \to \mathbb{C}^\times$ such that $\pi(g)\cdot v = \omega(\det g)\cdot v \ \forall\ g \in GL(2,\mathbb{Q}_p), v \in V$, where det is the usual determinant.*

[34]The original Harish-Chandra's admissibility theorem [210, 211, 212] only works for real reductive Lie groups.

[35]In this set of lecture notes, all adjectives "irreducible" should be interpreted in the category of unitary representations.

[36]It is absent on usual Lie groups, such as $SU(2)$.

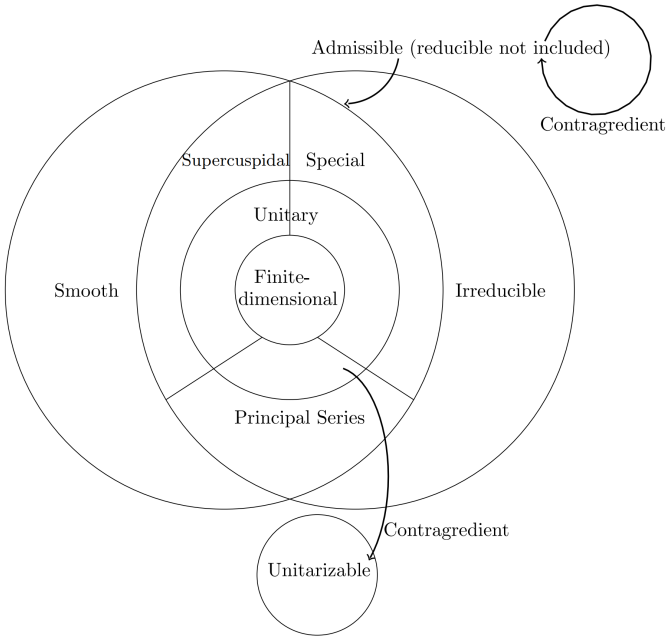

Figure 4.13: Relations between different types of representations for $GL(2, \mathbb{Q}_p)$.

For the group $SL(2, \mathbb{Q}_p)$, its linear character is 1. On the other hand, $PGL(2, \mathbb{Q}_p)$ consists of group elements of $GL(2, \mathbb{Q}_p)$ identified up to a scalar factor so that the linear character ω must be constant on the determinant in order to be consistent with this identification. Since ω is trivial, the dilatation transformation cannot be realized in this finite-dimensional admissible representation. Hence it is not a desirable physical Hilbert space. However, it would be interesting to see if an *ensemble* of primaries can be viewed as a tensor product of one-dimensional representations.

One of the simplest examples is presented in Section 4.1 of [168], the free boson on the boundary is viewed as a scalar representation of $PGL(2, \mathbb{Q}_p)$, and conformal dimensions of ϕ and Vladimirov derivative of ϕ are 0 and 1. However, we hope for more. One hint may come from the recent work on Green's functions of Vladimirov in the context of p-adic holography [221].

Infinite-dimensional admissible representations

According to the Langlands-like classification theorem [169], there are three classes of infinite-dimensional admissible representations for $GL(2, \mathbb{Q}_p)$: supercuspidal, principal series, and special.[37] Certainly, all of them contain non-unitary cases which do not fall into this classification, and those non-unitary cases are not of physical interests, because p-adic CFTs

[37] All of them enjoy so-called Kirillov models and Whittaker models, which we will not explain or pursue for now. For an accessible exposition on Whittaker models, see these notes [213].

satisfying Melzer's axioms are automatically unitary. Nevertheless, we will introduce their unitarity-independent definitions, and save unitarity-specific definitions to future work. In order to present the classification, we need to introduce the following object first.

Definition For an infinite-dimensional representation (π, V) and a unipotent subgroup $N = \left\{ \begin{pmatrix} 1 & * \\ 0 & 1 \end{pmatrix} \middle| * \in \mathbb{Q}_p \right\}$, consider the subspace

$$V_N = \{\pi(n)v - v | n \in N, v \in V\}, \tag{4.142}$$

then the quotient

$$V^N \equiv V/V_N \tag{4.143}$$

is called the *Jacquet module* of V. The classification of infinite-dimensional admissible representations is completely encoded by the dimension of V^N, which is at most two [219]. When $\dim_{\mathbb{C}} V^N = 0, 1, 2$, the representation is supercuspidal, special or principal series, respectively [222]. Incidentally, V^N also vanishes for finite-dimensional admissible representations.

For usual 2d CFTs, states with different Virasoro levels are orthogonal and obviously span an infinite-dimensional representation of the Virasoro algebra. Then in p-adic CFTs, one naïvely would think that different vectors in the representation space V have different energy levels. However, since we lack the necessary Casimir operators and algebra structure to define physical observables and quanta for the states, the realization of energy levels in a group representation is still mysterious.

Principal series and special representations

Principal series representations arise commonly in physics for non-compact semisimple Lie groups, and they are also present for $GL(2, \mathbb{Q}_p)$.

We start by defining the *normalized unitary character* of $GL_1(\mathbb{Q}_p) \simeq \mathbb{Q}_p^\times$, a continuous function $\omega : \mathbb{Q}_p^\times \to \mathbb{C}^\times$ such that [169]

1. $\omega(yy') = \omega(y)\omega(y'), \quad \forall y, y' \in \mathbb{Q}_p^\times$;
2. $|\omega(y)|_{\mathbb{C}} = 1, \quad \forall y \in \mathbb{Q}_p^\times$;
3. $\omega(p) = 1$.

Let $s_1, s_2 \in \mathbb{C}$. Then continuous characters χ_1, χ_2: $\mathbb{Q}_p^\times \to \mathbb{C}^\times$ are given by

$$\chi_i(x) \equiv \omega_i(x)|x|_p^{s_i}, \ s = 1, 2. \tag{4.144}$$

Consequently, $\chi = (\chi_1, \chi_2)$ extends to a character of the Borel subgroup B via

$$\chi\left[\begin{pmatrix} a & 0 \\ 0 & b \end{pmatrix} \begin{pmatrix} 1 & * \\ 0 & 1 \end{pmatrix} \right] = \chi_1(a)\chi_2(b). \tag{4.145}$$

Then the *normalized parabolic induction* of χ is the vector space:

$$V(\chi_1,\chi_2)=\Bigg\{f:GL\left(2,\mathbb{Q}_p\right)\to\mathbb{C}\,\Bigg|\,f\left[\begin{pmatrix}a&0\\0&b\end{pmatrix}\begin{pmatrix}1&*\\0&1\end{pmatrix}g\right]=\chi_1(a)\chi_2(b)\left|\frac{a}{b}\right|^{1/2}f(g),\\ \forall a,b\in\mathbb{Q}_p^{\times},\,*\in\mathbb{Q}_p,\,g\in GL\left(2,\mathbb{Q}_p\right),\,f\text{ is locally constant}\Bigg\},\tag{4.146}$$

called the *principal series representation* of $GL\left(2,\mathbb{Q}_p\right)$ induced from (χ_1,χ_2), and $GL\left(2,\mathbb{Q}_p\right)$ acts on $V(\chi_1,\chi_2)$ by right translation:

$$g\cdot f(h)=f(hg),\quad \forall g,h\in GL\left(2,\mathbb{Q}_p\right),\quad f\in V\left(\chi_1,\chi_2\right).\tag{4.147}$$

According to Jacquet-Langlands [223], this representation becomes reducible if $\chi_1\chi_2^{-1}=|\cdot|^{\pm1}$. If $\chi_1\chi_2^{-1}=|\cdot|^{-1}$, then $V(\chi_1,\chi_2)$ contains a 1D invariant subspace W such that $V(\chi_1,\chi_2)/W$ is an irrep called *special representation*; if $\chi_1\chi_2^{-1}=|\cdot|$, then $V(\chi_1,\chi_2)$ contains a 1D admissible subspace also called *special representation*.

Supercuspidal representations

If the Jacquet module V^N vanishes, then (π,V) is called a *supercuspidal representation.*[38] Although this one-line definition looks innocent, they are in general notoriously difficult to construct, and we present the simplest case via the so-called "*compact induction*" in Appendix B.4. We will use quite qualitative phrases in this short subsection.

However, supercuspidal representations are mathematically desirable due to its handful of nice properties. They are *the* "native" representations of $GL\left(2,\mathbb{Q}_p\right)$, because other admissible representations can all be constructed from them, by inducing a representation $\rho=(\rho_1,\rho_2)$ of a parabolic subgroup $P=MN$, where ρ_i is a supercuspidal representation of $GL_1\left(\mathbb{Q}_p\right)$, i.e., a character of $\mathbb{Q}_p^{\times}$, and the Levi subgroup $M\simeq GL_1\left(\mathbb{Q}_1\right)\times GL_1\left(\mathbb{Q}_1\right)\simeq\mathbb{Q}_p^{\times}\times\mathbb{Q}_p^{\times}$.

Another feature is that they have nicer inner products than the other two infinite-dimensional representations [219].

They are also the most well-behaved representations of $GL\left(2,\mathbb{Q}_p\right)$, i.e., that they behave much like representations of a compact group [225]. Finally, in familiar terms for $SL(2,\mathbb{R})$, supercuspidal and special representations are analogues of $SL(2,\mathbb{R})$ "discrete series" for $GL\left(2,\mathbb{Q}_p\right)$.

Key signature for physical representations

In previous subsections, we enumerated all candidate representations for the p-adic CFT Hilbert space. Although we made cogent arguments on the nonexistence of conformal algebra

[38] The adjective "super" stands for the p-adic version of "cuspidal" in the finite field $\mathbb{F}_q$ case [224], which is presented in Appendix B.4. For an equivalent definition in terms of integrals, see Section 6.13 of [169]. Equivalently, any irrep of $GL\left(2,\mathbb{Q}_p\right)$ which is not a subrepresentation of any representation induced from the Borel subgroup is *supercuspidal*.

and triviality of finite-dimensional admissible representations, there are still three classes of infinite-dimensional irreps remaining. There is no simple reasoning we could present to determine which one of them is the most suitable physical representation, and the difficulty of explicit construction of supercuspidal representations makes the computation over it tough. Fortunately, we find an important signature which could show clues as to which are true physical representations.

In the Virasoro character formula for normal chiral CFT on a torus $\chi(q) = \mathrm{Tr}_{\mathcal{H}} q^{L_0 - \frac{c}{24}}$, q is related to the modulus of T^2 torus via $q = e^{2\pi i \tau}$. However in Section 4.2, we saw the impossibility of defining a p-adic modulus $\tau \in \mathbb{Q}_p$. Moreover, the dilatation generator L_0 does not exist as discussed in Section 4.5, so the ordinary Virasoro character apparently makes no sense in p-adic CFTs. Nevertheless, $q^{L_0 - \frac{c}{24}}$ viewed as a whole can be interpreted as the representation of the dilatation transformation:

$$\begin{pmatrix} q^{\frac{1}{2}} & 0 \\ 0 & q^{-\frac{1}{2}} \end{pmatrix}, \tag{4.148}$$

which is exactly the same as the Schottky parameter in (4.16). Meanwhile, a genus-1 curve over $\mathbb{Q}_p$ was similarly constructed via p-adic Schottky group $q^{\mathbb{Z}}, q \in \mathbb{Q}_p^{\times}$. Intuitively, we could generalize the Virasoro character to p-adic CFTs by considering the image of the Schottky group generator under a $GL(2, \mathbb{Q}_p)$ representation (π, V), and using the new character to write down an analogous partition function for genus-1 p-adic CFT:

$$Z_{p-\text{adic CFT}} = \mathrm{Tr}_V \, \pi \left[\begin{pmatrix} q^{\frac{1}{2}} & 0 \\ 0 & q^{-\frac{1}{2}} \end{pmatrix} \right], \tag{4.149}$$

where the trace function always exists because $GL(2, \mathbb{Q}_p)$ is a TDLC group [218]. One thing worth looking at is to define a bounded-from-below V in terms of the Jacquet module.

In Section 4.3 we have explicitly calculated p-adic CFT partition functions from bulk path integral. In principle, we could check results there against (4.149) for all three classes of infinite-dimensional admissible representations. This check would yield a key signature of physical representations $\mathcal{H}$, and may also demystify the connections between $GL(2, \mathbb{Q}_p)$ representations and Chebyshev polynomials. Another ambitious thought is to apply group representations to possibly classify p-adic CFTs, just like ordinary minimal models, etc.

4.6 Summary and Outlook

We end with a summary of our results and several open questions for future exploration.

Discussion

In this chapter, we found the density of states of genus-1 p-adic BTZ black holes. Avoiding the assumption on the existence of a state-operator correspondence, we provide a new way

to calculate the genus-1 p-adic BTZ black hole partitions function via linear recurrence in scalar fields on vertices. Regarding both accounts, we have shown several similarities to their continuum analogues, but still realized features from Melzer's axioms for *non-Archimedean* CFTs.

Our analytical study on density of states in the high-temperature limit suggest that scalars in BTZ background obey a Bekenstein-Hawking-like area law and the results are analogous to the semiclassical genus-one partition function by Maloney and Witten [5]. However, one subtlety with our results are that they are unstable when $p = 3$. Possibly, this might be explained from our semi-classical analysis omitting gravitational contributions. Including gravitational effects for p-adic AdS/CFT was proposed by [187] via edge length dynamics, however, will be saved to future work,

Additionally, we calculated the averaged three-point coefficient in a p-adic BTZ black hole background and showed similarity with its ordinary counterpart by Kraus and Maloney, but notion of p-adic modular transformations remain unknown [145], so that one is unable to study the thermal p-adic AdS. We hope this calculation could initiate future work on n-point coefficients of p-adic CFTs on higher-genus Mumford curves, such as heavy-heavy-heavy three-point functions on regular genus-2 surfaces investigated in [143]. In fact, higher genus p-adic BTZ black holes were already developed by [168] using higher rank Schottky groups and Mumford curves.

Finally, we aim to narrow down the list of candidate Hilbert spaces for p-adic CFTs and provide hints for quantization. From the bulk point of view, the Hilbert space over $\mathbb{C}$ seems to be a very exotic one, due to Chebyshev polynomials showing up in Section 4.3.

Open questions

We provide a few open questions that would be interesting to explore in future work on p-adic AdS/CFT.

We have only considered the same species of bulk scalar fields but not the possibility of different species. Extending our bulk techniques to an ensemble of different species of bulk scalars ϕ_i would not only be interesting (due to the existence of multi-particle states in ordinary $\mathrm{AdS}_3/\mathrm{CFT}_2$ [54]), but might also shed light on p-adic CFT Hilbert space representations. A naïve guess for the boundary partition function with an ensemble of primaries χ_i dual to ϕ_i would be similar to that of ordinary 2d CFTs, with multiplicities M_{ij} of highest-weight states $|i, j\rangle$:

$$Z = \sum_{i,j} M_{ij} \chi_i(\tau) \chi_j(\overline{\tau}), \tag{4.150}$$

i.e., summation over primaries. While from the bulk point of view, since different scalars in the action (4.20) decouple from each other, the total partition function should be a simple product of individual partition functions like (4.36) for Bruhat-Tits trees, or (4.61) for BTZ black holes. The absence of descendants in p-adic CFT obscures the connection between

the summation over primaries on boundary and the product over them in bulk, which are transparently related in ordinary $\mathrm{AdS}_3/\mathrm{CFT}_2$.

As we have mentioned earlier, the $\mathcal{S}$-transformation on genus-1 Tate curve is still missing, so there is no good analogue of thermal p-adic AdS. We would like to study these potential p-adic modular transformation, and even p-adic MCGs.

Another question is about the role of $GL\left(n,\mathbb{Q}_p\right)$ in "p-adic" holography or in "higher-dimensional" p-adic CFTs, the latter being somewhat studied in [226]. For ordinary higher-dimensional CFTs, their fields can organize into Virasoro representations by *parabolic (generalized) Verma modules*, as stressed in [227]; they have also been used in ordinary affine Lie algebras [228]. Although Verma modules are absent in complex representations of p-adic groups, they have been constructed as representations on p-adic vector spaces instead of Hilbert spaces [206]. Then maybe it is worthwhile looking into the former vector spaces.

As to the connection between calculations in Section 4.3 and $GL(2,\mathbb{Q}_p)$ representations, unexpected coincidence showed up: the determinant of Laplacian on Bruhat-Tits tree (4.31) agrees with the volume of the following double coset [169] (Theorem 8.10.19 and Chapter 9.2 therein):

$$GL\left(2,\mathbb{Z}_p\right)\cdot\begin{pmatrix}p^N & 0\\ 0 & 1\end{pmatrix}\cdot GL\left(2,\mathbb{Z}_p\right) \tag{4.151}$$

with respect to a Haar measure in the context of principal series representations of $GL(2,\mathbb{Q}_p)$. We will present one explanation for this seeming coincidence in using the graph Laplacian on a Bruhat-Tits tree in Appendix B.1.

There are more ambitious questions. Since our auxiliary cutoff N is necessary in Section 4.3, then it is natural to ask what will happen to the boundary p-adic CFT when one introduce a real cut-off on the Bruhat-Tits tree? Since there is not yet a stress tensor in p-adic CFT [178], an analogue $T\bar{T}$ deformation $\mathrm{AdS}_3/\mathrm{CFT}_2$ [229] seems to be unrealistic.

Finally, beyond AdS/CFT, is it possible to formulate a p-adic dS/CFT correspondence? A precursor was given by [177] in the context of eteranal inflation with dS vacua, but not in the context of string theory.

Chapter 5

Double-Janus linear σ-models and generalized reciprocity for Gauss sums

5.1 Introduction

In this chapter, we study the torus partition function of a supersymmetric 2d linear σ-model with T^2 target space (a free theory) whose complex structure varies along one of the worldsheet directions (parametrized by $0 \leq \sigma_1 < 1$) and whose Kähler modulus varies along the other direction (parametrized by $0 \leq \sigma_2 < 1$). The periodic boundary conditions can be twisted both with an element in the MCG of the target T^2 (we choose to do that twist along the σ_1 direction) and with a T-duality transformation (along σ_2). The partition function thus depends on (the conjugacy classes of) $M, \widetilde{M} \in SL(2, Z)$ that respectively describe the MCG "geometrical" element and the T-duality transformation. We represent the complex structure of the target space by τ (taking values in the upper half-plane $\mathbb{H}$), which is allowed to vary as a function of σ_1. More concretely, as we complete a loop around the first cycle of the worldsheet (by varying σ_1 from 0 to 1), the variable τ may undergo a $PSL(2,\mathbb{Z})$ transformation $\tau \to (\mathbf{a}\tau + \mathbf{b}) / (\mathbf{c}\tau + \mathbf{d})$, and in order to prevent a discontinuity at $\sigma_1 = 0$ we need to impose boundary conditions (connecting the fields at $\sigma_1 = 0$ to the fields at $\sigma_1 = 1$) that involve an element of the MCG of the target space, encoded by

$$M = \begin{pmatrix} \mathbf{a} & \mathbf{b} \\ \mathbf{c} & \mathbf{d} \end{pmatrix} \in SL(2,\mathbb{Z}).$$

Similarly, the Kähler structure of the target space is represented by $\rho = \rho_1 + i\rho_2$ on the upper half-plane (with ρ_2 proportional to the area of the T^2 target and ρ_1 proportional to the Kalb-Ramond flux). As σ_2 varies from 0 to 1, the variable ρ may undergo a $PSL(2,\mathbb{Z})$ transformation $\rho \to \left(\tilde{\mathbf{a}}\rho + \tilde{\mathbf{b}}\right) \Big/ \left(\tilde{\mathbf{c}}\rho + \tilde{\mathbf{d}}\right)$, and in order to prevent a discontinuity at $\sigma_2 = 0$ we need to impose boundary conditions (connecting the fields at $\sigma_2 = 0$ to the fields at

$\sigma_2 = 1$) that involve a "T-duality wall" labeled by

$$\widetilde{M} = \begin{pmatrix} \tilde{\mathbf{a}} & \tilde{\mathbf{b}} \\ \tilde{\mathbf{c}} & \tilde{\mathbf{d}} \end{pmatrix} \in SL(2,\mathbb{Z}).$$

The motivation for considering such a setup is that it arises as a limit of a sort of "double-Janus" configuration of 4d $\mathcal{N} = 4$ SYM theory. Janus configurations are 4d SYM theories with a coupling constant that varies along one direction of space. They were first introduced by Bak, Gutperle and Hirano [230] in a non-supersymmetric dilatonic deformation of AdS_5, an exact solution to the Type IIB SUGRA equations, as a way to create a discontinuous jump in the *real* Yang-Mills coupling constant (which is related to the asymptotic boundary value of the dilaton according to the standard AdS/CFT dictionary) across a codimension-1 interface. A supersymmetric Janus configuration was introduced in [231], and later, the jump was "smoothed out" in [232], but still without a θ-angle. Subsequently, Gaiotto and Witten presented [233] the action of a deformation of $\mathcal{N} = 4$ SYM that preserves half of the supersymmetries with a *complex* coupling constant $\tau = \frac{4\pi i}{g^2_{\rm ym}} + \frac{\theta}{2\pi}$ that varies as a function of one spatial direction, say $\tau(x_3)$. Janus configurations have been further explored in [234, 235] and have been introduced into sphere partition functions in [236, 237]. They can also be constructed for theories in other dimensions [238]. Configurations for 2d σ-models have been proposed earlier in [239] and sphere partition functions with Janus configurations have been calculated in [237, 240].

Taking the gauge group to be $U(n)$, the Gaiotto-Witten action allows us to smoothly introduce an $SL(2,\mathbb{Z})$ duality twist (sometimes referred to as a "duality wall" or "S-fold" and studied in various string theory and gauge theory contexts, for example, in [241, 242, 243, 244, 245, 246]) in an S^1 compactification of 4d SYM. Parameterizing S^1 by $0 \le x_3 < 1$, the duality twist is an unconventional boundary condition that sets

$$\tau(1) = \frac{\mathbf{a}\tau(0) + \mathbf{b}}{\mathbf{c}\tau(0) + \mathbf{d}} \tag{5.1}$$

for $M \in SL(2,\mathbb{Z})$, together with the implied electric-magnetic duality action on the fields. We will refer to this theory as a *closed Janus configuration.* This setup was studied in [247] for $U(1)$ gauge group, where the low energy limit is easily shown to be described by a Chern-Simons action with an abelian gauge group, determined (not uniquely) by a decomposition of M into

$$T = \begin{pmatrix} 1 & 1 \\ 0 & 1 \end{pmatrix} \quad \text{and} \quad S = \begin{pmatrix} 0 & -1 \\ 1 & 0 \end{pmatrix}$$

generators. Furthermore, it was shown in [247] that a T-dual string theory background provides a geometrical interpretation for the quantum algebra of Wilson loops. A similar setup was also studied in [248], from the perspective of the holographic dual. Duality walls have also been studied in [249], and recently a gravitational anomaly was discovered [250] in such compactifications.

The Gaiotto-Witten Janus configuration can be constructed as a limit of a compactification of the 6d $(2,0)$-theory on a T^2-fibration over $\mathbb{R}$ when the area of the T^2 fiber shrinks to zero. We will review this construction in Section 5.2. To construct the closed Janus configuration requires us to first take the limit where the area of the T^2 fiber shrinks to zero, since otherwise the area will be discontinuous along S^1 (as we will explain in Section 5.2), and so we are back to $\mathcal{N}=4$ SYM with the S-fold twist M. In the context of 3d-3d correspondence [251], this configuration is related to the 6d $(2,0)$ theory on an (auxiliary) 3d mapping torus studied in [39, 252, 253, 254], where a higher-genus fiber is also considered. The setup for the present chapter is derived from an abelian double-Janus configuration that is a prelude to the study of a nonabelian theory. It can be obtained as a limit of a Gaiotto-Witten Janus configuration by compactifying on a small torus and allowing its complex structure parameter to vary as a function of time. In other words, we compactify the closed 4d Janus configuration on another (auxiliary) mapping torus labeled by another $SL(2,\mathbb{Z})$ element $\widetilde{M}$. We are interested in the partition function $\mathcal{Z}(M,\widetilde{M})$ which is a function of the two duality twists. Here M is the S-duality element that acts on the $\mathcal{N}=4$ SYM coupling constant, while $\widetilde{M}$ is the MCG element of the T^2 in the *geometrical* mapping torus. To preserve SUSY, it is again convenient to take the limit where the area of the T^2 fiber shrinks to zero first. Thus, we first reduce the 4d gauge theory to 2d, which for $U(1)$ gauge group becomes a σ-model with a $T^2\times\mathbb{R}^6$ target space. The $\mathbb{R}^6$ factor does not play much of a role in what follows, so we ignore it. We are thus led to study "double-Janus" configurations for a linear σ-model with T^2 target space where the complex structure varies in one direction and the Kähler structure (i.e., the complexified area) varies in the other direction, with M- and $\widetilde{M}$-boundary conditions respectively [where $M\in SL(2,\mathbb{Z}_\tau)$ and $\widetilde{M}\in SL(2,\mathbb{Z}_\rho)$]. We will show that $\mathcal{Z}(M,\widetilde{M})$ is essentially a finite sum over certain roots of unity, and by calculating it in two different limits, respectively corresponding to different limits of the shape of the (physical) T^2 target, we arrive at a number-theoretic identity known as the *Landsberg-Schaar* identity.

The rest of this chapter is organized as follows. We begin in Section 5.2 by reviewing our key motivation, the Gaiotto-Witten Janus configuration of 4d SYM, and its various connections to the 6d (2,0) theory. Then we deviate a little bit in Section 5.3 with a brief review of Quadratic Reciprocity, Gauss sums, and the Landsberg-Schaar identity. We then construct the double-Janus σ-model in the 2d bulk in Section 5.4, where we present the general constraints from supersymmetry, and various solutions. In Section 5.5 we compactify the double-Janus solution on a torus and introduce the twisted boundary conditions (with both geometrical and T-duality twists, M and $\widetilde{M}$, respectively). In Section 5.6 we calculate the double-Janus partition function, including both bosonic and fermionic one-loop determinants, which cancel each other out, leaving only a number-theoretic quadratic Gauss sum. In Section 5.7 we discuss connections with abelian Chern-Simons theory partition functions and the dual "strings on mapping tori" introduced in [247] in the context of 4d closed Janus configurations. We use this dual formulation to determine the precise normalization of the partition function. In Section 5.8 we show how the basic Landsberg-Schaar relation follows

with a Berry phase factor included, and in Section 5.9 we derive its multivariate generalizations, along with a comparison against known generalizations in the mathematical literature. Finally we conclude in Section 5.10.

5.2 Janus compactifications and mapping tori

The key motivation of our construction is a supersymmetric configuration of $\mathcal{N}=4$ SYM with a complex coupling constant $\tau=\tau_1+i\tau_2$ that varies along one of the directions, say $x_3\equiv y$, which for the time being we take to be $\mathbb{R}$ (but we will later compactify it to S^1). An explicit supersymmetric Lagrangian has been constructed by Gaiotto and Witten in [233].

Gaiotto-Witten Janus configuration

Now we review the Gaiotto-Witten construction in [233]. We adopt their notations, so that the action of the ordinary $\mathcal{N}=4$ SYM introduced in (1.47) now reads

$$\begin{aligned} I_0=\int d^4x\frac{1}{g_{YM}^2}\,\mathrm{Tr}\,\bigg(&\frac{F_{ij}F^{ij}}{2}+F_{3i}F^{3i}+D_3X_aD^3X^a+D_3Y_pD^3Y^p+D^iX^aD_iX_a+D^iY^pD_iY_p\\ &+\frac{1}{2}[X_a,X_b][X^a,X^b]+\frac{1}{2}[Y_p,Y_q][Y^p,Y^q]+[X_a,Y_p][X^a,Y^p]-i\overline{\Psi}\Gamma^ID_I\Psi\bigg)\\ &-\frac{\theta}{8\pi^2}\int F\wedge F, \end{aligned} \tag{5.2}$$

where the spacetime indices $i=0,1,2$, and we denote the six scalars as X_a for $a=4,5,6$ and Y_p for $p=7,8,9$, and $I=(i,3,a,p)=0,\cdots,9$. The action is invariant under the supersymmetry transformation

$$\delta A_I=i\bar{\varepsilon}\Gamma_I\Psi,\quad \delta\Psi=\frac{1}{2}\Gamma^{IJ}F_{IJ}\varepsilon, \tag{5.3}$$

where $A_I=(A_i,X_a,Y_p)$.

The Gaiotto-Witten Janus configuration is a deformation of the $\mathcal{N}=4$ SYM, such that the coupling $\tau=\theta/2\pi+4\pi i/g_{YM}^2$ as in (1.45) varies continuously over the x_3-direction as

$$\frac{1}{g_{YM}^2}=D\sin 2\psi,\quad \theta=2\pi a+8\pi^2D\cos 2\psi, \tag{5.4}$$

where ψ is an arbitrary function of x_3. This deformation preserves half of the 16 supercharges of the original theory, that satisfy the equation

$$(\Gamma^{3456}\sin\psi+\Gamma^{3789}\cos\psi)\varepsilon=\varepsilon, \tag{5.5}$$

where ε is a 10D chiral spinor. The deformed supersymmetry transformation of the gaugino Ψ is given by (5.3) plus

$$\widetilde{\delta}\Psi=\left(-\Gamma^3\Gamma^aX_a\psi'\tan\psi+\Gamma^3\Gamma^pY_p\psi'\cot\psi\right)\varepsilon. \tag{5.6}$$

The deformed action, that is invariant under the deformed supersymmetry transformation, is

$$I_{tot} = I_0 + I' + I'' + I''' \tag{5.7}$$

where

$$I' = \int d^4x \frac{i}{g_{YM}^2} \operatorname{Tr} \overline{\Psi} \left(\frac{1}{2}\psi' \Gamma_{012} - \frac{\psi'}{2\cos\psi}\Gamma_{456} + \frac{\psi'}{2\sin\psi}\Gamma_{789} \right) \Psi \tag{5.8}$$

includes additional fermionic bilinear terms, and

$$\begin{aligned} I'' = \int d^4x \operatorname{Tr} \Big[& -2\psi' \epsilon^{\mu\nu\lambda} \operatorname{Tr} \left(A_\mu \partial_\nu A_\lambda + \frac{2}{3} A_\mu A_\nu A_\lambda \right) + \frac{2\psi'}{3\cos\psi} \epsilon^{abc} \operatorname{Tr} X_a [X_b, X_c] \\ & - \frac{2\psi'}{3\sin\psi} \epsilon^{pqr} \operatorname{Tr} Y_p [Y_q, Y_r] \Big] \end{aligned} \tag{5.9}$$

includes additional dimension 3 bosonic terms, and

$$\begin{aligned} I''' &= \int d^4x \frac{1}{g_{YM}^2} \operatorname{Tr} \left\{ \left[(\psi' \tan\psi)' + (\psi')^2 \right] X^2 + \left[-(\psi' \cot\psi)' + (\psi')^2 \right] Y^2 \right\} \\ &= \int d^4x \frac{1}{g_{YM}^2} \operatorname{Tr} \left\{ \left[-2\psi' \tan\psi X^a X'_a + (\psi')^2 \tan^2\psi X^2 \right] \right. \\ &\qquad \left. + \left[2\psi' \cot\psi Y^p Y'_p + (\psi')^2 \cot^2\psi Y^2 \right] \right\}, \end{aligned} \tag{5.10}$$

includes additional dimension 2 terms. Notice that for the last equality in (5.10), we have used (5.4) and integration by parts. I''' can be absorbed into the kinetic term of X and Y,

$$\begin{aligned} \widetilde{I} &= \int d^4x \frac{1}{g_{YM}^2} \operatorname{Tr} \left[+D_3 X_a D^3 X^a + D_3 Y_p D^3 Y^p \right] + I''' \\ &= \int d^4x \frac{1}{g_{YM}^2} \operatorname{Tr} \left[\sec^2\psi D_3 \widetilde{X}_a D^3 \widetilde{X}^a + \csc^2\psi D_3 \widetilde{Y}_p D^3 \widetilde{Y}^p \right], \end{aligned} \tag{5.11}$$

where $\widetilde{X} = X\cos\psi$ and $\widetilde{Y} = Y\sin\psi$.

We include an attempt to topologically twist the in Appendix C.1.

To understand the supersymmetric Janus configurations, it is convenient to start in 6d with the $(2,0)$-theory. In fact, most of this chapter is about the free $U(1)$ gauge theory, so we will start with a free tensor multiplet in 6d. This theory has a basis of 16 supersymmetry charges, but to construct a supersymmetric Janus configuration we need to compactify on a suitable space and twist the supersymmetry. We can do this in two different ways.

Its connection to 6d (2,0)

Here we show how to get the Gaiotto-Witten Janus configuration [233] from the 6d $(2,0)$ theory. We begin with the 6d $(2,0)$ theory on a spacetime with metric given by

$$ds^2 = -dt^2 + dx_1^2 + dx_2^2 + dy^2 + R_4(y)^2 dx_4^2 + R_5^2 dx_5^2,$$

where R_5 is a constant and R_4 varies with periodicities $x_4 \sim x_4 + 2\pi$ and $x_5 \sim x_5 + 2\pi$, and noncompact $-\infty < y < \infty$. Note that direction x_4 forms an S^1-fibration over $\mathbb{R}$, the direction y, whose total space is a noncompact Riemann surface. The 6d $(2,0)$-theory compactification therefore falls within the class of theories studied by Gaiotto in [255]. To preserve 8 supersymmetries we introduce, as in [255], an R-symmetry twist that matches the holonomy of the Riemann surface. This is done with a background gauge field for an $SO(2)$ subgroup of the $Spin(5)$ R-symmetry group. Dimensional reduction along directions x_4, x_5 gives rise to a Janus configuration with $\tau(y) = iR_5/R_4$ varying with y and taking values along the imaginary axis. Now, apply an $SL(2,\mathbb{R})$ transformation that acts as

$$h : \tau \to \frac{\alpha\tau + \beta}{\gamma\tau + \delta}, \qquad h = \begin{pmatrix} \alpha & \beta \\ \gamma & \delta \end{pmatrix} \in SL(2,\mathbb{R}), \tag{5.12}$$

and linearly transforms x_4, x_5 to obtain the metric

$$ds^2 = dt^2 + dx_1^2 + dx_2^2 + dy^2 + R_4(y)^2 \left(\delta dx_4' - \beta dx_5'\right)^2 + R_5^2 \left(\alpha dx_5' - \gamma dx_4'\right)^2 . \tag{5.13}$$

We also modify the periodicity condition so that the new coordinates x_4', x_5' are periodic with periodicity 2π. The 3-manifold in directions y, x_4', x_5' still has a holonomy group $SO(2)$, and we can construct a twisted compactification of the 6d $(2,0)$-theory along x_4', x_5' to preserve supersymmetry by embedding $SO(2) \subset Spin(5)$. If we view the 6d $(2,0)$-theory as the low-energy description of M5-branes, we can let $SO(2)$ correspond to rotations in 2 out of the 5 transverse directions to the worldvolume. This compactification preserves half of the supersymmetry. In the limit $R \to 0$ we get the 4d Gaiotto-Witten Janus configuration with a complex Yang-Mills coupling constant given by $\tau' = \frac{\alpha\tau+\beta}{\gamma\tau+\delta}$, varying along a semicircle in the upper half-plane. The semicircle is the image of the imaginary axis under (5.12). The R-symmetry twist creates additional mass terms for the R-charged fields, as discovered in [233].

Dimofte-Gaiotto-Gukov configuration

Define the 3d mapping torus $\mathcal{M}_{\text{TF}}$, parametrized by (y, x_4, x_5) with periodic coordinates $0 \le x_4, x_5 < 1$, and unrestricted $-\infty < y < \infty$, and with metric

$$ds^2 = dy^2 + \rho\tau_2(y)^{-\frac{1}{2}} |dx_4 + \tau(y) dx_5|^2 . \tag{5.14}$$

Here ρ is the constant area of $\mathcal{M}_{\text{TF}}$. Compactifying the 6d $(2,0)$-theory on $\mathcal{M}_{\text{TF}}$ and taking the limit $\rho \to 0$ leads to a 4d $\mathcal{N} = 4$ SYM with a coupling constant τ that varies with y. However, the holonomy group of $\mathcal{M}_{\text{TF}}$ is the entire $SO(3)$, and $\mathcal{M}_{\text{TF}}$ therefore does not have a nonzero covariantly constant spinor. So, as it stands, compactification of the 6d $(2,0)$-theory on $\mathcal{M}_{\text{TF}}$ breaks supersymmetry entirely. The solution to this problem is to twist the supersymmetry in 6d. Consider a subgroup $Spin(3) \subset Spin(5)_R$ of the R-symmetry group, under which the spinors of $Spin(5)$ decompose as two copies of the fundamental

representation of $Spin(3) \simeq SU(2)$. If the $(2,0)$-theory is understood as the low-energy description of an M5-brane in M-theory [36], then such a subgroup can be realized as the group of rotations in 3 of the 5 directions transverse to the M5-brane. The twisting identifies this $Spin(3)$ with the (double cover of the) holonomy group of $\mathcal{M}_{\rm TF}$, or more geometrically, by letting 3 of the 5 transverse directions be fibered over $\mathcal{M}_{\rm TF}$ in a rank-3 vector bundle whose structure group is the holonomy group. Dimofte, Gaiotto, and Gukov (DGG) studied this system in [251, 39], as part of a comprehensive theory, 3d-3d correspondence, that they developed for analyzing the $(2,0)$-theory on 3-manifolds. After the twisting operation, the 6d supersymmetry generators transform as two copies of $\mathbf{2} \otimes \mathbf{2} = \mathbf{1} \oplus \mathbf{3}$ of the holonomy group. The singlet survives as a covariantly constant generator, and therefore one quarter of the supersymmetry is preserved. The DGG theory therefore preserves 4 supercharges, and $\tau(y)$ is an arbitrary function.

Now consider the twisting operation applied to the $U(1)$ version of the theory, i.e., a free tensor multiplet. Denote by $Spin(3)_H$ the holonomy group of $\mathcal{M}_{\rm TF}$. Before the twisting, the fermions are in the $(\mathbf{2},\mathbf{4})$ of $Spin(3)_H \otimes Spin(5)_R$, and the scalars are in the $(\mathbf{1},\mathbf{5})$ where $\mathbf{5}$ is the vector representation of $Spin(5)_R$. After the twist, we replace $\mathbf{4}$ of $Spin(5)_R$ with $\mathbf{2}\oplus\mathbf{2}$ of $Spin(3)_H$, and $\mathbf{5}$ of $Spin(5)_R$ with $2(\mathbf{1})\oplus\mathbf{3}$ (3 singlets and one vector). The spinors then transform as $\mathbf{2}\otimes(\mathbf{2}\oplus\mathbf{2}) = 2(\mathbf{1})\oplus 2(\mathbf{3})$. At low-energy the mode of the 2-form B that is proportional to the top form of the fiber $dx_4 \wedge dx_5$ becomes a third scalar, and the low-energy 4d R-symmetry is enhanced to $SU(2)_R$. Under $Spin(3)_H \times SU(2)_R$ the scalars transform as $(\mathbf{1},\mathbf{3})\oplus(\mathbf{3},\mathbf{1})$ and the spinors transform as $(\mathbf{1},\mathbf{2})\oplus(\mathbf{3},\mathbf{2})$. The equations of motion of the $Spin(3)_H$ vector fields are equivalent to those of a $U(1)$ gauge field in Lorenz gauge.

We stress that the above constructions are only a motivation for the σ-model that we will study starting from Section 5.4, which is a supersymmetric 2d σ-model with varying parameters. Now we review a key number-theoretic concept, to which we will connect Janus configurations.

5.3 Quadratic Reciprocity

Quadratic Reciprocity is a classic duality in elementary number theory. In order to introduce it, we first set up the context and review a few related concepts. If p is an odd prime number and q is an integer, then q is called a *quadratic residue* (mod p) if $x^2 \equiv q \pmod p$ has integer solutions x. The information on solutions to this equation is packaged inside the *Legendre symbol* $\left(\frac{q}{p}\right)$ defined as follows:

$$\left(\frac{q}{p}\right) \equiv \begin{cases} -1 & \text{if } \sqrt{q} \pmod p \text{ doesn't exist;} \\ 0 & \text{if } q \equiv 0 \pmod p; \\ 1 & \text{if } \pm\sqrt{q} \pmod p \text{ exist and are distinct.} \end{cases}$$

The *Law of Quadratic Reciprocity* states that if p and q are odd primes, then

$$\left(\frac{p}{q}\right)\left(\frac{q}{p}\right) = (-1)^{\left(\frac{p-1}{2}\right)\left(\frac{q-1}{2}\right)}. \tag{5.15}$$

It is a nontrivial statement that connects the existence of solutions to $x^2 \equiv q \pmod{p}$ with the existence of solutions to the dual equation $x^2 \equiv p \pmod{q}$. Quadratic Reciprocity was originally conjectured by Euler and Legendre in the late 18^{th} century, and then proved by Gauss in 1801. It was a catalyst for subsequent modern developments in Algebraic Number Theory, such as Artin's Reciprocity Law [256].

A *Quadratic Gauss Sum* is the discrete Fourier transform of the Legendre symbol:

$$\chi_p(a) \equiv \sum_{b=0}^{p-1} e^{2\pi i a b/p}\left(\frac{b}{p}\right) = \sum_{n=0}^{p-1} e^{2\pi i a n^2/p}\,, \qquad a\not\equiv 0 \pmod{p}\,, \tag{5.16}$$

where the last equality follows from the identity $\sum_{b=0}^{p-1} e^{2\pi i a b/p} = 0$ for $a\not\equiv 0 \pmod{p}$. It is not hard to prove that $\chi_p(a) = \left(\frac{a}{p}\right)\chi_p(1)$, so the quadratic Gauss sum is proportional to the quadratic residue. It can also be shown that $\chi_p(1) = \sqrt{p}$ if $p \equiv 1 \pmod 4$ and $\chi_p(1) = i\sqrt{p}$ if $p \equiv 3 \pmod 4$ (see [257]). Quadratic Reciprocity is then a statement about the relation between quadratic Gauss sums. For example, if both p and q are 1 (mod 4) then $\chi_p(q)/\sqrt{p} = \chi_q(p)/\sqrt{q}$.

A convenient way to prove the Quadratic Reciprocity (5.15) is via the Landsberg-Schaar identity [258, 259]

$$\frac{e^{\pi i/4}}{\sqrt{2p}} \sum_{n=0}^{2p-1} e^{-\pi i n^2 q/2p} = \frac{1}{\sqrt{q}} \sum_{n=0}^{q-1} e^{2\pi i n^2 p/q}\,, \qquad 1 \le p, q \in \mathbb{Z}. \tag{5.17}$$

The identity can easily be proved using the modular transformation properties of the Jacobi theta function $\vartheta(0;\tau) \equiv \sum_{n=-\infty}^{\infty} \exp\left(\pi i \tau n^2\right)$ evaluated at zero[1] and its asymptotic behavior as the argument τ vertically approaches the real axis [260, 261].[2] In this chapter, we will describe a physical system with a finite number of quantum ground states that reproduces (5.17) directly.

If p and q are both even, say $p = 2p'$ and $q = 2q'$ then it is easy to see that (5.17) reduces to

$$\frac{e^{\pi i/4}}{2\sqrt{p'}} \sum_{n=0}^{2p'-1} e^{-\pi i n^2 q'/2p'} = \frac{1}{\sqrt{2q'}} \sum_{n=0}^{q-1} e^{2\pi i n^2 p'/q'}\,.$$

[1] In Riemann and Mumford's notations, $\vartheta(z;\tau) \equiv \vartheta_{00}(z;\tau)$ is denoted as $\theta_3(z;q)$, where $q \equiv e^{2\pi i \tau}$.

[2] The Landsberg-Schaar identity was also recently proved using a non-analytical method [262]. For the history of development of various proofs other than Gauss's after 1801, see [263].

(This is seen by first summing the terms with n and $n+2p'$ on the LHS and n and $n+q'$ on the RHS.)

Before proceeding to the physical system, we note that for odd primes p and q, the Landsberg-Schaar identity is a slightly modified version of Quadratic Reciprocity. To see this, define

$$\varrho_p(a) \equiv \sum_{n=0}^{2p-1} e^{\pi i a n^2/2p}\,, \tag{5.18}$$

which is periodic in a with period $4p$, and satisfies $\varrho_p(a+2p) = (-i)^{ap}\varrho_p(a)$ (as can easily be seen by relabeling $n \to n+p$). In fact, it is elementary to check (by splitting the sum over n into sums over odd and even numbers) that

$$\varrho_p(a) = (1+i^{pa})\,\chi_p(a)\,. \tag{5.19}$$

It then follows from Quadratic Reciprocity and the results quoted above for quadratic Gauss sums that if $p \neq q$ are odd primes,

$$\frac{1}{\sqrt{2p}}\varrho_p(q) = \frac{1}{\sqrt{q}} e^{\frac{1}{4}(2q-1)i\pi}\chi_q(p)\,. \tag{5.20}$$

Taking the complex conjugate and noting the known result $\left(\frac{-1}{q}\right) = (-1)^{(q-1)/2}$, the Landsberg-Schaar identity (5.17) follows in the form

$$\frac{1}{\sqrt{2p}}\varrho_p(-q) = \frac{1}{\sqrt{q}} e^{-\frac{1}{4}i\pi}\chi_q(p)\,. \tag{5.21}$$

We will now construct a (p,q)-dependent quantum field theory whose partition function can be calculated in two different ways; one gives an expression proportional to $\chi_q(p)$ while the other gives an expression proportional to $\varrho_p(-q)$.

In the next sections we will show how (5.21) and generalizations of it arise from studying the partition function on T^2 of supersymmetric 2d σ-models whose target space is (also) a T^2 with complex structure τ and Kähler modulus ρ that vary along the T^2 worldsheet. We will include boundary conditions with duality twists along two independent cycles of the worldsheet, acting as

$$\tau \to \frac{\mathbf{a}\tau + \mathbf{b}}{\mathbf{c}\tau + \mathbf{d}}\,, \qquad \text{and} \qquad \rho \to \frac{\tilde{\mathbf{a}}\rho + \tilde{\mathbf{b}}}{\tilde{\mathbf{c}}\rho + \tilde{\mathbf{d}}}\,,$$

So that the partition function $\mathcal{Z}(M, \widetilde{M})$ will depend on two $SL(2,\mathbb{Z})$ elements

$$M \equiv \begin{pmatrix} \mathbf{a} & \mathbf{b} \\ \mathbf{c} & \mathbf{d} \end{pmatrix} \in SL(2,\mathbb{Z})_\tau\,, \qquad \widetilde{M} \equiv \begin{pmatrix} \tilde{\mathbf{a}} & \tilde{\mathbf{b}} \\ \tilde{\mathbf{c}} & \tilde{\mathbf{d}} \end{pmatrix} \in SL(2,\mathbb{Z})_\rho\,.$$

The basic Landsberg-Schaar relation (5.21) will be recovered in the special case where

$$M = \begin{pmatrix} 0 & -1 \\ 1 & q+2 \end{pmatrix}, \qquad \widetilde{M} = \begin{pmatrix} 0 & -1 \\ 1 & 2p+2 \end{pmatrix}. \tag{5.22}$$

We now present the details.

5.4 Double-Janus σ-models

In this section we construct a 2d σ-model whose target space is a T^2 with complex structure τ and Kähler modulus ρ that vary along the worldsheet so as to preserve some amount of supersymmetry. We use the terms "worldsheet" and "target-space", borrowed from string-theory, but we emphasize that we are dealing only with a 2d CFT. In particular, we will be working with a fixed metric

$$ds^2 = (d\sigma_1)^2 + (d\sigma_2)^2 = dz d\overline{z}\,,$$

where we denote the (Euclidean) worldsheet coordinates by (σ_1, σ_2), and we set

$$z \equiv \sigma_1 + i\sigma_2\,, \quad \overline{z} \equiv \sigma_1 - i\sigma_2\,, \quad \partial \equiv \frac{\partial}{\partial z} = \frac{1}{2}(\partial_1 - i\partial_2)\,, \quad \overline{\partial} \equiv \frac{\partial}{\partial \overline{z}} = \frac{1}{2}\left(\partial_1 + i\partial_2\right)\,.$$

Dimensional reduction of the Gaiotto-Witten action [233], in the special case of a $U(1)$ gauge group, is one way to obtain such a double-Janus Lagrangian, with both τ and ρ varying along the worldsheet. Now we present the details of this construction.

Following the compactification of 6d $(2,0)$ theory to 4d in the background (5.13), we further compactify the y direction by identifying $y \sim y+1$. This would be possible if we could find an $SL(2,\mathbb{Z})$ MCG transformation acting on x_4', x_5' that relates $\tau(y)$ to $\tau(y+1)$. The $SL(2,\mathbb{Z})$ element will then be identified with M, the S-duality twist in (5.1), and one of the eigenvalues of M has to be $R_4(1)/R_4(0)$ [and the other eigenvalue will be $R_4(0)/R_4(1)$]. Note, however, that the area of the T^2 in directions x_4', x_5', which is $(2\pi)^2 R_4(y) R_5$, is not generally a periodic function of y, and so we can only compactify y after the limit $R_4, R_5 \to 0$ has been taken to reach the 4d SYM low-energy limit.

From the 4d SYM theory we can proceed to 2d by compactifying directions x_1, x_2 on another T^2 and taking the low-energy limit. If the gauge group is $U(1)$ then we obtain a σ-model with T^2 target space from the gauge fields, whose complex structure is $\tau(y)$. We can now proceed in a parallel fashion to (5.13) and replace the so far untouched 3d part of the metric with

$$dt^2 + dx_1^2 + dx_2^2 \to dt^2 + R_1(t)^2\left(\delta' dx_1' - \beta' dx_2'\right)^2 + R_2^2\left(\alpha' dx_2' - \gamma' dx_1'\right)^2\,, \tag{5.23}$$

where

$$\begin{pmatrix} \alpha' & \beta' \\ \gamma' & \delta' \end{pmatrix} \in SL(2,\mathbb{R}).$$

In the low-energy limit, the $U(1)$ gauge field will reduce to a 2d σ-model with T^2 target space whose complex structure varies with y and whose Kähler structure varies with t. We can then compactify t by imposing the periodicity $t \sim t+1$ together with an associated linear transformation on (x_1', x_2') given by $\widetilde{M} \in SL(2,\mathbb{Z})$. This is possible in the limit $R_1, R_2 \to 0$ provided that $R_1(0)/R_1(1)$ is one of the eigenvalues of $\widetilde{M}$ [the other eigenvalue being $R_1(1)/R_1(0)$].

In this way we can preserve 4 supersymmetries, but we also get additional massive non-compact scalar fields. For our purposes of deriving the quadratic reciprocity, it will be sufficient to work with a minimally supersymmetric model which we describe in the following subsection.

Minimally supersymmetric double-Janus model

Our starting point is a supersymmetric σ-model with target-space T^N (later we will set $N = 2$). We let $I, J = 1, \ldots, N$ label target-space coordinates. The scalar fields will be denoted by $\mathbf{X}^I$, the left-moving fermionic fields will be denoted by Ψ^I, and the right-moving fermionic fields will be denoted by $\overline{\Psi}^I$. We combine them into $(2N)$-component column vectors, denoted by X, Ψ and $\overline{\Psi}$, with transposed row-vectors denoted by X^t, Ψ^t, and $\overline{\Psi}^t$. We assume that $\mathbf{X}^I \sim \mathbf{X}^I + 2\pi$ is a periodic field. All fields are functions of (σ_1, σ_2).

The components of the target-space metric and Kalb-Ramond field will be denoted by G_{IJ} and B_{IJ}, respectively, and combined into the $(2N) \times (2N)$ matrices G and B, with $G^t = G$ and $B^t = -B$. We denote

$$E \equiv G + B.$$

This matrix will appear in the kinetic term of the scalar fields X, and we allow E to vary with (σ_1, σ_2), in a predetermined way, as in a Janus configuration. E is thus a (σ_1, σ_2)-dependent background. To preserve supersymmetry, the action requires additional "mass terms" and "background gauge field terms" and takes the general form:

$$I = \frac{1}{\pi} \int \left(\partial X^t E \bar{\partial} X + i \Psi^t \Sigma \bar{\partial} \Psi + i \overline{\Psi}^t \overline{\Sigma} \partial \overline{\Psi} + i \Psi^t \mathcal{K} \Psi + i \overline{\Psi}^t \overline{\mathcal{K}} \overline{\Psi} + \overline{\Psi}^t \mathcal{W} \Psi \right) d^2\sigma \,. \tag{5.24}$$

Σ, $\overline{\Sigma}$, $\mathcal{K}$, $\overline{\mathcal{K}}$, and $\mathcal{W}$ are background $(2N) \times (2N)$ matrices with, possibly, (σ_1, σ_2)-dependent elements. $\Sigma = \Sigma^t$ and $\overline{\Sigma} = \overline{\Sigma}^t$ are symmetric matrices that define the fermionic kinetic terms, $\mathcal{K} = -\mathcal{K}^t$ and $\overline{\mathcal{K}} = -\overline{\mathcal{K}}^t$ are antisymmetric and enter in effective "background $SO(2N)$ gauge field terms", and $\mathcal{W}$ is an effective "mass term".

The supersymmetry transformations take the form

$$\widetilde{\delta} X = \eta \left(\Psi - \overline{\Psi} \right) , \qquad \widetilde{\delta} \Psi = i \eta \Sigma^{-1} G \partial X \,, \qquad \widetilde{\delta} \overline{\Psi} = -i \eta \overline{\Sigma}^{-1} G \bar{\partial} X \,, \tag{5.25}$$

where η is an anticommuting parameter. η is real, and complex conjugation acts as

$$\eta^\star = \eta, \qquad \Psi^\star = \overline{\Psi}, \qquad \overline{\Psi}^\star = \Psi, \qquad (\eta\Psi)^\star = \Psi^\star \eta^\star = -\eta \overline{\Psi}, \qquad \left(\Psi^I \Psi^J \right)^\star = \overline{\Psi}^J \overline{\Psi}^I . \tag{5.26}$$

Note that invariance of the action under the $(\cdots)^\star$ operation requires $B = 0$, $\Sigma^\star = \overline{\Sigma}$, $\mathcal{K}^\star = \overline{\mathcal{K}}$ and $\mathcal{W}^\star = \mathcal{W}^t$ (but we will not require this except in special cases below). Invariance of the action under the SUSY transformations (5.25) requires the following relations among G, E,

Σ and $\overline{\Sigma}$:

$$\begin{aligned} 0 &= 2\overline{\partial}\Sigma - \overline{\partial}EG^{-1}\Sigma - \Sigma G^{-1}\overline{\partial}E^t, && (5.27)\\ 0 &= 2\partial\overline{\Sigma} - \partial E^t G^{-1}\overline{\Sigma} - \overline{\Sigma}G^{-1}\partial E, && (5.28)\\ 0 &= \Sigma G^{-1}\overline{\partial}E + \partial E G^{-1}\overline{\Sigma}. && (5.29) \end{aligned}$$

Then, $\mathcal{K}$, $\overline{\mathcal{K}}$, and $\mathcal{W}$ are determined in terms of E, Σ, and $\overline{\Sigma}$ by

$$\begin{aligned} \mathcal{K} &= \frac{1}{2}\left(\overline{\partial}\Sigma - \overline{\partial}EG^{-1}\Sigma\right) = \frac{1}{4}\Sigma G^{-1}\overline{\partial}E^t - \frac{1}{4}\overline{\partial}EG^{-1}\Sigma, && (5.30)\\ \overline{\mathcal{K}} &= \frac{1}{2}\left(\partial\overline{\Sigma} - \partial E^t G^{-1}\overline{\Sigma}\right) = \frac{1}{4}\overline{\Sigma}G^{-1}\partial E - \frac{1}{4}\partial E^t G^{-1}\overline{\Sigma}, && (5.31)\\ \mathcal{W} &= i\overline{\Sigma}G^{-1}\partial E^t = -i\overline{\partial}E^t G^{-1}\Sigma. && (5.32) \end{aligned}$$

For future reference, we list the linear equations of motion that follow from (5.24). The bosonic equations are

$$0 = \overline{\partial}\left(E^t\partial X\right) + \partial\left(E\overline{\partial}X\right) = 2G\overline{\partial}\partial X + \left(\overline{\partial}E^t\right)\partial X + (\partial E)\,\overline{\partial}X, \tag{5.33}$$

and the fermionic equations of motion are

$$\overline{\partial}\Psi = -\frac{1}{2}G^{-1}\overline{\partial}E\overline{\Psi} - \Sigma^{-1}\left(\mathcal{K} + \frac{1}{2}\overline{\partial}\Sigma\right)\Psi\,, \qquad \partial\overline{\Psi} = -\frac{1}{2}G^{-1}\partial E^t\Psi - \overline{\Sigma}^{-1}\left(\overline{\mathcal{K}} + \frac{1}{2}\partial\overline{\Sigma}\right)\overline{\Psi}\,, \tag{5.34}$$

which can be simplified, using (5.30)-(5.32), to

$$0 = 2G\overline{\partial}\Psi + \left(\overline{\partial}E\right)\overline{\Psi} + \left(\overline{\partial}E^t\right)\Psi\,, \qquad 0 = 2G\partial\overline{\Psi} + \left(\partial E^t\right)\Psi + (\partial E)\,\overline{\Psi}\,. \tag{5.35}$$

The supersymmetry constraint equations (5.27)-(5.29) simplify somewhat when G is expressed in terms of a "vielbein" V as

$$G = V^t V. \tag{5.36}$$

Here V is a $(2N)\times(2N)$ matrix, which is not uniquely defined in terms of G, but different choices differ by $V \to \Omega V$, where Ω is $O(2N)$-valued. We also define

$$S \equiv \left(V^t\right)^{-1}\Sigma V^{-1} \qquad \overline{S} \equiv \left(V^t\right)^{-1}\overline{\Sigma}V^{-1}, \tag{5.37}$$

and

$$\begin{aligned} \mathcal{A}_z &\equiv \frac{1}{2}\left[\left(V^t\right)^{-1}\partial V^t - \partial V V^{-1}\right] + \frac{1}{2}\left(V^t\right)^{-1}\partial B V^{-1}, && (5.38)\\ \overline{\mathcal{A}}_{\bar{z}} &\equiv \frac{1}{2}\left[\left(V^t\right)^{-1}\overline{\partial}V^t - \overline{\partial}V V^{-1}\right] - \frac{1}{2}\left(V^t\right)^{-1}\overline{\partial}B V^{-1}. && (5.39) \end{aligned}$$

Then, $S = S^t$ and $\overline{S} = \overline{S}^t$ are symmetric matrices transforming under $V \to \Omega V$ as $S \to \Omega S \Omega^t$ and $\overline{S} \to \Omega \overline{S} \Omega^t$, while $\mathcal{A}_z$ and $\overline{\mathcal{A}}_{\overline{z}}$ are antisymmetric and transform like a gauge field:

$$\mathcal{A}_z \to \Omega \mathcal{A}_z \Omega^t + \Omega \partial \Omega^t, \qquad \overline{\mathcal{A}}_{\overline{z}} \to \Omega \overline{\mathcal{A}}_{\overline{z}} \Omega^t + \Omega \overline{\partial} \Omega^t.$$

The constraints (5.27)-(5.28) can then be written as

$$0 = \overline{\partial} S + \left[\overline{\mathcal{A}}_{\overline{z}}, S\right], \qquad 0 = \partial \overline{S} + \left[\mathcal{A}_z, \overline{S}\right]. \tag{5.40}$$

Next, we define the symmetric matrices

$$\mathcal{Y} \equiv \left(V^t\right)^{-1} \left(\partial E^t\right) V^{-1} = \left(V^t\right)^{-1} \left(\partial V^t\right) + \left(\partial V\right) V^{-1} - \left(V^t\right)^{-1} \left(\partial B\right) V^{-1}, \tag{5.41}$$

$$\overline{\mathcal{Y}} \equiv \left(V^t\right)^{-1} \left(\overline{\partial} E^t\right) V^{-1} = \left(V^t\right)^{-1} \left(\overline{\partial} V^t\right) + \left(\overline{\partial} V\right) V^{-1} - \left(V^t\right)^{-1} \left(\overline{\partial} B\right) V^{-1}. \tag{5.42}$$

Then, (5.29) can be written as

$$0 = \overline{S} \mathcal{Y} + \overline{\mathcal{Y}} S. \tag{5.43}$$

Thus, given V and B, we can find S and $\overline{S}$ by solving (5.40), and then (5.43) yields a constraint on V and B. We do not know the general solution $\left(G, B, S, \overline{S}\right)$ to (5.27)-(5.29), but below we will discuss a special class of solutions that will suffice for our needs. We restrict to $N = 1$ and begin with a simple class of solutions where G is diagonal and $B = 0$. We then apply solution generating transformations (i.e., T-duality) to obtain a wider class of solutions.

σ_1-independent solutions

A simple way to satisfy (5.40) is to set

$$S = \overline{S} = \mathbb{I},$$

where $\mathbb{I}$ is the identity matrix. Then, (5.43) becomes $\mathcal{Y} = \overline{\mathcal{Y}}$, which by (5.41)-(5.42) requires $0 = \partial E + \overline{\partial} E = \partial_1 E$. Thus, E, and hence G and B are functions of σ_2 only. How they vary with σ_2 is arbitrary, and any pair of $G(\sigma_2)$ and $B(\sigma_2)$ determines a supersymmetric action (5.24). The remaining couplings in (5.24) can then easily be calculated from (5.37) and (5.30)-(5.32):

$$\Sigma = \overline{\Sigma} = G, \qquad \mathcal{K} = \overline{\mathcal{K}} = -\frac{i}{4} \partial_2 B, \qquad \mathcal{W} = \frac{1}{2} \partial_2 E^t.$$

By setting $S = -\overline{S} = i\mathbb{I}$ we similarly get a solution with couplings that are functions of σ_1 only. In this chapter, however, we are more interested in solutions where G and B vary nontrivially with both σ_1 and σ_2.

Holomorphic solutions

For the T^2 target space, another class of solutions can be obtained by requiring ρ to be constant and allowing τ to vary holomorphically with z. The setup is then an elliptic fibration, reminiscent of F-theory [264]. We can take[3]

$$V = \rho_2^{\frac{1}{2}} \tau_2^{-\frac{1}{2}} \begin{pmatrix} 1 & -\tau_1 \\ 0 & \tau_2 \end{pmatrix},$$

and using (5.38)-(5.39), we calculate

$$\mathcal{A}_z = -\frac{\partial \tau_1}{2\tau_2}\epsilon\,, \qquad \overline{\mathcal{A}}_{\overline{z}} = -\frac{\overline{\partial}\tau_1}{2\tau_2}\epsilon\,,$$

where

$$\epsilon \equiv \begin{pmatrix} 0 & -1 \\ 1 & 0 \end{pmatrix}. \tag{5.44}$$

Since $\overline{\partial}\tau = 0$, we can substitute $\partial\tau_1 = i\partial\tau_2$ and $\overline{\partial}\tau_1 = -i\overline{\partial}\tau_2$ and write

$$\mathcal{A}_z = -i\frac{\partial \tau_2}{2\tau_2}\epsilon\,, \qquad \overline{\mathcal{A}}_{\overline{z}} = i\frac{\overline{\partial}\tau_2}{2\tau_2}\epsilon.$$

Then, (5.40) has the general solution

$$S = e^{-\frac{i}{2}(\log\tau_2)\epsilon} F(z) e^{\frac{i}{2}(\log\tau_2)\epsilon}, \qquad \overline{S} = e^{\frac{i}{2}(\log\tau_2)\epsilon} \overline{F}(\overline{z}) e^{-\frac{i}{2}(\log\tau_2)\epsilon}, \tag{5.45}$$

where $F(z)$ and $\overline{F}(\overline{z})$ are arbitrary holomoprhic and antiholomorphic (symmetric) matrix-valued functions on the worldsheet. We also calculate from (5.41)-(5.42),

$$\mathcal{Y} = \frac{1}{\tau_2}\begin{pmatrix} -\partial\tau_2 & -\partial\tau_1 \\ -\partial\tau_1 & \partial\tau_2 \end{pmatrix} = \frac{\partial\tau_2}{\tau_2}\begin{pmatrix} -1 & -i \\ -i & 1 \end{pmatrix}, \qquad \overline{\mathcal{Y}} = \frac{1}{\tau_2}\begin{pmatrix} -\overline{\partial}\tau_2 & -\overline{\partial}\tau_1 \\ -\overline{\partial}\tau_1 & \overline{\partial}\tau_2 \end{pmatrix} = \frac{\overline{\partial}\tau_2}{\tau_2}\begin{pmatrix} -1 & i \\ i & 1 \end{pmatrix}.$$

We set $\varkappa \equiv \begin{pmatrix} -1 & -i \\ -i & 1 \end{pmatrix}$, $\overline{\varkappa} \equiv \begin{pmatrix} -1 & i \\ i & 1 \end{pmatrix}$, and noting that $\varkappa\epsilon = -\epsilon\varkappa = i\varkappa$ and $\epsilon\overline{\varkappa} = -\overline{\varkappa}\epsilon = i\overline{\varkappa}$ imply $e^{-\frac{i}{2}(\log\tau_2)\epsilon}\varkappa e^{-\frac{i}{2}(\log\tau_2)\epsilon} = \varkappa$ and $e^{-\frac{i}{2}(\log\tau_2)\epsilon}\overline{\varkappa} e^{-\frac{i}{2}(\log\tau_2)\epsilon} = \overline{\varkappa}$, we find that (5.43) yields

$$0 = (\partial\tau_2)\,\overline{F}\varkappa + \left(\overline{\partial}\tau_2\right)\overline{\varkappa}F. \tag{5.46}$$

Since, for a holomorphic τ we have $\partial\tau_2 = -\frac{i}{2}\partial\tau$, which is also holomorphic, while $\overline{\partial}\tau_2 = \frac{i}{2}\overline{\partial}\overline{\tau}$ is antiholomoprhic, we see that (5.46) is possible only if

$$F = (\partial\tau_2)\,\varpi, \qquad \overline{F} = \left(\overline{\partial}\tau_2\right)\overline{\varpi}, \tag{5.47}$$

[3]The minus sign in front of τ_1 is in order for equations (5.62)-(5.63) to be simpler.

for some constant symmetric matrices ϖ, $\overline{\varpi}$ that satisfy

$$0 = \overline{\varpi}\varkappa + \overline{\varkappa}\varpi. \tag{5.48}$$

Since $\varkappa$ and $\overline{\varkappa}$ are nilpotent ($\varkappa^2 = \overline{\varkappa}^2 = 0$), (5.48) requires $\overline{\varkappa}\overline{\varpi}\varkappa = \overline{\varkappa}\varpi\varkappa = 0$ which is equivalent to

$$\operatorname{Tr}\varpi = \operatorname{Tr}\overline{\varpi} = 0. \tag{5.49}$$

If we also require $\overline{\varpi}$ to be the complex conjugate of ϖ then (5.48) is satisfied provided

$$\operatorname{Re}\varpi_{12} = -\operatorname{Im}\varpi_{11}. \tag{5.50}$$

Once we choose a 2×2 matrix ϖ (and its complex conjugate $\overline{\varpi}$) that satisfies (5.49) and (5.50), we calculate F and $\overline{F}$ from (5.47), and then we calculate S and $\overline{S}$ from (5.45). We then find Σ and $\overline{\Sigma}$ from (5.37).

These holomorphic solutions might be interesting to explore, but we will not discuss them further in the present chapter, since our focus is the closed double-Janus solutions to be described in Section 5.4. We will construct these solutions by first finding solutions where E is diagonal.

Diagonal solutions

We get another simple class of solutions to (5.27)-(5.29) [or, equivalently, to (5.40) and (5.43)] by setting $B = 0$ and requiring G to be diagonal. We can then choose a diagonal $V = G^{1/2}$ in (5.36) and we calculate from (5.38)-(5.39) that $\mathcal{A}_z = \overline{\mathcal{A}}_{\overline{z}} = 0$, and from (5.41)-(5.42) we calculate $\mathcal{Y} = \partial \log G$ and $\overline{\mathcal{Y}} = \overline{\partial}\log G$. Then, (5.40) and (5.43) require

$$0 = \partial\overline{S} = \overline{\partial}S = \left(\overline{\partial}\log G\right) S + \overline{S}\left(\partial \log G\right) .$$

We will make the further assumption that S and $\overline{S}$ are constant matrices, as is the case if the worldsheet is γ and we require S and $\overline{S}$ to be bounded, or if the worldsheet is T^2 with periodic boundary conditions. We also assume that $\overline{S}$ is the complex conjugate of S, and for simplicity we proceed to analyze the case $N = 2$, i.e., a T^2 target space.

If S is also diagonal, we proceed as follows. We first assume without loss of generality that $S_{11} > 0$ (since we can always rotate z by a phase to make it so). Then $0 = \left(\overline{\partial}\log G_{11}\right) S_{11} + \overline{S}_{11}\left(\partial \log G_{11}\right)$ says that G_{11} is a function of σ_2 only. If S_{22} is also real then a similar conclusion about G_{22} shows that we have a special case of Section 5.4. If S_{22} is not real, then G_{22} is a function of a different linear combination of σ_1 and σ_2. In any case, this seems to be a rather restricted system, and we will not pursue this further in this chapter.

If S is not diagonal, we can assume that $\overline{S}_{12} = S_{12} > 0$ (again achieved by rotating z if necessary). The off-diagonal components of

$$0 = \left(\overline{\partial}\log G\right) S + \overline{S}\left(\partial \log G\right) \tag{5.51}$$

yield

$$\overline{\partial}\log G_{11} = -\partial\log G_{22} \qquad \text{and} \qquad \overline{\partial}\log G_{22} = -\partial\log G_{11}, \tag{5.52}$$

from which it follows that $\partial^2\log G_{11} = \overline{\partial}^2\log G_{11}$ and similarly for G_{22}. Since $\partial^2 - \overline{\partial}^2 = i\partial_1\partial_2$, and combined with (5.52), we find that G takes the form

$$G = \begin{pmatrix} \frac{\rho_2}{\tau_2} & 0 \\ 0 & \rho_2\tau_2 \end{pmatrix}, \qquad \tau_2 = \tau_2(\sigma_1), \qquad \rho_2 = \rho_2(\sigma_2),$$

where we have written the metric in terms of the Kähler modulus $\rho = \rho_1 + i\rho_2$ (with $\rho_1 = 0$ since $B = 0$) and the complex structure $\tau = \tau_1 + i\tau_2$ (with $\tau_1 = 0$ since G is diagonal), and the analysis above shows that (for $S_{12} > 0$) $\tau_2 = \tau_2(\sigma_1)$ is a function of σ_1 only, and $\rho_2 = \rho_2(\sigma_2)$ is a function of σ_2 only. For the future, we denote

$$\tau_2' \equiv \frac{d\tau_2}{d\sigma_1}, \qquad \dot{\rho}_2 \equiv \frac{d\rho_2}{d\sigma_2}.$$

Then, since we assume that S and $\overline{S}$ are constant, the diagonal components of (5.51) imply that either $S_{11} = S_{22} = 0$, or both τ_2'/τ_2 and $\dot{\rho}_2/\rho_2$ are constant. We will first consider the more general case that τ_2 and ρ_2 are arbitrary functions of σ_1 and σ_2 and we therefore assume that $S_{11} = S_{22} = 0$. Although later on we will discuss the case that $\log\tau_2$ and $\log\rho_2$ are linear functions of σ_1 and σ_2, respectively, we will still keep the assumption $S_{11} = S_{22} = 0$, since it leads to the simpliest model. We can take $S_{12} = 1$ without loss of generality (by rescaling z if necessary). The action (5.24) then takes the form

$$\begin{aligned} I \;=\; & \frac{1}{\pi}\int\left[\frac{\rho_2}{\tau_2}\partial\mathbf{X}^1\overline{\partial}\mathbf{X}^1 + \rho_2\tau_2\partial\mathbf{X}^2\overline{\partial}\mathbf{X}^2 + i\rho_2\Psi^1\overline{\partial}\Psi^2 + i\rho_2\Psi^2\overline{\partial}\Psi^1 + i\rho_2\overline{\Psi}^1\partial\overline{\Psi}^2 + i\rho_2\overline{\Psi}^2\partial\overline{\Psi}^1\right. \\ & \left. + \frac{i\rho_2\tau_2'}{2\tau_2}\Psi^1\Psi^2 + \frac{i\rho_2\tau_2'}{2\tau_2}\overline{\Psi}^1\overline{\Psi}^2 + \left(\frac{\dot{\rho}_2}{2} + \frac{i\rho_2\tau_2'}{2\tau_2}\right)\overline{\Psi}^1\Psi^2 + \left(\frac{\dot{\rho}_2}{2} - \frac{i\rho_2\tau_2'}{2\tau_2}\right)\overline{\Psi}^2\Psi^1\right] d^2\sigma. \end{aligned} \tag{5.53}$$

Note that this action is real, in the sense defined below (5.26). The fermionic part of the action (5.53) can be simplified with a change of variables, but we will defer that to Section 5.6.

$SL(2,\mathbb{R})$-generated double-Janus solutions

The action (5.53) describes a special solution to (5.27)-(5.29) [substituted into (5.24)] where the complex structure $\tau = \tau_1 + i\tau_2$ and Kähler parameter $\rho_1 + i\rho_2$ of the T^2 target space are each allowed to vary along the imaginary axes of their respective upper half-planes. We will now apply fractional linear transformations, acting as

$$\tau \to \frac{\alpha\tau + \beta}{\gamma\tau + \delta}, \qquad \rho \to \frac{\tilde{\alpha}\rho + \tilde{\beta}}{\tilde{\gamma}\rho + \tilde{\delta}}, \qquad \text{for some} \quad \begin{pmatrix} \alpha & \beta \\ \gamma & \delta \end{pmatrix}, \begin{pmatrix} \tilde{\alpha} & \tilde{\beta} \\ \tilde{\gamma} & \tilde{\delta} \end{pmatrix} \in SL(2,\mathbb{R}),$$

to generate new solutions. In general, we expect an $O(n,n,\mathbb{R})$ group of transformations acting on the parameters $\left(E,\Sigma,\overline{\Sigma}\right)$, and converting a solution of (5.27)-(5.29) to a new solution $\left(E',\Sigma',\overline{\Sigma}'\right)$. This is an extension of the well-known $O(n,n,\mathbb{R})$ action on σ-models with T^n target space, parametrized by a Narain lattice in the isotropic (i.e., non-Janus) case. (See [265] for a review.) Such transformations are genererated by linear coordinate reparameterizations (which modify the boundary conditions since the new coordinates are still required to obey the same 2π periodicity conditions as the old ones) and T-dualities. The geometrical transformations act as

$$X' = PX, \qquad \Psi' = P\Psi, \qquad \overline{\Psi}' = P\overline{\Psi}\,,$$

and therefore

$$E' = \left(P^{-1}\right)^t E P^{-1}, \qquad \Sigma' = \left(P^{-1}\right)^t \Sigma P^{-1}, \qquad \overline{\Sigma}' = \left(P^{-1}\right)^t \overline{\Sigma} P^{-1}, \tag{5.54}$$

where $P \in GL(n,\mathbb{R})$ is a constant matrix. (Later, we will restrict to the case $n=2$.)

T-duality on all directions acts as

$$E' = E^{-1}, \qquad \Sigma' = E^{-1}\Sigma\left(E^t\right)^{-1}, \qquad \overline{\Sigma}' = \left(E^t\right)^{-1}\overline{\Sigma}E^{-1}. \tag{5.55}$$

The terms in the action (5.53) can then easily be calculated from (5.30)-(5.32). For example, after some algebra, we get

$$\begin{aligned}
\overline{\mathcal{K}}' &= \left(E^t\right)^{-1}\left[\overline{\mathcal{K}} + \frac{1}{2}\partial E^t\left(E^t\right)^{-1}\overline{\Sigma} - \frac{1}{2}\overline{\Sigma}E^{-1}\partial E\right]E^{-1}, \\
\mathcal{K}' &= E^{-1}\left[\mathcal{K} + \frac{1}{2}\left(\overline{\partial}E\right)E^{-1}\Sigma - \frac{1}{2}\Sigma\left(E^t\right)^{-1}\overline{\partial}E^t\right]\left(E^t\right)^{-1}.
\end{aligned}$$

For the case of T^2 target space, we can define two commuting $PSL(2,\mathbb{R})$ actions. We take the target space metric to be

$$G_{IJ}d\mathbf{X}^I d\mathbf{X}^J = \frac{\rho_2}{\tau_2}\left|\tau d\mathbf{X}^2 - d\mathbf{X}^1\right|^2,$$

so that the geometrical $PSL(2,\mathbb{R})_\tau$ acts as

$$E' = \left(P^{-1}\right)^t E P^{-1}, \quad \Sigma' = \left(P^{-1}\right)^t \Sigma P^{-1}, \quad \overline{\Sigma}' = \left(P^{-1}\right)^t \overline{\Sigma} P^{-1}, \qquad \tau \to \tau' = \frac{\alpha\tau+\beta}{\gamma\tau+\delta},$$

where

$$P = \begin{pmatrix} \alpha & \beta \\ \gamma & \delta \end{pmatrix} \in SL(2,\mathbb{R}). \tag{5.56}$$

The other group, $PSL(2,\mathbb{R})_\rho$, acts as

$$\rho \to \frac{\tilde{\alpha}\rho+\tilde{\beta}}{\tilde{\gamma}\rho+\tilde{\delta}},$$

combined with

$$\epsilon E' = \left(\tilde{\gamma}\epsilon E + \tilde{\delta}\mathbb{I}\right)^{-1}\left(\tilde{\alpha}\epsilon E + \tilde{\beta}\mathbb{I}\right), \tag{5.57}$$

$$\Sigma' = \left(\tilde{\gamma}E\epsilon + \tilde{\delta}\mathbb{I}\right)^{-1}\Sigma\left[\left(\tilde{\gamma}E\epsilon + \tilde{\delta}\mathbb{I}\right)^{-1}\right]^{t}, \tag{5.58}$$

$$\overline{\Sigma}' = \left[\left(\tilde{\gamma}\epsilon E + \tilde{\delta}\mathbb{I}\right)^{-1}\right]^{t}\overline{\Sigma}\left(\tilde{\gamma}\epsilon E + \tilde{\delta}\mathbb{I}\right)^{-1}, \tag{5.59}$$

where ϵ is the antisymmetric matrix defined in (5.44), and

$$\begin{pmatrix}\tilde{\alpha} & \tilde{\beta}\\ \tilde{\gamma} & \tilde{\delta}\end{pmatrix} \in SL(2,\mathbb{R}). \tag{5.60}$$

Applying these transformations to the solution (5.53), we get a new solution with $\tau(\sigma_1)$ taking values on a semicircle of radius $1/2|\gamma\delta|$ in the upper half-plane that intersects the real axis at the points α/γ and β/δ, and similarly, $\rho(\sigma_2)$ takes values on a semicircle of radius $1/2|\tilde{\gamma}\tilde{\delta}|$ that intersects the real axis at the points $\tilde{\alpha}/\tilde{\gamma}$ and $\tilde{\beta}/\tilde{\delta}$. This behavior of the modular parameters is similar to that derived by Gaiotto and Witten in [233] for the supersymmetric Janus configurations of $\mathcal{N}=4$ SYM.

The solutions discussed above are more suitable for our needs, since for suitably chosen parameters, the semicircles will be invariant under some $SL(2,\mathbb{Z})$ duality transformations. The worldsheet of such models can then be compactified on a torus, thus making σ_1 and σ_2 periodic, and the periodicities $\sigma_1 \to \sigma_1 + 1$ and $\sigma_2 \to \sigma_2 + 1$ are accompanied by duality twists. In the context of 4d $\mathcal{N}=4$ SYM, such a setup has been used in [247, 248] to compactify the Gaiotto-Witten solution to 3d. A generic $SL(2,\mathbb{Z})$ matrix

$$M = \begin{pmatrix}\mathbf{a} & \mathbf{b}\\ \mathbf{c} & \mathbf{d}\end{pmatrix}$$

with $|\mathbf{a}+\mathbf{d}| > 2$ (a hyperbolic element[4]) preserves the semicircle of radius $\sqrt{(\mathbf{a}+\mathbf{d})^2-4}/2|\mathbf{c}|$ that intersects the real axis at

$$\tau = \frac{1}{2\mathbf{c}}\left(\mathbf{a}-\mathbf{d} \pm \sqrt{(\mathbf{a}+\mathbf{d})^2-4}\right).$$

We will now discuss in detail how to incorporate the duality twists, and the "interaction" between the τ and ρ twists.

[4]Or equivalently, a *pseudo-Anosov homeomorphism* of T^2, the fiber of the non-geometric mapping torus, which turns out to be hyperbolic.

5.5 Duality twists

At the end of Section 5.4 we obtained a model with τ varying as a function of σ_1 while taking values on a semicircle that is preserved by

$$M = \begin{pmatrix} \mathbf{a} & \mathbf{b} \\ \mathbf{c} & \mathbf{d} \end{pmatrix},$$

and with ρ varying as a function of σ_2 while taking values on another semicircle that is preserved by

$$\widetilde{M} = \begin{pmatrix} \tilde{\mathbf{a}} & \tilde{\mathbf{b}} \\ \tilde{\mathbf{c}} & \tilde{\mathbf{d}} \end{pmatrix}.$$

We will now compactify the worldsheet. To begin with, we put the theory on a noncompact rectangular worldsheet with

$$0 \leq \sigma_1, \sigma_2 < 1\,.$$

Geometrical twist

Let us first discuss the boundary conditions relating $\sigma_1 = 0$ to $\sigma_1 = 1$. The complex structure τ of the target space T^2 depends on σ_1, and if $\tau(0) \neq \tau(1)$, we can insert an MCG element that acts nontrivially, but geometrically, on X. We then require $\tau(0)$ to be related to $\tau(1)$ by the element $M \in SL(2,\mathbb{Z})$ so that

$$\tau(1) = \frac{\mathbf{a}\tau(0) + \mathbf{b}}{\mathbf{c}\tau(0) + \mathbf{d}}\,. \tag{5.61}$$

The boundary conditions on the fermionic fields are

$$\Psi(1,\sigma_2) = M\Psi(0,\sigma_2)\,, \qquad \overline{\Psi}(1,\sigma_2) = M\overline{\Psi}(0,\sigma_2)\,. \tag{5.62}$$

For the bosonic fields, we require $X(1,\sigma_2)$ to be related to $MX(0,\sigma_2)$, up to a vector whose components are integer multiples of 2π:

$$X(1,\sigma_2) - MX(0,\sigma_2) \in 2\pi\mathbb{Z}^2\,. \tag{5.63}$$

Denote

$$\mathcal{N} \equiv \frac{1}{2\pi}\left[X(1,\sigma_2) - MX(0,\sigma_2)\right] \in \mathbb{Z}^2\,, \tag{5.64}$$

which can be thought of as a vector of "winding numbers", and being a vector of integers, it is independent of σ_2. We can construct a vector with a simpler boundary condition by removing a constant piece from X,

$$Z \equiv X - 2\pi\left(\mathbb{I} - M\right)^{-1}\mathcal{N}\,, \tag{5.65}$$

which satisfies the periodicity condition

$$Z(1,\sigma_2) = MZ(0,\sigma_2)\,. \tag{5.66}$$

Note that Z is also invariant under the discrete translations that are parametrized by a vector of integers K as:

$$X \to X + 2\pi K\,, \quad \mathcal{N} \to \mathcal{N} + (\mathbb{I} - M)K\,, \qquad (K \in \mathbb{Z}^2)\,. \tag{5.67}$$

In Minkowski (worldsheet) signature, the minimum energy configuration would be $Z = 0$ which corresponds to $X = 2\pi(\mathbb{I}-M)^{-1}\mathcal{N}$. These are the fixed points of the action $X \to MX$ (acting on the T^2 target). Moreover, the equivalence

$$X \sim X + 2\pi K\,, \qquad (K \in \mathbb{Z}^2)\,,$$

which is required to describe a T^2 target space (instead of $\mathbb{R}^2$), acts on $\mathcal{N}$ as

$$\mathcal{N} \sim \mathcal{N} + (\mathbb{I} - M)K\,. \tag{5.68}$$

The lattice $\mathbb{Z}^2$ subject to the identification (5.68) is a finite abelian group with $\det(\mathbb{I} - M) = |\mathbf{a} + \mathbf{d} - 2|$ elements. (This abelian group played an important role in [247], where it was related to a group of symmetry operators in a related context.) We denote this group by

$$\Xi_0 \equiv \left\{\mathcal{N} \text{ subject to } \mathcal{N} \sim \mathcal{N} + (\mathbb{I} - M)K \text{ for all } K \in \mathbb{Z}^2\right\} = (\mathbb{Z}^2)/(\mathbb{I} - M)(\mathbb{Z}^2). \tag{5.69}$$

The path integral over field configurations X (for any worldsheet signature) subject to the periodicity condition (5.63) is equivalent to a path integral over Z, subject to the boundary condition (5.66), and a sum over the finite group Ξ_0.

T-duality twist

Now, we introduce an $SL(2,\mathbb{Z})$ duality twist in the σ_2 direction. This twist acts on the $\rho(\sigma_2)$ parameter by an element $\widetilde{M} \in SL(2,\mathbb{Z})$ so that

$$\rho(1) = \frac{\tilde{\mathbf{a}}\rho(0) + \tilde{\mathbf{b}}}{\tilde{\mathbf{c}}\rho(0) + \tilde{\mathbf{d}}}\,, \qquad \widetilde{M} = \begin{pmatrix} \tilde{\mathbf{a}} & \tilde{\mathbf{b}} \\ \tilde{\mathbf{c}} & \tilde{\mathbf{d}} \end{pmatrix}\,, \tag{5.70}$$

resulting in an asymmetric orbifold [266]. The $\widetilde{M}$-twist induces certain nontrivial boundary conditions for the fields X, Ψ and $\overline{\Psi}$. To describe them, we denote

$$X_1(\sigma_1,\sigma_2) \equiv X(\sigma_1, 1{+}\sigma_2), \quad \Psi_1(\sigma_1,\sigma_2) \equiv \Psi(\sigma_1, 1{+}\sigma_2), \quad \overline{\Psi}_1(\sigma_1,\sigma_2) \equiv \overline{\Psi}(\sigma_1, 1{+}\sigma_2). \tag{5.71}$$

These fields will be used to describe the fields in the vicinity of $\sigma_2 = 1$. In the same vein, we also denote

$$X_0 \equiv X, \quad \Psi_0 \equiv \Psi, \quad \overline{\Psi}_0 \equiv \overline{\Psi}, \tag{5.72}$$

when referring to fields in the vicinity of $\sigma_2 = 0$. (Note that X_0 is identical to X, but the subscript "0" is useful for clarity when we couple X_0 to X_1 and restrict the fields to $\sigma_2 = 0$.) We use a similar subscript notation for the background fields, i.e., $E_0 \equiv E$, $E_1(\sigma_1, \sigma_2) \equiv E(\sigma_1, 1+\sigma_2)$, etc. On the level of equations of motion, the boundary conditions on the bosonic fields are

$$\overline{\partial} X_1 = \left(\tilde{\mathbf{c}}\epsilon E_0 + \tilde{\mathbf{d}}\mathbb{I}\right)\overline{\partial} X_0, \qquad \partial X_1 = \left(\tilde{\mathbf{c}} E_0\epsilon + \tilde{\mathbf{d}}\mathbb{I}\right)^t \partial X_0. \tag{5.73}$$

This is a special case of Bäcklund transformation (for Cauchy-Riemann-like equations), whereby the equations of motion for the fields at $\sigma_2 = 1$ get mapped to the integrability conditions for the fields at $\sigma_2 = 0$:

$$\partial\left(\overline{\partial} X_1\right) - \overline{\partial}\left(\partial X_1\right) = 0 = \tilde{\mathbf{c}}\epsilon\left[\overline{\partial}\left(E_0^t \partial X_0\right) + \partial\left(E_0 \overline{\partial} X_0\right)\right],$$

which vanishes thanks to the equation of motion (5.33).

The fermionic boundary conditions can be derived from the SUSY transformations (5.25), together with the boundary conditions on the background parameters (5.57)-(5.59), and they are

$$\overline{\Psi}_1 = \left(\tilde{\mathbf{c}}\epsilon E_0 + \tilde{\mathbf{d}}\mathbb{I}\right)\overline{\Psi}_0, \qquad \Psi_1 = \left(\tilde{\mathbf{c}} E_0\epsilon + \tilde{\mathbf{d}}\mathbb{I}\right)^t \Psi_0. \tag{5.74}$$

When applied to (5.74), the SUSY variation (5.25) gives the bosonic boundary conditions (5.73), and using the fermionic equations of motion (5.35), one can easily check that the SUSY variation of (5.73) is also satisfied. In deriving (5.74) we also used the relations

$$\epsilon E_1 = \left(\tilde{\mathbf{c}}\epsilon E_0 + \tilde{\mathbf{d}}\mathbb{I}\right)^{-1}\left(\tilde{\mathbf{a}}\epsilon E_0 + \tilde{\mathbf{b}}\mathbb{I}\right), \tag{5.75}$$

$$\Sigma_1 = \left(\tilde{\mathbf{c}} E_0\epsilon + \tilde{\mathbf{d}}\mathbb{I}\right)^{-1}\Sigma_0\left[\left(\tilde{\mathbf{c}} E_0\epsilon + \tilde{\mathbf{d}}\mathbb{I}\right)^{-1}\right]^t, \tag{5.76}$$

$$\overline{\Sigma}_1 = \left[\left(\tilde{\mathbf{c}}\epsilon E_0 + \tilde{\mathbf{d}}\mathbb{I}\right)^{-1}\right]^t\overline{\Sigma}_0\left(\tilde{\mathbf{c}}\epsilon E_0 + \tilde{\mathbf{d}}\mathbb{I}\right)^{-1}, \tag{5.77}$$

which mirror (5.57)-(5.59), but with integers $\tilde{\mathbf{a}}, \ldots, \tilde{\mathbf{d}}$ instead of real numbers $\tilde{\alpha}, \ldots, \tilde{\delta}$, and we also used the identity

$$G_1 = \left[\left(\tilde{\mathbf{c}}\epsilon E_0 + \tilde{\mathbf{d}}\mathbb{I}\right)^t\right]^{-1} G_0\left(\tilde{\mathbf{c}}\epsilon E_0 + \tilde{\mathbf{d}}\mathbb{I}\right)^{-1} = \left(\tilde{\mathbf{c}} E_0\epsilon + \tilde{\mathbf{d}}\mathbb{I}\right)^{-1} G_0\left[\left(\tilde{\mathbf{c}} E_0\epsilon + \tilde{\mathbf{d}}\mathbb{I}\right)^t\right]^{-1},$$

which easily follows from $2G = E + E^t$.

Quantum mechanically, the boundary conditions (5.73) are introduced by inserting a "duality wall" (see for instance [267] and the supersymmetric case discussed in [268]). The T-duality wall can be thought of as the dimensional reduction of the $T(U(1))$ theory,[5] and

[5] $T(U(1))$, or more generally $T(G)$, is the 3d action introduced in [269] to capture the action of S-duality in the $\mathcal{N} = 4$ Super-Yang-Mills theory, and see also [270, 271, 272, 273, 274, 249] for related ideas.

in general, to incorporate the $\widetilde{M}$ twist into the action we have to decompose $\widetilde{M}$ in terms of the generators

$$\widetilde{T} = \begin{pmatrix} 1 & 1 \\ 0 & 1 \end{pmatrix}, \qquad \widetilde{S} = \begin{pmatrix} 0 & -1 \\ 1 & 0 \end{pmatrix},$$

as

$$\widetilde{M} = \widetilde{S}\widetilde{T}^{\mathbf{k}_1} \cdots \widetilde{S}\widetilde{T}^{\mathbf{k}_r}, \tag{5.78}$$

where $\mathbf{k}_1, \ldots, \mathbf{k}_r$ are integers. The decomposition (5.79) is not unique, but for our purposes it will be sufficient to consider the case $r = 1$, so we will just set

$$\widetilde{M} = \widetilde{S}\widetilde{T}^{\mathbf{k}}. \tag{5.79}$$

(We will comment on the general case in Section 5.9.) The $\widetilde{M}$-twist can then be inserted by adding a 1-dimensional term I' and a 0-dimensional term I'' to the action as follows. I' is defined as the integral over σ_1 at $\sigma_2 = 0$, and is a sum

$$I' = I'_b + I'_f$$

of bosonic and fermionic terms. The bosonic term is given by

$$I'_b = -\frac{i\mathbf{k}}{4\pi} \int_0^1 X_0^t \epsilon dX_0 \Big|_{\sigma_2=0} + \frac{i}{2\pi} \int_0^1 X_1^t \epsilon dX_0 \Big|_{\sigma_2=0}. \tag{5.80}$$

The first term in (5.80) implements the $\widetilde{T}^{\mathbf{k}}$ component of (5.79) while the second term couples the fields at $\sigma_2 = 1$ to the fields at $\sigma_2 = 0$ and implements the $\tilde{S}$ component of $\widetilde{M}$. From now own, any field with a subscript "0" or "1" will be implicitly understood to be evaluated at $\sigma_2 = 0$.

The fermionic 1-dimensional action I'_f can be designed so that if we denote by I_f the fermionic part of the bulk action I given in (5.24), then the equations of motion derived from $I_f + I'_f$ at $\sigma_2 = 0$ and $\sigma_2 = 1$ will be equivalent to the boundary conditions (5.74). We take the ansatz[6]

$$I'_f = -\frac{i}{2\pi} \int \left(\overline{\Psi}_1^t R \overline{\Psi}_0 + \Psi_1^t \overline{R} \Psi_0 + \overline{\Psi}_1^t J \overline{\Psi}_1 + \Psi_1^t \overline{J} \Psi_1 + \overline{\Psi}_0^t H \overline{\Psi}_0 + \Psi_0^t \overline{H} \Psi_0 \right) d\sigma_1 , \tag{5.81}$$

where R, $\overline{R}$, J, $\overline{J}$, H and $\overline{H}$ are 2×2 antisymmetric matrices:

$$J^t = -J , \qquad \overline{J}^t = -\overline{J} , \qquad H^t = -H , \qquad \overline{H}^t = -\overline{H} . \tag{5.82}$$

To be compatible with (5.74), the following relations must hold:

$$2\overline{J} = -i\Sigma_1 - \overline{R} \left(-\epsilon E_0^t + \mathbf{k}\mathbb{I} \right)^{-1} , \tag{5.83}$$

$$2J = i\overline{\Sigma}_1 - R \left(\epsilon E_0 + \mathbf{k}\mathbb{I} \right)^{-1} , \tag{5.84}$$

$$2\overline{H} = i\Sigma_0 + \overline{R}^t \left(-\epsilon E_0^t + \mathbf{k}\mathbb{I} \right) , \tag{5.85}$$

$$2H = -i\overline{\Sigma}_0 + R^t \left(\epsilon E_0 + \mathbf{k}\mathbb{I} \right) . \tag{5.86}$$

[6] In I'_f we did not include mixed chirality terms of the form $\overline{\Psi}_1^t L \Psi_0$, $\Psi_1^t \overline{L} \overline{\Psi}_0$, $\overline{\Psi}_1^t Q \Psi_1$, $\overline{\Psi}_0^t O \Psi_0$ (with 2×2 matrices L, $\overline{L}$, Q and O) since they are not necessary.

Requiring H and $\overline{H}$ to be antisymmetric [as in (5.82)], and using (5.76)-(5.77)] we get two equations for R and $\overline{R}$:

$$-2i\Sigma_0 = (E_0\epsilon + \mathbf{k}\mathbb{I})\overline{R} + \overline{R}^t\left(-\epsilon E_0^t + \mathbf{k}\mathbb{I}\right), \tag{5.87}$$

$$2i\overline{\Sigma}_0 = \left(-E_0^t\epsilon + \mathbf{k}\mathbb{I}\right)R + R^t\left(\epsilon E_0 + \mathbf{k}\mathbb{I}\right). \tag{5.88}$$

It can easily be checked that if (5.87)-(5.88) are satisfied, J and $\overline{J}$ as given by (5.83)-(5.86) are also antisymmetric.

In order to solve (5.87)-(5.88) it is convenient to change variables as follows. Since Σ and $\overline{\Sigma}$ are symmetric and G is symmetric and nondegenerate (as we assume), we can find matrices $\mathfrak{Y}$ and $\overline{\mathfrak{Y}}$ so that

$$\Sigma = \mathfrak{Y}^t G\mathfrak{Y}\,, \qquad \overline{\Sigma} = \overline{\mathfrak{Y}}^t G\overline{\mathfrak{Y}}. \tag{5.89}$$

We can also require the boundary conditions

$$\mathfrak{Y}_1 = (E_0\epsilon + \mathbf{k}\mathbb{I})^t\mathfrak{Y}_0\left[(E_0\epsilon + \mathbf{k}\mathbb{I})^{-1}\right]^t, \qquad \overline{\mathfrak{Y}}_1 = (\epsilon E_0 + \mathbf{k}\mathbb{I})\overline{\mathfrak{Y}}_0(\epsilon E_0 + \mathbf{k}\mathbb{I})^{-1}, \tag{5.90}$$

which are compatible with (5.76)-(5.77). Then, it is not hard to check that

$$\overline{R} = i\mathfrak{Y}_1^t\epsilon\mathfrak{Y}_0 = i(E_0\epsilon + \mathbf{k}\mathbb{I})^{-1}\mathfrak{Y}_0^t(E_0\epsilon + \mathbf{k}\mathbb{I})\epsilon\mathfrak{Y}_0\,, \tag{5.91}$$

$$R = i\overline{\mathfrak{Y}}_1^t\epsilon\overline{\mathfrak{Y}}_0 = i\left[(\epsilon E_0 + \mathbf{k}\mathbb{I})^{-1}\right]^t\overline{\mathfrak{Y}}_0^t\left(\epsilon E_0 + \mathbf{k}\mathbb{I}\right)^t\epsilon\overline{\mathfrak{Y}}_0 \tag{5.92}$$

are solutions to (5.87)-(5.88).

The meaning of (5.91)-(5.92) becomes clearer if we change field variables to

$$\widehat{\Psi} \equiv \mathfrak{Y}\Psi, \qquad \widehat{\overline{\Psi}} \equiv \overline{\mathfrak{Y}}\widehat{\overline{\Psi}}.$$

In terms of the new variables, the kinetic terms $i\Psi^t\Sigma\overline{\partial}\Psi$ and $i\overline{\Psi}^t\overline{\Sigma}\partial\overline{\Psi}$ of (5.24) become $i\Psi^tG\overline{\partial}\Psi + (\cdots)$ and $i\overline{\Psi}^tG\partial\overline{\Psi} + (\cdots)$, where $(\cdots)$ are corrections to the $\Psi^t\mathcal{K}\Psi$ and $\overline{\Psi}^t\overline{\mathcal{K}\Psi}$ terms. In terms of the new field variables, (5.81) can be written as

$$\begin{aligned} I'_f = \frac{1}{2\pi}\int\Bigg(&\widehat{\overline{\Psi}}_1^t\epsilon\widehat{\overline{\Psi}}_0 + \widehat{\Psi}_1^t\epsilon\widehat{\Psi}_0 - \frac{1}{2}\widehat{\overline{\Psi}}_1^tB_1\widehat{\overline{\Psi}}_1 - \frac{1}{2}\widehat{\Psi}_1^tB_1\widehat{\Psi}_1 \\ &+\frac{1}{2}\widehat{\overline{\Psi}}_0^tB_0\widehat{\overline{\Psi}}_0 - \frac{1}{2}\mathbf{k}\widehat{\overline{\Psi}}_0^t\epsilon\widehat{\overline{\Psi}}_0 + \frac{1}{2}\widehat{\Psi}_0^tB_0\widehat{\Psi}_0 - \frac{1}{2}\mathbf{k}\widehat{\Psi}_0^t\epsilon\widehat{\Psi}_0\Bigg)\,d\sigma_1. \end{aligned} \tag{5.93}$$

Thus, the coupling between $\widehat{\Psi}_1$ and $\widehat{\Psi}_0$ is given by the constant matrix ϵ. However, the disadvantage of the new variables is that formulae (5.25), (5.27)-(5.29) and (5.30)-(5.32) become more cumbersome.

We also note that the total action $I + I'_b + I'_f$ is not invariant under the SUSY transformation (5.25), but this is expected with a duality wall, and a similar problem occurs with translations. Consider, for example, an $\widetilde{S}$-duality wall with $\rho = i$ (which does not require a Janus configuration to match the field values at $\sigma_2 = 0$ to those at $\sigma_2 = 1$). In that case, the

system is translationally invariant under $\sigma_2 \to \sigma_2 + \varepsilon$, but not manifestly so, because under a translation the duality wall is moved from $\sigma_2 = 0$ to $\sigma_2 = \varepsilon$, and demonstrating invariance requires an additional duality transformation within the strip $0 < \sigma_2 < \varepsilon$.

Finally, to complete the action we need to add a 0-dimensional term that couples the field $X(0,0)$ to $X(1,0)$. It takes the form

$$I'' = \frac{i}{4\pi}(\mathbf{k}-2)X(1,0)^t \epsilon M X(0,0). \tag{5.94}$$

This term is necessary to reproduce the correct equations of motion at the intersection $(0,0)$ of the two duality walls. Indeed, if we denote by I_b the bosonic part of I from (5.24), then $I_b + I_b' + I''$ leads to the bosonic boundary conditions (5.73). Note that $X(1,0)$ is related to $X(0,0)$ by (5.64). Without I'', the variation of the action $I_b + I_b'$ will have an unwanted term $\frac{i}{2}(\mathbf{k}-2)\delta X(0,0)^t \epsilon M^{-1}\mathcal{N}$, which would be too restrictive (leading to $\mathcal{N} = 0$). Thanks to (5.64) and the identity $M^t \epsilon M = \epsilon$ (which follows from $\det M = 1$), we can rewrite I'' as

$$I'' = \frac{i}{2}(\mathbf{k}-2)\mathcal{N}^t \epsilon M X(0,0). \tag{5.95}$$

If $\mathbf{k}$ is odd then $I_b' + I''$ might not be invariant under (5.67). This is clearer after rewriting $I_b' + I''$ as

$$I_b' + I'' = -\frac{i\mathbf{k}}{4\pi}\int_0^1 Z_0^t \epsilon dZ_0\Big|_{\sigma_2=0} + \frac{i}{2\pi}\int_0^1 Z_1^t \epsilon dZ_0\Big|_{\sigma_2=0} + i\pi(\mathbf{k}-2)\mathcal{N}^t\epsilon(\mathbb{I}-M)^{-1}\mathcal{N}, \tag{5.96}$$

where Z and $\mathcal{N}$ where defined in (5.65) and (5.64), and subscripts of Z_0 and Z_1 are defined similarly to those of X_0 and X_1 in (5.72) and (5.71). Z is invariant under the discrete shift (5.67), but the last term on the RHS of (5.96) changes by $i\pi(\mathbf{k}-2)\left(\mathcal{N}^t - K^t\right)\epsilon(\mathbb{I}-M)K$ (mod $2\pi i\mathbb{Z}$), which might be an odd multiple of $i\pi$ if $\mathbf{k}$ is odd. We therefore require $\mathbf{k}$ to be even.[7] (We will see another aspect of this requirement in Section 5.7.)

At this point one may wonder if an additional term quadratic in $\mathcal{N}$ can be added to the action. This, however, will violate locality, since $\mathcal{N}$ can only be calculated by continuously following the value of X from $\sigma_1 = 0$ to $\sigma_1 = 1$. We will address the issue of locality in more details in Appendix C.2, where we will also argue that I'' is necessary to incorporate the discrete target space periodicity (5.67) in a local way, at least for even $\mathbf{k}$.

The partition function

Thus, we have completed the construction of the action, which is given by the sum of (5.24), (5.80), (5.81) and (5.94):

$$I_{\text{tot}} = I + I_b' + I_f' + I'',$$

[7] We can, in fact, allow $\mathbf{k}$ to be odd if we require $M \in \Gamma(2)$, where $\Gamma(2)$ is the *principal congruence subgroup* of $SL(2,\mathbb{Z})$ with $\mathbf{a} \equiv \mathbf{d} \equiv 1 \pmod 2$ and $\mathbf{b} \equiv \mathbf{c} \equiv 0 \pmod 2$, and it has index 6 inside $SL(2,\mathbb{Z})$.

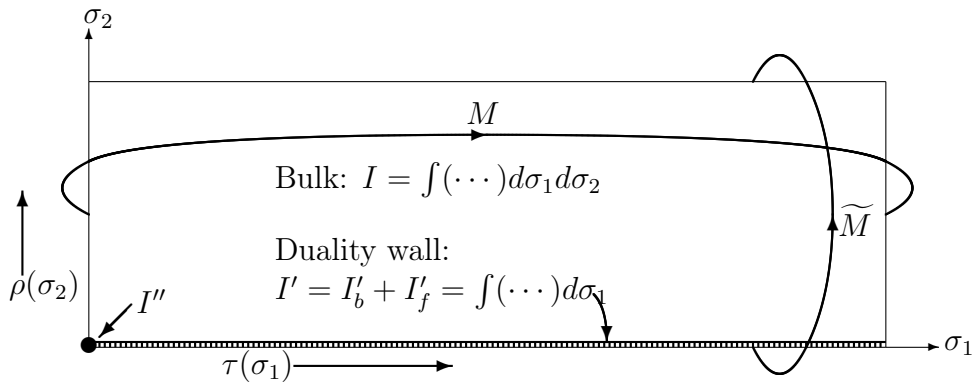

Figure 5.1: Our field theory is defined on a T^2 parametrized by $0 \leq \sigma_1, \sigma_2 \leq 1$, with τ varying as a function of σ_1, and ρ varying as a function of σ_2. Duality walls connect $\sigma_1 = 0$ to $\sigma_1 = 1$ [with the geometrical $M \in SL(2,\mathbb{Z})$] and $\sigma_2 = 0$ to $\sigma_2 = 1$ [with the T-duality $\widetilde{M} \in SL(2,\mathbb{Z})$], and their intersection supports a 0d action I''.

where I is obtained by $SL(2,\mathbb{R})_\rho \times SL(2,\mathbb{R})_\tau$ transformations on the diagonal model (5.53). The model we have constructed consists of the bulk 2d action (5.24) and two duality walls inserted between $\sigma_1 = 0$ and $\sigma_1 = 1$ and between $\sigma_2 = 0$ and $\sigma_2 = 1$. The wall at $\sigma_1 = 0$ is given by nontrivial boundary conditions (5.62)-(5.63), and the wall at $\sigma_2 = 0$ is described by the 1d action I' given by (5.80)-(5.81). At the intersection of the walls we have the additional 0d term I'' given by (5.94). This is depicted in Figure 5.1.

The partition function is defined as

$$\mathcal{Z} = \frac{1}{\sqrt{|\Xi_0|}} \int e^{-I - I'_b - I'_f - I''} \mathcal{D}X \mathcal{D}\Psi \mathcal{D}\overline{\Psi}. \tag{5.97}$$

The prefactor $1/\sqrt{|\Xi_0|}$ is necessary in order to have a properly normalized T-duality wall at $\sigma_2 = 1$. This can be argued by considering σ_2 as the time direction and realizing the T-duality wall at $\sigma_2 = 1$ as a unitary transformation on the Hilbert space. We will outline this approach in more detail in the Section 5.7, but first we will calculate $\mathcal{Z}$ by evaluating the one-loop determinants in the action.

5.6 Calculating the partition function

We will now calculate the partition function for the model we have constructed in Sections 5.5-5.5. First, it is convenient to express the bosonic 1d and 0d terms $I'_b + I''$ in terms of Z and $\mathcal{N}$ as in (5.96). The advantage is that Z satisfies linear boundary conditions (5.63) at σ_1, unlike X whose boundary conditions include an affine term (5.64). The discrete $\mathcal{N}$

decouples and the partition function now takes the form

$$\mathcal{Z} = \frac{1}{\sqrt{|\Xi_0|}} \left(\frac{\Delta_f}{\Delta_b}\right) \sum_{\mathcal{N}\in\Xi_0} \exp\left[i\pi(2-\mathbf{k})\mathcal{N}^t\epsilon(\mathbb{I}-M)^{-1}\mathcal{N}\right], \tag{5.98}$$

where the finite abelian group Ξ_0 was defined in (5.69), and where Δ_b^{-1} is the result of integrating over fluctuations of Z and Δ_f is the result of integrating over Ψ and $\overline{\Psi}$.

The bosonic one-loop determinant

Let us discuss the bosonic part first. To compute Δ_b we need a metric on the space of fluctuations, which we take to be

$$\|\delta Z\|^2 = \int \delta Z^t G \delta Z d^2\sigma\,. \tag{5.99}$$

Given a choice of vielbein V as in (5.36), we can change variables to $\widetilde{Z} \equiv VZ$, which brings the metric $\|\delta Z\|^2$ into the normal form. We will now show how to calculate Δ_b for the model whose 2d bulk is obtained by acting with $SL(2,\mathbb{R})_\tau \times SL(2,\mathbb{R})_\rho$ transformations, defined in Section 5.4, on the diagonal model of (5.53). Since Z, Ψ and $\overline{\Psi}$ are unaware of the periodicity of the target space T^2, their boundary conditions do not require the transformations to be restricted to $SL(2,\mathbb{Z})$, and so we can return to the diagonal model and calculate the fluctuations there.

In this way the model constructed at the end of Section 5.4, with τ and ρ varying along semicircles that are invariant under M and $\widetilde{M}$, respectively, gets converted to a model in which τ and ρ vary along the imaginary axis. In this model, whose bulk action is given by (5.53), the boundary conditions along the σ_1 and σ_2 directions are determined by the eigenvalues of M and $\widetilde{M}$,

$$M = \begin{pmatrix} \mathbf{a} & \mathbf{b} \\ \mathbf{c} & \mathbf{d} \end{pmatrix} \to \begin{pmatrix} e^{\varsigma} & 0 \\ 0 & e^{-\varsigma} \end{pmatrix}, \qquad \widetilde{M} = \begin{pmatrix} \tilde{\mathbf{a}} & \tilde{\mathbf{b}} \\ \tilde{\mathbf{c}} & \tilde{\mathbf{d}} \end{pmatrix} \to \begin{pmatrix} e^{\widetilde{\varsigma}} & 0 \\ 0 & e^{-\widetilde{\varsigma}} \end{pmatrix},$$

where

$$e^{\varsigma} = \frac{1}{2}\left(\mathbf{a}+\mathbf{d}+\sqrt{(\mathbf{a}+\mathbf{d})^2-4}\right), \qquad e^{\widetilde{\varsigma}} = \frac{1}{2}\left(\tilde{\mathbf{a}}+\tilde{\mathbf{d}}+\sqrt{\left(\tilde{\mathbf{a}}+\tilde{\mathbf{d}}\right)^2-4}\right).$$

Then, (5.61) and (5.70) become

$$\tau(1) = e^{2\varsigma}\tau(0)\,, \qquad \rho(1) = e^{2\widetilde{\varsigma}}\rho(0)\,, \tag{5.100}$$

and the boundary conditions (5.66) become

$$\mathbf{Z}^1(0,\sigma_2) = e^{\varsigma}\mathbf{Z}^1(1,\sigma_2)\,, \qquad \mathbf{Z}^2(0,\sigma_2) = e^{-\varsigma}\mathbf{Z}^2(1,\sigma_2)\,, \tag{5.101}$$

where $\mathbf{Z}^1$ and $\mathbf{Z}^2$ are the components of Z, while (5.73) becomes

$$\overline{\partial} Z(\sigma_1, 1) = e^{-\widetilde{\varsigma}} \overline{\partial} Z(\sigma_1, 0)\,, \qquad \partial Z(\sigma_1, 1) = e^{-\widetilde{\varsigma}} \partial Z(\sigma_1, 0), \tag{5.102}$$

which we can solve simply by requiring

$$Z(\sigma_1, 1) = e^{-\widetilde{\varsigma}} Z(\sigma_1, 0).$$

In (5.53), we can take the vielbein to be diagonal as well, so that the change of variables from Z to the normalized $\widetilde{Z}$ is given by

$$\widetilde{\mathbf{Z}}^1 = \rho_2^{\frac{1}{2}} \tau_2^{-\frac{1}{2}} \mathbf{Z}^1\,, \qquad \widetilde{\mathbf{Z}}^2 = \rho_2^{\frac{1}{2}} \tau_2^{\frac{1}{2}} \mathbf{Z}^2\,. \tag{5.103}$$

The boundary conditions (5.100), (5.101) and (5.102) imply that $\widetilde{Z}$ is periodic in σ_1 and σ_2. Substituting (5.103) into the bosonic part of (5.53), and integrating by parts, we get the bosonic part of the action in the form

$$I_b \;=\; \frac{1}{\pi} \int \left(\partial Z^t \overline{\partial} Z + \tfrac{1}{4} Z^t \mathfrak{M}^2 Z \right) d^2\sigma\,, \tag{5.104}$$

where the effective mass matrix (squared) is defined as

$$\mathfrak{M}^2 = \begin{pmatrix} \mathfrak{m}_1^2 & 0 \\ 0 & \mathfrak{m}_2^2 \end{pmatrix} \tag{5.105}$$

with the eigenvalues given in terms of $\tau_2(\sigma_1)$ and $\rho_2(\sigma_2)$ by

$$\mathfrak{m}_1^2 \;=\; \frac{\ddot{\rho}_2}{2\rho_2} - \frac{\dot{\rho}_2^2}{4\rho_2^2} - \frac{\tau_2''}{2\tau_2} + \frac{3\tau_2'^2}{4\tau_2^2}\,, \tag{5.106}$$

$$\mathfrak{m}_2^2 \;=\; \frac{\ddot{\rho}_2}{2\rho_2} - \frac{\dot{\rho}_2^2}{4\rho_2^2} + \frac{\tau_2''}{2\tau_2} - \frac{\tau_2'^2}{4\tau_2^2}\,. \tag{5.107}$$

The contribution of the fluctuations of Z to the partition function are now expressed in terms of the product of the eigenvalues of the operator $-2\partial\overline{\partial} + \mathfrak{M}^2$. These take the form of sums of two 1d Schrödinger problems as follows. Define

$$\mathbf{V}(\sigma_2) \equiv \frac{\ddot{\rho}_2}{2\rho_2} - \frac{\dot{\rho}_2^2}{4\rho_2^2}\,, \qquad \mathbf{U}_1(\sigma_1) \equiv -\frac{\tau_2''}{2\tau_2} + \frac{3\tau_2'^2}{4\tau_2^2}\,, \qquad \mathbf{U}_2(\sigma_1) \equiv \frac{\tau_2''}{2\tau_2} - \frac{\tau_2'^2}{4\tau_2^2}\,. \tag{5.108}$$

The boundary conditions (5.100) ensure that $\mathbf{V}$, $\mathbf{U}_1$ and $\mathbf{U}_2$ are periodic. We now need to solve three separate 1d Schrödinger problems with the following periodic potentials defined on the circle parametrized by the periodic coordinate $0 \le \mathbf{x} < 1$:

$$\begin{aligned} &-\frac{d}{d\mathbf{x}^2} + \mathbf{V}(x) \text{ with eigenvalues } \mu_0, \mu_1, \mu_2, \dots \\ &-\frac{d}{d\mathbf{x}^2} + \mathbf{U}_1(x) \text{ with eigenvalues } \varepsilon_0, \varepsilon_1, \varepsilon_2, \dots \\ &-\frac{d}{d\mathbf{x}^2} + \mathbf{U}_2(x) \text{ with eigenvalues } \vartheta_0, \vartheta_1, \vartheta_2, \dots \end{aligned} \tag{5.109}$$

Then, $\mu_i + \varepsilon_j$ are the eigenvalues of the fluctuations of $\widetilde{\mathbf{Z}}^1$, and $\mu_i + \vartheta_j$ are the eigenvalues of the fluctuations of $\widetilde{\mathbf{Z}}^2$ (with $0 \leq i, j < \infty$). We will see below that the eigenvalues of $\mathbf{U}_1$ and $\mathbf{U}_2$ are the same, $\varepsilon_j = \vartheta_j$, so that, formally, we can write

$$\Delta_b = \prod_{i,j} \{(\mu_i + \varepsilon_j)(\mu_i + \vartheta_j)\}^{1/2} = \prod_{i,j} (\mu_i + \varepsilon_j). \tag{5.110}$$

The eigenvalues μ_j, $\varepsilon_j = \vartheta_j$ are all positive. That the eigenvalues are nonnegative is a consequence of supersymmetry, and the fact that the σ_1-Schrödinger problem and σ_2-Schrödinger problem are decoupled. Thus, to show that $\mu_j \geq 0$ we can look at the model with constant τ_2 and $M = \mathbb{I}$. This model is translationally invariant in σ_1, which we can identify as time. Because of supersymmetry, all energy states are nonnegative, and therefore all single-particle eigenvalues μ_j must be nonnegative. Similarly, to argue that ε_j and ϑ_j are nonnegative we take ρ_2 to be constant and $\widetilde{M} = \mathbb{I}$ and identify σ_2 as the time direction. We can also argue more directly that the eigenvalues are positive, by noting that each of the potentials $\mathbf{V}$, $\mathbf{U}_1$ and $\mathbf{U}_2$ can be written in terms of a superpotential $\mathbf{W}$ as $\mathbf{W}^2 + d\mathbf{W}/d\mathbf{x}$, with

$$\mathbf{W} \to \frac{\dot{\rho}_2}{2\rho_2}, \text{ or } \pm\frac{\tau_2'}{2\tau_2}. \tag{5.111}$$

The Hamiltonian can then be expressed in terms of the superpotential as [275, 276, 277]

$$-\frac{d}{d\mathbf{x}^2} + \mathbf{W}^2 + \frac{d\mathbf{W}}{d\mathbf{x}} = q^\dagger q, \qquad \text{where} \qquad q \equiv \frac{d}{d\mathbf{x}} - \mathbf{W}(\mathbf{x}), \quad q^\dagger = -\frac{d}{d\mathbf{x}} - \mathbf{W}(\mathbf{x})\,.$$

It is now clear that the eigenvalues are nonnegative, and it is also clear that a zero eigenvalue would require a nontrivial kernel for either q or $q^\dagger$, but for ς and $\widetilde{\varsigma}$ both nonzero, and for $\mathbf{W}$ given in (5.111), there are no periodic zero eigenvalues for q or $q^\dagger$. This 1d supersymmetry is also the reason why $\varepsilon_j = \vartheta_j$. Setting

$$\mathbf{W} = \frac{\tau_2'}{2\tau_2},$$

we find

$$qq^\dagger = -\frac{d}{d\mathbf{x}^2} + \mathbf{U}_1(x)\,, \qquad q^\dagger q = -\frac{d}{d\mathbf{x}^2} + \mathbf{U}_2(x),$$

and since we have established that the kernels of both q and $q^\dagger$ are trivial, it follows that the eigenvalues of $qq^\dagger$ and $q^\dagger q$ are equal, as is well-known. Thus, the double-Janus σ-model realizes a second quantized version of supersymmetric quantum mechanics.

We note that there is a special case where the three effective Schrödinger potentials are positive constants. For this we take

$$\tau(\sigma_1) = e^{2\varsigma\sigma_1}, \qquad \rho(\sigma_2) = e^{2\widetilde{\varsigma}\sigma_2}, \tag{5.112}$$

which satisfies the boundary conditions (5.100) and leads to

$$\mathbf{V} = \widetilde{\varsigma}^2, \qquad \mathbf{U}_1 = \mathbf{U}_2 = \varsigma^2,$$

and the action (5.104) becomes that of two free, translationally invariant, massive bosons:

$$I_b = \frac{1}{\pi}\int\left(\partial Z^t\overline{\partial}Z+\frac{1}{4}m^2Z^tZ\right)d^2\sigma\,, \tag{5.113}$$

with constant mass squared given in terms of the eigenvalues of the $SL(2,\mathbb{Z})$ twist matrices M and $\widetilde{M}$ by

$$m^2=\widetilde{\varsigma}^2+\varsigma^2. \tag{5.114}$$

Up to an unimportant constant, then

$$\Delta_b=\det\left(-\partial\overline{\partial}+\frac{1}{4}m^2\right). \tag{5.115}$$

The fermionic one-loop determinant

To define the fermionic determinant we again need a metric on the space of fluctuations, similarly to (5.99). We choose it to be given in terms of Σ and $\overline{\Sigma}$, for Ψ and $\overline{\Psi}$, respectively. Then, using (5.89), and the vielbein, we can redefine

$$\widetilde{\widetilde{\Psi}}\equiv V\mathfrak{Y}\Psi,\qquad \widetilde{\widetilde{\overline{\Psi}}}\equiv V\overline{\mathfrak{Y}\Psi},$$

for which the kinetic term in the bulk action is normalized. As in Section 5.6, we can then change variables to the diagonal model (5.53). It is convenient to use, instead of $\widetilde{\widetilde{\Psi}}$ which has kinetic term $i\widetilde{\widetilde{\Psi}}^t\overline{\partial}\widetilde{\widetilde{\Psi}}$, another set of variables

$$\widetilde{\Psi^1}\equiv\rho_2^{1/2}\tau_2^{-1/2}\Psi^1,\quad \widetilde{\Psi^2}\equiv\rho_2^{1/2}\tau_2^{1/2}\Psi^2,\qquad \widetilde{\overline{\Psi}^1}\equiv\rho_2^{1/2}\tau_2^{-1/2}\overline{\Psi}^1,\quad \widetilde{\overline{\Psi}^2}\equiv\rho_2^{1/2}\tau_2^{1/2}\overline{\Psi}^2, \tag{5.116}$$

similarly to (5.103). These new fields are periodic in σ_1 and σ_2 and the fermionic part of (5.53) is given in terms of them by

$$I_f = \frac{1}{\pi}\int\left[2i\widetilde{\Psi^1}\overline{\partial}\widetilde{\Psi^2}+2i\widetilde{\overline{\Psi}^1}\partial\widetilde{\overline{\Psi}^2}+\left(\frac{i\tau_2'}{2\tau_2}+\frac{\dot{\rho}_2}{2\rho_2}\right)\widetilde{\overline{\Psi}^1}\widetilde{\Psi^2}+\left(\frac{i\tau_2'}{2\tau_2}-\frac{\dot{\rho}_2}{2\rho_2}\right)\widetilde{\Psi^1}\widetilde{\overline{\Psi}^2}\right]d^2\sigma\,. \tag{5.117}$$

The fermionic determinant is now expressed, formally, as

$$\Delta_f=\det\begin{pmatrix} i\overline{\partial} & \frac{i\tau_2'}{4\tau_2}-\frac{\dot{\rho}_2}{4\rho_2}\\ \frac{i\tau_2'}{4\tau_2}+\frac{\dot{\rho}_2}{4\rho_2} & i\partial\end{pmatrix}. \tag{5.118}$$

To calculate the determinant, we use the well known identity for the determinant of a $(2N)\times(2N)$ matrix given in 4 blocks of $N\times N$ matrices A,B,C,D, with C invertible, as

$$\det\begin{pmatrix}A & B\\ C & D\end{pmatrix}=\det\left(AC^{-1}DC-BC\right)\xrightarrow{\text{if } CD=DC}\det(AD-CB). \tag{5.119}$$

By choosing a different representation of 2d Dirac matrices[8] we rewrite (5.118) as

$$\Delta_f = \det \begin{pmatrix} \frac{i}{2}\partial_1 + \frac{i\tau_2'}{4\tau_2} & \frac{1}{2}\partial_2 - \frac{\dot\rho_2}{4\rho_2} \\ \frac{1}{2}\partial_2 + \frac{\dot\rho_2}{4\rho_2} & \frac{i}{2}\partial_1 - \frac{i\tau_2'}{4\tau_2} \end{pmatrix}. \tag{5.120}$$

Applying the identity (5.119) to (5.118) (with commuting $C \equiv \frac{1}{2}\partial_2 + \frac{\dot\rho_2}{4\rho_2}$ and $D \equiv \frac{i}{2}\partial_1 - \frac{i\tau_2'}{4\tau_2}$), we get

$$\Delta_f \;=\; \det\left(-\frac{1}{4}\partial_1^2 - \frac{1}{4}\partial_2^2 + \frac{\ddot\rho_2}{8\rho_2} + \frac{\tau_2''}{8\tau_2} - \frac{{\tau_2'}^2}{16\tau_2^2} - \frac{\dot\rho_2^2}{16\rho_2^2}\right) = \det\left(-\overline\partial\partial + \frac{1}{4}\mathfrak{m}_2^2\right), \tag{5.121}$$

where $\mathfrak{m}_2^2$ was defined in (5.107). Following the arguments at the end of Section 5.6, and using (5.110), we find that

$$\Delta_f = \prod_{i,j}(\mu_i + \varepsilon_j) = \Delta_b.$$

For example, in the special case (5.112), we get constant

$$\frac{i\tau_2'}{4\tau_2} + \frac{\dot\rho_2}{4\rho_2} = \frac{1}{2}\left(\widetilde\varsigma + i\varsigma\right),$$

and then

$$\Delta_f = \det\left(-\overline\partial\partial + \frac{1}{4}m^2\right), \tag{5.122}$$

with m^2 given by (5.114). Comparing (5.122) to (5.115), we find $\Delta_f = \Delta_b$, as expected.

We conclude that the partition function (5.98) reduces to

$$\boxed{\mathcal{Z} = \frac{1}{\sqrt{|\Xi_0|}}\sum_{\mathcal{N}\in\Xi_0}\exp\left[i\pi(2-\mathbf{k})\mathcal{N}^t\epsilon(\mathbb{I}-M)^{-1}\mathcal{N}\right]}. \tag{5.123}$$

This is essentially a quadratic Gauss sum, and we will now see how this double-Janus configuration naturally leads to the Quadratic Reciprocity.

5.7 Connections with abelian Chern-Simons theory and strings on a mapping torus

We now return to the matter of normalization of the partition function $\mathcal{Z}$. In particular, we need to explain the prefactor $1/\sqrt{|\Xi_0|}$ that appears in (5.97) and (5.123). This factor will be necessary to reproduce the Landsberg-Schaar identity in Section 5.8, and it can be

[8]The matrix in (5.118) can be written in terms of Pauli matrices as $\frac{i}{2}\mathbb{I}\partial_1 - \frac{1}{2}\boldsymbol{\sigma}_3\partial_2 + i\boldsymbol{\sigma}_1\frac{\tau_2'}{4\tau_2} - i\boldsymbol{\sigma}_2\frac{\dot\rho_2}{4\rho_2}$ and we got (5.120) by rotating $\boldsymbol{\sigma}_1 \to \boldsymbol{\sigma}_3$ and $\boldsymbol{\sigma}_3 \to -\boldsymbol{\sigma}_1$.

argued by treating σ_2 and "time" and realizing the T-duality $\widetilde{M}$ in (5.78) as an operator on a Hilbert space of dimension $|\Xi_0|$.

We will argue that, up to a known phase, (5.123) can be recast as the trace of the operators representing $M = ST^{\mathbf{k}} \in SL(2,\mathbb{Z})$ in a certain $|\Xi_0|$-dimensional representation of $SL(2,\mathbb{Z})$. We will give two equivalent constructions and physical interpretations for this representation, as a Hilbert space of ground states, one in terms of low-energy strings on a mapping-torus target space, and another in terms of an effective abelian Chern-Simons theory on T^2. The first construction can be expressed in terms of the element in M explicitly, and it directly leads to (5.123), but the construction of matrix elements of $\mathcal{S}$ and $\mathcal{T}$, representing S and T in $SL(2,\mathbb{Z})$ respectively, will only be given up to independent $(\pm)$ signs – an ambiguity that has a physical origin. The second construction relies on a particular decomposition of M as

$$M = ST^{l_1}ST^{l_2}\cdots ST^{l_s}. \tag{5.124}$$

We note that this decomposition is unique if M belongs to the subgroup $\langle S, T^2\rangle$ generated by S and T^2 [and isomorphic to the *Hecke congruence subgroup* $\Gamma_0(2) \subset SL(2,\mathbb{Z})$], as we will assume in Section 5.9.

The $SL(2,\mathbb{Z})$ representations that we will need belong to the subclass of representations that appear in the theory of *modular tensor category*[9], i.e., the representations one obtains by studying Chern-Simons theory with a compact abelian gauge group. The physical interpretation presented in this section is partly based on results from [247]. More recently a much deeper theory related to nonabelian Chern-Simons was developed in [278, 279], related to the study of the 6d $(2,0)$-theory on plumbed 3-manifolds, including mapping tori, but our case is somewhat different. We will begin with a few generalities about such representations, which are defined through a quadratic form on a finite abelian group. (In general, the classification of unimodular, symmetric quadratic forms on finite abelian groups [280] is equivalent to a classification of *pointed modular tensor categories*, i.e., theories of "abelian anyons" in physical terminology [281, 282]. For additional recent insight on abelian Chern-Simons theory and abelian anyons, see [283, 284, 285].)

Representations of $SL(2,\mathbb{Z})$ from quadratic forms on abelian groups

In this subsection we will denote the standard $SL(2,\mathbb{Z})$ generators by $\mathcal{S}$ and $\mathcal{T}$, in order to distinguish the abstract discussion from the concrete S, T. The construction, known as the *Weil representation*[10] [286, 287, 279] begins with a finite abelian group $\mathcal{A}$ on which a quadratic form $\mathfrak{q}(\cdot)$ is defined. In our case the abelian group is $\mathcal{A} \simeq \Xi_0$ and the complex vector space of the representation is the group algebra $\gamma[\mathcal{A}]$, which we identify with the Hilbert space spanned by a basis of states of the form $|\mathbf{v}\rangle$, with $\mathbf{v} \in \mathcal{A}$. The quadratic form $\mathfrak{q}(\cdot)$ is required to take values in $\mathbb{Q}/\mathbb{Z}$, i.e., $\mathfrak{q}(\mathbf{v})$ is a rational number up to an undetermined

[9] Mathematically it is equivalent defined as a *ribbon fusion category*, or a *braided fusion category* with a *spherical structure*, whose modular $\mathcal{S}$ matrix is invertible.

[10] Most generally it is defined for $Mp(2n)$, a double cover of $Sp(2n)$, over an arbitrary local or finite field.

integer part. Thus, the phase $\exp[2\pi i\mathfrak{q}(\mathbf{v})]$ is well-defined for every element $\mathbf{v}\in\mathcal{A}$. From $\mathfrak{q}(\cdot)$ we then construct a symmetric *bilinear form*[11]:

$$\mathfrak{b}(\mathbf{u},\mathbf{v})\equiv\mathfrak{q}(\mathbf{u}+\mathbf{v})-\mathfrak{q}(\mathbf{u})-\mathfrak{q}(\mathbf{v}),\qquad \mathbf{u},\mathbf{v}\in\mathcal{A}.$$

We assume that the abelian group $\mathcal{A}$ is given as a quotient of a lattice by a sublattice $\mathcal{A}=\widetilde{\Lambda}/\widetilde{\Lambda}'$ and $\mathfrak{q}$ descends from a quadratic form q on $\widetilde{\Lambda}$ that takes integer values on $\widetilde{\Lambda}'$ [so that for any basis $\{\mathbf{V}_i\}$ of $\widetilde{\Lambda}'$, the associated bilinear form $\mathbf{B}$ is represented by a symmetric matrix with integer elements and even integers on the diagonal]. Then, the Weil representation constructed from this data is given by the action of the $SL(2,\mathbb{Z})$ generators $\mathcal{S}$ and $\mathcal{T}$ on the basis vectors $|\mathbf{v}\rangle$ of Hilbert space as follows:

$$\mathcal{T}\,|\mathbf{v}\rangle=e^{-i\phi}e^{2\pi i\mathfrak{q}(\mathbf{v})}\,|\mathbf{v}\rangle\,,\qquad \mathcal{S}\,|\mathbf{v}\rangle=\frac{1}{\sqrt{|\mathcal{A}|}}\sum_{\mathbf{u}\in\mathcal{A}}e^{-2\pi i\mathfrak{b}(\mathbf{v},\mathbf{u})}\,|\mathbf{u}\rangle\,, \tag{5.125}$$

where $|\mathcal{A}|$ is the number of elements in $\mathcal{A}$ and the phase ϕ is given by $\frac{\pi}{12}\sigma(\mathfrak{q})$ [282, 288], where $\sigma(\mathfrak{q})$ is the *signature* of the quadratic form (i.e., the difference between the number of positive and negative eigenvalues of the matrix representing the bilinear form $\mathbf{B}$ in any basis $\{\mathbf{V}_i\}$ of $\widetilde{\Lambda}'$). The phase is also given by the cubic root of the *Gauss-Milgram sum* [289]: [286, 288]:

$$e^{-3i\phi}=e^{-\frac{1}{4}\pi i\sigma(\mathfrak{q})}=\frac{1}{\sqrt{|\mathcal{A}|}}\sum_{\mathbf{v}\in\mathcal{A}}e^{-2\pi i\mathfrak{q}(\mathbf{v})}\,.$$

In our case, there are two ways to describe $\mathfrak{q}(\cdot)$ on $\mathcal{A}$. In the first, we decompose $M\in SL(2,\mathbb{Z})$ into S and T generators as in (5.124), and we assume that all the powers are even, so that $l_i=2v_i$ for $v_i\in\mathbb{Z}$. We then construct the $s\times s$ symmetric matrix

$$K\equiv\begin{pmatrix} l_1 & -1 & 0 & & -1\\ -1 & \ddots & \ddots & \ddots & \\ 0 & \ddots & \ddots & \ddots & 0\\ & \ddots & \ddots & \ddots & -1\\ -1 & & 0 & -1 & l_s\end{pmatrix}, \tag{5.126}$$

with $\{l_i\}$ along the diagonal, and (-1)'s on the $(i,i+1)$ and $(1,s)$ places. For the special case $s=2$ we take instead

$$K\equiv\begin{pmatrix} l_1 & -2\\ -2 & l_2\end{pmatrix}, \tag{5.127}$$

and for $s=1$ we take $K\equiv(l_1-2)$.

[11] Conversely, given a bilinear form $\mathfrak{b}(\cdot,\cdot)$ (not necessarily symmetric), if a function $\mathfrak{q}$ on $\mathcal{A}$ satisfies $\mathfrak{b}(\mathbf{u},\mathbf{v})=\mathfrak{q}(\mathbf{u}+\mathbf{v})-\mathfrak{q}(\mathbf{u})-\mathfrak{q}(\mathbf{v})+\mathfrak{q}(0)$, $\forall\,\mathbf{u},\mathbf{v}\in\mathcal{A}$, then $\mathfrak{q}$ is called a *quadratic refinement* of $\mathfrak{b}(\cdot,\cdot)$ [283, 284, 285].

We then define $\widetilde{\Lambda} = \mathbb{Z}^s$ and $\widetilde{\Lambda}' \subset \widetilde{\Lambda}$ to be the sublattice generated by the columns of K, i.e.,

$$\widetilde{\Lambda}' = \{K\mathbf{W} : \mathbf{W} \in \mathbb{Z}^s\} \equiv K(\mathbb{Z}^s).$$

One can show [247] that $\widetilde{\Lambda}/\widetilde{\Lambda}'$ is isomorphic to Ξ_0, and we therefore take $\mathcal{A} = \widetilde{\Lambda}/\widetilde{\Lambda}'$, and define

$$\mathfrak{q}(\mathbf{v}) = \mathbf{V}^t K^{-1}\mathbf{V}, \qquad \text{for any representative } \mathbf{V} \in \widetilde{\Lambda} \text{ of } \mathbf{v} \in \widetilde{\Lambda}/\widetilde{\Lambda}'. \tag{5.128}$$

This quadratic form on $\mathcal{A}$ then defines, through (5.125), a $|\mathcal{A}|$-dimensional Weil representation of $SL(2,\mathbb{Z})$. We will elaborate on its physical interpretation (related to Chern-Simons theory with $U(1)^s$ gauge group) in Section 5.7.

The expression (5.128) and the associated Weil representation (5.125) is not yet satisfactory for us, since it is not yet clear how it is related to (5.123). We would like to argue that, up to a phase, (5.128) can be written as $\mathrm{Tr}(\mathcal{S}\mathcal{T}^{\mathbf{k}})$ (corresponding to $\widetilde{M} = \widetilde{S}\widetilde{T}^{\mathbf{k}}$) in the Weil representation, but to see this we will need to recast the expressions for the matrix elements of $\mathcal{S}$ and $\mathcal{T}$ directly in terms of M. We will see that this can be achieved only up to $\pm$ signs on elements in $\mathcal{S}$ and $\mathcal{T}$. Nevertheless, these signs drop out of the expression for $\mathrm{Tr}(\mathcal{S}\mathcal{T}^{\mathbf{k}})$. This leads us to the *second* way to describe $\mathfrak{q}(\cdot)$, which we now present.

First, it is convenient to introduce a new lattice $(M-\mathbb{I})^{-1}(\mathbb{Z}^2)$, and for $\mathcal{N} \in \Xi_0 = \mathbb{Z}^2/(M-\mathbb{I})\mathbb{Z}^2$ [see (5.69)], we define

$$v \equiv (M-\mathbb{I})^{-1}\mathcal{N} \pmod{\mathbb{Z}^2}, \qquad \text{so that } v \in (M-\mathbb{I})^{-1}(\mathbb{Z}^2)/\mathbb{Z}^2. \tag{5.129}$$

The quotient $(M-\mathbb{I})^{-1}(\mathbb{Z}^2)/\mathbb{Z}^2$ is canonically identified with Ξ_0 in this way. As mentioned above, there is an isomorphism $\widetilde{\varphi} : \Xi_0 \cong \widetilde{\Lambda}/\widetilde{\Lambda}'$ (which we will describe in detail in Section 5.7). Using it, we can define a quadratic form on Ξ_0 simply as

$$\widetilde{\mathfrak{q}}(v) \equiv \mathfrak{q}\left(\widetilde{\varphi}(v)\right), \qquad \text{for } \mathcal{N} \in \Xi_0. \tag{5.130}$$

Using $\widetilde{\mathfrak{q}}$ we can then define the action of $\mathcal{S}$ and $\mathcal{T}$ on the states $|v\rangle$ in Ξ_0 as

$$\mathcal{T}\,|v\rangle = e^{-i\phi}e^{2\pi i\widetilde{\mathfrak{q}}(v)}\,|v\rangle\,, \qquad \mathcal{S}\,|v\rangle = \frac{1}{\sqrt{|\Xi_0|}}\sum_{u\in\Xi_0} e^{-2\pi i\widetilde{\mathfrak{b}}(v,u)}\,|u\rangle\,, \qquad \text{for } v \in \Xi_0, \tag{5.131}$$

where

$$\widetilde{\mathfrak{b}}(u,v) \equiv \widetilde{\mathfrak{q}}(u+v) - \widetilde{\mathfrak{q}}(u) - \widetilde{\mathfrak{q}}(v), \qquad u, v \in \Xi_0.$$

We claim that (at least for $s \le 2$) the doubled quadratic form $2\widetilde{\mathfrak{q}}(\cdot)$ has a simple expression in terms of M:

$$2\widetilde{\mathfrak{q}}(v) = v^t \epsilon M v \pmod{\mathbb{Z}}, \tag{5.132}$$

and therefore

$$\mathcal{T}^2\,|v\rangle = e^{-2i\phi}e^{2\pi i v^t\epsilon M v}\,|v\rangle\,. \tag{5.133}$$

We will prove (5.132) in Appendix C.3 for $s \leq 2$. It implies that the matrix elements of $\mathcal{T}$ and $\mathcal{S}$ can be expressed as follows (with undetermined $\pm$ signs that depend on $u, v \in \Xi_0$, as well as other input data):

$$\langle u| \mathcal{T} |v\rangle = \pm\delta_{uv} e^{-i\phi} e^{\pi i v^t \epsilon M v}, \qquad \langle u| \mathcal{S} |v\rangle = \pm \frac{1}{\sqrt{|\Xi_0|}} e^{-\pi i (u^t \epsilon M v + v^t \epsilon M u)}. \tag{5.134}$$

(In Appendix C.3 we will show what the $\pm$ signs are in a particular example.) Fortunately, for even $\mathbf{k} = 2u$, the trace $\mathrm{Tr}\,(\mathcal{S}\mathcal{T}^{2u})$ is independent of the unknown $\pm$ signs in (5.134):

$$\mathrm{Tr}\left(\mathcal{S}\mathcal{T}^{2u}\right) = \frac{e^{-2iu\phi}}{\sqrt{|\Xi_0|}} \sum_v e^{2(u-1)\pi i v^t \epsilon M v}\,. \tag{5.135}$$

Using (5.129), we easily check[12] that (5.135) reproduces (5.123), up to the phase $e^{-2iu\phi}$.

In Section 5.9 we will also need to calculate $\mathrm{Tr}(\mathcal{S}\mathcal{T}^{2u_1}\mathcal{S}\mathcal{T}^{2u_2})$, and luckily again, this is independent of the ambiguous $\pm$ signs in (5.134):

$$\mathrm{Tr}\left(\mathcal{S}\mathcal{T}^{2u_1}\mathcal{S}\mathcal{T}^{2u_2}\right) = \frac{e^{-2i(u_1+u_2)\phi}}{|\Xi_0|} \sum_{u,v} e^{2\pi i (u_2 v^t \epsilon M v + u_1 u^t \epsilon M u - u^t \epsilon M v - v^t \epsilon M u)}\,. \tag{5.136}$$

We will now offer a physical interpretation for (5.132).

Low-energy strings on a mapping torus

There is a simple geometrical interpretation of (5.133) in terms of the topology of (an auxiliary) *mapping torus* – a manifold formed by fibering T^2 over S^1. Let $\theta \in \mathbb{R}$ be a periodic coordinate on the S^1 base with periodicity 1, and let $\mathbf{x} \in \mathbb{R}^2$ be coordinates that will soon parametrize a torus, after additional periodicity conditions are imposed. The mapping torus is defined as the set of points $(\theta, \mathbf{x})$ with identification,

$$(\theta, \mathbf{x}) \sim (\theta, \mathbf{x} + \mathbf{K}) \sim \left(\theta + 1, M^{-1}\mathbf{x}\right)\,, \qquad \forall\, \mathbf{K} \in \mathbb{Z}^2, \tag{5.137}$$

for a fixed $M \in SL(2,\mathbb{Z})$, which acts as an MCG element on the fiber. In our case, a mapping torus is formed by fixing σ_2 and considering the configuration space of the fields $X(\sigma_1, \sigma_2)$ as σ_1 (which we identified as θ above) varies from 0 to 1. A *ground state* of the string corresponds to a point on the T^2 fiber that is invariant modulo $\mathbb{Z}^2$ under the geometrical M-twist. Representing this point by $v \in \mathbb{R}^2$, we thus require $v - Mv \in \mathbb{Z}^2$. This has a discrete set of rational solutions $v \in \mathbb{Q}^2$, and we formally define a Hilbert space $\mathcal{H}_M$ of states with basis $\{|v\rangle\}$ comprising of states $|v\rangle$ such that

$$(M - \mathbb{I})v \in \mathbb{Z}^2 \tag{5.138}$$

[12] Using $\mathcal{N}^t \epsilon \mathcal{N} = 0$ and $\epsilon M = (M^t)^{-1}\epsilon$.

in which $|v\rangle = |u\rangle$ if $v - u \in \mathbb{Z}^2$. Now we define the lattice

$$\Lambda \equiv (M - \mathbb{I})^{-1}\left(\mathbb{Z}^2\right) = \left\{v \in \mathbb{Q}^2 : (M - \mathbb{I})v \in \mathbb{Z}^2\right\} \supset \mathbb{Z}^2\,. \tag{5.139}$$

Then a solution to (5.138) with the identification "$v \sim u$ whenever $v - u \in \mathbb{Z}^2$" defines an element of the coset space $\Lambda/\mathbb{Z}^2$, which map to a basis of the Hilbert space $\mathcal{H}_M$. This coset space is a finite abelian group, i.e., the cokernal of $M - \mathbb{I}$, which can be identified with isometries of the mapping torus. (See [247] for more details.) It is easy to see that $\Lambda/\mathbb{Z}^2$ is isomorphic to Ξ_0 [defined in (5.69)] and that the number of states is

$$|\Lambda/\mathbb{Z}^2| = |\det(M - \mathbb{I})| = |\mathrm{Tr}\, M - 2|.$$

We need to know the action of $SL(2,\mathbb{Z})$, generated by S and T, on those quantum states. It can be described as T-duality on the T^2 fiber and, as we argued in (5.132), (at least for $M = ST^{2v_1}$ or $M = ST^{2v_1}ST^{2v_2}$) is given by

$$\mathcal{S}\,|v\rangle = \frac{1}{\sqrt{|\Lambda/\mathbb{Z}^2|}} \sum_{u\in\Lambda/\mathbb{Z}^2} (\pm) e^{-\pi i(v^t\epsilon M u + u^t\epsilon M v)}\,|u\rangle\,, \tag{5.140}$$

$$\mathcal{T}^{\overline{k}}\,|v\rangle = \pm e^{-i\overline{k}\phi} e^{\overline{k}\pi i v^t\epsilon M v}\,|v\rangle\ , \tag{5.141}$$

where all the $(\pm)$ signs in (5.140) and (5.141) are independent of u and v respectively, and where ϕ in (5.141) has been defined in Section 5.7 [e.g., (5.125)] and is a constant phase chosen so that $(\mathcal{S}\mathcal{T})^3 = \mathcal{S}^2$ equals the charge conjugation operator [which represents the $-\mathbb{I} \in SL(2,\mathbb{Z})$], which acts as

$$\mathcal{S}^2\,|v\rangle = |-v\rangle\,.$$

$\mathcal{T}^{\overline{k}}$ is ill-defined for odd $\overline{k}$ [unless M is such that $v^t\epsilon M v$ is an even integer for all $v \in \mathbb{Z}^2$, which is when $M \in \Gamma(2)$, as mentioned in Footnote 7], so to avoid extra complications we assume $\overline{k} \in 2\mathbb{Z}$. Note that the definitions (5.140) and (5.141) are independent of the representatives v and u, because for $\mathbf{K} \in \mathbb{Z}^2$ we have $\mathbf{K}^t\epsilon(M - \mathbb{I})u \in \mathbb{Z}$ when $(M - \mathbb{I})v \in \mathbb{Z}^2$, and also $u^t\epsilon(M - \mathbb{I})\mathbf{K} = [(\mathbb{I} - M)u]^t\epsilon M\mathbf{K} \in \mathbb{Z}$. Note also that since ϵ is antisymmetric as in (5.44), we have $v^t\epsilon M v = v^t\epsilon(M - \mathbb{I})v$.

The phase $\exp\left(-\overline{k}\pi i v^t\epsilon M v\right)$ has a nice geometrical interpretation (analogous to the one discussed in §3.7 of [274] for $M = S$). The expression

$$-\frac{1}{2}v^t\epsilon M v = \frac{1}{2}v^t\epsilon M^{-1}v$$

is the area of a triangle in $\mathbb{R}^2$ with sides given by the vectors v and $M^{-1}v$. To see how this is related to $\mathcal{T}$, consider a string worldsheet (i.e., an X field configuration) that interpolates between the states $|0\rangle$ (a string at $v = 0$ for say $\sigma_2 = 0$) and $|v\rangle$ (for $v \neq 0$ and $\sigma_2 > 0$). We can realize it by constructing a section of the mapping torus with $\mathbf{x} = \zeta v$ and then letting $\zeta \in [0,1]$ and $\theta \in (0,1)$ be the coordinates of the worldsheet (i.e., identify θ with σ_1, and ζ

with σ_2). If we attach to this surface Σ the triangle with vertices $\{0, v, M^{-1}v\}$, we obtain a surface whose boundary is the union of three loops: the loop corresponding to string state $|0\rangle$, the loop corresponding to string state $|v\rangle$, and the loop from $(0, v)$ to $(0, M^{-1}v) \sim (1, v)$ at constant $\theta = 0$, which is a closed loop thanks to (5.137) and (5.138). If we now consider the scattering amplitude of an inelastic scattering process with two string states $|0\rangle$ going into two final string states $|v\rangle$ and $|-v\rangle$:

$$|0\rangle \otimes |0\rangle \to |v\rangle \otimes |-v\rangle \,, \tag{5.142}$$

then it is calculated in string theory by a path integral over worldsheets Σ with four boundary components corresponding to the four string states $|v\rangle$, $|-v\rangle$ and $|0\rangle$'s (wrapped twice with opposite orientation). Since the duality operation $\mathcal{T}^{\overline{k}}$ acts on the Kalb-Ramond field B as $B \to B + \pi\overline{k} d\mathbf{x}^t \wedge \epsilon d\mathbf{x}$, it multiplies the scattering amplitude by the phase

$$\exp\left(i \int_\Sigma B\right).$$

The construction above shows that this phase is $4\pi\overline{k}$ times the area of the triangle with vertices $\{0, v, M^{-1}v\}$, which corresponds to a wavefunction normalization of each of the $|\pm v\rangle$ states by $\exp\left(\overline{k}\pi i v^t \epsilon M^{-1} v\right)$, as required by (5.141). This explains the physical origin of the $\pm$ sign ambiguity in (5.134), since the process (5.142) requires two states for charge conservation.[13]

We can now recover the partition function (5.123) by calculating

$$\mathrm{Tr}_{\mathcal{H}_M}\left(\mathcal{S}\mathcal{T}^{\overline{k}}\right) = \sum_v \langle v| \mathcal{S}\mathcal{T}^{\overline{k}} |v\rangle = \frac{e^{-i\overline{k}\phi}}{\sqrt{|\Lambda/\mathbb{Z}^2|}} \sum_v e^{\left(2-\overline{k}\right)\pi i v^t \epsilon (M-\mathbb{I})v}. \tag{5.143}$$

Up to the phase ϕ, this equals (5.123) after the substitution

$$\mathcal{N} = (\mathbb{I} - M)v.$$

Connection with $U(1)^s$ Chern-Simons theory

The quadratic Gauss sum (5.123) can also be expressed as a trace similar to (5.143), but with $\mathcal{S}$ and $\mathcal{T}$ defined as MCG representation generators acting on the Hilbert space of an abelian Chern-Simons theory placed on T^2 [247]. To see this, let us first consider Chern-Simons theory at level $\mathbf{k}_{\rm cs} \in \mathbb{Z}$ with a $U(1)$ gauge group, compactified on $T^2 \times \mathbb{R}$, where $\mathbb{R}$ is the Euclidean time direction and T^2 is a torus parametrized by periodic coordinates $0 \le x_1, x_2 < 1$. The action is

$$I = \frac{\mathbf{k}_{\rm cs}}{2\pi} \int A \wedge dA,$$

where A is the $U(1)$ gauge field. It is well-known [290] that the Hilbert space $\mathcal{H}_{U(1)}$ of the ground states of the theory has a $\mathbf{k}_{\rm cs}$-fold degeneracy[14], which we will denote by $|a\rangle$

[13] As explained in [247], the "charges" correspond to the first homology group $H_1(\mathbb{Z})$ of the mapping torus, which is isomorphic to Ξ_0, and $|v\rangle$ has charge v.

[14] Its ground-state degeneracy is $(\mathbf{k}_{\rm cs})^g$ on a genus-g Riemann surface instead [291].

$(a = 0, \ldots, \mathbf{k}_{\rm cs} - 1)$. Let α and β be two fundamental 1-cycles of T^2, where α corresponds to a loop at constant x_2, with x_1 varying from 0 to 1, and β corresponds to a similar loop at constant x_1 with x_2 varying from 0 to 1. Consider the Wilson loop operators

$$W_1 \equiv \exp\left(i \oint_\alpha A\right) \quad \text{and} \quad W_2 \equiv \exp\left(i \oint_\beta A\right). \tag{5.144}$$

Their action on the ground states is given by the "clock" and "shift" matrices:

$$W_1 \left|a\right\rangle = e^{2\pi i a/\mathbf{k}_{\rm cs}} \left|a\right\rangle \ , \qquad W_2 \left|a\right\rangle = \left|a+1\right\rangle \ . \tag{5.145}$$

We will need the action of large diffeomorphisms, generated by $\widehat{\mathcal{T}}$ and $\widehat{\mathcal{S}}$,

$$\widehat{\mathcal{S}} \left|a\right\rangle = \frac{1}{\sqrt{\mathbf{k}_{\rm cs}}} \sum_{b=0}^{\mathbf{k}_{\rm cs}-1} e^{-2\pi i a b/\mathbf{k}_{\rm cs}} \left|b\right\rangle \ , \qquad \widehat{\mathcal{T}} \left|a\right\rangle = e^{-i\pi/12} e^{\pi i a^2/\mathbf{k}_{\rm cs}} \left|a\right\rangle \ . \tag{5.146}$$

Up to the constant phase $e^{-i\pi/4}$, this can be checked by making sure that the commutation relations $\widehat{\mathcal{S}}^{-1} W_i \widehat{\mathcal{S}}$ and $\widehat{\mathcal{T}}^{-1} W_i \widehat{\mathcal{T}}$ are as they should be (for $i = 1, 2$), given the geometrical interpretation of $\widehat{\mathcal{T}}$ and $\widehat{\mathcal{S}}$ as torus MCG generators. The phase $e^{-i\pi/4}$ is determined by requiring $(\widehat{\mathcal{S}}\widehat{\mathcal{T}})^3 = \widehat{\mathcal{S}}^2$, which is the charge conjugation operator, so that we obtain a *linear* instead of a *projective* $SL(2,\mathbb{Z})$ representation. It can be derived more systematically by explicitly writing the ground-state wavefunctions as a function of holonomies of the gauge fields [292, 293], or by recalling the connection between the $U(1)$ Chern-Simons theory and the 2d CFT of a free chiral boson [25]. Note that the equation for $\widehat{\mathcal{T}}$ is ill-defined for odd $\mathbf{k}_{\rm cs}$ (because it is inconsistent with $\left|a\right\rangle = \left|a + \mathbf{k}_{\rm cs}\right\rangle$). In that case only even powers of $\widehat{\mathcal{T}}$ are well-defined.

We now set $\mathbf{k}_{\rm cs} \equiv q$. Up to an $e^{\pi i/4}$ phase, the (complex conjugate of) quadratic Gauss sum appearing on the RHS of (5.17) can then be written as

$$\frac{1}{\sqrt{q}} \sum_{n=0}^{q-1} e^{-2\pi i n^2 p/q} = e^{(p+1)\pi i/12} \sum_{n=0}^{q-1} \left\langle n\right| \widehat{\mathcal{S}}\widehat{\mathcal{T}}^{2+2p} \left|n\right\rangle = e^{(p+1)\pi i/12} \mathrm{Tr}_{\mathcal{H}_{U(1)}} \left(\widehat{\mathcal{S}}\widehat{\mathcal{T}}^{2+2p}\right). \tag{5.147}$$

We will see in Section 5.8 that, up to a phase, (5.147) is also the partition function $\mathcal{Z}$ that we calculated in (5.123), for $M = ST^{q+2}$. In Section 5.8 we will calculate the phase of the partition function in a T-dual formulation and observe that it receives a contribution from a Berry phase that depends on the details of how the complex structure varies with time. We also note that a much deeper analysis of the partition function of Chern-Simons theory on a mapping torus with $SU(2)$ gauge group has been carried out by Jeffrey (see §4 of [294] and §4 of [295]), where the result[15] is similarly given by a trace of the action of M on the Hilbert space and yields a quadratic Gauss sum.

[15] With a particular "canonical" choice of *2-framing* of the mapping torus M_3, i.e., the choice of a homotopy equivalence class of trivialization of of $TM_3 \oplus TM_3$ [296], so that the theory is free of framing anomaly.

To move from the special case of (5.17) to the general case (5.123), we need $U(1)^{\overline{r}}$ Chern-Simons theory on T^2. We first recall some basic facts, and then we explain in Section 5.7 why it is related to (5.123). The Chern-Simons coupling constants are given by a symmetric matrix, which for $\overline{r} > 2$ takes the tri-diagonal form with corners[16]

$$K \equiv \begin{pmatrix} \overline{k}_1 & -1 & 0 & & -1 \\ -1 & \ddots & \ddots & \ddots & \\ 0 & \ddots & \ddots & \ddots & 0 \\ & \ddots & \ddots & \ddots & -1 \\ -1 & & 0 & -1 & \overline{k}_{\overline{r}} \end{pmatrix}, \tag{5.148}$$

and for $\overline{r} = 2$ takes the form

$$K \equiv \begin{pmatrix} \overline{k}_1 & -2 \\ -2 & \overline{k}_2 \end{pmatrix}. \tag{5.149}$$

(It is conventionally called *the K-matrix* in condensed matter literature[17], and is used to describe the $\overline{r}$-component abelian fractional quantum Hall effect [299].) The Hilbert space of $U(1)^{\overline{r}}$ Chern-Simons theory on T^2 with coupling constant matrix K has a basis of states $|\widetilde{v}\rangle$ parametrized by $\widetilde{v} \in \mathbb{Z}^{\overline{r}}$ such that $|\widetilde{v}\rangle = |\widetilde{u}\rangle$ if $\widetilde{v} - \widetilde{u} = K\overline{\mathcal{N}}$ for some $\overline{\mathcal{N}} \in \mathbb{Z}^{\overline{r}}$. Define the lattice

$$\Lambda' \simeq K\left(\mathbb{Z}^{\overline{r}}\right) \equiv \left\{K\widetilde{w} : \widetilde{w} \in \mathbb{Z}^{\overline{r}}\right\} \subset \mathbb{Z}^{\overline{r}}. \tag{5.150}$$

So Λ' is the sublattice of $\mathbb{Z}^{\overline{r}}$ that is generated by the columns of the matrix K. The coset $\mathbb{Z}^{\overline{r}}/\Lambda'$ is a finite abelian group. The Hilbert space of $U(1)^{\overline{r}}$ Chern-Simons theory on T^2 with coupling constant matrix K has a basis of states which can be identified with elements of $\mathbb{Z}^{\overline{r}}/\Lambda'$. Pick a nontrivial generator of $\pi_1(T^2)$, and consider the corresponding $\overline{r}$ Wilson loops acting on the Hilbert space. They form an abelian group which can be identified with $\mathbb{Z}^{\overline{r}}/\Lambda'$.

Next, we define the action of $SL(2,\mathbb{Z})$ on the Hilbert space, as a physical realization of (5.131). From the Chern-Simons perspective, this is the action of the MCG of T^2. We assume that K is even, i.e., all $\overline{k}_i \in 2\mathbb{Z}$ $(i = 1, \ldots, \overline{r})$. The generators act on states as:

$$\mathcal{S}\,|\widetilde{v}\rangle = \frac{1}{\sqrt{|\mathbb{Z}^{\overline{r}}/\Lambda'|}} \sum_{\widetilde{u} \in \mathbb{Z}^{\overline{r}}/\Lambda'} e^{-2\pi i \widetilde{u}^t K^{-1} \widetilde{v}}\,|\widetilde{v}\rangle\,, \quad \mathcal{T}\,|\widetilde{v}\rangle = e^{-i\phi} e^{\pi i \widetilde{v}^t K^{-1} \widetilde{v}}\,|\widetilde{v}\rangle\,, \tag{5.151}$$

generalizing the previous $\widehat{\mathcal{S}}$ and $\widehat{\mathcal{T}}$ actions in $U(1)$ Chern-Simons theory, given by (5.146). The phase ϕ equals $\pi i\overline{r}/12$ if all $\overline{k}_i > 0$, and in general it is $\pi i/12$ times the signature of K. Note that $\mathcal{T}$ is well-defined when K defines an even bilinear form. We will now show how the Chern-Simons picture is isomorphic to the mapping-torus picture.

[16] $U(1)^{\overline{r}}$ Chern-Simons on more general 3-manifolds, such as plumbed 3-manifolds, has been considered in [297, 298].

[17] The ground-state degeneracy of this Chern-Simons theory on a genus-g Riemann surface is $|\det K|^g$ [299].

Isomorphism between the Chern-Simons and mapping torus descriptions

We take the powers $\overline{k}_1, \ldots, \overline{k}_{\overline{r}}$ to match the powers in one of the (non-unique) decompositions of $M \in SL(2,\mathbb{Z})$ into S and T generators:

$$M = ST^{\overline{k}_1} ST^{\overline{k}_2} \cdots ST^{\overline{k}_{\overline{r}}}.$$

Then, it can be shown, using elementary row and column operations, that there exist $P, Q \in PSL(\overline{r},\mathbb{Z})$ (unimodular) so that

$$PKQ = \begin{pmatrix} M-\mathbb{I} & & & & \\ & 1 & & & \\ & & 1 & & \\ & & & \ddots & \\ & & & & 1 \end{pmatrix}$$

is a unique block-diagonal matrix. In other words, $M - \mathbb{I}$ and K have the same *Smith normal form*[18], i.e., according to (5.139) and (5.150), $\Lambda/\mathbb{Z}^2$ is isomorphic to $\mathbb{Z}^{\overline{r}}/\Lambda'$. Now let us construct an explicit isomorphism between them. Define the $(2\overline{r}) \times 2$ matrix

$$\mathcal{J} \equiv \begin{pmatrix} 1 & 0 \\ 0 & 1 \\ 0 & 0 \\ \vdots & \vdots \\ 0 & 0 \end{pmatrix} \in \mathrm{Hom}\left(\mathbb{Z}^2, \mathbb{Z}^{\overline{r}}\right).$$

Now, suppose v satisfies $(M-\mathbb{I})v \in \mathbb{Z}^2$ and define

$$\widetilde{\varphi}(v) = KQ\mathcal{J}v = P^{-1} \begin{pmatrix} M-\mathbb{I} & & & & \\ & 1 & & & \\ & & 1 & & \\ & & & \ddots & \\ & & & & 1 \end{pmatrix} \begin{pmatrix} v \\ 0 \\ 0 \\ \vdots \\ 0 \end{pmatrix} = P^{-1}\mathcal{J}(M-\mathbb{I})v \in \mathbb{Z}^{\overline{r}},$$

implying that $\widetilde{\varphi}(v) \in \mathbb{Z}^{\overline{r}}$ if $(M-\mathbb{I})v \in \mathbb{Z}^2$, so $\widetilde{\varphi}$ is surjective. Its injectivity is due to both P and $M - \mathbb{I}$ being invertible, and $\mathcal{J}^t\mathcal{J} = \mathbb{I}$. Therefore $\widetilde{\varphi}$ is an isomorphism between finite abelian groups $\widetilde{\varphi} : \Lambda/\mathbb{Z}^2 \cong \mathbb{Z}^{\overline{r}}/\Lambda'$ with $\widetilde{\varphi}(v) \equiv \tilde{v}$ (see Appendix A in [247] for more details).

We take (5.151) as the definition of the action of $SL(2,\mathbb{Z})$ on the states. In the basis $|v\rangle$ of Section 5.7 we define the $SL(2,\mathbb{Z})$ action using the isomorphism $\widetilde{\varphi}$. We conjecture that

[18]Here we adopt the uncommon convention that on the diagonal, each lower-right element divides the element upper-left to it, opposite to that in [247].

this definition is the same as formulae (5.140) and (5.141) for the $\mathcal{T}$ and $\mathcal{S}$ generators [with a suitable choice of $\pm$ signs in the matrix elements of (5.140) and (5.141)], and we prove it explicitly in the case $\overline{r} = 2$ in Appendix C.3, with numerical evidence for the $\overline{r} = 3$ case in Appendix C.3.

5.8 Quadratic Reciprocity from double-Janus σ-models

The partition function of the double-Janus σ-model that we discussed in Section 5.6 reduces to a sum (5.123) over the finite abelian group Ξ_0 defined in (5.69). We will now show how, in a special case, $\mathcal{Z}$ reduces to the Gauss sum defined in Section 5.3, and we will follow with a discussion on the general case. We will give a Hilbert space interpretation of (5.123), with σ_2 identified as "time", and we will subsequently argue that the Landsberg-Schaar identity (5.21) can be understood by switching the role of "time" from σ_2 to σ_1.

Quadratic Gauss sum as a special case of $\mathcal{Z}(M, \widetilde{M})$

Taking the special case (5.22):

$$M = ST^{q+2} = \begin{pmatrix} 0 & -1 \\ 1 & q+2 \end{pmatrix}, \qquad \widetilde{M} = \widetilde{S}\widetilde{T}^{2+2p} = \begin{pmatrix} 0 & -1 \\ 1 & 2p+2 \end{pmatrix},$$

we can identify Ξ_0 with $\mathbb{Z}_q$ as follows. Setting

$$\mathcal{N} = \begin{pmatrix} \mathbf{x} \\ \mathbf{y} \end{pmatrix}, \qquad K = \begin{pmatrix} \mathbf{m} \\ \mathbf{n} \end{pmatrix},$$

the identification $\mathcal{N} \sim \mathcal{N} + (\mathbb{I} - M)K$ [see (5.68)] becomes

$$\mathbf{x} \sim \mathbf{x} + \mathbf{m} + \mathbf{n}, \qquad \mathbf{y} \sim \mathbf{y} - \mathbf{m} - \mathbf{n} - q\mathbf{n}.$$

We define $\mathbf{z} \equiv \mathbf{x} + \mathbf{y}$, and use the freedom to choose $\mathbf{m} = -\mathbf{x} - \mathbf{n}$ to set $\mathbf{x} = 0$. Then, $\mathbf{z} \sim \mathbf{z} - q\mathbf{n}$, and so $\mathbf{z}$ can be identified with an element of $\mathbb{Z}_q$. Setting $\mathbf{k} = 2 + 2p$, we then calculate

$$\mathcal{Z} = \frac{1}{\sqrt{q}} \sum_{\mathcal{N} \in \Xi_0} \exp\left[i\pi(2 - \mathbf{k})\mathcal{N}^t \epsilon (\mathbb{I} - M)^{-1} \mathcal{N} \right] = \frac{1}{\sqrt{q}} \sum_{\mathbf{z}=0}^{q-1} \exp\left(-\frac{2\pi i p \mathbf{z}^2}{q} \right), \tag{5.152}$$

as the standard quadratic Gauss sum.

Berry phase

The Landsberg-Schaar identity (5.17) relates Gauss sum of $(4p)^{\text{th}}$ roots of unity to Gauss sum of q^{th} roots of unity. The partition function $\mathcal{Z}$, derived in (5.123), reproduces the

latter sum, as we saw in Section 5.8, and this form is closely associated with a Hilbert space interpretation whereby time is identified with σ_2. We will now show that the other side of the Landsberg-Schaar identity can be interpreted in terms of a different Hilbert space, with time identified with σ_1. In such a Hilbert space interpretation the duality wall at $\sigma_1 = 0$ contributes a trace of M, which has to be multiplied by a Berry phase resulting from the variation of complex structure τ (which we can take to be adiabatic).[19] We will see that the phase of $e^{\pi i/4}$ that appears in (5.17) can be reproduced by a combination of the representation of M on the low-energy Hilbert space and the Berry phase. In calculating the Berry phase, the form of the profile $\tau(\sigma_1)$ is important, and we will see that when $\tau(\sigma_1)$ takes values along a semi-circle in its upper half-plane, as in Section 5.4, the correct phase is reproduced.

In Section 5.4 we have chosen the radii of the σ_1 and σ_2 circles to be equal (and given by $1/2\pi$). This was mostly to avoid a cumbersome notation, and indeed, we can easily allow the radii to be different. The partition function $\mathcal{Z}$ is independent of the radii, thanks to supersymmetry. We will now take the limit that the σ_2 direction is much smaller than the σ_1 circle. In this limit, we can study the Hilbert space of the problem at a fixed σ_1, reduce to ground states, and then introduce the wall at $\sigma_1 = 0$ by inserting the operator representing M on the subspace of ground states. For $0 < \sigma_1 < 1$, the most relevant terms in the action are given by the single-derivative terms (5.80), and we can set $X_0 = X_1$, since the σ_2 circle is assumed to be small, and momentum modes along it are suppressed. Writing $\xi(\sigma_1)$ instead of both X_0 and X_1, we are therefore left with

$$I'_b = \frac{i(2-\mathbf{k})}{4\pi}\int \xi^t \epsilon d\xi, \tag{5.153}$$

where the integral is over σ_1 and ξ is independent of σ_2. We set $q \equiv \mathbf{k} - 2$, and assume $q > 0$. ξ describes a coordinate on T^2, and the Hilbert space of ground states can be identified with that of geometric quantization at level q (i.e., with a symplectic form $\frac{q}{4\pi} d\xi^t \epsilon \wedge d\xi = \frac{q}{2\pi} d\xi^1 \wedge d\xi^2$).

Quantization on a torus at level q is one of the simplest examples of geometric quantization [301, 302, 303]. Our T^2 is parametrized by (ξ^1, ξ^2) with $0 \le \xi^1, \xi^2 < 2\pi$. It is convenient to add the kinetic term to get the Lagrangian of a Landau problem (a particle in a uniform and constant magnetic field) on T^2:

$$I_L = \frac{1}{2\pi}\int \left(\frac{1}{2} m G_{IJ}\dot{\xi}^I\dot{\xi}^J - \frac{iq}{2}\epsilon_{IJ}\xi^I\dot{\xi}^J\right) dt\,, \tag{5.154}$$

where for G_{IJ} we take the metric $ds^2 = \frac{1}{\tau_2}|\tau d\xi^2 - d\xi^1|^2$. The ground states of (5.154) are

[19] A similar Berry phase for fermions (either Dirac or Majorana) on a 3d mapping torus under an adiabatic diffeomorphism appeared in [300].

normalized Landau wavefunctions[20] (independent of m and the area of the T^2):

$$\begin{aligned}\Psi_{j,q}\left(\xi^1,\xi^2\right) &= \frac{1}{2\pi}\left(2q\tau_2\right)^{\frac{1}{4}} e^{-\frac{iq\xi^1\xi^2}{4\pi}} \sum_{n=-\infty}^{\infty} e^{i(nq+j)\xi^1+\pi iq\tau\left(n+\frac{j}{q}-\frac{\xi^2}{2\pi}\right)^2} \\ &= \frac{1}{2\pi}\left(2q\tau_2\right)^{\frac{1}{4}} e^{-\frac{iq\xi^1\xi^2}{4\pi}} e^{\pi i\tau q\left(\frac{\xi^2}{2\pi}\right)^2} \Theta_{j,q}\left(\frac{\xi^1-\tau\xi^2}{2\pi};\tau\right) \end{aligned} \tag{5.155}$$

where the Θ-function is defined as

$$\Theta_{j,q}(u,\tau) \equiv \sum_{n=-\infty}^{\infty} e^{\pi iq\tau\left(n+\frac{j}{q}\right)^2+2\pi iq\left(n+\frac{j}{q}\right)u} \tag{5.156}$$

and is holomorphic in u and τ. In the low-energy limit, the kinetic term in (5.154) can be dropped, and as is well-known, we are left with the Lagrangian that describes a noncommutative T^2 with a symplectic form $\omega = \frac{q}{2\pi} d\xi^1 \wedge d\xi^2$.

Defining the Berry connection in a standard way as

$$(\mathcal{A}_\tau)_{lj} = i\left\langle \Psi_{j,q}\right| \partial_\tau \left|\Psi_{l,q}\right\rangle , \qquad (\mathcal{A}_{\overline{\tau}})_{lj} = i\left\langle \Psi_{j,q}\right| \partial_{\overline{\tau}} \left|\Psi_{l,q}\right\rangle ,$$

we calculate

$$(\mathcal{A})_{lj} = (\mathcal{A}_\tau)_{lj} d\tau + (\mathcal{A}_{\overline{\tau}})_{lj} d\overline{\tau} = -\frac{1}{4\tau_2}\delta_{lj} d\tau_1.$$

We need to calculate the Berry phase along the path that τ takes, as σ_1 varies from 0 to 1. We parametrize the arc of the semicircle described at the end of Section 5.4 (see [233, 247, 248]) in terms of the variable ψ and parameters a and D, introduced in [233]:

$$\tau = a + 4\pi D e^{2i\psi},$$

where

$$a = \frac{\mathbf{a}-\mathbf{d}}{2\mathbf{c}}, \qquad 4\pi D = \frac{\sqrt{(\mathbf{a}+\mathbf{d})^2-4}}{2|\mathbf{c}|},$$

Defining ψ_0 and ψ_1 as the values of the phase ψ at the start and end of the arc, i.e.,

$$\tau(0) = a + 4\pi D e^{2i\psi_0}, \qquad \tau(1) = \frac{\mathbf{a}\tau(0)+\mathbf{b}}{\mathbf{c}\tau(0)+\mathbf{d}} = a + 4\pi D e^{2i\psi_1},$$

we calculate the phase difference as [247]:

$$e^{i(\psi_1-\psi_0)} = \mathrm{sgn}(\mathbf{a}+\mathbf{d})\frac{|\mathbf{c}\tau(0)+\mathbf{d}|}{\mathbf{c}\tau(0)+\mathbf{d}},$$

and the total Berry phase is easily calculated to be

$$e^{i\int_0^1 \mathcal{A}} = e^{\frac{i}{2}(\psi_1-\psi_0)} = \left[\mathrm{sgn}(\mathbf{a}+\mathbf{d})\frac{|\mathbf{c}\tau(0)+\mathbf{d}|}{\mathbf{c}\tau(0)+\mathbf{d}}\right]^{1/2}. \tag{5.157}$$

The sign of the square root is determined so that $-\frac{\pi}{2} < \frac{1}{2}(\psi_1-\psi_0) < \frac{\pi}{2}$.

[20] They are essentially $1/q$ Laughlin states on a torus as proposed in [301].

Modular transformations of the Landau wavefunctions

To introduce the M-duality wall, we need to examine the behavior of the wavefunction under an $SL(2,\mathbb{Z})$ transformation that acts as

$$\xi^1 \to \mathbf{a}\xi^1 + \mathbf{b}\xi^2\,, \qquad \xi^2 \to \mathbf{c}\xi^1 + \mathbf{d}\xi^2\,, \qquad \tau \to \frac{\mathbf{a}\tau+\mathbf{b}}{\mathbf{c}\tau+\mathbf{d}}\,.$$

The general $SL(2,\mathbb{Z})$ transformation can be composed from the S and T generators, which act on wavefunctions as

$$S: \quad \Psi_{j,q}\left(-\xi^2,\xi^1;-\tfrac{1}{\tau}\right) = e^{-\frac{\pi i}{4}}\left(\frac{\tau}{|\tau|}\right)^{\frac{1}{2}}\frac{1}{\sqrt{q}}\sum_{l=0}^{q-1} e^{-\frac{2\pi i}{q}jl}\Psi_{l,q}(\xi^1,\xi^2;\tau)\,, \tag{5.158}$$

and for even q we have

$$T: \quad \Psi_{j,q}\left(\xi^1+\xi^2,\xi^2;\tau+1\right) = e^{\frac{\pi i j^2}{q}}\Psi_{j,q}\left(\xi^1,\xi^2;\tau\right). \tag{5.159}$$

We note that for any $q\in\mathbb{Z}$ we have

$$\Psi_{j,q}\left(\xi^1+\xi^2,\xi^2;\tau+1\right) = e^{\frac{i\pi j^2}{q}}\frac{1}{2\pi}\left(2q\tau_2\right)^{\frac{1}{4}}e^{-\frac{iq\xi^1\xi^2}{4\pi}}\sum_{n=-\infty}^{\infty} e^{i(qn+j)\xi^1+\pi iq\tau\left(n+\frac{j}{q}-\frac{\xi^2}{2\pi}\right)^2}(-1)^{qn}. \tag{5.160}$$

This is well-defined on the q-dimensional Hilbert space for $q\in 2\mathbb{Z}$, since the RHS is a linear combination of the $\Psi_{j,q}$'s, but for odd $q\in\mathbb{Z}$ only the square T^2 is a well-defined operator on the Hilbert space.

Recovering the Landsberg-Schaar relation

For $M=ST^{q+2}$ and $q=2p$ we combine the two modular transformations (5.158)-(5.159) to get

$$\Psi_{j,2p}\to\left(\frac{\tau}{|\tau|}\right)^{\frac{1}{2}}\frac{e^{-\frac{\pi i}{4}}}{\sqrt{2p}}e^{\frac{\pi i(q+2)j^2}{2p}}\sum_{l=0}^{2p-1}e^{-\frac{\pi i}{p}jl}\Psi_{l,2p}\,. \tag{5.161}$$

In this expression τ is a shorthand for $\tau(0)+q+2$ [since this is the value of τ after T^{q+2} acts on $\tau(0)$], and $\Psi_{l,2p}$ on the RHS is a shorthand for $\Psi_{l,2p}\big(\xi^2+(q+2)\xi^1,-\xi^1;\tau(0)\big)$. The RHS of (5.161) represents the wavefunction at $\sigma_1=1$ (not including the Berry phase yet) after the action by M. To complete the calculation of the partition function, we must multiply the RHS of (5.161) by $e^{-I''}$ [with I'' given in (5.95)], take its inner product with $\Psi_{j,2p}$, sum over j, and multiply by the Berry phase (5.157). Note that the role of I'' is to ensure periodicity in (ξ^1,ξ^2), since the arguments in $\Psi_{l,2p}$ correspond to X at $\sigma_1=1$, while those in $\Psi_{j,2p}$ correspond to X at $\sigma_1=0$, and they can differ by $\mathcal{N}$, as defined in (5.64). Moreover, since

$\Psi_{j,2p}$ is periodic only up to a gauge transformation (in the language of the Landau problem of a particle in a uniform magnetic field), periodicity in (ξ^1, ξ^2) can only be restored by including $e^{-I''}$ which plays the role of a gauge factor. The resulting partition function is

$$\mathcal{Z}' = \frac{e^{-\frac{\pi i}{4}}}{\sqrt{2p}} \sum_{j=0}^{2p-1} e^{\frac{\pi i q j^2}{2p}} = \frac{e^{-\frac{\pi i}{4}}}{\sqrt{2p}} \varrho_p(q)\,.$$

Equating $\mathcal{Z}$ calculated in (5.123) with $\mathcal{Z}'$, we recover the (complex conjugate of the) basic Landsberg-Schaar relation (5.21).

5.9 Identities for generalizations of Gauss sums

In previous sections we saw how the Landsberg-Schaar identity (5.17) is recovered for duality twists of the form $M = ST^{q+2}$ and $\widetilde{M} = \widetilde{S}\widetilde{T}^{2+2p}$, as in Section 5.8. We can get more complicated identities by looking at $SL(2,\mathbb{Z})$ elements which are expressed as longer words, with more S generators in M or $\widetilde{S}$ generators in $\widetilde{M}$. In all cases, the identities that we get are of the schematic form

$$\mathrm{Tr}_{\mathcal{H}_M}(\widetilde{M}) = e^{i\varphi}\mathrm{Tr}_{\mathcal{H}_{\widetilde{M}}}(M),$$

where $\mathrm{Tr}_{\mathcal{H}_M}$ is a trace over the $|\det(\mathbb{I}-M)|$-dimensional Hilbert space $\mathcal{H}_M$ of ground states of the M-twisted circle compactification [whose states correspond to the finite abelian group Ξ_0 defined in (5.69)], and $\mathrm{Tr}_{\mathcal{H}_{\widetilde{M}}}$ is a similar trace over the $|\det\left(\mathbb{I}-\widetilde{M}\right)|$-dimensional Hilbert space $\mathcal{H}_{\widetilde{M}}$ of ground states of the $\widetilde{M}$-twisted circle compactification, and φ is a phase correction (arising from the Berry phase[21] as in Section 5.8).

In some cases we will be able to rewrite the sum (5.123) explicitly, which requires identifying the abelian group Ξ_0 as a direct sum of cyclic groups, and turns out to be of the form $\mathbb{Z}_{d_1} \oplus \mathbb{Z}_{d_2}$. To achieve this we need to calculate the "Smith normal form" of the matrix $\mathbb{I}-M$, i.e., to find matrices $P, Q \in SL(2,\mathbb{Z})$ and unique integers $d_1, d_2 \in \mathbb{Z}$ such that

$$\mathbb{I} - M = P \begin{pmatrix} d_1 & 0 \\ 0 & d_2 \end{pmatrix} Q.$$

We will present a few examples below.

M generated by S and T^2 and $\widetilde{M} = \widetilde{S}\widetilde{T}^{2+q}$

Let us assume that M can be expanded as the word

$$M = ST^{2v_1}ST^{2v_2}\cdots ST^{2v_s}, \qquad \text{with } v_1, \ldots, v_s \text{ nonzero integers.} \tag{5.162}$$

[21] The first place where a Berry phase appears as a multiplicative factor in the partition function is in [304], where each "hedgehog" defect, a singular configuration, of a spin field in a $(2+1)$d antiferromagnet, described by an $O(3)$ NLSM, carries a Berry phase. It is also directly related to the Wess-Zumino term [305]

We will also assume that $\widetilde{M} = \widetilde{S}\widetilde{T}^{2+q}$, with q even. We recall that in $SL(2,\mathbb{Z})$ there are no relations among S and T^2, other than those that follow from inserting an even number of $S^2 = -\mathbb{I}$ in expressions, and therefore if M is of the form (5.162), the decomposition is unique. In fact the subgroup of $SL(2,\mathbb{Z})$ freely generated by S and T^2 is isomorphic to the *Hecke congruence subgroup* $\Gamma_0(2)$. (See Example 3.7 of [30].)

We now get an identity that equates the partition function $\mathcal{Z}$ given in the form (5.123) (with $\mathbf{k} = q-2$), to a partition function calculated by combining the modular transformations of the q ground-state wavefunctions and the Berry phase, as in Sections 5.8-5.8. The result of the latter is

$$\left(\frac{e^{\frac{\pi i}{4}}}{\sqrt{q}}\right)^s \sum_{l_1,\ldots,l_s=0}^{q-1} \exp\left\{-\frac{2\pi i}{q}\left(\sum_{j=1}^{s} v_j l_j^2 + \sum_{j=1}^{s-1} l_j l_{j+1} + l_1 l_s\right)\right\}.$$

The generalized identity for Gauss sums then takes the form

$$\frac{1}{\sqrt{|\Xi_0|}} \sum_{\mathcal{N}\in\Xi_0} \exp\left[-i\pi q \mathcal{N}^t \epsilon (\mathbb{I}-M)^{-1}\mathcal{N}\right] = \frac{e^{\frac{\pi i s}{4}}}{q^{s/2}} \sum_{l_1,\ldots,l_s=0}^{q-1} e^{-\frac{2\pi i}{q}\left(\sum_{j=1}^{s} v_j l_j^2 + \sum_{j=1}^{s-1} l_j l_{j+1} + l_1 l_s\right)}. \tag{5.163}$$

For example, we take $s = 2$ and

$$M = ST^{2v_1}ST^{2v_2} = \begin{pmatrix} -1 & -2v_2 \\ 2v_1 & 4v_1v_2 - 1 \end{pmatrix}.$$

For simplicity, we assume that $v_1, v_2 \geq 1$. Then

$$|\Xi_0| = |\det(\mathbb{I} - M)| = 4(v_1v_2 - 1).$$

The Smith normal form of $\mathbb{I} - M$ is given by

$$\mathbb{I} - M = \begin{pmatrix} 1 & v_2 \\ -2v_1 & 1 - 2v_1v_2 \end{pmatrix} \begin{pmatrix} 2(1 - v_1v_2) & 0 \\ 0 & 2 \end{pmatrix} \begin{pmatrix} 1 & 0 \\ v_1 & 1 \end{pmatrix}.$$

[Note that the leftmost matrix on the RHS is in $SL(2,\mathbb{Z})$.] An element of $\Xi_0 \cong \mathbb{Z}^2/(\mathbb{I} - M)(\mathbb{Z}^2)$ can then be parametrized as

$$\mathcal{N} = \begin{pmatrix} 1 & v_2 \\ -2v_1 & 1 - 2v_1v_2 \end{pmatrix} \begin{pmatrix} \mathbf{n} \\ \mathbf{a} \end{pmatrix} = \begin{pmatrix} \mathbf{n} + v_2\mathbf{a} \\ (1 - 2v_1v_2)\mathbf{a} - 2v_1\mathbf{n} \end{pmatrix},$$

with

$$\mathbf{a} = 0, 1\,, \qquad \mathbf{n} = 0, \ldots, 2(v_1v_2 - 1) - 1.$$

And then we calculate

$$\mathcal{N}^t \epsilon (\mathbb{I} - M)^{-1}\mathcal{N} = \frac{v_1\mathbf{n}^2}{2(v_1v_2 - 1)} - \frac{v_2\mathbf{a}^2}{2}, \tag{5.164}$$

so the LHS of (5.163) can be expressed as

$$\frac{1}{\sqrt{|\Xi_0|}}\sum_{\mathcal{N}\in\Xi_0}\exp\left[-i\pi q\mathcal{N}^t\epsilon(\mathbb{I}-M)^{-1}\mathcal{N}\right]=\frac{1+i^{-qv_2}}{2\sqrt{v_1v_2-1}}\sum_{\mathbf{n}=0}^{2(v_1v_2-1)-1}\exp\left(\frac{i\pi qv_1\mathbf{n}^2}{2(v_1v_2-1)}\right).$$

Setting $a=v_1$, $b=v_2$, and taking the complex conjugate, we find that (5.163) becomes

$$\boxed{-\frac{i}{q}\sum_{m,n=0}^{q-1}e^{\frac{2\pi i}{q}(am^2+bn^2-2mn)}=\frac{1+i^{qb}}{2\sqrt{ab-1}}\sum_{\mathbf{n}=0}^{2ab-3}\exp\left(-\frac{\pi iqa\mathbf{n}^2}{2(ab-1)}\right)}\tag{5.165}$$

for $a,b\in\mathbb{Z}$, $ab>1$, and $q\in 2\mathbb{Z}_+$. This is our first concrete generalization of the Landsberg-Schaar relation, whose proof we include in Appendix C.4. Identity (5.165) is actually a special case of a collection of generalizations of the basic Landsberg-Schaar identity derived by Krazer in the year of 1912 [306] and other authors from then onwards, and the requirement for even q also appears there. In our case it is a requirement that appeared at the end of Section 5.5. We will discuss Krazer's and others' work in Section 5.9. We also note that double quadratic Gauss sums with denominators [q in (5.165)] that are powers of a prime have been evaluated in [307] in terms of the Legendre symbol.

More generalizations

We can obtain more identities by allowing $\widetilde{M}$ to take the more general form

$$\widetilde{M}=\widetilde{S}\widetilde{T}^{2u_1}\widetilde{S}\widetilde{T}^{2u_2}\cdots\widetilde{S}\widetilde{T}^{2u_r},\tag{5.166}$$

with $u_1,\ldots,u_s$ nonzero integers.

We recall that $\widetilde{S}$ and $\widetilde{T}^2$ generate the *theta subgroup* with index-3 in $SL(2,\mathbb{Z})$, as introduced in 1.3.[22].

Inserting the $\widetilde{M}$-twist in the σ_2 direction amounts to inserting r duality walls of the type (5.80), one for each $\widetilde{S}\widetilde{T}^{2u_j}$ factor ($j=1,\ldots,r$). The combined phase factor of modular transformations and the Berry phase, as in Sections 5.8-5.8, now comes out to $\exp\left(\frac{i\pi}{4}sr\right)$.

If we repeat the analysis of Section 5.8 for the system with r duality walls, we get instead of (5.153), a reduced (0+1)d system that describes geometric quantization of T^{2r} with an action given by

$$-\frac{i}{4\pi}\int\sum_{\mathbf{i},\mathbf{j}=1}^{r}\widetilde{K}_{\mathbf{ij}}\xi^t_{\mathbf{i}}\epsilon d\xi_{\mathbf{j}},$$

[22]However, any subgroup $\langle S,T^m\rangle$ with $m>2$ does not have a finite index inside $SL(2,\mathbb{Z})$.

where $\widetilde{K}$ is an $r \times r$ integer coupling constant matrix given by an expression similar to (5.148)-(5.149), which for r takes the form

$$\widetilde{K} \equiv \begin{pmatrix} 2u_1 & -1 & 0 & & -1 \\ -1 & \ddots & \ddots & \ddots & \\ 0 & \ddots & \ddots & \ddots & 0 \\ & \ddots & \ddots & \ddots & -1 \\ -1 & & 0 & -1 & 2u_r \end{pmatrix} , \tag{5.167}$$

and $\xi_{\mathbf{i}}$ ($\mathbf{i} = 1, \ldots, r$) are coordinates on the $\mathbf{i}^{th}$ T^2 factor. For $r = 2$, $\widetilde{K}$ takes the form

$$\widetilde{K} \equiv \begin{pmatrix} 2u_1 & -2 \\ -2 & 2u_2 \end{pmatrix} . \tag{5.168}$$

For example, for $s = r = 2$ we obtain the identity

$$\frac{1}{pq-1}\left[1+(-1)^{sq}\right] \sum_{m,n=0}^{2pq-3} e^{-\frac{\pi i p}{pq-1}(sm^2+tn^2-2mn)} \tag{5.169a}$$

$$= -\frac{1}{st-1}\left[1+(-1)^{tp}\right] \sum_{m,n=0}^{2st-3} e^{\frac{\pi i s}{st-1}(pm^2+qn^2-2mn)} , \qquad \text{for } tq \in 2\mathbb{Z}. \tag{5.169b}$$

where we have set $p = u_1$, $q = u_2$, $s = v_1$, $t = v_2$. The requirement that tq must be even arises as follows. The abelian group Ξ_0 defined in (5.69) turns out to be isomorphic to $\mathbb{Z}_{st-1} \oplus \mathbb{Z}_2^2$ in this case, and the sum over the $\mathbb{Z}_2^2$ factor produces a factor of $\left[1+(-1)^{tq}\right]\left[1+(-1)^{sq}\right]$ on the LHS of (5.169a), while the RHS receives a factor of $\left[1+(-1)^{tq}\right]\left[1+(-1)^{tp}\right]$ instead. We cancelled the common factor of $\left[1+(-1)^{tq}\right]$ by assuming $tq \in 2\mathbb{Z}$. For t and q both odd, the relation in (5.169a) is not generally correct, for example for $s = p = 2$ and $t = q = 1$ the two sides differ by a $(-)$ sign, and for $s = 1$, $p = 3$, $t = q = 1$, the LHS is 8 while the RHS is 0.

Relation to Krazer's, Jeffrey's, Deloup's, and Turaev's reciprocity formulae

Let us now briefly discuss the relationship among the identities we found in Sections 5.9-5.9 and a few known results in the mathematical literature spanning centuries. In the late 19$^{\text{th}}$ century, a univariate formula which slightly generalizes the Landsberg-Schaar identity (5.17) was discovered independently by Cauchy, Dirichlet, and Kronecker [308]:

$$|b|^{-1/2} \sum_{x \in \mathbb{Z}/b\mathbb{Z}} e^{\frac{\pi i a}{b}(x+\omega)^2} = e^{\frac{\pi i}{4}\text{sign}(ab)} |a|^{-1/2} \sum_{x \in \mathbb{Z}/a\mathbb{Z}} e^{-\frac{\pi i b}{a}x^2 - 2\pi i \omega x} , \tag{5.170}$$

where a, b are nonzero integers and $\omega \in \mathbb{Q}$ such that $ab + 2a\omega \in 2\mathbb{Z}$. Later, a version of (5.170) for multivariate Gauss sums was obtained around 1912 by A. Krazer [306, 309, 310]:

$$d^{-\frac{m}{2}} \sum_{x \in (\mathbb{Z}/d\mathbb{Z})^m} e^{\frac{\pi i x^t A x}{d}} = \frac{d^{\frac{m-r}{2}} e^{\frac{\pi i}{4}\sigma(A)}}{|\det A|^{\frac{1}{2}}} \sum_{y \in \mathbb{Z}/A'\mathbb{Z}^m} e^{-\pi i d y^t A'^{-1} y}, \tag{5.171}$$

where d is again a nonzero integer, A is a symmetric $m \times m$ matrix with integer entries, $\sigma(A) \in \mathbb{Z}$ is the signature of A (i.e., the difference between numbers of positive and negative eigenvalues), and either d or A is *even* (i.e., all diagonal entries of A are even). The $r \times r$ symmetric invertible matrix A' with integer entries is determined from A by finding a unimodular matrix P such that $P^t A P = A' \oplus (0_{m-r})$, where 0_{m-r} is the zero matrix of size $m - r$. Equation (5.171) generalizes the case $\omega = 0$ of (5.170) by replacing one of the numbers a and b in the exponents there by an integer-valued quadratic form given by A. Note that the input to the identity is a single bilinear form A and an integer d, because A' is determined by A.

In 1992, Jeffrey studied the semiclassical expansion of $SU(2)$ Chern-Simons partition functions on Lens spaces and torus bundles [294], and discovered a generalization (which was slightly corrected by Deloup and Turaev [311] in 2005):

$$\mathrm{vol}\,(\Lambda^*) \sum_{\lambda \in \Lambda/r\Lambda} e^{i\pi\langle\lambda, B\lambda/r\rangle + 2\pi i\langle\lambda,\psi\rangle} = \left(\frac{\det B}{r^l}\right)^{-1/2} e^{i\pi\sigma(g)/4} \sum_{\mu \in \Lambda^*/B\Lambda^*} e^{-i\pi\langle\mu+\psi, rB^{-1}(\mu+\psi)\rangle}, \tag{5.172}$$

where Λ is a lattice of finite rank l with Λ^* being its dual, $\langle\cdot,\cdot\rangle$ is the inner product on the real vector space $\Lambda_{\mathbb{R}} = \Lambda \otimes_{\mathbb{Z}} \mathbb{R}$, $\psi \in \Lambda_{\mathbb{R}}$, $r \in \mathbb{Z}_{>0}$, and B is a self-adjoint automorphism on $\Lambda_{\mathbb{R}}$ (i.e., a bilinear form). The volume $\mathrm{vol}(\Lambda^*)$ is the absolute value of the determinant of a matrix obtained by expanding a basis of Λ^* in terms of an orthonormal basis of $\Lambda_{\mathbb{R}}$. The symmetric bilinear form $g : \Lambda \times \Lambda \to \mathbb{Z}$ is defined by $g(x, y) = \langle x, B(y)\rangle$ for all $x, y \in \Lambda$, and $\sigma(g)$ is the signature of a diagonal matrix presenting the bilinear extension $\Lambda_{\mathbb{R}} \times \Lambda_{\mathbb{R}} \to \mathbb{R}$ of g. Formula (5.172) extends Krazer's formula in that the lattice to be summed over is now arbitrary, and on both sides there are additional linear terms in ψ in the exponents, whose significance will be discussed in the next paragraph. Notice that there is still only *one single* bilinear form B.

In 1996, independently of Jeffrey, Deloup [312, 313] geometrically generalized Krazer's formula (5.171) (as well as Jeffrey's) by essentially replacing *both* integers a and b in (5.170) with bilinear forms, and applied his result to calculate topological invariants of 3-manifolds, such as Witten-Reshetikhin-Turaev (WRT) invariants (i.e., Chern-Simons partition functions). For integral quadratic forms determined by *two* invertible, even, symmetric matrices $\mathbf{A}$ and $\mathbf{B}$, Deloup's reciprocity theorem relates a Gauss sum with bilinear form $\mathbf{A} \otimes \mathbf{B}^{-1}$ to another Gauss sum with bilinear form $-\mathbf{A}^{-1} \otimes \mathbf{B}$.[23] This identity appears as Theorem 3 in

[23]For an $m \times m$ matrix $\mathbf{A}$ and $n \times n$ matrix $\mathbf{B}^{-1}$, the $(mn) \times (mn)$ matrix $\mathbf{A} \otimes \mathbf{B}^{-1}$ denotes the tensor (Kronecker) product.

[312], and we do not present it here, since it would require quite a few new notations and definitions. In the context of our Section 5.9, $\mathbf{A}$ can be identified with the coupling constant matrix $\widetilde{K}$ (derived from $\widetilde{M}$) of abelian Chern-Simons theory, while $\mathbf{B}$ can be identified with a similar but independent matrix derived from $M = ST^{2v_1}\cdots ST^{2v_s}$:

$$K \equiv \begin{pmatrix} 2v_1 & -1 & 0 & & -1 \\ -1 & \ddots & \ddots & \ddots & \\ 0 & \ddots & \ddots & \ddots & 0 \\ & \ddots & \ddots & \ddots & -1 \\ -1 & & 0 & -1 & 2v_s \end{pmatrix} . \tag{5.173}$$

We note that in a Gauss sum with a bilinear form governed by K^{-1}, the sum would be over the finite abelian group $\mathbb{Z}^n/K(\mathbb{Z}^n)$ [where $K(\mathbb{Z}^n)$ is the sublattice of $\mathbb{Z}^n$ generated by the columns of K]. This abelian group is equivalent to Ξ_0 in (5.69), as shown in Appendix A of [247]. Deloup's reciprocity relation is actually more general, allowing non-even $\mathbf{A}$ and $\mathbf{B}$ by introducing arithmetic "Wu classes". For a quadratic form $\mathbf{x}^t\mathbf{A}\mathbf{x}$ (with $\mathbf{x}\in\mathbb{Z}^n$), a *Wu class* is realized by a constant vector $\mathbf{w}\in\mathbb{Z}^n$ such that $\mathbf{x}^t\mathbf{A}\mathbf{x}+\mathbf{w}^t\mathbf{x}\in 2\mathbb{Z}$ for all $\mathbf{x}\in\mathbb{Z}^n$ [312]. By adding such linear terms (also similarly in Jeffrey's), one overcomes the ambiguity in the definition of Gauss sums in (5.171) for a non-even $\mathbf{A}$. In our context, this suggests a possible extension to twists M and $\widetilde{M}$ beyond the $SL(2,\mathbb{Z})$ form given by (5.166), by inserting operators linear in the bosonic field X introduced in Section 5.4, which would correspond to "vertex operators", but we will not explore this possibility in the present chapter.

In 1998, Turaev further generalized [308] Deloup's formula to capture an arbitrary "rational Wu class" (which means that the Gauss sums are sums of exponentials in quadratic forms on a lattice plus linear terms with rational coefficients that ensure that the exponents are well-defined up to $2\pi i$). Overall, the place of our construction and generalization in Sections 5.9-5.9 is somewhere in between Krazer's/Jeffrey's formula and Deloup's theorem – for example, if we set the duality twists to be $M = ST^{2v_1}ST^{2v_2}$ and $\widetilde{M} = \widetilde{S}\widetilde{T}^{2u_1}\widetilde{S}\widetilde{T}^{2u_2}$, we get bivariate quadratic forms on both sides of the identity (5.169a); the result is a special case of Deloup's formula, but beyond Krazer's formula. In other words, our physical system is able to accommodate two independent bilinear forms, and the identities obtained in (5.165) and (5.169a) are slightly more general than Jeffrey's formula (5.172).

Recently, the corrected formula (5.172) has been extensively used in studying the categorification of WRT invariants [298, 314, 279, 254]. It plays an essential role in the derivation of $\hat{Z}$-invariants, or "*homological blocks*", of plumbed 3-manifolds M_3. The topology of M_3 is encoded in its plumbing graph, hence the linking matrix of the link corresponding to the graph. The colored Jones polynomials of this link, or equivalently the WRT invariant of M_3, is a Laurent polymonial $J[q,q^{-1}]$ in variable[24] $q \equiv \exp\left(\frac{2i\pi}{\mathbf{k}_{\rm cs}+h^\vee}\right)$, which are raised to powers dictated by linking matrix elements. Formula (5.172) then basically converts $J[q,q^{-1}]$

[24] $h^\vee$ is the dual Coxeter number of the gauge group of the pure Chern-Simons theory defined on M_3.

into a linear combination of homological blocks, i.e., a summation over the lattice defined by the linking matrix, whose cokernel determines $H^1(M_3)$.

Finally, for a more comprehensive and technical historical account of the long sequence of Quadratic Reciprocity formulae up to the early 20^{th} century [i.e., just prior to Krazer's formula (5.171)], consult Chapter 1 of [315] or Chapter 4 of [316].

5.10 Discussion and outlook

We have constructed a supersymmetric double-Janus configuration for a 2d σ-model with T^2 target space, where all the moduli are allowed to vary along both coordinates, and we focused on a particular solution of the SUSY conditions whereby the complex structure varies along one direction and the Kähler structure varies along the other. We then placed the 2d double-Janus configuration on T^2 with periodic boundary condition that include $SL(2,\mathbb{Z})$-duality walls. We discovered a nontrivial interaction at the intersection of the duality walls, and we calculated the partition function and showed that it can be expressed as a quadratic Gauss sum. The fermionic and bosonic modes generally describe what might be called "a second quantized supersymmetric quantum mechanics", where the single-particle energy levels are those of a $0+1d$ supersymmetric system with an arbitrary periodic superpotential. The fermionic and bosonic determinants cancel each other, leaving only a number-theoretic quadratic Gauss sum, which we could compute in two different ways, verifying the Landsberg-Schaar relation and obtaining generalizations. Our derivation of the Landsberg-Schaar relation contains somewhat similar ingredients to a method introduced by Armitage and Rogers [317], where quantum mechanics with a toroidal phase space was also considered, although in their approach the physical time was quantized.

Our work here is a prelude to the problem of an $\mathcal{N}=4$ Super-Yang-Mills theory with nonabelian $U(n)$ gauge group compactified on a closed double-Janus configuration with an $SL(2,\mathbb{Z})$-duality twist. As suggested in [247], such a system can be studied by realizing it in terms of a stack of D3-branes and then mapping it to a system of weakly-coupled strings in Type-IIA on a mapping torus. That system can be compactified on another mapping torus, and the work in this chapter provides the partition function of a sector of the weakly-coupled Type-IIA strings. It suggests interesting connections between number theory and partition functions with $SL(2,\mathbb{Z})$-duality walls.

Appendix A

3d Gravity

A.1 Bipartition for the full partition function

In this appendix we justify that inputting j-invariant into the replica trick formula is a legal operation. We need to make sure that the horizon in the $SL(2,\mathbb{Z})$ family of Euclidean BTZ black holes is still at the central cord of their solid tori, so that we can cut along it. Although j-function contains contribution from thermal AdS_3 which contains no black holes, we will see later that this configuration contributes nothing at a high enough finite temperature. For convenience we set $l = 1$.

To see how Euclidean BTZ Schwarzschild coordinates transform under the $SL(2,\mathbb{Z})$ action on τ, we need an intermediate FRW metric for the unexcited (before being quotiented by Γ) AdS_3 with cylindrical topology, similar to the one mainly used in [5]:

$$\begin{aligned} ds^2 &= \cosh^2\rho\, d\Sigma^2 + d\rho^2 \\ &= -\sinh^2\rho\,(du - d\bar{u})^2 + \cosh^2\rho(du + d\bar{u})^2 + d\rho^2 \\ &= \sinh^2\rho\, d\phi^2 + \cosh^2\rho\, dt'^2 + d\rho^2, \end{aligned} \tag{A.1}$$

where $2u \equiv i\phi - t$ and $2\bar{u} \equiv -i\phi - t$ parametrize the domain of discontinuity Σ, and ρ indicates the radial direction.

To obtain a Euclidean BTZ from this, we demand $2u \equiv (t - i\phi)/\tau'$, with $\tau' \equiv -1/\tau = \Phi + i\beta$ the modular parameter for BTZ black hole, and τ the modular parameter of thermal AdS_3. The identification in the BTZ spatial direction is automatic due to the periodicity in the $\mathbb{H}^3$ metric; $\mathrm{Im}\tau'$ represents the time identification because it is the length of the time cycle, and $\mathrm{Re}\tau'$ offers a spatial twist upon that identification, inducing an angular momentum by "tilting" the meridian.[1] Define the Schwarzschild radial coordinate r:

$$\sinh^2\rho = \frac{r^2 - (\mathrm{Im}(1/\tau'))^2}{|\tau'|^2}, \tag{A.2}$$

[1]Situation is almost identical in the thermal AdS_3 (A.1), where $\mathrm{Im}\tau$ specifies the time identification, upon which $\mathrm{Re}\tau$ indicates a spatial twist.

we obtain the Euclidean BTZ black hole in Schwarzschild coordinates for $r \geq \mathrm{Im}(1/\tau')$:

$$ds^2 = N^2 dt^2 + N(r)^{-2} dr^2 + r^2[d\phi + N^\phi(r)dt]^2, \tag{A.3}$$

where

$$N^2(r) = \frac{1}{r^2}\left[r^2 - \left(\mathrm{Im}\,\frac{1}{\tau'}\right)^2\right]\left[r^2 + \left(\mathrm{Re}\,\frac{1}{\tau'}\right)^2\right], \quad N^\phi(r) = \frac{1}{r^2}\left(\mathrm{Re}\,\frac{1}{\tau'})\right)\left(\mathrm{Im}\,\frac{1}{\tau'}\right). \tag{A.4}$$

Now the outer horizon is at $r_+ = \mathrm{Im}(1/\tau')$. When an $SL(2,\mathbb{Z})$ transformation is applied $\tau' \to \tau'' = 1/(c\tau' + d) = \tau/(d\tau - c)$, r becomes

$$r''^2 \to \frac{(c\ \mathrm{Re}\tau' + d)^2 \sinh^2\rho + (c\ \mathrm{Im}\tau')^2 \cosh^2\rho}{|c\tau' + d|^4}. \tag{A.5}$$

It is enough to just think of $1/(c\tau' + d)$ because there are only three independent parameters in (a, b, c, d) due to the constraint $ad - bc = 1$. One has the freedom to choose $a = 0$, which fixes $-bc = 1$, consequently $(a\tau' + b)/(c\tau' + d) = -1/(c^2\tau' + cd)$. Redefine $-c^2 = c$ and $-cd = d$, then we arrive at $1/(c\tau' + d)$. The minus sign in both c and d is not a problem, because (c, d) is equivalent to $(-c, -d)$.

Since $\sinh^2\rho = r^2\beta^2 - 1$, we have $\mathrm{Im}\tau'' = -c\beta/(c^2\beta^2 + d^2)$, $\mathrm{Re}\tau'' = d/(c^2\beta^2 + d^2)$, implying a rotating black hole. Now we need to see if the new r'' is still at the horizon in the Schwarzschild coordinates associated to τ', and it suffices to check that $r''_+ = \mathrm{Im}\tau''$. This is indeed true. Hence no matter what (c, d) we change into, as long as τ and τ'' are $SL(2,\mathbb{Z})-$equivalent, $r'' = r''_+ \equiv \mathrm{Im}\tau$ will be mapped to a segment on z-axis of spherical coordinate system for the upper half $\mathbb{H}^3$, so our cut is still valid.

A.2 TEE from the whole $J(q)$ function

Now we plug the entire J-function as the canonical partition function into (2.29). We start from the definition of j-invariant $j(\tau) = J(\tau) - 744 \equiv E_4^3(\tau)/\Delta(\tau)$, where $\Delta = \eta^{24}(\tau)$ is the normalized modular discriminant. To find the derivative of $J(\tau)$, we make use of the Jacobi theta function $\vartheta(f) \equiv f' - \frac{m}{12}E_2(\tau)f$ [318], where $E_j(\tau)$ is Eisenstein series of weight j and m is the weight of an arbitrary modular form f. Substituting $j(\tau)$ for f, we obtain

$$\frac{d}{d\tau}j(\tau) = \vartheta(j(\tau)) + E_2(\tau)j(\tau). \tag{A.6}$$

We have made use of the fact that the weight of $j(\tau)$ is three times the weight of $E_4(\tau)$ by definition. One easily observes from the right hand side of above equation that the weight of $j(\tau)$ becomes $12 + 2 = 14$ after differentiation. Since the vector space of $SL(2,\mathbb{Z})$ modular forms of weight 14 is spanned by $E_4^2(\tau)E_6(\tau)$ and has complex dimension 1, we must have

$\frac{d}{d\tau}j(\tau) \propto \frac{E_6(\tau)}{E_4(\tau)}j(\tau)$, up to a constant prefactor. This factor can be found by plugging in the first several terms of the $j(\tau)$ function and we finally arrive at[2]

$$\frac{d}{d\tau}j(\tau) = -2\pi i \frac{E_6(\tau)}{E_4(\tau)}j(\tau). \tag{A.7}$$

Plugging into the replica trick equation (2.29) we obtain for the holomorphic part

$$S_{\text{full}}(\tau) = \ln J(\tau) + 2\pi\beta \frac{j(\tau)}{J(\tau)} \frac{E_6(\tau)}{E_4(\tau)}. \tag{A.8}$$

To calculate the ration E_6/E_4, we use the asymptotic formula for the holomorphic Einstein series $G_s(\tau) \equiv 2\zeta(s)E_s(\tau)$, assuming $0 < |\arg\tau| < \pi$ and $\text{Re}(s) > -N+1$ for any positive integer N [319] (Theorem 2):

$$G_s(\tau) = (1+\tau^{-s})(1+e^{\pi i s})\zeta(s) + 2\sin(s\pi)\frac{\zeta(s-1)}{s-1}\tau^{-1} - (1+\cos(s\pi))\,\zeta(s) \tag{A.9}$$

$$+ \sum_{k=1,\,k\text{ odd}}^{N-1} 2\sin(s\pi)\binom{-s}{k}\zeta(s+k)\zeta(-k)\tau^k + \mathcal{O}(|\tau|^N), \quad |\tau| \le 1. \tag{A.10}$$

For both $s = 4, 6$, the second term vanishes at high temperatures $|\tau| \to 0$, and $\sin(s\pi)$ in the summation over k vanishes as well. Switching to the real variable $\beta = -i\tau$, we have $G_4(i\beta) \approx 2\beta^4\zeta(4)$ and $G_6(i\beta) \approx -2\beta^6\zeta(6)$ as $\beta \to 0$. And since in this limit, $j(i\beta) \approx J(i\beta)$, we have for $k = 1$

$$S_{full}(\tau, \bar{\tau}) \approx 2\ln J(\tau) - 4\pi\beta^3, \tag{A.11}$$

where we have taken into account the anti-holomorphic part.

Now we see that if we consider the entire $SL(2,\mathbb{Z})$ family of black holes as well as thermal AdS_3 (the later contributes little at small β), the one-loop contribution to TEE is negative, agreeing with our previous calculations.

A.3 Towards a formulation of Bekenstein-Hawking entropy in strongly coupled AdS_3

In this appendix, we use the proposed duality to compute a gravitational entropy. The resulting expressions, reported in (A.27) at the end of this appendix, resemble the form of the universal subleading correction to the entanglement entropy of the ground states of long-range entangled topological phases in $(2+1)$ dimensions [17, 18].

For this purpose, we consider the genus-one case and use the fact that the gravitational partition function equals that of the modular invariant 2d Ising CFT at the asymptotic

[2]It is also a consequence of applying Ramanujan's identities on E_2, E_4 and E_6 [66].

boundary. We then use Cardy's method [198, 199, 320] to extract a variant of the familiar expression for the entropy. Our suggested expressions are listed in (A.27) below. We first briefly review familiar manipulations of the modular invariant 2d CFT partition function for general central charge c, and specialize to $c = 1/2$ at a suitable point below when we exhibit the new features.

The partition function can be written as

$$Z(\tau,\bar{\tau}) = \mathrm{Tr}_{\mathcal{H}}\; e^{2\pi i\tau(L_0-c/24)}e^{-2\pi i\bar{\tau}\left(\bar{L}_0-c/24\right)} \equiv \mathcal{Z}(\tau,\bar{\tau})e^{-2\pi ic\tau/24}e^{2\pi ic\bar{\tau}/24}, \tag{A.12}$$

where $\mathcal{H}$ denotes the Hilbert space of the CFT (i.e., a choice of pairs of holomorphic and anti-holomorphic primaries), and, when denoting the eigenvalues of L_0 and $\overline{L}_0$ as Δ and $\overline{\Delta}$, the quantity $\mathcal{Z}(\tau,\overline{\tau})$ is related to the density of states $\rho\left(\Delta,\overline{\Delta}\right)$ of the CFT by

$$\mathcal{Z}(\tau,\bar{\tau}) = \sum_{\Delta,\overline{\Delta}} \rho(\Delta,\overline{\Delta})e^{2\pi i\Delta\tau}e^{-2\pi i\bar{\Delta}\bar{\tau}}. \tag{A.13}$$

We can extract the density of states ρ from the partition function by contour integration via the inverse Laplace transformation going from the canonical to the microcanonical ensemble

$$\rho\left(\Delta,\overline{\Delta}\right) = \frac{1}{(2\pi i)^2}\left(\int_{i\epsilon-\infty}^{i\epsilon+\infty} d\tau\right)\left(\int_{i\epsilon-\infty}^{i\epsilon+\infty} d\bar{\tau}\right) q^{-1-\Delta}\overline{q}^{-1-\overline{\Delta}} Z(q,\bar{q}), \tag{A.14}$$

where $q = e^{2\pi i\tau}$ and $\bar{q} = e^{2\pi i\bar{\tau}}$. Using modular invariance $Z(\tau,\bar{\tau}) = Z(-1/\tau,-1/\bar{\tau})$, as well as the definition of $\mathcal{Z}(\tau,\bar{\tau})$ from (A.12), we obtain

$$\begin{aligned}\mathcal{Z}(\tau,\bar{\tau}) &= e^{\frac{2\pi ic}{24}\tau}e^{-\frac{2\pi ic}{24}\bar{\tau}}Z(\tau,\bar{\tau}) = e^{\frac{2\pi ic}{24}\tau}e^{-\frac{2\pi ic}{24}\bar{\tau}}\mathcal{Z}\left(-\frac{1}{\tau},-\frac{1}{\bar{\tau}}\right)\\ &= e^{\frac{2\pi ic}{24}\tau}e^{\frac{2\pi ic}{24}\frac{1}{\tau}}e^{-\frac{2\pi ic}{24}\bar{\tau}}e^{-\frac{2\pi ic}{24}\frac{1}{\bar{\tau}}}\mathcal{Z}\left(-\frac{1}{\tau},-\frac{1}{\bar{\tau}}\right),\end{aligned} \tag{A.15}$$

and we can rewrite the density of states as

$$\rho\left(\Delta,\overline{\Delta}\right) = \int_{i\epsilon-\infty}^{i\epsilon+\infty} d\tau \int_{i\epsilon-\infty}^{i\epsilon+\infty} d\bar{\tau}\; e^{-2\pi i\Delta\tau}e^{2\pi i\overline{\Delta}\bar{\tau}}e^{\frac{2\pi ic\tau}{24}}e^{-\frac{2\pi ic\bar{\tau}}{24}}e^{\frac{2\pi ic}{24\tau}}e^{-\frac{2\pi ic}{24\bar{\tau}}}\mathcal{Z}\left(-\frac{1}{\tau},-\frac{1}{\bar{\tau}}\right). \tag{A.16}$$

The asymptotic form of the density of states for large Δ and $\bar{\Delta}$, of interest to us here, is then obtained from (A.16) by steepest descend: Assuming first that $\mathcal{Z}(-1/\tau,-1/\bar{\tau})$ varies slowly near the saddle point (a fact that we subsequently check to be correct), one finds the saddle point τ_*, $\bar{\tau}_*$ to be located at

$$\tau_* \approx i\sqrt{\frac{c}{24\Delta}}, \quad \bar{\tau}_* \approx i\sqrt{\frac{c}{24\bar{\Delta}}}, \tag{A.17}$$

where $\Delta/c \gg 1$, $\bar{\Delta}/c \gg 1$ was used[3], implying $|\tau_*|, |\bar{\tau}_*| \ll 1$. Substituting back into the integral above yields the "Cardy formula"

$$\log \rho\left(\Delta, \overline{\Delta}\right) \sim 2\pi c \left(\sqrt{\frac{\Delta}{6c}} + \sqrt{\frac{\bar{\Delta}}{6c}}\right), \qquad \left(\text{when } \frac{\Delta}{c} \gg 1, \frac{\bar{\Delta}}{c} \gg 1\right). \tag{A.18}$$

Now we discuss the Ising case with $c = 1/2$. For convenience we make the identification $\{\chi_{1,1}, \chi_{1,2}, \chi_{2,1}\} = \{\chi_1, \chi_\sigma, \chi_\psi\}$. With $\tau = i\,(\beta/L)$, the partition function in (A.12) describes the quantum partition function of thermal AdS_3 , where the spatial cycle has circumference L. In the low-temperature limit (small q, $\tau \to i\infty$), the gravitational system is dominated by the thermal AdS_3 solution, i.e., $Z(\tau, \bar{\tau}) \sim |\chi_{1,1}(\tau)|^2$. In the opposite high-temperature limit, the black hole solutions dominate. Specifically, the BTZ saddle point can be obtained from the thermal AdS_3 saddle by an S modular transformation $\tau \to -1/\tau$. Considering the high-temperature ($\beta \to 0$) limit $\tau \to 0$, where $-1/\tau = i(L/\beta) \to i\infty$, we obtain

$$\begin{aligned} &|\chi_1(\tau)|^2 + |\chi_\sigma(\tau)|^2 + |\chi_\psi(\tau)|^2 = Z_{\text{Ising}}(\tau) = Z_{\text{Ising}}(-1/\tau) \\ &= |\chi_1(-1/\tau)|^2 + |\chi_\sigma(-1/\tau)|^2 + |\chi_\psi(-1/\tau)|^2 \sim |\chi_1(-1/\tau)|^2, \ (-1/\tau \to i\infty). \end{aligned} \tag{A.19}$$

Now we re-write the first line using the action of the modular transformation on the characters

$$\chi_a(\tau) = \sum_{b=1,\sigma,\psi} \mathcal{S}_{a,b}\ \chi_b(-1/\tau). \tag{A.20}$$

The *normalized* modular matrices are

$$\mathcal{S} = \frac{1}{2}\begin{pmatrix} 1 & \sqrt{2} & 1 \\ \sqrt{2} & 0 & -\sqrt{2} \\ 1 & -\sqrt{2} & 1 \end{pmatrix}, \quad \mathcal{T} = e^{-2\pi i/48}\begin{pmatrix} 1 & 0 & 0 \\ 0 & e^{2\pi i/16} & 0 \\ 0 & 0 & -1 \end{pmatrix}. \tag{A.21}$$

Collecting the leading terms in the limit $-1/\tau \to i\infty$,

$$|\chi_a(\tau)|^2 \sim |\mathcal{S}_{a,1}|^2\ |\chi_1(-1/\tau)|^2 + \ldots, \tag{A.22}$$

the first line of (A.19) then reads in this limit

$$\begin{aligned} &|\chi_1(\tau)|^2 + |\chi_\sigma(\tau)|^2 + |\chi_\psi(\tau)|^2 \\ \sim\ &\frac{d_1^2}{\mathcal{D}^2}\ |\chi_1(-1/\tau)|^2 + \frac{d_\sigma^2}{\mathcal{D}^2}\ |\chi_1(-1/\tau)|^2 + \frac{d_\psi^2}{\mathcal{D}^2}|\chi_1(-1/\tau)|^2, \qquad (-1/\tau \to i\infty) \end{aligned} \tag{A.23}$$

where we have made use of the relationship of the quantum dimensions $d_a = \mathcal{S}_{1,a}/\mathcal{S}_{1,1}$, and the total quantum dimension $\mathcal{D}^2 = \sum_a {d_a}^2 = 1/(\mathcal{S}_{1,1})^2$ of the Ising TQFT, with the modular $\mathcal{S}$-matrix (from the Verlinde formula). (A.23) suggests that the three summands in the

[3]Thus $(-1/\tau_*) \to i\infty$ and $(-1/\bar{\tau}_*) \to i\infty$, implying that $\mathcal{Z}(-1/\tau, -1/\bar{\tau}) \to 1$ varies slowly, in agreement with the assumption made above.

second line arise from the corresponding three summands in the first line. Using (A.12), (A.13) and (A.18), we have

$$\begin{aligned} & Z(\tau,\bar{\tau}) = \mathcal{Z}(\tau,\bar{\tau})\; e^{-\frac{2\pi i c}{24}\tau}\; e^{-\frac{2\pi i c}{24}\bar{\tau}} \\ = \;& Z(-1/\tau,-1/\bar{\tau}) = \mathcal{Z}(-1/\tau,-1/\bar{\tau})\; e^{-\frac{2\pi i c}{24}(-1/\tau)}\; e^{-\frac{2\pi i c}{24}(-1/\bar{\tau})} \end{aligned} \tag{A.24}$$

which, in the limit $-1/\tau \to i\infty$, yields

$$\sum_{\Delta,\bar{\Delta}} \rho\left(\Delta,\bar{\Delta}\right) e^{2\pi i\Delta\tau} e^{2\pi i\bar{\Delta}\bar{\tau}} \sim e^{-\frac{2\pi i c}{24}(-1/\tau)}\; e^{-\frac{2\pi i c}{24}(-1/\bar{\tau})} \sim |\chi_1(-1/\tau)|^2, \quad (-1/\tau \to i\infty), \tag{A.25}$$

and we need these expressions here with $c = 1/2$. Comparison with (A.23) suggests that we can identify three different densities of states,

$$\rho_1\left(\Delta,\bar{\Delta}\right) \equiv \frac{d_1^2}{\mathcal{D}^2}\rho\left(\Delta,\bar{\Delta}\right),\; \rho_\sigma\left(\Delta,\bar{\Delta}\right) \equiv \frac{d_\sigma^2}{\mathcal{D}^2}\rho\left(\Delta,\bar{\Delta}\right),\; \rho_\psi\left(\Delta,\bar{\Delta}\right) \equiv \frac{d_\psi^2}{\mathcal{D}^2}\rho\left(\Delta,\bar{\Delta}\right) \tag{A.26}$$

in the regime of large Δ/c and $\bar{\Delta}/c$. Taking the logarithm of (A.26), we arrive at

$$S_a = \left\{\log\rho\left(\Delta,\bar{\Delta}\right) - \log D^2\right\} + \log d_a^2, \qquad \text{where } a = \sigma,\psi. \tag{A.27}$$

Following the interpretation in [51] that non-trivial primaries in the dual CFT correspond to black holes, the expression (A.27) suggests that the different types of black holes labeled by σ and ψ can be distinguished by a subleading constant term in their entropy, apart from the extensive contribution [the term in curly brackets in (A.27)] arising from boundary gravitons dressing the black hole. Here, a black hole dressed by boundary gravitons corresponds to descendant states in the dual CFT. The term in curly brackets in (A.27) is independent of the labels a and, hence, is universal.

We note that, as already mentioned above, these expressions resemble the form of the universal subleading correction to the entanglement entropy of the ground states of long-range entangled topological phases of matter in $(2+1)$ dimensions [17, 18]. Earlier studies of connections between "topological entanglement entropies" and Bekenstein-Hawking entropy of BTZ black holes, from different perspectives, include [44, 321].

A.4 Superselection sectors of angular momenta

In this appendix, we explain the nature of rotation of BTZ black holes at genus one, which is not usually discussed in the literature. The lesson will be general enough to extend to higher genus.

It is well-known that given a modular parameter τ on a torus, which is the asymptotic boundary of the BTZ black hole, its temperature is $\mathrm{Im}\,\tau$, and the angular potential is $\mathrm{Re}\,\tau$, and if $\mathrm{Re}\,\tau = 0$, then it is not rotating. Then what if we shift the purely imaginary τ by an

integer under T? Apparently it becomes rotating, but it is not true, because the Einstein-Hilbert actions of all semiclassical saddles are invariant under T, and we have excluded them when summing over $\Gamma_\infty\backslash SL(2,\mathbb{Z})$. Then what about more general images in $\Gamma_c\backslash SL(2,\mathbb{Z})$? The answer is actually that most of them are rotating due to their real parts.[4]

Since the modulus τ of the boundary torus is only defined up to $SL(2,\mathbb{Z})$ transformations [5], we say that both τ and the shifted τ are in same superselection sector of rotation, which obtains its name due to the following. Generically, different τ's on the upper half plane $\mathbb{H}$ are not connected by $SL(2,\mathbb{Z})$ transformations. For example, take $\tau_1 = i$ and $\tau_2 = 1/3+i/2$. For them to be connected, we need some $\gamma \in SL(2,\mathbb{Z})$, such that

$$\gamma\tau = \frac{ai+b}{ci+d} = 1/3 + i/2 = \tau_2$$

for some $\gamma \in SL(2,\mathbb{Z})$.

However, this is not possible, because this requires

$$\frac{bd+ac}{c^2+d^2} = \frac{1}{3}, \quad \frac{ad-bc}{c^2+d^2} = \frac{1}{2}.$$

The second equation implies that $c, d = \pm 1$. Substituting them into the first equation, we obtain $bd + ac = 2/3$, which is impossible.

A more obvious example is to consider $\tau_1 = i$ and τ_3 with an irrational real or imaginary part. Hence we say that disconnected τ's belong to different superselection sectors, or mathematically speaking, they are in different conformal classes, i.e., they are different points in the moduli space of the boundary torus.

The above description of BTZ angular momentum is consistent with the phase diagram for 3d quantum gravity (not necessarily pure or Einstein) shown in Figure 3b in [5]. Based on the standard tessellation of $\mathbb{H}$ by $SL(2,\mathbb{Z})$ fundamental regions, this phase diagram is a subtessellation obtained by erasing curves which can be crossed without changing the dominant geometry $M_{c,d}$, so all degree 6 vertices become fixed points of $SL(2,\mathbb{Z})$ of order 3. Rotating and non-rotating BTZ black holes can coexist in the same phase, since dominant geometries $M_{c,d}$ for them can have the same 2-tuple (c,d), e.g., all $\operatorname{Im}\tau \geq 1$ saddles belong to one single phase, where $M_{1,0}$ dominates.

For genus two, in a different geometrical limit than the one in Appendix A.8 (e.g., when two regions where three cylinders join each other are folded around the axis perpendicular to the $\mathbb{Z}_2$-symmetry plane in an opposite way[5]), the period matrix Ω develops a real part and the spacetime rotates, but our $Z^{\rm cl}_{\rm vac}$ will stay the same. Analytic continuation of a rotating asymptotic AdS_3 into the Euclidean signature requires a more complicated version

[4]The angular momenta of the "seed" and its $SL(2,\mathbb{Z})$ images are denoted by J and j respectively in [322], and also implicitly in (3.21) in [5]. Spin j is obtained from Fourier transform on $\hat{j}$, defined by $d = d' + \hat{j}c$ where $d' \in \mathbb{Z}/c\mathbb{Z}, \hat{j} \in \mathbb{Z}$, and from (3.19) in [5] it easy to see that j generically exists even if $\operatorname{Re}\tau = 0$.

[5]Simply twisting cylinders along the axis perpendicular to the $\mathbb{Z}_2$-symmetry plane, or tilting them with respect to the same plane will not introduce rotation.

of Schottky double [129], and there is no longer time-reversal symmetry with respect to the $t = 0$ slice. However, as long as the doubling remains, one can calculate Ω using the same replica trick for $\mathbb{Z}_2$ symmetry as in Appendix A.8.

A.5 Partition function of Ising CFT at genus two

The partition function of the 2d Ising CFT can be computed on a Riemann surface Σ_g with arbitrary genus g as the square root of that of the $\mathbb{Z}_2$-orbifold CFT of a free scalar field at central charge $c = 1$ with compactification radius $R = 1$ [141, 142]. It is given by the product of $Z^{\rm qu}$, representing the quantum fluctuations of the compactified scalar field, and a classical part $Z^{\rm cl}$. The latter is the partition sum over the classical solutions in $2g$ winding or soliton sectors [142] around the α and β cycles depicted in Figure 3.3 in Section 3.3 above, and turns out to be given by [141]

$$Z^{\rm cl}(\Omega,\bar\Omega) = 2^{-g} \sum_{\mathbf{a},\mathbf{b}\in\left(\frac{1}{2}\mathbb{Z}\right)^g} \left|\vartheta\begin{bmatrix}\mathbf{a}\\ \mathbf{b}\end{bmatrix}(\Omega)\right|. \tag{A.28}$$

The more subtle quantum factor is [142, 323, 324]

$$Z^{\rm qu}(\Omega,\bar\Omega) = \left(\frac{\det'(-\Delta_G)}{\int_{\Sigma_g}\sqrt{h}\det\left(\mathrm{Im}\Omega\right)}\right)^{-1/4}. \tag{A.29}$$

Here Δ_G is defined as

$$\Delta_G \equiv -\frac{1}{\sqrt{G}}\partial_\mu\sqrt{G}G^{\mu\nu}\partial_\nu. \tag{A.30}$$

It is the scalar Laplacian on real functions[6], i.e., the Laplace-Beltrami operator, and G is the metric on Σ_g. The prime in $\det'$ indicates regularization by omitting zero modes of Δ_G. For genus one, with the standard metric $|d\sigma_1 + \tau d\sigma_2|^2$, the entire expression in (A.29) is simply $Z^{\rm qu}(\tau,\bar\tau) = 1/\left(\sqrt{2}|\eta(\tau)|\right)$, as it appears in standard texts, such as e.g., [135]. For genus $g > 1$, the determinant alone is evaluated as [325, 326, 327, 328]

$$\det{}'\Delta_G = \zeta_S'(1)\exp\left\{(g-1)\left[\ln 2\pi - 1/2 + 4\zeta'(-1)\right]\right\} \approx \zeta_S'(1)e^{0.6762(g-1)}, \tag{A.31}$$

[6] Δ_G equals the natural covariant Laplacians $\Delta_0^\pm$ on $\mathbb{T}^n$, the space of all weight $(n,0)$ tensor fields on Σ_g [325]. Generally $\Delta_n^+ = -2\nabla_{n+1}^z\nabla_z^n = 2\bar\partial_{n+1}\bar\partial_{n+1}^\dagger$ and $\Delta_n^- = -2\nabla_z^{n-1}\nabla_n^z = 2\bar\partial_n^\dagger\bar\partial$, where the covariant derivatives are

$$\nabla_z^n : \mathbb{T}^n \to \mathbb{T}^{n+1}, \quad \nabla_z^n\left(T(dz)^n\right) \equiv (G_{z\bar z})^n\frac{\partial}{\partial z}\left(\left(G^{z\bar z}\right)^n T\right)(dz)^{n+1};$$
$$\nabla_n^z : \mathbb{T}^n \to \mathbb{T}^{n-1}, \quad \nabla_n^z\left(T(dz)^n\right) \equiv G^{z\bar z}\frac{\partial}{\partial\bar z}T(dz)^{n-1},$$

This subtlety is explained here, because in the original papers, the numerator in (A.29) is $\det'(-\nabla^2)$ [142, 324] or $\det'\Delta_0^\pm$ [326, 327], instead of $\det'\Delta_G$.

where $\zeta_S(s)$ and $\zeta(s)$ are Selberg and Riemann zeta functions, respectively. The Selberg zeta function for Σ_g is defined as

$$\zeta_S(s) = \prod_{p \text{ primitive}} \prod_{k=1}^{\infty} \left[1 - e^{-(s+k)l(p)}\right], \tag{A.32}$$

where the primitive p's are the simple closed oriented geodesics on Σ_g annd $l(p)$ is the hyperbolic length of p.

Since the Ising CFT can also be expressed in terms of the CFT of a single non-interacting Majorana fermion species, the classical part in (A.28) is simply proportional to the summation over the partition function for the free Majorana fermion theory of the corresponding spin structure. For example in the case of torus, we have [135]

$$\begin{aligned}
2\sqrt{\eta(\tau)}\ \chi_{1,1}(\tau) &= 2\sqrt{\eta(\tau)}\ \chi_1(\tau) = \vartheta^{1/2}\begin{bmatrix}0\\0\end{bmatrix}(\tau) + \vartheta^{1/2}\begin{bmatrix}0\\1/2\end{bmatrix}(\tau),\\
\sqrt{2\eta(\tau)}\ \chi_{1,2}(\tau) &= \sqrt{2\eta(\tau)}\ \chi_\sigma(\tau) = \vartheta^{1/2}\begin{bmatrix}1/2\\0\end{bmatrix}(\tau),\\
2\sqrt{\eta(\tau)}\ \chi_{2,1}(\tau) &= 2\sqrt{\eta(\tau)}\ \chi_\psi(\tau) = \vartheta^{1/2}\begin{bmatrix}0\\0\end{bmatrix}(\tau) - \vartheta^{1/2}\begin{bmatrix}0\\1/2\end{bmatrix}(\tau).
\end{aligned} \tag{A.33}$$

At genus $g = 2$, there turn out to be ten holomorphic conformal blocks of the Ising theory. As shown in Figure A.1, the three primary fields $a, b, c \in \{1, \sigma, \psi\}$ satisfy the following fusion rules,

$$a \times \bar{a} \to b, \quad c \times \bar{c} \to b, \tag{A.34}$$

where the overbar denotes the anti-particle (and all particles $1, \sigma, \psi$ are their own anti-particle).

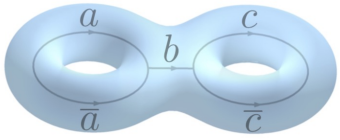

Figure A.1: All possible admissible label sets are $\{a, b, c\} = \{1, 1, 1\}$, $\{\psi, 1, 1\}$, $\{1, 1, \psi\}$, $\{\psi, 1, \psi\}$, $\{\sigma, 1, 1\}$, $\{1, 1, \sigma\}$, $\{\sigma, 1, \psi\}$, $\{\psi, 1, \sigma\}$, $\{\sigma, 1, \sigma\}$, $\{\sigma, \psi, \sigma\}$.

There are sixteen $g = 2$ Riemann theta functions corresponding to the different possible choices of characteristic vectors $\mathbf{a}$ and $\mathbf{b}$, where $\mathbf{a}, \mathbf{b} \in (\frac{1}{2}\mathbb{Z}_2)^2$ - compare with Section 3.3 above. Only the ten even ones are non-vanishing, which are listed in (A.43). In Table A.1,

we present the matrix of basis change[7] from the "free Majorana fermion basis" of square-roots of theta functions (right part of Table) to the classical parts of the basis of the genus-two Ising characters (left part of Table).

$4\chi^{\rm cl}_{111}$	$\vartheta^{1/2}\begin{bmatrix}0&0\\0&0\end{bmatrix}+\vartheta^{1/2}\begin{bmatrix}0&0\\0&1/2\end{bmatrix}+\vartheta^{1/2}\begin{bmatrix}0&0\\1/2&0\end{bmatrix}+\vartheta^{1/2}\begin{bmatrix}0&0\\1/2&1/2\end{bmatrix}$
$4\chi^{\rm cl}_{\psi 11}$	$\vartheta^{1/2}\begin{bmatrix}0&0\\0&0\end{bmatrix}+\vartheta^{1/2}\begin{bmatrix}0&0\\0&1/2\end{bmatrix}-\vartheta^{1/2}\begin{bmatrix}0&0\\1/2&0\end{bmatrix}-\vartheta^{1/2}\begin{bmatrix}0&0\\1/2&1/2\end{bmatrix}$
$4\chi^{\rm cl}_{11\psi}$	$\vartheta^{1/2}\begin{bmatrix}0&0\\0&0\end{bmatrix}-\vartheta^{1/2}\begin{bmatrix}0&0\\0&1/2\end{bmatrix}+\vartheta^{1/2}\begin{bmatrix}0&0\\1/2&0\end{bmatrix}-\vartheta^{1/2}\begin{bmatrix}0&0\\1/2&1/2\end{bmatrix}$
$4\chi^{\rm cl}_{\psi 1\psi}$	$\vartheta^{1/2}\begin{bmatrix}0&0\\0&0\end{bmatrix}-\vartheta^{1/2}\begin{bmatrix}0&0\\0&1/2\end{bmatrix}-\vartheta^{1/2}\begin{bmatrix}0&0\\1/2&0\end{bmatrix}+\vartheta^{1/2}\begin{bmatrix}0&0\\1/2&1/2\end{bmatrix}$

$2\sqrt{2}\chi^{\rm cl}_{\sigma 11}$	$\vartheta^{1/2}\begin{bmatrix}1/2&0\\0&0\end{bmatrix}+\vartheta^{1/2}\begin{bmatrix}1/2&0\\0&1/2\end{bmatrix}$	$2\sqrt{2}\chi^{\rm cl}_{\sigma 1\psi}$	$2\vartheta^{1/2}\begin{bmatrix}1/2&0\\0&0\end{bmatrix}-\vartheta^{1/2}\begin{bmatrix}1/2&0\\0&1/2\end{bmatrix}$
$2\sqrt{2}\chi^{\rm cl}_{11\sigma}$	$\vartheta^{1/2}\begin{bmatrix}0&1/2\\0&0\end{bmatrix}+\vartheta^{1/2}\begin{bmatrix}0&1/2\\1/2&0\end{bmatrix}$	$2\sqrt{2}\chi^{\rm cl}_{\psi 1\sigma}$	$\vartheta^{1/2}\begin{bmatrix}0&1/2\\0&0\end{bmatrix}-\vartheta^{1/2}\begin{bmatrix}0&1/2\\1/2&0\end{bmatrix}$

$2\chi^{\rm cl}_{\sigma 1\sigma}$	$\vartheta^{1/2}\begin{bmatrix}1/2&1/2\\0&0\end{bmatrix}$	$2\chi^{\rm cl}_{\sigma\psi\sigma}$	$\vartheta^{1/2}\begin{bmatrix}1/2&1/2\\1/2&1/2\end{bmatrix}$

Table A.1: The correspondence between (the classical parts of) Ising characters (left) and free fermion characters (right).

The table can be understood intuitively in the pinching limit, where the off-diagonal entries of the period matrix Ω vanish. When $\Omega_{12}\to 0$, all of the above characters except $\chi_{\psi\sigma\psi}$ factorize into a product of two genus-one characters:

$$\chi_{\mu 1\nu}(\Omega)\to\chi_\mu(\Omega_{11})\chi_\nu(\Omega_{22}), \tag{A.35}$$

with $\mu,\nu\in\{1,\sigma,\psi\}$. (For simplicity, we use the notations $\chi_{1,1}\equiv\chi_1$, $\chi_{1,2}\equiv\chi_\sigma$, and $\chi_{2,1}\equiv\chi_\psi$.) The factorization is not possible for $\chi_{\psi\sigma\psi}$ because when the particle b in Figure A.1 is non-trivial, the character is intrinsically genus-two and cannot be viewed as disjoint union of

[7]Table A.1 is the result of an educated guess based on (A.35) below, and its content passed all the consistency checks to our best knowledge. Perhaps it could be derived by considering six-point functions of twist operators of conformal dimension $\frac{c}{6}\left(2-\frac{1}{2}\right)=\frac{1}{8}$ in the orbifold CFT Ising$^{\otimes 2}/\mathbb{Z}_2$ on the Riemann sphere in the spirit of [51, 143].

two genus-one components, even from a topological point of view. For the other nine sectors, (A.35) can be traced back to the factorization of Jacobi theta functions in such a limit:

$$\vartheta \begin{bmatrix} a_1 & a_2 \\ b_1 & b_2 \end{bmatrix} (\Omega) \to \vartheta \begin{bmatrix} a_1 \\ b_1 \end{bmatrix} (\Omega_{11})\ \vartheta \begin{bmatrix} a_2 \\ b_2 \end{bmatrix} (\Omega_{22}). \tag{A.36}$$

A.6 Genus one modular sum revisited

This appendix presents some new results concerning the genus-one case, which aim to explain the mathematical meaning of the factor of eight in (3.20). We will first introduce several necessary concepts.

As discussed in [122], for any 2d rational CFT $\mathcal{C}$ with a finite set $\mathcal{I}$ of primaries, the field extension F of $\mathbb{Q}$ by adjoining the all matrix elements of the modular $\mathcal{S}$ matrix as in (A.21) [329, 330] is a subfield of a cyclotomic field $\mathbb{Q}[\zeta_n]$ for some positive integer n, where $\zeta_n \equiv e^{2\pi i/n}$ is the primitive $n^{\mathbf{th}}$ root of unity, by the Kronecker-Weber theorem in number theory. Following the terminology in algebraic number theory, the smallest n for which $F \subseteq \mathbb{Q}[\zeta_n]$ is called the *conductor* of $\mathcal{C}$ (also defined in [331]), and can be shown [122] to be equal to the *order* N of modular $\mathcal{T}$ matrix. For the Ising CFT of interest to us here, the modular $\mathcal{T}$ matrix is listed in (A.21).

Another important player for us is the *kernel* $\mathcal{K}$ of the *linear* representation of $SL(2,\mathbb{Z})$, defined as the set of modular transformations represented by the identity matrix,

$$\mathcal{K} = \{\gamma \in SL(2,\mathbb{Z}) |\, M_{ij}(\gamma) = \delta_{ij}\}\,, \tag{A.37}$$

where $i, j \in \mathcal{I}$, and $M_{ij}(\gamma)$ is the representation matrix of γ transforming between characters:

$$\chi_i\left(\gamma \cdot \tau\right) = \sum_j M_{ij}(\gamma)\chi_j(\tau). \tag{A.38}$$

$\mathcal{K}$ can be shown [122, 123] to be a congruence subgroup of level N, whose meaning will be clear soon.

Now one can consider the index of the *principal* congruence subgroup $\Gamma(N)$ of $SL(2,\mathbb{Z})$ of level N, as already defined in (1.34), inside the kernel $\mathcal{K}$, i.e., the quantity $|\mathcal{K} : \Gamma(N)|$.[8] Bantay then showed [122], using solely the knowledge of the modular $\mathcal{S}$ matrix, that the conductor of the 2d Ising CFT is $N = 48$, and he further proved[9] that the index $|\mathcal{K} : \Gamma(48)| = 64$.

On the other hand, the formula for the index of $\Gamma(N)$ inside $SL(2,\mathbb{Z})$ is

$$|SL(2,\mathbb{Z}) : \Gamma(N)| = N^3 \prod_{p|N} \left(1 - \frac{1}{p^2}\right), \tag{A.39}$$

[8]For the *principal congruence subgroup* of a Siegel modular group $Sp(2g,\mathbb{Z})$ of level N, the definition is the group of diagonal matrices with entries being 1 mod N [332, 333].

[9]Bantay proved that the index $|\mathcal{K} : \Gamma(N)|$ equals the order of the image of $\mathcal{K}$ under a group homomorphism $\mu_N : SL(2,\mathbb{Z}) \to SL(2,\mathbb{Z})/\Gamma(N)$.

where the product is (as indicated) over all prime numbers p that divide the level N. The above equation gives 73728 for $N = 48$.

Then by the Lagrange's theorem in group theory, we have

$$|SL(2,\mathbb{Z}) : \Gamma(48)| = |SL(2,\mathbb{Z}) : \mathcal{K}| \cdot |\mathcal{K} : \Gamma(48)|, \tag{A.40}$$

so one would naïvely expect that the index $|SL(2,\mathbb{Z}) : \mathcal{K}|$ for the 2d Ising CFT should be $73728/64 = 1152$.

However, there is a subtlety: There exist three distinct ways of lifting a projective representation of $SL(2,\mathbb{Z})$ to a linear representation (i.e., three distinct "linearizations"), see for example [31, 334]. Bantay considered a linear representation in [122], while we are focusing on projective ones because a TQFT (in our case as discussed in Section 3.4, the 3d Ising TQFT, whose algebraic theory is described by the Ising MTC [31]) gives rise to a *projective* representation of the MCG of a Riemann surface [compare with (3.35) and (A.46)-(A.49)], partially due to the non-degeneracy axiom for the modular $\mathcal{S}$ matrix of the TQFT [162, 335, 160]. This is also consistent with the (projective) transformations of Jacobi theta functions under $SL(2,\mathbb{Z})$ mentioned in Appendix A.7 below. After linearization of the projective representation, the order of the image of the $SL(2,\mathbb{Z})$ generator T changes from 16 to 48. Taking into account this factor of three, we finally arrive at the index $384 = 1152/3$, which agrees with the result from our *Mathematica* code.[10]

Now we notice that $\mathcal{K}$ in [122] is *not* the enhanced symmetry group $\Gamma_c^{[g=1]}$ for genus 1 discussed in [119], since the latter is defined as in (3.18), in a similar but different way than in (A.37), i.e., only preserving the vacuum character up to a $U(1)$ phase. $\Gamma_c^{[g=1]}$ turns out to be an index-24 subgroup of $SL(2,\mathbb{Z})$, consistent with Footnote 9, and in [119] Bantay's $\mathcal{K}$ is merely used as an argument justifying the finiteness of the genus one modular sum.

Up to now, our entire discussion is about genus one. Our final remark is that the mathematical meaning of the prefactor 384 in (3.24) in the genus two case is the analogue of the prefactor 8 for the genus one partition function in (3.20).[11]

The factor 384 arises because the subgroup $\Gamma_c^{[g=2]}$ of the MCG $\Gamma_{g=2}$ is the immediate counterpart of the subgroup $\Gamma_c^{[g=1]}$ of the MCG $\Gamma_{g=1} = SL(2,Z)$, both subgroups being denoted by Γ_c in (3.18) as well as below (3.21).

[10] The indices of the $SL(2,\mathbb{Z})$ subgroups which preserve *only one of the three* characters $\chi_{1,1}$, $\chi_{1,2}$, or $\chi_{2,1}$ are 384, 384 and 48, respectively. If the characters are required to be preserved only up to a $U(1)$ phase, then these indices become 24, 24 and 3, respectively.

[11] The fact that the numerical prefactor "384" in (3.24) is the same number as the above-mentioned *index* "384" $= 1152/3$ is probably a coincidence.

A.7 Generators for $Sp(4,\mathbb{Z})$ and the algorithm

The group $Sp(4,\mathbb{Z})$ is minimally generated by K and L with the following representations:

$$K=\begin{pmatrix}1&0&0&0\\1&-1&0&0\\0&0&1&1\\0&0&0&-1\end{pmatrix},\quad L=\begin{pmatrix}0&0&-1&0\\0&0&0&-1\\1&0&1&0\\0&1&0&0\end{pmatrix}. \tag{A.41}$$

They satisfy $K^2=L^{12}=\mathbb{1}_4$ and the following six additional relations [147],

$$\begin{array}{l}\left(L^2X\right)^2=\left(XL^2\right)^2,\quad L\left(L^6X\right)^2=\left(L^6X\right)^2L,\quad \left(KL^5\right)^5=\left(L^6X\right)^2,\\ \left(KL^7KL^5K\right)L=LX,\quad \left(L^2KL^4\right)X=X\left(L^2KL^4\right),\quad \left(L^3KL^3\right)X=X(L^3KL^3),\end{array} \tag{A.42}$$

with $X\equiv KL^5KL^7K=\mathbb{1}_2\otimes\sigma_x$, $L^6=\mathbb{1}_2\otimes\sigma_z$, where σ_i denote the standard three Pauli matrices. Its generalization to arbitrary genus $Sp(2g,\mathbb{Z})$ with at most 3 generators and $3g+5$ relations can be found in [148]. In the following basis of Riemann theta functions

$$\begin{array}{l}\vartheta^{1/2}\begin{bmatrix}0&0\\0&0\end{bmatrix}(\Omega),\ \vartheta^{1/2}\begin{bmatrix}\frac12&0\\0&0\end{bmatrix}(\Omega),\ \vartheta^{1/2}\begin{bmatrix}0&0\\\frac12&0\end{bmatrix}(\Omega),\ \vartheta^{1/2}\begin{bmatrix}0&0\\\frac12&\frac12\end{bmatrix}(\Omega),\ \vartheta^{1/2}\begin{bmatrix}0&\frac12\\0&0\end{bmatrix}(\Omega),\\ \vartheta^{1/2}\begin{bmatrix}\frac12&0\\0&\frac12\end{bmatrix}(\Omega),\ \vartheta^{1/2}\begin{bmatrix}0&\frac12\\\frac12&0\end{bmatrix}(\Omega),\ \vartheta^{1/2}\begin{bmatrix}0&0\\0&\frac12\end{bmatrix}(\Omega),\ \vartheta^{1/2}\begin{bmatrix}\frac12&\frac12\\0&0\end{bmatrix}(\Omega),\ \vartheta^{1/2}\begin{bmatrix}\frac12&\frac12\\\frac12&\frac12\end{bmatrix}(\Omega),\end{array} \tag{A.43}$$

the projective representations of K and L are:

$$\mathcal{K}=\begin{pmatrix}1&0&0&0&0&0&0&0&0&0\\0&1&0&0&0&0&0&0&0&0\\0&0&0&1&0&0&0&0&0&0\\0&0&1&0&0&0&0&0&0&0\\0&0&0&0&0&0&0&0&1&0\\0&0&0&0&0&1&0&0&0&0\\0&0&0&0&0&0&0&0&0&1\\0&0&0&0&0&0&0&1&0&0\\0&0&0&0&1&0&0&0&0&0\\0&0&0&0&0&0&1&0&0&0\end{pmatrix},\quad \mathcal{L}=\begin{pmatrix}0&0&1&0&0&0&0&0&0&0\\1&0&0&0&0&0&0&0&0&0\\0&e^{\pi i/8}&0&0&0&0&0&0&0&0\\0&0&0&0&0&0&0&0&e^{\pi i/8}&0\\0&0&0&1&0&0&0&0&0&0\\0&0&0&0&1&0&0&0&0&0\\0&0&0&0&0&e^{\pi i/8}&0&0&0&0\\0&0&0&0&0&0&1&0&0&0\\0&0&0&0&0&0&0&1&0&0\\0&0&0&0&0&0&0&0&0&e^{3\pi i/8}\end{pmatrix}, \tag{A.44}$$

where $\mathcal{L}$ is of order 24 and $\mathcal{K}$ is of order 2. $Z_{\rm vac}^{\rm cl}$ in (3.22) is invariant under the action of $\mathcal{K}$, just like the torus vacuum seed $Z_{\rm vac}$ is invariant under T of $SL(2,\mathbb{Z})$. Additionally, $Z_{\rm vac}^{\rm cl}$ is also invariant under $\mathcal{L}^6$.

We ignore the factor $\det(C\Omega+D)^{-1}$ in the modular transformation of Riemann theta functions (3.35), because it is expected to be absorbed in the overall quantum factor for the characters (A.29), similar to the Dedekind eta function in the torus case [135]. The phase $\epsilon(\gamma)$ in (3.35) has no effect because it is an overall factor independent of Ω, which drops out when taking the norm in the expression for $Z_{\rm vac}^{\rm cl}$.

Below we present the pseudocode similar to those used in an arbitrary solvable "word problem" for the MCG [150]. $\mathcal{K}[\,\cdot\,]$ or $\mathcal{L}[\,\cdot\,]$ means that $\mathcal{K}$ or $\mathcal{L}$ acts on the period matrix Ω in all *seed*, *seed*1 and *seed*2.

Algorithm 1

1: Inititalize $\mathcal{K}$, $\mathcal{L}$, $seed1 := \chi_{1,1}$
2: $seed = \mathcal{K}[seed1]$
3: **for** $n = 0$, $n \leq 23$, $n++$ **do**
4: $\quad temp = \mathcal{L}[seed]$
5: $\quad$ **if** $temp \notin seed$, **then** do nothing
6: $\quad$ **else** $seed$ =Append [$seed$, $temp$]
7: $seed2 = seed$
8: **if** Length [Intersection [$seed1$, $seed2$]]<Length [$seed2$] **then** $seed1 = seed2$, and repeat from 2 to 8
9: **else** stop
10: Print Z_{grav} :=Total [$seed2$]

Finally, we comment on the "translational" subgroup $\Gamma_\infty^{[g=2]}$ of $Sp(4,\mathbb{Z})$. The group gets its name from its genus-one counterpart, where $\Gamma_\infty^{[g=1]}$ is generated by the translation $T : \tau \to \tau + 1$. (The superscripts $\cdot^{[g=1]}$ and $\cdot^{[g=2]}$ specify the corresponding genus.) As in the genus one case, the group $\Gamma_\infty^{[g=2]}$ is the "classical analogue" of $\Gamma_c^{[g=2]}$. There is no canonical choice for $\Gamma_\infty^{[g=2]}$ on genus two surfaces, but one possibility is generated (not necessarily minimally) by

$$\begin{aligned} &\tilde{S} = \left(L^6 X\right)^3, \quad \tilde{T} = XKL^6X, \\ &T_1 = XT_2X, \quad T_2 = L^{-1}XL^{-2}XL^{-2}, \quad T_3 = L^8KL^4X\tilde{S}, \end{aligned} \tag{A.45}$$

with the same X as before. Here T_1, T_2 and T_3 respectively shift the entries Ω_{11}, Ω_{22} and Ω_{12} by 1; each of $\tilde{S}$ and $\tilde{T}$ acting on Ω as in (3.30) performs the conjugation $\Omega \to M\Omega M^{-1}$, where M denotes the generator S or T of $SL(2,\mathbb{Z})$ [52]. In the same basis (A.43), the 10-dimensional projective representations of the generators listed in (A.45) are:

$$\tilde{\mathcal{T}}_1 = \begin{pmatrix} 0 & 0 & 1 & 0 & 0 & 0 & 0 & 0 & 0 & 0 \\ 0 & e^{\pi i/4} & 0 & 0 & 0 & 0 & 0 & 0 & 0 & 0 \\ 1 & 0 & 0 & 0 & 0 & 0 & 0 & 0 & 0 & 0 \\ 0 & 0 & 0 & 0 & 0 & 0 & 0 & 1 & 0 & 0 \\ 0 & 0 & 0 & 0 & 0 & 0 & 1 & 0 & 0 & 0 \\ 0 & 0 & 0 & 0 & 0 & e^{\pi i/4} & 0 & 0 & 0 & 0 \\ 0 & 0 & 0 & 0 & 1 & 0 & 0 & 0 & 0 & 0 \\ 0 & 0 & 0 & 1 & 0 & 0 & 0 & 0 & 0 & 0 \\ 0 & 0 & 0 & 0 & 0 & 0 & 0 & 0 & e^{\pi i/4} & 0 \\ 0 & 0 & 0 & 0 & 0 & 0 & 0 & 0 & 0 & e^{\pi i/4} \end{pmatrix}, \tag{A.46}$$

$$\tilde{\mathcal{T}}_2 = \begin{pmatrix} 0&0&0&0&0&0&0&1&0&0\\ 0&0&0&0&0&1&0&0&0&0\\ 0&0&0&1&0&0&0&0&0&0\\ 0&0&1&0&0&0&0&0&0&0\\ 0&0&0&0&e^{\pi i/4}&0&0&0&0&0\\ 0&1&0&0&0&0&0&0&0&0\\ 0&0&0&0&0&0&e^{\pi i/4}&0&0&0\\ 1&0&0&0&0&0&0&0&0&0\\ 0&0&0&0&0&0&0&0&e^{\pi i/4}&0\\ 0&0&0&0&0&0&0&0&0&e^{\pi i/4} \end{pmatrix}, \tag{A.47}$$

$$\tilde{\mathcal{T}}_3 = \begin{pmatrix} 1&0&0&0&0&0&0&0&0&0\\ 0&0&0&0&0&1&0&0&0&0\\ 0&0&1&0&0&0&0&0&0&0\\ 0&0&0&1&0&0&0&0&0&0\\ 0&0&0&0&0&0&1&0&0&0\\ 0&1&0&0&0&0&0&0&0&0\\ 0&0&0&0&1&0&0&0&0&0\\ 0&0&0&0&0&0&0&1&0&0\\ 0&0&0&0&0&0&0&0&0&-i\\ 0&0&0&0&0&0&0&0&-i&0 \end{pmatrix}, \tag{A.48}$$

$$\tilde{\mathcal{S}} = \begin{pmatrix} 1&0&0&0&0&0&0&0&0&0\\ 0&0&0&0&1&0&0&0&0&0\\ 0&0&0&0&0&0&0&1&0&0\\ 0&0&0&1&0&0&0&0&0&0\\ 0&1&0&0&0&0&0&0&0&0\\ 0&0&0&0&0&0&1&0&0&0\\ 0&0&0&0&0&1&0&0&0&0\\ 0&0&1&0&0&0&0&0&0&0\\ 0&0&0&0&0&0&0&0&1&0\\ 0&0&0&0&0&0&0&0&0&1 \end{pmatrix}, \quad \tilde{\mathcal{T}} = \begin{pmatrix} 1&0&0&0&0&0&0&0&0&0\\ 0&0&0&0&0&0&0&0&1&0\\ 0&0&1&0&0&0&0&0&0&0\\ 0&0&0&0&0&0&0&1&0&0\\ 0&0&0&0&1&0&0&0&0&0\\ 0&0&0&0&0&0&0&0&0&1\\ 0&0&0&0&0&0&1&0&0&0\\ 0&0&0&1&0&0&0&0&0&0\\ 0&1&0&0&0&0&0&0&0&0\\ 0&0&0&0&0&1&0&0&0&0 \end{pmatrix}. \tag{A.49}$$

A.8 Genus two long-cylinder limit

In this appendix, we provide some details regarding the low-temperature or the long-cylinder limit of the Ising and the $c = 3l/2G_N = 1/2$ gravity partition functions on genus two. As reviewed in (3.23), a genus-two Riemann surface with a $\mathbb{Z}_2$ time-reflection symmetry can be constructed as a complex curve by the "replica trick" on two copies of real lines with six branch points, i.e., three finite intervals [144, 336]. For computational convenience, we

choose an alternative but equivalent expression other than (3.23):

$$y(z)^2 = u(z)v(z), \quad u(z) = \prod_{i=1}^{3}(z - x_{2i-2}), \quad v(z) = \prod_{i=1}^{2}(z - x_{2i-1}), \tag{A.50}$$

where $y, z \in \mathbb{C}^2$, and we have used a conformal map to fix three of the six branch points as cross ratios:

$$x(z) \equiv \frac{(u_1 - z)(u_2 - u_3)}{(u_1 - u_2)(z - u_3)}, \tag{A.51}$$

such that $x(u_1) = 0$, $x(u_2) = 1$, and $x(u_3) \mapsto$ infinity, which we denote as z_∞. For simplicity we have denoted $x(u_n) \equiv x_{2n-2}$, $x(v_n) \equiv x_{2n-1}$, $n = 1, 2, 3$.

This curve has a non-normalized basis of holomorphic 1-forms:

$$\omega_i = \frac{z^{i-1}}{y(z)}dz, \quad i = 1, 2. \tag{A.52}$$

Given the canonical homology basis $\{\alpha_i, \beta_j\}$ on the Riemann surface as in (3.27), two 2-by-2 non-symmetric matrices can be defined on the surface

$$\mathcal{A}_{j,i} \equiv \oint_{\alpha_i} \omega_j, \quad \mathcal{B}_{j,i} \equiv \oint_{\beta_i} \omega_j. \tag{A.53}$$

The corresponding period matrix of the surface can then be expressed as

$$\Omega = \mathcal{A}^{-1} \cdot \mathcal{B}, \tag{A.54}$$

separating the contributions from integrals along the α and β cycles. (Notice that here we used a different normalization on ω than the one in (3.28).)

Next, we perform a basis transformation by decomposing $\{\alpha_i, \beta_i\}$ into auxiliary cycles $\{\alpha_i^{\rm aux}, \beta_i^{\rm aux}\}$,

$$\alpha_i = \sum_{k=1}^{i} \alpha_k^{\rm aux}, \quad \beta_i = \beta_i^{\rm aux}. \tag{A.55}$$

Correspondingly, one can define following the matrices, which are simply integrals of the one-forms (A.52) along the auxiliary cycles

$$\mathcal{A}_{j,i} = \sum_{k=1}^{i} \left(\mathcal{A}^{\rm aux}\right)^{j,k}, \quad \mathcal{B}_{j,i} = \left(\mathcal{B}^{\rm aux}\right)^{j,k}. \tag{A.56}$$

and finally [144, 336],

$$\begin{aligned} \left(\mathcal{A}^{\rm aux}\right)_{j,i} &\equiv \oint_{\alpha_i^{\rm aux}} \omega_j = -2(-1)^{3-i}\mathcal{F}_j \,|_{x_{2i-2}}^{x_{2i-1}}, \\ \left(\mathcal{B}^{\rm aux}\right)_{j,i} &\equiv \oint_{\beta_i^{\rm aux}} \omega_b = -2i(-1)^{3-i}\mathcal{F}_j \,|_{x_{2i-1}}^{x_{2i}}, \quad i = 1, 2. \end{aligned} \tag{A.57}$$

Here $\mathcal{F}_j\,|_a^b$ can be expressed in terms of the fourth Lauricella function $F_D^{(3)}$ [337], a generalization of the hypergeometric function ${}_2F_1$,

$$\begin{aligned}\mathcal{F}_j\,|_a^b &= \int_0^1 dt\ \frac{(b-a)[(b-a)t+a]^{j-3/2}}{\prod_{k=2}^3 |(b-a)t-(x_{2k-2}-a)|^{1/2}\prod_{k=1}^2 |(b-a)t-(x_{2k-1}-a)|^{1/2}}\\ &= \frac{\pi a^{j-3/2}}{\prod^3_{\substack{k=2\\ x_{2k-2}\neq a}} |x_{2k-2}-a|^{1/2}\prod^2_{\substack{l=1\\ x_{2k-2}\neq a}} |x_{2l-1}-a|^{1/2}} F_D^{(3)}\left(\frac{1}{2},\frac{3}{2}-j,\frac{1}{2},\frac{1}{2};1;\mathbf{q}^{(a,b)}\right),\end{aligned} \tag{A.58}$$

where the 3-dimensional vector $\mathbf{q}^{(a,b)}$ has components:

$$\mathbf{q}_\xi^{(a,b)} \equiv \frac{b-a}{x_\xi - a}, \quad \xi \in \{0,1,2,3,4\}\backslash\{\eta | x_\eta \neq a,b\}, \tag{A.59}$$

and $F_D^{(3)}$ has the integral representation:

$$F_D^{(3)}(a,b_1,b_2,b_3;c;q_1,q_2,q_3) = \frac{\Gamma(c)}{\Gamma(a)\Gamma(c-a)}\int_0^1 dt \frac{t^{a-1}(1-t)^{c-a-1}}{\prod_{j=1}^3(1-q_j t)^{b_j}}. \tag{A.60}$$

Taking all $(x_{2i-1}-x_{2i-2}) \equiv \epsilon_i$ to be small for $i \in \{1,2,3\}$, which is required by the long-cylinder limit, we obtain

$$\mathcal{A} = -\frac{2\pi}{\sqrt{z_\infty}}\begin{pmatrix}1 & 0\\ 0 & -1\end{pmatrix}, \quad \mathcal{B} = \frac{2i}{\sqrt{z_\infty}}\begin{pmatrix}\log\epsilon_1\epsilon_2 & -\log\epsilon_2\\ \log\epsilon_2 & -\log\epsilon_2\end{pmatrix}, \tag{A.61}$$

and the period matrix is

$$\Omega = \frac{i}{\pi}\begin{pmatrix}-\log\epsilon_1\epsilon_2 & \log\epsilon_2\\ \log\epsilon_2 & -\log\epsilon_2\end{pmatrix}. \tag{A.62}$$

Inserting this into the equations (A.28) and (3.22), we find that they match each other at leading order, which further justifies our expression for $Z^{\rm cl}_{\rm vac}$. The subleading terms will not agree, because the contribution of other sectors will enter.

One remark is that, in this appendix we have used a non-rotating, i.e., purely imaginary period matrix for convenience. Adding an angular potential complicates the calculations but does not affect the match between the low temperature limits of $Z^{\rm cl}_{\rm vac}$ and $Z^{\rm cl}$, which is robust against arbitrarily large angular momenta due to the cancellation between fast oscillating phases in Riemann theta functions. For a review of the rotating case in general, see the following Appendix A.4.

For genus greater than 2 with $\mathbb{Z}_2$ symmetry, one can allow for more branch points and take two copies, and follow the general treatment in [144] to obtain Ω similarly.

A.9 Extended property F of the Ising theory

Unitary $(2+1)$d-TQFTs are well-captured, physically, by anyon models, or, mathematically, by unitary modular tensor categories. The *extended property F conjecture* asserts that all representations of MCGs from a TQFT would have finite images if the total quantum dimension $D^2 = \sum_i d_i^2$ is an integer. For the original non-extended *property F conjecture* on braid groups instead of MCGs, see [338, 339]. In this appendix, we prove the Ising TQFT extended case.

The Ising theory has three labels or anyon types $\{1, \sigma, \psi\}$. The same fusion rule can be realized by 8 different anyon models [340] with chiral central charges $c = \frac{a}{2}, a = 1, 3, ..., 15$, where $c = \frac{1}{2}$ for Ising TQFT. The results in this appendix apply to all 8 theories.

The Ising TQFT can be constructed explicitly using Temperley-Lieb algebras and Jones-Wenzl (JW) projectors with $A = ie^{\pm\frac{2\pi i}{16}}$. The three anyon types $\{1, \sigma, \psi\}$ then correspond to the JW projectors $\{p_i\}, i = 0, 1, 2$. For the notations and terminologies, see for example [161]. The MCG representations are explicitly described in [341].

To understand the representations of MCGs Γ_g from the Ising TQFT, we will use four different bases of the Hilbert spaces $V_{\text{iTQFT}}(\Sigma_g)$: the defining basis $\{e^{\mathbf{a}}_{\mathbf{b}}\}$, the standard basis $\{v^{\mathbf{i}}_{\mathbf{k}}\}$, the geometric basis $\{u^{\mathbf{i}}_{\mathbf{k}}\}$, and the spin basis $\{\omega^{\mathbf{m}}_{\mathbf{l}}\}$—the last three bases are defined and used in [146], and the defining basis is used in [341]. The defining basis and standard basis consist of labeled fusion graphs using $\{1, \sigma, \psi\}$. The defining basis is the one as in Figure 3.7, while the standard basis can be obtained from Figure 3.7 by performing F-moves at all w_i-labeled edges. The geometric basis consists of skeins of simple closed curves; the spin basis consists of even spin structures (those with Arf invariant 0) or even quadratic enhancements of the intersection forms.

The four bases can be changed to each other through the following explicit formulae [146]. From the geometric to the standard, $v^{\mathbf{i}}_{\mathbf{k}} = \sum_{\mathbf{i}' \leq \mathbf{i}} \alpha_{\mathbf{i}'} u^{\mathbf{i}'}_{\mathbf{k}}$, where $\alpha_{\mathbf{i}'} = (-[2]_A)^{\frac{g-\sum(i_n - i'_n)}{2}}$, where $[k]_A \equiv \frac{A^{2k}-A^{-2k}}{A^2-A^{-2}}$ is the quantum integer, and $A = ie^{-2\pi i/16}$ for Ising TQFT. From the standard to the spin, $\omega^{\mathbf{m}}_{\mathbf{l}} = \sum_{\mathbf{k}} \alpha_{\mathbf{k}} v^{\mathbf{i}}_{\mathbf{k}}$, where $i_n = m_n l_n + 1$, $k_n = 2$ if $m_n = 1$, $k_n = 1$ or 3 if $m_n = 0$, and $\alpha_{\mathbf{k}} = (-1)^l 2^{\frac{\sum m_n - g}{2}}, l = \sum \delta_{3,k_n} l_n$. To go from the defining to the standard, we first note that the label w_1 in Figure 3.7 would be either 1 or ψ. Inductively, we obtain a change of basis by applying F moves.

Any self-diffeomorphism f of a surface Σ_g induces an action on the $\mathbb{Z}_2$-homology group $H_1(\Sigma_g; \mathbb{Z}_2)$ of Σ_g. The images of all such $\{f\}$ form $Sp(2g, \mathbb{Z}_2)$. The kernel consists all diffeomorphims that fix $H_1(\Sigma_g; \mathbb{Z}_2)$, which form a subgroup D_g of Σ_g. It is proved in [146] that D_g is generated by all squares of Dehn twists on simple closed curves.

Any simple closed curve s on Σ_g defines a function from the set of spin structures ω of Σ_g to $\mathbb{Z}_2$ by sending ω to $\omega(s)$. To prove the finiteness of all representations, it is convenient to use the spin basis. In this basis, the square of Dehn twist on any simple closed curve s is a diagonal matrix with non-zero entries $(-A^6)^{\omega(s)}$. Since A^6 is of order 8, the image of D_g is an abelian group inside $\mathbb{Z}_8^N$ for some N.

It follows that we have an exact sequence:

$$1 \to \rho_{\text{iTQFT}}(D_g) \to \rho_{\text{iTQFT}}(\Gamma_g) \to Sp(2g, \mathbb{Z}_2) \to 1,$$

where $\rho_{\text{iTQFT}}(D_g)$ is a subgroup of $\mathbb{Z}_8^N$ for some N.

A.10 Proof of the theorem on page 71

Here we fill out the full details of the proof on page 71 of this thesis.

Theorem Suppose that the group representation $\rho_g(\Gamma_g)$ of Γ_g is an infinite set of $U(N_g)$ matrices, then for any small $\epsilon > 0$, either

(1) $\exists \gamma, \gamma' \in \Gamma_g$ such that

$$0 < |\operatorname{Tr} \rho_g(\gamma) - \operatorname{Tr} \rho_g(\gamma')| < \epsilon, \tag{A.63}$$

or (2) $\exists \gamma'' \in \Gamma_g$ such that

$$N_g - \epsilon < |\operatorname{Tr} \rho_g(\gamma'')| < N_g. \tag{A.64}$$

Proof The compactness of $U(N_g)$ ensures the existence of $\gamma, \gamma' \in \Gamma_g$ such that[12]

$$0 < \big|\big|\rho_g(\gamma) - \rho_g(\gamma')\big|\big| < \epsilon', \tag{A.65}$$

where ϵ' is small. Now we discuss two situations:

(1) If $\rho_g(\gamma') = \rho_g(\gamma) \cdot e^{i\theta} \cdot \mathbb{1}$, then (A.65) implies

$$0 < \{\operatorname{Tr}[(\rho_g(\gamma) - \rho_g(\gamma'))(\rho_g(\gamma) - \rho_g(\gamma'))^*]\}^{1/2} < \epsilon' \tag{A.66}$$

$$\Longrightarrow\ 0 < \left\{\operatorname{Tr}\left[\rho_g(\gamma)(1 - e^{i\theta})\rho_g^*(\gamma)(1 - e^{-i\theta})\right]\right\}^{1/2} < \epsilon' \tag{A.67}$$

but $\rho_g(\gamma)\rho_g(\gamma)^* = \mathbb{1}$, so

$$0 < [(2 - 2\cos\theta)N_g]^{1/2} < \epsilon' \tag{A.68}$$

On the other hand, (A.63) now means

$$0 < \left|\operatorname{Tr}\left[\rho_g(\gamma)(1 - e^{i\theta})\mathbb{1}\right]\right| < \epsilon \tag{A.69}$$

$$\Longrightarrow\ 0 < \left|1 - e^{i\theta}\right| \cdot \left|\operatorname{Tr} \rho_g(\gamma)\right| < \epsilon. \tag{A.70}$$

But

$$\left|1 - e^{i\theta}\right| \cdot \left|\operatorname{Tr} \rho_g(\gamma)\right| \le N_g\sqrt{2 - 2\cos\theta} < \epsilon, \tag{A.71}$$

so by comparing with (A.69), we can choose $\boxed{\epsilon' \equiv \epsilon/\sqrt{N_g}}$ in (A.65) to achieve (A.63).

(2) If $\rho_g(\gamma') \neq \rho_g(\gamma) \cdot e^{i\theta} \cdot \mathbb{1}$.

[12]Here $\gamma \neq \gamma'$ not necessarily implies that $\rho_g(\gamma) \neq \rho_g(\gamma')$, because ρ_g may not be faithful.

Notice that the Frobenius norm $||\cdot||$ is invariant under multiplying $\cdot$ with a unitary matrix, so we multiply terms inside $||\cdot||$ in (A.65) by $\rho_g(\gamma')^{-1}$ to get

$$0 < \big|\big|\rho_g(\gamma'') - \mathbb{1}\big|\big| < \epsilon', \tag{A.72}$$

where $\rho_g(\gamma'') \equiv \rho_g(\gamma)\rho_g(\gamma')^{-1}$. Consequently

$$0 < \{\mathrm{Tr}\,[(\rho_g(\gamma'') - \mathbb{1})(\rho_g(\gamma'') - \mathbb{1})^*]\}^{1/2} < \epsilon'. \tag{A.73}$$

We use $\rho_g(\gamma'')\rho_g(\gamma'')^* = \mathbb{1}$ to get

$$0 < (2N_g - 2\,\mathrm{Re}\,C)^{1/2} < \epsilon', \tag{A.74}$$

where $C \equiv \mathrm{Tr}\,\rho_g(\gamma'')$. But $\mathrm{Im}\,C \leq N$ and $\mathrm{Re}\,C < |C|$, from (A.74) we have

$$0 < N_g - \mathrm{Re}(c) < \epsilon'^2/2 \tag{A.75}$$

$$\implies N_g - |c| < \epsilon'^2/2 \tag{A.76}$$

Recall that (A.64) is equivalent to

$$0 < N_g - |C| < \epsilon. \tag{A.77}$$

so we pick $\epsilon = \epsilon'^2/2$, namely $\boxed{\epsilon' = \sqrt{2\epsilon}}$ in (A.65) to achieve (A.64). ■

Appendix B

p-Adics

B.1 Laplacian matrix on a multigraph, and its relation to volume of (4.151)

Here we use a graph-theoretic method to obtain the determinant of Laplacian operator on the Bruhat-Tits tree[1], which has already been calculated in Section 4.3.

Let us recall that the result (4.31) is the product of all nonzero eigenvalues of a directed multigraph Laplacian $\widetilde{\Box}$. This multigraph G contains:

- $N+1$ vertices, labelled by $0, \ldots, N$;
- One arrow from the i^{th} vertex to $(i+1)^{\text{th}}$ vertex, where $i = 0, \ldots, N-2$;
- p arrows from the j^{th} vertex to the $(j-1)^{\text{th}}$ vertex, where $j = N, N-1, \ldots, 2$;
- $p+1$ arrows from the vertex 1 to the vertex 0.

The product of eigenvalues of equals the determinant of the adjacency matrix of G, with the $(N+1)^{\text{th}}$ row and the $(N+1)^{\text{th}}$ column removed, because there is no arrow going from anywhere else to the vertex N. By Kirchhoff's theorem, this determinant equals the number of spanning trees starting from the vertex N, which is

$$\underbrace{p \cdot p \cdot \ldots \cdot p}_{N-1} \cdot (p+1) = p^N + p^{N-1}. \tag{B.1}$$

In fact, G can be obtained by "compressing" the truncated Bruhat-Tits tree in Section 4.3 onto one ray using the rotational symmetry, so a spanning tree starting from the vertex N is equivalent to a path originating from the origin 0 to the cut-off boundary of the Bruhat-Tits tree, which in turn is equivalent to choosing a point at depth N on the tree.

[1]I thank Yehao Zhou for helpful comments.

Finally, all points at depth N on the Bruhat-Tits tree form an orbit of the Iwahori subgroup of $GL(2,\mathbb{Z}_p)$, called the *Iwahori orbit*. Under the Haar measure, the orbit has volume 1, so the volume of the double coset (4.151) equals the number of elements in the quotient of (4.151) by the right action of Iwahori subgroup. This quotient is exactly the Iwahori orbit representing elements

$$\begin{pmatrix} p^N & 0 \\ 0 & 1 \end{pmatrix}, \tag{B.2}$$

namely, points at depth N. As we discussed on the previous page, there are $p^N + p^{N-1}$ of them.

However, for the BTZ graph, there is no good rotational symmetry which allows for a "compression", so a similar analysis obtaining $\det \widetilde{\Box}$ cannot be done.

It would also be interesting to understand this volume purely in terms of p-adic integration using Haar measure, say, in Appendix A of [168].

B.2 BTZ graphs revisited

In Section 4.3, if we do not use the periodic linear recurrence on the horizon (4.44), without loss of generality, we start from the initial condition at the $\phi_{0,s}$ vertex:

$$(p-1)(\phi_{0,s} - \phi_{1,s}) + (\phi_{0,s} - \phi_{0,s-1}) + (\phi_{0,s} - \phi_{0,s+1}) = \lambda\phi_{0,s}, \tag{B.3}$$

where $\phi_{1,s}$ denotes the field value on the outward vertex one edge away from the horizon point $(0,s)$, and hence

$$\phi_{1,s} = \frac{(p+1-\lambda)\phi_{0,s} - (\phi_{0,s-1} + \phi_{0,s+1})}{p-1}. \tag{B.4}$$

Similar to what we have shown in Section 4.3, all field values $\phi_{n,s}, n > 1$, away from the event horizon only depend on their depths n and hence isotropic in each subtree rooted at one horizon vertex $(0,s)$. There is no change in the linear recurrence (4.26) for all $n > 2$, and for $n = 2$ we have

$$\begin{aligned} \phi_{2,s} &= \frac{(p+1-\lambda)\phi_{1,s} - \phi_{0,s}}{p} \\ &= \frac{[\lambda(\lambda-2p-2) + p(p+1) + 2]\phi_{0,s} + (\lambda - p - 1)(\phi_{0,s+1} + \phi_{0,s-1})}{p(p-1)}, \end{aligned} \tag{B.5}$$

then the coefficients get uncontrollably complicated as the depth n increases.

B.3 Review on the ordinary BTZ parameters

In ordinary Eulcidean AdS_3, for a genus-1 gravitational saddle configuration, the modular parameter is $\tau = \theta + i\beta$, defined on the upper-half plane $\mathbb{H}^2$, where θ is the angular potential

and β is the inverse temperature, then the tree-level partition function is [64]

$$Z = e^{\pi k \frac{\mathrm{Im}\tau}{|\tau|^2}}, \tag{B.6}$$

where k is the inverse 3d Newton's constant. For a non-rotating black hole, as in our case $\theta = 0$, so

$$Z = e^{\frac{\pi k}{\beta}} = e^{\pi k r_+}. \tag{B.7}$$

If corrected by the one-loop contribution as in [5], we have:

$$Z = \mathcal{Z}(\tau)\bar{\mathcal{Z}}(\bar{\tau}), \tag{B.8}$$

where the holomorphic piece is

$$\mathcal{Z}(\tau) = \frac{q_-^{-(k-1/24)}(1-q_-)}{\eta(-1/\tau)}, \tag{B.9}$$

and $q_- \equiv e^{-2\pi i/\tau}$. Since the partition function of 3d pure gravity is 1-loop exact [5], the combined result is

$$Z_{\mathrm{tot}} = \frac{e^{\frac{4\pi \mathrm{Im}\tau}{|\tau|^2}\left(k-\frac{1}{24}\right)}}{\eta\left(-\frac{1}{\tau}\right)\bar{\eta}\left(-\frac{1}{\bar{\tau}}\right)}\left[1 + e^{-\frac{4\pi\mathrm{Im}\tau}{|\tau|^2}} - 2\cos\left(\frac{2\pi\mathrm{Im}\tau}{|\tau|^2}\right)e^{-\frac{2\pi\mathrm{Im}\tau}{|\tau|^2}}\right] \tag{B.10}$$

We will use the q-Pochhammer symbol specified at q itself

$$(q;q)_\infty \equiv \prod_{n=1}^{\infty}\left(1-q^n\right), \tag{B.11}$$

as well as the fact that $q_-\bar{q}_- = e^{-4\pi\frac{\mathrm{Im}\tau}{|\tau|^2}}$ and $\eta(-1/\tau) \equiv q_-^{1/24}(q_-;q_-)_\infty$, a useful expression when $q \in \mathbb{R}$.

Hence for a non-rotating BTZ black hole, $q_- = \bar{q}_-$, and at large $r_+ = 1/\beta$, we have

$$\frac{e^{4\pi k\frac{\mathrm{Im}\tau}{|\tau|^2}}}{(q_-;q_-)_\infty(\bar{q}_-;\bar{q}_-)_\infty} \approx \boxed{e^{4k\pi r_+}}. \tag{B.12}$$

Instead when r_+ is very small, we use the asymptotics [342]:

$$(q;q)_\infty \approx \sqrt{\frac{2\pi}{t}}e^{\frac{t}{24}-\frac{\pi^2}{6t}}, \text{for } q = e^{-t}, t \to 0, \tag{B.13}$$

so that the partition function is approximately $\boxed{r_+ e^{(4k-1/6)\pi r_+}}$.

B.4 An appetizer to compact induction

Compact induction is among the very first constructions of supercuspidal representations. The standard philosophy is to induce an irrep of the group G from a representation of a *compact* subgroup $H \subset G$. Avoiding most technicalities, we demonstrate this for the simplest case, the symmetric group S_3, adopting the approach from [343]. We will not define terms not shown in our main text.

It is known that for a given p, there are $p(p-1)/2$ distinct supercuspidal representations for $SL(2,\mathbb{Q}_p)$ [344] (Theorem 2.5), so the supercuspidal representation for $SL(2,\mathbb{Q}_2)$ is unique. We start from the *cuspidal representation* of $SL(2,\mathbb{F}_2) \cong S_3$, i.e., the character ρ with mappings:

$$\begin{array}{cccccccc} \begin{pmatrix} 1 & 0 \\ 0 & 1 \end{pmatrix}, & \begin{pmatrix} 0 & 1 \\ 1 & 0 \end{pmatrix}, & \begin{pmatrix} 1 & 1 \\ 0 & 1 \end{pmatrix}, & \begin{pmatrix} 1 & 0 \\ 1 & 1 \end{pmatrix}, & \begin{pmatrix} 1 & 1 \\ 1 & 0 \end{pmatrix}, & \begin{pmatrix} 0 & 1 \\ 1 & 1 \end{pmatrix}, \\ \downarrow & \downarrow & \downarrow & \downarrow & \downarrow & \downarrow \\ 1 & -1 & -1 & -1 & 1 & 1 \end{array} \tag{B.14}$$

and preform compact induction on S_3 to obtain the supercuspidal representation of $SL(2,\mathbb{Q}_2)$.

We use the fact that there is a unique *tamely ramified extension* $\mathbb{Q}_2\left(\zeta_3, \sqrt[3]{2}\right)/\mathbb{Q}_2$ whose Galois group is exactly S_3, where ζ_3 is a 3^{rd} root of unity. Then the *Langlands parameter*

$$\phi : \mathrm{Gal}\left(\mathbb{Q}_2\left(\zeta_3, \sqrt[3]{2}\right)\Big/\mathbb{Q}_2\right) \to S_3 \subseteq PGL(2,\mathbb{C}) \tag{B.15}$$

corresponds to two irreps of $SL(2,\mathbb{Q}_2)$ given by compact induction from

$$K_1 = SL(2,\mathbb{Z}), \quad \text{and } K_2 = \begin{pmatrix} 2 & 0 \\ 0 & 1 \end{pmatrix} K_1 \begin{pmatrix} 1/2 & 0 \\ 0 & 1 \end{pmatrix} = \begin{pmatrix} * & 2* \\ */2 & * \end{pmatrix} \tag{B.16}$$

of the characters $K_i \to S_3 \xrightarrow{\text{sgn}} \{\pm 1\}$.

More generally and abstractly, compact induction can be performed on $\mathbb{Z}_p/p\mathbb{Z}_p \sim \mathbb{Z}/\mathbb{Z}_p \sim \mathbb{F}_p$ as well, and supercuspidal representations obtained are called *depth-zero* [219]. With this, one can actually enumerate all supercuspidal representations of $GL(2,\mathbb{Q}_p)$ [345].

Appendix C

Reciprocity

C.1 Topological twists

In this appendix, we attempt to topologically twist the Gaiotto-Witten Janus confuguration we introduced in .

Twisting the Gaiotto-Witten Janus configuration

In this subsection, all spinors and vectors are in Euclidean signature. The 10D spinor decompose into the $Spin(4)_L \times Spin(6) \cong SU(2)_+ \times SU(2)_- \times Spin(6)$ representation as

$$(\mathbf{2},\mathbf{1};\ \bar{\mathbf{4}}) \oplus (\mathbf{1},\mathbf{2};\mathbf{4}). \tag{C.1}$$

They decompose into representation of $SU(2)_+ \times SU(2)_- \times Spin(3)_X \times Spin(3)_Y$ as

$$(\mathbf{2},\mathbf{1};\mathbf{2},\mathbf{2}) \oplus (\mathbf{1},\mathbf{2};\mathbf{2},\mathbf{2}), \tag{C.2}$$

where $Spin(4)_L$ is generated by Γ^i for $i = 0,1,2,3$, $Spin(3)_X$ is generated by Γ^a for $a = 4,5,6$, and $Spin(3)_Y$ is generated by Γ^p for $p = 7,8,9$. The spinors further decompose into the representation of $Spin(3)_D \times Spin(3)_Y \times \mathbb{Z}_2$ as

$$(\mathbf{1},\mathbf{2})^+ \oplus (\mathbf{3},\mathbf{2})^+ \oplus (\mathbf{1},\mathbf{2})^- \oplus (\mathbf{3},\mathbf{2})^-, \tag{C.3}$$

where $Spin(3)_D$ is the diagonal subgroup of $SU(2)_+ \times SU(2)_- \times Spin(3)_X$, and the $\mathbb{Z}_2$ is generated by Γ^{0123}. There are four spinors invariant under the $Spin(3)_D$. They satisfy three equations

$$\Gamma^{0145}\varepsilon = \varepsilon, \quad \Gamma^{0246}\varepsilon = \varepsilon, \quad i\Gamma^{0123456789}\varepsilon = \varepsilon. \tag{C.4}$$

The four solutions form a pair of doublets under the $Spin(3)_Y$, which have ± 1 eigenvalue under Γ^{0123}. we denote them by $\varepsilon_{\pm,\alpha}$, which satisfy

$$\Gamma^{0123}\varepsilon_{\pm,\alpha} = \pm\varepsilon_{\pm,\alpha}, \qquad \Gamma^{pq}\varepsilon_{\pm,\alpha} = i\epsilon^{pqr}(\sigma_r)_\alpha{}^\beta\varepsilon_{\pm,\beta}, \tag{C.5}$$

where $(\sigma_r)_\alpha{}^\beta$ are Pauli matrices.[1] A choice of $\varepsilon_{-,\alpha}$ determines a natural choice of $\varepsilon_{+,\alpha}$,

$$\varepsilon_{-,\alpha} = N\varepsilon_{+,\alpha}, \quad \varepsilon_{+,\alpha} = -N\varepsilon_{-,\alpha}, \quad N = \frac{1}{3}\sum_{i=0}^{2}\Gamma^i\Gamma^{i+4}. \tag{C.7}$$

One can further show that $\varepsilon_{\pm,\alpha}$ satisfy

$$\Gamma^{i+4}\varepsilon_{+,\alpha} = \Gamma^i\varepsilon_{-,\alpha}, \quad \Gamma^{i+4}\varepsilon_{-,\alpha} = -\Gamma^i\varepsilon_{+,\alpha} \quad \text{for } i = 0, 1, 2. \tag{C.8}$$

We would like to consider Gaiotto-Witten Janus configuration. The supersymmetry transformation preserved by the Gaiotto-Witten Janus configuration must satisfy the condition

$$(\Gamma^{3456}\sin\psi + \Gamma^{3789}\cos\psi)\varepsilon = \varepsilon. \tag{C.9}$$

We could construct solutions from $\varepsilon_{\pm,\alpha}$ by

$$\varepsilon_\alpha = \varepsilon_{+,\alpha} + \varepsilon_{-,\alpha}ie^{i\psi}. \tag{C.10}$$

Let us decompose the gaugino field Ψ as

$$\Psi = (\eta^{+\alpha} + \Gamma^{ij}\chi_{ij}^{+\alpha})\varepsilon_{+,\alpha} + (\eta^{-\alpha} + \Gamma^{ij}\chi_{ij}^{-\alpha})\varepsilon_{-,\alpha}. \tag{C.11}$$

The Gaiotto-Witten supersymmetry transformation on the gaugino is

$$\begin{aligned}(\delta+\widetilde{\delta})\Psi = \Big(&\frac{1}{2}\Gamma^{ij}F_{ij} + \Gamma^3\Gamma^i F_{3i} + \frac{1}{2}\Gamma^{ab}[X_a, X_b] + \frac{1}{2}\Gamma^{pq}[Y_p, Y_q] \\ &+ \Gamma^i\Gamma^a D_i X_a + \Gamma^3\Gamma^a D_3 X_a + \Gamma^i\Gamma^p D_i Y_p + \Gamma^3\Gamma^p D_3 Y_p + \Gamma^a\Gamma^p[X_a, Y_p] \\ &- \Gamma^3\Gamma^a X_a\psi'\tan\psi + \Gamma^3\Gamma^p Y_p\psi'\cot\psi\Big)\varepsilon.\end{aligned} \tag{C.12}$$

Let us denote $\delta_{\pm,\alpha}$ being the supersymmetry transformations with the parameters $\varepsilon_{\pm,\alpha}$. We

[1] Our convention for the $SU(2)$ spinors u_α is such that we raise and lower the index α by the antisymmetric invariant tensors $\epsilon_{\alpha\beta}$ and $\epsilon^{\alpha\beta}$ as

$$u^\alpha = \epsilon^{\alpha\beta}u_\beta, \quad u_\alpha = u^\beta\epsilon_{\beta\alpha}. \tag{C.6}$$

$\epsilon_{\alpha\beta}$ and $\epsilon^{\alpha\beta}$ are normalized by $\epsilon_{12} = \epsilon^{12} = 1$. When the spinor indices are implicit, they are always contracted as an upper left index contracting with an lower right index, $uv = u^\alpha v_\alpha$.

obtain

$$\begin{aligned}
(u^+\delta_+ + u^-\delta_-)\chi^+_{ij} =& \frac{u^+}{2}(F_{ij} + \epsilon_{ijk}F^{3k} - [X_i, X_j] - \epsilon_{ijk}[X^k, Y^p]\sigma_p) \\
&+ \frac{u^-}{2}(-D_{[i}X_{j]} - \epsilon_{ijk}D_3X^k - \epsilon_{ijk}D^kY^p\sigma_p + \epsilon_{ijk}X^k\psi' \tan\psi), \\
(u^+\delta_+ + u^-\delta_-)\chi^-_{ij} =& \frac{u^-}{2}(F_{ij} - \epsilon_{ijk}F^{3k} - [X_i, X_j] + \epsilon_{ijk}[X^k, Y^p]\sigma_p) \\
&+ \frac{u^+}{2}(D_{[i}X_{j]} - \epsilon_{ijk}D_3X^k - \epsilon_{ijk}D^kY^p\sigma_p + \epsilon_{ijk}X^k\psi' \tan\psi), \\
(u^+\delta_+ + u^-\delta_-)\eta^+ =& \frac{u^+}{2}(i\epsilon^{pqr}\sigma_r[Y_p, Y_q]) + \frac{u^-}{2}(-D^iX_i + D^3Y^p\sigma_p + Y^p\sigma_p\psi' \cot\psi), \\
(u^+\delta_+ + u^-\delta_-)\eta^- =& \frac{u^-}{2}(i\epsilon^{pqr}\sigma_r[Y_p, Y_q]) + \frac{u^+}{2}(D^iX_i - D^3Y^p\sigma_p - Y^p\sigma_p\psi' \cot\psi).
\end{aligned} \tag{C.13}$$

Consider the supersymmetry transformation generated by (C.10), i.e. setting

$$u^+ = u, \quad u^- = -ie^{-i\psi}u, \tag{C.14}$$

where u^α is a fixed two-component spinor, which specified the twisting. The vanishing of the supersymmetry transformation on $\eta^\pm$ gives

$$u\sigma_r[Y_p, Y_q]\epsilon^{pqr} = 0, \quad u(D^iX_i - D^3Y^p\sigma_p - Y^p\sigma_p\psi' \cot\psi) = 0 \tag{C.15}$$

The vanishing of the supersymmetry transformation on $\chi^\pm$ gives

$$\begin{aligned}
u\big[&- (F_{ij} - [X_i, X_j]) \sin\psi + i\epsilon_{ijk}(F^{3k} - [X^k, Y^p]\sigma_p)\cos\psi \\
&- \epsilon_{ijk}\left(D_3X^k - X^k\psi' \tan\psi + D^kY^p\sigma_p\right)\big] = 0, \\
u\big[&i(F_{ij} - [X_i, X_j])\cos\psi - \epsilon_{ijk}(F^{3k} - [X^k, Y^p]\sigma_p)\sin\psi - D_{[i}X_{j]}\big] = 0,
\end{aligned} \tag{C.16}$$

The BPS equations take the form as

$$u^\alpha A + (u\sigma_p)^\alpha B^p = 0. \tag{C.17}$$

Contracting this equation by u_α and $(\sigma_q u)_\alpha$ gives

$$U_pB^p = 0, \quad U_pA + i\epsilon_{pqr}B^pU^r = 0, \tag{C.18}$$

where $U_p = u\sigma_p u$ is a null vector, $U_pU^p = 0$. The possible choices of twisting is parametrized by a hyperplane inside $\mathbb{CP}^2$, which is parametrized by U_1, U_2, U_3 with $U_p \sim xU_p$ for $x \in \mathbb{C}$, and the hyperplane is defined by the equation $U_pU^p = 0$.

Any choice of the twisting U_p breaks the $Spin(3)_Y$ symmetry. If we required that the BPS equations are satisfied for *all* the choice of the u^α, we have

$$\begin{aligned}
&D^kY^p = 0, \quad D^3Y^p + Y^p\psi' \cot\psi = 0, \quad [Y_p, Y_q] = 0, \\
&D^iX_i = 0, \quad D_{[i}X_{j]} = 0, \quad D_3X^k - X^k\psi' \tan\psi = 0, \\
&F_{ij} - [X_i, X_j] = 0, \quad F^{3k} = 0, \quad [X^k, Y^p] = 0.
\end{aligned} \tag{C.19}$$

This preserves the $Spin(3)_Y$ symmetry.

Next, we work out the supersymmetry transformation of the bosonic fields. One could normalize the spinors as

$$\begin{aligned}\bar{\varepsilon}_{\mp,\alpha}\Gamma_3\varepsilon_{\pm,\beta} &= \pm\epsilon_{\alpha\beta},\\ \bar{\varepsilon}_{\pm,\alpha}\Gamma_3\varepsilon_{\pm,\beta} &= 0.\end{aligned} \tag{C.20}$$

The supersymmetry variations of the bosonic fields are

$$\begin{aligned}&(u^+\delta_+ + u^-\delta_-)A_i = \epsilon^{ijk}(u^+\chi^-_{jk} + u^-\chi^+_{jk}),\\ &(u^+\delta_+ + u^-\delta_-)A_3 = u^+\eta^- - u^-\eta^+,\\ &(u^+\delta_+ + u^-\delta_-)X_i = \epsilon^{ijk}(u^+\chi^+_i - u^-\chi^-_i),\\ &(u^+\delta_+ + u^-\delta_-)Y_p = u^+\sigma_p\eta^+ + u^-\sigma_p\eta^-.\end{aligned} \tag{C.21}$$

Deriving the BPS equations

Here we derive the BPS equations for abelian and non-ablelian gauge groups respectively

The abelian case

For simplicity, let us first consider the case that the gauge group is $U(1)$.

$$\begin{aligned}&u(\partial^i X_i - \partial^3 Y^p\sigma_p - Y^p\sigma_p\psi'\cot\psi) = 0,\\ &u\big[-F_{ij}\sin\psi + i\epsilon_{ijk}F^{3k}\cos\psi - \epsilon_{ijk}\left(\partial_3 X^k - X^k\psi'\tan\psi + \partial^k Y^p\sigma_p\right)\big] = 0,\\ &u\left[iF_{ij}\cos\psi - \epsilon_{ijk}F^{3k}\sin\psi - \partial_{[i}X_{j]}\right] = 0.\end{aligned} \tag{C.22}$$

The last equation implies (setting the real and imaginary part to zero saparately)

$$F_{ij} = 0, \quad -\epsilon_{ijk}F^{3k}\sin\psi - \partial_{[i}X_{j]} = 0. \tag{C.23}$$

Now, we assume that $u = (1,0)$, and we have $u\sigma_p Y^p = (Y^9, Y^-)$, where $Y^\pm = Y_7 \pm iY^8$. The first equation then reads

$$\begin{aligned}&\partial^i X_i - \partial^3 Y^9 - Y^9\psi'\cot\psi = 0,\\ &\partial^3 Y^- + Y^-\psi'\cot\psi = 0.\end{aligned} \tag{C.24}$$

The second equation reads

$$\begin{aligned}&F^{3k} = 0, \quad \partial^k Y^- = 0,\\ &\partial_3 X^k - X^k\psi'\tan\psi + \partial^k Y^9 = 0.\end{aligned} \tag{C.25}$$

The BPS equations can be written in terms of $\widetilde{X} = X\cos\psi$ and $\widetilde{Y} = Y\sin\psi$ as

$$\begin{aligned}&F_{ij} = 0, \quad F_{3k} = 0, \quad \partial_{[i}\widetilde{X}_{j]} = 0, \quad \partial_3\widetilde{Y}^- = 0, \quad \partial_k\widetilde{Y}^- = 0,\\ &(\partial^i\widetilde{X}_i)\tan\psi - \partial^3\widetilde{Y}^9 = 0, \quad (\partial_3\widetilde{X}^k)\tan\psi + \partial_k\widetilde{Y}^9 = 0.\end{aligned} \tag{C.26}$$

The non-abelian case

Let us consider the BPS equation for non-abelian gauge group. The BPS equations are

$$\begin{aligned} u\sigma_r[Y_p,Y_q]\epsilon^{pqr}=0,\quad u(D^iX_i-D^3Y^p\sigma_p-Y^p\sigma_p\psi'\cot\psi)=0,\\ u\big[-(F_{ij}-[X_i,X_j])\sin\psi+i\epsilon_{ijk}(F^{3k}-[X^k,Y^p]\sigma_p)\cos\psi-\\ \epsilon_{ijk}\left(D_3X^k-X^k\psi'\tan\psi+D^kY^p\sigma_p\right)\big]=0,\\ u\big[i(F_{ij}-[X_i,X_j])\cos\psi-\epsilon_{ijk}(F^{3k}-[X^k,Y^p]\sigma_p)\sin\psi-D_{[i}X_{j]}\big]=0. \end{aligned} \tag{C.27}$$

Also assuming $u=(1,0)$, the equations on the first line of (C.27) give

$$\begin{aligned} &[Y^+,Y^-]=0,\quad [Y^-,Y^9]=0,\\ &(D^i\widetilde{X}_i)\tan\psi-D_3\widetilde{Y}^9=0,\quad D_3\widetilde{Y}^-=0. \end{aligned} \tag{C.28}$$

The equation on the second line of (C.27) give

$$\begin{aligned} &i[X^k,Y^-]\cos\psi+D^kY^-=0,\quad F^{3k}-[X^k,Y^9]=0,\\ &(F_{ij}-[X_i,X_j])\sin\psi+\epsilon_{ijk}\left(D_3X^k-X^k\psi'\tan\psi+D^kY^9\right)=0. \end{aligned} \tag{C.29}$$

The equation on the last line of (C.27) give

$$\begin{aligned} &[X^k,Y^-]=0,\quad F_{ij}-[X_i,X_j]=0,\\ &\epsilon_{ijk}(F^{3k}-[X^k,Y^9])\sin\psi+D_{[i}X_{j]}=0. \end{aligned} \tag{C.30}$$

In summary, we have the BPS equations,

$$\begin{aligned} &F_{ij}-[X_i,X_j]=0,\quad F^{3k}-[X^k,Y^9]=0,\quad D_{[i}X_{j]}=0,\\ &[X^k,Y^-]=0,\quad D^kY^-=0,\quad [Y^+,Y^-]=0,\quad [Y^-,Y^9]=0,\quad D_3\widetilde{Y}^-=0.\\ &(D_3\widetilde{X}^k)\tan\psi+D^k\widetilde{Y}^9=0,\quad (D^i\widetilde{X}_i)\tan\psi-D_3\widetilde{Y}^9=0. \end{aligned} \tag{C.31}$$

Some comments are as follows:

- The scalar Y^+ only shows up in the commutator $[Y^+,Y^-]=0$, otherwise is unconstrained by the BPS equations;
- By (C.21), the scalar Y^- is invariant under our choice of supercharge, as $u=(1,0)$;
- In deriving (C.26) and (C.31), we assume the bosonic fields (A_i,A_3,X_i,Y_p) are all real, and set the real part and the pure imaginary part of a equation to zero separately.

Compactifying the Janus configuation

In this appendix, we only consider the twisting that preserve the $Spin(3)_Y$. Let us consider the Janus configuration on an interval $[0, 2\pi]$. The coupling constant τ on the two ends of the interval are related by an S-transformation

$$\tau(0) = -\frac{1}{\tau(2\pi)}. \tag{C.32}$$

We can then compatify the x_3-direction.

Recall that the Janus configuration is parametrized by a function $\psi(x_3)$ as $\tau = a + 4\pi D e^{2i\psi}$. Now, suppose the angle ψ near $x_3 = 0$ is a constant, and the action reduces to the $\mathcal{N} = 4$ SYM action. For simplicity, we also assume that the θ-angle is zero near $x_3 = 0$. Consider the kinetic term of the scalar Y_a in the x_3-direction,

$$\frac{1}{g_{YM}^2} \operatorname{Tr}(\partial_3 Y_a \partial_3 Y^a). \tag{C.33}$$

Let us denote $Y_i = Y|_{x_3=0}$, $Y_f = Y|_{x_3=2\pi}$, and $g_{YM,i} = g_{YM}(2\pi)$, $g_{YM,f} = g_{YM}(2\pi)$. For (C.33) to be invariant under the S-transformation, we must have

$$Y_f = \frac{1}{g_{YM,i}^2} Y_i, \quad g_{YM,f} = \frac{1}{g_{YM,i}}. \tag{C.34}$$

Recall that $Y = \widetilde{Y}/\sin\psi$ and $\widetilde{Y}$ is a constant by the BPS equations (C.19). If $\widetilde{Y}$ is nonzero, then (C.34) gives

$$\frac{1}{\sin\psi_i \sin\psi_f} = 2D = \frac{1}{\cos\psi_i \cos\psi_f}, \tag{C.35}$$

which implies

$$g_{YM,f} = \frac{1}{D \sin 2\psi_f} = 1, \tag{C.36}$$

and the S-transformation acting trivially.

C.2 Locality and action I'' at the intersection of the $SL(2,\mathbb{Z})$ duality walls

The bosonic part of the duality wall corresponding to $\widetilde{M} = \overline{ST}^{\overline{k}}$ was given by the sum of I'_b and I'' from (5.80) and (5.94):

$$I'_b + I'' = \frac{i}{4\pi} \int_0^1 \left(2X_1^t \epsilon dX_0 - \overline{k} X_0^t \epsilon dX_0\right)\Big|_{\sigma_2=0} + \frac{i}{4\pi} \left(\overline{k} - 2\right) X(1,0)^t \epsilon M X(0,0)\,. \tag{C.37}$$

We mentioned below (5.94) that I'' is necessary to incorporate the periodic identification (5.67) in a local way. Let us now explain in what sense (C.37) is a local action. For one, it is crucial that the coefficient in (5.94) is $\left(2-\overline{k}\right)$. The key point is that X_0 and X_1 are only one set of representative functions on $\mathbb{R}^2$ that represent a map to the coset $T^2 \simeq \mathbb{R}^2/\mathbb{Z}^2$. In order to analyze the locality of the expression, let us divide the range $0 \le \sigma_1 < 1$ into $\mathfrak{n}$ segments labeled by $\mathfrak{g} = 0, \ldots, \mathfrak{n}-1$ with endpoints

$$0 = \sigma_{1,0} < \sigma_{1,1} < \cdots < \sigma_{1,\mathfrak{n}-1} < \sigma_{1,\mathfrak{n}} = 1\,.$$

In each segment $[\sigma_{1,\mathfrak{g}}, \sigma_{1,\mathfrak{g}+1}]$, we define fields $X_{0,\mathfrak{g}}(\sigma_1)$, with $\sigma_{1,\mathfrak{g}} \le \sigma_1 \le \sigma_{1,\mathfrak{g}+1}$. Similarly, at $\sigma_2 = 1$ we have another sequence of vector functions $\{X_{1,\mathfrak{g}}\}_{\mathfrak{g}=1}^{\mathfrak{n}}$. Thanks to the equivalence (5.67), there is an infinite number of ways to pick $X_{0,\mathfrak{g}}$ and $X_{1,\mathfrak{g}}$ in each segment, but different choices differ by a constant vector K. To incorporate that ambiguity in a local way, we allow the boundary conditions at the point were $\sigma_{1,\mathfrak{g}+1}$, where one segment touches the next one, to include a shift by $\mathcal{N}_{\mathfrak{g}} \in \mathbb{Z}^2$ [which plays the role of K in (5.67)]:

$$X_{i,\mathfrak{g}}(\sigma_{1,\mathfrak{g}+1}) = M^{\nu_{\mathfrak{g}}} X_{i,\mathfrak{g}+1}\left(\sigma_{1,\mathfrak{g}+1}\right) + 2\pi\mathcal{N}_{\mathfrak{g}}\,, \qquad i = 0, 1. \tag{C.38}$$

In (C.38), we also allow a twist by an integer power $\nu_{\mathfrak{g}} \in \mathbb{Z}$ of M between the $\mathfrak{g}^{th}$ and $(\mathfrak{g}+1)^{th}$ segment. In order to comply with (5.63), we require that the net twist be M, so that:

$$\sum_{\mathfrak{g}=0}^{\mathfrak{n}-1} \nu_{\mathfrak{g}} = 1.$$

Our convention is that $\mathfrak{n} \sim 0$ so that $\mathcal{N}_{\mathfrak{n}} = \mathcal{N}_0$. We require that the action be a sum of local expressions, and we start by replacing the first two terms in (C.37) with

$$\tilde{I}'_b \equiv -\frac{i}{4\pi} \sum_{\mathfrak{g}=0}^{\mathfrak{n}-1} \int_{\sigma_{1,\mathfrak{g}}}^{\sigma_{1,\mathfrak{g}+1}} \left(\overline{k} X_{0,\mathfrak{g}}^t \epsilon dX_{0,\mathfrak{g}} - 2X_{1,\mathfrak{g}}^t \epsilon dX_{0,\mathfrak{g}}\right)\,. \tag{C.39}$$

Next, we require local gauge invariance. The gauge transformations are labeled by $\mathfrak{n}$ vectors $K_{\mathfrak{g}} \in \mathbb{Z}^2$ and act as

$$X_{i,\mathfrak{g}} \to X_{i,\mathfrak{g}} + 2\pi K_{\mathfrak{g}} \quad (i = 0, 1)\,, \qquad \mathcal{N}_{\mathfrak{g}} \to \mathcal{N}_{\mathfrak{g}} + K_{\mathfrak{g}} - M^{\nu_{\mathfrak{g}}} K_{\mathfrak{g}+1}\,, \qquad \mathfrak{g} = 0, \ldots, \mathfrak{n}-1. \tag{C.40}$$

Under this gauge transformation the action transforms as

$$\tilde{I}'_b \;\to\; \tilde{I}'_b - \frac{i}{2}\left(\overline{k}-2\right) \sum_{\mathfrak{g}=0}^{\mathfrak{n}-1} K_{\mathfrak{g}}^t \epsilon \left[M^{\nu_{\mathfrak{g}}} X_{0,\mathfrak{g}+1}(\sigma_{1,\mathfrak{g}+1}) - X_{0,\mathfrak{g}}(\sigma_{1,\mathfrak{g}})\right] - i\left(\overline{k}-2\right)\pi \sum_{\mathfrak{g}=0}^{\mathfrak{n}-1} K_{\mathfrak{g}}^t \epsilon \mathcal{N}_{\mathfrak{g}} \tag{C.41}$$

Since we assume that $\overline{k} \in 2\mathbb{Z}$, the last term is in $2\pi\mathbb{Z}$ and we can drop it, since the path integral is over e^{-I}. For the remaining terms, we can rearrange the sum to read

$$\sum_{\mathfrak{g}=0}^{\mathfrak{n}-1} K_{\mathfrak{g}}^t \epsilon \left[M^{\nu_{\mathfrak{g}}} X_{0,\mathfrak{g}+1}(\sigma_{1,\mathfrak{g}+1}) - X_{0,\mathfrak{g}}(\sigma_{1,\mathfrak{g}})\right] = \sum_{\mathfrak{g}=1}^{\mathfrak{n}} \left[K_{\mathfrak{g}-1}^t \left(M^{-\nu_{\mathfrak{g}-1}}\right)^t - K_{\mathfrak{g}}^t\right] \epsilon X_{0,\mathfrak{g}}(\sigma_{1,\mathfrak{g}}),$$

where we used the identity $(M^{\nu_{\mathfrak{g}-1}})^t \epsilon M^{\nu_{\mathfrak{g}-1}} = (\det M)^{\nu_{\mathfrak{g}-1}}\epsilon = \epsilon$. Thus, (C.41) can be rewritten as

$$\tilde{I}'_b \to \tilde{I}'_b - \frac{i}{2}\left(\overline{k}-2\right)\sum_{\mathfrak{g}=1}^{\mathfrak{n}}\left[K^t_{\mathfrak{g}-1}\left(M^{-\nu_{\mathfrak{g}-1}}\right)^t - K^t_{\mathfrak{g}}\right]\epsilon X_{0,\mathfrak{g}}(\sigma_{1,\mathfrak{g}}) \qquad (\text{mod } 2\pi\mathbb{Z})\,.$$

So, $\tilde{I}'_b$ is not gauge invariant on its own. To fix it, we can add to $\tilde{I}'_b$ the term

$$\tilde{I}'' \equiv \frac{i}{2}\left(\overline{k}-2\right)\sum_{\mathfrak{g}=0}^{\mathfrak{n}-1}\mathcal{N}^t_{\mathfrak{g}-1}\left(M^{-\nu_{\mathfrak{g}-1}}\right)^t \epsilon X_{0,\mathfrak{g}}(\sigma_{1,\mathfrak{g}}). \tag{C.42}$$

We can now check that $\tilde{I}'_b + \tilde{I}''$ is invariant, using (C.40) to calculate

$$\mathcal{N}_{\mathfrak{g}} \to \mathcal{N}_{\mathfrak{g}} + K_{\mathfrak{g}} - M^{\nu_{\mathfrak{g}}}K_{\mathfrak{g}+1}\,, \qquad \mathcal{N}^t_{\mathfrak{g}-1} \to \mathcal{N}^t_{\mathfrak{g}-1} + K^t_{\mathfrak{g}-1} - K^t_{\mathfrak{g}}\left(M^{\nu_{\mathfrak{g}-1}}\right)^t\,,$$

and thus

$$\mathcal{N}^t_{\mathfrak{g}-1}\left(M^{-\nu_{\mathfrak{g}-1}}\right)^t \to \mathcal{N}^t_{\mathfrak{g}-1}\left(M^{-\nu_{\mathfrak{g}-1}}\right)^t + K^t_{\mathfrak{g}-1}\left(M^{-\nu_{\mathfrak{g}-1}}\right)^t - K^t_{\mathfrak{g}}\,.$$

Now, if we set

$$\nu_{-1} \equiv \nu_{\mathfrak{n}-1} = 1\,, \qquad \nu_0 = \nu_1 = \cdots = \nu_{\mathfrak{n}-2} = 0\,,$$

and

$$\mathcal{N}_{-1} \equiv \mathcal{N}_{\mathfrak{n}-1} = \mathcal{N}\,, \qquad \mathcal{N}_0 = \mathcal{N}_1 = \cdots = \mathcal{N}_{\mathfrak{n}-2} = 0\,,$$

then we recover the action (5.96).

C.3 On the equivalence between $2\widetilde{\mathfrak{q}}(\cdot)$ and $v^t\epsilon M v$ in (5.132)

Proof for $M = ST^{2v_1}$ and $M = ST^{2v_1}ST^{2v_2}$

We now show that (5.132) holds for the cases $M = ST^{2v_1}$ and $M = ST^{2v_1}ST^{2v_2}$. Equation (5.132) states that the quadratic form $2\widetilde{\mathfrak{q}}(v)$ can be written as $v^t\epsilon M v$ up to an integer.

The case $M = ST^{2v_1}$ is simple. The group Ξ_0, defined in (5.69), is isomorphic to the cyclic group $\mathbb{Z}_{(2v_1-1)}$, and an element of $(M-\mathbb{I})^{-1}(\mathbb{Z}^2)/\mathbb{Z}^2$ can be expressed as

$$v = \frac{\mathbf{n}}{2v_1-2}\begin{pmatrix}1\\-1\end{pmatrix}, \qquad \text{for } \mathbf{n} = 0,\ldots,2(v_1-1)-1.$$

Then (half) the RHS of (5.132) is equal to

$$\tfrac{1}{2}v^t\epsilon M v = \frac{\mathbf{n}^2}{4(v_1-1)}.$$

The coupling constant matrix K is 1×1 and given by $(2v_1 - 2)$ which results in the same expression. Thus, in this case $\widetilde{\mathfrak{q}}(v)$ equals $\frac{1}{2}v^t\epsilon Mv$.

For the case $M = ST^{2v_1}ST^{2v_2}$, (half) the RHS of (5.132) was calculated in (5.164) as

$$\tfrac{1}{2}v^t\epsilon Mv = \frac{v_1\mathbf{n}^2}{4(v_1v_2-1)} - \frac{v_2\mathbf{a}^2}{4} \tag{C.43}$$

using an identification of Ξ_0 with $\mathbb{Z}_{2(v_1v_2-1)} \oplus \mathbb{Z}_2$ via

$$v \mapsto \begin{pmatrix}\mathbf{n}\\ \mathbf{a}\end{pmatrix}, \qquad \mathbf{a} = 0, 1\,, \qquad \mathbf{n} = 0, \ldots, 2(v_1v_2-1) - 1.$$

[The relation $v = (M - \mathbb{I})^{-1}\mathcal{N}$ is needed to relate (5.164) to (C.43).]

To calculate $\mathfrak{q}(\cdot)$ we note that

$$K = \begin{pmatrix}2v_1 & -2\\ -2 & 2v_2\end{pmatrix} = \begin{pmatrix}0 & -1\\ 1 & v_2\end{pmatrix}\begin{pmatrix}2(v_1v_2-1) & 0\\ 0 & 2\end{pmatrix}\begin{pmatrix}1 & 0\\ -v_1 & 1\end{pmatrix}.$$

Thus, we can define the isomorphism $\widetilde{\varphi}$ by

$$\widetilde{\varphi}(v) = \mathbf{v} = \begin{pmatrix}0 & -1\\ 1 & v_2\end{pmatrix}\begin{pmatrix}\mathbf{n}\\ \mathbf{a}\end{pmatrix},$$

and use (5.130) to calculate

$$\widetilde{\mathfrak{q}}(v) = \mathfrak{q}(\widetilde{\varphi}(v)) = \tfrac{1}{2}\mathbf{v}^tK^{-1}\mathbf{v} = \frac{v_2}{4}\mathbf{a}^2 + \frac{v_1}{4(v_1v_2-1)}\mathbf{n}^2 + \frac{1}{2}\mathbf{an}. \tag{C.44}$$

Comparing (C.44) to (C.43) we see that in general

$$\widetilde{\mathfrak{q}}(v) \neq \tfrac{1}{2}v^t\epsilon Mv \pmod{\mathbb{Z}}$$

but

$$2\widetilde{\mathfrak{q}}(v) \equiv v^t\epsilon Mv \pmod{\mathbb{Z}},$$

as stated.

Example for M with three $ST^{\#}$ factors

Although we did not prove the equivalence of $2\mathfrak{q}(v)$ and $v^t\epsilon Mv$ (mod 1) for the case with three factors of $ST^{\#}$ inside the decomposition of M, we here present a numerical example to support our conjecture that signs could be added by hand to the *naïve*[2] $\widetilde{\mathcal{T}}$ to satisfy $(\mathcal{S}\widetilde{\mathcal{T}})^3 = \mathcal{S}^2$. The naïve $\widetilde{\mathcal{T}}$ is defined as

$$\widetilde{\mathcal{T}}\,|v\rangle \equiv e^{-\pi i v^t\epsilon Mv}\,|v\rangle\,, \quad v \in \Xi_0.$$

[2]In this section, by "naïve" we mean that we do not consider any $\pm$ sign shown in (5.141), or the phase ϕ predicted by the signature σ of the quadratic form $v^t\epsilon Mv$ in (5.132).

Let us consider

$$M = ST^2ST^2ST^4 = \begin{pmatrix} -2 & -7 \\ 3 & 10 \end{pmatrix}, \tag{C.45}$$

which yields a cyclic group $\Xi_0 \cong \mathbb{Z}_6$ with an ordered basis

$$\left\{ \left(\frac{5}{6}, \frac{1}{2}\right), \left(\frac{2}{3}, 0\right), \left(\frac{1}{2}, \frac{1}{2}\right), \left(\frac{1}{3}, 0\right), \left(\frac{1}{6}, \frac{1}{2}\right), (0,0) \right\}.$$

Here we do not calculate $\mathcal{S}$ according to the definition (5.140). The reason is as follows: without knowing the correct $\pm$ sign in front of each matrix element beforehand, if one were to choose all signs to be, say, $+$, then it is a numerical observation that almost always one would obtain a singular $\mathcal{S}$ where at least two rows are identical, and furthermore $\mathcal{S}^2$ would not be the charge conjugation. Hence, we start by using the unsymmetrized[3]/naïve definition:

$$\widetilde{\mathcal{S}} \left| v \right\rangle \equiv \frac{1}{\sqrt{|\Xi_0|}} \sum_{u \in \Lambda/\mathbb{Z}^2} e^{2\pi i v^t \epsilon (M - \mathbb{I}) u} \left| u \right\rangle, \quad u, v \in \Xi_0. \tag{C.46}$$

Then we calculate

$$\widetilde{\mathcal{T}} = \begin{pmatrix} e^{\frac{5i\pi}{6}} & & & & & \\ & e^{-\frac{2i\pi}{3}} & & & & \\ & & -1 & & & \\ & & & -e^{\frac{i\pi}{3}} & & \\ & & & & e^{-\frac{5i\pi}{6}} & \\ & & & & & -1 \end{pmatrix},$$

and

$$\widetilde{\mathcal{S}} = \frac{1}{\sqrt{6}} \begin{pmatrix} e^{\frac{i\pi}{3}} & e^{\frac{2i\pi}{3}} & -1 & e^{-\frac{2i\pi}{3}} & e^{-\frac{i\pi}{3}} & 1 \\ e^{\frac{2i\pi}{3}} & e^{-\frac{2i\pi}{3}} & 1 & e^{\frac{2i\pi}{3}} & e^{-\frac{2i\pi}{3}} & 1 \\ -1 & 1 & -1 & 1 & -1 & 1 \\ e^{-\frac{2i\pi}{3}} & e^{\frac{2i\pi}{3}} & 1 & e^{-\frac{2i\pi}{3}} & e^{\frac{2i\pi}{3}} & 1 \\ e^{-\frac{i\pi}{3}} & e^{-\frac{2i\pi}{3}} & -1 & e^{\frac{2i\pi}{3}} & e^{\frac{i\pi}{3}} & 1 \\ 1 & 1 & 1 & 1 & 1 & 1 \end{pmatrix}.$$

We can easily check that $\widetilde{\mathcal{S}}^2$ is the Sylvester's "shift" matrix in the canonical basis

$$\begin{pmatrix} 0 & 0 & 0 & 0 & 1 & 0 \\ 0 & 0 & 0 & 1 & 0 & 0 \\ 0 & 0 & 1 & 0 & 0 & 0 \\ 0 & 1 & 0 & 0 & 0 & 0 \\ 1 & 0 & 0 & 0 & 0 & 0 \\ 0 & 0 & 0 & 0 & 0 & 1 \end{pmatrix},$$

[3]The exponent is unsymmetrized, but $\mathcal{S}$ is still a symmetric matrix.

i.e., the charge conjugation sending $|v\rangle$ to $|-v\rangle$, and $\widetilde{\mathcal{S}}^4 = \mathbb{I}$.

We found four solutions to $\left|(\widetilde{\mathcal{S}}\mathcal{T})^3\right| = \widetilde{\mathcal{S}}^2$, and below is the list of phases[4] required to multiply the entire $\mathcal{T}$ to possibly become the *refined* $\mathcal{T}$ as in (5.141) satisfying $(\widetilde{\mathcal{S}}\mathcal{T})^3 = \widetilde{\mathcal{S}}^2$, along with positions on the diagonal of $\widetilde{\mathcal{T}}$ where signs are flipped in each solution:

- phase: $e^{-\frac{i\pi}{12}}$, positions: 1, 2, 3, 5, 6;
- phase: $e^{\frac{i\pi}{12}}$, positions: 1, 3, 4, 5;
- $\boxed{\text{phase: } e^{-\frac{i\pi}{4}},\ \text{positions:2, 6}}$;
- phase: $e^{\frac{i\pi}{4}}$, position: 4.

We see that the third sign configuration yields a phase matching ϕ in $\mathcal{T}$ in (5.125), since the signature of the K-matrix (5.148) in this example

$$\begin{pmatrix} 2 & -1 & 0 \\ -1 & 2 & -1 \\ 0 & -1 & 4 \end{pmatrix} \tag{C.47}$$

is 3 [because exponents in $ST^{\#}$ factors of M in (5.125) are all positive].

Our final comment is that the naïve $\widetilde{\mathcal{T}}$ and unsymmetrized $\widetilde{\mathcal{S}}$ matrices here also enable us to find the correct sign configuration on the refined $\mathcal{T}$ in (5.141), with a phase matching the signature of K-matrix for cases with two $ST^{\#}$ factors in M, as expected from Appendix C.3. We also conjecture that the correct sign configuration on $\mathcal{S}$ in (5.134) and $\mathcal{S}$ in (5.140) is exactly given by $\widetilde{\mathcal{S}}$ on the face value.

Concrete exercises for M with two $ST^{\#}$ factors

The purpose of this subsection is to provide examples for Appendix C.3. Our first example is

$$M = ST^2ST^4 = \begin{pmatrix} -1 & -4 \\ 2 & 7 \end{pmatrix},$$

[4] Up to multiplications by $e^{\frac{2\pi i}{3}}$ and $e^{\frac{4\pi i}{3}}$, due to the three distinct ways of lifting a projective representation of $SL(2,\mathbb{Z})$ to a linear representation (i.e., three distinct "linearizations"), see for example [31, 334].

which generate Ξ_0 as $\mathbb{Z}_2 \oplus \mathbb{Z}_2$, the Klein 4-group[5]. Since everything is mod 1 here, we choose the ordered basis $\{(1/2,1/2),(1/2,0),(0,1/2),(0,0)\}$. Then its naïve $\widetilde{\mathcal{T}}$ matrix is

$$\mathcal{T} = \begin{pmatrix} -i & 0 & 0 & 0 \\ 0 & i & 0 & 0 \\ 0 & 0 & -1 & 0 \\ 0 & 0 & 0 & 1 \end{pmatrix},$$

If we were to following the customs to symmetrize the quadratic form on the exponent in (5.140) to be a quadratic refinement (a symmetric bilinear form) [283, 281], then we would get a candidate "$\mathcal{S}$-matrix" with *symmetrized* exponents $e^{-\pi i(v^t \epsilon M u + u^t \epsilon M v)}$ in its summation:

$$\mathcal{S}' = \frac{1}{2}\begin{pmatrix} -1 & -1 & 1 & 1 \\ -1 & -1 & 1 & 1 \\ 1 & 1 & 1 & 1 \\ 1 & 1 & 1 & 1 \end{pmatrix}.$$

However, as we have claimed in Appendix C.3, it is singular and its square is not a charge conjugation matrix.

On the other hand, another candidate "$\mathcal{S}$-matrix" whose summands are *antisymmetrized* exponents $e^{-\pi i(v^t \epsilon M u - u^t \epsilon M v)}$ is

$$\mathcal{S}'' = \frac{1}{2}\begin{pmatrix} 1 & -1 & -1 & 1 \\ -1 & 1 & -1 & 1 \\ -1 & -1 & 1 & 1 \\ 1 & 1 & 1 & 1 \end{pmatrix}, \tag{C.48}$$

which now squared to be the identity, but one cannot achieve $\left|(\mathcal{S}''\widetilde{\mathcal{T}})^3\right| = \mathcal{S}''^2$ by flipping signs on elements in $\widetilde{\mathcal{T}}$, and the best one could possibly do is to flip the lower right entry in $\widetilde{\mathcal{T}}$ so that

$$\left[\mathcal{S}''\begin{pmatrix} -i & 0 & 0 & 0 \\ 0 & i & 0 & 0 \\ 0 & 0 & -1 & 0 \\ 0 & 0 & 0 & \boxed{-1} \end{pmatrix}\right]^3 = \begin{pmatrix} 1 & 0 & 0 & 0 \\ 0 & 1 & 0 & 0 \\ 0 & 0 & -1 & 0 \\ 0 & 0 & 0 & -1 \end{pmatrix},$$

which is fine because we are working with (mod 1) for MCG actions in (5.140) and (5.141). However, in the upcoming example we will not be so lucky with antisymmetrization, which would fail there.

Now let us consider

$$M = ST^4ST^6 = \begin{pmatrix} -1 & -6 \\ 4 & 23 \end{pmatrix},$$

[5]Incidentally, we note that

$$M = ST^{-1}ST^{-3}ST = \begin{pmatrix} 3 & 4 \\ 2 & 3 \end{pmatrix}$$

also give the same $\mathbb{Z}_2 \oplus \mathbb{Z}_2$ with the same basis.

which generate Ξ_0 with the basis of the following order

$$\begin{aligned}\Big\{&(0,0)\,,\left(\frac{7}{10},\frac{1}{10}\right),\left(\frac{2}{5},\frac{1}{5}\right),\left(\frac{1}{10},\frac{3}{10}\right),\left(\frac{4}{5},\frac{2}{5}\right),\left(\frac{1}{2},\frac{1}{2}\right),\left(\frac{1}{5},\frac{3}{5}\right),\left(\frac{9}{10},\frac{7}{10}\right),\\ &\left(\frac{3}{5},\frac{4}{5}\right),\left(\frac{3}{10},\frac{9}{10}\right),\left(\frac{9}{10},\frac{1}{5}\right),\left(\frac{3}{5},\frac{3}{10}\right),\left(\frac{3}{10},\frac{2}{5}\right),\left(0,\frac{1}{2}\right),\left(\frac{7}{10},\frac{3}{5}\right),\\ &\left(\frac{4}{5},\frac{9}{10}\right),\left(\frac{1}{10},\frac{4}{5}\right),\left(\frac{1}{2},0\right),\left(\frac{2}{5},\frac{7}{10}\right),\left(\frac{1}{5},\frac{1}{10}\right)\Big\},\end{aligned} \tag{C.49}$$

so its naïve $\widetilde{\mathfrak{T}}$ matrix is

$$\begin{aligned}\widetilde{\mathfrak{T}} = \operatorname{diag}\Big(&1, e^{-\frac{3\pi}{10}i}, e^{\frac{4\pi}{5}i}, e^{-\frac{7\pi}{10}i}, e^{-\frac{4\pi}{5}i}, i, e^{-\frac{4\pi}{5}i}, e^{-\frac{7\pi}{10}i}, e^{\frac{4\pi}{5}i}, e^{-\frac{3\pi}{10}i}, e^{-\frac{\pi}{5}i}, e^{-\frac{3\pi}{10}i}, e^{\frac{\pi}{5}i}, -i,\\ &e^{\frac{\pi}{5}i}, e^{\frac{7\pi}{10}i}, e^{-\frac{\pi}{5}i}, -1, e^{\frac{3\pi}{10}i}, e^{\frac{7\pi}{10}i}\Big)\,.\end{aligned} \tag{C.50}$$

The antisymmatrization proposal similar to (C.48) will yield a candidate

$$\mathcal{S}'' = \frac{1}{2\sqrt{5}}\begin{pmatrix}
1 & 1 & 1 & 1 & 1 & 1 & 1 & 1 & 1 & 1 & 1 & 1 & 1 & 1 & 1 & 1 & 1 & 1 & 1 & 1\\
1 & 1 & 1 & 1 & 1 & 1 & 1 & 1 & 1 & 1 & -1 & -1 & -1 & -1 & -1 & -1 & -1 & -1 & -1 & -1\\
1 & 1 & 1 & 1 & 1 & 1 & 1 & 1 & 1 & 1 & 1 & 1 & 1 & 1 & 1 & 1 & 1 & 1 & 1 & 1\\
1 & 1 & 1 & 1 & 1 & 1 & 1 & 1 & 1 & 1 & -1 & -1 & -1 & -1 & -1 & -1 & -1 & -1 & -1 & -1\\
1 & 1 & 1 & 1 & 1 & 1 & 1 & 1 & 1 & 1 & 1 & 1 & 1 & 1 & 1 & 1 & 1 & 1 & 1 & 1\\
1 & 1 & 1 & 1 & 1 & 1 & 1 & 1 & 1 & 1 & -1 & -1 & -1 & -1 & -1 & -1 & -1 & -1 & -1 & -1\\
1 & 1 & 1 & 1 & 1 & 1 & 1 & 1 & 1 & 1 & 1 & 1 & 1 & 1 & 1 & 1 & 1 & 1 & 1 & 1\\
1 & 1 & 1 & 1 & 1 & 1 & 1 & 1 & 1 & 1 & -1 & -1 & -1 & -1 & -1 & -1 & -1 & -1 & -1 & -1\\
1 & 1 & 1 & 1 & 1 & 1 & 1 & 1 & 1 & 1 & 1 & 1 & 1 & 1 & 1 & 1 & 1 & 1 & 1 & 1\\
1 & 1 & 1 & 1 & 1 & 1 & 1 & 1 & 1 & 1 & -1 & -1 & -1 & -1 & -1 & -1 & -1 & -1 & -1 & -1\\
1 & -1 & 1 & -1 & 1 & -1 & 1 & -1 & 1 & -1 & 1 & -1 & 1 & -1 & 1 & -1 & 1 & 1 & -1 & -1\\
1 & -1 & 1 & -1 & 1 & -1 & 1 & -1 & 1 & -1 & -1 & 1 & -1 & 1 & -1 & 1 & -1 & -1 & 1 & 1\\
1 & -1 & 1 & -1 & 1 & -1 & 1 & -1 & 1 & -1 & 1 & -1 & 1 & -1 & 1 & -1 & 1 & 1 & -1 & -1\\
1 & -1 & 1 & -1 & 1 & -1 & 1 & -1 & 1 & -1 & -1 & 1 & -1 & 1 & -1 & 1 & -1 & -1 & 1 & 1\\
1 & -1 & 1 & -1 & 1 & -1 & 1 & -1 & 1 & -1 & 1 & -1 & 1 & -1 & 1 & -1 & 1 & 1 & -1 & -1\\
1 & -1 & 1 & -1 & 1 & -1 & 1 & -1 & 1 & -1 & -1 & 1 & -1 & 1 & -1 & 1 & -1 & -1 & 1 & 1\\
1 & -1 & 1 & -1 & 1 & -1 & 1 & -1 & 1 & -1 & 1 & -1 & 1 & -1 & 1 & -1 & 1 & 1 & -1 & -1\\
1 & -1 & 1 & -1 & 1 & -1 & 1 & -1 & 1 & -1 & 1 & -1 & 1 & -1 & 1 & -1 & 1 & 1 & -1 & -1\\
1 & -1 & 1 & -1 & 1 & -1 & 1 & -1 & 1 & -1 & -1 & 1 & -1 & 1 & -1 & 1 & -1 & -1 & 1 & 1\\
1 & -1 & 1 & -1 & 1 & -1 & 1 & -1 & 1 & -1 & -1 & 1 & -1 & 1 & -1 & 1 & -1 & -1 & 1 & 1
\end{pmatrix},$$

whose square and the fourth power are nothing close to a charge conjugation operator or the identity matrix.

Following the unsymmetrized definition (C.46), we have the $\widetilde{\mathcal{S}}$ matrix

$$\widetilde{\mathcal{S}} = \frac{1}{2\sqrt{5}} \begin{pmatrix}
1 & 1 & 1 & 1 & 1 & 1 & 1 & 1 & 1 & 1 & 1 & 1 & 1 & 1 & 1 & 1 & 1 & 1 & 1 & 1 \\
1 & e^{\frac{3i\pi}{5}} & e^{-\frac{4i\pi}{5}} & e^{-\frac{i\pi}{5}} & e^{\frac{2i\pi}{5}} & -1 & e^{-\frac{2i\pi}{5}} & e^{\frac{i\pi}{5}} & e^{\frac{4i\pi}{5}} & e^{-\frac{3i\pi}{5}} & e^{\frac{i\pi}{5}} & e^{\frac{4i\pi}{5}} & e^{-\frac{3i\pi}{5}} & 1 & e^{\frac{3i\pi}{5}} & e^{\frac{2i\pi}{5}} & e^{-\frac{i\pi}{5}} & -1 & e^{-\frac{4i\pi}{5}} & e^{-\frac{2i\pi}{5}} \\
1 & e^{-\frac{4i\pi}{5}} & e^{\frac{2i\pi}{5}} & e^{-\frac{2i\pi}{5}} & e^{\frac{4i\pi}{5}} & 1 & e^{-\frac{4i\pi}{5}} & e^{\frac{2i\pi}{5}} & e^{-\frac{2i\pi}{5}} & e^{\frac{4i\pi}{5}} & e^{\frac{2i\pi}{5}} & e^{-\frac{2i\pi}{5}} & e^{\frac{4i\pi}{5}} & 1 & e^{-\frac{4i\pi}{5}} & e^{\frac{4i\pi}{5}} & e^{-\frac{2i\pi}{5}} & 1 & e^{\frac{2i\pi}{5}} & e^{-\frac{4i\pi}{5}} \\
1 & e^{-\frac{i\pi}{5}} & e^{-\frac{2i\pi}{5}} & e^{-\frac{3i\pi}{5}} & e^{-\frac{4i\pi}{5}} & -1 & e^{\frac{4i\pi}{5}} & e^{\frac{3i\pi}{5}} & e^{\frac{2i\pi}{5}} & e^{\frac{i\pi}{5}} & e^{\frac{3i\pi}{5}} & e^{\frac{2i\pi}{5}} & e^{\frac{i\pi}{5}} & 1 & e^{-\frac{i\pi}{5}} & e^{-\frac{4i\pi}{5}} & e^{-\frac{3i\pi}{5}} & -1 & e^{-\frac{2i\pi}{5}} & e^{\frac{4i\pi}{5}} \\
1 & e^{\frac{2i\pi}{5}} & e^{\frac{4i\pi}{5}} & e^{-\frac{4i\pi}{5}} & e^{-\frac{2i\pi}{5}} & 1 & e^{\frac{2i\pi}{5}} & e^{\frac{4i\pi}{5}} & e^{-\frac{4i\pi}{5}} & e^{-\frac{2i\pi}{5}} & e^{\frac{4i\pi}{5}} & e^{-\frac{4i\pi}{5}} & e^{-\frac{2i\pi}{5}} & 1 & e^{\frac{2i\pi}{5}} & e^{-\frac{2i\pi}{5}} & e^{-\frac{4i\pi}{5}} & 1 & e^{\frac{4i\pi}{5}} & e^{\frac{2i\pi}{5}} \\
1 & -1 & 1 & -1 & 1 & -1 & 1 & -1 & 1 & -1 & -1 & 1 & -1 & 1 & -1 & 1 & -1 & -1 & 1 & 1 \\
1 & e^{-\frac{2i\pi}{5}} & e^{-\frac{4i\pi}{5}} & e^{\frac{4i\pi}{5}} & e^{\frac{2i\pi}{5}} & 1 & e^{-\frac{2i\pi}{5}} & e^{-\frac{4i\pi}{5}} & e^{\frac{4i\pi}{5}} & e^{\frac{2i\pi}{5}} & e^{-\frac{4i\pi}{5}} & e^{\frac{4i\pi}{5}} & e^{\frac{2i\pi}{5}} & 1 & e^{-\frac{2i\pi}{5}} & e^{\frac{2i\pi}{5}} & e^{\frac{4i\pi}{5}} & 1 & e^{-\frac{4i\pi}{5}} & e^{-\frac{2i\pi}{5}} \\
1 & e^{\frac{i\pi}{5}} & e^{\frac{2i\pi}{5}} & e^{\frac{3i\pi}{5}} & e^{\frac{4i\pi}{5}} & -1 & e^{-\frac{4i\pi}{5}} & e^{-\frac{3i\pi}{5}} & e^{-\frac{2i\pi}{5}} & e^{-\frac{i\pi}{5}} & e^{-\frac{3i\pi}{5}} & e^{-\frac{2i\pi}{5}} & e^{-\frac{i\pi}{5}} & 1 & e^{\frac{i\pi}{5}} & e^{\frac{4i\pi}{5}} & e^{\frac{3i\pi}{5}} & -1 & e^{\frac{2i\pi}{5}} & e^{-\frac{4i\pi}{5}} \\
1 & e^{\frac{4i\pi}{5}} & e^{-\frac{2i\pi}{5}} & e^{\frac{2i\pi}{5}} & e^{-\frac{4i\pi}{5}} & 1 & e^{\frac{4i\pi}{5}} & e^{-\frac{2i\pi}{5}} & e^{\frac{2i\pi}{5}} & e^{-\frac{4i\pi}{5}} & e^{\frac{2i\pi}{5}} & e^{\frac{2i\pi}{5}} & e^{-\frac{4i\pi}{5}} & 1 & e^{\frac{4i\pi}{5}} & e^{-\frac{4i\pi}{5}} & e^{\frac{2i\pi}{5}} & 1 & e^{-\frac{2i\pi}{5}} & e^{\frac{4i\pi}{5}} \\
1 & e^{-\frac{3i\pi}{5}} & e^{\frac{4i\pi}{5}} & e^{\frac{i\pi}{5}} & e^{-\frac{2i\pi}{5}} & -1 & e^{\frac{2i\pi}{5}} & e^{-\frac{i\pi}{5}} & e^{-\frac{4i\pi}{5}} & e^{\frac{3i\pi}{5}} & e^{-\frac{i\pi}{5}} & e^{-\frac{4i\pi}{5}} & e^{\frac{3i\pi}{5}} & 1 & e^{-\frac{3i\pi}{5}} & e^{-\frac{2i\pi}{5}} & e^{\frac{i\pi}{5}} & -1 & e^{\frac{4i\pi}{5}} & e^{\frac{2i\pi}{5}} \\
1 & e^{\frac{i\pi}{5}} & e^{\frac{2i\pi}{5}} & e^{\frac{3i\pi}{5}} & e^{\frac{4i\pi}{5}} & -1 & e^{-\frac{4i\pi}{5}} & e^{-\frac{3i\pi}{5}} & e^{-\frac{2i\pi}{5}} & e^{-\frac{i\pi}{5}} & e^{\frac{2i\pi}{5}} & e^{\frac{3i\pi}{5}} & e^{\frac{4i\pi}{5}} & -1 & e^{-\frac{4i\pi}{5}} & e^{-\frac{i\pi}{5}} & e^{-\frac{2i\pi}{5}} & 1 & e^{-\frac{3i\pi}{5}} & e^{\frac{i\pi}{5}} \\
1 & e^{\frac{4i\pi}{5}} & e^{-\frac{2i\pi}{5}} & e^{\frac{2i\pi}{5}} & e^{-\frac{4i\pi}{5}} & 1 & e^{\frac{4i\pi}{5}} & e^{-\frac{2i\pi}{5}} & e^{\frac{2i\pi}{5}} & e^{-\frac{4i\pi}{5}} & e^{\frac{3i\pi}{5}} & e^{-\frac{3i\pi}{5}} & e^{\frac{i\pi}{5}} & -1 & e^{-\frac{i\pi}{5}} & e^{\frac{i\pi}{5}} & e^{-\frac{3i\pi}{5}} & -1 & e^{\frac{3i\pi}{5}} & e^{-\frac{i\pi}{5}} \\
1 & e^{-\frac{3i\pi}{5}} & e^{\frac{4i\pi}{5}} & e^{\frac{i\pi}{5}} & e^{-\frac{2i\pi}{5}} & -1 & e^{\frac{2i\pi}{5}} & e^{-\frac{i\pi}{5}} & e^{-\frac{4i\pi}{5}} & e^{\frac{3i\pi}{5}} & e^{\frac{4i\pi}{5}} & e^{\frac{i\pi}{5}} & e^{-\frac{2i\pi}{5}} & -1 & e^{\frac{2i\pi}{5}} & e^{\frac{3i\pi}{5}} & e^{-\frac{4i\pi}{5}} & 1 & e^{-\frac{i\pi}{5}} & e^{-\frac{3i\pi}{5}} \\
1 & 1 & 1 & 1 & 1 & 1 & 1 & 1 & 1 & -1 & -1 & -1 & -1 & -1 & -1 & -1 & -1 & -1 & -1 & -1 \\
1 & e^{\frac{3i\pi}{5}} & e^{-\frac{4i\pi}{5}} & e^{-\frac{i\pi}{5}} & e^{\frac{2i\pi}{5}} & -1 & e^{-\frac{2i\pi}{5}} & e^{\frac{i\pi}{5}} & e^{\frac{4i\pi}{5}} & e^{-\frac{3i\pi}{5}} & e^{-\frac{4i\pi}{5}} & e^{-\frac{i\pi}{5}} & e^{\frac{2i\pi}{5}} & -1 & e^{-\frac{2i\pi}{5}} & e^{-\frac{3i\pi}{5}} & e^{\frac{4i\pi}{5}} & 1 & e^{\frac{i\pi}{5}} & e^{\frac{3i\pi}{5}} \\
1 & e^{\frac{2i\pi}{5}} & e^{\frac{4i\pi}{5}} & e^{-\frac{4i\pi}{5}} & e^{-\frac{2i\pi}{5}} & 1 & e^{\frac{2i\pi}{5}} & e^{\frac{4i\pi}{5}} & e^{-\frac{4i\pi}{5}} & e^{-\frac{2i\pi}{5}} & e^{-\frac{i\pi}{5}} & e^{\frac{i\pi}{5}} & e^{\frac{3i\pi}{5}} & -1 & e^{-\frac{3i\pi}{5}} & e^{\frac{3i\pi}{5}} & e^{\frac{i\pi}{5}} & -1 & e^{-\frac{i\pi}{5}} & e^{-\frac{3i\pi}{5}} \\
1 & e^{-\frac{i\pi}{5}} & e^{-\frac{2i\pi}{5}} & e^{-\frac{3i\pi}{5}} & e^{-\frac{4i\pi}{5}} & -1 & e^{\frac{4i\pi}{5}} & e^{\frac{3i\pi}{5}} & e^{\frac{2i\pi}{5}} & e^{\frac{i\pi}{5}} & e^{-\frac{2i\pi}{5}} & e^{-\frac{3i\pi}{5}} & e^{-\frac{4i\pi}{5}} & -1 & e^{\frac{4i\pi}{5}} & e^{\frac{i\pi}{5}} & e^{\frac{2i\pi}{5}} & 1 & e^{\frac{3i\pi}{5}} & e^{-\frac{i\pi}{5}} \\
1 & -1 & 1 & -1 & 1 & -1 & 1 & -1 & 1 & -1 & 1 & -1 & 1 & -1 & 1 & -1 & 1 & 1 & -1 & -1 \\
1 & e^{-\frac{4i\pi}{5}} & e^{\frac{2i\pi}{5}} & e^{-\frac{2i\pi}{5}} & e^{\frac{4i\pi}{5}} & 1 & e^{-\frac{4i\pi}{5}} & e^{\frac{2i\pi}{5}} & e^{-\frac{2i\pi}{5}} & e^{\frac{4i\pi}{5}} & e^{-\frac{3i\pi}{5}} & e^{\frac{3i\pi}{5}} & e^{-\frac{i\pi}{5}} & -1 & e^{\frac{i\pi}{5}} & e^{-\frac{i\pi}{5}} & e^{\frac{3i\pi}{5}} & -1 & e^{-\frac{3i\pi}{5}} & e^{\frac{i\pi}{5}} \\
1 & e^{-\frac{2i\pi}{5}} & e^{-\frac{4i\pi}{5}} & e^{\frac{4i\pi}{5}} & e^{\frac{2i\pi}{5}} & 1 & e^{-\frac{2i\pi}{5}} & e^{-\frac{4i\pi}{5}} & e^{\frac{4i\pi}{5}} & e^{\frac{2i\pi}{5}} & e^{\frac{i\pi}{5}} & e^{-\frac{i\pi}{5}} & e^{-\frac{3i\pi}{5}} & -1 & e^{\frac{3i\pi}{5}} & e^{-\frac{3i\pi}{5}} & e^{-\frac{i\pi}{5}} & -1 & e^{\frac{i\pi}{5}} & e^{\frac{3i\pi}{5}}
\end{pmatrix},$$

which squared to be the charge conjugation operator – the "shift" matrix in a non-canonical basis.

It is not hard to use *Mathematica* to find 8 solutions to $\left|(\widetilde{\mathcal{S}}\mathcal{T})^3\right| = \widetilde{\mathcal{S}}^2$, out of $2^{20} = 1,048,576$ possible sign configurations of $\widetilde{\mathcal{T}}$'s diagonal elements. Below for each solution, we list positions of entries in $\widetilde{\mathcal{T}}$ whose signs are flipped, as well as the phase needs to be added by hand to convert the naïve $\widetilde{\mathcal{T}}$ matrix into the refined $\mathcal{T}$ so that $(\widetilde{\mathcal{S}}\mathcal{T})^3 = \widetilde{\mathcal{S}}^2$:

- phase: $e^{\frac{i\pi}{6}}$ or $e^{\frac{5i\pi}{6}}$ or $e^{-\frac{i\pi}{2}}$, positions: 1–11, 13, 15, 17, 18;
- phase: 1 or $e^{\frac{2i\pi}{3}}$ or $e^{\frac{4i\pi}{3}}$, positions 1–10, 12, 14, 15, 19, 20;
- $\boxed{\text{phase: } e^{\frac{i\pi}{2}} \text{ or } e^{\frac{7i\pi}{6}} \text{ or } e^{-\frac{i\pi}{6}}, \text{ positions: 1, 3, 5, 7, 9, 11–20}}$;
- phase: 1 or $e^{\frac{2i\pi}{3}}$ or $e^{\frac{4i\pi}{3}}$, positions: 1, 3, 5, 7, 9;
- phase: -1 or $e^{\frac{i\pi}{3}}$ or $e^{-\frac{i\pi}{3}}$, positions: 2, 4, 6, 8, 10–20;
- phase: $e^{\frac{i\pi}{6}}$ or $e^{\frac{5i\pi}{6}}$ or $e^{-\frac{i\pi}{2}}$, positions: 2, 4, 6, 8, 10;
- phase: -1 or $e^{\frac{i\pi}{3}}$ or $e^{-\frac{i\pi}{3}}$, positions: 11, 13, 15, 17, 18;
- $\boxed{\text{phase: } e^{\frac{i\pi}{2}} \text{ or } e^{\frac{7i\pi}{6}} \text{ or } e^{-\frac{i\pi}{6}}, \text{ positions: 12, 14, 16, 19, 20}}$.

Now in this case, the K-matrix defined as (5.127) is

$$\begin{pmatrix} 4 & -2 \\ -2 & 6 \end{pmatrix}, \tag{C.51}$$

whose signature is 2, meaning that the third and the last solutions yield the right phase as dictated by comments following (5.125) and (5.151).

A concrete exercise for M with 4 factors of $ST^{\#}$

In fact, our above procedure goes beyond 3 factors of $ST^{\#}$ in M. To support this claim, we finally consider

$$M = ST^2ST^3ST^2ST^3 = \begin{pmatrix} -5 & -12 \\ 8 & 9 \end{pmatrix} \tag{C.52}$$

with four $ST^{\#}$ factors.

In the ordered basis of Ξ_0

$$\left\{(0,0), \left(0,\frac{1}{2}\right), \left(\frac{1}{2},\frac{2}{3}\right), \left(\frac{1}{2},\frac{1}{6}\right), \left(0,\frac{1}{3}\right), \left(0,\frac{5}{6}\right), \left(\frac{1}{2},0\right), \left(\frac{1}{2},\frac{1}{2}\right), \left(0,\frac{2}{3}\right), \left(0,\frac{1}{6}\right), \left(\frac{1}{2},\frac{1}{3}\right), \left(\frac{1}{2},\frac{5}{6}\right)\right\}, \tag{C.53}$$

the naïve $\widetilde{\mathcal{T}}$ matrix is

$$\widetilde{\mathcal{T}} = \mathrm{diag}\left(1,-1,e^{-\frac{2i\pi}{3}},e^{\frac{i\pi}{3}},e^{-\frac{2i\pi}{3}},e^{\frac{i\pi}{3}},1,-1,e^{-\frac{2i\pi}{3}},e^{\frac{i\pi}{3}},e^{-\frac{2i\pi}{3}},e^{\frac{i\pi}{3}}\right). \tag{C.54}$$

The unsymmetrized $\widetilde{\mathcal{S}}$ matrix is

$$\widetilde{\mathcal{S}} = \frac{1}{2\sqrt{3}} \begin{pmatrix} 1 & 1 & 1 & 1 & 1 & 1 & 1 & 1 & 1 & 1 & 1 & 1 \\ 1 & 1 & -1 & -1 & 1 & 1 & -1 & -1 & 1 & 1 & -1 & -1 \\ 1 & -1 & e^{-\frac{2i\pi}{3}} & e^{\frac{i\pi}{3}} & e^{\frac{2i\pi}{3}} & e^{-\frac{i\pi}{3}} & 1 & -1 & e^{-\frac{2i\pi}{3}} & e^{\frac{i\pi}{3}} & e^{\frac{2i\pi}{3}} & e^{-\frac{i\pi}{3}} \\ 1 & -1 & e^{\frac{i\pi}{3}} & e^{-\frac{2i\pi}{3}} & e^{\frac{2i\pi}{3}} & e^{-\frac{i\pi}{3}} & -1 & 1 & e^{-\frac{2i\pi}{3}} & e^{\frac{i\pi}{3}} & e^{-\frac{i\pi}{3}} & e^{\frac{2i\pi}{3}} \\ 1 & 1 & e^{\frac{2i\pi}{3}} & e^{\frac{2i\pi}{3}} & e^{-\frac{2i\pi}{3}} & e^{-\frac{2i\pi}{3}} & 1 & 1 & e^{\frac{2i\pi}{3}} & e^{\frac{2i\pi}{3}} & e^{-\frac{2i\pi}{3}} & e^{-\frac{2i\pi}{3}} \\ 1 & 1 & e^{-\frac{i\pi}{3}} & e^{-\frac{i\pi}{3}} & e^{-\frac{2i\pi}{3}} & e^{-\frac{2i\pi}{3}} & -1 & -1 & e^{\frac{2i\pi}{3}} & e^{\frac{2i\pi}{3}} & e^{\frac{i\pi}{3}} & e^{\frac{i\pi}{3}} \\ 1 & -1 & 1 & -1 & 1 & -1 & 1 & -1 & 1 & -1 & 1 & -1 \\ 1 & -1 & -1 & 1 & 1 & -1 & -1 & 1 & 1 & -1 & -1 & 1 \\ 1 & 1 & e^{-\frac{2i\pi}{3}} & e^{-\frac{2i\pi}{3}} & e^{\frac{2i\pi}{3}} & e^{\frac{2i\pi}{3}} & 1 & 1 & e^{-\frac{2i\pi}{3}} & e^{-\frac{2i\pi}{3}} & e^{\frac{2i\pi}{3}} & e^{\frac{2i\pi}{3}} \\ 1 & 1 & e^{\frac{i\pi}{3}} & e^{\frac{i\pi}{3}} & e^{\frac{2i\pi}{3}} & e^{\frac{2i\pi}{3}} & -1 & -1 & e^{-\frac{2i\pi}{3}} & e^{-\frac{2i\pi}{3}} & e^{-\frac{i\pi}{3}} & e^{-\frac{i\pi}{3}} \\ 1 & -1 & e^{\frac{2i\pi}{3}} & e^{-\frac{i\pi}{3}} & e^{-\frac{2i\pi}{3}} & e^{\frac{i\pi}{3}} & 1 & -1 & e^{\frac{2i\pi}{3}} & e^{-\frac{i\pi}{3}} & e^{-\frac{2i\pi}{3}} & e^{\frac{i\pi}{3}} \\ 1 & -1 & e^{-\frac{i\pi}{3}} & e^{\frac{2i\pi}{3}} & e^{-\frac{2i\pi}{3}} & e^{\frac{i\pi}{3}} & -1 & 1 & e^{\frac{2i\pi}{3}} & e^{-\frac{i\pi}{3}} & e^{\frac{i\pi}{3}} & e^{-\frac{2i\pi}{3}} \end{pmatrix}. \tag{C.55}$$

We find 8 solutions to $(\widetilde{\mathcal{S}}\mathcal{T})^3 = \widetilde{\mathcal{S}}^2$ by flipping signs and multiplying phases on the diagonal of $\mathcal{T}$:

- phase: $e^{\frac{i\pi}{3}}$, positions: 1, 2, 3, 5, 6, 7, 9, 10, 11;
- phase: $e^{\frac{-i\pi}{3}}$, positions: 1, 2, 4, 5, 6, 8, 9, 10, 12;
- phase: $e^{\frac{i\pi}{3}}$, positions: 1, 3, 4, 5, 7, 8, 9, 11, 12;
- phase: $e^{\frac{i\pi}{3}}$, positions: 2, 3, 4, 6, 7, 8, 10, 11, 12;

- $\boxed{\text{phase: } e^{\frac{-i\pi}{3}},\ \text{positions: } 1,\ 5,\ 9}$;
- $\boxed{\text{phase: } e^{\frac{-i\pi}{3}},\ \text{positions: } 1,\ 3,\ 4,\ 5,\ 7,\ 8,\ 9,\ 11,\ 12}$;
- phase: $e^{\frac{i\pi}{3}}$, positions: 1, 2, 4, 5, 6, 8, 9, 10, 12;
- $\boxed{\text{phase: } e^{\frac{-i\pi}{3}},\ \text{positions: } 1,\ 2,\ 3,\ 5,\ 6,\ 7,\ 9,\ 10,\ 11}$.

The K-matrix of M is

$$\begin{pmatrix} 2 & -1 & 0 & -1 \\ -1 & 3 & -1 & 0 \\ 0 & -1 & 2 & -1 \\ -1 & 0 & -1 & 3 \end{pmatrix} \tag{C.56}$$

with signature 4, and again all phases are up to multiplications by $e^{\frac{2i\pi}{3}}$ and $e^{-\frac{2i\pi}{3}}$, so we see that the second, the fifth, the sixth and the last solutions yield the correct results.

Finally, we propose the following conjecture:

Conjecture For any $M \in SL(2,\mathbb{Z})$ built from a finite number of $ST^{\#}$ factors with any integer power $\#$, we perform the following steps:

- Compute the unsymmetrized $\widetilde{\mathcal{S}}$ and the naïve $\widetilde{\mathcal{T}}$ à la (5.134), or à la (5.140) and (5.141);
- Flip signs on $\widetilde{\mathcal{T}}$'s diagonal to get $\mathcal{T}$ satisfying $\left|(\widetilde{\mathcal{S}}\mathcal{T})^3\right| = \widetilde{\mathcal{S}}^2$;
- Multiply $\mathcal{T}$ with a necessary phase ϕ to satisfy $(\widetilde{\mathcal{S}}\mathcal{T})^3 = \widetilde{\mathcal{S}}^2$.

We claim that the resulting $\widetilde{\mathcal{S}}$ and $\mathcal{T}$ always exist, and they give the correct sign configurations for $\mathcal{S}$ and $\mathcal{T}$ in (5.134); as well as $\mathcal{S}$ in (5.140) and $\mathcal{T}$ in (5.141). Moreover, ϕ equals $e^{-i\pi\sigma(K)/12}$ as mentioned below (5.125) and (5.151), where K is defined by (5.126) together with (5.127).

C.4 Proof of the bivariate Landsberg-Schaar relation in (5.165)

The identity to be proved is:

$$\boxed{-\frac{i}{q}\sum_{m,n=0}^{q-1} e^{-\frac{2\pi i}{q}\left(2mn-am^2-bn^2\right)} = \left(\frac{1+i^{qb}}{2\sqrt{ab-1}}\right)\sum_{n=0}^{2ab-3}\exp\left(-\frac{\pi i q a n^2}{2(ab-1)}\right)}, \tag{C.57}$$

for $q \in 2\mathbb{Z}_+$, $a, b \in \mathbb{Z}$, $ab > 1$.

In the following subsections, we will prove this by discussing two separate situations, in which $q = 4r$ and $q = 4r+2$, respectively, where r is an odd integer.

Analysis for $q = 4r$

To prove this identity (C.57) we start with the Poisson resummation in two variables:

$$\sum_{m,n\in\mathbb{Z}} f(m,n) = \sum_{x,y\in\mathbb{Z}} \hat{f}(x,y),$$

where the Fourier transform is defined with normalization as:

$$\hat{f}(x,y) \equiv \int_{-\infty}^{\infty}\int_{-\infty}^{\infty} e^{-2\pi i(mx+ny)} f(u,v)dudv$$

We choose the function to be

$$f(u,v) \equiv e^{2\pi i\tau\left(au^2+bv^2-2uv\right)}, \qquad \mathrm{Im}\tau > 0, \qquad a,b>1,$$

then

$$\begin{aligned}\hat{f}(x,y) &= \int_{-\infty}^{\infty}\int_{-\infty}^{\infty} e^{2\pi i\left(a\tau x^2+b\tau y^2-2\tau xy-ux-vy\right)}dxdy \\ &= -\frac{1}{2i\sqrt{ab-1}}\exp\left[-\frac{\pi i\left(bu^2+av^2+2uv\right)}{2(ab-1)\tau}\right].\end{aligned} \tag{C.58}$$

So, we have

$$-\frac{1}{2i\sqrt{ab-1}}\sum_{m,n\in\mathbb{Z}}\exp\left[-\frac{\pi i\left(bm^2+an^2+2mn\right)}{2(ab-1)\tau}\right] = \sum_{m,n\in\mathbb{Z}} e^{2\pi i\tau\left(am^2+bn^2-2mn\right)}. \tag{C.59}$$

Now, we set

$$\tau = \frac{1}{q} + i\epsilon, \quad q = 4r, \tag{C.60}$$

and take the limit $\epsilon \to 0$, so that[6]

$$-\frac{1}{\tau} = -q + iq^2\epsilon + O\left(\epsilon^2\right). \tag{C.61}$$

The expression on the RHS of (C.59) can be expanded by setting

$$m \equiv m_1 q + m_0, \qquad n \equiv n_1 q + n_0, \qquad m_0, n_0 = 0,\ldots,q-1, \qquad m_1, n_1 \in \mathbb{Z},$$

so that with (C.60),

$$\exp\left[2\pi i\tau\left(am^2+bn^2-2mn\right)\right] \approx \exp\left[\frac{2\pi i}{q}\left(am_0^2+bn_0^2-2m_0n_0\right)\right] e^{-2\pi q^2\epsilon\left(am_1^2+bn_1^2-2m_1n_1\right)},$$

[6]This is similar to the standard complex-analytical technique in proving the basic univariate Landsberg-Schaar relation (5.17), shown for example in [260].

where in the exponent of the second factor on the RHS, we have ignored terms $2am_0m_1q$, bm_0^2, $2bn_0n_1q$, bn_0^2, $-2m_1n_0q$, $-2m_0n_1q$, and $-2m_0n_0$, which are proportional to either q or 1, because both m_0 and n_0 are only comparable to q at most.

Then

$$\sum_{m,n\in\mathbb{Z}} e^{2\pi i\tau\left(am^2+bn^2-2mn\right)} = \left(\sum_{m,n=0}^{q-1} e^{\frac{2\pi i}{q}\left(am^2+bn^2-2mn\right)}\right) \sum_{m,n\in\mathbb{Z}} e^{-2\pi q^2\epsilon\left(am^2+bn^2-2mn\right)}. \quad \text{(C.62)}$$

In the limit $\epsilon \to 0$, the leftmost sum on RHS of (C.62) can be evaluated by converting it into an integral with a change of variables $u \equiv m\sqrt{\epsilon}$ and $v \equiv n\sqrt{\epsilon}$:

$$\lim_{\epsilon\to 0} \sum_{m,n\in\mathbb{Z}} e^{-2\pi q^2\epsilon\left(am^2+bn^2-2mn\right)} \approx \frac{1}{\epsilon}\int_{-\infty}^{\infty} du \int_{-\infty}^{\infty} dv e^{-2\pi q^2\left(am^2+bn^2-2mn\right)} = \frac{1}{2\epsilon q^2\sqrt{ab-1}}.$$

So, we have

$$\lim_{\epsilon\to 0} \sum_{m,n\in\mathbb{Z}} e^{2\pi i\tau\left(am^2+bn^2-2mn\right)} \approx \frac{1}{2\epsilon q^2\sqrt{ab-1}} \sum_{m,n=0}^{q-1} e^{\frac{2\pi i}{q}\left(am^2+bn^2-2mn\right)}. \quad \text{(C.63)}$$

Now to approximate the LHS of (C.59), we need to perform a similar manipulation on the double sum

$$\sum_{m,n\in\mathbb{Z}} \exp\left[-\frac{\pi i\left(bm^2+an^2+2mn\right)}{2(ab-1)\tau}\right]. \quad \text{(C.64)}$$

It would help to know the Smith Normal Form of the matrix $\begin{pmatrix} a & -1 \\ -1 & b \end{pmatrix}$, which is related to the inverse of the quadratic form in the exponent of (C.64) by

$$\begin{pmatrix} a & -1 \\ -1 & b \end{pmatrix} = (ab-1)\begin{pmatrix} b & 1 \\ 1 & a \end{pmatrix}^{-1}.$$

Its decomposition into the Smith Normal Form is:

$$\begin{pmatrix} a & -1 \\ -1 & b \end{pmatrix} = \begin{pmatrix} 1 & -a \\ 0 & 1 \end{pmatrix}\begin{pmatrix} ab-1 & 0 \\ 0 & 1 \end{pmatrix}\begin{pmatrix} 0 & 1 \\ -1 & b \end{pmatrix}.$$

We want to convert the sum over $(m,n) \in \mathbb{Z}^2$ in (C.64) into a sum over a finite number of points in the fundamental cell generated by the columns of $\begin{pmatrix} a & -1 \\ -1 & b \end{pmatrix}$, times a sum over the lattice points generated by these columns. So, we write (m,n) as

$$\begin{pmatrix} m \\ n \end{pmatrix} = \begin{pmatrix} m_0 \\ n_0 \end{pmatrix} + \begin{pmatrix} a & -1 \\ -1 & b \end{pmatrix}\begin{pmatrix} m_1 \\ n_1 \end{pmatrix} = \begin{pmatrix} m_0+am_1-n_1 \\ n_0+bn_1-m_1 \end{pmatrix},$$

where (m_0, n_0) take $ab-1$ possible integer values.

Replacing

$$\begin{pmatrix} m_1 \\ n_1 \end{pmatrix} \to \begin{pmatrix} 0 & 1 \\ -1 & b \end{pmatrix} \begin{pmatrix} m_1 \\ n_1 \end{pmatrix},$$

we can write

$$\begin{pmatrix} m \\ n \end{pmatrix} = \begin{pmatrix} m_0 \\ n_0 \end{pmatrix} + \begin{pmatrix} 1 & -a \\ 0 & 1 \end{pmatrix} \begin{pmatrix} ab-1 & 0 \\ 0 & 1 \end{pmatrix} \begin{pmatrix} m_1 \\ n_1 \end{pmatrix}.$$

Setting

$$\begin{pmatrix} m_0 \\ n_0 \end{pmatrix} = \begin{pmatrix} 1 & -a \\ 0 & 1 \end{pmatrix} \begin{pmatrix} j \\ 0 \end{pmatrix}, \qquad j = 0, \ldots, ab-2\,,$$

we find

$$\begin{pmatrix} m \\ n \end{pmatrix} = \begin{pmatrix} j + m_1(ab-1) - n_1 a \\ n_1 \end{pmatrix}.$$

So, we set $n \equiv n_1$ and $m \equiv j + (ab-1)k - na$, where $j = 0, \ldots, ab-2$. Then,

$$bm^2 + an^2 + 2mn = bj^2 + (ab-1)\left[a(bk-n)^2 - b(k-j)^2 + 2(k-j)n + bj^2\right],$$

and (C.64) becomes

$$\sum_{j=0}^{ab-2} \left(e^{-\frac{\pi i b j^2}{2(ab-1)\tau}} \sum_{n,k\in\mathbb{Z}} \exp\left[-\frac{\pi i \left[a(bk-n)^2 - b(k-j)^2 + 2(k-j)n + bj^2\right]}{2\tau} \right] \right)$$

In the limit $\tau = 1/q + i\epsilon$ (C.61) with $\epsilon \to 0$, we can approximate the exponent

$$\begin{aligned} &-\frac{\pi i}{2\tau}\left[a(bk-n)^2 - b(k-j)^2 + 2(k-j)n + bj^2\right] \\ &\approx \; -\frac{\pi i}{2} q \left[a(bk-n)^2 - b(k-j)^2 + 2(k-j)n + bj^2\right] - \frac{\pi}{2} q^2 \epsilon \left[a(bk-n)^2 - bk^2 + 2kn\right]. \end{aligned} \tag{C.65}$$

Because $4|q$, the first term on the last line in (C.65) is an integer multiple of $2\pi i$ and can be dropped, so we are left with

$$\begin{aligned} &\sum_{m,n\in\mathbb{Z}} \exp\left[-\frac{\pi i \left(bm^2 + an^2 + 2mn\right)}{2(ab-1)\tau} \right] \\ &= \left(\sum_{j=0}^{ab-2} e^{-\frac{\pi i q b j^2}{2(ab-1)}} \right) \lim_{\epsilon\to 0} \sum_{n,k\in\mathbb{Z}} e^{-\frac{\pi}{2} q^2 \epsilon \left[a(bk-n)^2 - bk^2 + 2kn\right]}. \end{aligned} \tag{C.66}$$

The limit $\epsilon \to 0$ can be evaluated by converting (C.66) into an integral with a change of variables $u \equiv k\sqrt{\epsilon}$ and $v \equiv n\sqrt{\epsilon}$:

$$\begin{aligned}&\lim_{\epsilon\to 0}\sum_{n,k\in\mathbb{Z}} e^{-\frac{\pi}{2}q^2\epsilon\left[a(bk-n)^2-bk^2+2kn\right]}\\ &= \frac{1}{\epsilon}\int_{-\infty}^{\infty}du\int_{-\infty}^{\infty}dve^{-\frac{\pi}{2}q^2\left[a(bu-v)^2-bu^2+2uv\right]} = \frac{2}{q^2(ab-1)\epsilon}.\end{aligned}$$

Finally, we need to show that in (C.66),

$$\sum_{j=0}^{ab-2} e^{-\frac{\pi iqbj^2}{2(ab-1)}} = \sum_{j=ab-1}^{2ab-3} e^{-\frac{\pi iqbj^2}{2(ab-1)}}. \tag{C.67}$$

In order to achieve this, we consider the pairings between exponents of forms

$$-\frac{qbj^2}{ab-1}\frac{\pi i}{2} \quad \text{and} \quad -\frac{qb(ab-1+j)^2}{ab-1}\frac{\pi i}{2}, \quad j=0,\ldots,ab-2,$$

then the difference between j^2 and $(ab-1+j)^2$ is $a^2b^2-2ab+1+2j(ab-1) = (ab-1)^2+2j(ab-1)$, so the difference between two exponents is $(ab-1+2j)qb\pi i/2$, which is an integer multiple of $2\pi i$ because $4|q$. So the summands in (C.67) can be paired using the one-to-one correspondence between j and $ab-1+j$, and (C.67) is true.

At this point, we have results (C.59), (C.63), and the newly proved:

$$\lim_{\epsilon\to 0}\sum_{m,n\in\mathbb{Z}} \exp\left[-\frac{\pi i\left(bm^2+an^2+2mn\right)}{2(ab-1)\tau}\right] \tag{C.68}$$

$$\approx \frac{2}{q^2(ab-1)\epsilon}\sum_{j=0}^{ab-2} e^{-\frac{\pi iqbj^2}{2(ab-1)}} = \frac{2}{q^2(ab-1)\epsilon}\sum_{j=0}^{2ab-3} e^{-\frac{\pi iqbj^2}{2(ab-1)}}. \tag{C.69}$$

Combining these three equations, by inspection, (C.57) holds if $4|q$.

Analysis for $q = 4r+2 = 2s$

The case of odd b

In this case, the RHS of (C.57) is obviously zero. Hence we need to show that the LHS of (C.57) also vanishes, i.e., for fixed q and m,

$$\sum_{n=0}^{q-1} e^{-\frac{2\pi i}{q}\left(2mn-am^2-bn^2\right)} = 0.$$

We need to show that with m fixed, for every n, there is always a single $n' = n+t$ such that am^2+bn^2-2mn and $am^2+b(n+t)^2-2m(n+t)$ differ by an odd multiple of s, hence the pairing $e^{\frac{\pi i}{s}\left(am^2+bn^2-2mn\right)} + e^{\frac{\pi i}{s}\left(am^2+bn'^2-2mn'\right)}$ is 0.

We calculate this difference $am^2 + b(n+t)^2 - 2m(n+t) - (am^2 + bn^2 - 2mn) = bt^2 + 2bnt - 2mt$, and set it to be $-\delta s$. Then we only need to show that δ can be odd for every n. We start from the quadratic equation in t:

$$bt^2 + 2(bn - m)t + \delta s = 0, \tag{C.70}$$

with solutions $t_\pm = -n + \dfrac{m \pm \sqrt{(bn-m)^2 - b\delta s}}{b}$. We set the discriminant Δ to be x^2, $x \in \mathbb{Z}$, then it follows that

$$(bn - m - x)(bn - m + x) = b\delta s. \tag{C.71}$$

We also denote $\dfrac{m \pm \sqrt{\Delta}}{b} \equiv y$, leading to $m = by \pm x$. Then (C.71) becomes

$$(n - y)(bn - by \pm 2x) = \delta s.$$

In order to establish the pairing between n and n' for all n and n', we have to require $-n+y$, a solution to (C.70), be exactly $s = q/2$ [so that the pairings are all "diagonal" in the irregular q-sided polygon on the complex plane, whose vertices are $e^{-\frac{2\pi i}{q}\left(2mn - am^2 - bn^2\right)}$]. So we have

$$bn - by \pm 2x = -bs \pm 2x = -\delta.$$

Since both b and s are odd, δ has to be odd, as expected. Hence, for $q = 4r + 2$ and odd b, both sides of (C.57) are zero.

The case of even b and odd a

In this case, we do not construct pairings as before, but resort to an analytic method. The first term in (C.65) expands as

$$s\pi i \left[ab^2k^2 - 2abnk + an^2 - bk^2 + 2bjk + 2(k - j)n\right].$$

Since all terms in the square brackets, except for an^2, are even, the overall contributing exponent provided by (C.65) is

$$-\frac{\pi}{2}q^2\epsilon \left[a(bk - n)^2 - bk^2 + 2kn\right] - asn^2\pi i.$$

So the sum concerning n and k following (C.65) becomes

$$\lim_{\epsilon \to 0} \sum_{n,k \in \mathbb{Z}} e^{-\frac{\pi}{2}q^2\epsilon\left[a(bk-n)^2 - bk^2 + 2kn\right]} e^{-asn^2\pi i}, \tag{C.72}$$

where the second factor is just $(-1)^n$. We evaluate the first factor again by converting it into a single integral via a change of variables $u \equiv k\sqrt{\epsilon}$ and $v \equiv n\sqrt{\epsilon}$:

$$\frac{1}{\epsilon}\int_{-\infty}^{\infty} du \int_{-\infty}^{\infty} dv e^{-\frac{\pi}{2}q^2\left[a(bu-v)^2 - bu^2 + 2uv\right]} du dv = \frac{1}{q}\sqrt{\frac{2}{b(ab-1)\epsilon}} \sum_{n \in \mathbb{Z}} e^{-\frac{\pi q^2 \epsilon n^2}{2b}}, \tag{C.73}$$

where we only performed the u-integral and have converted v back to n after the equal sign. Then we consider the remaining infinite sum in (C.72):

$$\frac{1}{q}\lim_{\epsilon\to 0}\sqrt{\frac{2}{b(ab-1)\epsilon}}\sum_{n\in\mathbb{Z}}(-1)^n e^{-\frac{\pi q^2\epsilon n^2}{2b}},$$

which is zero because this is an alternating Riemann sum, and the decay in the exponent is $\sim\epsilon\to 0$, while the denominator of here goes as $\sim 1/\sqrt{\epsilon}$.

Notice that the result here agrees with the symmetry between a and b which is manifest on the LHS of (C.57), as well as the fact that both sides vanishes for an odd b as shown in Section C.4.

If both a and b are even

Then again the first term in (C.65) is an integer multiple of $2\pi i$, and the remaining argument conincide with that in the previous subsection Section C.4. ■

Bibliography

[1] Ana Achucarro and Paul K. Townsend. "A Chern-Simons action for three-dimensional anti-de Sitter supergravity theories". *Phys. Lett. B* 180.1-2 (1986), pp. 89–92.

[2] Edward Witten. "$2+1$ dimensional gravity as an exactly soluble system". *Nucl. Phys. B* 311.1 (1988), pp. 46–78.

[3] Steven Carlip. "Conformal field theory, $(2+1)$-dimensional gravity and the BTZ black hole". *Class. Quant. Grav.* 22.12 (2005), R85.

[4] Alexander B. Zamolodchikov. ""Irreversibility" of the Flux of the Renormalization Group in a 2D Field Theory". *J. Exp. Theor. Phys.* 43.12 (1986), pp. 730–732.

[5] Alexander Maloney and Edward Witten. "Quantum gravity partition functions in three dimensions". *J. High Energy Phys.* 2010.2 (2010), p. 29.

[6] Edward Witten. "APS Medal for Exceptional Achievement in Research: Invited article on entanglement properties of quantum field theory". *Rev. Mod. Phys.* 90.4 (2018), p. 045003.

[7] Hisaharu Umegaki. "Conditional expectation in an operator algebra, IV (Entropy and information)". *Kodai Mathematical Seminar Reports*. Vol. 14. 2. Department of Mathematics, Tokyo Institute of Technology. 1962, pp. 59–85.

[8] Pasquale Calabrese and John L. Cardy. "Entanglement entropy and quantum field theory". *J. Stat. Mech.: Theory. Exp.* 2004.06 (2004), P06002.

[9] Vladimir E. Korepin. "Universality of Scaling of Entropy in 1D Gapless Models". *Phys. Rev. Lett.* 92.9 (2004), p. 096402.

[10] Pasquale Calabrese and John L. Cardy. "Entanglement entropy and conformal field theory". *J. Phys. A: Math. Theor.* 42.50 (2009), p. 504005.

[11] Pasquale Calabrese, John L. Cardy, and Erik Tonni. "Entanglement entropy of two disjoint intervals in conformal field theory: II". *J. Stat. Mech.: Theory. Exp.* 2011.01 (2011), P01021.

[12] Maurizio Fagotti and Pasquale Calabrese. "Entanglement entropy of two disjoint blocks in XY chains". *J. Stat. Mech.: Theory. Exp.* 2010.04 (2010), P04016.

[13] Pasquale Calabrese, John L. Cardy, and Erik Tonni. "Entanglement entropy of two disjoint intervals in conformal field theory". *J. Stat. Mech.: Theory. Exp.* 2009.11 (2009), P11001.

[14] Vincenzo Alba, Luca Tagliacozzo, and Pasquale Calabrese. "Entanglement entropy of two disjoint blocks in critical Ising models". *Phys. Rev. B* 81.6 (2010), p. 060411.

[15] Shinsei Ryu and Tadashi Takayanagi. "Holographic derivation of entanglement entropy from the anti–de Sitter space/conformal field theory correspondence". *Phys. Rev. Lett.* 96.18 (2006), p. 181602.

[16] Jens Eisert, Marcus Cramer, and Martin B. Plenio. "*Colloquium*: Area laws for the entanglement entropy". *Rev. Mod. Phys.* 82.1 (2010), p. 277.

[17] Alexei Y. Kitaev and John Preskill. "Topological entanglement entropy". *Phys. Rev. Lett.* 96.11 (2006), p. 110404.

[18] Michael Levin and Xiao-Gang Wen. "Detecting topological order in a ground state wave function". *Phys. Rev. Lett.* 96.11 (2006), p. 110405.

[19] Pavan Hosur et al. "Chaos in quantum channels". *J. High Energy Phys.* 2016.2 (2016), p. 4.

[20] Massimiliano Rota. "Tripartite information of highly entangled states". *J. High Energy Phys.* 2016.4 (2016), p. 75.

[21] Yi Zhang et al. "Quasiparticle statistics and braiding from ground-state entanglement". *Phys. Rev. B* 85.23 (2012), p. 235151.

[22] Steven R. White. "Density matrix formulation for quantum renormalization groups". *Phys. Rev. Lett.* 69.19 (1992), p. 2863.

[23] Hong-Chen Jiang, Zhenghan Wang, and Leon Balents. "Identifying topological order by entanglement entropy". *Nat. Phys.* 8.12 (2012), pp. 902–905.

[24] Max Dehn. "Die Gruppe der Abbildungsklassen (Das arithmetische Feld auf Flächen)". *Acta Math.* 69 (1938), pp. 135–206.

[25] Edward Witten. "Quantum field theory and the Jones polynomial". *Commun. Math. Phys.* 121.3 (1989), pp. 351–399.

[26] Edward Witten. "Gauge theories and integrable lattice models". *Nucl. Phys. B* 322.3 (1989), pp. 629–697.

[27] Edward Witten. "Gauge theories, vertex models, and quantum groups". *Nucl. Phys. B* 330.2-3 (1990), pp. 285–346.

[28] Kenneth Intriligator and Nathan Seiberg. "Mirror symmetry in three dimensional gauge theories". *Phys. Lett. B* 387.3 (1996), pp. 513–519.

[29] Giancarlo Camilo et al. "Circuit complexity of knot states in Chern-Simons theory". *J. High Energy Phys.* 2019.7 (2019), p. 163.

[30] Keith Conrad. $SL_2(\mathbb{Z})$. Available at `https://kconrad.math.uconn.edu/blurbs/grouptheory/SL(2,Z).pdf`.

[31] Parsa Bonderson et al. "Congruence subgroups and super-modular categories". *Pac. J. Math.* 296.2 (2018), pp. 257–270.

[32] Juan Maldacena. "The large-N limit of superconformal field theories and supergravity". *Adv. Theor. Math. Phys.* 2.2 (1998), pp. 231–252.

[33] Martin Ammon and Johanna Erdmenger. *Gauge/gravity duality: Foundations and applications*. Cambridge University Press, 2015.

[34] Werner Nahm. "Supersymmetries and their Representations". *Nucl. Phys. B* 135 (1978), pp. 149–166.

[35] Edward Witten. "Some comments on string dynamics". *Future perspectives in string theory. Proceedings, Conference, Strings'95, Los Angeles, USA, March 13-18, 1995*. World Scientific, 1995, pp. 501–523.

[36] Andrew Strominger. "Open p-branes". *Phys. Lett. B* 383.1 (1996), pp. 44–47.

[37] Cumrun Vafa. "Geometric origin of Montonen-Olive duality". *Adv. Theor. Math. Phys.* 1 (1997), pp. 158–166.

[38] Luis F. Alday, Davide Gaiotto, and Yuji Tachikawa. "Liouville correlation functions from four-dimensional gauge theories". *Lett. Math. Phys.* 91.2 (2010), pp. 167–197.

[39] Tudor Dimofte, Davide Gaiotto, and Sergei Gukov. "3-manifolds and 3d indices". *Adv. Theor. Math. Phys.* 17.5 (2013), pp. 975–1076.

[40] Boris Feigin and Sergei Gukov. "VOA[M_4]". *J. Math. Phys.* 61.1 (2020), p. 012302.

[41] Ori J. Ganor et al. "Q-balls of quasi-particles in a (2, 0)-theory model of the fractional quantum Hall effect". *J. High Energy Phys.* 09.181 (2015), p. 181.

[42] Shiying Dong et al. "Topological entanglement entropy in Chern-Simons theories and quantum Hall fluids". *J. High Energy Phys.* 2008.05 (2008), p. 016.

[43] Sergei Gukov. "Three-dimensional quantum gravity, Chern-Simons theory, and the A-polynomial". *Commun. Math. Phys.* 255.3 (2005), pp. 577–627.

[44] Lauren McGough and Herman Verlinde. "Bekenstein-Hawking entropy as topological entanglement entropy". *J. High Energy Phys.* 2013.11 (2013), p. 208.

[45] Máaximo Bañados, Claudio Teitelboim, and Jorge Zanelli. "Black hole in three-dimensional spacetime". *Phys. Rev. Lett.* 69.13 (1992), p. 1849.

[46] Máximo Bañados et al. "Geometry of the $2+1$ black hole". *Phys. Rev. D* 48.4 (1993), p. 1506.

[47] Alexander B. Zamolodchikov and Alexei B. Zamolodchikov. "Liouville field theory on a pseudosphere". *6th Workshop on Supersymmetries and Quantum Symmetries (SQS'05)*. 2001, pp. 280–299.

[48] Oliver Coussaert, Marc Henneaux, and Peter van Driel. "The asymptotic dynamics of three-dimensional Einstein gravity with a negative cosmological constant". *Class. Quant. Grav.* 12.12 (1995), p. 2961.

[49] Kirill Krasnov. "Three-dimensional gravity, point particles and Liouville theory". *Class. Quant. Grav.* 18.7 (2001), p. 1291.

[50] Jörg Teschner. "Liouville theory revisited". *Class. Quant. Grav.* 18.23 (2001), R153.

[51] Edward Witten. *Three-Dimensional Gravity Revisited*. 2007. arXiv: `0706.3359 [hep-th]`.

[52] Xi Yin. "Partition functions of three-dimensional pure gravity". *Commun. Num. Theor. Phys.* (2008).

[53] Bin Chen and Jie-qiang Wu. "1-loop partition function in AdS_3/CFT_2". *J. High Energy Phys.* 2015.12 (2015), pp. 1–29.

[54] Simone Giombi, Alexander Maloney, and Xi Yin. "One-loop partition functions of 3D gravity". *J. High Energy Phys.* 2008.08 (2008), p. 007.

[55] Taylor Barrella et al. "Holographic entanglement beyond classical gravity". *J. High Energy Phys.* 2013.9 (2013), p. 01.

[56] Kirill Krasnov. "Holography and Riemann surfaces". *Adv. Theor. Math. Phys.* 4.4 (2000), pp. 929–979.

[57] Juan Maldacena. "Eternal black holes in anti-de Sitter". *J. High Energy Phys.* 2003.04 (2003), p. 021.

[58] Mark Van Raamsdonk. "Building up spacetime with quantum entanglement". *Gen. Relativ. Gravit.* 42.10 (2010), pp. 2323–2329.

[59] Juan Maldacena and Leonard Susskind. "Cool horizons for entangled black holes". *Fortschritte der Phys.* 61.9 (2013), pp. 781–811.

[60] Tatsuo Azeyanagi, Tatsuma Nishioka, and Tadashi Takayanagi. "Near extremal black hole entropy as entanglement entropy via AdS_2/CFT_1". *Phys. Rev. D* 77.6 (2008), p. 064005.

[61] John W. Milnor. "A procedure for killing the homotopy groups of differentiable manifolds". *Proc. Sympos. Pure Math. AMS*. Vol. 3. 1962, pp. 39–55.

[62] Curtis Callan and Frank Wilczek. "On geometric entropy". *Phys. Lett. B* 333.1-2 (1994), pp. 55–61.

[63] William P. Thurston. "Three dimensional manifolds, Kleinian groups and hyperbolic geometry". *Bull. Am. Math. Soc.* 6.3 (1982), pp. 357–381.

[64] Juan Maldacena and Andrew Strominger. "AdS_3 black holes and a stringy exclusion principle". *J. High Energy Phys.* 1998.12 (1999), p. 005.

[65] Robbert Dijkgraaf et al. *A Black Hole Farey Tail*. 2000. arXiv: `hep-th/0005003 [hep-th]`.

[66] Diptarka Das, Shouvik Datta, and Sridip Pal. "Monstrous entanglement". *J. High Energy Phys.* 2017.10 (2017), p. 147.

[67] Steven Carlip and Claudio Teitelboim. "Aspects of black hole quantum mechanics and thermodynamics in $2+1$ dimensions". *Phys. Rev. D* 51.2 (1995), p. 622.

[68] Steven J. Carlip. *Quantum gravity in* $2+1$ *dimensions*. Vol. 50. Cambridge University Press, 2003.

[69] Vijay Balasubramanian et al. "Multiboundary wormholes and holographic entanglement". *Class. Quant. Grav.* 31.18 (2014), p. 185015.

[70] Norihiro Iizuka, Akinori Tanaka, and Seiji Terashima. "Exact path integral for 3D quantum gravity". *Phys. Rev. Lett.* 115.16 (2015), p. 161304.

[71] Sergey N. Solodukhin. "Entanglement entropy of black holes". *Living Rev. Relativ.* 14.1 (2011), p. 8.

[72] Jan Manschot. "AdS_3 partition functions reconstructed". *J. High Energy Phys.* 2007.10 (2007), p. 103.

[73] Gerald Höhn. "Selbstduale vertexoperatorsuperalgebren und das babymonster (self-dual vertex operator super algebras and the baby monster)". *Bonner Math. Schriften* 286 (1996). Ph.D. thesis (Bonn 1995), pp. 1–85.

[74] John F.R. Duncan and Igor B. Frenkel. "Rademacher sums, moonshine and gravity". *Commun. Num. Theor. Phys.* 5.4 (2011), pp. 849–976.

[75] John H. Conway et al. *Atlas of finite groups: maximal subgroups and ordinary characters for simple groups*. Oxford University Press, 1985, pp. 220–227.

[76] John G. Thompson. "Some numerology between the Fischer-Griess Monster and the elliptic modular function". *Bull. London Math. Soc.* 11.3 (1979), pp. 352–353.

[77] John H. Conway and Simon P. Norton. "Monstrous moonshine". *Bull. London Math. Soc.* 11.3 (1979), pp. 308–339.

[78] Richard E. Borcherds. "Monstrous moonshine and monstrous Lie superalgebras". *Invent. Math.* 109.1 (1992), pp. 405–444.

[79] J. David Brown and Marc Henneaux. "Central charges in the canonical realization of asymptotic symmetries: an example from three dimensional gravity". *Commun. Math. Phys.* 104.2 (1986), pp. 207–226.

[80] Igor B. Frenkel, James Lepowsky, and Arne Meurman. "A natural representation of the Fischer-Griess Monster with the modular function J as character". *Proc. Natl. Acad. Sci. U.S.A.* 81.10 (1984), pp. 3256–3260.

[81] Jin-Beom Bae, Kimyeong Lee, and Sungjay Lee. *Bootstrapping Pure Quantum Gravity in* AdS_3. 2016. arXiv: `1610.05814 [hep-th]`.

[82] Davide Gaiotto. *Monster symmetry and Extremal CFTs*. 2008. arXiv: `0801.0988 [hep-th]`.

[83] John F.R. Duncan, Michael J. Griffin, and Ken Ono. "Moonshine". *Res. Math. Sci.* 2.11 (2015).

[84] Don N. Page. "Density matrix of the universe". *Phys. Rev. D* 34.8 (1986), p. 2267.

[85] Stephen H. Hawking. "The density matrix of the universe". 1987.T15 (1987), pp. 151–153.

[86] John C. Baez and Jamie Vicary. "Wormholes and entanglement". *Class. Quant. Grav.* 31.21 (2014), p. 214007.

[87] Song He et al. "Quantum dimension as entanglement entropy in two dimensional conformal field theories". *Phys. Rev. D* 90.4 (2014), p. 041701.

[88] Paweł Caputa and Alvaro Veliz-Osorio. "Entanglement constant for conformal families". *Phys. Rev. D* 92.6 (2015), p. 065010.

[89] Bin Chen et al. "Entanglement entropy for descendent local operators in 2D CFTs". *J. High Energy Phys.* 2015.10 (2015), p. 173.

[90] Floyd L. Williams. "Remainder formula and zeta expression for extremal CFT partition functions". *In Symmetry: representation theory and its applications*. Springer, 2014, pp. 505–518.

[91] Igor B. Frenkel, James Lepowsky, and Arne Meurman. *Vertex operator algebras and the Monster*. Academic Press Inc., 1989.

[92] Edward Frenkel and David Ben-Zvi. *Vertex algebras and algebraic curves*. 88. American Mathematical Society, 2004.

[93] Chongying Dong, Xiangyu Jiao, and Feng Xu. "Quantum dimensions and quantum Galois theory". *Trans. Am. Math. Soc.* 365.12 (2013), pp. 6441–6469.

[94] Terry Gannon. *Moonshine beyond the Monster: The bridge connecting algebra, modular forms and physics*. Cambridge University Press, 2006.

[95] Simon P. Norton. "Generalized moonshine". *Proc. Symp. Pure Math.* Vol. 47. 1987, pp. 208–209.

[96] Scott Carnahan and Masahiko Miyamoto. *Regularity of fixed-point vertex operator subalgebras*. 2016. arXiv: `1603.05645 [math.RT]`.

[97] Masahiko Miyamoto. "$C2$-cofiniteness of cyclic-orbifold models". *Commun. Math. Phys.* 335 (2015), pp. 1279–1286.

[98] Yi-Zhi Huang. "Vertex operator algebras, the Verlinde conjecture, and modular tensor categories". *Proc. Natl. Acad. Sci. U.S.A.* 102.15 (2005), pp. 5352–5356.

[99] Gregory W. Moore and Nathan Seiberg. "Classical and quantum conformal field theory". *Commun. Math. Phys.* 123.2 (1989), pp. 177–254.

[100] Jürgen Fuchs, Ingo Runkel, and Christoph Schweigert. "TFT construction of RCFT correlators I: Partition functions". *Nucl. Phys. B* 646.3 (2002), pp. 353–497.

[101] Stephen W. Hawking and Don N. Page. "Thermodynamics of black holes in anti-de Sitter space". *Commun. Math. Phys.* 87.4 (1983), pp. 577–588.

[102] Paul C. W. Davies. "The thermodynamic theory of black holes". *Proc. Royal Soc. A* 353.1675 (1977), pp. 499–521.

[103] Juan Crisóostomo, Ricardo Troncoso, and Jorge Zanelli. "Black hole scan". *Phys. Rev. D* 62.8 (2000), p. 084013.

[104] Yun Soo Myung. "No Hawking-Page phase transition in three dimensions". *Phys. Lett. B* 624.3-4 (2005), pp. 297–303.

[105] Paweł Caputa et al. "Liouville action as path-integral complexity: from continuous tensor networks to AdS/CFT". *J. High Energy Phys.* 2017.11 (2017), p. 97.

[106] Myungseok Eune, Wontae Kim, and Sang-Heon Yi. "Hawking-Page phase transition in BTZ black hole revisited". *J. High Energy Phys.* 2013.3 (2013), p. 20.

[107] Luigi Cappiello and Wolfgang Mück. "On the phase transition of conformal field theories with holographic duals". *Phys. Lett. B* 522.1-2 (2001), pp. 139–144.

[108] Yasunari Kurita and Masa-aki Sakagami. "CFT Description of the three-dimensional Hawking-Page transition". *Prog. Theor. Phys.* 113.6 (2005), pp. 1193–1213.

[109] Leszek M. Sokolowski and Pawel Mazur. "Second-order phase transitions in black-hole thermodynamics". *J. Phys. A: Math. Gen.* 13.3 (1980), p. 1113.

[110] Grant J. Stephens and Bei-Lok Hu. "Notes on black hole phase transitions". *Int. J. Theor. Phys.* 40.12 (2001), pp. 2183–2200.

[111] Zhu-Xi Luo and Hao-Yu Sun. *Work in progress.*

[112] Patrick Hayden, Matthew Headrick, and Alexander Maloney. "Holographic mutual information is monogamous". *Phys. Rev. D* 87.4 (2013), p. 046003.

[113] Diptarka Das and Shouvik Datta. "Universal features of left-right entanglement entropy". *Phys. Rev. Lett.* 115.13 (2015), p. 131602.

[114] Ben Craps, Matthias R. Gaberdiel, and Jeffrey A. Harvey. "Monstrous branes". *Commun. Math. Phys.* 234.2 (2003), pp. 229–251.

[115] Curtis T. Asplund et al. "Entanglement scrambling in 2d conformal field theory". *J. High Energy Phys.* 2015.9 (2015), p. 110.

[116] Paweł Caputa et al. "Scrambling time from local perturbations of the eternal BTZ black hole". *J. High Energy Phys.* 2015.8 (2015), p. 11.

[117] Vaughan F.R. Jones. "Index for subfactors". *Invent. Math.* 72.1 (1983), pp. 1–25.

[118] Vaughan F.R. Jones. "Knots, groups, subfactors and physics". *Jpn. J. Math.* 11.1 (2016), pp. 69–111.

[119] Alejandra Castro et al. "Gravity dual of the Ising model". *Phys. Rev. D* 85.2 (2012), p. 024032.

[120] Alexander A. Belavin, Alexander M. Polyakov, and Alexander B. Zamolodchikov. "Infinite conformal symmetry in two-dimensional quantum field theory". *Nucl. Phys. B* 241.2 (1984), pp. 333–380.

[121] Daniel Friedan, Zongan Qiu, and Stephen Shenker. "Conformal invariance, unitarity, and critical exponents in two dimensions". *Phys. Rev. Lett.* 52.18 (1984), p. 1575.

[122] Peter Bantay. "The kernel of the modular representation and the Galois action in RCFT". *Commun. Math. Phys.* 233.3 (2003), pp. 423–438.

[123] Siu-Hung Ng and Peter Schauenburg. "Congruence subgroups and generalized Frobenius-Schur indicators". *Commun. Math. Phys.* 300.1 (2010), pp. 1–46.

[124] Mikhail A. Vasiliev. "Nonlinear equations for symmetric massless higher spin fields in (A)dS$_d$". *Phys. Lett. B* 567.1-2 (2003), pp. 139–151.

[125] Matthias R. Gaberdiel and Rajesh Gopakumar. "An AdS$_3$ dual for minimal model CFTs". *Phys. Rev. D* 83.6 (2011), p. 066007.

[126] Andrew Strominger. "Black hole entropy from near-horizon microstates". *J. High Energy Phys.* 1998.02 (1998), p. 009.

[127] Stefan Åminnneborg et al. "Black holes and wormholes in $2+1$ dimensions". *Mathematical and quantum aspects of relativity and cosmology*. Springer, 2000, pp. 143–179.

[128] Dieter Brill. "Black holes and wormholes in $2+1$ dimensions". *In: S. Cotsakis, G.W. Gibbons (eds.) Mathematical and quantum aspects of relativity and cosmology, vol. 537*. Springer, 2000, pp. 143–179.

[129] Kirill Krasnov. "Analytic continuation for asymptotically AdS 3D gravity". *Class. Quant. Grav.* 19.9 (2002), p. 2399.

[130] Kostas Skenderis and Balt C. van Rees. "Holography and wormholes in $2+1$ dimensions". *Commun. Math. Phys.* 301.3 (2011), pp. 583–626.

[131] Xi Yin. "On non-handlebody instantons in 3D gravity". *J. High Energy Phys.* 2008.09 (2008), p. 120.

[132] Dennis Sullivan. "On the ergodic theory at infinity of an arbitrary discrete group of hyperbolic motions". *Riemann surfaces and related topics: Proceedings of the 1978 Stony Brook Conference, State Univ. New York, Stony Brook, ed. I. Kra and B. Maskit, Ann. Math. Studies 97*. Princeton University Press. 1981, pp. 465–496.

[133] Curtis T. McMullen. "Iteration on Teichmüller space". *Invent. Math.* 99.1 (1990), pp. 425–454.

[134] Danny Birmingham et al. "Geometrical finiteness, holography, and the Bañados-Teitelboim-Zanelli black hole". *Phys. Rev. Lett.* 82.21 (1999), p. 4164.

[135] Philippe Francesco, Pierre Mathieu, and David Sénéchal. *Conformal field theory*. Springer Science & Business Media, 1997.

[136] Alvany Rocha-Caridi. "Vacuum vector representations of the Virasoro algebra". *Vertex operators in mathematics and physics, Proc. Conf., November 10-17, 1983, ed. Lepowsky, S. Mandelstam and I. M. Singer*. Springer, 1985, pp. 451–473.

[137] Andrea Cappelli, Claude Itzykson, and Jean-Bernard Zuber. "The A-D-E classification of minimal and $A_1^{(1)}$ conformal invariant theories". *Commun. Math. Phys.* 113.1 (1987), pp. 1–26.

[138] Charles Fefferman and C. Robin Graham. "Conformal invariants". *"Elie Cartan et les Mathématiques d'Aujourd'hui," Astérisque, hors serie* (1985), pp. 95–116.

[139] Charles Fefferman and C. Robin Graham. *The Ambient Metric (AM-178)*. Princeton University Press, 2012.

[140] Matthew Headrick et al. "Rényi entropies, the analytic bootstrap, and 3D quantum gravity at higher genus". *J. High Energy Phys.* 2015.7 (2015), p. 59.

[141] Robbert Dijkgraaf, Erik Verlinde, and Herman Verlinde. "$C = 1$ conformal field theories on Riemann surfaces". *Commun. Math. Phys.* 115.4 (1988), pp. 649–690.

[142] Luis Alvarez-Gaumé, Gregory W. Moore, and Cumrun Vafa. "Theta functions, modular invariance, and strings". *Commun. Math. Phys.* 106.1 (1986), pp. 1–40.

[143] John L. Cardy, Alexander Maloney, and Henry Maxfield. "A new handle on three-point coefficients: OPE asymptotics from genus two modular invariance". *J. High Energy Phys.* 2017.10 (2017), p. 136.

[144] Andrea Coser, Luca Tagliacozzo, and Erik Tonni. "On Rényi entropies of disjoint intervals in conformal field theory". *J. Stat. Mech.: Theory. Exp.* 2014.1 (2014), P01008.

[145] Per Kraus and Alexander Maloney. "A cardy formula for three-point coefficients or how the black hole got its spots". *J. High Energy Phys.* 2017.5 (2017), pp. 1–22.

[146] Gretchen Wright. "The Reshetikhin-Turaev representation of the mapping class group". *J. Knot Theory Ramif.* 3.04 (1994), pp. 547–574.

[147] Peter Bender. "Eine Präsentation der symplektischen Gruppe $Sp(4, \mathbb{Z})$ mit 2 Erzeugenden und 8 definierenden Relationen". *J. Algebra* 65.2 (1980), pp. 328–331.

[148] Ning Lu. "A simple presentation of the Siegel modular groups". *Linear Algebra Its Appl.* 166 (1992), pp. 185–194.

[149] Allen Hatcher and Dan Margalit. "Generating the Torelli group". *Enseign. Math.* 58.1-2 (2011), pp. 165–188.

[150] Benson Farb and Dan Margalit. *A primer on mapping class groups (PMS-49)*. Princeton University Press, 2011.

[151] David B. Mumford. *Tata Lectures on Theta. I*. Modern Birkhäuser classics. Birkhäuser Boston Incorporated, 1983.

[152] David B. Mumford. *Tata lectures on theta II: Jacobian theta functions and differential equations*. Progress in Mathematics, volume 43. Birkhäuser Boston Incorporated, 1984.

[153] John D. Fay. *Theta functions on Riemann surfaces*. Vol. 352. Springer, 1973.

[154] Jun-ichi Igusa. *Theta functions*. Vol. 194. Springer Science & Business Media, 1972.

[155] Shu-Heng Shao and Edward Witten. "Private communications" (2020).

[156] Kevin Walker. *On Witten's 3-manifold invariants*. Avaliable at `http://canyon23.net/math/1991TQFTNotes.pdf`.

[157] Robion Kirby and Paul Melvin. "The 3-manifold invariants of Witten and Reshetikhin-Turaev for sl(2, C)". *Invent. Math.* 105.1 (1991), pp. 473–545.

[158] Allen Hatcher. *Algebraic topology*. [Example 2.48]. Cambridge University Press, 2002.

[159] Henry Maxfield, Simon F. Ross, and Benson Way. "Holographic partition functions and phases for higher genus Riemann surfaces". *Class. Quant. Grav.* 33.12 (2016), p. 125018.

[160] Bojko Bakalov and Alexander A. Kirillov Jr. *Lectures on tensor categories and modular functors*. American Mathematical Society, 2001.

[161] Zhenghan Wang. *Topological quantum computation*. American Mathematical Society, 2010.

[162] Michael Müger. "On the structure of modular categories". *Proc. London Math. Soc.* 87.2 (2003), pp. 291–308.

[163] Michael H. Freedman, Michael J. Larsen, and Zhenghan Wang. "The two-eigenvalue problem and density of Jones representation of braid groups". *Commun. Math. Phys.* 228 (2002), pp. 177–199.

[164] Peter G.O. Freund and Edward Witten. "Adelic string amplitudes". *Phys. Lett. B* 199.2 (1987), pp. 191–194.

[165] Lee Brekke et al. "Non-archimedean string dynamics". *Nucl. Phys. B* 302.3 (1988), pp. 365–402.

[166] Anton V. Zabrodin. "Non-archimedean strings and Bruhat-Tits trees". *Commun. Math. Phys.* 123.3 (1989), pp. 463–483.

[167] Steven S. Gubser et al. "p-adic AdS/CFT". *Commun. Math. Phys.* 352.3 (2017), pp. 1019–1059.

[168] Matthew T. E. Heydeman et al. "Tensor networks, p-adic fields, and algebraic curves: arithmetic and the $\mathrm{AdS}_3/\mathrm{CFT}_2$ correspondence". *Adv. Theor. Math. Phys.* 22.1 (2016), pp. 93–176.

[169] Dorian Goldfeld and Joseph Hundley. *Automorphic Representations and L-Functions for the General Linear Group: Volume 1*. Vol. 129. Cambridge University Press, 2011.

[170] Matthew Heydeman et al. *Nonarchimedean Holographic Entropy from Networks of Perfect Tensors*. 2018. arXiv: `1812.04057 [hep-th]`.

[171] Ling-Yan Hung, Wei Li, and Charles M. Melby-Thompson. "p-adic CFT is a holographic tensor network". *J. High Energy Phys.* 2019.4 (2019), p. 170.

[172] Steven S. Gubser, Christian Jepsen, and Brian Trundy. "Spin in p-adic AdS/CFT". *J. Phys. A: Math. Theor.* 52.14 (2019), p. 144004.

[173] Steven S. Gubser et al. "Melonic theories over diverse number systems". *Phys. Rev. D* 98.12 (2018), p. 126007.

[174] Steven S. Gubser et al. "Higher melonic theories". *J. High Energy Phys.* 2018.9 (2018), p. 49.

[175] An Huang, Dan Mao, and Bogdan Stoica. *From p-adic to Archimedean Physics: Renormalization Group Flow and Berkovich Spaces*. 2020. arXiv: `2001.01725 [hep-th]`.

[176] Ezer Melzer. "Nonarchimedean conformal field theories". *Int. J. Mod. Phys. A* 4.18 (1989), pp. 4877–4908.

[177] Daniel Harlow et al. "Eternal symmetree". *Phys. Rev. D* 85.6 (2012), p. 063516.

[178] Steven S. Gubser and Sarthak Parikh. "Geodesic bulk diagrams on the Bruhat–Tits tree". *Phys. Rev. D* 96.6 (2017), p. 066024.

[179] James S. Milne. *Algebraic number theory*. Available at `https://www.jmilne.org/math/CourseNotes/ANT.pdf`.

[180] Neal Koblitz. *p-adic Numbers, p-adic Analysis, and Zeta-Functions*. Springer Science & Business Media, 1984.

[181] Geunho Gim. *Ostrowski's Theorem*. Available at `https://www.math.ucla.edu/~ggim/F12-205A.pdf`.

[182] Lee Brekke and Peter G.O. Freund. "p-Adic numbers in physics". *Phys. Rep.* 233.1 (1993), pp. 1–66.

[183] Feng Qu and Yi-hong Gao. "Scalar fields on pAdS". *Phys. Lett. B* 786 (2018), pp. 165–170.

[184] Victor Gurarie. "c-Theorem for disordered systems". *Nucl. Phys. B* 546.3 (1999), pp. 765–778.

[185] Victor Gurarie and Andreas W. W. Ludwig. "Conformal field theory at central charge $c = 0$ and two-dimensional critical systems with quenched disorder". *From Fields to Strings: Circumnavigating Theoretical Physics: Ian Kogan Memorial Collection (In 3 Volumes)*. World Scientific, 2005, pp. 1384–1440.

[186] Per Kraus, Hirosi Ooguri, and Stephen Shenker. "Inside the horizon with AdS/CFT". *Phys. Rev. D* 67.12 (2003), p. 124022.

[187] Steven S. Gubser et al. "Edge length dynamics on graphs with applications to p-adic AdS/CFT". *J. High Energy Phys.* 2017.6 (2017), p. 157.

[188] Shuliang Bai et al. *On the Sum of Ricci-Curvatures for Weighted Graphs*. 2020. arXiv: 2001.01776 [math.CO].

[189] An Huang et al. *Bounds on the Ricci curvature and solutions to the Einstein equations for weighted graphs*. 2020. arXiv: 2006.06716 [math-ph].

[190] Steven S. Gubser, Igor R. Klebanov, and Alexander M. Polyakov. "Gauge theory correlators from non-critical string theory". *Phys. Lett. B* 428.1-2 (1998), pp. 105–114.

[191] Edward Witten. "Anti-de Sitter space and holography". *Adv. Theor. Math. Phys.* 2.2 (1998), pp. 253–291.

[192] Alexander Lubotzky. *Discrete groups, expanding graphs and invariant measures*. Springer Science & Business Media, 1994.

[193] Daniel Zwillinger. *CRC standard mathematical tables and formulae, 30th Edition*. CRC Press, 1995.

[194] Romesh K. Kaul and Parthasarathi Majumdar. "Logarithmic correction to the Bekenstein-Hawking entropy". *Phys. Rev. Lett.* 84.23 (2000), p. 5255.

[195] Steven Carlip. "Logarithmic corrections to black hole entropy, from the Cardy formula". *Class. Quant. Grav.* 17.20 (2000), p. 4175.

[196] Rafael D. Sorkin. "On the entropy of the vacuum outside a horizon". *B. Bertotti, F. de Felice, A. Pascolini (eds.), Tenth International Conference on General Relativity and Gravitation (held Padova, 4-9 July, 1983), Contributed Papers*. Vol. 2. Consiglio Nazionale delle richerche (Rome), 1983, pp. 734–736.

[197] John L. Cardy. "Operator content of two-dimensional conformally invariant theories". *Nucl. Phys. B* 270 (1986), pp. 186–204.

[198] John L. Cardy. "Effect of boundary conditions on the operator content of two-dimensional conformally invariant theories". *Nucl. Phys. B* 275.2 (1986), pp. 200–218.

[199] Henk W.J. Blöte, John L. Cardy, and M. Peter Nightingale. "Conformal invariance, the central charge, and universal finite-size amplitudes at criticality". *Phys. Rev. Lett.* 56.7 (1986), p. 742.

[200] Yong Lin, Linyuan Lu, and Shing-Tung Yau. "Ricci curvature of graphs". *Tohoku Math. J.* 63.4 (2011), pp. 605–627.

[201] Zeph Landau, Umesh Vazirani, and Thomas Vidick. "A polynomial time algorithm for the ground state of one-dimensional gapped local Hamiltonians". *Nat. Phys.* 11.7 (2015), pp. 566–569.

[202] Itai Arad et al. "Rigorous RG algorithms and area laws for low energy eigenstates in 1D". *Commun. Math. Phys.* 356.1 (2017), pp. 65–105.

[203] Luca V. Iliesiu et al. "An exact quantization of Jackiw-Teitelboim gravity". *J. High Energy Phys.* 2019.11 (2019), p. 91.

[204] Alexei Y. Kitaev. *Notes on* $\widetilde{\mathrm{SL}}(2,\mathbb{R})$ *representations*. 2017. arXiv: 1711.08169 [hep-th].

[205] Helge Glöckner. *Lectures on Lie groups over local fields*. 2008. arXiv: 0804.2234 [math.GR].

[206] Sascha Orlik and Matthias Strauch. "On the irreducibility of locally analytic principal series representations". *Represent. Theory* 14.20 (2010), pp. 713–746.

[207] Owen T. R. Jones. "An analogue of the BGG resolution for locally analytic principal series". *J. Number Theory* 131.9 (2011), pp. 1616–1640.

[208] Allan G. Silberger. *Introduction to harmonic analysis on reductive p-adic groups.(MN-23): Based on lectures by Harish-Chandra at The Institute for Advanced Study, 1971-73*. Princeton University Press, 2016.

[209] Jonathan D. Rogawski. *Modular forms, the Ramanujan conjecture and the Jacquet-Langlands correspondence*. Appendix to "Discrete groups, expanding graphs and invariant measures" by A. Lubotzky.

[210] Harish-Chandra. "Representations of Semisimple Lie Groups on a Banach Space". *Proc. Natl. Acad. Sci. U.S.A.* 37.3 (1956), pp. 170–173.

[211] Harish-Chandra. "Representations of semi-simple Lie groups. III. Characters". *Proc. Natl. Acad. Sci. U.S.A.* 37.6 (1951), pp. 366–369.

[212] Harish-Chandra. "Representations of semi-simple Lie groups. IV". *Proc. Natl. Acad. Sci. U.S.A.* 37.10 (1951), pp. 691–694.

[213] Paul Garrett. *Representations of* $GL(2)$ *and* $SL(2)$ *over finite fields*. Available at http://www-users.math.umn.edu/~garrett/m/v/toy_GL2.pdf.

[214] Matvei Libine. *Introduction to Representations of Real Semisimple Lie Groups*. 2012. arXiv: 1212.2578 [math.RT].

[215] I.N. Bernšteın. "All reductive p-adic groups are of type I". *Funkcional. Anal. i Priložen* 8.2 (1974), pp. 3–6.

[216] Karl E. Rumelhart. *Representations of p-adic groups, Lectures by Joseph Bernstein, Harvard University, Fall 1992*. Available at http://www.math.harvard.edu/~gaitsgde/Jerusalem_2010/GradStudentSeminar/p-adic.pdf.

[217] Uriya A. First and Thomas Rüd. "On uniform admissibility of unitary and smooth representations". *Arch. Math.* 112.2 (2019), pp. 169–179.

[218] Thomas Rüd. "Admissibility of representations of totally disconnected locally compact groups". Available at http://www.math.ubc.ca/~thomas/TeXthings/Projet_Master_Thomas_Rud_v3.pdf. MA thesis. École polytechnique fédérale de Lausanne and University of British Columbia, 2016.

[219] Kimball Martin. *Automorphic Representation, Fall 2011 Notes (and beyond)*. Available at `http://www2.math.ou.edu/~kmartin/autreps/autreps.pdf`.

[220] Jonathan D. Rogawski. *Admissible Representations of $GL_2(F)$: p-adic case*. Avaliable at `https://www.math.ucla.edu/~jonr/eprints/padic.pdf`.

[221] An Huang et al. *Green's Functions for Vladimirov Derivatives and Tate's Thesis*. 2020. arXiv: `2001.01721 [hep-th]`.

[222] Hervé Jacquet. "Représentations des groupes linéaires p-adiques". *Gherardelli, F. (ed.), Theory of group representations and Fourier analysis (Centro Internaz. Mat. Estivo (C.I.M.E.), II Ciclo, Montecatini Terme, 1970), Rome: Edizioni cremonese*. Springer, 1971, pp. 119–220.

[223] Robert P. Langlands and Hervé Jacquet. *Automorphic forms on $GL(2)$*. Springer-Verlag, 1970.

[224] Michael C. Woodbury. *Representation theory and number theory*. Available at `http://www.mi.uni-koeln.de/~woodbury/research/Grossnotes.pdf`.

[225] Oliver Taïbi. *The Jacquet-Langlands correspondence for $GL_2(\mathbb{Q}_p)$, Notes for the M2 course*. Available at `https://otaibi.perso.math.cnrs.fr/notesJL.pdf`.

[226] Jean-Loup Gervais. "p-adic analyticity and Virasoro algebras for conformal theories in more than two dimensions". *Phys. Lett. B* 201.3 (1988), pp. 306–310.

[227] Masahito Yamazaki. "Comments on determinant formulas for general CFTs". *J. High Energy Phys.* 2016.10 (2016), p. 35.

[228] Christoph Schweigert. *Introduction to conformal field theory, Universität Hamburg, 65-405, Winter 2013/14*. Available at `https://www.math.uni-hamburg.de/home/schweigert/ws13/cft.html`.

[229] Lauren McGough, Márk Mezei, and Herman Verlinde. "Moving the CFT into the bulk with $T\overline{T}$". *J. High Energy Phys.* 2018.4 (2018), p. 10.

[230] Dongsu Bak, Michael Gutperle, and Shinji Hirano. "A dilatonic deformation of AdS5 and its field theory dual". *J. High Energy Phys.* 2003.05 (2003), p. 072.

[231] Adam B. Clark and Andreas Karch. "Super Janus". *J. High Energy Phys.* 2005.10 (2005), p. 094.

[232] Eric D'Hoker, John Estes, and Michael Gutperle. "Interface Yang-Mills, supersymmetry, and Janus". *Nucl. Phys. B* 753.1-2 (2006), pp. 16–41.

[233] Davide Gaiotto and Edward Witten. "Janus Configurations, Chern-Simons Couplings, And The Theta-Angle in $\mathcal{N} = 4$ Super Yang-Mills Theory". *J. High Energy Phys.* 2010.6 (2010), p. 97.

[234] Chanju Kim, Eunkyung Koh, and Ki-Myeong Lee. "Janus and multifaced supersymmetric theories". *J. High Energy Phys.* 2008.06 (2008), p. 040.

[235] Chanju Kim, Eunkyung Koh, and Ki-Myeong Lee. "Janus and multifaced supersymmetric theories. II". *Phys. Rev. D* 79.12 (2009), p. 126013.

[236] Yuji Terashima and Masahito Yamazaki. "$SL(2,\mathbb{R})$ Chern-Simons, Liouville, and Gauge Theory on Duality Walls". *J. High Energy Phys.* 2011.8 (2011), p. 135.

[237] Nadav Drukker, Davide Gaiotto, and Jaume Gomis. "The virtue of defects in 4D gauge theories and 2D CFTs". *J. High Energy Phys.* 2011.6 (2011), p. 25.

[238] Joseph A. Minahan and Usman Naseer. "Gauge theories on spheres with 16 supercharges and non-constant couplings". *J. Phys. A: Math. Theor.* 52.23 (2019), p. 235401.

[239] Davide Gaiotto. "Surface Operators in $\mathcal{N} = 2$ 4d Gauge Theories". *J. High Energy Phys.* 2012.11 (2012), p. 90.

[240] Kanato Goto and Takuya Okuda. "Janus interface in two-dimensional supersymmetric gauge theories". *J. High Energy Phys.* 2019.10 (2019), p. 45.

[241] Dabholkar, Atish and Harvey, Jeffrey A. "String islands". *J. High Energy Phys.* 1999.02 (1999), p. 006.

[242] Ori J. Ganor. "U-duality twists and possible phase transitions in 2+1 D supergravity". *Nucl. Phys. B* 549.1-2 (1999), pp. 145–180.

[243] Simeon Hellerman, John McGreevy, and Brook Williams. "Geometric constructions of nongeometric string theories". *J. High Energy Phys.* 2004.01 (2004), p. 024.

[244] Atish Dabholkar and Chris Hull. "Duality twists, orbifolds, and fluxes". *J. High Energy Phys.* 2003.09 (2003), p. 054.

[245] Atish Dabholkar and Chris Hull. "Generalised T-duality and non-geometric backgrounds". *J. High Energy Phys.* 2006.05 (2006), p. 009.

[246] Abhijit Gadde, Sergei Gukov, and Pavel Putrov. *Duality Defects*. 2014. arXiv: `1404.2929 [hep-th]`.

[247] Ori J. Ganor et al. "Janus configurations with $SL(2,\mathbb{Z})$-duality twists, strings on mapping tori and a tridiagonal determinant formula". *J. High Energy Phys.* 2014.7 (2014), p. 10.

[248] Benjamin Assel and Alessandro Tomasiello. "Holographic duals of 3d S-fold CFTs". *J. High Energy Phys.* 2018.6 (2018), p. 19.

[249] Luca Martucci. "Topological duality twist and brane instantons in F-theory". *J. High Energy Phys.* 2014.6 (2014), p. 180.

[250] Chang-Tse Hsieh, Yuji Tachikawa, and Kazuya Yonekura. "Anomaly of the electromagnetic duality of Maxwell theory". *Phys. Rev. Lett.* 123.16 (2019), p. 161601.

[251] Tudor Dimofte, Davide Gaiotto, and Sergei Gukov. "Gauge theories labelled by three-manifolds". *Commun. Math. Phys.* 325.2 (2014), pp. 367–419.

[252] Dongmin Gang et al. "Aspects of defects in 3d-3d correspondence". *J. High Energy Phys.* 2016.10 (2016), p. 62.

[253] Dongmin Gang et al. "Taming supersymmetric defects in 3d–3d correspondence". *J. Phys. A: Math. Theor.* 49.30 (2016), 30LT02.

[254] Sungbong Chun et al. *3d-3d correspondence for mapping tori*. 2019. arXiv: `1911.08456 [hep-th]`.

[255] Davide Gaiotto. "$N = 2$ dualities". *J. High Energy Phys.* 2012.8 (2012), p. 34.

[256] Emil Artin. "Beweis des allgemeinen Reziprozitätsgesetzes". *Abhandlungen aus dem Mathematischen Seminar der Universität Hamburg*. Vol. 5. 1. Springer. 1927, pp. 353–363.

[257] Kenneth Ireland and Michael Rosen. *A Classical Introduction to Modern Number Theory. 1990*. Graduate Texts in Mathematics. 1990.

[258] Mathias Schaar. *Mémoire sur la théorie des résidus quadraticues*. Vol. 24. 5. 1850, pp. 1–14.

[259] Georg Landsberg. *Zur Theorie der Gauss' schen Summen und der linearen Transformation der Thetafunctionen*. Vol. 111. G. Reimer, 1893, pp. 234–253.

[260] Harry Dym and Henry P. McKean. *Fourier series and integrals*. Academic Press, 1972.

[261] Jonathan M. Borwein and Peter B. Borwein. *Pi and the AGM: a study in the analytic number theory and computational complexity*. Wiley-Interscience, 1987.

[262] Ben Moore. "A proof of the Landsberg-Schaar relation by finite methods". *Ramanujan J.* (2020), pp. 1–13.

[263] Bruce C. Berndt and Ronald J. Evans. "The determination of Gauss sums". *Bull. Am. Math. Soc.* 5.2 (1981), pp. 107–129.

[264] Cumrun Vafa. "Evidence for F-theory". *Nucl. Phys. B* 469.3 (1996), pp. 403–415.

[265] Amit Giveon, Massimo Porrati, and Eliezer Rabinovici. "Target space duality in string theory". *Phys. Rep.* 244.2-3 (1994), pp. 77–202.

[266] Kumar S. Narain, M. Hossein Sarmadi, and Cumrun Vafa. "Asymmetric orbifolds". Vol. 288. Elsevier, 1987, pp. 551–577.

[267] Anton Kapustin and Mikhail Tikhonov. "Abelian duality, walls and boundary conditions in diverse dimensions". *J. High Energy Phys.* 2009.11 (2009), p. 006.

[268] Ori J. Ganor, Sharon Jue, and Shannon McCurdy. "Ground states of duality-twisted sigma-models with K_3 target space". *J. High Energy Phys.* 2013.2 (2013), p. 17.

[269] Davide Gaiotto and Edward Witten. "S-duality of boundary conditions in $\mathcal{N} = 4$ super Yang-Mills theory". *Adv. Theor. Math. Phys.* 13.3 (2008), pp. 721–896.

[270] Yolanda Lozano. "S-duality in gauge theories as a canonical transformation". *Phys. Lett. B* 364.1 (1995), pp. 19–26.

[271] Ori J. Ganor. "A note on zeroes of superpotentials in F-theory". *Nucl. Phys. B* 499.1-2 (1997), pp. 55–66.

[272] Edward Witten. "$SL(2,\mathbb{Z})$ action on three-dimensional conformal field theories with Abelian symmetry". *In Shifman, M. (ed.) et al.: From Fields to Strings: Circumnavigating Theoretical Physics. Ian Kogan Memorial Collection (3 volume set), vol.2.* World Scientific, 2005, pp. 1173–1200.

[273] Ori J. Ganor and Yoon Pyo Hong. *Selfduality and Chern-Simons Theory*. 2008. arXiv: `0812.1213 [hep-th]`.

[274] Ori J. Ganor, Yoon Pyo Hong, and Hai Siong Tan. "Ground states of S-duality twisted $N = 4$ super Yang-Mills theory". *J. High Energy Phys.* 2011.3 (2011), p. 99.

[275] Edward Witten. "Dynamical breaking of supersymmetry". *Nucl. Phys. B* 188.3 (1981), pp. 513–554.

[276] Fred Cooper and Barry Freedman. "Aspects of supersymmetric quantum mechanics". *Ann. Phys.* 146.2 (1983), pp. 262–288.

[277] Fred Cooper, Avinash Khare, and Uday Sukhatme. "Supersymmetry and quantum mechanics". *Ann. Phys.* 146.2 (1982), pp. 262–288.

[278] Sergei Gukov, Marcos Marino, and Pavel Putrov. *Resurgence in complex Chern-Simons theory*. 2016. arXiv: `1605.07615 [hep-th]`.

[279] Miranda C.-N. Cheng et al. "3d modularity". *J. High Energy Phys.* 2019.10 (2019), p. 10.

[280] Charles T. C. Wall. "Quadratic forms on finite groups, and related topics". *Topology* 2.4 (1963), pp. 281–298.

[281] César Galindo and Nicolás Jaramillo. "Solutions of the hexagon equation for abelian anyons". *Rev. Colomb. de Mat.* 50.2, (2016), pp. 277–298.

[282] Modjtaba S. Zini. "Lecture notes on vector-valued modular forms by Zhenghan Wang at University of California, Santa Barbara, Math 227C, Spring 2019". *unpublished* ().

[283] Dmitriy Belov and Gregory W. Moore. *Classification of abelian spin Chern-Simons theories*. 2005. arXiv: `hep-th/0505235 [hep-th]`.

[284] Yasunori Lee and Yuji Tachikawa. "A study of time reversal symmetry of abelian anyons". *J. High Energy Phys.* 2018.7 (2018), p. 90.

[285] Diego Delmastro and Jaume Gomis. *Symmetries of Abelian Chern-Simons Theories and Arithmetic*. 2019. arXiv: `1904.12884 [hep-th]`.

[286] Brandon Williams. "Computing modular forms for the Weil representation". PhD thesis. University of California, Berkeley, 2018.

[287] Florian Deloupe. *Topological Quantum Field Theory, Reciprocity and the Weil representation*. Available at `http://www.math.univ-toulouse.fr/~deloup/Weil-book10.pdf`.

[288] Jennifer Cano et al. "Bulk-edge correspondence in $(2+1)$-dimensional abelian topological phases". *Phys. Rev. B* 89.11 (2014), p. 115116.

[289] M. Lawrence Glasser and Michael Milgram. "On quadratic Gauss sums and variations thereof". *Cogent Mathe.* 2.1 (2015), p. 1021187.

[290] Xiao-Gang Wen. "Vacuum degeneracy of chiral spin states in compactified space". *Phys. Rev. B* 40.10 (1989), p. 7387.

[291] Xiao-Gang Wen and Qian Niu. "Ground-state degeneracy of the fractional quantum Hall states in the presence of a random potential and on high-genus Riemann surfaces". *Phys. Rev. B* 41.13 (1990), p. 9377.

[292] Shmuel Elitzur et al. "Remarks on the canonical quantization of the Chern-Simons-Witten theory". *Nucl. Phys. B* 326.1 (1989), pp. 108–134.

[293] Scott Axelrod, Steve A. Della Pietra, and Edward Witten. "Geometric quantization of Chern Simons gauge theory". *J. Diff. Geom.* 33.3 (1991), pp. 787–902.

[294] Lisa C. Jeffrey. "Chern-Simons-Witten invariants of lens spaces and torus bundles, and the semiclassical approximation". *Commun. Math. Phys.* 147.3 (1992), pp. 563–604.

[295] Lisa C. Jeffrey. "Symplectic quantum mechanics and Chern-Simons gauge theory. II. Mapping tori of tori". *J. Math. Phys.* 54.5 (2013), p. 052305.

[296] Michael Atiyah. "On framings of 3-manifolds". *Topology* 29.1 (1990), pp. 1–7.

[297] Abhijit Gadde, Sergei Gukov, and Pavel Putrov. "Fivebranes and 4-manifolds". *In: W. Ballmann, C. Blohmann, G. Faltings, P. Teichner, D. Zagier (eds.) Arbeitstagung Bonn 2013. Progress in Mathematics, vol 319. Birkhäuser, Cham.* Springer, 2016, pp. 155–245.

[298] Sergei Gukov, Pavel Putrov, and Cumrun Vafa. "Fivebranes and 3-manifold homology". *J. High Energy Phys.* 2017.7 (2017), p. 71.

[299] Xiao-Gang Wen and Anthony Zee. "Classification of Abelian quantum Hall states and matrix formulation of topological fluids". *Phys. Rev. B* 46.4 (1992), p. 2290.

[300] Edward Witten. "Fermion path integrals and topological phases". *Rev. Mod. Phys.* 88.3 (2016), p. 035001.

[301] F. Duncan M. Haldane and Edward H. Rezayi. "Periodic Laughlin-Jastrow wave functions for the fractional quantized Hall effect". *Phys. Rev. B* 31.4 (1985), p. 2529.

[302] Mauro Spera. "Quantization on Abelian varieties". *Rend. Semin. Mat. Univ. Politec. Torino* 44 (1986), pp. 383–392.

[303] John R. Klauder and Enrico Onofri. "Landau levels and geometric quantization". *Int. J. Mod. Phys. A* 4.15 (1989), pp. 3939–3949.

[304] F. Duncan M. Haldane. "$O(3)$ nonlinear σ-model and the topological distinction between integer-and half-integer-spin antiferromagnets in two dimensions". *Phys. Rev. Lett.* 61.8 (1988), p. 1029.

[305] Alexander Altland and Ben D. Simons. *Condensed matter field theory*. Cambridge University Press, 2010.

[306] Adolf Krazer. "Zur Theorie der mehrfachen Gaußschen Summen". *Festschrift Heinrich Weber zu seinem siebzigsten Geburtstag am 5. März 1912*. Leipzitg und Berlin, B. G. Teubner, 1912, p. 181.

[307] Şaban Alaca and Greg Doyle. "Explicit Evaluation of Double Gauss Sums". *J. Comb. Number Theory* 8.1 (2016), pp. 47–61.

[308] Vladimir G. Turaev. "Reciprocity for Gauss sums on finite abelian groups". *Math. Proc. Camb. Phil. Soc.* Vol. 124. 2. Cambridge University Press. 1998, pp. 205–214.

[309] Hel Braun. "Geschlechter quadratischer Formen." *J. reine angew. Math.* 1940.182 (1940), pp. 32–49.

[310] Carl L. Siegel. *Über das quadratische Reziprozitätsgesetz in algebraischen Zahlkörpern*. Vandenhoeck & Ruprecht, 1960.

[311] Florian Deloup and Vladimir G. Turaev. "On reciprocity". *J. Pure and Appl. Algebra* 208.1 (2007), pp. 153–158.

[312] Florian Deloup. "Linking forms, reciprocity for Gauss sums and invariants of 3-manifolds". *Trans. Am. Math. Soc.* 351.5 (1999), pp. 1895–1918.

[313] Florian Deloup. "On abelian quantum invariants of links in 3-manifolds". *Math. Ann.* 319.4 (2001), pp. 759–795.

[314] Sergei Gukov et al. *BPS spectra and 3-manifold invariants*. 2017. arXiv: `1701.06567 [hep-th]`.

[315] Greg Doyle. "Quadratic Form Gauss Sums". PhD thesis. Carleton University, 2016.

[316] Franz Lemmermeyer. *Reciprocity laws: from Euler to Eisenstein*. Springer Science & Business Media, 2000.

[317] Vernon Armitage and Alice Rogers. "Gauss sums and quantum mechanics". *J. Phys. A: Math. Gen.* 33.34 (2000), p. 5993.

[318] Masanobu Kaneko and Don Zagier. "Supersingular j-invariants, hypergeometric series, and Atkin's orthogonal polynomials". *AMS/IP Studies in Advanced Mathematics* 7 (1998), pp. 97–126.

[319] Takumi Noda. "Some asymptotic expansions of the Eisenstein series". *RIMS Kôkyûroku* 1659 (2009), p. 106.

[320] Steven Carlip. "What we don't know about BTZ black hole entropy". *Class. Quant. Grav.* 15.11 (1998), p. 3609.

[321] Zhu-Xi Luo and Hao-Yu Sun. "Topological entanglement entropy in Euclidean AdS_3 via surgery". *J. High Energy Phys.* 2017.12 (2017), p. 116.

[322] Christoph A. Keller and Alexander Maloney. "Poincaré series, 3D gravity and CFT spectroscopy". *J. High Energy Phys.* 2015.2 (2015), p. 80.

[323] Daniel S. Freed. "Determinants, torsion, and strings". *Commun. Math. Phys.* 107.3 (1986), pp. 483–513.

[324] Jean-Benoît Bost and Philip C. Nelson. "Spin-1/2 nosonization on compact surfaces". *Phys. Rev. Lett.* 57 (1986), p. 795.

[325] Eric D'Hoker and Duong H. Phong. "The geometry of string perturbation theory". *Rev. Mod. Phys.* 60.4 (1988), p. 917.

[326] Eric D'Hoker and Duong H. Phong. "Multiloop amplitudes for the bosonic Polyakov string". *Nucl. Phys. B* 269.1 (1986), pp. 205–234.

[327] Eric D'Hoker and Duong H. Phong. "On determinants of Laplacians on Riemann surfaces". *Commun. Math. Phys.* 104.4 (1986), pp. 537–545.

[328] David Fried. "Analytic torsion and closed geodesics on hyperbolic manifolds". *Invent. Math.* 84.3 (1986), pp. 523–540.

[329] Jan de Boer and Jacob Goeree. "Markov traces and II_1 factors in conformal field theory". *Commun. Math. Phys.* 139.2 (1991), pp. 267–304.

[330] Antoine Coste and Terry Gannon. "Remarks on Galois symmetry in rational conformal field theories". *Phys. Lett. B* 323.3-4 (1994), pp. 316–321.

[331] Sergei Gukov and Cumrun Vafa. "Rational conformal field theories and complex multiplication". *Commun. Math. Phys.* 246.1 (2004), pp. 181–210.

[332] Max Koecher. "Zur Theorie der Modulformenn-ten Grades. I". *Math. Z.* 59.1 (1953), pp. 399–416.

[333] Aloys Krieg. *Modular forms on half-spaces of quaternions*. Springer, 1985.

[334] James E. Tener and Zhenghan Wang. "On classification of extremal non-holomorphic conformal field theories". *J. Phys. A: Math. Theor.* 50.11 (2017), p. 115204.

[335] Vladimir G. Turaev. *Quantum invariants of knots and 3-manifolds*. Walter de Gruyter GmbH & Co KG, 1994.

[336] Victor Z. Enolski and Tamara Grava. "Singular $\mathbb{Z}_N$-curves and the Riemann-Hilbert problem". *Int. Math. Res. Not.* 2004.32 (2004), pp. 1619–1683.

[337] Harold Exton. "Multiple hypergeometric functions and applications" (1976).

[338] Pavel Etingof, Eric C. Rowell, and Sarah Witherspoon. "Braid group representations from twisted quantum doubles of finite groups". *Pac. J. Math.* 234.1 (2008), pp. 33–41.

[339] Deepak Naidu and Eric C. Rowell. "A finiteness property for braided fusion categories". *Algebr. Represent. Theor.* 14.5 (2011), pp. 837–855.

[340] Alexei Y. Kitaev. "Anyons in an exactly solved model and beyond". *Ann. Phys.* 321.1 (2006), pp. 2–111.

[341] Wade Bloomquist and Zhenghan Wang. "On topological quantum computing with mapping class group representations". *J. Phys. A: Math. Theor.* 52.1 (2018), p. 015301.

[342] George N. Watson. "The final problem: an account of the mock theta functions". *J. London Math. Soc.* s1-11.1 (1936), pp. 55–80.

[343] Chao Li. *"Lecture notes on representation theory and number theory'' by Benedict Gross at Columbia University in the City of New York, Fall 2011*. Available at `http://www.math.columbia.edu/~chaoli/docs/EilenbergLectures.html`.

[344] Andrew Knightly and Carl Ragsdale. "Matrix coefficients of depth-zero supercuspidal representations of $GL(2)$". *Involve* 7.5 (2014), pp. 669–690.

[345] Alexander Youcis. *Notes for p-adic representations*. Available at `https://ayoucis.files.wordpress.com/2016/10/notes-p-adic.pdf`.